

Lowland Maya Lime Plaster Technology: a Diachronic Approach

A thesis submitted as partial fulfillment of the requirements for the degree of
Doctor of Philosophy

Institute of Archaeology, University College London

by

María Isabel Villaseñor Alonso

Abstract

Lime plasters are mixtures of burnt lime, aggregates and other materials that are employed in masonry architecture. Lime plasters were widely used by the ancient Maya in public monumental buildings and constitute important elements of ancient Maya material culture.

This research analyses archaeological samples of lime plasters from three different lowland Maya sites: Palenque, Calakmul and Lamanai. The thesis examines how these building materials changed through time, and includes samples from ca. 400 BC to the 16th century AD.

In addition to the analysis of archaeological samples, the research also reviews various sources of information, including ethnographic and ethnohistorical descriptions, for the understanding of ancient Maya lime plaster production.

The results demonstrate that plasters from the three sites have different characteristics that are due to different access to raw materials and different building traditions at each of the sites. Some of the changes seem to be related to changing economic and political conditions, which is very clear in the use of clays instead of lime for the manufacture of architectural plasters during the Terminal Classic periods at Calakmul and Palenque. Other observations include the use of local meteoritic deposits in the lime mixtures of Palenque, the use of non-local volcanic materials in the late plasters from Lamanai, and the likely use of volcanic ash at Calakmul for the production of hydraulic plasters.

In addition to the technological analyses of ancient plasters, the research also provides suggestions for future research and recommends those analytical methods that are most suitable for the examination of Maya lime plasters.

ACKNOWLEDGMENTS

I warmly thank my supervisors, Prof. Clifford Price, Dr. Elizabeth Graham, Dr. Ruth Siddall and Dr. James Aimers for their very sensible comments and advice throughout the PhD, as well as for the timely feedback during the last stage of the writing up. I thank them for their support and their great expertise and professionalism, without which the completion of this thesis would not have been possible. I also want to acknowledge the commitment of Clifford Price, who willingly continued supervising my research after his retirement, as well as Elizabeth Graham, who kindly supervised me during her sabbatical years.

I thank the laboratory technicians of the Archaeological Science Laboratories at the Institute of Archaeology UCL, who provided substantial training and advice on the analyses of samples: Kevin Reeves and Philip Connolly for their assistance with the SEM/EDS, microprobe and Raman spectroscopy equipments; James Hales for his support with the preparation of samples; Ms. Sandra Bond for her assistance with optical microscopy; and Simon Groom for the operation of the XRF equipment.

I also thank the panel of examiners and readers of my upgrade, who gave me sensible feedback and constructive criticism: Dr. Dafydd Griffiths, Dr. Ken Thomas and Dr. Marcos Martín-Torres. I also thank the latter for his advice on many aspects of analyses and data interpretation throughout the PhD.

I am grateful to Prof. Thilo Rehren for his help with the interpretation of XRF data and to Prof. Clive Orton for his advice on sampling and statistics, as well as to many members of the Institute of Archaeology staff who had important input into my research and were generous with their time and expertise, in particular Dr. Dorian Fuller, Dr. Arlene Rosen, and Mr. Tim Williams.

I am also grateful to Dr. Adrian Jones, UCL Earth Sciences, and Dr. Andrew Beard, School of Earth Sciences Birkbeck, for their specialised advice on the analyses and identification of meteoritic materials and for providing access to the microprobe equipment.

I thank Dr. Emmanuel Pantos, the Daresbury Laboratory, as well as the Council for the Central Laboratory of the Research Councils (CCLRC), for funding and facilitating access to the XRD equipment, and for providing assistance on the interpretation of XRD spectra. I also want to thank Dr. Steve Firth and Dr. Geoffrey Hyatt, Department of Chemistry UCL, for the training and assistance provided for the operation of the Raman spectroscopy and XRD equipments respectively.

I thank INAH –Instituto Nacional de Antropología e Historia– and the Consejo de Arqueología, for providing sampling and export permits of archaeological samples

I am also very grateful to the investigators and staff of the archaeological site of Palenque, as well as to the archaeologists of Calakmul, Ramon Carrasco Vargas, Omar Rodriguez Campero and Veronica Vázquez López, who kindly provided assistance for the sampling of materials and without whom the collection of samples would not have been possible.

I equally thank the Institute of Archaeology and the National Institute of Culture and History of Belize, in particular Jaime Awe and John Morris, for providing sampling and export permits of archaeological materials. My sincere thanks go to the staff working at the site of Lamanai, who provided assistance with the sampling: Dr. Elizabeth Graham, Dr. Scott Simmons and Ms. Laura Howard. I am also grateful to Rutilia, Ricardo and Jorge for investing some hours of hard labour under the Belizean sun digging for the samples, as well as Michael Pendergast for bringing the Lamanai samples to London. My deep thanks go to Dr. David Pendergast, who very generously provided information and assistance for the dating of the samples from Lamanai and many other aspects related to the archaeology of the site and the characteristics of plasters.

Many thanks go to various researchers from different institutions who were enthusiastic about my research and who generously shared their knowledge, views and ideas on many topics. I deeply thank Dr. Martha Cuevas García, INAH, for the interesting exchange in ideas on the archaeology of Palenque. The same goes to Christophe Helmke, University of Copenhagen, on the archaeology and plasters of Pook's Hill. I also thank Dr. Luis Barba, IIA-UNAM, and Dr. Thomas Schreiner, University of California at Berkeley, for sharing their knowledge of Mesoamerican lime production and other topics. I thank Dr. Rodrigo Liendo, IIA-UNAM, for his input into the archaeology of Palenque, as well as Valeria García and Claudia García, CNCPC-INAH, for sharing their views and observations on the characteristics of Maya plasters. I also thank Dr. Linda Howie, University of Western Ontario, Dr. Patrick Quinn, University of Sheffield, and Dr. Richar McPhail, UCL, for their assistance with the petrography of my samples. I am equally grateful to Dr. Elizabeth Baquedano, Birkbeck College, for her ideas and interest on my research, to Alejandra Alonso, University of Calgary, for her advice on plant remains, and to Renata García Moreno, Universtité de Liège, for her ideas about the pigments from Calakmul.

I also want to express my gratitude to CONACYT for providing a three-year funding for my PhD, and the people involved in the communication concerning payments, academic reports and other matters.

I would like to thank the administrative staff of the Institute of Archaeology, who were always helpful, as well as the Institute of Archaeology and the Graduate School of UCL for the funding provided for congresses and conferences.

I am most grateful to my UCL classmates and colleagues, who had a direct input into my research and with whom I shared enjoyable moments during my years in London: Fatma Marii, Maria Dikomitou, Roseleen Bains, Isabel Galina, Marilena Alivizatou, Margarita Nazou, Claire Cohen, Aude Mongiatti, Lorna Anguilano, Angela Wallace, Elizabeth Markou, Melina Smirniou, Duygu Cleere, Maria Cardoso, Nadine Schibille, Ray Burke, Philip Connolly, Sarah Wolferstain, Paolo Guarino, Brenda Valdés, Pablo Mateos, Alejandra del Río, Alfonso Vega, Emiliano Zolla and Ennio Michelis.

I also thank my family and friends back in Mexico, who were always very supportive. I especially thank my siblings, who prevented me from jeopardising the submission of my thesis. I am, of course, very grateful to Emmanuel, who was patient with me and my thesis and gave me unlimited support in every possible way during the years of my PhD.

CONTENTS

| | |
|--|----|
| Abstract..... | 1 |
| Acknowledgments..... | 2 |
| 1. Introduction..... | 5 |
| Presentation | |
| Justification and approach | |
| Research questions | |
| Aims and objectives | |
| Contribution and originality | |
| Structure of the thesis | |
| 2. Environment and Cultural Setting of the Maya area..... | 11 |
| 2.1 Environment | |
| Geology | |
| Geological History of the Maya area | |
| The nature of outcrops and procurement of raw materials | |
| 2.2 Cultural setting | |
| Palenque | |
| Calakmul | |
| Lamanai | |
| 3. Use and production of lime in the Maya area..... | 38 |
| 3.1. Chemistry of lime production | |
| 3.2. Brief overview of the use of lime in the Old World | |
| 3.3. Maya and Mesoamerican lime production | |
| Ethnohistoric sources | |
| Ethnographic sources | |
| Archaeological deposits and artefactual evidence | |
| Epigraphic and literary sources | |
| Characterisation of archaeological lime plasters and experimental work | |
| Cultural, economic and environmental implications of the use of lime in Maya culture | |
| 4. The cultural practices of architectural technology..... | 65 |
| <i>Chaîne Opératoire</i> | |
| The framework of technological choices | |
| The social and political organisation of labour: Neo-Marxist approaches | |

| | |
|---|-----|
| 5. Methodology..... | 74 |
| 5.1. Sampling criteria | |
| 5.2. Selection of analytical techniques and experimental procedures | |
| Optical reflected microscopy (ORM) | |
| Petrography | |
| Microprobe and scanning electron microscopy with energy dispersive spectrometry (SEM/EDS) | |
| Raman spectroscopy | |
| X-ray diffraction (XRD) | |
| X-ray fluorescence (XRF) | |
| Statistical analyses | |
| Inventory of samples analysed | |
| Analyses carried out in the samples | |
| 6. Results..... | 93 |
| 6.1. Palenque | |
| 6.2. Calakmul | |
| 6.3. Lamanai | |
| 7. Discussion of results | 115 |
| 7.1 Palenque | |
| Variation in Ca and Mg contents | |
| The use of clays and the decline of plaster technology | |
| The use of meteoritic material | |
| Soot layers, replastering and the evidence of ritual activity | |
| 7.2 Calakmul | |
| Craft specialisation and technological variation through time | |
| The use of unburnt clays and the decline in plaster technology | |
| Hydraulic plasters and the identification of volcanic ash | |
| The use of compacted sascab | |
| Crystals of binders as evidence of slaking practices | |
| The identification of ascidians, carbonate pellets and amorphous silica plant remains | |
| Characterisation of pigments | |
| 7.3 Lamanai | |
| The variability in aggregate materials | |
| Use of non-local materials during the Late Postclassic/ Early colonial periods | |
| Use of compacted sascab in floors | |
| Secondary rhombohedral calcite crystals | |
| Replastering applications | |
| Recycling of plasters | |
| Characterisation of pigments | |

| | |
|---|-----|
| 8. Conclusions and future research..... | 159 |
| Palenque | |
| Calakmul | |
| Lamanai | |
| Concluding remarks | |
| Future research | |
| References..... | 171 |
| Appendices | |
| A. Plasters | |
| A.1. Munsell Colours..... | 193 |
| A.2. Petrography..... | 196 |
| A.2.1. Petrographic observations | |
| A.2.2. Photomicrographs and fabric groups | |
| A.3. Scanning Electron Microscopy (SEM/EDS)..... | 224 |
| A.3.1. EDS analyses | |
| A.3.2. Analyses of crystals in binders | |
| A.4. Microprobe analyses of glass and other inclusions..... | 232 |
| A.5. X-ray diffraction..... | 240 |
| A.6. X-ray fluorescence..... | 246 |
| A.6.1. Quality of the data | |
| A.6.2. Bulk XRF data | |
| A.6.3. Cluster Analyses of bulk XRF data | |
| A.6.4. Principal Component Analyses of bulk XRF data | |
| B. Analyses of pigments | |
| B.1. Polarizing microscopy of paint layers and pigment dispersions..... | 262 |
| B.2. Raman spectroscopy..... | 266 |
| Glossary..... | 272 |
| Abbreviations and acronyms | 276 |
| List of figures and tables..... | 278 |

1. Introduction

This chapter introduces my research and explains how the thesis is organised. Firstly, the chapter presents the project and provides a justification for the research. Secondly, it outlines the research questions as well as the aims and objectives of the thesis. Finally, the contributions and originality of this research are explained, followed by the description of the structure of the thesis.

Presentation

This thesis is a study of ancient lime plaster¹ production in the Maya lowlands and how technology changed through time. The research makes use primarily of material analyses of archaeological plasters from three case studies of various chronological periods. Palenque, Calakmul and Lamanai were the sites selected as case studies, and the samples analysed date from the Middle Preclassic period (ca. 400 BC) to the Early Spanish Colonial period (AD 16th century) (see fig. 1.1. and table 1.1).



Fig. 1.1. Location of case studies and other Maya sites.

¹ The term plaster is used in my thesis as an umbrella term for all lime-based materials employed in architecture. See glossary for definitions and use of the different terms employed in the literature.

Samples from Palenque included material from the Late and Terminal Classic periods. Calakmul samples spanned the Late Middle Preclassic period to Terminal Classic periods. Finally, Lamanai comprised samples from the Late Preclassic to the Early Spanish Colonial periods (see table 1.1).

| | Middle Preclassic | Late Preclassic | Early Classic | Late Classic | Terminal Classic | Early Postclassic | Late Postclassic | Spanish Colonial |
|----------|-------------------|-----------------|----------------|----------------|---------------------|-------------------|------------------|------------------|
| Site | 1000/ 400 BC | 400 BC/ AD 250 | AD 250/ AD 600 | AD 600/ AD 800 | AD 800/900- AD 1100 | AD 900/ AD 1200 | AD 1200/ AD 1500 | AD 16th century |
| Palenque | | | | | | | | |
| Calakmul | | | | | | | | |
| Lamanai | | | | | | | | |

Table 1.1. Plaster samples analysed in this research.

The three sites selected as case studies shared cultural traditions and were contemporaneous for some centuries. However, the sites went through different socio-political trajectories and had access to different raw materials for lime production. Palenque and Calakmul constituted powerful sites that dominated peripheral centres and they both experienced a socio-political decline and were eventually abandoned at the end of the Terminal Classic Period (Demarest et al 2004). Conversely, the site of Lamanai, although smaller than the other two sites, remained inhabited even after the Spanish Colonial Period in the 16th century (Pendergast 1985a, 1990).

Justification and approach

Maya monumental architecture was one of the most important elements of ancient Maya civilisation and developed to the highest degree in the Maya Lowlands. Architecture is therefore an important source of information for Maya archaeology, and given that lime plasters constitute one of the main components of Maya monumental architecture, the characterisation of architectural plasters is therefore important in understanding Maya technology.

Although lime plaster production was a common characteristic of Maya Lowland cultural traditions, it is worth mentioning that my research emphasises diachronic comparisons within each of the case studies and makes less emphasis on comparisons between sites. This is justified by the fact that each of the three centers had the necessary raw materials for lime production and because the Maya Lowlands never constituted a unified political kingdom, but consisted of independent polities, each of which went through different paths of socio-political development (Hammond 1982b:199-220). Future studies, however, could emphasise the synchronic approach in order to tackle aspects such as interaction and technological influences.

Research questions

The main research question of this project is how lime plaster technology developed in the Maya Lowlands through time, and how this technology relates to large-scale architectural practices. The research also examines the way in which the changing economic, socio-political and environmental contexts had an impact on lime plaster technology in the three case studies.

A more specific question relates to the nature of raw materials that were employed in the manufacture of plasters and whether they were locally available. In addition to this, an important question is how lime plasters were employed in architecture.

In the case of Palenque, lime plasters from the Late and Terminal Classic periods (AD 600-800/ AD 800-900) were analysed with the purpose of assessing how the ultimate collapse and abandonment of this polity might be reflected earlier in lime plaster production and the use of this material in monumental architecture. It is worth saying that the demise of Palenque occurred soon after large architectural programs were carried out, and that this site was one of the first and most dramatic examples of the demographic collapse during the Terminal Classic period (Demarest et al 2004).

Calakmul was chosen because the site was one of the most powerful and highly populated sites in the Maya area and underwent a collapse that led to its eventual abandonment after the Terminal Classic period; the research questions therefore are concerned with how these important changes were reflected in lime plaster technology. In addition, research questions focus on how lime production changed throughout the 13 centuries in which the site was inhabited, and include an examination of lime production during the Late Preclassic period, which in the case of Calakmul exhibits some of the earliest and most ambitious examples of Maya monumental architecture.

The research questions of the third case study, Lamanai, are concerned with how lime plaster production changed at a site that was uninterruptedly inhabited. Lamanai was one of the few lowland sites that do not show clear evidence of decline at the end of the Classic period, and Lamanai itself remained inhabited even beyond European contact. A specific question in the case of Lamanai, therefore, is how lime technology changed in the transitions between periods, in particular during the Late Postclassic/ Spanish Colonial transition.

In addition to the general questions that have been outlined, a specific question is whether hydraulic lime plasters were produced by the ancient Maya. Hydraulic plasters are mixtures of lime and pozzolanic aggregates, as explained in Chapter 3, which have higher mechanical strength than non-hydraulic plasters and the ability to set under water.

Although hydraulic plasters have not been decisively reported so far in Mesoamerican archaeology, the identification of volcanic materials—pozzolanic materials often employed in hydraulic

plasters—in Maya Lowland ceramics has been proposed, as explained in Chapter 2 and 7. Therefore, the identification of hydraulic plasters would not only be of interest from a technological point of view, but would also be relevant for understanding the use of volcanic materials in the Maya lowlands.

A secondary question, not related to the technology of plasters, is the identification of materials deposited over the surface of the plasters and the information they can provide regarding the use of architecture.

Aims and objectives

My research aims, first, at systematically analysing archaeological plasters by making use of a variety of analytical techniques, as well as at providing the necessary technical information in order for the thesis to be consulted by future studies.

Secondly, the study aims at interpreting the analysed data using an anthropological perspective by contextualising the information using theoretical frameworks of anthropology of technology. In the same way, the research aims at having a comprehensive approach by considering different sources of evidence that inform Maya lime and plaster production.

Thirdly, the research aims at having a wide scope in terms of sites and periods under study. Although it is not expected that the conclusions drawn for the three case studies are representative of all lowland Maya lime production, the thesis aims at providing a general overview of how this industry emerged and developed in three important lowland sites.

Additionally, my research aims at describing the most appropriate analytical methods for the examination of Maya lime plasters, as well as at outlining potential methodological problems.

Finally, this study aims at suggesting future lines of research based on the gaps found in the literature review.

Contribution and originality

Although Maya architecture is one the most informative sources of information for Maya archaeology, very few studies of building materials have been carried out so far, in comparison to those focusing, for instance, on ceramics.

The original contribution of this research to Maya archaeology is that it presents a systematically collected body of data of samples from different sites with a wide time span. Although some studies have been carried out on the characterisation of Maya lime plasters (Littman 1957, Villegas et al 1995, Hansen et al 1997, Magaloni 1995, Goodall et al 2007), none of them have included more than one site, and each of them has focused only in one chronological horizon.

Secondly, and in contrast with previous characterisations of archaeological plasters, this research reviews different sources of evidence, from ethnohistorical accounts to glyphic evidence, as well as previous studies on materials analyses. Although two systematic studies of modern Maya lime production have been carried out recently using ethnographic approaches (Schreiner 2002, Mathews 2002), neither examined archaeological materials. By studying different sources of information, this research has a more comprehensive approach.

Another contribution of this research regards the combination of methods for the analysis of archaeological plasters. Previous studies have used isolated methods, mainly either scanning electron microscopy with energy dispersive spectrometry (SEM/EDS) or X-ray diffraction (XRD), which has resulted sometimes in misleading or inconclusive data. By using a combination of methods, my research provides complementary data about the chemical and mineralogical compositions of the plasters, as well as their micromorphological characteristics; the resulting body of data is therefore more complete than in the case of previous studies. Additionally, the research makes use of statistical analyses for the examination of the quantitative data, which had not been done before with Maya plasters.

Structure of the thesis

The first two chapters of the thesis provide a general background of the sites under study, and background information of lime production. Chapter 2 explains the physical and cultural characteristics of the Maya area, especially the three sites that comprise my case studies, in order to understand the context in which the lime plaster industry emerged and developed. The first part of the chapter deals with the environmental context and describes the available geological resources that constitute the raw materials for lime production. The second part of the chapter gives an overview of the cultural developments of the three sites, in particular regarding monumental architecture and dynastic histories.

Chapter 3 provides a description of lime technology, including the chemistry of the lime cycle and the steps involved in the manufacture of plasters. The chapter provides an overview of lime production in the Old World and the most representative achievements of this technology. The chapter also provides a literature review of the different sources that inform Maya lime and plaster production; these include archaeological, epigraphic, ethnohistoric and ethnographic sources. Finally, the chapter discusses the implications of the use and production of lime in ancient Maya times.

Chapter 4 is a description of the theoretical frameworks that I employed in my research and which helped to structure my research questions and my approach to collecting the data and interpreting the results.

Chapter 5 explains the criteria for sample selection and analysis. It describes each of the analytical techniques, as well as the sample preparation methods and how analytical procedures were carried out.

Chapter 6 presents the results from the various analyses carried out on the archaeological samples. The chapter presents the results for each of the case studies individually.

Chapter 7 discusses the data presented in Chapter 6 and analyses this information in terms of technological characteristics and in relation to ancient Maya culture.

Finally, Chapter 8 summarises and concludes the analyses and discussion of the previous chapters. It is organised according to case studies but it also provides general concluding remarks and lines of research for future studies.

2. *Environment and Cultural Setting of the Maya Area*

In this chapter I explain briefly the environmental and cultural variability in the Maya area. These are important aspects to be reviewed, since they have an impact on the choice of plaster manufacturing.

2.1 *Environment*

There are numerous studies on the natural and cultural subdivisions of the Maya area that have been carried out in order to understand subsistence, adaptation and evolution of Maya culture and the emergence of social complexity. These studies (Hansen et al 2002, Sanders 1977, Graham 1987) recognise the environmental variability of the Maya area, which was overlooked by previous studies (Rathje 1971), and which is thought to have influenced settlement patterns. Many studies have also focused on long-distance trade of commodities, but emphasis has also been made on the availability of local resources to understand local procurement of basic and prestige needs (Graham 1987).

Broadly speaking, the Maya area is divided into three main physiographic zones: the Lowlands at the North, the Highlands at the centre, and the Pacific Coastal plain at the south. Rainfall, drainage, vegetation and geological resources show noticeable differences in these three areas. See fig. 2.1.

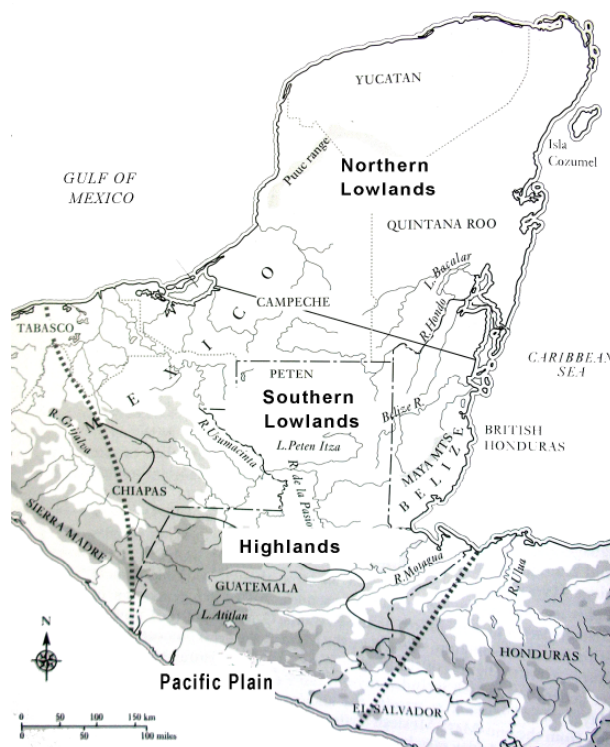


Fig 2.1. Physiography of the Maya area. Coe 2005.

Regarding the availability of water, the higher rainfall indexes are seen in the Pacific Coastal Plain, the southwestern lowlands and in some areas of the Highlands, with up to 4000 mm/yr. However, rainfall drops considerably to the north, with less than 500 mm/yr in the Northwestern Yucatan Peninsula (Grube 2006). Despite the high precipitation in some areas, most of the Maya area has a long dry season that can last up to six months. As sources of water, the northern Lowlands have dissolution pits of karstic terrain with a shallow water table, locally known as cenotes, which were also places of rituals (Siemens 1978:117). The main bodies of water in central zones are seasonally-inundated swamps (*bajos*) and perennial reservoirs (*aguadas*). Although only the latter are sources of drinking water at present, the *bajos* may have held water more efficiently than they do today (Siemens 1978:137). Ancient canals have been mapped by satellites, which were probably built for wetland agriculture around the *aguadas* (Pope and Dahlin 1989). In addition, some areas of the southern lowlands, such as the Gulf Coast and Belize, are traversed by rivers and streams. However, despite the presence of bodies of water in some areas, most of the Maya settlements relied on rainfall, without access to river or lakes, and therefore, the difficulties for the subsistence of large populations imposed by the long dry season have puzzled many archaeologists, some of whom believe that prolonged droughts played a major role in the demise of the Lowlands at the end of the Classic period (Hoddell et al 1995, Haug et al 2003, Gill 2000, Gunn et al 2002b, Demarest et al 2004).

Vegetation varies considerably across the Maya area. While the southern Lowlands and especially the Highlands have taller evergreen vegetation, the northern Lowlands are characterised by shrubby vegetation, with a higher proportion of semi-deciduous trees (INEGI 2006), see fig. 2.2. Despite the fact that the Maya area is now heavily forested, ancient anthropogenic deforestation may have been considerable. There is clear evidence of deforestation in some areas during Prehispanic times, notably the valley of Copan (Abrams 1988, Paine and Freter 1996) and some authors have even proposed that severe deforestation may have generated regional droughts (Shaw 2003).

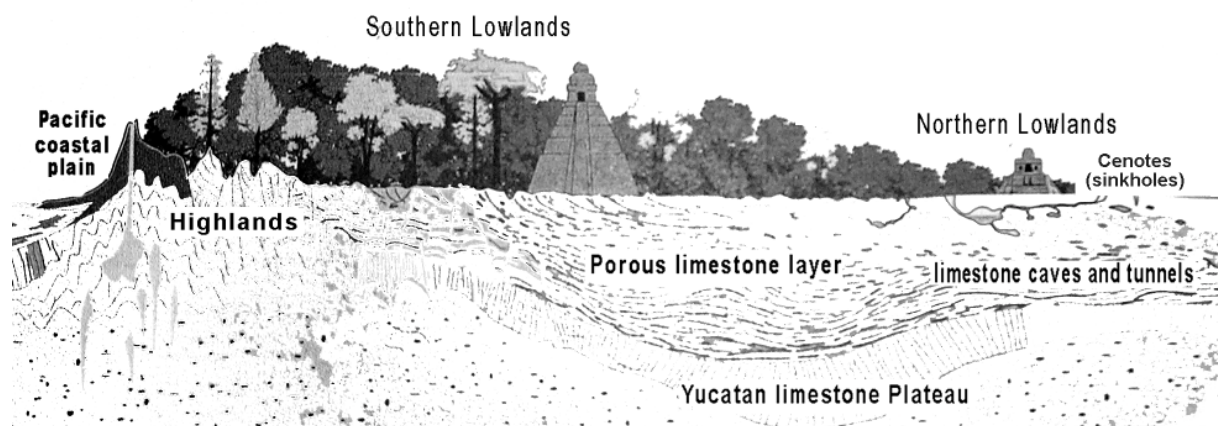


Fig. 2.2. Physiographic variation in the Maya area. Cross section South-North. Grube 2006.

Drainage is very much determined by geology. The karstic terrain of the northern Lowlands, north of 19°N of the equator is highly permeable, allowing only underground streams, whereas the southern lowlands and the highlands are drained with the Motagua, the Usumacinta and the Belize River as the main systems (Weidie 1985:3).

Geology

There are no extensive geological surveys of the Maya area, due in part to the limited exposures of bedrock and the lack of reliable biostratigraphic data (Schönian 2005). Starting from the mid 20th century, British commissioners carried out some studies in order to document the mineral resources of the colonies of the British Empire, when Belize was still British Honduras (Dixon 1955 Ower, 1928, Bateson 1977, Wright et al 1959).

There have also been important geological surveys carried out by PEMEX (Petróleos Mexicanos), who drilled several wells in the Maya area and the Gulf coast of Mexico, some of them over 3000 meters deep, as part of its exploration of oil resources (Bartolini et al 2001, Bartolini et al 2003, Salvador 1991). Anschutz Minerals Corporations also carried out surveys in the 1970s (Anschutz 1976). These wells have exposed thick stratigraphies that have been used to understand the geological past of the area.

More recently, the region has prompted much geological research focusing on the Chicxulub meteorite, which landed in the Northern Yucatan Peninsula around 65 million years ago when the platform was still submerged, as described below.

Geological surveys for archaeological purposes (Dull et al 2001, Roberts and Irving 1957, Siemens 1978, Ward et al 1985) tend to concentrate in small areas of the Maya area. Mathews (2002) reviewed the literature of the different geological regions of the Maya in order to explain

variation in modern Maya lime production. However, she only analysed a small number of geological samples from the Three Rivers Region of Northwestern Belize, which constitutes a very small area of the Lowlands.

Geologically speaking, the Yucatan peninsula is part of the Yucatan Platform and constitutes the emerged half of the carbonate shelf, whereas the submerged half is known as the Campeche Bank (see fig. 2.3).

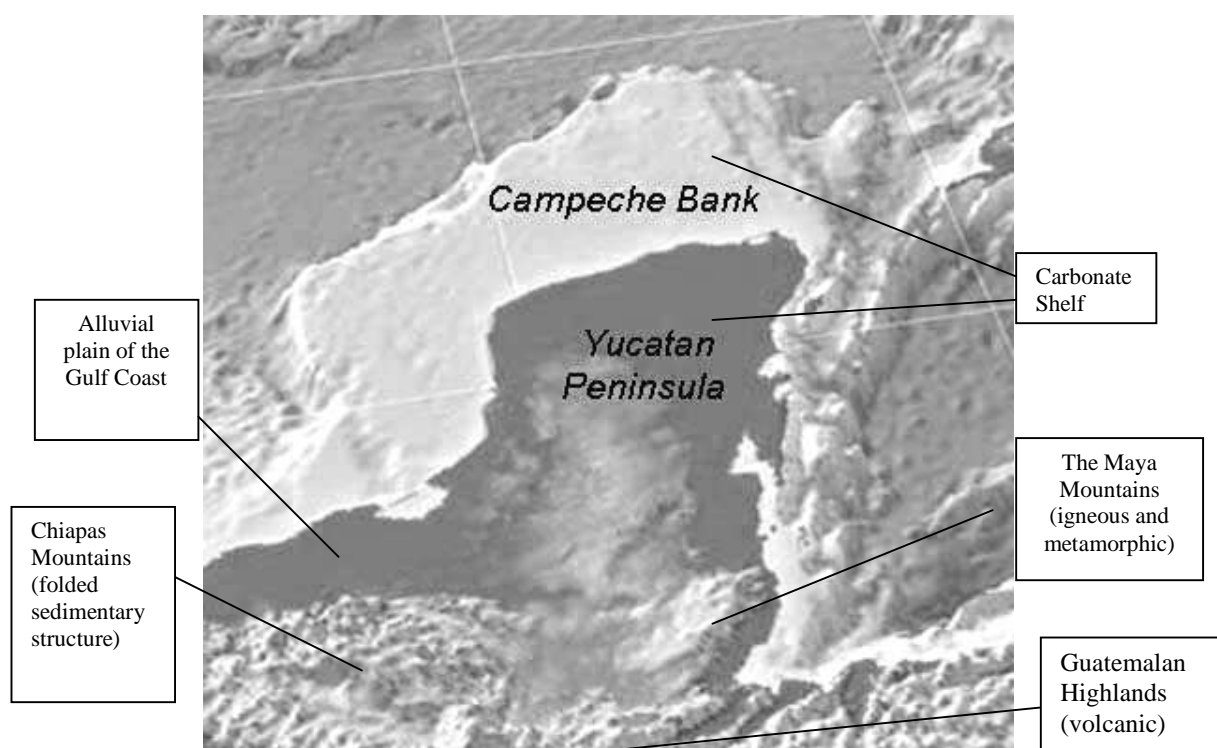


Fig.2.3 Geology of the Maya area. Nipper et al (2008)

The Yucatan Peninsula is usually divided into four main geological areas: the Northern Pitted Karst Plain, the Sierrita de Ticul, the Southern Hilly Karst Plain, and the Eastern Block-Fault District. The Northern Pitted Karst Plain is located at the North of the Sierrita de Ticul, and shows elevations that slowly increase inland. The Sierrita de Ticul is a formation that resulted from normal faulting and shows maximum elevations of 150 meters. The Southern Hilly Karst Plain is south of the Sierrita de Ticul bordering the Sierra de Chiapas, La Libertad Arch in northern Guatemala and the Maya Mountains of Belize. This plain shows maximum elevations of around 300 m, and its western part shows folding of the carbonates that result in topographic undulations. The Eastern Block Fault District runs along the Caribbean coast to Tulum and comprises folded structures that form ridges and depressions and causes the alignment of streams and lakes (Weidie 1985:3). See fig. 2.4. To the

East of the Hondo River, Northern Belize also consists of low-lying folded limestones aligned along the river, but the south of the country is dominated by the igneous and metamorphic Maya mountains. The Maya mountains were the source of many raw materials, such as granites, quartzites and sandstones that are not available in the limestone lowlands. They are also the source of alluvial soils and ceramic clays found along the rivers that drain the mountains (Graham 1994, Hammond 1982a).

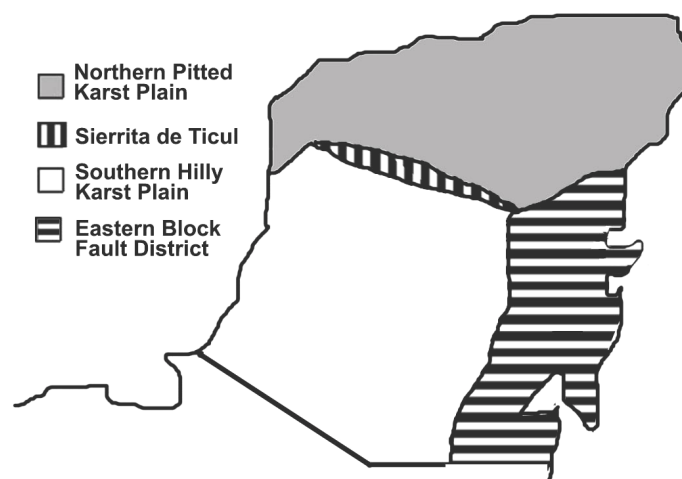


Fig.2.4. Physiographic areas of the Yucatan Peninsula. Based on Weidie 1985.

The Guatemalan Highlands are more geologically diverse than the Lowlands. They consist of Tertiary and Quaternary volcanic formations to the south and Paleozoic formations in the north, which are known as the Central American Volcanic Arc (CAVA). In the southern highlands, active and extinct volcanoes have resulted in the deposition of thick layers of pumice and ash, which are overlain by thin soils (Hodell et al 2004). Based on the abundance of volcanic glass as tempering material in Maya ceramics, Ford and Rose (1995) propose that volcanic activity during ancient Maya times was intense and that numerous ash falls occurred, although this has not been supported by the documentation of extensive deposits of ash in the Maya lowlands.

Other volcanic formations relevant for the Maya area are the Chiapanecan Volcanic Arch (CVA) in Chiapas, Mexico; the Tuxtlas Volcanic Field (TVF) in the Gulf Coast of Mexico; and the Trans-Mexican Volcanic Belt (TMVB) in the Central Mexican Highlands (Macías et al 2003). Some of the igneous deposits of these formations provided raw materials for the Maya lowlands and promoted interaction with other areas of Mesoamerica.

Geological history of the Maya area

Generally speaking, the age of the Yucatan peninsula's rocks increases southwards, with Pleistocene sediments at the Northern area, and Mesozoic rocks in the southern Lowlands (see fig. 2.5).

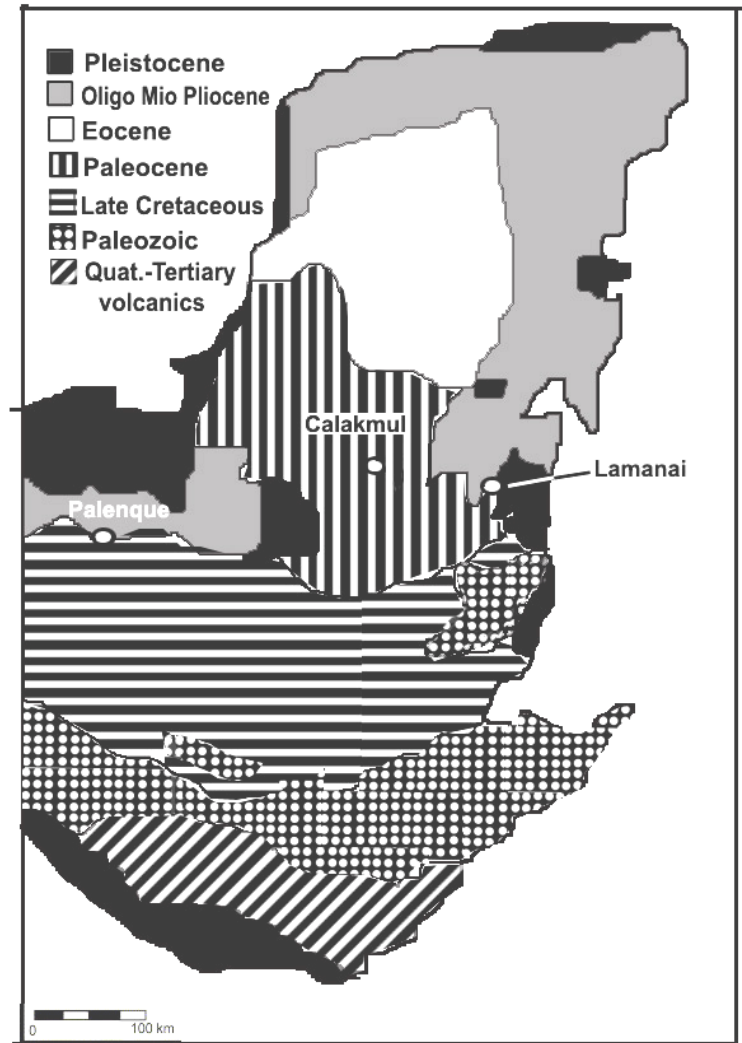


Fig.2.5. Age of the rocks and sediments in the Maya area and locations of the three case studies.
Based on Hodell and colleagues (2004).

2. Environment and Cultural Setting of the Maya Area

| Era | Period | | Epoch | Began million years ago |
|------------|---------------|-----------|--------------|--------------------------------|
| Cenozoic | Quaternary | | Holocene | 0.01 |
| | | | Pleistocene | 1.6 |
| | Tertiary | Neogene | Pliocene | 5.3 |
| | | | Miocene | 23.7 |
| | | | Oligocene | 36.6 |
| | Paleogene | Eocene | 57.8 | |
| | | Paleocene | 66.4 | |
| Mesozoic | Cretaceous | | | 144 |
| | Jurassic | | | 208 |
| | Triassic | | | 245 |
| Paleozoic | Permian | | | 286 |
| | Carboniferous | | | 360 |
| | Devonian | | | 408 |
| | Silurian | | | 438 |
| | Ordovician | | | 505 |
| | Cambrian | | | 570 |

Table 2.1. Geologic timescale of the Phanerozoic Eon. Based on Tarbuck and Lutgens 2002.

Although the geological history of the Maya area is better known from the Mesozoic period onwards, it is known that Paleozoic metasediments are found in Chiapas, Oaxaca, Guatemala, Belize, and Honduras. Deep coring done by Pemex has exposed chlorite schists in Yucatan and Quintana Roo over 2000 meters depth (Weidie 1985:5).

During the Mesozoic, the dominant formation is *Todos los Santos*, which is found in Oaxaca, Chiapas, Guatemala and Honduras, and is characterised by conglomerates, sandstones and shales. The Cretaceous period saw extensive evaporite and carbonate deposition in the entirety of the Maya lowlands, which has continued until the present day. The lowermost strata of the Cretaceous are quartz silty dolomites over which miliolid biosparites were deposited. There is a thick anhydrite layer interbedded with the dolomite, which indicates that at least the central and Northeastern areas of the Yucatan peninsula, from the Guatemalan Petén to the Yucatan, were evaporitic areas. After this, open shelf conditions returned and micrites were deposited over the evaporites (Weidie 1985:5).

During the Early Cretaceous, limestones of rudists (a type of bivalves) developed along the margins of the peninsula and interbedded with pelleted biomicrites (Weidie 1985:8). Upper Cretaceous strata at the north of the peninsula are composed of pelletoid micrites with laminated fossiliferous dolomites. The pelletoid limestones contain fossils that are indicative of deposition on a shallow open shelf (Weidie 1985:7).

The geology of the Chiapas Mountains dates from the Cretaceous period and forms a carbonate platform with a synclinal structure, that is, a series of folds that dip into the centre of the

structure. This formation crops out in the central and northern part of the State of Chiapas, forming steep mountains (Cros et al 1998).

At the end of the Cretaceous Period, the Yucatan Peninsula was hit by the Chicxulub meteorite, when the peninsula was still submerged. Many studies have been done in order to date the impact but it is usually agreed that it occurred at the end of the Cretaceous period, around 65 million years ago. The crater is the third largest in the world and measures 180 km in diameter. Although it is covered by thick layers of rock, its size is marked by a ring of sinkholes or *cenotes*, which are thought to have formed as the result of a subduction zone caused by the presence of the crater (Connors et al 1996). Although there has been some debate, it is also generally agreed that the impact is related to the mass extinction that occurred at this time, therefore constituting a major event of the geological past (Arenillas et al 2006, Connors et al 1996, Pope et al 1993, Ward et al 1995, Hildebrand et al 1991).

Many studies have focused on the characterisation of impact materials from the Chicxulub meteorite, which have been observed as far as Haiti and Northeastern Mexico (Kring and Boynton 1991, Hough et al 1997). There are also reports of impact material in many exposures of the southern Maya lowlands. In the Actela section in Guatemala, close to San Luis in the Petén, outcrops of breccias can be seen with altered glass spherules (meteoritic glass) and elevated concentrations of iridium, which are characteristic features of the Chicxulub impact material (Fourcade et al 1998). Similar breccias that are stratigraphically related with these Guatemalan materials can be seen in the Guayal and Bochil sections in the Mexican states of Tabasco and Chiapas respectively (Arenillas et al 2006). In the Cretaceous/Tertiary (K/T) boundary of these sections, a bed of dark clays can be seen, overlain by a limestone layer of the Paleocene (Arenillas et al 2006). In southern Quintana Roo, numerous impact deposits have been found west of the Rio Hondo Fault System (Schönian et al 2005). Impact materials in Belize are also abundant at Albion Island (King and Petryny 2003, Pope et al 1999), and close to the town of Armenia, where impact deposits cover weathered Cretaceous dolomites (Ocampo et al 2003, Pope et al 2005). See fig. 2.6 and 2.7.

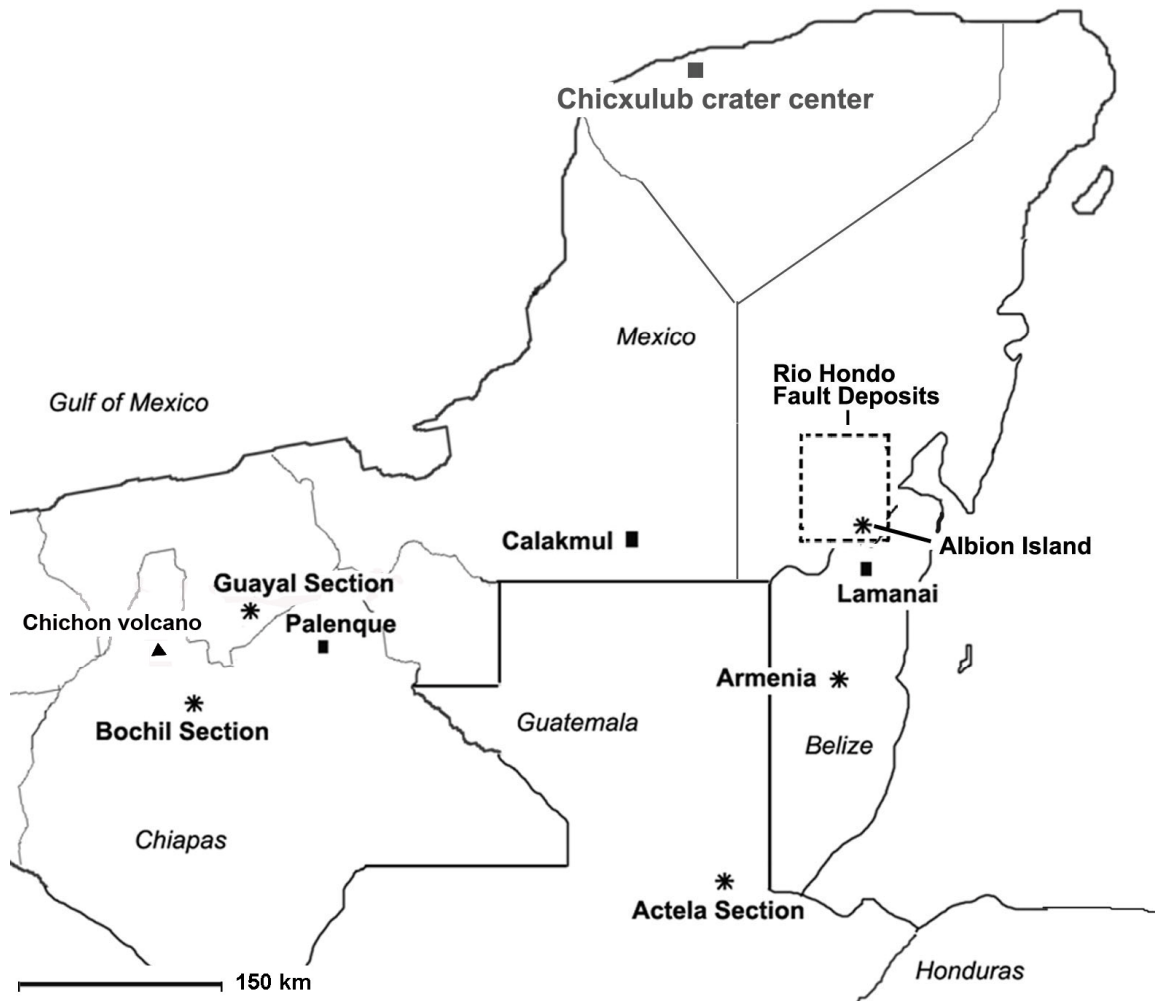


Fig.2.6. Chicxulub crater center and outcrops of impact ejecta. Location of Chichón volcano.

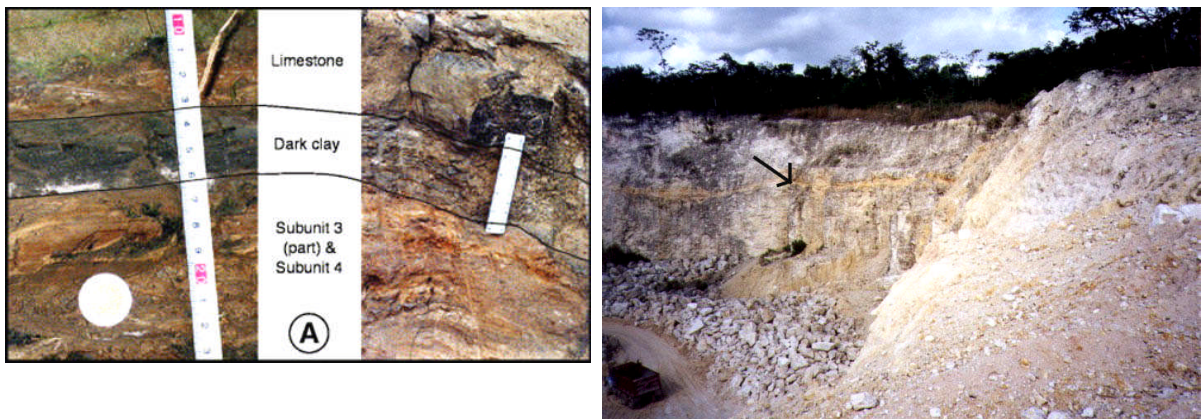


Fig. 2.7. Chicxulub ejecta deposits. Left: Cretaceous/Palaeogene boundary at Guayal and Boyil showing the Chicxulub related Complex Clastic Unit, dark clays and Palaeogene limestone (Arenillas et al 2006). Right. Quarry at Albion Island with visible K/T deposits. Picture: Paul Daudley.

After the Chicxulub impact, the Cenozoic period continued with extensive carbonate deposition in the whole of the Maya area. The Northwestern area of the peninsula has the maximum thickness of Cenozoic rocks, about 1000m, which consists of dolomites, limestones, and marls. The Lower Cenozoic contains a considerable amount of evaporites in central and east central Yucatan.

The upper Cenozoic, especially the Pleistocene, shows extensive deposits of eolites, which are sedimentary rocks formed by clastic material deposited by the wind (Brook 2001). Neogene rocks crop out in a belt along the northern coast of the peninsula and along the Caribbean coast (Weidie 1985:10).

During the Cenozoic period in Chiapas, igneous and sedimentary rocks were deposited over the Mesozoic strata. Two episodes of strong igneous activity have been recognised. The first one occurred during the Miocene and can be seen as intrusions of igneous rocks into the rocks of the Chiapas Massif, whereas the second one occurred during the Late Cenozoic and consisted of strong volcanic activity in the central and northern part of Chiapas, exemplified by the El Chichón, Tzontehutiz and Nicolás Ruiz volcanoes (Moraa et al 2007). The Chichón volcano is well known in the area by its eruption in 1982, which spread volcanic ash in a 100 km diameter, reaching the states of Chiapas, Campeche, Oaxaca, Veracruz and Tabasco (Peralta 2004). Tilling and colleagues (1984) propose that the Chichón volcano also erupted at least three times around 600, 1250 and 1700 years BP, during ancient Maya times (see fig. 2.6 for location of Chichón volcano).

The nature of the outcrops and procurement of raw materials

Given that the Maya lowlands are part of the Yucatan carbonate platform, raw materials for lime production were widely available, although these materials are not found universally: the Gulf Coast Plain to the Southwest is mainly alluvial with fertile soils; the Maya Mountains of southern Belize are composed of three large granitic intrusions with the Bladen volcanic series at the south of the Mountains (Graham 1987); Quirigua, Pusilha, Altar de Sacrificios and Toniná had sandstones that they employed in architecture (Sharer 2006); and finally Copan, in Western Honduras, has a volcanic geology and its green tuff is famous for having been carved into sculptures (Webster 1999). It is worth saying however, that even in sites where there were no local limestones, the Maya produced lime for architecture. In the case of Copan, despite the volcanic lithology, Classic period buildings were built with lime plaster (Goodall et al 2007). The site of Comalcalco, located in Tabasco's alluvial plain is another example where despite the lack of limestone, lime was used as buildings material, presumably obtained from shells (Littman 1958b). In the same way, the site of

Kendal in Stann Creek made use of a non-local white clay as rendering material in order to simulate lime plastered surfaces (Graham 1994).

The areas of the lowlands with limestone bedrock show a high variation in the physical, mechanical and chemical characteristics of the different carbonate sediments and rocks. This is due to the different diagenetic environments involved in their formation, which is typical of limestones formed in shallow tropical seas with an abundance of reefs and corals (Espinosa et al 1996). These different environments include the deposition of lime detritus as a consequence of natural processes of the flora and fauna of the waters, and to a minor degree, the dredging of beach particles, swamps and coastal lagoons. Moreover, after the slow emergence of the continental platform as the waters receded during the Pleistocene, there has been continuous dissolution of the carbonates due to pluvial and underground currents of water (Espinosa et al 1996), which accounts for another factor of variability in the characteristics of carbonate rocks.

The calcareous sediments exist as outcrops over more than 60% of the Lowlands and show an 80-100 cm hardpan of limestone that overlies soft unconsolidated carbonates, locally known as sascab (Espinosa et al 1996). Sascab is an important geological material that was widely used and is still used today for building purposes, as described in Chapter 3. However, the nature and properties of these sediments vary considerably.

As Espinosa and colleagues (1996) describe, sascab is found in the Yucatan Peninsula as a soft unconsolidated deposit up to several meters thick that is located between the indurated or petrocalcic horizon—a hard and dense limestone carapace around 1 meter thick—and the limestone bedrock. Isphording and Wilson (1973) report that the sascab layer has a higher content in dolomite, talc and chlorite in comparison to the overlying limestone. For this reason, the authors consider that this particular stratigraphy is caused by selective dissolution of high-magnesium calcite from the upper limestones and its subsequent deposition in the sascab stratum below, which occurs during the rainy season. In contrast, during the dry season when the water migrates to the surface for evaporation, low magnesium calcite is transported from the sascab layer to the upper limestone, where it crystallises.

However, in Belize and other areas of the southern lowlands, these crumbly calcareous deposits are found directly under a thin soil profile and not under hardened carapaces (Darch and Furley 1983), which is why previous studies referred to this material simply as marl and not as sascab (McDonald 1978). Nodules of chert usually occur in sascab deposits as a replacement mineral during diagenesis (see fig. 2.8.)

Littman (1958a) describes the different characteristics of sascab deposits. He mentions that whereas at Uxmal and Sayil the sascab has a red colour, it is yellow at Chichén Itzá and white at

Jaina. Sascab from Palenque, on the other hand, is present in low hills and is very soft. Although sascab shows considerable variations in morphology, composition and appearance, the term is used as a generic throughout the Maya lowlands to refer to these locally weathered carbonate deposits.



Fig. 2.8. Left. View of a sascab quarry (sascabera) in Indian Church, Lamanai, Belize. Right: detail of chert nodule in sascab quarry at Indian Church.

Beach (1998) claims that sascaberas (sascab extraction pits) were used as a source of water and may have been an important element in wetland agriculture. Beach also mentions that sascab may have been used as a fertilizer.

Regarding the sites selected as case studies for this thesis, Palenque is located along the margin of the alluvial plain of Tabasco and the foothills of the folded Cretaceous sedimentary structure of the Chiapas Mountains. It is therefore a site that shows some physiographic and geological diversity. Neither the Sierras nor the plains consist of a homogenous environment; the low Sierras show a range in altitudes between 100 and 1000 meters AMSL, and show different exposures of limestone, sandstone and shale (Rands and Bishop 1980) (see fig. 2.9).

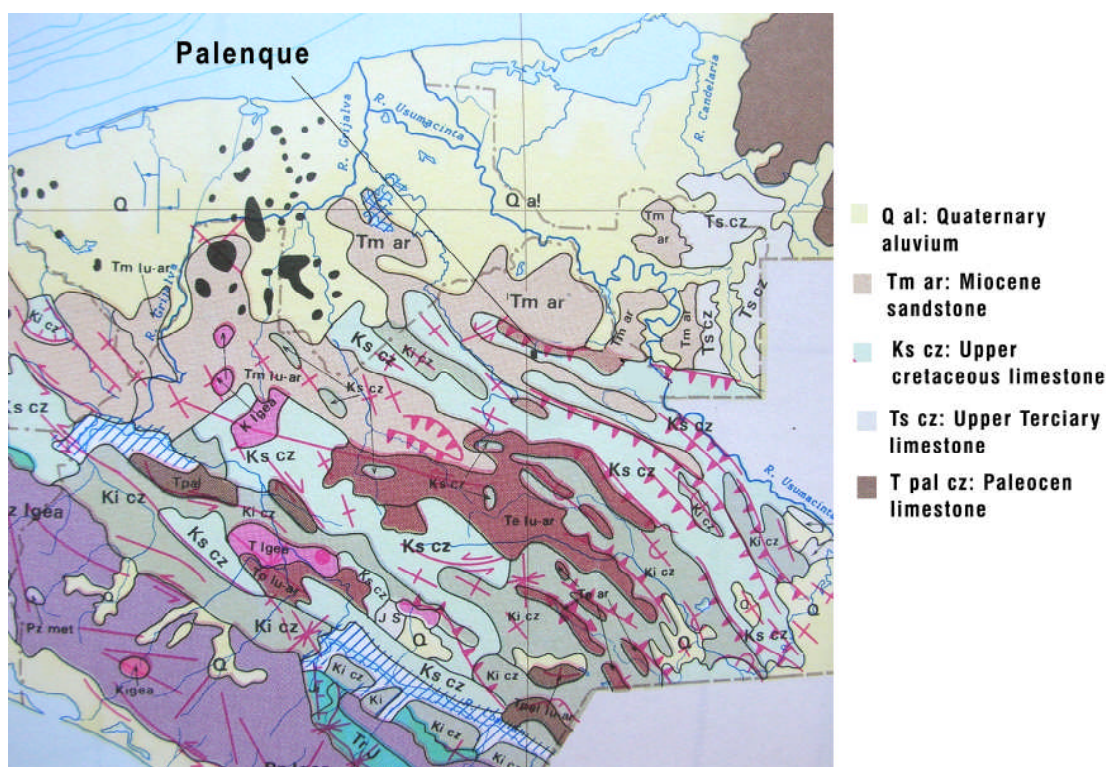


Fig. 2.9. Location of Palenque showing the geological diversity of the region (UNAM 1990).

Geological samples that were analysed from the sites under study contribute additional information toward the understanding of the lithology of the sites' surroundings. Petrographic observations and X-ray fluorescence analyses of limestone samples taken from buildings of Palenque, which presumably represent the lithology of the zone, revealed the presence of dolostones (see appendix A.2 and A.5).

In contrast to Palenque, Calakmul is located on the carbonate shelf of the Yucatan Peninsula, in an area of Paleocene limestones (see fig. 2.5). The Paleocene limestones have layers of gypsum from the Xpujil formation, and above these rocks there are carbonate strata with clay layers dating from the Eocene (Castro Mora 2002). Calakmul's lithology is very porous and results in a very permeable terrain, with the water table found more than 200m below (Morales and Magara 2001 cited in Parkswatch 2004).

Limestone samples taken from buildings and quarries in Calakmul's center and analysed as part of my research show pelmicrites, that is, limestones with high proportion of pellets in a micritic cement. A sample of sascab was also analysed, showing subrounded and subspherical sediments of micritic calcite with high contents in silicon, presumably caused by a high proportion of clay minerals (see appendix A.2 and A.5).

2. Environment and Cultural Setting of the Maya Area

Lamanai is located in Northern Belize, in an area of folded crystalline limestones dating from the Cretaceous to the Eocene Periods. The stratigraphy consists of soft limestones and unconsolidated calcareous sediments as well as quartz sand that date from the Miocene to the Pleistocene, and cover the hard crystalline limestones of the Cretaceous period (McDonald 1978). Limestones from buildings at the site were also analysed. They proved to be peloidal and micritic limestones almost entirely composed of calcium carbonate. Local sascab from the nearest quarry showed rounded and subrounded sediments of micritic calcite, although chert nodules were also visible in the quarry.

2.2. *Cultural Setting*

In this section, I explain briefly the cultural setting of the Maya area. This background is important for understanding the cultural and technological choices involved in construction and plaster manufacturing.

The cultural development of the Maya is inserted within the broader chronological framework of Mesoamerica, which is divided into five main horizons (see table 2.2).

| Period | Subperiod | Dates |
|-------------|-----------|---------------------------|
| Paleoindian | | 20,000/10,000 BC- 8000 BC |
| Archaic | | 8000 BC – 2000 BC |
| Preclassic | Early | 2000 BC -1000 BC |
| | Middle | 1000 BC - 400 BC |
| | Late | 400 BC – AD 250 |
| Classic | Early | AD 250 – AD 600 |
| | Late | AD 600 – AD 800 |
| | Terminal | AD 800 – AD 900/1000 |
| Postclassic | Early | AD 900/1000 – AD 1200 |
| | Late | AD 1200 – AD 1519 |

Table 2.2. Mesoamerican chronology (Sharer 2006).

The Archaic Period saw the transition from nomadic hunting and gathering to the beginning of agriculture and settled life. Pope and colleagues (2001) claim that the earliest evidence of domesticated maize comes from the Gulf of Tabasco, with pollen dating from 7,000 BP, which is 1000 years earlier than the first crops found in the Highlands of Central Mexico and the valley of Oaxaca.

By the beginning of the Preclassic period, Mesoamerican people had already domesticated many crops, with numerous agricultural settlements spreading across the area. In the Maya area the Preclassic period saw the emergence of the first complex societies, together with the development of the institution of kingship and writing. Rapid population growth and massive architecture were seen during this period in the Petén, which demonstrates that sociopolitical complexity was far greater than originally thought. It has been estimated, for instance, that the Danta pyramid and the western group in Nakbé each have a total volume of over 1 million m³, which must have required centralised organization of labour (Hansen 2000). However, towards the end of the Preclassic period, many centres experienced a decline, similar to the more famous collapse of the Classic period (Coe 2005:82).

During the Classic period there was a development of more complex forms of political organisation and an expansion of pre-industrial states as the central lowland polities reached their

sociopolitical, cultural and demographic peaks. As a consequence, early research gave the name of “Classic” to this period, which has marked Maya archaeology and created biases towards the study of other periods. However, it was during the Terminal Classic Period when major changes in the political and demographic life of the Maya area occurred. These changes affected mainly the core of the southern Lowlands, but not its coastal margins. Extensive research has been produced in trying to explain the decline and abandonment of the sites, but archaeological evidence suggests there were many processes and factors involved, with different patterns and timing of decline across the different areas in the lowlands (Aimers 2007). As Demarest and colleagues (2004) clarify however, there was no “collapse” of the Maya civilisation, but just a decrease in power of the institution of kingship, and a change in the social and political structures.

Many of the cultural traits of Maya civilisation, such as writing, monumental architecture and religious beliefs continued to be part of the life of the Postclassic period. This period saw the emergence of new centers with a new political system and an emphasis on trade, all of which were abruptly disrupted by the Spanish conquest in the early 16th century (Sharer 2006: 156).

Palenque

Palenque is located in the southwestern Lowlands, in the foothills of the Sierra de Chiapas, over the margin of the alluvial plain of Tabasco. It was one of the Lowland sites that was abandoned during the Terminal Classic period. It therefore remained undetected until the 18th century, when a group of explorers first reported the site. Later in the 19th century European interest in Palenque increased, with numerous explorers and travelers documenting the site, including John Stephens and Frederick Catherwood.

Palenque continued to be extensively investigated during the 20th century. In 1952 Alberto Ruz Lhuillier discovered the funerary crypt inside the Temple of the Inscriptions, built for the Maya ruler K'inich Janaab' Pakal, also known as Pakal II (Ruz-Lhuillier 1973). But it was with the beginning of Palenque's round tables in 1973 that prolific research on Palenque was generated (Robertson 1974, 1976, 1979, 1980, Benson 1980, Fields 1985, 1991,1994, Macri and McHargue 1996).

Epigraphic research in Palenque has been particularly fruitful for Maya archaeology and has yielded valuable information on Maya cosmology and on the dynastic history of the site (see table 2.3).

2. Environment and Cultural Setting of the Maya Area

| Ruler | Took power (AD) | Died (AD) |
|----------------------------------|-----------------|-----------|
| K'uk' B'Alam I | 431 | 435 |
| "Casper II" | 435 | 487 |
| B'utz'aj Sak Chiik | 489 | ~ 501 |
| Akul Mo' Nab' I | 501 | 524 |
| Kan Joy Chitam I | 529 | 565 |
| Akul Mo' Nab' II | 565 | 570 |
| Kan B'alam I | 572 | 583 |
| Ix Yol Ik'nal | 593 | 604 |
| Ajen Yok Mat | 605 | 612 |
| Ix Sak K'uk? | 612? | 640 |
| K'inich Janaab Pakal I | 615 | 683 |
| K'inich Kan Balam II | 684 | 702 |
| K'inich Kan Joy Chitam II | 702 | 721? |
| K'inich Akul Mo' Nab' III | 721 | ~740 |
| U Pakal K'inich Janaab' Pakal II | 742 | ~750 |
| K'inich Kan Balam III | 751 | ~783 |
| K'inich K'uk Balam II | 764 | ~799 |
| Wak Kimi Janaab' Pakal III | 799 | ? |

Table 2.3. Dynastic history of Palenque (Mathews 2000).

Recent research has documented newly discovered royal tombs and inscriptions, and has demonstrated that the site was much larger and densely populated than originally thought. The *Palenque Mapping Project* (Barnhart 2000) identified 1478 structures in the urban centre, where only 329 had been mapped before. The project also identified the Picota Plaza as a public focus point earlier than the Classic Palace Plaza. The settlement pattern proved to be dictated by the landforms, with seasonally flooded plains at the north, high hills to the south, and narrow ridges to the east and west. The mapping project also documented the water management works, which were oriented towards avoiding seasonal inundation in the most densely populated areas (Barnhart 2000). See fig. 2.10.



Fig. 2.10. Palenque Map (Image: Barnhart 2000). Scale bar 500 meters.

Palenque's architecture shows a characteristic style, marked by a smaller scale in the size of monumental architecture compared to other Maya sites, its delicate proportions, the fine lime plaster sculptures, and the use of distinctive cresterías, or roof combs (see Hernandez Reyes and Peralta Bárcenas 1974, Robertson 1975). As Griffin (1978) suggests, the roof combs at Palenque, together with the inscriptions tablets, may have served the purposes of stelae, which are abundant at many other Maya sites but were not used in Palenque.

Although Palenque was occupied from Early Classic times, it was during the Late Classic that the site reached its political and demographic heyday. Little archaeological evidence has been found regarding the activities of the rulers before K'inich Janaab' Pakal I, but the inscriptions associate previous rulers with the supernatural world, which has been interpreted as a way of justifying and reinforcing political power of later rulers (Martin and Grube 2000). It is known that in AD 611, Calakmul sacked Palenque during the reign of Ajen Yok Mat, after which a period of political instability followed.

Pakal II, who reigned from AD 615 to 683, suffered a defeat by Piedras Negras in AD 628 (Martin and Grube 2000). After this defeat, Pakal quickly established himself as a powerful ruler and was famous for commanding architectural programs dictated by his political agenda. He built the Olvidado Temple, which was the model to follow for later buildings. Pakal also renovated the Palace complex, but the culmination of his architectural programs was the Temple of the Inscriptions with his own funerary crypt inside it (Ruz Lhuillier 1973). In the midst of this prosperity, Palenque was sacked once again by Calakmul in AD 654 (Martin and Grube 2000).

Pakal's son, K'inich Kan Balam II succeeded his father in AD 684 and remained in power until AD 702. According to the inscriptions, he continued with his father's architectural programs and ordered the construction of the Cross Group, which includes the Temples of the Sun, Cross and Foliated Cross, recalling the triadic arrangement of Preclassic Petén architecture (see fig. 2.11).

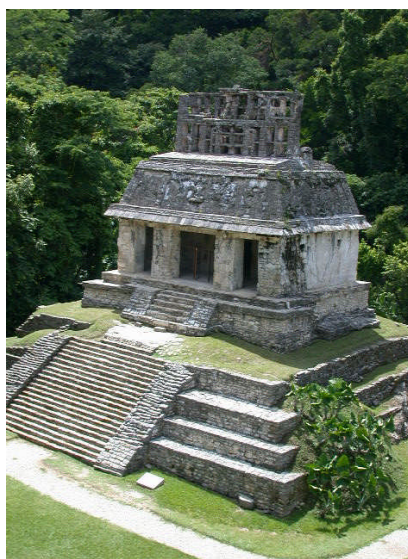


Fig. 2.11. Temple of the Sun, Palenque.

However, it is worth noting that the dating of buildings at Palenque have usually relied on the interpretation of inscriptions, although this is not infallible since the inscriptions could have been incorporated by later rulers; only recently have researchers stressed the relevance of complementing architectural typologies, ceramic assemblages, epigraphy and stratigraphy (Marken 2006).

The Cross Group was an important ritual location in the ancient city of Palenque, which has been proposed based on the tablets present inside the sanctuaries of the Temples, as well as on the numerous effigy incense burners that have been found buried inside the stepped platforms of the buildings (Rands and Rands 1959, Cuevas García 2000, Cuevas García 2007).

Building activities after K'inich Kan Balam II are less clear, but it is known that Kan Balam II and perhaps his younger brother and successor, Kan Joy Chitam II (AD 702-721), were in charge of renovating the northern part of the palace (Tovalín Ahumada and López Bravo 2001).

Palenque's decline and abandonment was one of the earliest in the Maya area, and occurred as a very quick process. It is believed, based on the ceramics of the site, that this demise took place around AD 800 – 830 (Rands 1974). The last date of Palenque was recorded in AD 799 on a ceramic vessel that was recovered from the Bats Group (Martin and Grube 2000).

Cuevas García and González Cruz (2007) documented subtle traces left during the final stages of the site, as well as earth layers that separate the strata of the dynastic periods from later occupations that presumably took place during a period of pilgrimage.

Calakmul

Calakmul is located in the Mexican state of Campeche, 30 km north of the Guatemalan border. The climate of the site is hot and humid, with a well-defined rainy season from May to November. The vegetation is semideciduous rain forest, with canopy as tall as 15 and 20 metres (Rojas González-Castilla 2000).

The site was first reported in 1931 by Cyrus L. Lundell and explored soon after by Sylvanus Morley from the Carnegie Institute of Washington. It then remained unexplored for several decades until 1982, when the University of Campeche launched a project under the direction of William Folan that lasted until 1994. The site is now being investigated by the Instituto Nacional de Antropología e Historia—INAH—under the direction of Ramón Carrasco.

Although the site is now heavily forested, more than 6000 buildings have been mapped so far, indicating the intensive human transformation of the landscape in ancient times (see fig. 2.1.2). It was occupied from the Middle Preclassic until the Postclassic period (Folan et al 1995).

The monumental core of Calakmul was built over a limestone dome adjacent to a number of seasonal wetlands, locally known as *bajos*. The central area is also encircled by a 22 km diameter hydraulic system of canal and reservoirs, which demonstrates the ability of the managerial elite to coordinate these projects (Folan et al 1995:311) (see fig. 2.13).

Calakmul was also well connected with other sites, and seven roads or *sacbeob* have been associated with the site, one of them probably linking Calakmul and El Mirador (Folan et al 1995).



Fig. 2.12. Calakmul. View of Structure I.

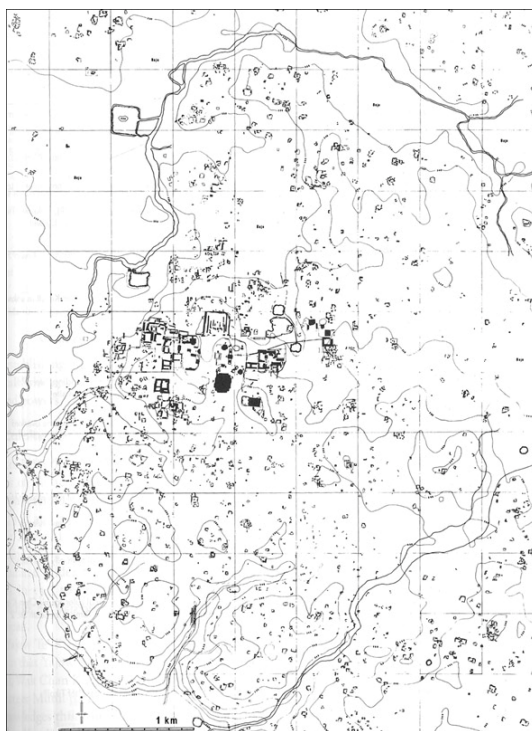


Fig.2.13. Central area of Calakmul with hydraulic system of canals and reservoirs. Scale bar: 1 km. Drawing: Gonzalez-Heredia in Sharer 2006.

The Late Preclassic Period in Calakmul saw a rapid population growth and extensive architectural programs. Despite these impressive architectural programs, Calakmul may have been subjected to El Mirador during Preclassic times, a massive Preclassic polity of the Petén (Sharer 2006:279).

It was perhaps the demise of El Mirador at the end of the Preclassic which allowed Calakmul to emerge as a major centre in the Lowlands. Despite the fact that the early history of Calakmul is not clear, due in part to the bad preservation of hieroglyphic texts, it is evident that by the sixth century AD the site had become an expansionist state, as attested by many texts in other lowland sites (Sharer 2006:356). Soon after, Calakmul established alliances with other lowland sites, particularly with Caracol, and became the most important rival of Tikal. The rivalry between Calakmul and Tikal was a determinant force of the political life of the Classic Maya lowlands, and involved many alliances of both polities with secondary centres.

Calakmul and its allies defeated Tikal in AD 562, but Calakmul's apogee was not reached until the reign of Yuknoom Ch'een II (AD 636-86) (Simon and Grube 2000:108). Under this ruler, more victories were recorded over Tikal, but Calakmul was eventually defeated by its rival in AD 695. Despite the final victory over Calakmul, Yuknoom Took' K'awiil's reign from 702 to 736 saw the construction of impressive arrays of monuments and dedicatory stelae. However, after this ruler, the number of dedicated stelae suffered a steep decline, and the last recorded ruler, Aj Took, was mentioned in 909 as part of the celebrations of the K'atun ending. After this, Calakmul's dynasty soon disappeared (Sharer 2006:415).

Regarding architectural programs, Calakmul represents one of the longest time spans of monumental architectural programs, ranging from the Late Middle Preclassic Period (ca. 400 BC) to the 9th century AD. The Preclassic Period saw the construction of massive monumental architecture, of which Structure II is one outstanding example. It reached a height of 55 m, and was one of the highest buildings ever built in Mesoamerica (Folan et al 1995:316). It is also known that the Preclassic acropolis of Calakmul showed a triadic arrangement, in which the main platforms, Structure II, IV, V and VII, were topped by three temples (Folan et al 2001). The Preclassic acropolis or Gran Plaza established the configuration that we see today, and the massive structures, in particular Structure II, were conceived as sacred mountains and were likely used to reinforce the power of the ruling lineages (Rodríguez Campero 2000).

However, as at all Maya sites, Calakmul was repeatedly transformed through additions, renovations, and sometimes destruction of earlier buildings. Recent excavations have revealed the existence of a large Preclassic frieze sealed inside structure II, which corresponds to Substructure IIc-1. The frieze was modeled in lime plaster and its iconography is related to the mountain as a

gateway to Xibalbá, or the Underworld (Rodríguez Campero 2008), a widespread notion in Mesoamerican cosmogony (see figs. 2.14 and 2.15).

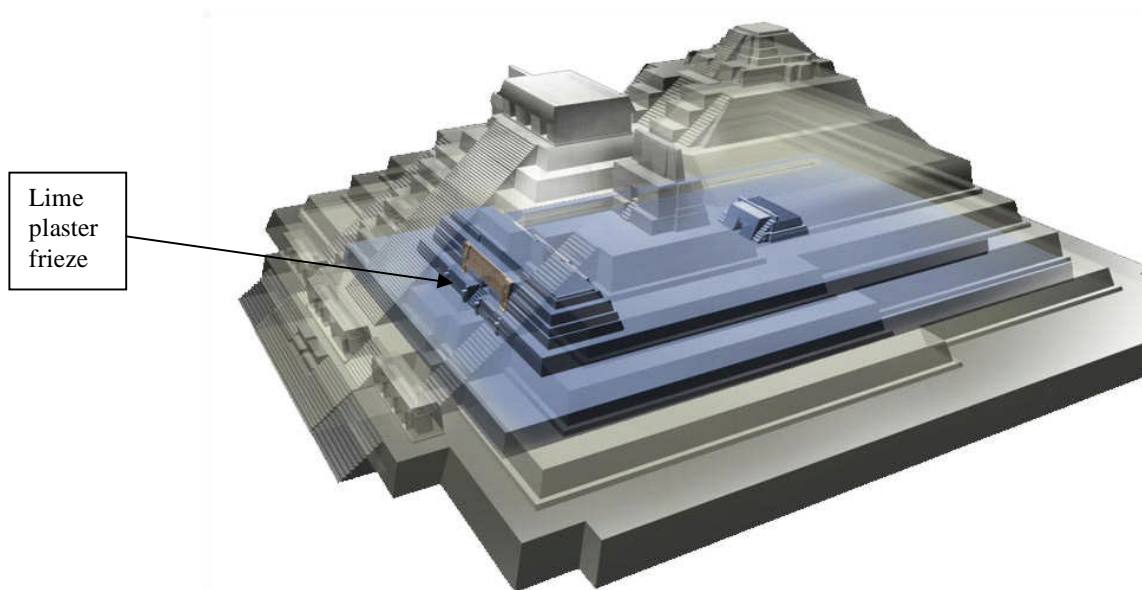


Fig.2.14. Building phases of Structure II with Late Middle Preclassic Substructure II c-1 shown in blue and Late Classic buildings in gray. Image: Rodríguez Campero (2008).

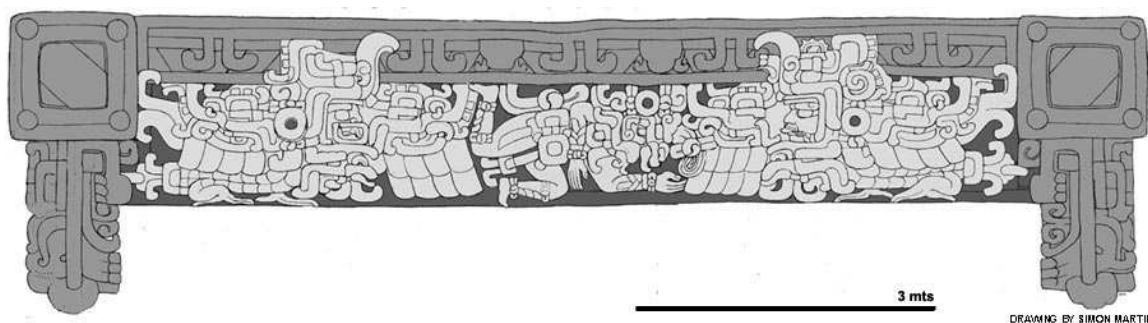


Fig. 2.15. Drawing of lime plaster frieze in substructure IIc1. Scale: 3 mts.
Drawing: Simon Martin, reproduced in Rodríguez Campero (2008).

Important architectural innovations were achieved during the Preclassic period at Calakmul. Substructure IIc, for instance, shows a unique example of a barrel vault, in which the principle for distributing the forces downwards seems to have been discovered during the Late Middle Preclassic Period. For some reason, however, this vault did not evolve in Maya architecture, and the common Maya corbel vault was used in later periods at Calakmul (see figure 2.16).



Fig. 2.16. Barrel vault of Substructure IIc, showing later fill. Image: Rodríguez Campero2008.

These architectural features were covered by a Late Preclassic structure, known as Substructure II-b. During the Early Classic period the structure was modified twice. The first modification involved covering of the front area of the Substructure II-b and the construction of two buildings on top, which reflect changes in the power balance of the city, but also changes in style in Maya architecture (Rodríguez Campero 2008). With the second modification during the Early Classic, a monumental stairway and four zoomorphic masks were built to form the façade, but they too were later buried during the Late Classic period (Carrasco et al 1999).

Structure VII also saw periodic transformations, with its earliest phases dating to the Late Preclassic, the central superstructure dating to the Late Classic, and the latest modifications Terminal Classic in date (Braswell et al 2004:172).

Another important structure is the Chik Naab' acropolis, which has been preliminarily dated to the Early Classic period. In this building, wall paintings were unearthed and conserved in 2004. The paintings show images of daily life such as cooking, drinking and smoking, and are therefore a rare example in Maya imagery (Miller 2006, Pacheco 2007). It is known that the ruler Yuknoom Yic'haak' K'ak' took place at the Chiik Naab' acropolis (Carrasco Vargas and Colón González 2005). Despite the construction of this important building, the understanding of the Early Classic period at Calakmul is to some extent fragmentary and the ongoing excavations aim to advance our knowledge in this respect (Carrasco Vargas and Colón González 2005)

The Late Classic period was also a very prolific period in architecture. More than 100 structures were built, and more than 40 during the century between AD 652 and 752 alone (Folan et al 1995). The presence of complex burial assemblages of the ruling elite and the inscriptions

associated to them also demonstrate the socio-political complexity of the Late Classic period at Calakmul (Carrasco Vargas 1999, García Moreno and Granados 2000).

Settlement data show that Calakmul's population during the Late Classic reached more than 50,000 individuals, and perhaps up to 200,000 when including its secondary sites. However, Calakmul suffered a steep demographic decline in the Terminal Classic, losing perhaps 90% of its rural population (Braswell et al 2004: 188). Major social and political changes also occurred during the Terminal Classic, with former sacred temples, such as Structure II, being used for residential and administrative purposes (Braswell et al 2004). Researchers have also suggested that drying of the *bajos*, caused by prolonged drought, may have been the result of anthropogenic deforestation, all of which may have constituted a factor in the collapse of this city (Gunn et al 2002).

Lamanai

Lamanai is located in the modern district of Orange Walk, Northern Belize, on the western bank of the New River Lagoon and at the head of the New River. The site was first excavated between 1974 and 1986 under the direction of David Pendergast. Investigations began again in 1998 under the direction of Elizabeth Graham who was joined by Scott Simmons as co- principal investigator in 2003. The site continues to be investigated.

The earliest date for the occupation of Lamanai is a fragment of wood associated with maize agriculture, radiocarbon-dated to 1500 BC (Graham 2000:53). This occupation continued from the Preclassic period through to the Postclassic, surviving the collapse that affected most of the Maya Lowland sites in the transition between the Classic and Postclassic periods. Lamanai also survived the Spanish conquest and remained occupied until the 17th century during the Spanish Colonial period (Pendergast 1985a, 1998:55, Graham 2008).

During Preclassic times, Lamanai may have dominated Cerros, one of the earliest Maya centres, but Lamanai was perhaps subjugated by El Mirador, the most powerful polity of the Preclassic Lowlands (Sharer 2006: 279). In any case, Lamanai was a vibrant site during the Late Preclassic, with the construction of one structure, Str. N10-43, the "High Temple", reaching 33m – one of the highest structures built during this period in the Maya area (see fig. 2.17).



Fig. 2.17. Structure N10-43, the High Temple



Fig. 2.18. Plan of Lamanai. Drawing: Pendergast 1985a. Scale bar in image at the left: 100 m.

Pendergast (1985b) states that a common problem affecting many sites in Belize during the Late Classic was the scarcity of stone suitable for facing. The difficulty in obtaining suitable stone may have been the reason for the recycling of materials, as in the case of Structure N10-12, where Terminal Classic stones were reused in the Early Postclassic construction. There is also evidence that stone from the Plaza Group N10 [3] was re-used in the facing of Late Classic buildings (Graham 2004:235).

Despite the scarcity of building materials and in contrast to earlier interpretations that

presented Lamanai as a site where monumental public construction was drastically reduced after the Classic period (Pendergast 1981), later excavations showed important architectural programs going on during the Terminal Classic. The courtyard filling of the Ottawa Group N10[3] is an example, where more than 21,000 tons of material raised the level of the plaza (Pendergast 1985b, Graham 2004). As part of the infilling work, the buildings around the courtyard were razed and covered, and the whole area of the Ottawa Group was extended northwards. The infilling began shortly after the frieze of Str. N10-28 was destroyed at the end of the Late Classic. This phase was nicknamed “Boulders” owing to the stones of the infilling work (Graham 2004:232). It is worth mentioning however, that the stone employed in the filling of the courtyard was a hard stone not suitable for facing (E. Graham, personal communication 2007). This hard stone most likely corresponds to the crystalline limestones of the Cretaceous and Paleogene periods (McDonald 1978).

Construction activity in this area continued through the Early Postclassic period, although buildings were constructed in part or mostly of wood rather than stone (Graham 2004:234). The existence of a mercury offering underneath the ball court, built at the end of the Classic (Pendergast 1990:172), shows an active ritual life and long-distance trade with the Maya Highlands. Structure N10-9, the Jaguar temple, located south of the Ottawa Group, is another example of continuity in architectural practices during the transition between the Classic and Postclassic periods. Although this building was originally built during the Classic period, it was continuously transformed and renovated until the 12th century, with minor modifications probably until the 15th and 16th centuries (Pendergast 1985b:98).

Despite the fact that construction activities suggest that Lamanai was a society with functioning political and economic structures during the Terminal Classic, the northern area of the site, as a zone of ritual focus, was largely abandoned in this period, and the life of the site turned southwards, especially to the lagoon littoral (Pendergast 1985b, Graham 2004: 239).

The Stela Temple, N10-27, was one of the structures that was abandoned but left standing at the end of the Classic Period, although it has ritual refuse from Terminal Classic and Early Postclassic times (Graham 2004:230). Str. N10-77 and the other buildings of the Ottawa Group, however, as described above, were razed and buried by later construction phases (Graham 2004:236).

As mentioned before, not only did Lamanai continue to be occupied in the transition between the Late Classic and the Postclassic periods, but it also remained inhabited after Spanish contact. Structure N12-12, The Rectory, has different sources of evidence that suggest that this building was used during and perhaps beyond the Spanish colonial period. Structures YDLI and YDLII (fig. 2.19) were built by the Spaniards as Christian temples and remained in use until 1641,

2. Environment and Cultural Setting of the Maya Area

when a Maya uprising occurred (Pendergast 1990:177). The church zone was transformed during the British period and YDLII was even used as a smithy (Graham 2004:228). The church area was excavated in 2003 and 2004, and consolidated in 2007. These investigations unearthed a *plaza-atrio* associated with the first church (YDLI), where open-air gatherings most likely took place. Colonial caches (offerings) and postholes indicate the original dimension of the second church (YDLII) (Graham 2008).

Maya occupation in Lamanai may have ceased in the seventeenth century or the early eighteenth century (Pendergast 1990:177).



Fig. 2.19. Structure YDLII. Remains of the 16th century Spanish church.

3. Use and Production of Lime in the Maya Area

In this chapter I describe the principles of lime production and plaster manufacture, including the chemistry of the lime cycle. I also give a brief overview of lime production in the Old World and review the literature of Mesoamerican lime and lime plaster production.

3.1. Chemistry of lime production

Lime is produced when limestone or another calcium carbonate-rich material is burnt over 900° C, after which this compound is transformed into calcium oxide. This material is then slaked with water or moist air, forming a white powder or paste depending on the amount of water, and transforming into calcium hydroxide. The slaked product is sometimes stored for several months to promote hydration and to improve plasticity and other working properties of the lime. During setting and following exposure to air, calcium hydroxide reacts with carbon dioxide to form calcium carbonate (Boynton 1980). The chemical reactions of the lime cycle are as following:

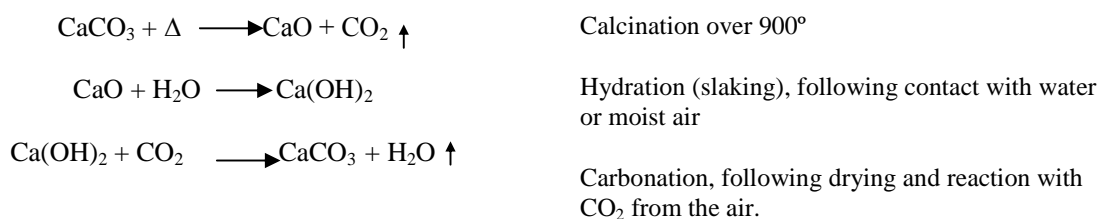


Fig. 3.1. Chemical reactions that occur in the lime cycle.

Lime is the cementing material of plasters, but it requires aggregates to create a material that is stable after drying and hardening, and which confers specific mechanical properties to the mixtures (Stefanidou and Papayiani 2005). Aggregate materials are added once the lime is slaked in the form of a paste; after thorough mixing, the plaster can be applied or modelled over architectural surfaces (see glossary for definition of terms including plaster, mortar, concrete and stucco). Another way of mixing the aggregates is known as “hot mixing” and consists on mixing moist aggregates with the quicklime; this technique has been identified in Greek archaeological plasters by Karkanias (2007).

More durable lime materials can be obtained with hydraulic plasters, which can be produced with natural hydraulic limes, artificial hydraulic limes or with the use of pozzolanic aggregates. Natural hydraulic limes are produced when limestones with clay impurities are burnt below sintering temperature, whereas artificial hydraulic limes are obtained by deliberately adding siliceous materials to the limestone before calcination. Pozzolanic aggregates, on the other hand,

confer hydraulic properties when they are added to non-hydraulic limes during slaking (Charola and Henriques 1999). Pozzolanic aggregates are named after the volcanic ash from Pozzuoli, near Naples, which the Romans used systematically in their lime mixtures. In addition to volcanic ash, brick dust has been used historically as a pozzolanic aggregate, and more recently fly ash and condensed silica fume have also been used. The former is a residue from coal-fired power plants and the latter a waste material in the production of silicon alloys (King 2000).

Generally speaking, hydraulic plasters are characterised by the formation of calcium silicate and aluminate hydrates. The resulting material is a mortar that sets under water and is therefore known as “hydraulic”. In the case of non-hydraulic limes, setting is produced solely by drying and carbonation, during which calcium hydroxide reacts with carbon dioxide to form calcium carbonate. In contrast, the hardening of natural and artificial hydraulic limes results when calcium silicates and aluminates react with water. In a similar way, when pozzolanic aggregates are added to non-hydraulic limes during slaking, chemical reactions occur between the calcium hydroxide and the reactive silica and alumina, resulting also in the formation of hydraulic phases (Gibbons 2003). Broadly speaking, hydraulic limes have higher hardness and compressive strength in comparison to non-hydraulic limes, as well as lower porosity and therefore lower permeability. However, performance characteristics of non-hydraulic limes can be improved with specific manufacturing techniques, such as the controlled burning of the lime, the use of adequate lime/aggregate proportions as well as thorough slaking and mixing (Constantinides 1995, Kerstin et al 2002).

A general way for calculating hydraulicity index is the cementation index formula (C.I), on which the three degrees of hydraulicity are established (Boynton 1980:313). However, it is important to consider that there may be siliceous aggregates in the plasters, such as quartz, that do not participate in hydraulic reactions, and for this reason the nature of the aggregates needs to be established beforehand.

$$\text{C.I.} = (2.8 \times \% \text{SiO}_2 + 1.1 \times \% \text{Al}_2\text{O}_3 + 0.7 \times \% \text{Fe}_2\text{O}_3) / (\% \text{CaO} + 1.4 \times \% \text{MgO}).$$

After calculating the C.I., hydraulicity of mortars can be established as:

- Feebly hydraulic: 0.30 to 0.50 of C.I.
- Moderately hydraulic: 0.50 to 0.70 of C.I.
- Eminently hydraulic: 0.70 to 1.10 of C.I.

Other techniques for estimating hydraulicity are thermal analysis, which is based on the different temperature at which hydraulic phases decompose (Ellis 1999), as well as pozzolanicity tests and the measurement of soluble silica contents (Van Balen et al 1999).

Modern Portland cement is manufactured by burning a calcium-rich material, usually chalk, together with clays rich in alumino-silicates, at temperatures between 1,300 and 1,450°C, during which sinterisation occurs. Sinterisation is the process by which the particles adhere to each other forming a clinker. This is then ground to powder and mixed with water, usually with a small amount of gypsum as a retarder (Davey 1961). The hardening is the result of the formation of water-containing compounds that result as the reaction of calcium silicate and aluminates with water. It is important to note that although the principle of modern Portland cement is the same as in natural hydraulic limes, the firing temperature is much higher in the former, which allows sinterisation, while this does not occur in natural hydraulic limes. The formation of a clinker as a result of sinterisation produces specific hydraulic phases, such as alite, which does not form at lower temperatures (Altun 1999). In the case of non-hydraulic limes, however, burning temperatures exceeding 1500°C are counterproductive, since they become dead-burnt, that is to say, the lime loses chemical reactivity with the water and presents difficulties for slaking (Boynton 1980:184).

3.2. Brief overview of the use of lime in the Old World

Lime has played an important role in many cultures around the world and has had a fundamental importance in the development of civilisations. Until the invention and widespread use of Portland cement in the 19th century, building activities across the world relied on lime or hydraulic lime as the main binding material in masonry construction, as well as for coating and finishing renders.

Gypsum was perhaps the first cement to be used in antiquity, since it only requires firing temperatures between 130° and 170°C. Gypsum was widely used in ancient Egypt during dynastic times, but its use in other early civilisations is less clear due to the fact that this material is affected by water and is not preserved well. However, gypsum may have been first used in the Middle East, where there are large outcrops of this mineral (Davey 1961:92).

The earliest lime production can be traced back perhaps to Epipaleolithic times, around 12000 BC and its use in architecture of the Natufian Period (10300-8500 BC) (Kingery et al 1988). However, more extensive use of lime plasters appeared in the Near East during the Neolithic in the 9th millennium BP, which predates ceramic production and coincides with the appearance of village life. Some examples are found in Asikli Hüyük and Çatal Hüyük in present day Turkey, Jericho in the West Bank (Goren et al 2001), in Jarmo, modern Iraq, and Tell Ramad in Syria (Goudin and Kingery 1975). Ain Ghazal in Jordan is an outstanding discovery of lime technology in the Near

East, where several anthropomorphic lime plaster statues were found, the technology of which is described by Grissom (2000).

Another early example of the use of lime was found in Lepenski Vir, Serbia, where lime-plastered floors dating from between 6200 and 5400 BC are contemporaneous with or predate early Neolithic ceramics. These architectural innovations are related to the origins of sedentism and the development of social and symbolic complexity (Borić 2002).

Much later, the Egyptians also employed lime for building purposes. The earliest report of Egyptian plaster dates from 1400-1200 BC from Timna (Gourdin and Kingery 1975). Thin lime plaster layers were also employed as preparation layers for painting in Egyptian sarcophagi during the XXVI dynasty, around 600 BC (Chiavari et al 1995).

Lime was also used in the Greek world. Analyses of the renders of wall painting from Knossos, the famous Minoan palace in Crete, have been characterised as lime plasters (Dandrau 2001). Many other Minoan sites including Amnissos, Hagia Triada, Chania, and Malia, ranging in date from 1750 to around 1200 BC, show lime plaster renders and floors.

It is likely that the hydraulic properties of the lime were discovered by the Greeks. Dandrau (2000) affirms that in the case of Malia in Crete, the lime mortars have hydraulic limes, but it is not clear whether the silicates originate from clay inclusions of the limestones that were used to produce the lime, or from Santorini earth added to the mortars (volcanic ash from the Santorini volcano in the Aegean Sea). Despite this apparent discovery by the Greeks, the Romans were without any doubt the first culture to use hydraulic lime extensively and to exploit its full potential. They built on Greek traditions and developed a monumental architecture of a previously unknown scale.

Vitruvius compiled Roman building traditions in his *Ten Books of Architecture* during the first century AD, where he described the use of Roman cement for the first time. The manufacture of Roman cement, known in Roman times as *opus caementicium*, was prepared with volcanic ash from Pozzuoli, the town with deposits of volcanic ash from the Vesuvius volcano. Vitruvius described the pozzolanas as a material that “when mixed with lime and rubble, it lends the strength to all the other sort of construction, but in addition, when piers are built into the sea, they solidify under water” (Vitruvius, book II).

This technology was extremely important for the construction of Roman harbours, since the concrete was poured in frameworks directly under the water, which replaced the time-consuming carved stones for the constructions of piers. The earliest example of Roman maritime concrete work is the port of Cosa, in southwestern Tuscany, which dates probably to the 1st century BC. In this site, five free-standing pillars were found and analysed, showing strong hydraulic reactions with the

binder, which was likely manufactured with volcanic material from the Vesuvius area traded by sea (Oleson et al 2004). Another important use of hydraulic plasters in the Roman world was the lining of cisterns, since hydraulic mortars are much less permeable and can therefore store water in a better way. The Romans made use of crushed and powdered ceramics as artificial pozzolanas for obtaining hydraulic sets for the lining of cisterns (Siddall 2000). This has been documented in the site of Uthina, a Roman city in northern Tunisia (Farci et al 2005).

In addition to the use of pozzolanas, Vitruvius also described the proportion in which aggregates should be mixed with lime to prepare plasters, and advised that sand from sand deposits should be preferred over sea and river sand for aggregates (Vitruvius, book II). He also mentioned that crushed potsherds can be added to the lime mortars, forming a harder material, which is known as *cocciopesto*, literally meaning “crushed earthenware” in modern Italian. The practice of adding crushed fired ceramics to lime mixtures became a widespread practice in the Roman provinces where volcanic ash was not available (Farci et al 2005), since ceramic powder is also a pozzolanic material that confers hydraulic properties to the plaster.

However, raw materials were not the only factor to consider in Roman mortar manufacturing. The Romans improved the technique by using graded plaster in sequences of progressively finer and thinner layers that conferred better mechanical characteristics to the renders, which has been documented by Benedetti and colleagues (2004).

After the collapse of the Western Roman Empire, much of the knowledge on lime plaster craftsmanship was lost, although the practice of adding brick dust to lime to produce hydraulic plasters continued (Charola and Henriques 1999). This technique also continued to be used in the Eastern Roman provinces during the Byzantine period, exemplified by the mortars employed in Hagia Sophia, which are considered to have played an important role in the structural stability of the building (Van Nice 1948, Moropolou et al 2002). Hydraulic lime was also occasionally used in Medieval European architecture, as in the case of the leaning tower of Pisa, where hydraulicity was obtained through the use of diatomaceous earth (Franzini et al 2000).

During the Italian Renaissance there was a general interest in Ancient Rome, and Roman building traditions were recovered. Palladio mentioned Vitruvius in his *Four Books of Architecture*, and followed Vitruvius' recipes for the manufacturing of mortars and the selection of raw materials. Palladio also described the pozzolanas and the way they improve the properties of the mortars (Palladio, book I).

However, it was not until the 19th century in Britain that major breakthroughs occurred in the fabrication of cementitious materials. In 1796, James Parker manufactured high-quality hydraulic limes, known at that time as “Roman cement”, by burning argillaceous limestones from

the Thames estuary. Later attempts were made to improve the recipe, and in 1833 Frost patented the “British cement”, which was burnt at higher temperatures. In 1845 Johnson produced the first Portland cement with burning temperatures high enough to produce sinterisation (Davey 1961).

3.3. Maya and Mesoamerican lime production

It is well known that lime was used extensively in Mesoamerica during Prehispanic times, which constituted an independent technological achievement that had important cultural implications for the development of civilisation in this cultural area. The Lowland Maya employed lime for structural and decorative purposes in architecture, partly because raw materials, limestone and firewood, were abundant (see Espinosa et al 1996, Hammond and Ashmore 1981). In addition to the use of lime for the manufacture of architectural plasters, there is strong ethnographic and ethnohistoric evidence of the use of lime for maize processing, the relevance of which for the subsistence of ancient populations is explained below. Lime was also used in the manufacture of codices (Prehispanic folded books), in which lime plasters were applied in thin layers over the paper substrates before writing (Escalante Gonzalbo 1999). It is also known that lime was used, and is still used today, amongst the lowland and highland Maya for tobacco chewing (Thomson 1970:110), whereby lime increases the hallucinogenic effect of the nicotine (Wilbert 1987). Lime may have had other uses in the Maya area, such as water purification, soil stabilisation and fiber softening for paper making, as is known for other cultural areas in modern uses, although there is no archaeological evidence for these activities in the Maya area.

Ethnohistoric sources

In the 16th century, the priest Diego de Landa described in his chronicles the abundance of limestone in the Yucatan Peninsula, and its suitability for producing lime (Tozzer 1966:186). In relation to the manufacturing of lime plasters, Landa described that plasters were prepared by mixing lime with a juice obtained from the bark of certain trees (Tozzer 1966:176).

Diego de Landa also described *sac cab*, or *sascab*¹ as it is known today, as an abundant white earth that is used as aggregate in the manufacture of plasters (Tozzer 1966:18,171). This material is a combination of soft chalk and calcareous sediments that is abundant in the karstic Yucatan Peninsula, and it is usually found between the superficial caliche and the limestone bedrock, or as weathered calcareous deposits below the soil profile in some areas of the southern

¹ The Colonial world *sascab* correspond to the *saskab* in modern orthography. The term is a compound noun of “white” *sak* and “earth” *kab* as *sak-kab*. The <k> in *sak* has shifted phonologically to <s>, transforming from *sakkab* to *saskab* (Helmke personal communication).

lowlands, as explained in Chapter 2 (Espinosa et al 1996, Beach 1998:765). The site of Cobá in the Northern Yucatán Peninsula has archaeological evidence of sascab mining, where small columns were left to support the upper limestone cap (Folan 1978) (see fig. 3.2).



Fig. 3.2. Drawing of a sascab mine or *sascabera*. Image: Folan (1978). Columns are around 1 meter high.

In the chronicles of Fray Diego Durán (d. 1588?) lime is mentioned several times, among many other products, to have been paid as tribute to the Aztecs by various towns under Aztec dominion. Durán described that Moctezuma Ilhuicamina sent messengers to several towns in order to gather lime and other building materials, as well as labour force, for the construction of the Huitzilopochtli Temple in Tenochtitlan. The Chalcas rejected any form of cooperation and the Aztecs attacked and defeated Chalco, after which many Chalcas captives were sacrificed to Huitzilopochtli (Duran d.1588: 140). Duran also reported that lime for the Aztec empire was provided by the Hot Lands, which refers to numerous towns in the low-laying areas surrounding Tenochtitlan (present-day Mexico City) such as Cuauhnahuac, Yauhtepec, Huaxtepec, Acapichtlan, Matlatzinca zone, Xocotlan, Xilotepec and Actopan (Duran d. 1588).

In the 17th century, Ruiz de Alarcon (1629:87-89) described ritual practices of indigenous people from the Central Mexican Highlands during lime burning. He described how men would conjure the white woman (lime) to be born out of the death (stone) with the help of the fire and the wind. These ritual practices are essentially the same as the ones carried out by Maya lime burners of the 20th century, as explained below.

Ethnographic sources

Due to the scarce archaeological evidence of Maya lime production, ethnographic research on this topic has aimed at having a better understanding of the cultural, technological and environmental implications that this industry may have had in Prehispanic times, given that modern practices presumably constitute an inherited tradition from the ancient Maya. Ethnographic research is a fruitful line of evidence since Maya knowledge can still be found not only in lime production but in

many other aspects of building traditions throughout southeastern Mexico, Belize and Guatemala. A clear example is the use of specific Maya terms that have permeated into local Spanish for referring to different building activities and materials, such as *bak ch'ich* and *bak pek* (quarrying waste), *pak luum* (earth for the manufacture of mud plasters), and many other terms.

Ethnographic research shows examples of highly sophisticated methods for lime production, especially regarding the construction of open pyres for lime burning, bringing to light living traditions that were thought to be extinct. Morris and colleagues (1931) describe how Maya men in the Yucatan Peninsula used to burn the lime in open pyres, also called *caleras*. The authors described in a detailed way the construction of a circular solidly-packed pyre of 2 meters height and 5.50 metres diameter, on top of which fragments of limestone were placed in a 50 cm-thick layer. They described that only green moist wood was used because the burning temperature obtained with it was higher, although now it is known that the purpose of using this type of wood was to produce a slow and controlled burn (Schreiner 2002:43), which may also have an effect on lowering the dissociation temperature of lime (Boyton 1980:183). However, green firewood may have fulfilled a ritual purpose as well; offerings of stacked green firewood were a well established Pre-Hispanic practice, commonly carried out by Aztec priests, and depictions can be found frequently in the Borgia codices (Berdan and Rieff Anawalt 1992: 155).

Regarding the use of aggregates, Morris and colleagues (1931:224) documented that Maya builders used three parts of sascab per each part of lime in the manufacture of plasters, although a particularly hard plaster could be obtained by mixing two parts of sascab and one part of lime. Other authors have also described the use of sascab for the production of lime plasters in modern Maya communities (Littman 1958a, Abrams and Freter 1996, Thomson 1974:68). In addition to the use of sascab, it is also known that quarrying waste is commonly incorporated as aggregate material in the plasters, and experimental works have shown that quarrying and stone dressing generate approximately 50% waste of limestone (Abrams 1994: 46, Morris et al 1931: 215). The stone powder that is produced during quarrying activities is called *bak ch'ich'* in Yucatec Maya, whereas the gravel-size waste is called *bak pek*. Both *bak ch'ich'* and *bak pek* are desirable as aggregate material because they have angular edges that result in plasters with good mechanical characteristics. For this reason, contemporary Maya masons add this type of quarrying waste to the plaster mixtures (V. García, personal communication).

Morris and colleagues (1931) also describe the practice of soaking the bark of the *chochom* or *chucum* tree (*Pithecolobium albicans*) for several days, adding the resulting solution to the lime plasters, presumably as an attempt to improve workability and strength of the lime and to avoid cracking after drying (Littman 1960:593). Magaloni (1997) states that the bark of the *holol* tree was

soaked to extract organic substances to use as additives for Maya mortars. It is also known that organic additives are often incorporated during lime slaking, which results in specific properties of the plasters (Benavides 2006). Another organic substance added to lime plasters in the Maya area is honey, as was observed during conservation works in Uxmal, most probably a practice with ancient origins (Littman 1957: 136).

Ethnographic studies have also reported the extensive use of snails for Maya dietary purposes, after which the shells are burnt to obtain lime for maize processing (Nations 1979, Healy et al 1990, Baer and Merrifield 1971:152, Mackinnon and May 1990, Mathews 2002). The burning technique for shells makes use of dry wood, usually *ramón* or poisonwood, and is performed by either gender, in contrast to the much bigger wet wood pyres, which are male-specific (Schreiner 2002). Although it is generally believed that shell lime is employed only for maize soaking, given the low quantities produced (Mathews 2002), the chronicles of the 16th century conqueror Hernán Cortés, in his expeditions to the Maya Lowlands, recorded that Cholti-Lacandón used to gather mountains of snail shells in their dwellings (Hellmuth 1977), probably to produce lime for building purposes.

More comprehensive studies of ethnographic descriptions of Maya lime production have been carried out by Schreiner (2002) and Rusell (2008). The authors compile detailed information on lime burning techniques in the Yucatan peninsula and the Petén. The reported techniques consist of seven regional variants of open pyres, both in pits and above ground, with various sizes and ways of stacking the firewood, on top of which fragments of limestones are placed. Elaborate methods of stacking the fuel comprise strategically placing dry pieces of wood between wet materials, with the use of vents that promote the passage of air drafts. The burns are always performed in the open air and the lime mixes with the ashes as the firewood is consumed (Schreiner 2002). It is worth noting in this respect that the modern Yucatec Maya term *taan* is employed to refer to both lime and ash (Alvarez 1984), which may originate from traditional Maya lime burning where lime is mixed with ash during its production. Moreover, modern Maya masons mix sacked lime with wood ash, because they consider that ash provide beneficial properties to the lime (Schreiner 2002).

The research carried out by Schreiner (2002) initially aimed at examining whether ancient lime production contributed significantly to environmental degradation in the Mirador Basin (northern Guatemala) during the Late Preclassic period. Although this hypothesis was not decisively supported in the thesis, calculations for wood requirements based on traditional Maya techniques did seem to support the idea that large quantities of wood were necessary as fuel. Rusell (2008) also describes the large amounts of firewood that are required, although he considers that forest exploitation for lime burning at the site of Mayapán was sustainable.

Regarding the use of firewood, ethnographic research reports that lime burning takes place wherever firewood is available; the limestone is taken to the forest where the burn will take place and the quicklime obtained after the firing is transported to the site of construction (Redfield and Villa 1934, Morris 1931:221). It is also known that gumbo-limbo (*Bursera simaruba*), locally known as *chacah*, is the preferred tree to use as fuel. Some advantages are that its wood burns very easily without leaving behind charcoal that could contaminate the lime. This species is also a fast growing tree that can be planted from cuttings to renew fuel supplies (Schreiner 2002:45).

In addition to ethnographic descriptions, experimental projects have been carried out in order to assess the time required to fell trees with stone axes, as it was done in Prehispanic times for the procurement of firewood. Lewenstein (1987:37-39) reports that three man-hours of hard labour are required to fell a medium size *chacah* tree with frequent resharpening and replacement of tools. This time requirements needs therefore to be considered when estimating ancient labour, since the use of stone tools requires longer times than the steel axes used in modern Maya practices on which ethnographic descriptions are based (see Schreiner 2002).

Archaeological deposits and artefactual evidence

Although lime plasters were extensively produced and used in Maya architecture, the archaeological evidence of its actual production is scarce, a fact noted by many authors (see Barba and Frunz 1999; Mazzullo et al 1994). Dearth of evidence is most likely related to the use of open pyres of wood for lime burning, the remains of which would be, to some extent, difficult to detect in the archaeological record. However, a more likely reason for the few reports of lime production may be related to the fact that lime burning used to take place in the outskirts of the sites where firewood was abundant (Russell and Dahlin 2007), but these areas have not been excavated extensively. For this reason, ethnohistorical and ethnographic evidence constitute the most informative source for the study of ancient Maya lime production, as explained above.

The difficulties in detecting lime production in the archaeological record mean that the origins of lime production in the Maya area are far from clear. For this reason, the observation of lime-based materials in architecture constitutes the earliest clear evidence for the use of lime. However, the practice of producing lime may have long preceded its use in architecture, very likely following the accidental discovery of the properties of lime by the observation of the contact between water and hot limestones from hearths. Another possible discovery might have been related to the practice of cooking with hot stones, which consists of boiling water by placing a hot stone inside a container filled with water. Cooking with hot stones may have been a common practice

3. Use and Production of Lime in the Maya Area

during the Early Preclassic period, since ceramics from this period do not show any firing evidence (Coe 1994, Sharer 2006:161).

One of the earliest reports of the use of lime in the Maya lowlands comes from plastered platforms at Cuello, Belize, which are associated with the earliest ceramics at the site, during the Swasey and Bladen phases, ranging in date from 1100 BC to 600 BC (Gerhardt 1988: 140, Hammond and Gerhardt 1990, Andrews and Hammond 1990:571, Littman 1979) (see fig. 3.3).

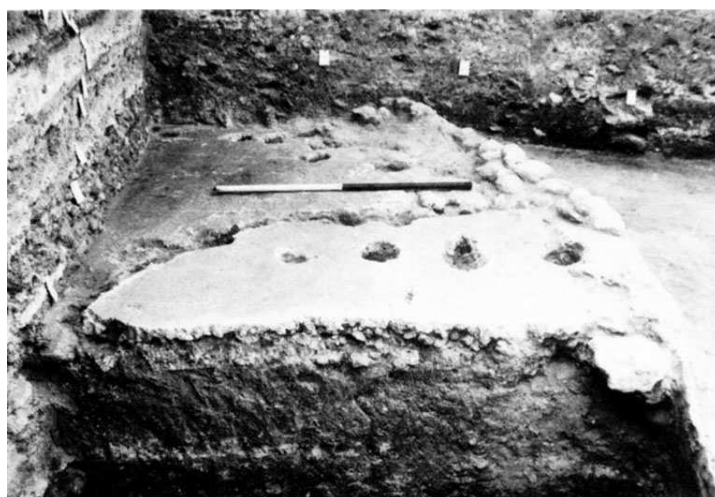


Fig. 3.3. Structure 327 at Cuello showing postholes and numerous applications of lime plasters dating from the Swasey and Bladen phases (Hammond and Gerhardt 1990).

Other early examples of architectural lime plasters are dated to the Early Middle Preclassic period, between 900 and 600 BC, in Nakbé, Guatemala (Hansen et al 1995, Hansen et al 1997). Soon after this, lime-based architecture is in evidence in the Middle Preclassic period at Uaxactun, Calakmul and El Mirador. This area of the central lowlands shows the most ambitious monumentality in Maya architecture, and is precisely where the main traits of Maya lowland civilisation would be later developed (Carrasco-Vargas 2000:14). There is also evidence for the use of lime in other areas of Mesoamerica, as in the valley of Oaxaca, Mexico, as early as 900 BC (Flannery and Marcus 1990:23).

Some examples of archaeological evidence of lime production have been reported in the literature. Descriptions include the case of the Tepeaca region (Castanzo 2004; Castanzo and Anderson 2004); Chalcatzingo (Grove and Guillen 1987, Grove 1987); Watson's island and Stann Creek (Graham 1994). The reports describe deposits with charred limestone, dark carbon-rich soil, charcoal and recarbonated lime, although none of these reports describe the remains of enclosed ovens. Abrams (1996:203) reports five burning pits at Copan, Honduras, which he believes were

3. Use and Production of Lime in the Maya Area

used to produce lime in small quantities for maize processing. Morris and colleagues (1931:225) mention that farmers in the Northern Lowlands used to state that remains of lime burning from the “ancients” could be found very easily when clearing land for agriculture.

Abrams and Freter (1996) report the only presumed enclosed lime oven in the Maya area, located also in Copan. The circular structure of 17 m³ capacity, built with grass-tempered clay, was dated to the Late Classic period. This evidence does not correspond with the descriptions of ethnographic and ethnohistorical sources of traditional Maya lime production, which describe lime burning in open pyres without any permanent structure for heat containment. Abrams and Freter (1996:426) claim that the oven was a technological development as a means for improving fuel efficiency in circumstances of a degraded environment. However, Schreiner (2002:96) states that this oven has the characteristics of Chorti Maya pottery kilns and that little heat containment would have been achieved if wet wood was used. Other arguable features are the 20 cm opening described by Abrams and Freter, which would make wood loading difficult. Furthermore, the interpretation that lime production had a low level of specialisation and a low socio-economic status based on the fact that the kiln was close to non-elite houses (Abrams and Freter 1996: 426) seems also problematic since it does not take into account the fact that lime burning was produced where firewood was available (Morris 1931:221, Redfield and Villa 1934:55), which was likely the periphery of the site.

Mackinnon and May (1990) excavated a 40 cm-thick layer of calcium carbonate associated with cemented lumps of calcium carbonate, sherds, shells and charcoal in the Early Classic site of Placencia Lagoon. This evidence was compared to the excavation of a pit next to a modern lime production site in Placencia Lagoon, Belize. Based on the similarities of both pits, Mackinnon and May argue that it is possible to obtain a thick recarbonated layer formed by leached material from the slaked heap of lime. They also carried out experimental firings of shells with the Lacandon small pyre dry-wood method of lime burning. The authors believe that shell lime is more suitable for household consumption since limestone quarrying requires considerably higher amounts of labour. Although much higher quantities of lime are obtained with limestone, a 50 pound sack per year is enough for household consumption; shell burning for lime production is therefore an adequate technique for household requirements.

Other likely archaeological evidence of lime production has been found in the Mexican state of Puebla, where more than 80 probable open lime kilns have been reported and dated for the Middle Preclassic Period, 1000-400BC, (Castanzo 2004, Castanzo and Anderson 2004). Although in a non-Maya region, the evidence reported, consisting of pits, charcoal and burnt limestone, suggests the use of open pyres in the central Puebla-Tlaxcala Basin.

In the southern part of Chalcatzingo, central Mexico, Grove and Guillen (1987) report a layer of manufactured lime dated in the Cantera Phase (700-500 BC) of the Middle Preclassic Period. There are also three open lime kilns from the Classic period in this site (Grove 1987:385).

A rather different perspective for detecting Maya lime processing in the archaeological record was carried out by Mazullo et al (1994) in materials from Santa Cruz, Belize on Ambergris Caye. According to the authors, based on mineralogical and micromorphological characteristics, it is possible to differentiate geological calcite from secondary calcite (obtained after calcination, slaking and recarbonation). In their work, archaeological samples were compared with modern manufactured lime and naturally occurring carbonate deposits. They observed that archaeological calcite was similar to calcite crystals of modern manufactured lime, and clearly different from natural carbonate deposits

Other aspects of lime production remain little known, as in the case of limestone provenance. Although it is usually assumed that raw materials for lime production were locally obtained, this seems reasonable for the sites located on the Yucatan limestone plateau, but is not the case for many sites of the Southwestern lowlands, the highlands, western Honduras and the Pacific coastal plain where limestone is not available.

Regarding the use of tools, many authors (Willys 1973, Eaton 1991, Lewenstein 1987, 1995) report artefacts made of chert, such as hammers and chisels for quarrying and tree felling. Experimental use of similar tools has demonstrated their functionality and wear marks (Lewenstein 1987), as well as working times (Abrams 1984). Folan (1982:155) reports two wooden clubs recovered in a *sascabera* at Cobá, as well as a terrapin shell that may have been used as an ancient scoop.

Regarding the technology for the manufacturing of lime plaster relief sculpture, Robertson (1983) has noted that many Maya sculptures have limestone cores that are embedded in the walls and provide the structural nucleus for the sculptures. However, this is not always the case and sculptures can be fully modelled with lime plasters, as in the case of the sculptures of the crypt of Palenque (Robertson 1983:19).

Robertson also describes that in the stratigraphy of Palenque sculptures, each plaster layer corresponds to a clothing element; that is to say, the persons were modelled naked and successive plaster layers were applied for each of the garments (Robertson 1983:19).

In the case of the sculptures of House B of the Palace at Palenque, Robertson notes that a drawing was scratched over the wall before the application of the lime plaster (see Fig. 3.4). In other cases, the design was done in black paint (Robertson 1983:19).



Fig. 3.4. Partially lost lime plaster relief sculpture showing scratched design on the wall.
(Robertson 1979: 157).

Epigraphic and literary sources

Maya writing is based on a combination of a logographic component (glyphs that represent words or concepts) and syllabic components that stand for sounds. Attempts to decipher Maya writing started after the Second World War but it was not until the 1980s that real and systematic progress on the decipherment was achieved by scholars (Coe 1999).

Most Maya inscriptions relate to the political history of the biggest and most powerful sites. However, epigraphic research has recently shown that the Maya also recorded more ordinary things, some of them relating to architecture.

The House E of the Palace at Palenque shows a glyph that has been interpreted by Martin and Grube (2000) and Mathews and Biro (2007) as Sak Nuk[ul] Naah (see fig. 3.5), which means the House of the White Skin. It seems that this name was given to this area of the Palace in reference to the lime plaster, since it was the only one without a red paint (Martin and Grube 2000:163). It is interesting to note the term “skin” in the glyph, since the Maya may have conceived wall renders and floors as a proper skin for the building.



Fig. 3.5. Sak Nuk[ul] Naah glyph (Mathews and Biró 2007).

Vault number 19 of Ek' Balam shows a similar glyph, which Lacadena García Gallo (2004) has interpreted as Sak Xok Naah (see fig. 3.6), meaning either “the Reading White House” or “White House of Respect/Obedience”. It seems that this glyph is the proper noun for room 35 of the Acropolis, the building with the distinctive lime plaster sculptures in its façade. In this building no traces of coloured paint layers have been found, in contrast to the rest of the structures of this site (Lacadena García-Gallo 2004).



Fig. 3.6. Left: Sak Xok Naah glyph (The white house for counting) in Vault number 19, Ek' Balam: Drawing: Lacadena García-Gallo (2004). Right: Detail of Ek' Balam's structure 35, referred to as Sak Xok Naah because of its unpainted lime plaster.

Lime plasters are mentioned in the Popol Vuh. This book is the sacred book of the Quiché Maya and was written in Quiché with the Latin alphabet just after Spanish contact in the early 16th century. The Popol Vuh is the written account of former oral traditions in which Maya mythology and religiosity was passed down through generations (Christenson 2003:37). Many of the mythological accounts described in the Popol Vuh have been detected in pictorial representations that date from the Classic Period.

The Popol Vuh describes the foundation of Chi Izmachi, a mountain-citadel, the ruins of which can be found on a hill to the southwest of Cumarcah, the ancient Quiché capital. In this account, the authors of the Popol Vuh describe:

“Chi Izmachi then, was the name of the mountain of which they dwelt as their citadel. There they settled and tested their glory. They ground their lime plaster and their whitewash in the fourth generation of lords. It is said that Co Nache and Beleheb Queh ruled then, along with the Lord Magistrate”. (Christenson 2003:262).

Later in the book, the use of lime plaster is also mentioned when relating the glory of the Lords of Cumarcah, where it is clear that lime-plastered architecture is associated with glory and sovereignty:

“Thus were established the twenty-four lords as well as the twenty-four great houses.

Then their glory and their sovereignty were increased in Quiché. The grandeur and importance of the Quichés was glorified and made sovereign. Then as well the canyon-citadel was whitewashed and plastered. The nations came there, the small and the great. Thus the lord who made Quiché great has his name.” (Christenson 2003:274).

Lime is also depicted in the Mendoza Codex, a book written with Aztec pictograms a couple of decades after the Spanish Conquest of Tenochtitlan. This codex documents the tribute paid to the Aztec capital by the different provinces under its dominion. Four thousand loads of lime (160-168 tons) are said to have been paid annually by the Province of Tepeac, which comprises the central and southern parts of the modern state of Puebla (Berdan and Rieff Anawalt 1992) (see Fig. 3.7).

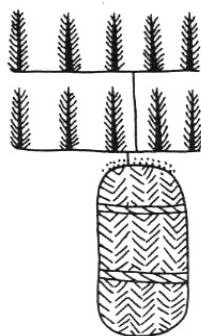


Fig. 3.7. Depiction of 4,000 loads of lime in the Mendoza codex.
Each of the branches represents 400 units.

Characterisation of archaeological lime plasters and experimental work

Several studies of lime plaster analysis have been carried out, many of which are summarised in reviews (Hughes and Válek 2003, Elsen 2006). There are also standard procedures for the analysis

of lime plasters (ASTM 2004, BSI 1997), although they are designed for industrial purposes and not always suitable for the analysis of archaeological materials.

Hansen (2005) summarises the main characteristics of Maya lime plasters and Maya lime production. He points out the importance of relating archaeological evidence (contextual information), ethnographic studies and ethnohistoric accounts to the information derived from the material analyses of Maya archaeological plasters. He also recognises the difficulties for recovering archaeological information relating to burning and slaking practices but believes that crystal fabrics observed in high magnifications may shed some light in this respect.

The first studies of Mesoamerican lime plasters were carried out by Littman (1957, 1958, 1959, 1959b, 1960, 1960b, 1962, 1966, 1967, 1979), after which little interest in this material was shown in Mesoamerican archaeology. Littman was the first to document the most relevant features of Maya lime plasters, such as the use of calcareous aggregates, wash coats, and the colours of paint layers. However, Littman employs confusing terminology as in the case of the term “lime-aggregate” to refer to a specific type of plaster (Littman 1957: 136, 1959:265).

Littman’s methods for measuring insoluble content also seems inadequate at present, since dissolution with hydrochloric acid equally dissolves the lime matrix and the calcareous aggregates that are characteristic of Maya plasters, giving erroneous figures for the estimation of the aggregates/binder ratio. However, as Elsen (2006) notes, the use of wet chemistry methods in the initial stages of the characterisation of historic and archaeological plasters was a common practice that was later replaced by microscopic studies often combined with X-ray diffraction. Nevertheless, wet chemistry is still used today for measuring soluble silica contents, which are indicative of hydraulic phases (Middendorf and Knöfel 1998).

There has been some interest from Maya archaeologists in having lime plasters analysed by specialists. David Pendergast commissioned a private consultant to study building materials from Belize and Quintana Roo (Brown 1986a, 1986b, 1986d and 1986e). The studies carried out included mechanical tests, absorption measurements and phenolphthalein dyeing to observe uncarbonated lime. Brown (1986c) also proposed a methodology for the analysis of archaeological building materials.

More recent studies of lime plaster analysis have been carried out at the site of Nakbé in the Guatemalan Petén. Hansen (1994, 2002) and Hansen and colleagues (1997) document an evolution in lime plaster floors at this site from the Middle Preclassic to the Classic period; they consider that this technical evolution was propelled by economic development (Hansen 2000:86). Hansen (1994) notes a drastic increase in the thickness and the quality of plasters throughout the Late Preclassic period, when massive architecture was built in this area. However, he notes that after 100 BC the

quality and quantity of plasters falls sharply, probably due to difficulties in accessing raw materials and firewood, or the logistics of managing the requisite labour force. Late Classic plasters from the same site, however, show considerable hardness, which Hansen and colleagues (1997:215) consider is due to the semi-hydraulic characteristics conferred by clays; however, the authors only report the presence of smectite, which is a non-reactive clay that does not result in the formation of hydraulic phases.

In the case of Uaxactún, Littman (1990) notes an improvement in the quality of the floors from Chicanel to Tepeu phases (Late Preclassic to Late Classic), and the substitution of rounded aggregates to man-made angular aggregates, which he attributes to changes in economic conditions.

Villegas and colleagues (1995) in their study of Late Classic plasters from Palenque, Mexico, report that the technical evolution shows an increase in the aggregate/binder ratio. They also describe an improvement in mixing, the reduction in the size of aggregates, and the addition of siliceous aggregates. The authors attribute the reduction of aggregate size to the improvement of grinding methods, although they relied on secondary electron images at high magnifications, which may have prevented them from observing larger aggregates.

Another technological sequence in Mesoamerican lime plaster production was carried out by Magaloni and colleagues (1992) at Teotihuacan. The authors describe a decrease in the aggregate/binder ratio, which they considered as an improvement in technique. Based on the properties of the material, they consider that it is possible to identify five technical periods in the plasters.

Goodall and colleagues (2007) carried out Raman spectroscopy analyses and optical microscopy observations of lime plasters from Copan, Honduras. They documented phases of incomplete carbonation (CaO and Ca(OH)_2), as well as a decrease in layer thickness through time.

X-ray diffraction has also been used to characterise mineral phases of lime plasters and associated materials. García-Solís and colleagues (2006) analysed lime plaster and fills of the substructure IIc-1 from Calakmul, as well as raw materials and soils. The predominant phase proved to be calcium carbonate in all samples, which masked other mineral phases. After the removal of CaCO_3 , with hydrochloric acid, quartz, illite, aragonite and cristobalite were identified in the plasters. In the case of limestones from local quarries, the authors also identified quartz and montmorillonite clays. In the filling material of the structure, feldspars were also identified, which according to them were minerals related to the presence of volcanic ash deposits that have been detected in cores of seasonally inundated swamps at Calakmul (Gunn et al 2002).

Another line of research concerns the characterisation of organic additives in plasters and binders in paint layers. Magaloni and colleagues (1995) identified high levels of glutamic and

aspartic acids in Maya mortars from 16 different sites, which they believe show the presence of an organic additive in the lime mixtures, employed in order to improve mechanical properties. A later study by Magaloni (1998) identified specific monosaccharides and aminoacids with gas chromatography/ mass spectrometry and high performance liquid chromatography (HPLC). Based on this, Magaloni considers that the organic substances in the Bonampak paint layers are a mixture of orchid bulbs and *holol* bark extracts. However, it is important to note that organic substances degrade through time, which results in changes of the chromatography spectra. The difficulties in characterising organic additives in Maya archaeological plasters have also been noted by Hansen (2005). In a similar line of research, Benavides (2006) has tested the workability properties of lime plasters when mixed with extracts from *chacah*, *jabin* and *holol* trees and complement in this way Landa's ethnohistoric accounts on the use of these additives (Tozzer 1966: 176)

Another attempt to characterise organic substances was made by Hansen and colleagues (1995). An organic substance forming part of cream-colour layers of plasters from Nakbé showed similar infrared spectra to those of the *relbunium* plant. However, Hansen and colleagues are explicitly aware of the complexity involved in the characterisation of organic compounds, as well as the likely alteration suffered by these compounds through time. A cream-coloured layer was also observed in the frieze inside substructure II-cI of Calakmul, also from the Preclassic period. When analysed by X-ray diffraction, the paint layer showed no pattern other than the calcium carbonate of the lime plaster, which may support Hansen's hypothesis about the use of an organic dye (García-Solís et al 2006).

There are no clear reports of hydraulic plasters in the Maya area. It is worth noting, however, that the description of the term "lime-aggregate" by Littman (1957, 1959) and Roys (1934) as "monolithic" lime mixtures that were poured into shells of facing stones in Postclassic architecture of the northern lowlands does suggest the existence of hydraulic mixtures. Although no recent studies have been done on this, the descriptions suggest the use of a hydraulic material since non-hydraulic limes usually show high shrinkage during setting that do not allow them to be poured in large volumes, although some application techniques, such as repeated tamping, can reduce shrinkage. The description that these "lime aggregates" are rich in silicon (Littman 1957) may also support the presence of hydraulic plasters.

Barba and colleagues (2006) studied lime plasters from Teotihuacan in Central Mexico. According to the authors, volcanic glass was detected as an aggregate and analysed by microscopic techniques and ICP-MS laser ablation although, surprisingly, the authors state that the plasters have no hydraulic properties.

Barba and colleagues (in press) studied the provenance of the limestone employed in lime production for the manufacture of Teotihuacan plasters, since the geology of the Teotihuacan valley is volcanic and the nearest limestone source is 60 km away. They employed laser ablation inductively coupled plasma mass spectrometry (LA-ICP-MS) to measure trace and rare elements in the lime lumps and compare them against samples from three possible quarries, and concluded that lime was produced with limestone from Tula, Hidalgo.

Radiocarbon dating of lime plaster was first attempted in the 1960s and improvements of the technique are summarised by Hale and colleagues (2003). Some examples include Folk and Balastro (1976), Cherf (1984) and Heinemeir and colleagues (1997). The principle of radiocarbon dating of lime plasters is based on the dissolution of the lime matrix by acidic solutions, which liberates the carbon dioxide that was incorporated during the carbonation of the plasters, therefore constituting a datable event. Dating of Mesoamerican plasters with this technique include Murakami and colleagues (2006) at Teotihuacan, and Mathews (2001) in the Yalahau Region, Northern Quintana Roo. The latter study made use of Accelerator Mass Spectrometry (AMS) to date the lime matrix of plasters and charcoal inclusions in the Northern Maya area. However it is worth saying that dating Maya plasters with this technique is highly problematic. This is because, as in any plaster, it is possible to have lime binder that was not fully calcined and consequently that contains CO₂ from the time of the rock formation; which results in a much older dating. In a similar way, the carbonation process often takes decades to complete in full, which results in the incorporation of more recent CO₂. However, a more important problem is that Maya plasters have calcareous aggregates that are dissolved in acids, which liberates CO₂ dating from geological times rather than from the anthropogenic event. Moreover, the mechanical separation of the calcareous aggregates is virtually impossible, given that sascab, the widely used calcareous sediment in the Maya area, has a silt and clay-size particle fraction (Littman 1958).

Archaeomagnetism is another innovative dating technique for lime plasters that has been attempted in Classic and Postclassic materials from Teotihuacan and Tenochtitlan (Hueda-Tanabe et al 2004). With this technique, iron-rich particles, in this case volcanic scoria employed as aggregates, are analysed for remanent magnetism, assuming that such particles would align themselves with the earth's magnetic field during the setting process of the plasters. However, experimental work is perhaps required to prove that directional changes of magnetic particles do occur during the setting of lime plasters in order to demonstrate that this technique is reliable.

Another interesting field of research in Mesoamerican archaeology has been the analysis of chemical signatures in floors. Although not related to lime plaster technology, this research has generated interesting patterns of data to interpret ancient household activities based on

concentrations of organic substances, phosphorous, iron and other metallic ions present in lime plaster floors (Barba and Manzanilla 1987, Barba et al 1996, Terry et al 2004).

A different field of research regards the study and preparation of high-quality plasters for conservation and other purposes. The study of consolidants for lime plaster materials has gained importance in recent years, not only in Mesoamerican archaeology, but in many other areas of the world. Baglioni and Giorgi (2006) have tested, with good results, the consolidation effect of Maya wall paintings from Calakmul using nanoparticles of calcium hydroxide dispersed in alcohol. There are also many aspects of the technology of lime that are still not fully understood. Researchers have experimented with slaking, and have described the benefits of long slaking in the resulting calcite crystals (Cazalla et al 2000, Navarro et al 1998). The study of lime carbonation has proved to be an important and complex field of research and the kinetics of the reactions involved in this process has been studied by Van Balen and Van Gemert (1994), and Van Balen (2005).

Outside the Maya area, there is substantial published research on characterizations of lime plasters. The review of this literature is therefore beyond the scope of my thesis but a good compilation of research can be found in Hughes and Valek (2003).

Cultural, economic and environmental implications of the use of lime in Maya culture

Lime was extensively used in Maya architecture and the implications for this ancient industry need to be explored beyond the mere description of lime-based materials found in the archaeological record. Labour and material requirements, as well as the cultural significance of this material need to be understood within the specific social, economic and environmental contexts of ancient Maya societies.

Subsistence

In addition to the extensive use of lime in architectural plasters, lime was also used for maize processing and played an important role in subsistence across ancient Mesoamerica. Maize is still a staple crop in indigenous communities throughout Mexico and Central America. The process of soaking the maize in limewater is still extensively used and it is known by the Náhuatl word *nixtamal*. By soaking the maize in limewater, the grain softens and the pericarp can be removed. The nutritional properties of the grain are also considerably improved by the increase of calcium, lysine and tryptophan contents. Although similar nutritional benefits can be obtained by soaking the maize in vegetable ashes, the increase in calcium is not present (Katz 1974, Bressanni et al 1990, Wright 1999: 206). Many authors have stressed the role of lime or alkali-processed maize as an important feature for Maya subsistence, because populations would have suffered from widespread

pellagra, an illness caused by vitamin deficiency. Coe (2005:13) has gone so far as to state that no settled life in Mesoamerica would have been possible without the use of lime for maize processing.

Lime may also have been critical for the storage of water, which was a central aspect of subsistence in the Maya area, especially in the Northern Lowlands, where surface water was not available and where the dry season can last up to six months. The Maya of the northern lowlands built many *chultunoob'*, which are cisterns carved in the limestone that are usually associated with water collection surfaces, such as plazas, roofs and platform surfaces. The *chultunoob'* were usually lined on their inner surfaces with lime plasters (Matheny 1982). However, no studies have been carried out regarding the specific properties of such plasters on the manufacturing techniques that would render them waterproof and consequently more suitable for water storage and collection. The scarcity of water may have been so acute in the Northern Lowlands that Adams (1991) believes that elite classes may have managed this resource as an instrument of social control through the construction and use of these cisterns. Cisterns internally lined with lime plaster were widespread in antiquity, as in the case of Minoan Crete during the Bronze Age (Cadogan 2007). This internal lining was necessary to provide adequate storage of water. In the Maya case, the high porosity of the limestone in the northern lowlands resulted in rapid absorption of the liquid.

Another aspect related to subsistence is the increase of the quality of life when lime is employed in domestic architecture. The use of lime plaster floors, for instance, may have been more hygienic than tamped earthen surfaces. Lime plasters must have played also an important role in providing protection to the walls in the tropical environment (Abrams 1994:34). It is known, for instance, that limewashed earthen architecture, which is the traditional Maya house, lasts about 15 to 25 years if whitewashed with lime, in comparison to 3 to 7 years if it does not have a limewash (Bryant et al 1988).

Economic and social implications

Given that raw materials for lime production were widely available in the Maya Lowlands, lime was employed by all social strata for different building purposes. However, the extent of lime consumption for architecture varied considerably according to social strata. In non-elite architecture, for instance, only a limewash was applied over the wattle and daub structure, whereas the use of lime in masonry lime-based architecture of public structures and elite residences was considerably higher.

The high energy investment of lime production and its consequent association with a higher social and political status has been noted by Abrams (1994: 32) and Abrams and Freter (1996: 427). However, most of the literature on Maya archaeology does not specifically relate social status with

the use of lime plasters but instead with monumental architecture in general and the presence of elite household assemblages.

There have been interesting theoretical works on energy investment in architecture and its social and economic implications, where labour invested in the procurement and transformation of materials reflect the social status of the individuals in command of the works (White 1949, Adams 1975, Trigger 1990). There are also studies on Maya architecture, in which energy investments are calculated in terms of person-days, although they do not deal specifically with lime and lime plaster production (Erasmus 1986, Abrams 1987, 1989, 1998, 1994, Abrams and Boland 1999, Carelli 2004, Cheek 1986, Webster and Kirker 1995).

Abrams (1994: 74) briefly mentions that lime is one of the most energy-intensive materials in Maya architecture, although he does not describe Maya lime production in detail. Despite this assertion, Abrams (1994:44) considers that the time required for lime plastering is not significant, since one man can plaster 80 m² in one day; however, this is an underestimation as can be seen in the description of modern practices of lime rendering (see Sykes 1985:32). In any case, it is clear that masonry lime-based architecture is much more labour-intensive than traditional Maya wattle and daub architecture (Redfield and Villa 1934).

As mentioned above, Maya masonry architecture, which necessarily requires the use of lime plasters, has been associated with upper social and political strata, but its connection with power and lineages is also sometimes straightforward. Many authors have established this clear relationship by claiming that changes in rulers usually had an impact on building activities (Demarest et al 2004: 566). In the case of Copán, it is clear that masonry architecture began just at the time of Copan's dynastic foundation in the Early Classic Period. This type of architecture renewed and expanded earlier earthen architecture in the initial royal centre, and a masonry architecture tradition gradually replaced the tradition of earthen architecture (Sharer et al 1999 cited in Sharer 2002). It is therefore clear that the institution of divine kingship required powerful symbols, and monumental architecture was one of the most important ones. This is also supported by the fact that many public buildings have inscriptions which record the names of the rulers that ordered their construction, as well as the participation of these rulers in the dedication rituals of the structures (See Martin and Grube 2000).

Other authors have claimed that increasing demands for public masonry architecture and monuments as a result of increased rituality, coordinated by the political and religious elites, must have had an important labour component in the Classic period (Demarest et al 2004:567), and thus, demands on labour were high. Russell and Dahlin (2007) and Russell (2008) consider that at least 215 persons would have been needed to work full-time throughout the year to meet the lime

requirements of the ancient site of Mayapán, although these estimates are considered conservative because they are based on modern burns which make use of metal tools and modern means of transportation. In contrast, Abrams (1987) claims that public architecture and its demand for materials created little if any stress during the Late Classic. It is worth saying in this respect that even if high demands of labour were required for the supply of materials and building activities, this was available during the dry season, which was a period when agricultural activities required little labour and during which ruling elites benefited from the non-elite population through the use of *corvée* labour (Sharer 2007: 85, Erasmus 1965).

Environmental implications

There are few studies of firewood requirements for lime production with traditional Maya burning techniques, and data are both ambiguous and conflicting. This has generated different attitudes about the role of lime production in ancient deforestation.

Morris and colleagues (1931:225) first described the amount of wood required for lime burning, stating that 200 loads or *cargas* (8000-8400 kg) of lime are yielded by a standard 2 m high calera that contains 11.9 cords of wood (ca. 43 m³). It is not clear however, whether the reported “lime” is quicklime or slaked lime, and it is also difficult to obtain ratios of firewood/lime since volume and weight are not comparable when specific weights of materials are unknown. In any case, as Schreiner (2002:66) analyses, there is an overestimation of the lime yield in Morris’ calculations.



Fig. 3.8. Left: Calera construction in the early 20th at Chichén Itzá. Right: After the burn the lime is left to slake in the open air. Pictures: Morris and colleagues (1931).



Fig. 3.9. Lime burning at Chan Kom. Picutre: Refield and Villa (1934).

Based on Morris' calculations and despite the picture of a *calera* construction shown in their book (see Fig. 3.8), Abrams (1988) considers that 11 m³ of wood are required to produce 10 m³ of lime. Making use of these data, Abrams estimates that 0.13 ha of forest would have been annually cleared for construction activities of Classic Copan, which he considers negligible. A drastically different quantity is reported by Bradley and Dahlin (2007), who consider that around 400 ha of forest would have been annually cleared in the case of Mayapán.

The ethnographic observations and experimental burns with Maya caleras carried out by Schreiner (2002) established a new methodology, in which ratios of firewood/lime are obtained by weighing the wood and measuring its moisture content, adjusting the firewood weight to 0% humidity in order to compare different wood species, and the reported lime is always quicklime. The average efficiency of Maya lime caleras reported by Schreiner is 5:1 wood:lime w/w; that is, nearly 5 times less fuel-efficient than Abrams' estimations. This fuel efficiency is considerably lower than the enclosed ovens introduced by the Spaniards in the 16th century.

Despite the problems for the estimation of firewood consumption, many authors believe that lime production may have caused considerable deforestation, contributing to the collapse of the centres of the Central Lowlands at the end of the Late Classic (Henderson 1997, MacKinnon and May 1990, Shaw 2003).

It is worth saying, however, that regardless of the firewood requirements for lime production, Maya architecture varied highly through time and across the different areas and architectural traditions, and therefore lime requirements also varied. The firewood requirements for the massive thick-plastered Preclassic architecture of the Mirador Basin, for instance, cannot be compared to the demands imposed by the smaller architecture of most of the Northern Lowlands in later periods, where carved stone prevailed over plastered surfaces.

It is also worth saying that even if traditional Maya lime production has a low thermal efficiency when compared to enclosed ovens, this does not mean it is not a good technological option. It may have been more suitable not to depend upon permanent structures for lime burning, especially considering the large amounts of wood that needed to be transported and the lack of wheeled transport in Prehispanic times.

Symbolism and cultural aspects

It is also known that traditional Maya lime production is a ritually-laden technology that is only performed by men. Schreiner (2002: 104-116) describes Maya lime production as associated with rebirth, transformation and fertility, attributes that are also described in ethnohistoric descriptions of the 17th century (Ruiz de Alarcon 1629).

Schreiner (2002:104) describes that lime is perceived as a young woman born from the fire, although women are banned from participating in the burn. The fertility symbolism permeates all aspects of lime production, and pyres of firewood are even conceived as wombs (Schreiner 2002). Russell and Dahlin (2007) describe ritual offerings consisting of chili, rock salt, cobs and other materials, that are placed towards the four cardinal directions before the ignition of the pyres.

It is possible that the symbolism of rebirth and fertility associated with lime is related to re-plastering applications. There is widespread evidence of ritual activity regarding dedication and termination rituals in both public and residential Maya architecture, (Garber et al 1998, Tozzer 1966), which often involved new constructive phases and re-plastering. There is also considerable evidence that the ancient Maya perceived the buildings as animated structures that go through stages of life (Garber et al 1998, Houston 1998). Replastering events carried out as part of dedication rituals may also represent an attempt to revitalise the buildings, which correlates well with the rebirth and fertility symbolism of lime in Maya culture.

Another important cultural aspect, as mentioned above, was the use of lime for maize processing, which is an important feature for the subsistence of Mesoamerican populations. It is likely that the fertility symbolism associated with lime perhaps originated from the association of this material with maize, since fertility and rebirth connotations have always been associated with maize and agricultural practices.

As mentioned above, the construction of lime plaster floors is described in the Popol Vuh in the foundation of Chi Izmachi, the capital of the Quichés. According to Recinos (1957, cited in Anderson 2003:262) the foundation of this citadel was the beginning of the *ajawarem* or lordship of the Quichés. In this sense, the mention of lime plaster may be associated with settlement, power and establishment, and stands in clear opposition to domestic wattle and daub earthen architecture. It is

3. Use and Production of Lime in the Maya Area

likely therefore, that the authors of the Popol Vuh associated lime-based masonry architecture with the origin of the Quiché lineages.

4. The Cultural Practices of Architectural Technology

This chapter describes the theoretical framework that informed my research questions and helped to structure my approach to the collection and interpretation of the data. My intent is to make explicit the assumptions underpinning my descriptions, interpretation and analysis of the data.

The central aspect of my research is the study of the technology of architectural plasters and the significance of technological variation. Continuity and change in the technology of architectural practices, however, occur in a wider socio-cultural context. With regard to ancient cultures, explaining change and continuity has been a long-standing problem in archaeology that has resulted in debates about the nature of traditions, inventions, influences or the rejection of practices formally followed. Therefore in this chapter I explain the frameworks I have used to contextualise the forces of change and continuity in technological and architectural practices.

Technological studies of artefacts have been part of mainstream archaeology since the very beginning of the discipline. The use of sophisticated analytical techniques has resulted in rich quantitative databases of all kinds of artefacts from all over the world. Equally important has been the development of theoretical approaches, mainly from the 1980s onwards, which have aimed to contribute an anthropological perspective. Whereas early studies emphasised material aspects of artefacts, such as functionality and performance characteristics, more recent studies have emphasised the importance of the broader cultural context, including the social, economic and ideological realms, and have put humans and human agency back in the centre of discussion.

There are a number of valid arguments and ideas in the different theoretical strands which are not contradictory but complementary. I consider that making use of arguments and ideas taken from different theoretical perspectives for specific problems is a valid and sensible approach. Therefore I draw from different schools of thought for the interpretation of results.

Chaîne Opératoire

An important framework for understanding technology is the *chaîne opératoire*, an approach developed by André Leroi-Gourhan (1964). Although Leroi-Gourhan's ideas were originally developed for the study of reductive technologies, especially stone knapping, this approach constitutes a central and widely accepted aspect of the anthropology of technology that aims to identify the different stages that are carried out throughout the sequence of artefact production. By hypothetically reconstructing a sequence of production, often with experimental work, archaeologists consider the selection, transportation and modification of raw materials for the production of a finished object. Although this notion can seem obvious, technological studies that do not attempt to reconstruct the *chaîne opératoire* risk ignoring the production processes and thus

the social aspects behind them, something that has frequently happened in technological studies of Mesoamerican plasters. How raw materials were exploited and transported, how they were transformed and manufactured and how production was organised constitute essential aspects of technological studies. It is worth noting, however, that there is very limited archaeological evidence for the ancient production of Maya lime plasters, and this constitutes a challenge for the reconstruction of the *chaîne opératoire* and the understanding of this technology. However, my research draws examples from ethnographic and ethnohistoric sources in an attempt to understand the sequence of production, as well as from general material aspects involved in lime technology as reported in other cultural areas.

Lime production requires a specific sequence in which materials are collected, prepared and put together. Broadly speaking, as described in Chapter 3, lime plaster technology requires the collection of calcareous materials that are later calcined to obtain quicklime. The quicklime is in turn slaked with water and mixed with aggregate materials to produce plasters. Once the plasters are mixed, they are applied over architectural surfaces using a variety of manufacturing techniques. Despite this apparent simplicity, some of the steps can be carried out in a different order or sequence, demonstrating that lime production is a complex industry. Furthermore, each of the steps in the sequence can be affected by a variety of technological choices. A schematic representation of the *chaîne opératoire* of lime plaster production with particular reference to the Maya area can be seen in Fig. 4.1.

Awareness of the possible steps involved in the sequence of plaster production helped to structure my research during the collection and interpretation of the data and also influenced my selection of analytical techniques. An example of how the *chaîne opératoire* can enhance sensitivity to the implication of technological choices is the recycling of previous plasters as aggregate materials of new plasters, which constitutes a specific step in the cycle of a plaster and the manufacture of a new one (see fig. 4.1). The basis for such a choice may be taken as evidence of a specific symbolic, social or political agenda. By understanding the sequence of production, it is possible to know that previous plasters can be recycled either as aggregates by mixing them with the slaked lime, or as calcareous raw materials by burning them again to produce quicklime. The recycling of plasters as aggregate materials, for instance, can only be identified by means of petrography—which could be done in the case of Lamanai (see discussion p. 145) —, since a bulk compositional analysis would not identify the phenomenon. On the other hand, it is also important to know the chemistry of the lime cycle and the limitations of the available analytical techniques; the recycling of plasters as new raw materials for lime production, for instance, cannot be identified in the examination of plaster samples because the recycled plasters lose all morphological

characteristics during burning, and the resulting chemistry may also be indistinguishable from other calcareous raw materials.

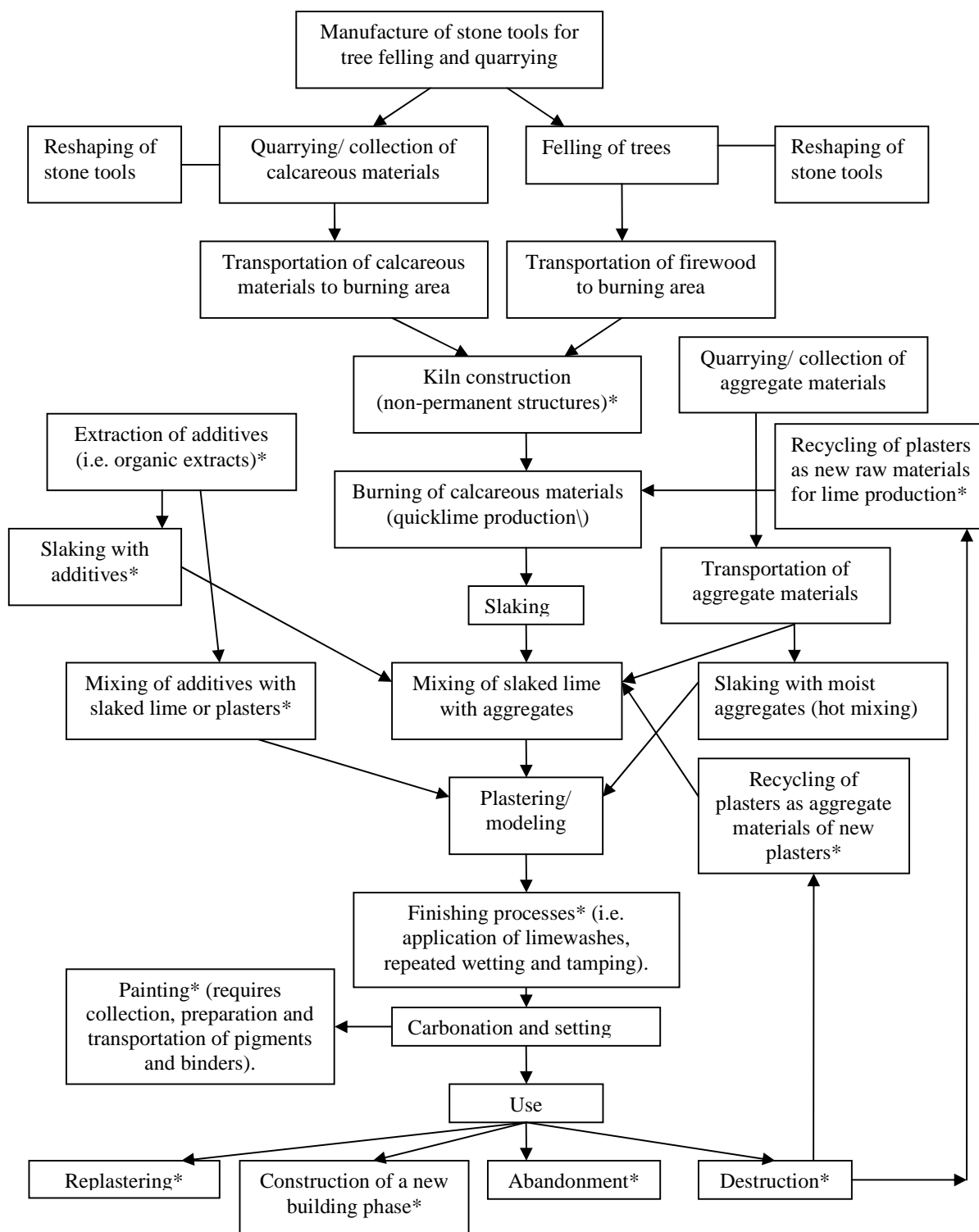


Fig. 4.1. Possible sequence or *chaîne opératoire* of lime plaster production with particular reference to the Maya area. (*) indicates optional processes.

One example of the sequence of plaster production that is often overlooked in Maya archaeology is the burning process, which is perhaps the result of the very few cases in which lime burning has been identified in the archaeological record. By looking at the sequence of lime plaster production, it is easy to see that this step is fundamental and very labour-intensive, since it requires felling large numbers of trees, transporting the firewood and constructing a kiln (in the case of non-permanent structures). Without the understanding of this particular step in the sequence of production the manufacture of plasters is severely underestimated. The notion of *chaîne opératoire* is therefore a critical step in understanding social and cultural practices behind the technology of plasters.

The framework of technological choices

My research also makes use of the approach of technological choices. This theoretical position recognises that individuals are capable of making choices during all stages of technological processes, including the procurement of raw materials and the manufacturing of objects (Lemonier 1993:4). A central aspect of this theoretical strand is the concept of agency, which is understood as the active and creative roles of individuals. Despite the fact that individuals' roles are often impossible to detect in the archaeological record, the analytical concept of individuals can still be applied. Agency can be understood as those innovations brought about by individuals in a particular group who adopt specific technological choices in a situation in which other choices could have been made (Sillar and Tite 2000:8). Material culture and technology are not passive results of humans adapting to the world around them, as evolutionary approaches suggest, but are activities in which humans are actively engaged. This does not mean that technological choices do not follow traditions but, rather, that traditions are actively followed and/or re-invented by individuals.

The technological traits that are reported and discussed throughout the thesis are interpreted as the choices of individuals acting within specific cultural, social and environmental contexts. This means that technological choices are not made in an abstract context, but rather, in a specific set of environmental settings with specific natural resources, which takes place under specific social and cultural conditions of which craftsmanship is a part. In this way, the economic, social, environmental and technological circumstances constitute a background which influences the decision-making during all steps of plaster production.

The concept of technological choices also emphasises the role of world views and social dynamics as important components of technology. In contrast to earlier approaches, it recognises the material and symbolic/ritual aspects of technology, and acknowledges the active role of individuals in technological events. This approach considers material culture as a central element of

social reproduction and engagement, and technology is examined and conceived beyond the material means of making artefacts. Therefore, material culture is considered to be meaningfully-constituted (Dobres 2000, Dobres and Hoffman 1994, Sillar and Tite 2000, Pfaffenberger 1988). In considering the social and symbolic implications, technology is consequently understood as a culturally-specific phenomenon.

Related to the roles of world views and social dynamics, as described in Chapter 3, there is valuable ethnographic research that sheds light on the social practices and ritual activities related to ancient Maya lime production. Moreover, there is strong cultural continuity between pre-conquest Maya societies and modern Maya communities, validating a direct historical approach that provides additional support for the understanding of this specific technology (Gould and Watson 1982).

An important notion discussed by Sillar and Tite (2000), also in the context of technological choices, is the way in which different industries and activities interact. An example applicable to my research is firing technology. Given their high demand on firewood, firing technologies cannot be understood without considering the competition of different pyrotechnologies, as well as woodland management and the broader social, environmental and economic context of which firewood is a part. As the authors state, firing methods depend on personal and group choices but are influenced by social, economic and environmental factors that go beyond the immediate production and use of artefacts.

A schematic representation of the different variables that influence decision-making in all stages of the sequence of production can be seen as follows:

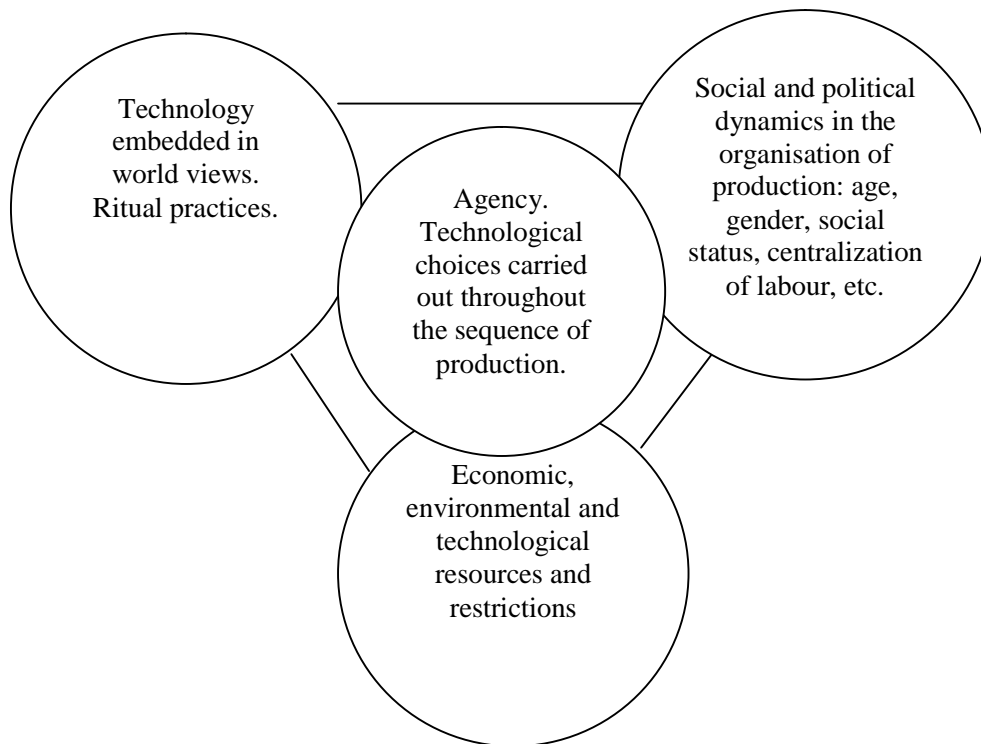


Fig. 4.2. Schematic representation of technological choices and the factors that influence decision-making throughout the sequence of production.

As mentioned above, individuals make choices in each of the steps of the sequence of production, and often these choices can be identified with specific techniques in the analysis of archaeological samples. One example is the collection or quarrying of aggregate materials and the way in which they are incorporated into the lime mixtures. Aggregates can be collected as natural sediments or they can be quarried. Destroyed fragments of previous plasters or quarrying waste can also be used as aggregates. Moist aggregates can also be mixed directly with the quicklime in order to slake it. All these different technological choices were available to the ancient Maya and each of them would have reflected the labour involved in the exploitation or collection of raw materials, as well as the specific workability and performance characteristics that each of the choices would produce in the plasters. In the same way, each of the technological choices leaves a specific characteristic in the plasters that may be detected by means of material analyses. Aggregates consisting of natural sediments, such as sascab, can be identified based on their rounded edges, whereas quarried material shows characteristic angular edges that can easily be seen under the petrographic microscope, and which was actually identified in the case of Lamanai (see discussion p. 138). There are also different types of raw materials that when mixed with the lime react in different ways, producing specific chemical and mechanical results in the plasters. Some of these raw materials have visual characteristics that can be recognised in the natural environment, and which, as a result

of human agency, were selected by the ancient Maya and other cultures to experiment with the lime mixtures (see Chapter 7 for discussion).

It was important for my research to consider all the different technological choices that were available to the ancient Maya for lime production, as well as the specific characteristics that particular choices would leave in the plasters. One example is the method of burning of calcareous materials. In the case of modern Maya lime production, for instance, the lime mixes with the ashes in the open kiln method. Due to the fact that the firewood most often employed, *chacah*, leaves no charcoal after burning, these types of limes are virtually charcoal-free. In this sense it is important to understand the possible methods of limestone burning, as well as the specific raw materials that the ancient Maya would have used; otherwise the analysis of the data would have resulted in misleading interpretations, such as the conclusion that due to the lack or virtual lack of fragments of charcoal observed in the samples analysed, the lime must have been produced in a structure which separated the lime from the firewood, such as some varieties of European enclosed ovens.

The social and political organisation of labour: Neo-Marxist approaches

Theoretical approaches that focus on the discussion of labour also find a place in the understanding of ancient Maya lime technology. As explained in Chapter 3, Mesoamerican lime production and lime plaster manufacturing were labour-intensive activities, and the exploitation, transportation and firing of raw materials resulted in high labour demands in societies without wheeled transport or the use of metal tools. Therefore, the labour required in this industry remains an important aspect to be considered.

As Ortiz (1994) observes, labour and production can generate or strengthen social relations, as well as reinforce power, prestige and status. The links between prestige and labour/production are important to explore in Maya material culture, in particular Maya monumental architecture, which was not only meaningfully constituted but sometimes clearly used by political and religious leaders as means for reaffirming power (Reese-Taylor and Koontz 2001). In Maya household architecture, as Carmean (1991) discusses, differential labour investments are directly related to the ability of some households to control the labour of others, and it is therefore a manifestation of the social and economic relationships of the individuals of a specific society. In Maya monumental architecture, this notion is even more important, and the number of people working for or obligated to elite groups or the state apparatus is much higher. The discussion of labour for the study of Maya monumental architecture is important due to the public character of this architecture, which necessarily requires centralised management and planning; changes in architectural practices therefore respond to changes in managerial conditions.

The selection of the three case studies of this research was stimulated by the notions of labour and production. My assumption was that social and political structures would have influenced plaster production. The case of Lamanai, for instance, has abundant evidence that shows that the site was not significantly affected by the socio-political collapse of the Terminal Classic period (Pendergast 1985b, Pendergast 1990, Graham 2004), which suggests that the political and economic organisation in which plaster production took place was different from other Maya sites. On the other hand, Calakmul was the largest site in the Maya area and one of the most powerful; the labour organisation required for the production of building materials in the case of such large-scale architectural programs was most probably centrally organised by the political elites.

It is important to mention that the archaeological samples analysed in my research were taken either from public ceremonial buildings or from elite residences. In this sense, the production of these plasters most probably took place in a public sphere and the examination of these plasters therefore sheds some light regarding the circumstances that were impacting the social and political elites, as well as the sites' public life. Future studies, however, could look at building materials from non-elite residences in order to assess household level production.

Other notions of neo-Marxist approaches with particular reference to the Maya area relate to the association of public buildings with the power and authorities of leaders (DeMarrais et al 2006), as well as the establishment of common cultural expressions (Kowalski 1999, Hansen 2000). The power represented by public buildings and the representation of cultural expression in architecture may have stimulated the continued use of specific architectural typologies, in particular the public monumental and ceremonial architecture which consisted almost invariably of lime-based masonry buildings, often with stucco sculpture, and which constituted a clear visual representation of social and political power in contrast to the smaller perishable non-elite domestic architecture. The cultural expressions associated with this type of architecture may have promoted the production of surfaces with a similar appearance to that of plastered surfaces in cases where lime technology was virtually abandoned, as in the case of limewashed mud plasters at Palenque during the Terminal Classic period (see discussion p. 108-111), or the use of white clays for rendering at sites without the necessary raw materials for lime production, as in the case of Kendal, Stann Creek district (Graham 1994).

Theoretical frameworks that emphasise power and social relations are highly relevant to the study of lime plaster production. The presence of monumental architecture and the significant numbers of masonry buildings that characterise the Classic period in the Maya area force us to ask how labour might have been organised under such conditions. A focus on the technology of plaster production itself, in fact, can be seen as a methodology that can address neo-Marxist questions.

4. The Cultural Practices of Architectural Technology

Although often the methods employed by archaeologists cannot get direct information about labour and production, focusing on the technology of plaster can yield indirect information on the social and political organisation of production and therefore on social relations of power. Although I do not deal directly with social relations of power, my research has discussed some aspects of production and has laid the ground for future studies to continue elucidating production and power relations.

In summary, three main ideas from interpretative archaeologies have informed my methodology: the *chaîne opératoire*, which highlights the stages of production; the framework of technological choices in which humans are seen as creative agents; and neo-Marxist approaches, in which labour and production are discussed in terms of social and power relations.

5. *Methodology*

My methodology is based on a range of analytical methods applied to the study of archaeological lime plasters. I made use of a variety of techniques, including microscopic and compositional methods of analysis, as explained below. In addition to the analytical work, a comprehensive literature review was carried out, as well as on-site observations of archaeological plasters.

In the literature review (Chapters 2 and 3) I examined previous studies of Maya lime plaster technology, including ethnographic and ethnohistoric descriptions of traditional Maya lime production, as well as experimental works. I also reviewed the reported examples of lime production in the archaeological record, as well as the epigraphic and literary sources that inform our knowledge of this ancient industry. I also described the three case studies and discussed general topics such as architectural programs and natural settings, in particular the geological resources available to the lime plaster industry. I also reviewed briefly the political history of the sites as recorded by inscriptions.

On-site observations aimed to describe the way in which lime plasters were used in Maya architecture, and to document the macroscopic characteristics of the plasters and the quantities in which these materials were used.

5.1. *Sampling criteria*

Chronology is a central aspect of this study, since well dated materials are necessary in order to provide adequate data for a diachronic study. In the case of Calakmul and Lamanai, sampling was carried out with the principal investigators of each of the sites, which provided a unique opportunity to achieve comprehensive, well dated sampling and to access unexcavated material that would not have been possible otherwise. Dating of the samples from Lamanai and Calakmul was based on the stratigraphic association of architectural features with diagnostic ceramic assemblages and/or radiocarbon dating of organic material. For this reason, plasters were dated to the broad periods of Mesoamerican chronology, each of which spans two to five centuries. In a few cases at Calakmul and Palenque, the dating was refined by long count dates from inscriptions of the buildings that have been converted to Gregorian dates, whereas in the case of Lamanai, direct radiocarbon dating complemented the dating based on ceramic typologies.

Palenque is a very different case regarding chronology. The main difference lies in architectural traditions, because most of the buildings of Palenque constitute a single construction episode. Another important difference is that the extant buildings in the core of Palenque probably

span only a little over 200 years during the Late/Terminal Classic periods (Rands 1974), owing to the fact that earlier buildings were razed, and the site was abandoned shortly after the architectural programs of the Late Classic period. Although epigraphy constitutes an important line of evidence for dating the buildings of Palenque, it is not infallible since later rulers may have added inscriptions and dates to earlier buildings. Likewise, dating with ceramic assemblages is generally too broad for the short time span of Palenque's architecture. Nonetheless, there is some literature on the chronology of Palenque that combines studies of architectural and stylistic attributes, epigraphic information and ceramic complexes, which allows an adequate discussion to date the architecture of the site (Robertson 1983a, 1983b, 1983c and 1983d, Tovalín Ahumada and López Bravo 2001, Tovalín Ahumada and Ceja Manrique 1993, Marken 2006, Martin and Grube 2000).

Uniformity in the sampled materials was a desirable factor and was aimed for in an attempt to account for variation in manufacturing techniques due to different functions of materials. Given their ubiquity, floors were favoured for sampling over wall renders and lime plaster sculpture. However, the presence of architectural remains proved to be very patchy and lime-based materials other than floors, such as wall renders, sculpture or joining mortars, were sampled when floors were missing for specific periods.

I also sought a balanced representation in my sampling in order to collect data that would inform us about technological characteristics of the different sites and periods; I tried therefore to collect equal numbers of samples for each period in all sites. In the case of Palenque, however, a higher number of samples from the Late and Terminal Classic were taken, as architecture from these periods only was available to sample. It is worth mentioning, however, that on-site observations at Palenque showed that there was a clear change in plaster manufacturing even within this short period of time. Palenque was chosen therefore to provide a shorter and more intensive diachronic case study.

Samples were taken with scalpels or with a hammer and chisel. Sizes clustered at around 2 cm long and samples were taken from edges or areas already damaged. It is worth mentioning that this was probably not the ideal method of sampling from a statistical point of view since the samples were perhaps not representative in some cases. However, this was the best it could be done in order to limit damage to the structures. A few samples consisted of collapsed material coming from known locations, as in the case of the plaster fragments from the frieze of Substructure IIc-1 of Calakmul. These samples were therefore bigger than the samples taken from buildings.

In addition to the sampling of archaeological plasters, some samples were taken from local raw materials, either from local calcareous deposits or from limestones of archaeological buildings. In the case of Palenque, I also analysed samples of snail shells from the river, since shells are

known to have been employed as raw materials for lime production, as explained in Chapter 3. The samples analysed, their chronology and location can be found in Table 5.1. Analyses carried out on each of the samples can be found in Table 5.2 at the end of this chapter.

5.2. Selection of analytical techniques and experimental procedures

Material analyses constitute the primary source of information of my research. Optical reflected-light microscopy (ORM), petrography, scanning electron microscopy and microprobe with energy dispersive spectrometry (SEM-EDS), X-ray fluorescence (XRF), Raman Spectrometry and X-ray diffraction (XRD) were selected as analytical techniques. The analytical techniques produced a variety of data on the nature and diagnostic features of lime plasters.

Optical reflected microscopy (ORM)

ORM aimed to document the microstratigraphic and micromorphological characteristics of plasters, especially coloured features such as paint and soot layers, complementing in this way the petrographic observations.

Microscopic observations were carried out with reflected light using a Leica DMLM polarising microscope at magnifications between 50X and 500X. Samples for optical microscopy were embedded in EpoThin® resin, cut and polished with carborundum (SiC) down to 5 µm (2500 grit).

Petrography

Petrography is one of the most important methods used in my research. It allows the identification of the different minerals that constitute the plasters, in addition to giving a clear observation of the micromorphological and microstratigraphic characteristics of the samples by documenting features not visible under reflected-light microscopy. Petrography is useful for allowing a clear observation of the different layers, including paint layers, limewashes and replastering events. It also allows the observation of the properties of the lime matrix, which was classified as hydraulic, non hydraulic, clayey and unburnt lime, as well as documenting pore characteristics and the presence of lime lumps, amorphous phases and alkali-silica gels. The technique was also useful for the characterisation of various materials and inclusions, such as fossils, secondary minerals, charcoal, plant remains and opaque minerals. The characteristics of aggregates, such as roundness, sphericity, sorting, size range and proportions against the binder were also documented with this technique. Minerals were identified by their characteristic optical properties under polarised light, including

pleochroism, birefringence, and twinning, which are specific of each mineral (Pichler and Schmitt-Riegraf 1997).

Petrography was also employed to characterise the colouring agents through the observation of size, shape and optical qualities of powder samples under transmitted polarised light (Eastaugh et al 2004)

Petrographic observations were made with a Leica CMLP transmitted-light microscope, under magnifications ranging between 40X and 630X. Photomicrographs of both reflected and transmitted light were taken with a digital Nikon-Coolpix camera attached to the microscope.

Samples for thin sectioning were vacuum-impregnated with EpoThin® resin and cut and polished with progressively finer carborundum (SiC). The samples were then ultrasound-cleaned and the polished sides were glued onto glass slides. Samples were then cut and ground until ca. 60 µm thick with a diamond saw and subsequently polished by hand using aluminum polishing powder (Al₂O₃) until 30 µm, as indicated by the birefringence of quartz. They were cleaned with an ultrasound bath and covered with glass slips using Canada balsam.

The preparation for pigment analysis consisted of scraping some powder from the paint layers onto glass slides. The samples were then covered with glass slips and fixed with MeltMount® resin. The resin has a refractive index of 1.662, which allows better observation of the pigment grains.

Microprobe and scanning electron microscopy with energy dispersive spectrometry (SEM-EDS)

Scanning electron microscopy (SEM) documented further micromorphological observations with higher magnifications, employing secondary electrons to observe relief, and backscattered electrons to observe compositional variation. It also yielded semi-quantitative elemental composition of the plasters by bombarding the area of interest with a beam of electrons, the resulting signal being detected by the energy dispersive detector (Pollard 2007:109). The latter characteristic allowed the analyses of the different components of the samples, discriminating between aggregates and binders.

The microprobe was a thin-film window Jeol superprobe JXA-8600 with energy-dispersive spectrometry and Oxford Link analytical equipment. Acceleration voltage was 15 and 20 kv with a working distance of 10 mm, and data were processed with INCA software. Elements were combined with oxygen by stoichiometry and carbon was excluded in the analyses, since samples were carbon-coated. Internal calibration was performed with cobalt. Microprobe analysis was used for the analysis of specific inclusions in the thin sections, the mineralogy of which could not be determined by means of petrography. In order to analyse the thin

sections, the glass cover slips were removed and the samples were polished with 1 μm diamond paste and ultrasound-cleaned before the analysis.

The SEM was a thin-film window Hitachi S-570 with Link Analytical Equipment. Photomicrographs of both secondary and backscattered electron modes were captured in magnifications between 50X and 1500X with an accelerating voltage of 20 kv. SEM was used with polished blocks or thin sections for imaging and compositional purposes. For the purpose of the study of crystal habits, samples were analysed without polishing, and images were taken with the secondary electron mode to observe relief.

Raman spectroscopy

Raman Spectroscopy, in contrast to the compositional information given by SEM and XRF, yields information about the molecules, reporting the compounds that constitute the materials. This technique was used specifically for the characterisation of the pigments of painted plasters.

Raman spectroscopy consists on the interaction between the incident radiation and the vibrational frequencies of the material that is analysed. The difference in wavelength between the incident radiation and the scattered radiation (inelastic) is characteristic of the material (Pollard 2007:83).

The equipment used was a Renishaw Raman spectrometer, and was operated with a wavelength of 875 nm. No sample preparation was required, and owing to the non-destructive nature of the analysis, samples analysed by Raman spectroscopy were subjected to other analyses.

X- Ray Diffraction (XRD)

X-ray diffraction (XRD) is a complementary technique to petrography and XRF. The technique was employed to characterise the mineralogy of pigments, local geological materials and bulk composition of archaeological plasters.

The technique consists of the irradiation of samples with X rays. Because each crystalline solid has a specific distance between crystal lattices, X rays are diffracted through specific angles depending on the minerals that are present in the sample. The identification of minerals is based on Bragg's law, which relates wavelength of the incident beam, distance between the crystal lattices and the angle of diffraction (Pollard 2007: 113).

XRD analyses were performed at the Daresbury Laboratory with a synchrotron radiation source and a wavelength of 0.87 \AA (8.7×10^{-2} nm). Sample preparation required only powdered samples to be mounted on self-adhesive tape in order to irradiate the samples with the X-ray beam.

Additional samples were analysed at the Ingold Laboratories of UCL in an attempt to identify more crystalline phases after acid dissolution of the samples, since the calcareous nature of the plasters resulted in strong peaks of calcite that masked other minerals. XRD analyses carried out at the Ingold laboratories made use of a Bruker-Axs D8 (GADDS) diffractometer with a Cu X-ray source (1.54056 Å) in an area of analysis around 3-4 mm². Analyses were done directly on flat surfaces of compressed powders and polished blocks.

Diffraction patterns were transformed into spectra of 2θ values vs. intensity and the strongest peaks in the spectra were compared with the peaks of suspected minerals reported in Crystalweb 2005 and ICDD mineral databases.

X-Ray fluorescence (XRF)

X-ray fluorescence aimed to obtain a more reliable bulk quantitative elemental analysis with lower detection limits than the SEM. In this way, XRF allowed the detection of major, minor and trace elements, and therefore documented the compositional variation of archaeological plasters of different periods and geological materials, which yielded information regarding the selection of raw materials for plaster manufacture.

The XRF technique uses X rays to irradiate the samples, which creates vacancies in the inner shells of atoms. These vacancies later de-excite and release X rays, which are characteristic of the elements that are present in the sample (Pollard 2007:101).

XRF analyses were carried with a wavelength-dispersive Spectro X-lab 2000. The elements detected were reported as oxides by stoichiometry. Samples for X-ray fluorescence were ground down to fine powders using an agate planetary ball mill. They were then oven-dried for 24 hours at 100° C and later mixed with analytical wax at a ratio 0.1125:1 wax/sample (wt/wt) and prepared as pressed pellets with a hydraulic press.

Reference materials (British Chemical Standards) were analysed together with the samples in order to evaluate the quality of the compositional data in terms of accuracy. Accuracy is a measure of how close the measurements are to the real values. Precision was also measured by carrying out three measurements of each of the samples and looking at this variation, since precision is a dispersion measurement between replicate measurements of the same sample (Pollard 2007:313).

The elements selected to be reported are: Mg, Al, Si, Ca because they constitute the major elements of the samples; Na, Mn, Fe, Sr, K and Rb for having significance in carbonate sedimentation; and Ni, Co, Zn and Cu, which were selected for containing palaeo-environmental

information (De-Vito et al 2004) and are therefore related to sources of raw materials. Ti, Co, Zr and Ba were selected since they co-vary with some of the elements.

All elements are reported as oxides combined by stoichiometry as given by the XRF spectrometer, except in the case of Ca and Mg and Ba, which were transformed from oxides to carbonates using stoichiometric calculations. This was carried out in order to account for the loss on ignition (CO₂) that is not reported by the equipment. By converting CaO, MgO and BaO into carbonates, the sum of concentration was increased, after which all elements were normalised to 100%. It is worth noting, however, that X-ray fluorescence is an elemental technique that reports the analysed elements in a standard way; therefore the elements may not be physically present in the way they are reported. However, a more detailed analysis of the loss on ignition and the different phases present in the samples, such as uncarbonated lime and hydraulic phases, could be obtained in the future with Thermal Analysis (see Ellis 1999).

Statistical analyses

Statistical analyses were employed to process the XRF data through classification and data reduction techniques (cluster analyses and principal component analyses) in order to examine whether groups of samples with similar chemistries could be related to archaeologically significant groups such as provenance (sites), type of samples (floors, wall renders, etc) and diachronic variation (chronological periods).

Cluster analysis and principal component analysis (PCA) were carried out as complementary methods, since the former is a classificatory analysis and is based on the similarities and distances between the different samples, whereas the latter reduces the variables to two or more uncorrelated variables (Shennan 1997:267). Cluster analysis yields a dendrogram with the visual representation of the samples in each of the groups. Principal component analysis (PCA), on the other hand, gives information about the relationship between units (samples) and variables and indicates which variables are involved in the trends, which can be plotted to produce a graphic representation (Shennan 1997:197).

Cluster analyses were carried out as hierarchical clusterings with agglomerative schedule using Ward's method and squared Euclidian distance. Variables were standardised to Z scores in order to give them equal weight regardless of their scale. The selected elements for the analyses were MgCO₃, Al₂O₃, SiO₂, CaCO₃, TiO₂, Fe₂O₃, NiO, Rb₂O, SrO. Co-varying variables were not selected since this method examines similarities between values and their selection would have obscured the patterns (Shennan 1997:265). Totals were normalised to 100% before carrying out the analysis. Dendrograms were obtained as a graphical representation of Cluster Analyses and are

shown in appendix A.6.3. Four dendrograms are presented, one with the data from all three sites, and three with the data of each of the case studies.

PCA analyses were carried out through the method of principal components, using a correlation matrix. After the reduction of the data, scatter plots were obtained with the two principal components in order to have a visual representation of the similarity of the samples and how samples cluster according to their chemistry. Given that the obtained factors are uncorrelated and therefore there is no risk that co-related variables would obscure the patterns, more elements were included in the analysis. The elements selected for the analysis were Na₂O, MgO, Al₂O₃, SiO₂, K₂O, CaCO₃, TiO₂, MnO, Fe₂O₃, NiO, CuO, ZnO, Rb₂O, SrO, ZrO₂ and BaO. Scatter plots of PCA analysis can be found in appendix A.6.4.

Inventory of samples analysed:

| Sample | Type | Period and source of dating | Dates | Structure | Observations |
|--------|----------------|--|--------------|------------------------------|---|
| Pa4 | Joining mortar | Cascada Phase (Marken 2006) | AD 500-620 | Temple XV | Filling material of the platform |
| Pa6 | Wall render | Otulum phase (Marken 2006) | AD 620/700 | Temple of the Count | Render from the ceiling of the Temple of the Conde (collapsed material) |
| Pa49 | Wall render | Otulum phase (Marken 2006) | AD 620/700 | Temple of the Count | West room, north wall. |
| Pa50 | Floor | Otulum phase (Marken 2006) | AD 620/700 | Temple of the Count | West room, south side. Upper layer. |
| Pa77 | Wall render | K'inich Janaab' Pakal I (Robertson 1983) | AD 615-683 | Palace, House K | Upper layer |
| Pa78 | Wall render | K'inich Janaab' Pakal I (Robertson 1983) | AD 615-683 | Palace, House K | Lower layer |
| Pa22 | Floor | K'inich Kan Balam II (Martin and Grube 2000) | AD 684-702 | Temple of the Sun | Interior. |
| Pa23 | Floor | K'inich Kan Balam II (Martin and Grube 2000) | AD 684-702 | Temple of the Sun | Interior. |
| Pa24 | Wall render | K'inich Kan Balam II (Martin and Grube 2000) | AD 684-702 | Temple of the Sun | Wall render from the external wall, northwest corner. |
| Pa27 | Wall render | K'inich Kan Balam II (Martin and Grube 2000) | AD 684-702 | Temple of the Cross | Wall render, external wall of south façade. |
| Pa28 | Floor | K'inich Kan Balam II (Martin and Grube 2000) | AD 684-702 | Temple of the Cross | Exterior area |
| Pa33 | Floor | K'inich Kan Balam II (Martin and Grube 2000) | AD 684-702 | Temple of the Foliated Cross | South façade, lower layer |
| Pa34 | Wall render | K'inich Kan Balam II (Martin and Grube 2000) | AD 684-702 | Temple of the Foliated Cross | South wall, exterior wall. |
| Pa35 | Floor (mud) | K'inich Kan Balam II (Martin and Grube 2000) | AD 684-702 | Temple of the Foliated Cross | East façade. lower layer (mud mortar) |
| Pa41 | Floor | K'inich Kan Balam II (Martin and Grube 2000) | AD 684-702 | Temple of the Foliated Cross | Northern room |
| Pa42 | Joining mortar | K'inich Kan Balam II (Martin and Grube 2000) | AD 684-702 | Temple of the Sun | Interior room, East wall. |
| Pa52 | Floor | K'inich Kan Balam II? (Tovalin and Ceja Manrique 1993) | AD 684-702 | Temple II, North Group | Central room |
| Pa59 | Floor | K'inich Kan Balam II (Martin and Grube 2000) | AD 684-702 | Temple of the Foliated Cross | Exterior floor (stairs) Layer no.15 (from top to bottom) |
| Pa60 | Floor | K'inich Kan Balam II (Martin and Grube 2000) | A AD 684-702 | Temple of the Foliated Cross | Exterior floor (stairs) Layer no.14 (from top to bottom) |
| Pa61 | Floor | K'inich Kan Balam II (Martin and Grube 2000) | AD 684-702 | Temple of the Foliated Cross | Exterior floor (stairs) Layer no.13 (from top to bottom) |
| Pa62 | Floor | K'inich Kan Balam II (Martin and Grube 2000) | AD 684-702 | Temple of the Foliated Cross | Exterior floor (stairs) Layer no.12 (from top to bottom) |
| Pa63 | Floor | K'inich Kan Balam II (Martin and Grube 2000) | AD 684-702 | Temple of the Foliated Cross | Exterior floor (stairs) Layer no.11 (from top to bottom) |
| Pa65 | Floor | K'inich Kan Balam II (Martin and Grube 2000) | AD 684-702 | Temple of the Foliated Cross | Exterior floor (stairs) Layer no.9 (from top to bottom) |
| Pa66 | Floor | K'inich Kan Balam II (Martin and Grube 2000) | AD 684-702 | Temple of the Foliated Cross | Exterior floor (stairs) Layer no.8 (from top to bottom) |
| Pa67 | Floor | K'inich Kan Balam II (Martin and Grube 2000) | AD 684-702 | Temple of the Foliated Cross | Exterior floor (stairs) Layer no.7 (from top to bottom) |
| Pa68 | Floor | K'inich Kan Balam II (Martin and Grube 2000) | AD 684-702 | Temple of the Foliated Cross | Exterior floor (stairs) Layer no.6 (from top to bottom) |

| Sample | Type | Period and source of dating | Dates | Structure | Observations |
|--------|----------------|--|---------------------|------------------------------|---|
| Pa70 | Floor | K'inich Kan Balam II. Martin and Grube (2000) | AD 684-702 | Temple of the Foliated Cross | Exterior floor (stairs) Layer no.4 (from top to bottom) |
| Pa71 | Floor | K'inich Kan Balam II. Martin and Grube (2000) | AD 684-702 | Temple of the Foliated Cross | Exterior floor (stairs) Layer no.3 (from top to bottom) |
| Pa72 | Floor | K'inich Kan Balam II. Martin and Grube (2000) | AD 684-702 | Temple of the Foliated Cross | Exterior floor (stairs) Layer no.2 (from top to bottom) |
| Pa75 | Wall render | K'inich Kan Balam II. Martin and Grube (2000) | AD 684-702 | Temple of the Foliated Cross | Wall render sequence. south wall, doorway of central room. |
| Pa17 | Wall render | Joy Chitam II or K'inich Kan Balam II Tovalin Ahumada and Lopez Bravo (2001), Robertson 1983d. | AD 702-711 | Palace, House D | |
| Pa18 | Floor | Joy Chitam II or K'inich Kan Balam II Tovalin Ahumada and Lopez Bravo (2001), Robertson (1983d). | AD 702-711 | Palace, House D | |
| Pa19 | Wall render | Joy Chitam II or K'inich Kan Balam II Tovalin Ahumada and Lopez Bravo (2001), Robertson (1983d). | AD 702-711 | Palace, House D | |
| Pa43 | Wall render | Joy Chitam II? Tovalin Ahumada and Lopez Bravo (2001), K'inich Kan Balam II (Robertson 1983) | AD 702-711? | Palace. House A | Northern side, west wall. |
| Pa47 | Floor | Joy Chitam II? (Tovalin Ahumada and Lopez Bravo 2001), K'inich Kan Balam II (Robertson 1983). | AD 702-711? | Palace. House D | Lower layer. Northernmost room. |
| Pa1 | Wall render | K'inich Kuk Bahlam II (Aka Kuk) (Robertson 1983d). | AD 764-799 | Palace, House I | North wall (interior wall). East side of the room. |
| Pa2a | Floor | K'inich Kuk Bahlam II (Aka Kuk) (Robertson 1983d). | AD 764-799 | Palace, House I | West side of the room. Upper layer of floor. |
| Pa2b | Floor | K'inich Kuk Bahlam II (Aka Kuk) (Robertson 1983d). | AD 764-799 | Palace, House I | West side of the room. Lower layer of floor. |
| Pa12 | Wall render | K'inich Kuk Bahlam II (Aka Kuk)? Balunte? | AD 764-799 | Temple of the Skull | South corridor, north wall |
| Pa53 | Wall render | Balunte phase (Rands 1974) | AD 770-850 | Bats Group. Structure MC2. | Interior room. |
| Pa56 | Floor | Balunte phase (Rands 1974) | AD 770-850 | Bats Group. Structure MC2. | Exterior corridor. |
| Pa86 | Wall render | Balunte phase (Tovalin 1999) | AD 770-850 | Temple IV, North Group | Original wall, south wall. Interior room. |
| Pa85 | Wall render | Architectural modifications (on-site observations) | AD 770-850 or later | Architectural Modification | East room. Late wall (architectural modification) |
| Pa40 | Joining mortar | Architectural modifications (on site observations). | AD 770-850 or later | Temple of the Foliated Cross | Northern room, interior west wall. |
| Pa44 | Wall render | Architectural modifications (on site observations). | AD 770-850 or later | Palace. House D | Penultimate room from south to north. Added wall (architectural interventions). |
| Pa45 | Joining mortar | Architectural modifications (on site observations). | AD 770-850 or later | Palace. House D | Penultimate room from south to north. Added wall (architectural interventions). |
| Pa80 | Joining mortar | Architectural modifications (on site observations). | AD 770-850 or later | Palace. House D | Central room. Added wall (architectural modifications). |
| Pa82 | Wall render | Architectural modifications (on site observations). | AD 770-850 or later | Temple of the Foliated Cross | Added wall in west façade. |
| Pa87 | Wall render | Architectural modifications (on site observations). | AD 770-850 or later | Temple IV, North Group | Dividing wall, central room. |

| Sample | Type | Period and source of dating | Dates | Structure | Observations |
|--------|-------------------------|---|--------------------|---|--|
| Pa26 | Limestone | K'inich Kan Balam II. Martin and Grube (2000) | AD 684-702 | Temple of the Cross | South façade, external wall. |
| Pa48 | Limestone | Joy Chitam II Martin and Grube (2000). | AD 702-711 | Palace, House A-D | From filling material of the platform. |
| Pa55 | Limestone | Balunte phase? | AD 770-850 | Bats Group. Structure MC2. | Interior room. |
| Pa3 | Limestone | Cascada Phase (Marken 2006) | AD 500-620 | Temple XV | From the filling material of the platform. |
| Pa5 | Limestone | Cascada Phase? (Marken 2006) | AD 500-620 | Ball court | North side of the structure. |
| Pa7 | Limestone | Otulum phase (620-700) (Marken 2006). | AD 620-700 | Temple of the Count | Interior room. |
| Pa89 | Limestone | Modern material | NA | From river. | |
| Pa-She | Snail shells | Modern material | NA | From river. | |
| La24 | Wall render | Late Preclassic (E. Graham and D Pendergast, personal communication). | ca. 100 BC | Str N10-43. Mask to the right of the central stairs, first floor. | Red paint layer. |
| La25 | Wall render | Late Preclassic (E. Graham and D. Pendergast, personal communication). | ca. 100 BC | Str N10-43. Render to the left of the mask, second level. | Red paint layer. |
| La28 | Floor | Late Preclassic (E. Graham and D Pendergast, personal communication). | 400-100 BC | Str. N10-4 | Floor from stone alignment, struct N10-4 |
| La29 | Floor | Late Preclassic (E. Graham and D Pendergast, personal communication). | 400-100 BC | Str. N10-4 | Pit in trench that is dug in N10-4 (trench to the north of the corridor/trench) |
| La30 | Floor | Late Preclassic (E. Graham and D Pendergast, personal communication). | 400-100 BC | Str. N10-4, pit 1 | Pit in trench that is dug in N10-4 (trench to the north of the corridor/trench). 30 cms depth. No continuous floor. Red paint in one of the fragments. |
| La31 | Floor | Late Preclassic (E. Graham and D Pendergast, personal communication). | 400-100 BC | Str. N10-4, pit 1 | Pit in trench that is dug in N10-4 (trench to the north of the corridor/trench). 30 cms depth. No continuous floor. |
| La32a | Floor | Late Preclassic (E. Graham and D Pendergast, personal communication). | 400-100 BC | Str. N10-4, pit 3 | Pit in corridor/trench. Lower layer of floor. |
| La32b | Floor | Late Preclassic (E. Graham and D Pendergast, personal communication). | 400-100 BC | Str. N10-4, pit 3 | Pit in corridor/trench. Upper layer of floor. |
| La34 | Floor | Late Preclassic (E. Graham and D Pendergast, personal communication). | 400-100 BC | Str. N10-4, pit 3 | Material on top of sample La32 |
| La15 | Floor | Late Preclassic (E. Graham and D Pendergast, personal communication). | ca. 100 BC | Str. N10-43 | Lower layer of 4th step at the level of the 1st platform, left stairs. |
| La46 | Floor | Late Preclassic/Early Classic (E. Graham and D Pendergast, personal communication). | ca. 100 BC- AD 300 | Str. P9-25 ("Holiday House") Hyatt floor | Upper layer. |
| La47 | Floor | Late Preclassic/Early Classic (E. Graham and D Pendergast, personal communication). | ca. 100 BC- AD 300 | Str. P9-25 ("Holiday House") (Hyatt floor) | Lower layer (floor 20 cm thick). |
| La48 | Sculpture (wall render) | Early Classic (E. Graham and D Pendergast, personal communication). | Ca. AD 450 | Str. N9-56 ("Mask Temple") | Wall render. |
| La44 | Floor | Early Classic (E. Graham and D Pendergast, personal communication). | AD 1 – AD 400 | Str. P9-24 ("Holiday House") | Compacted sascab? |

| Sample | Type | Period and source of dating | Dates | Structure | Observations |
|--------|------------------------|---|--------------------|--|---|
| La45 | Floor. | Early Classic (E. Graham and D Pendergast, personal communication). | AD 1 – AD 400 | Str. P9-24 ("Holiday House") | |
| La3 | Floor | Late Classic (Graham 2007) | AD 600-870 | Str. N10-78 | From cross section of Na10-78, East side. |
| La4 | Floor | Late Classic (Graham 2007) | AD 600-870 | Str. N10-78 | From cross section of Na10-78, East side. |
| La6 | Floor | Late Classic (Graham 2007) | AD 600-870 | Str. N10-78/ N10-79 | Floor between N10-78 y N10-79. Lower layer. When sampled, hard inclusions of plaster were seen. Red paint layer. |
| La7 | Floor | Late Classic (Graham 2007) | AD 600-870 | Str. N10-78/ N10-79 | Floor between N10-78 y N10-79. Upper layer. |
| La14 | Floor | Late Classic? (Graham 2007) | AD 600-870 | Str. N10-43 | Upper layer of 4th step at the level of the 1st platform, left stairs. Same renovation of platform added during this period? |
| La16 | Floor | Late Classic? (Graham 2007) | AD 600-870 | Str. N10-43 | Upper layer of 4th step at the level of the 1st platform, central stairs. Same renovation of platform added during this period? |
| La17 | Floor | Late Classic (Graham 2007) | AD 600-870 | Str. N10-43 | Platform built in front of stairs. Floor covered by a thick layer (ca 30 cms). |
| La35 | Floor | Late Classic (Graham 2007) | AD 600-870 | Str. N10-27 | 2nd level, left side, floor from Stela Temple |
| La9 | Floor | Late/ Terminal Classic or later (Graham 2007) | AD 650-890 | Str. N10-15 | Upper floor. Hard sample. Visible orange inclusions. |
| La10 | Floor | Late/Terminal Classic (Graham 2007) | AD 650-890 | Str. N10-15 | Lower layer. Very hard sample. |
| La11 | Floor | Terminal Classic/ Early Postclassic (Graham 2007) | AD 770-AD 950/1000 | N10-15 | North addition to Str. N10-15. Upper layer. Crumbly. |
| La12 | Floor | Terminal Classic/ Early Postclassic (Graham 2007) | AD 770-AD 950/1000 | N10-15 | North addition to Str. N10-15. Lower layer. Crumbly. |
| La2 | Floor | Early Middle Postclassic (Graham 2007) | ca. AD 1250 | Str. N10-2 | Probably a later addition to Buk. 15cms of plaster. |
| La22 | Wall render | Late Postclassic (Graham 2008) | AD 1250- 1540 | Str. N12-11, 2nd (YDLI). | 2 visible layers. West wall. |
| La36a | Wall render? | Late Postclassic? Early Spanish Colonial? (Graham 2008) | ca. AD 1540 | Pit west of Str. N12-11, 2nd (YDLI). | Upper layers of fragment. Crumbly layer. Visible mixture of materials. |
| La36b | Plaster layers (wall?) | Late Postclassic? (Graham 2008) | ca. AD 1540 | Pit west of Str. N12-11, 2nd (YDLI). | Lower layers of fragment. This sample may be Spanish Colonial. |
| La49 | Floor | Late Postclassic. (Graham 2008) | AD 1250- 1540 | Str. N12-11, 2 nd (YDLI). North façade. | Upper layer with red pigment. |
| La50 | Floor (lower layer) | Late Postclassic (Graham 2008) | AD 1250- 1540 | Str. N12-11, 2 nd (YDLI). North façade. | Lower layer with red pigment. Very hard. It has a large limestone fragment. |
| La19 | Floor | Early Spanish Colonial (Graham 2008) | AD 1540-1600 | Str. N12-12 | From corridor. |
| La20 | Joining mortar | Early Spanish Colonial (Graham 2008) | AD 1540-1600 | Str. N12-13 (YDL II) | Northern wall, at the entrance of the church |
| La21 | Wall render | Early Spanish Colonial (Graham 2008) | AD 1540-1600 | Str. N12-13 (YDL II) | Northern wall, at the entrance of the church. |
| La40 | Wall render | Early Spanish Colonial (Graham 2008) | AD 1540-1600 | Str. N12-13 (YDL II) South Wall | South wall |
| LaSas1 | Sascab | Modern geological material (Graham 2008) | NA | NA | Sascab collected from building works |

| Sample | Type | Period and source of dating | Dates | Structure | Observations |
|--------------|-----------------------|---|-----------------|--|--|
| LaSas2 | Sascab | Modern geological material | NA | NA | Sascab from the quarry in Indian Church Village |
| La23 | Limestone | Early Spanish Colonial | NA | Str. N12-13 (YDL II) | Limestone from the northern wall, at the entrance of the church |
| La39 | Limestone | Late Postclassic | NA | Str. N12-12 | Limestone from the southern wall of structure N12-12 |
| La13 | Limestone | Late Classic | NA | Str. N10-18 | |
| La27 | Limestone | Late Preclassic | NA | Str N10-43 | Limestone from the central stairs, first level. |
| Lamanai Cret | Limestone | Modern geological material | NA | NA | From building works |
| Ca9 | Floor | Middle Preclassic. (Rodríguez Campero, personal communication) | 1000-400 BC | Substructure II-d | Lower layer of sequence. Very crumbly. |
| Ca10 | Floor | Middle Preclassic. (Rodríguez Campero, personal communication) | 1000-400 BC | Substructure II-d | Upper layer of sequence. Very hard sample. |
| Ca11 | Wall render | Middle Preclassic. (Rodríguez Campero, personal communication) | 1000-400 BC | Substructure II-d | |
| Ca12 | Floor | Middle Preclassic. (Rodríguez Campero, personal communication) | 1000-400 BC | Substructure II-d | |
| Ca5 | Stucco sculpture | Late Middle Preclassic (Rodríguez Campero 2008) | ca. 390-250 BC | Basement, substructure IIc1, central part of tablero | Red paint layer. |
| Ca6 | Wall render | Late Middle Preclassic (Rodríguez Campero 2008) | ca. 390-250 BC | Basement, substructure IIc1, left part of tablero | Extremely hard sample. |
| Ca7 | Stucco sculpture | Late Middle Preclassic (Rodríguez Campero 2008) | ca. 390-250 BC | Substructure IIC1 | Red painting layer. Dislocated sample but most likely lower molding or panels of frieze. Very hard sample. |
| Ca8 | Stucco sculpture | Late Middle Preclassic (Rodríguez Campero 2000) | ca. 390-250 BC | Substructure IIc2 | Yellow paint layer |
| Ca29 | Floor (floor bed). | Late Preclassic (Carrasco and Rodríguez, personal communication). | 400 BC – AD 250 | Pit, structure VII | Very crumbly. Compacted layer below Ca30. |
| Ca30 | Floor | Late Preclassic (Carrasco and Rodríguez, personal communication). | 400 BC – AD 250 | Pit, structure VII | Upper layer (on top of Ca29). |
| Ca1 | Wall render, interior | Early Classic (Carrasco and Rodríguez, personal communication). | AD 250-600 | Structure III, south room, south area | |
| Ca31 | Floor | Early Classic (Carrasco and Rodríguez, personal communication). | AD 250-600 | Pit, structure VII | |
| Ca2 | Floor, interior | Early Classic (Carrasco and Rodríguez, personal communication). | AD 250-600 | Structure III, south room, south area | |

| Sample | Type | Period and source of dating | Dates | Structure | Observations |
|--------|---|---|------------|--|--|
| Ca13 | Floor | Early Classic (Carrasco and Rodriguez, personal communication). | AD 250-600 | Substructure I-4, structure I, Chiik Naab'acr., SE area | Very crumbly sample with visible brown inclusions. |
| Ca14 | Wall render with paint | Early Classic (Carrasco and Rodriguez, personal communication). | AD 250-600 | Substructure I-4, structure I, Chiik Naab'acropolis, SW area | Red paint layer (applied over yellow paint) |
| Ca15 | Wall render with paint | Early Classic (Carrasco and Rodriguez, personal communication). | AD 250-600 | Substructure I-4, structure I, Chiik Naab'acropolis SW area | Yellow paint layer (covered by red paint layer). |
| Ca19 | Floor | Early Classic (Carrasco and Rodriguez, personal communication). | AD 250-600 | Structure 1, patio B, Chan Chi'ich residential complex | |
| Ca20 | Wall | Early Classic (Carrasco and Rodriguez, personal communication). | AD 250-600 | Structure 1, patio B, Chan Chi'ich residential complex | |
| Ca22 | Floor | Early Classic (Carrasco and Rodriguez, personal communication). | AD 250-600 | Substructure IIB | |
| Ca23 | Wall render with paint | Early Classic (Carrasco and Rodriguez, personal communication). | AD 250-600 | Structure XIII | Red paint layer |
| Ca24 | Found in the fill of structure III. Prior to Early Classic. | Early Classic (Carrasco and Rodriguez, personal communication). | AD 250-600 | Structure XIII | Very hard sample. |
| Ca35 | Stucco, fill | Early Classic (Carrasco and Rodriguez, personal communication). | AD 250-600 | Substructure XX-b | Red and black paint layers. |
| Ca17 | Wall render | Late Classic (Carrasco and Rodriguez, personal communication). | AD 600-800 | Structure GN-1, Northeast structure | |
| Ca18 | Floor | Late Classic (Carrasco and Rodriguez, personal communication). | AD 600-800 | Structure GN-1, Northeast structure | |
| Ca21 | Floor | Late Classic, 702 AD according to epigraphy (Carrasco et al 1999:51) | AD 600-800 | Substructure IIB | |
| Ca26 | Wall render | Late Classic (Carrasco and Rodriguez, personal communication). | AD 600-800 | Structure XIII, east side, vaulted corridor | Very crumbly |
| Ca16 | Wall render, exterior | Late Classic, almost Terminal (Carrasco and Rodriguez, personal communication). | AD 600-800 | Substructure I-1, SE corner, 2nd body | |

| Sample | Type | Period and source of dating | Dates | Structure | Observations |
|-----------|---------------------|--|-----------------|---|--|
| Ca36 | Wall render, frieze | Late Classic (Carrasco and Rodriguez, personal communication). | AD 600-800 | Substructure XX-a | Very hard sample. |
| Ca3 | floor | Terminal Classic (Carrasco and Rodriguez, personal communication). | AD 800-900/1000 | Tok structure | Very dark colour (brown). Completely pulverized. |
| Ca4 | Floor | Terminal Classic (Carrasco and Rodriguez, personal communication). | AD 800-900/1000 | Tok structure | |
| Ca33 | Floor | Terminal Classic (Carrasco and Rodriguez, personal communication). | AD 800-900/1000 | Structure VI, upper building | Very dark colour (brown). Completely pulverized. |
| Ca34 | Wall render | Terminal Classic (Carrasco and Rodriguez, personal communication). | AD 800-900/1000 | Structure XX, 2nd corridor | Very crumbly |
| Ca Sascab | Sascab | Modern | NA | Calakmul biosphere | It has harder inclusions. |
| Ca25 | Limestone | Late Classic | NA | Structure XIII, east side, vaulted corridor | |
| Ca27 | Limestone | Modern | NA | Quarry, west of Chiik Naab | |
| Ca28 | Limestone | Modern | NA | Quarry, south of small acropolis | |

Table 5.1. Inventory of samples analysed.

Analyses carried out in the samples:

| Sample | Type | Period | ORM | SEM | Petrography | Petrography pigments | XRF, PCA and cluster analysis | XRD | Microprobe analysis of inclusions | Raman (pigments) |
|--------|------|-----------|-----|-----|-------------|----------------------|-------------------------------|-----|-----------------------------------|------------------|
| Pal_1 | JM | Cas | | | * | | | | | |
| Pal_2 | WR | Ot | | | | | * | | | |
| Pal_3 | WR | Ot | | | * | | * | | | |
| Pal_4 | F | Ot | | | * | | | | | |
| Pal_5 | WR | Pak II | | | * | | | | | |
| Pal_6 | WR | Pak II | | | * | | | | | |
| Pal_7 | F | Kam Bal | | | * | | | | | |
| Pal_8 | F | Kam Bal | | | * | | | | | |
| Pal_9 | WR | Kam Bal | * | | * | | * | | | |
| Pal_10 | WR | Kam Bal | * | | * | | | | | |
| Pal_11 | F | Kam Bal | | | * | | | | | |
| Pal_12 | F | Kam Bal | | | | | * | | | |
| Pal_13 | WR | Kam Bal | | | | | * | | | |
| Pal_14 | F | Kam Bal | | | | | * | | | |
| Pal_15 | F | Kam Bal | | | | * | | | | * |
| Pal_16 | JM | Kam Bal | | | | | | | | |
| Pal_17 | F | Kam Bal ? | | | * | | * | | | |
| Pal_18 | F | Kam Bal | | | * | | * | | | |
| Pal_19 | F | Kam Bal | | | * | | * | * | | |
| Pal_20 | F | Kam Bal | | | * | | | | | |
| Pal_21 | F | Kam Bal | | * | * | | | | | |
| Pal_22 | F | Kam Bal | | | * | | * | | | |
| Pal_23 | F | Kam Bal | | | * | | * | | | |
| Pal_24 | F | Kam Bal | | | * | | | * | | |
| Pal_25 | F | Kam Bal | | | * | | | | | |
| Pal_26 | F | Kam Bal | | * | * | | | | | |
| Pal_27 | F | Kam Bal | | * | * | * | * | | | |
| Pal_28 | F | Kam Bal | | * | * | * | | | | |
| Pal_29 | F | Kam Bal | * | | * | | | | | |
| Pal_30 | WR | Kam Bal | * | | * | | | | | * |
| Pal_31 | WR | Arch Mod | | | | | | | | * |
| Pal_32 | WR | Joy Chit? | | | | | | * | | |
| Pal_33 | F | Joy Chit? | | * | * | * | | * | | |
| Pal_34 | WR | Joy Chit? | | | * | | | | | |
| Pal_35 | WR | Joy Chit? | | | * | * | | | | |
| Pal_36 | F | Joy Chit | | | | * | | | | |
| Pal_37 | WR | Kuk Bahl | * | | * | * | | * | | |

Abbreviation sites: Pal: Palenque, Cal: Calakmul, Lam: Lamanai. **Abbreviations type of material:** F: Floor, JM: Joining mortar, WR: Wall render, S: sculpture, L: Limestone, S: sculpture, Sas: sascab. **Abbreviations rulers and periods:** Cas: Cascada Phase, Ot: Otulum Phase, Pak II: K'inich Janaab' Pakal, Kam Bal: K'inich Kam Balam II, Joy Chit: Joy Chitam II, Kuk Bahl: K'inich Kuk Bahlam II, Balun: Balunte Phase, Arch mod: architectural modifications, MPrec: Middle Preclassic, LPrec: Late Preclassic, EClas: Early Classic, LClas: Late Classic, TClas: Terminal Classic, EPos: Early Postclassic, LPost: Late Postclassic. SCol: Spanish Colonial

| Sample | Type | Period | ORM | SEM | Petrography | Petrography pigments | XRF, PCA and cluster analysis | XRD | Microprobe analysis of inclusions | Raman (pigments) |
|--------|--------|-------------|-----|-----|-------------|----------------------|-------------------------------|-----|-----------------------------------|------------------|
| Pal_38 | F | Kuk Bahl | | | * | | * | | | |
| Pal_39 | F | Kuk Bahl | | | * | | | | | |
| Pal_40 | WR | Kuk Bahl? | | | * | | | | * | |
| Pal_41 | WR | Balun? | | | * | | * | | | |
| Pal_42 | F | Balun? | | | * | | * | | * | |
| Pal_43 | WR | Balun? | | | * | | * | | | |
| Pal_44 | JM | Arch Mod | | | | | * | | | |
| Pal_45 | WR | Arch Mod | | | * | | * | * | | |
| Pal_46 | JM | Arch Mod | | | * | | * | | | |
| Pal_47 | JM | Arch Mod | | | | | * | | | |
| Pal_48 | WR | Arch Mod | | | | | * | | | |
| Pal_49 | WR | Arch Mod | | | * | | * | | | |
| Pal_50 | L | L/ Kam Bal | | | * | | | | | |
| Pal_51 | L | L/ Joy Chit | | | * | | | | | |
| Pal_52 | L | L/Balun? | | | * | | | | | |
| Pal_53 | L | L/Cas | | | | | * | | | |
| Pal_54 | L | L/Cas? | | | * | | * | | | |
| Pal_55 | L | L/Ot | | | | | * | | | |
| Pal_56 | L | L/NA | | | | | * | * | | |
| Pal_57 | Shells | NA | | | | | * | | | |
| Cal_1 | F | MPrec | | * | * | | * | * | | |
| Cal_2 | F | MPrec | | * | * | | * | * | | |
| Cal_3 | WR | MPrec | | | * | | | | * | |
| Cal_4 | F | MPrec | | | | | * | | | |
| Cal_5 | S | LMPrec | * | * | * | * | * | | | * |
| Cal_6 | WR | LMPrec | | * | * | | * | | * | |
| Cal_7 | S | LMPrec | * | * | * | * | * | * | | * |
| Cal_8 | S | LMPrec | * | * | * | * | * | | | * |
| Cal_9 | F | LPrec | | | * | | * | * | * | |
| Cal_10 | F | LPrec | | | * | | * | | * | |
| Cal_11 | WR | EClas | | | * | | | | | |
| Cal_12 | F | EClas | | | * | | | | | |
| Cal_13 | F | EClas | | | * | | * | * | | |
| Cal_14 | WR | EClas | * | * | * | * | | | * | * |
| Cal_15 | WR | EClas | | * | * | | | | | * |
| Cal_16 | F | EClas | | | * | | * | | | |
| Cal_17 | F | EClas | | | * | | * | * | | |
| Cal_18 | WR | EClas | * | | * | * | | | | * |
| Cal_19 | WR? | EClas? | * | * | * | | * | | | |

Abbreviation sites: Pal: Palenque, Cal: Calakmul, Lam: Lamanai. **Abbreviations type of material:** F: Floor, JM: Joining mortar, WR: Wall render, S: sculpture, L: Limestone, S: sculpture, Sas: sascab. **Abbreviations rulers and periods:** Cas: Cascada Phase, Ot: Otulum Phase, Pak II: K'inich Janaab' Pakal, Kam Bal: K'inich Kam Balam II, Joy Chit: Joy Chitam II, Kuk Bahl: K'inich Kuk Bahlam II, Balun: Balunte Phase, Arch mod: architectural modifications, MPrec: Middle Preclassic, LPrec: Late Preclassic, EClas: Early Classic, LClas: Late Classic, TClas: Terminal Classic, EPos: Early Postclassic, LPost: Late Postclassic. SCol: Spanish Colonial.

| Sample | Type | Period | ORM | SEM) | Petrography | Petrography pigments | XRF, PCA and cluster analysis | XRD | Microprobe analysis of inclusions | Raman (pigments) |
|--------|------|-------------|-----|------|-------------|----------------------|-------------------------------|-----|-----------------------------------|------------------|
| Cal_20 | S | EClas | * | | | * | | | | * |
| Cal_21 | WR | LClas | | * | * | | | | * | |
| Cal_22 | WR | LClas | | | | | * | | | |
| Cal_23 | F | LClas | | * | * | | * | * | * | |
| Cal_24 | F | LClas | | | * | | | * | | |
| Cal_25 | WR | LClas | | | * | | * | | * | |
| Cal_26 | WR | LClas | | * | * | | * | | | |
| Cal_27 | F | TClas | | | * | | * | * | | |
| Cal_28 | F | TClas | | * | * | | * | | | |
| Cal_29 | F | TClas | | | * | | * | * | | |
| Cal_30 | WR | TClas | | | * | | * | | | |
| Cal_31 | L | L/LClas | | | * | | | | | |
| Cal_32 | L | L/LClas | | | * | | * | | | |
| Cal_33 | L | L/LClas | | | * | | * | | | |
| Cal_34 | Sas | L/NA | | | * | | * | * | | |
| Lam_1 | WR | LPrec | | | * | | | | | |
| Lam_2 | WR | LPrec | | | * | | | * | | |
| Lam_3 | F | LPrec | | * | * | | | | | |
| Lam_4 | F | LPrec | | | * | | | | | |
| Lam_5 | F | LPrec | * | | * | | | | | |
| Lam_6 | F | LPrec | * | | * | | | | | |
| Lam_7 | F | LPrec? | | | * | | | | | |
| Lam_8 | F | LPrec? | | | * | | | | | |
| Lam_9 | F | LPrec? | | | * | | * | | | |
| Lam_10 | F | LPrec | | | * | | * | | | |
| Lam_11 | F | EClas? | | | * | | | | | |
| Lam_12 | F | EClas? | | | * | | | | | |
| Lam_13 | WR | EClas | | | * | | * | | | |
| Lam_14 | F | EClas | | | | | * | | | |
| Lam_15 | F | EClas | | | * | | * | | | |
| Lam_16 | F | LClas | | | * | | * | | | |
| Lam_17 | F | LClas | | * | * | | | * | | |
| Lam_18 | F | LClas | | | * | | * | | | |
| Lam_19 | F | LClas | | | * | | | | | |
| Lam_20 | F | LClas? | * | | * | | | * | | |
| Lam_21 | F | LClas? | | | * | | | | | |
| Lam_22 | F | LClas | * | | * | | * | | | |
| Lam_23 | F | LClas | * | | * | | | | | |
| Lam_24 | F | LClas/TClas | * | * | * | | * | | | |
| Lam_25 | F | LClas/TClas | * | * | * | | * | | | |
| Lam_26 | F | TClas/EPos | | | * | | * | | | |
| Lam_27 | F | TClas/EPos | | | * | | * | * | | |

Abbreviation sites: Pal: Palenque, Cal: Calakmul, Lam: Lamanai. **Abbreviations type of material:** F: Floor, JM: Joining mortar, WR: Wall render, S: sculpture, L: Limestone, S: sculpture, Sas: sascab. **Abbreviations rulers and periods:** Cas: Cascada Phase, Ot: Otulum Phase, Pak II: K'inich Janaab' Pakal, Kam Bal: K'inich Kam Balam II, Joy Chit: Joy Chitam II, Kuk Bahl: K'inich Kuk Bahlam II, Balun: Balunte Phase, Arch mod: architectural modifications, MPrec: Middle Preclassic, LPrec: Late Preclassic, EClas: Early Classic, LClas: Late Classic, TClas: Terminal Classic, EPos: Early Postclassic, LPost: Late Postclassic. SCol: Spanish Colonial.

| Sample | Type | Period | ORM | SEM | Petrography | Petrography pigments | XRF, PCA and cluster analysis | XRD | Microprobe analysis of inclusions | Raman (pigments) |
|--------|------|-----------|-----|-----|-------------|----------------------|-------------------------------|-----|-----------------------------------|------------------|
| Lam_28 | F | EPos/MPos | | | * | | * | | | |
| Lam_29 | WR | LPos | * | | * | | | * | | |
| Lam_30 | WR? | LPos | | | * | | * | | | |
| Lam_31 | WR? | LPos | * | | * | | * | | * | |
| Lam_32 | F | LPos | | | * | | * | * | * | |
| Lam_33 | F | LPos | | | * | | | | | |
| Lam_34 | F | SCol | * | * | * | | * | * | | |
| Lam_35 | JM | SCol | * | | * | | * | | * | |
| Lam_36 | WR | SCol | * | * | * | | * | * | | |
| Lam_37 | WR | SCol | | | * | | | | * | |
| Lam_38 | Sas | L/NA | | | * | | * | * | | |
| Lam_39 | Sas | L/NA | | | | | * | | | |
| Lam_40 | L | L/Scol | | | * | | * | | | |
| Lam_41 | L | L/LPos | | | * | | | * | | |
| Lam_42 | L | L/LClas | | | * | | * | | | |
| Lam_43 | L | L/Lprec | | | * | | | | | |
| Lam_44 | L | L/NA | | | | | * | | | |

Abbreviation sites: Pal: Palenque, Cal: Calakmul, Lam: Lamanai. **Abbreviations type of material:** F: Floor, JM: Joining mortar, WR: Wall render, S: sculpture, L: Limestone, S: sculpture, Sas: sascab. **Abbreviations rulers and periods:** Cas: Cascada Phase, Ot: Otulum Phase, Pak II: K'inich Janaab' Pakal, Kam Bal: K'inich Kam Balam II, Joy Chit: Joy Chitam II, Kuk Bahl: K'inich Kuk Bahlam II, Balun: Balunte Phase, Arch mod: architectural modifications, MPrec: Middle Preclassic, LPrec: Late Preclassic, EClas: Early Classic, LClas: Late Classic, TClas: Terminal Classic, EPos: Early Postclassic, LPost: Late Postclassic. SCol: Spanish Colonial.

Table 5.2. Analyses carried out.

6. Results

In this chapter I present the results of the analyses carried out on the plaster samples from the three case studies. The results are organised by case study, each of which presents the bulk elemental composition, the mineralogy of aggregates and inclusions, the microstratigraphy, the nature of the binder, pigments and coloured surfaces, as well as the nature of limestones and local raw materials. The discussion of results can be found in Chapter 7, and the full data are presented in the appendices.

6.1. Palenque

Bulk elemental Composition¹

The bulk composition of the plasters from Palenque showed noticeable differences. All samples have significant amounts of magnesium and roughly half of them can be considered as dolomitic plasters, that is to say, with more than 35% MgCO_3 ² (Seeley 2002).

Bulk elemental compositions obtained by XRF also showed that in all cases CaCO_3 and MgCO_3 were the major components and were negatively correlated with each other. The variation in the content of calcium and magnesium carbonates was very high; MgCO_3 contents ranged between 9 and 63%, whereas CaCO_3 contents ranged between 30 and 84% (see fig. 6.1 and appendix A.6 for XRF analysis).

¹ XRF is a bulk analysis and therefore does not distinguish between aggregates and binders. SEM-EDS analysis was employed in order to examine the chemistry of the different components of the samples (see appendix A.3.1).

² As mentioned in Chapter 5, CaO and MgO contents obtained by means of XRF analyses were converted into carbonates by stoichiometric calculations in order to account for the CO_2 that is not reported in the analyses. This was done because it is believed that most of the calcium and magnesium are present as carbonates, although there could be some content present as hydroxides due to incomplete carbonation of the lime. The conversion to carbonates was also done with the data collected with the EDS attached to the SEM and the microprobe.

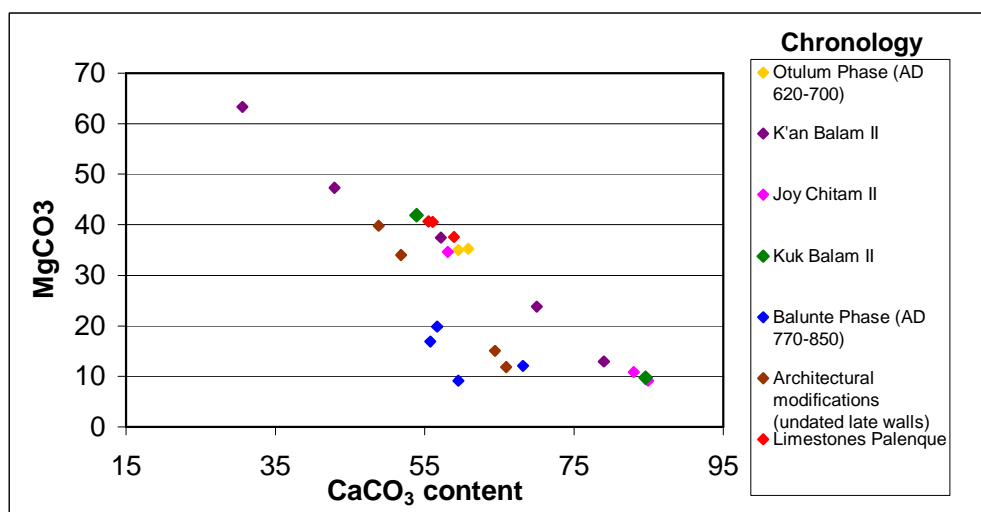


Fig. 6.1. CaCO₃ vs MgCO₃ scatter plot (weight %).

SiO₂ was also highly variable in the bulk compositions. Although the average content of SiO₂ was 7.8 wt%, plasters dating from the Balunté Phase (Terminal Classic Period) showed up to 21% of SiO₂ and up to 6% of Al₂O₃, which is higher than earlier plasters (see fig. 6.2 and appendix A.6). It was also clear that in some samples there was a co-variation of SiO₂ with Al₂O₃, TiO₂, Fe₂O₃, Na₂O and K₂O, as well as with trace elements such as CO₃O₄, NiO, ZnO, Rb₂O, ZrO₂ and BaCO₃. In contrast, high contents in SrO seemed to be correlated with high contents in CaCO₃ (see appendix A.7).

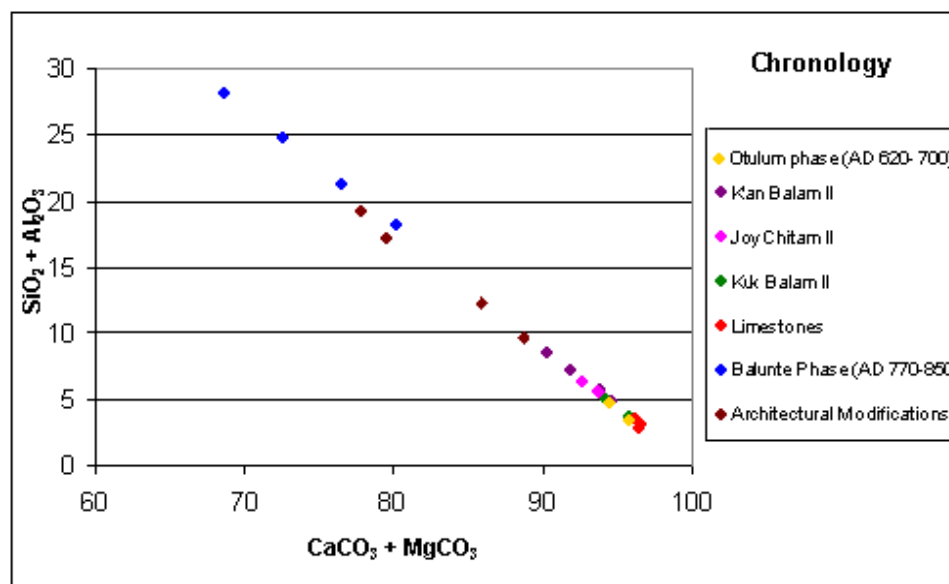


Fig. 6.2. CaCO₃ + MgCO₃ vs SiO₂ + Al₂O₃ scatter plot (weight %).

The cluster analysis of bulk elemental compositions distinguishes two main clusters, one of them with Balunté Phase samples (Terminal Classic) and samples from architectural interventions (walls added after the original plan of the buildings), and a second cluster with the rest of the samples. Exceptions to these clusters are samples Pa44 and Pa82, from architectural modifications, which were grouped together with earlier plasters (see appendix A.6.3).

Principal Component Analysis (PCA) also shows two main trends, as can be seen in fig. 6.3. By looking at the component plot in appendix A.6 (fig. A.6.4.6), it becomes clear that the vertical tendency is determined by the content in either CaCO_3 or MgCO_3 . This tendency groups all the samples except those from the Balunté Phase and the architectural modifications. This is a group low in SiO_2 and Al_2O_3 , and ranges between the samples with the highest MgCO_3 contents in the lower part of the graph to those with the highest CaCO_3 contents in the upper part. The diagonal tendency is determined by the content in SiO_2 and Al_2O_3 , and all the elements correlated with them. This trend defines the Balunté phase samples and the architectural interventions, which are located closer to SiO_2 and Al_2O_3 and away from the carbonates, and which is related to the clayey nature of the samples, as was also seen under the petrographic microscope.

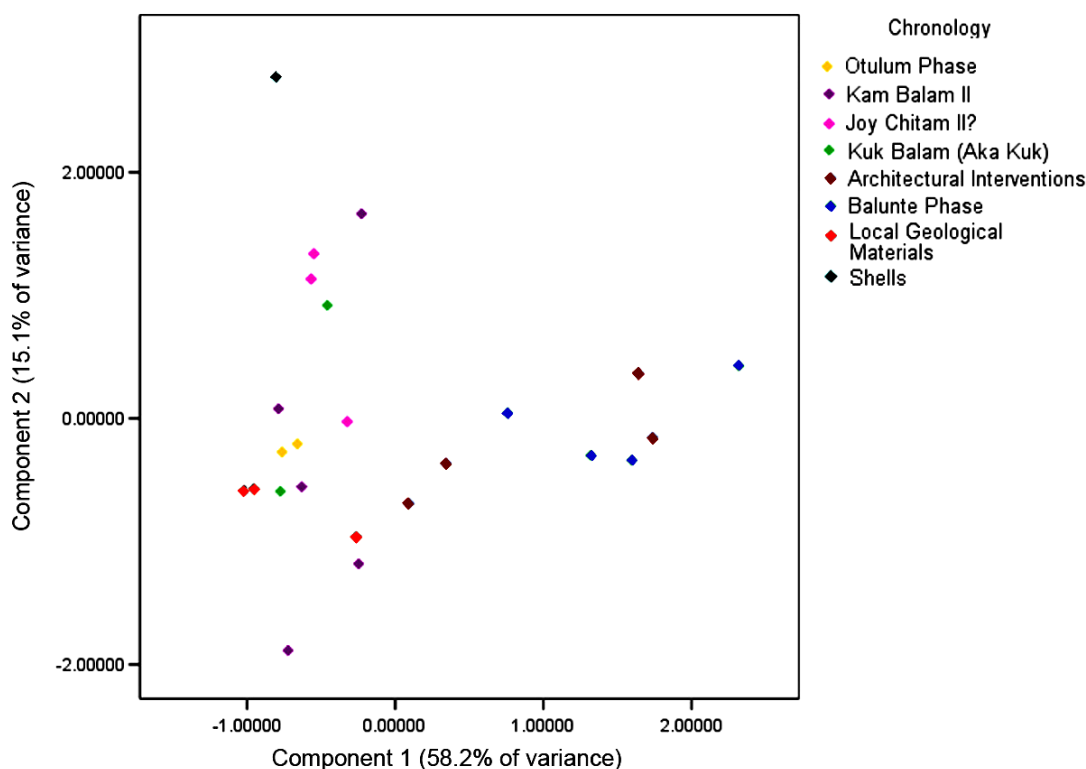


Fig. 6.3. Scatter plot of the two principal components (PCA) of bulk compositional data of Palenque samples (obtained by XRF).

Mineralogy and the nature of inclusions

Calcareous materials, constituted either by micritic or crystalline carbonates, were the most widely observed aggregates in the plasters from Palenque. In most of the cases the two types of carbonate aggregates occur together, although in some cases micritic calcite predominates (Pa 18, Pa77, Pa52, Pa2a), whereas in other samples crystalline carbonates prevail (Pa28, Pa23, Pa49).

Another frequently seen mineral, in addition to the carbonate phases, was quartz. Quartz was invariably angular or sub-angular. The presence of quartz in the plasters seems to be diagnostic. Although quartz is present in some of the plasters with calcareous non-clayey matrices, it constitutes only a secondary type of aggregate; in contrast, quartz was used as the main aggregate materials in the clayey plasters (see appendix A.2).

In most of the cases quartz grains were monocrystalline, but few exceptions of polycrystalline quartz could be seen (Pa12, Pa53 and Pa56). It was possible to see that some of the quartz grains were shocked—a distinctive feature of meteoritic material, as explained in Chapter 7—, showing distinctive sets of cleavages or planar deformation features (PDFs) (see Fig. 7.6 in Chapter 7 and appendix A.2.2). The identification of quartz was done on the basis of its optical properties, although in the case of shocked quartz its presence was confirmed with microprobe analysis in order to rule out alkali feldspars, which have similar optical properties.

Shocked quartz occurs together with or inside isotropic phases, as in the case of samples Pa22, Pa27, and Pa56. Sample Pa56 shows a clast of breccia with grains of shocked quartz that are supported by a partially isotropic matrix rich in SiO_2 and CaCO_3 (see fig. 6.4 and appendix A.4).

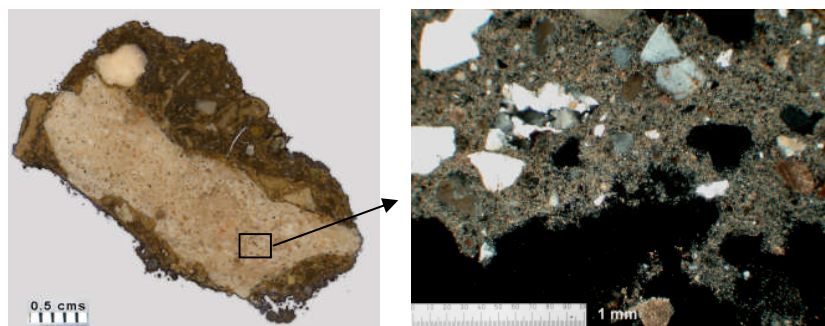


Fig. 6.4. Left: Pa56: clay-based plaster with a clast of breccia, scale bar: 0.5 cms. Right: clast of breccia with angular grains of shocked quartz supported by a partially isotropic matrix. XPL. Scale bar: 1 mm.

Other minerals frequently seen, although in small amounts, were muscovite mica (Pa28, Pa50, Pa53) and plagioclase feldspars (Pa44, Pa53, Pa56, Pa86), usually forming part of rounded fragments of volcanic rocks. Alkali feldspars were also occasionally seen (Pa12), and occur together or inside isotropic phases.

Two other minerals identified with the microprobe in sample Pa66 were zircon and moissanite (SiC), the latter also identified in sample Pa77. However, the presence of moissanite cannot be confirmed in the plasters since the grinding material for sample preparation was also composed of SiC.

In addition to these minerals, XRD showed the presence of dolomite (samples Pa63 and Pa88) and hydromagnesite (Pa63 and Pa70), and it also confirmed the presence of quartz in samples Pa60, Pa63, Pa70, and calcite in all the samples (see appendix A.5).

Isotropic phases were frequently seen in the plasters from Palenque (Pa12, Pa18, Pa27, Pa24 Pa52, Pa59, Pa60, Pa62, Pa70, Pa72 and Pa78). Some of these samples showed a reaction rim around them. On occasion these phases showed unusual bubbles and patterns of cracks, and when analysed with the microprobe, these phases showed exceptionally high concentrations of MgCO_3 (up to 56% in sample Pa27) with some SiO_2 and Al_2O_3 . In some cases, isotropic inclusions showed characteristic blebs of around 100 μm in diameter and some others showed partial devitrification, which is characterised by a yellow to red appearance under the polarising microscope (see fig. 6.5 and appendix A.2).

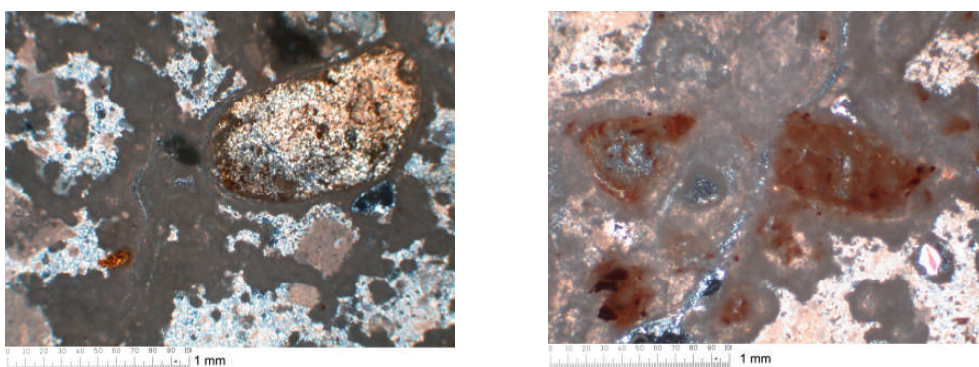


Fig. 6.5. Reaction rims around devitrified glass.
Left: sample Pa67 XPL. Scale bar: 1 mm. Right: sample Pa70, XPL. Scale bar 1 m.

Shells were seen in samples Pa4, Pa28, Pa44, Pa86, Pa87, which are plasters rich in clays, mainly from the Balunté Phase and from architectural modifications (dividing walls), as discussed below. Foraminifera fossils were also observed in late plasters, in samples Pa12, Pa56 and Pa87.

In addition to aggregates and inclusions that were incorporated in the lime mixtures, it was possible to observe the presence of materials, deposited in cracks and surfaces, which are related to the use of architecture and the decay of building materials (see Chapter 7 for discussion). Sample Pa28 shows a material with isotropic properties and a dark yellow colour under PPL, which suggests the presence of an organic material. This material is deposited along the cracks of the

plaster and it is in turn covered by secondary calcite (recrystallised calcite), showing that the isotropic material was deposited before the secondary calcite (see fig. 6.6).

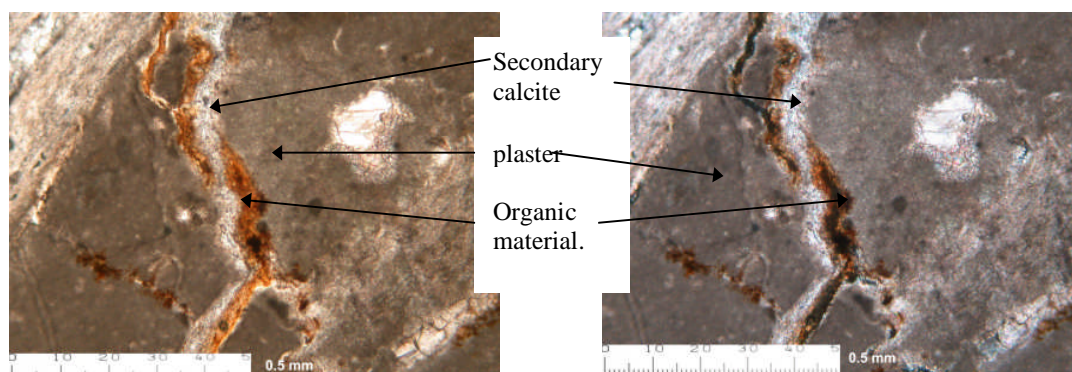


Fig. 6.6. Sample Pa28. Organic substance with secondary calcite recrystallised over it.

Secondary (recrystallised) minerals were also seen in samples Pa4, Pa53 and Pa66 (see appendix A.2). In addition to the secondary calcite—easily identified by its birefringence—another mineral with first order birefringence was also observed. This mineral is likely hydromagnesite, which has been previously identified by Villaseñor and Price (2008) as a secondary mineral in plasters from Palenque.

Few small fragments of charcoal were also observed in samples Pa24, Pa25, Pa27 and Pa28, although with no visible cellular structures, which prevented the identification of the wood species.

The nature of the binder

By means of petrography, it was possible to see that roughly half of the samples from Palenque show matrices with hydraulic areas, characterised by a dark and mottled appearance and a low optical activity. In some cases, these characteristics are evenly distributed throughout the lime matrix and in other cases they are localised or restricted to reaction rims around isotropic aggregates and SiO₂-rich phases. Samples with these characteristics include Pa1, Pa24, Pa27, Pa49, Pa50, Pa52, Pa59, Pa60, Pa61, Pa62, Pa63, Pa64, Pa65, Pa66, Pa67, Pa68, Pa69, Pa70, Pa71 and Pa77 (see appendix A.2 and fig. 6.5).

Lime lumps were observed in many plasters, although the biggest lumps, visible even with the naked eye, were from plasters dating from late periods (sample Pa53, Pa86) (see fig. 7.4 in chapter 7 and appendix A.2).

A distinctive characteristic in some of the plasters from Palenque is that they show many shrinkage cracks and clay pellets, as well as a red colour in the matrices. These characteristics were seen in samples Pa49, Pa53, Pa56, Pa86, Pa87 and Pa88, and the upper layer of Pa44, which are from the latest buildings in the sites, as discussed in chapter 7. Based on these characteristics, it is clear that the plasters from late periods have a more clayey nature than earlier plasters. Furthermore, elemental analyses carried out with the SEM/EDS showed up to 24% of SiO₂ and up to 4% of Al₂O₃ in the matrices of the plasters of the Balunté Phase, which supports this idea (see appendix A.3.1). Although it was not possible to characterise clay minerals by means of XRD, the presence of clays was also suggested by the way in which SiO, Al₂O₃, TiO, Fe₂O, Na₂O and K₂O co-varied (see appendix A.6).

Another characteristic that proved to be diagnostic of clayey matrices was the colour of the plasters, which was documented using the Munsell chart. Samples Pa12, Pa19, Pa26, Pa43, Pa44, Pa50, Pa52 show darker colours than the average of the samples, in the range of very pale browns, and samples Pa53, Pa56, Pa86, Pa87 and Pa88, show darker browns and yellowish brown colours (see appendix A.1), which are the samples with clay pellets and shrinkage cracks mentioned above.

Regarding the nature of the lime binder as observed by its crystallography, it was possible to observe agglomerations of platy hexagonal crystals of around 1 µm composed of 90% CaCO₃³ and 9% MgCO₃ in sample Pa62. Masses of anhedral crystals were also seen in Pa18 and Pa71 and few acicular crystals with up to 13% of SiO₂ were seen in sample Pa18. In addition to this, larger interlocking tabular crystals of around 10 µm, entirely composed of MgCO₃ were seen in samples Pa68 and Pa70. It is worth saying however, that although magnesium was combined by stoichiometry to MgCO₃, it is thought that these crystals are composed of brucite, Mg(OH)₂, which is the dominant phase in magnesian limes and forms the characteristic tabular crystals observed in the samples (see tabular crystals reported by Lamprecht 1993 and appendix A.3.2).

Microstratigraphy

Many samples of Palenque show one, two or three layers of limewashes (Pa 19, Pa60, Pa61, Pa62, Pa63, Pa66, Pa67, Pa68, Pa70, Pa71 and Pa72), which is a common feature in Maya plasters. However, other samples show many more layers of limewashes: Sample Pa1 shows 8 layers, Pa24 12 layers, Pa27 17 layers and Pa75 around 60 layers.

³ As was mentioned before, SEM data are reported as carbonates in the case of calcium and magnesium. However, the platy crystals rich in calcium are more likely portlandite, Ca(OH)₂, which shows an incomplete carbonation of the binder.

Moreover, samples Pa27 and Pa75 show extremely thin black layers alternating with the limewashes, which is clearly observed in optical reflected microscopy. Pa24, on the other hand, does not show black layers between the numerous limewashes (see fig. 6.7 and 6.8).

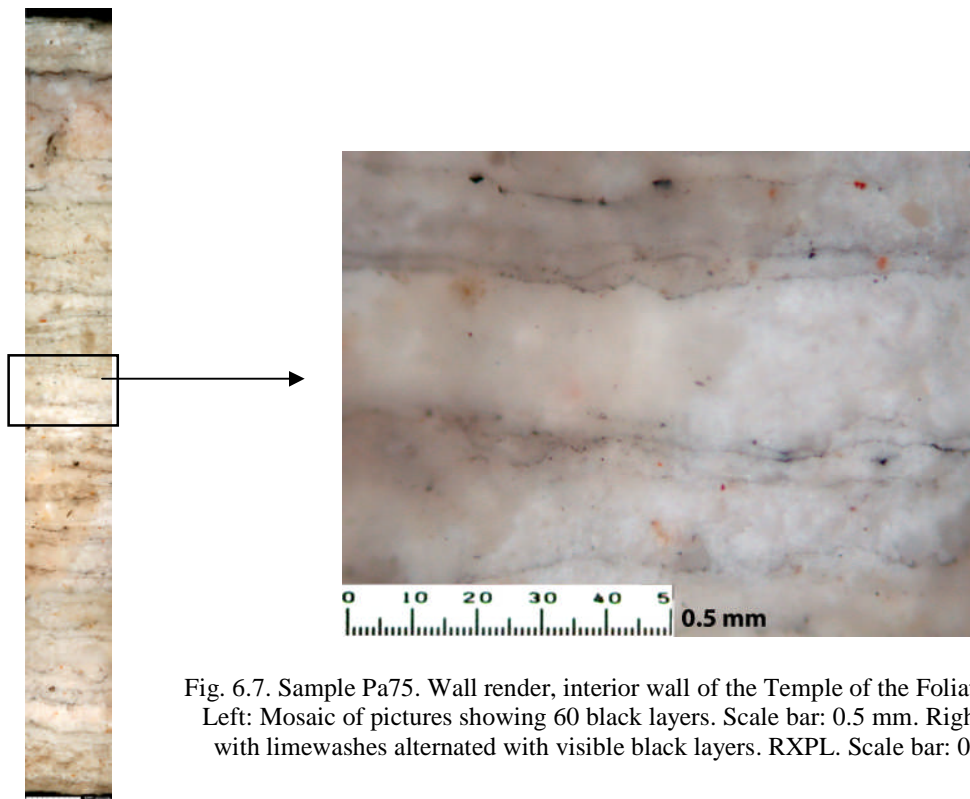


Fig. 6.7. Sample Pa75. Wall render, interior wall of the Temple of the Foliated Cross. Left: Mosaic of pictures showing 60 black layers. Scale bar: 0.5 mm. Right: detail with limewashes alternated with visible black layers. RXPL. Scale bar: 0.5 mm.

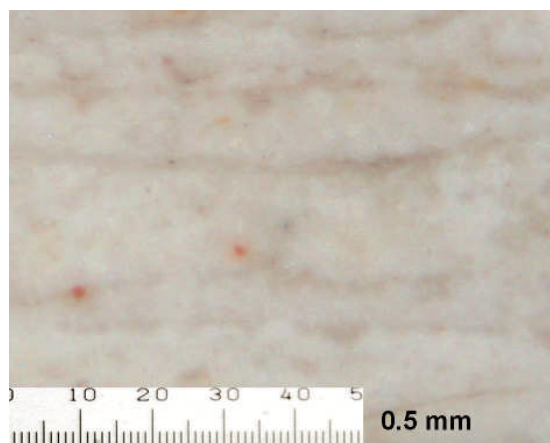


Fig.6.8. Sample Pa24. External wall from the rear façade of the Temple of the Sun. Limewashes with no visible black layers. RXPL. Scale bar: 0.5 mm.

It is not possible to measure the thickness of the black layers accurately with optical microscopy but they are less than 5 μm thick. They do not show on the SEM, very likely because they are composed of carbon (graphite) and therefore do not differentiate chemically from the lime plaster.

Sample Pa1 also shows a black layer, but it is thicker than the ones observed in the wall renders of the Temples of the Cross and the Foliated Cross, and measures around 10 μm .

In addition to the limewashes, some plasters of Palenque, mainly floors, showed replastering sequences, that is to say, the application of successive layers of lime plasters for renovation purposes. This was observed during on-site observations, as in the case of Pa2a and Pa2b, which correspond to two different floor applications of the House I of the Palace, and samples Pa77 and Pa78, which are wall renders corresponding to two plastering moments of House I. Replastering was also seen in the floor of the Temple of the Foliated Cross and the House D of the Palace. In some other cases, replastering became evident only when samples were prepared and observed under the petrographic microscope (Pa49, Pa59 and Pa77).

The Temple of the Foliated Cross is a very particular case regarding replastering. In addition to the 60 limewashes in the wall renders of the Temple, a sequence of 15 layers of floors was seen in the stepped platform of this building. Moreover, when each of these layers of floors was observed under the microscope, most of them showed two or more applications of limewashes (see appendix A.2.1). However, the stepped platform of the Temple of the Foliated Cross has not been excavated and it is not known the total number of floor layers and their distribution in the platform (see fig. 6.9).



Fig. 6.9. Sequence with 15 layers of floors in the stepped platform of the Temple of the Foliated Cross. Left: General view. Right: detail (scale bar 5 cms).

Pigments and coloured surfaces

Although many pigments have been reported to be present in the architectural surfaces of Palenque (see Robertson 1979), only black layers were observed in the sample analysed (samples Pa1, Pa27, Pa41, Pa75 and Pa85). It was not possible to analyse the black layers with the SEM, since they were not visible in the compositional images, and Raman spectroscopy was therefore employed for their analysis. Sample Pa41 showed peaks at 1300 and 1580 Raman shift (cm^{-1}), which correspond to the

peaks of graphite; sample Pa72 showed peaks at 1087 and 1782, representing the peaks of calcite and an unknown mineral; finally sample Pa85 yielded peaks at 1087, 1300 and 1580, confirming the presence of calcite and graphite (see appendix B.2).

The nature of limestones and local raw materials.

Four samples of limestones were analysed from Palenque. They all showed crystals of ca. 10 μm in size, and their bulk composition ranged between 37% and 40% of MgCO_3 , and between 55% and 58% CaCO_3 , indicating a dolomitic composition (see appendix A.6.2). Veins of iron oxides and small inclusions of detrital quartz were seen in some of the samples (see appendix A.2).

Shells from the Otulum River were also analysed, as they constitute alternative raw materials for lime production. They proved to be composed of 99% of CaCO_3 and 0.4% of Na_2O , as well as high contents in SrO (see appendix A.6). This is further discussed in Chapter 7.

6.2. Calakmul

Bulk elemental composition

The major component of the plasters from Calakmul was CaCO_3 , ranging between 56% and 95%, followed by SiO_2 , which ranged between 3% and 40%. Terminal Classic samples are higher in SiO_2 and Al_2O_3 than the rest of the samples, but samples Ca26 and Ca29, from the Late Classic and Late Preclassic periods respectively, show the highest content in SiO_2 (21% and 40% respectively) (see fig. 6.10).

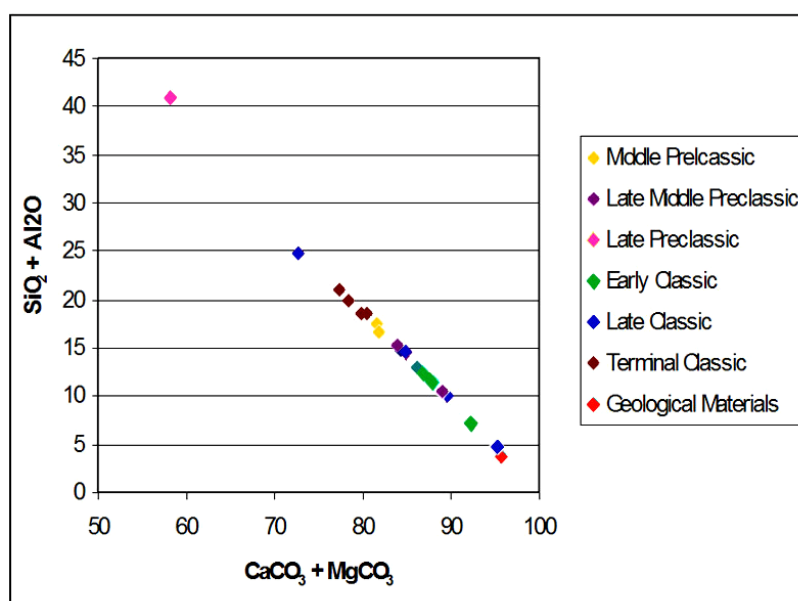


Fig. 6.10. $\text{CaCO}_3 + \text{MgCO}_3$ vs $\text{SiO}_2 + \text{Al}_2\text{O}_3$ scatter plot (weight %) of Calakmul samples. Carbonate contents were obtained by stoichiometric calculations of oxides, as obtained by XRF.

Only few samples show some content in alkaline oxides (Ca29, Ca36, Ca34, Ca13, Ca33), which were positively correlated with TiO₂, MnO, Fe₂O₃, CO₃O₄. In the case of Ca9, it shows the highest contents in MgCO₃, CO₃O₄, CuO, ZnO, RbO, and SrO. The composition of Ca26 was also unique and showed the lowest content in CaCO₃, and some of the highest in the rest of the elements (see appendix A.6).

The dendrogram obtained by cluster analysis of bulk elemental compositions shows that samples Ca9 (Middle Preclassic) and Ca29 (Late Preclassic) are the most dissimilar from the rest of the samples. The analysis also clearly distinguishes a group for the Terminal Classic samples, Ca33, Ca4, Ca34, but also includes Ca12, which is dated in the Middle Preclassic Period. The groups formed for the rest of the samples do not correspond clearly with any specific chronological period (see appendix A.6.3)

Principal component analysis (PCA) shows a relatively high dispersion, but Terminal Classic samples are clearly away from the average composition, and distant from the composition of local limestones (see fig. 6.11 appendix A.6.4).

As can be seen in the component plot (appendix A.6.4), CaCO₃ is strongly negatively correlated with the rest of the elements, and slightly correlated with BaCO₃. Al₂O₃ and SiO₂ are positively correlated with each other but not as strongly as in the case of Palenque. ZnO, and SrO are also correlated with each other (see appendix A.6.4)

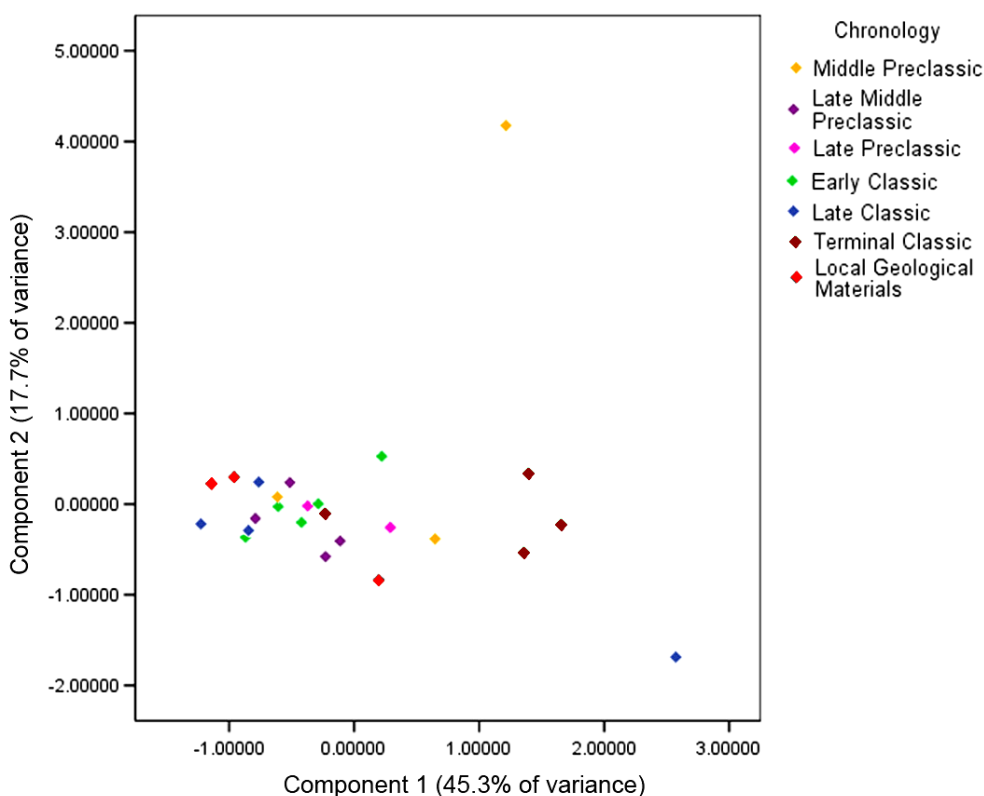


Fig. 6.11. Principal component analysis of XRF compositional data of Calakmul samples.

Mineralogy and the nature of inclusions

The mineralogy of the samples from Calakmul proved to be highly calcareous. XRD analyses identified calcite in all of the samples. Additionally, dolomite was characterised in Ca13, whereas quartz and possibly montmorillonite were identified in sample Ca33.

The aggregate material in Calakmul consisted, in the vast majority of the cases, of rounded particles of micritic calcite up to 20 mm in size. Aggregates of micritic calcite prevailed overwhelmingly over aggregates of crystalline calcite grains in all the samples.

In addition to calcareous aggregates, a few grains of quartz were seen in samples Ca1, Ca2, Ca4, Ca14, Ca23 and Ca26. Grains of polycrystalline quartz were observed in samples Ca5 and Ca24.

Other inclusions were seen as rounded aggregates of fibrous crystals of first order birefringence in samples Ca2, Ca3, Ca5, Ca6, Ca7, Ca8, Ca9, Ca15, Ca14, Ca14 and Ca30. Elemental analyses showed a composition between 54% and 77% of SiO_2 , between 7% and 20% of MgCO_3 , and between 2% and 13% of Al_2O_3 which indicates the presence of an aluminosilicate, likely cordierite (see fig. 6.12 and appendix A.2 and A.4). In addition to these inclusions, isolated fibrous crystals mixed with carbonate materials were observed in samples Ca29 and Ca9, although

their composition did not contain any Al_2O_3 , which suggests the presence of a mineral from the serpentine group (see chapter 7 for discussion).

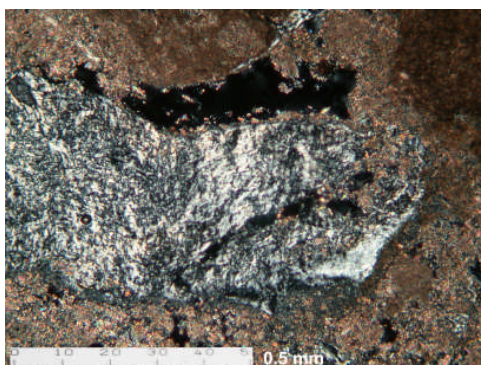


Fig. 6.12. Aggregate formed by aluminosilicate crystals, likely cordierite. Sample Ca9. XPL. Scale bar: 0.5 mm.

Yellow isotropic inclusions were observed in samples Ca5, Ca7, Ca8, Ca11, Ca13, Ca14, Ca16, Ca18, Ca19, Ca22 and Ca23.

A yellow inclusion in Ca16 was analysed with the microprobe and proved to be composed of 64% SiO_2 , followed by MgCO_3 and Al_2O_3 as the major components (see appendix A.4). In occasions this material was seen in apparent association with acicular phases (see fig. 6.13).

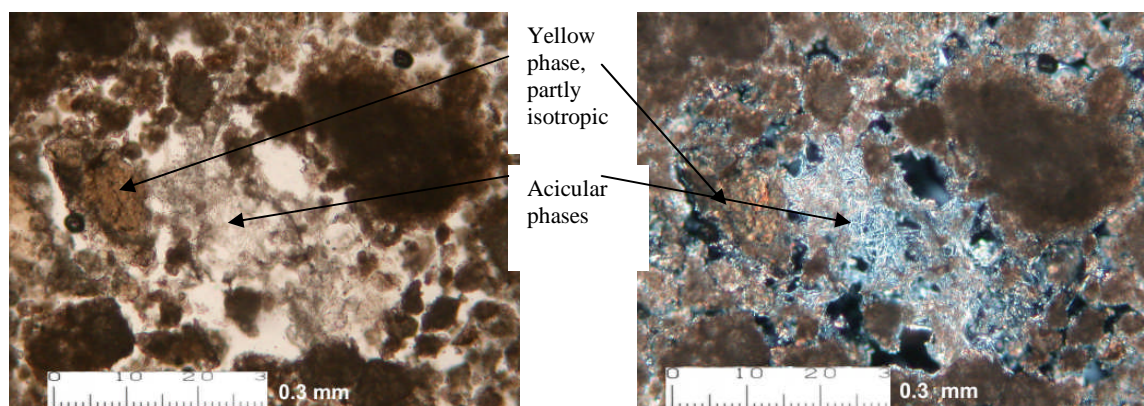


Fig. 6.13. Ca16. Yellow mineral associated with acicular phases. See appendix A.4. for composition.

Acicular phases, sometimes rich in SiO_2 and Al_2O_3 , were also seen in association with reaction rims (sample Ca11) and with phases rich in CaCO_3 and SO_3 (sample Ca18). SO_3 , however, was also a major component of the mounting resin and the analysis is therefore not conclusive in this respect (see appendix A.4).

Shells were observed in samples Ca4, Ca10, Ca16. The shell in Ca10 is a likely a *Cyrenia* shell (Schoelle and Ulmer-Schoelle 2003:164), but the species of shells in the rest of the samples were not identified (see appendix A.2.2).

Other interesting inclusions were isotropic materials with visible cellular structures. These inclusions were seen in many samples, but most frequently in the Late Middle Preclassic and the Terminal Classic periods. They were also present in the sascab sample. When analysed, they showed a composition of 100% SiO₂. It was also observed that these materials were forming part of carbonate aggregates (see fig. 6.14 and appendix A.2).

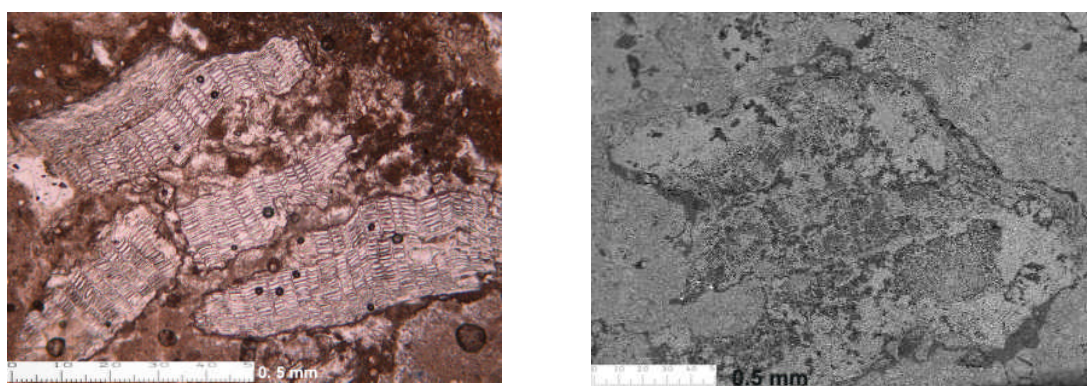


Fig. 6.14. Ca30. Inclusions with cellular structure. Left: PPL. Scale bar: 500 microns. Right: BSE image that shows they are part of a carbonate aggregate. Scale bar: 500 μ m.

In addition to the isotropic inclusions with visible cellular structures, few fragments of charcoal were seen in samples Ca2, Ca3, Ca5, Ca6, Ca10, Ca18, Ca24, Ca26 and Ca36. As in the case of Palenque, the fragments were too small to show a cellular structure and it was therefore not possible to identify the species of tree.

Ascidian fossils were also observed in most of the samples from Calakmul, although magnifications higher than 400x were required in order to observe them (see fig. 7.19)

The nature of the binder

The matrices of binders proved to be relatively high in CaCO₃ and with normal calcite birefringence. However, on occasion considerable amounts of SiO₂ were detected in the matrices by means of EDS attached to the SEM. Although the average content of SiO₂ in the matrices of Calakmul was 15%, samples Ca3 and Ca13, from the Terminal Classic and the Early Classic period, showed the highest contents with up to 21% and 47% of SiO₂ respectively, although variation in composition was very high depending on the area of analysis (see appendix A.3.1). By means of petrography, this was seen to be the result of clay and iron-rich matrices (see chapter 7 for discussion).

Samples from the Terminal Classic period (Ca3, Ca4 and Ca34), and to some extent samples from the Early Classic (Ca1, Ca13 and Ca22), show darker colours in comparison to the rest of the samples, ranging in pale browns and light grays (see appendix A.1). When observed

under the polarising microscope, the matrices of these plasters showed multiple cracks and plant roots inside the cracks (see appendix A.2.2).

Clear hydraulic areas and hydraulic reactions were seen with the petrographic microscope in samples Ca5, Ca7, Ca10, Ca11, Ca16. The reaction rims in sample Ca11 were analysed with the microprobe and proved to be composed of 38% SiO₂ and 60% CaCO₃. Acicular phases inside the reaction rims in this sample showed a composition rich in CaCO₃, SiO₂ and Al₂O₃ (see appendix A.4.)

The analyses of crystal fabrics of the binder showed agglomeration of hexagonal platy crystals (samples Ca10, Ca14, Ca15, Ca18), hexagonal prisms (Ca5, Ca8, Ca14, Ca15, Ca16) and agglomerations of euhedral or subhedral polyhedrons (Ca8, Ca14), all of them almost entirely composed of CaCO₃. Elongated, bladed and acicular crystals with up to 11% in SiO₂ were seen in samples Ca7, Ca8, Ca18 and Ca15, and foliated crystals with up to 70% in SiO₂ were present in sample Ca5. Sample Ca8 also showed elongated habits with rounded edges, whereas sample Ca5 showed globular and amorphous inclusions almost entirely composed of SiO₂ (see appendix A.3.2). In samples Ca3 and Ca 4, euhedral crystals were not observed, but only carbonate particles in a clay-size cement (see fig. 6.15 and appendix A.3.2).

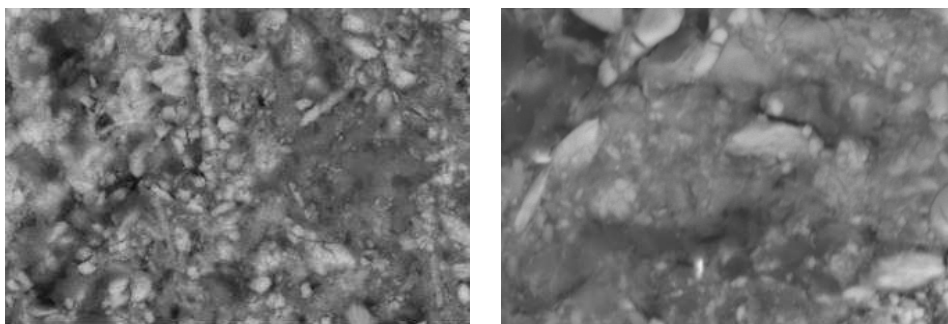


Fig. 6.15. Clay-size calcareous materials. Left: Ca3, BSE image, scale bar: 20 microns. Right: Ca4. BSE image, scale bar: 20 μ m.

Microstratigraphy

The presence of limewashes is a common feature in the samples from Calakmul. One layer of limewash could be seen in samples Ca5, Ca6, Ca7 and Ca10, and two layers were seen in sample Ca16.

Replastering was also seen on site in the floor sequence of structure VII (samples Ca29 and Ca30), and in substructure II-d (samples Ca9 and Ca10). In other cases, replastering was not observed until samples were observed under the microscope; samples Ca6 and Ca18 showed two layers of plasters, whereas Ca16 showed three layers.

Another interesting feature was the observation of isotropic layers of around 200 microns in thickness on the surface of samples Ca6, Ca18 and Ca31. The layer of sample Ca31 was analysed with the microprobe and showed a composition of 97% of SiO₂.

Pigments and coloured surfaces

Although pigments were not the main research question of my thesis, some of the plaster samples from Calakmul had painted surfaces and they were therefore analysed together with the plasters.

The plaster samples from the frieze of substructure II-c1 (Ca5 and Ca7) showed extremely thin paint layers, homogeneously applied over thin limewashes. Samples from later periods (Ca14 and Ca35) showed thicker layers less homogeneously applied (see appendix B.1).

Regarding the composition of the pigments with Raman spectroscopy, samples with red paint layers (Ca5, Ca7, Ca14 and Ca35) showed some of the characteristic peaks of hematite at 225, 292 and 409 Raman shifts (cm⁻¹), although in occasions with very weak signals. The observation of pigment dispersions of Preclassic red paint layers (Ca5 and Ca7) showed the presence of dark red birefringent particles and areas with a pink hue. Red paint layers from the Early Classic period (Ca14 and Ca35), on the other hand, showed red, yellow and black particles.

Sample Ca8, with a yellow paint layer, also yielded peaks at 294 and 409 Raman shifts (cm⁻¹), although many other peaks were not identified. Under the petrographic microscope, the dispersion of this yellow paint showed carbonate particles with yellow material with very small particle size. The sample also showed small orange and yellow isotropic particles.

The black paint layer of Ca35 showed the characteristic peaks of graphite at 1360 and 1580 Raman shifts (cm⁻¹), and under the petrographic microscope the black pigment proved to be composed of a mixture of dark brown, yellow and red particles, which indicates the presence of graphite (see appendix B.1 and B.2).

The nature of limestones and local raw materials.

All limestones from the quarries close to the centre of the site, and the one taken from structure XIII proved to be pelloidal limestones, that is to say, formed by pellets of micritic cement less than 2 mm in size supported by micritic cement. These limestones also showed a very calcitic composition, with 95% of CaCO₃ and 3% of SiO₂. The sascab consisted of reworked subrounded sediments of micritic calcite, with a bulk composition of 84% of CaCO₃ and 11 % of SiO₂ (see appendix A.2 and A.6).

6.3. Lamanai

Bulk elemental composition

All of the samples from Lamanai are highly calcitic, most of them with more than 90% CaCO_3 . MgCO_3 is lower than 1% in all of the samples, and many other elements such as Na_2O , K_2O , CO_3O_4 and NiO were below the detection limits of the equipment in most of the samples.

The samples with higher SiO_2 and Al_2O_3 contents proved to be in the majority of the cases Late Postclassic or Early Spanish Colonial, with up to 12% SiO_2 and 6% Al_2O_3 (see fig. 6.16).

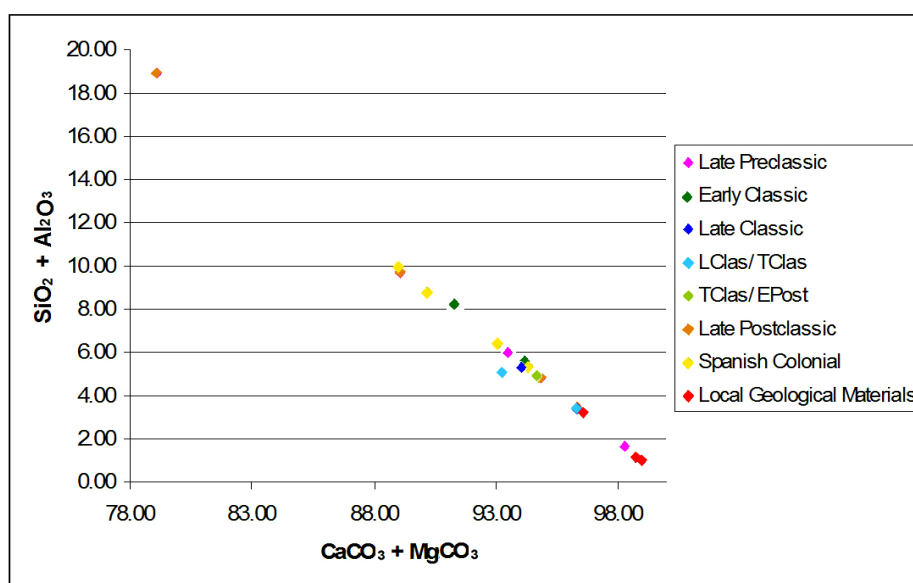


Fig. 6.16. $\text{CaCO}_3 + \text{MgCO}_3$ vs $\text{SiO}_2 + \text{Al}_2\text{O}_3$ scatter plot of bulk XRF data of Lamanai samples.

Samples La3 and La44, from compacted sascab floors (see discussion, chapter 7), also showed high contents in SiO_2 and Al_2O_3 .

Cluster analysis shows a short distance in the different groups, showing that the chemistry of Lamanai samples is very similar. The groups do not correspond clearly to the chronological periods (see appendix A.6.3).

Principal component analysis does not show any specific groups, but suggests that Late Postclassic and Spanish Colonial samples are the most dissimilar from the rest of the samples and are located away from the local raw materials (see fig. 6.17 and appendix A.6.4).

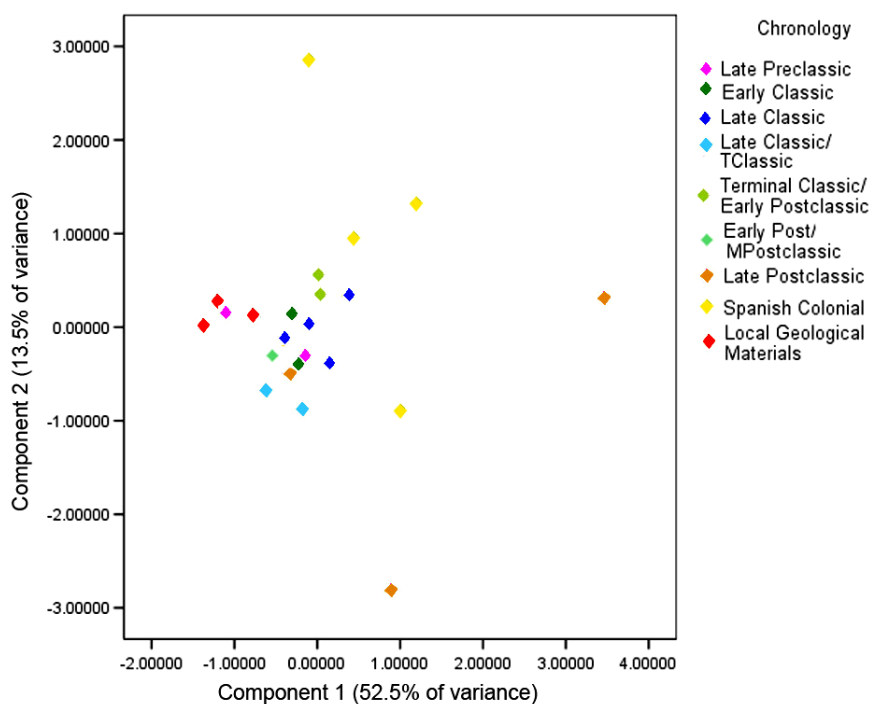


Fig. 6.17. Principal component analysis of bulk XRF compositional data of Lamanai samples.

The component plot of the PCA shows that AlSiO_2 , SiO_2 , Fe_2O_3 , ZnO , ZrO_2 and MnO are strongly correlated with each other. CaCO_3 is negatively correlated with the rest of the elements.

Mineralogy and the nature of inclusions

The mineralogy of Lamanai samples was also highly calcareous. XRD analyses showed the dominant peaks of calcite in all samples. The sascab sample, however, showed peaks at 44.8 and 50.9 of 2θ values that were not identified and which were not present in the archaeological plasters (see appendix A.5).

Petrographic observations showed that subrounded aggregates of micritic calcite were the most often employed material in early plasters (Late Postclassic, Early Classic and Late Classic), whereas larger aggregates of crystalline limestones (polycrystalline calcite) predominate over micritic calcite from the Terminal Classic period onwards (see appendix A.2).

Also by means of petrography, and in addition to calcareous materials, quartz was observed in Terminal Classic samples, but most abundantly in Late Postclassic and Spanish Colonial samples (La9, La5, La20, 32b, La45, La48). Some of the quartz grains are associated or embedded in isotropic phases, and some appeared to be shocked, although the latter characteristic cannot be

confirmed with certainty. The presence of quartz was also identified by XRD in samples La49 and La21, from Late Postclassic and Spanish Colonial architecture respectively.

Late Postclassic and Spanish Colonial samples also showed devitrified glass, which was characterised by angular edges and high content in SiO_2 . Devitrified glass was also accompanied by several isotropic phases with a characteristic yellow colour under PPL, which proved to have also a composition high in SiO_2 and Al_2O_3 (see appendix A.2.2 and A.4).

Foraminifera fossils were observed in samples La4 and La16, from the Late Classic period.

A very particular type of inclusion was seen in sample La6, which consisted in the apparent use of fragments of recycled plaster that were employed as aggregate material in the new plaster. In some of the recycled fragments it was possible to see a red paint layer overlain by a green/blue paint layer. Within the recycled plaster fragments, fragments of ceramics were observed, which were in turn tempered with quartz (see fig. 6.18).

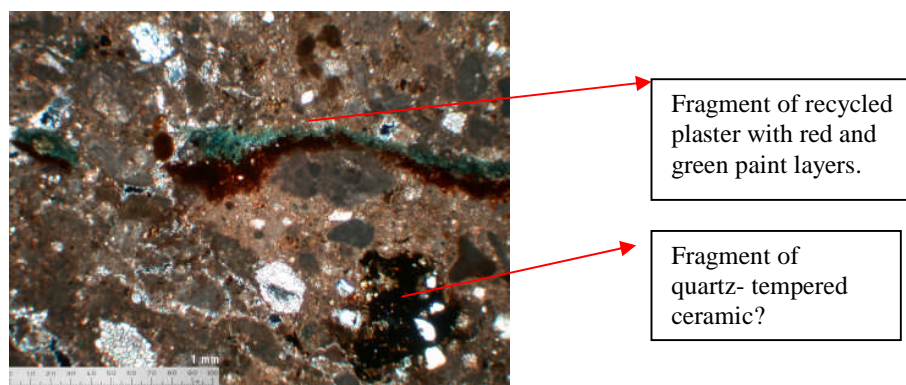


Fig. 6.18. Sample La6. Fragment of plaster recycled as aggregate. Red and blue/green paint layers can be seen, and possibly the use of ceramic as aggregate in the recycled plaster.

The nature of the binder

Most of the samples showed a very pure white non-hydraulic lime binder, although samples La29, La32a and La36a showed darker matrices with a clayey appearance.

Some of the samples from the Late/Terminal Classic, Late Postclassic and Spanish Colonial (La6, La9, La22, La36b, La49, La50, La19, La20 and La21) show areas with a slightly hydraulic matrix.

Some floor samples, ranging from the Late Preclassic period to the Early Middle Postclassic, proved to be entirely composed of micritic calcite, without the apparent use of aggregates (samples La31, La34, La46, La47, La3, La7, La13, La14, La35, La2). On occasion cracks running parallel to the surface were observed (see discussion in Chapter 7).

A very common feature in the samples from Lamanai was the observation of hexagonal prisms of calcite up to 100 μm in size. These crystals were seen in three forms: as isolated crystals

in the matrices; forming masses in lime lumps; and in bands or channels (see Fig. 6.19 and appendix A.2.2).

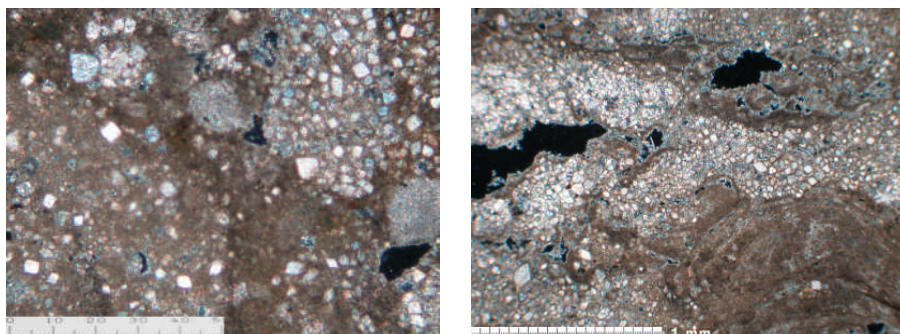


Fig. 6.19. Hexagonal prisms of calcite. Left: sample La9, isolated crystals in matrix. XPL, scale bar: 0.5 mm. Right: sample La31. Crystals in channel. XPL, Scale bar: 1 mm.

SEM/EDS analyses showed that the hexagonal prisms were entirely composed of CaCO_3 . In sample La21, it was clear that the large calcite prisms were cemented by a mass of smaller anhedral crystals. Sample La4 and La19 showed prisms with smaller platy crystals in the faces of hexagonal prisms.

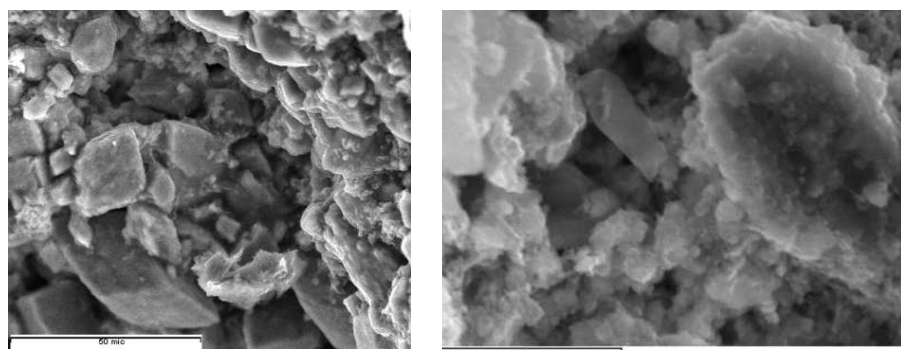


Fig. 6.20. Left: sample La21. Large rhombohedral prisms cemented by smaller crystals. SE image. Scale bar: 50 microns. Right: sample La19. Large rhombohedral crystal with smaller platy crystals in its faces. Scale bar: 10 microns.

Elongated crystals with up to 19% of SiO_2 were also observed in the binders of samples La4 and La28, and a large crystal with a foliated structure entirely composed of CaCO_3 was observed in sample La10 (see appendix A.3.2).

Microstratigraphy

Replastering applications were clearly seen on site in structure N10-43, which showed two layers of floors. Structure N10-15 (Late/Terminal Classic) and the additions in the northern part of this structure (Terminal Classic/Early Postclassic) also showed two layers of very hard floors. Structure P9-25 (Holiday House) showed two visible floors too, the lower one being 20 cm thick. Structure

N12-11 was observed to have two layers of floors in the steps of the north facade, each of them with a red paint layer. Finally, the fragment of plaster recovered from a pit west to structure N12-11 (YDLI) showed 5 thick layers of variable appearance (samples La36a and La36b). See fig. 6.21.



Fig. 6.21. Left: two layers of floors in Str. N10-15. The picture looks south. Right: five thick layers in debris recovered in the pit west of Str. N12-11 (YDLI) (samples La36a and La36b).

In addition to these re-plasterings, limewashes were frequently seen when the samples were observed under the petrographic microscope, especially in the Late Postclassic period (see appendix A.2.1).

In addition to the application of floor layers and as mentioned in Chapter 2, the architecture of Lamanai showed numerous renovations, which is a common characteristic of ancient Maya architecture. Structures N10-78 and N10-79, for example, show several construction phases during the Late Classic, with many floors and fill material (see Graham 2004).

Pigments and coloured surfaces

Red paint layers were seen in samples La6, La24, La25, La49 and La50. When observed in cross section, sample La6 showed an orange layer underlying the red paint layer.

The red and orange paint layers of the thin section in sample La6 were prepared as pigment dispersions. The pigment proved to be a mixture of dark red and orange particles mixed with calcite.

As mentioned above, sample La6 showed a plaster fragment with a red and a green/blue layer that was recycled as aggregate. Further sampling from these paint layers taken with the scalpel from the thin section was carried out in order to prepare pigment dispersions. The blue layer showed a homogenous translucent bright blue, and under crossed polars the substrate proved to be a clay mineral, indicating the presence of Maya blue. The red layers showed red, orange and pink

hues under plane polarised light and were observed to be birefringent under XPL (see appendix B.1).

The nature of limestones and local raw materials.

Samples of sascab also showed a very calcitic composition, with CaCO_3 as the major component (96-98%), followed by SiO_2 (1-2%). Under the petrographic microscope, they proved to be subrounded sediments of reworked micritic carbonates materials on occasion with recrystallised calcite.

Sample La23, a limestone sample from Spanish Colonial architecture was composed of 93% CaCO_3 and 4% SiO_2 , but a crystalline limestone employed in the restoration work of YDLI (sample LaCret) showed a composition of 99% CaCO_3 .

7. Discussion of Results

In this chapter I discuss the results presented in Chapter 6. The discussion is organised by each of the sites under study and revolves around the interpretation of the chemistry, mineralogy and micromorphological characteristics of the plasters, which is in turn discussed in terms of ancient technology and its significance in ancient Maya culture.

7.1. Palenque

The discussion of the results of Palenque involves many interesting features and it is divided into: variation in calcium and magnesium contents; the use of clays and the decline in plaster technology; the use of meteoritic material; and the evidence of ritual practices in the plasters.

Variation in Ca and Mg contents

As mentioned in Chapter 6, all of the plasters show a significant content in MgCO_3 in their bulk chemistry, but some samples have low contents in MgCO_3 and high contents in CaCO_3 (see fig. 6.1). A relevant aspect of this phenomenon is that the variation in CaCO_3 and MgCO_3 indicates whether calcitic or dolomitic limestones were employed as raw materials for lime production and aggregate materials.

Given that XRF was a bulk compositional analysis, it is necessary to discuss whether MgCO_3 contents occur in the lime matrices, in the aggregates or in both. Regarding the aggregates, the vast majority of the plasters from Palenque showed crystalline calcareous aggregates when observed under the petrographic microscope. Given that dolomite and calcite have similar optical properties, only distinguishable with the use of staining techniques, some of the crystalline aggregates were analysed with EDS and proved to be dolomite. In addition to the use of dolomitic aggregates, and as mentioned in Chapter 6, the binder of the samples that was analysed by SEM/EDS proved to have the characteristic tabular crystals of brucite, entirely composed of MgCO_3 ¹, which indicates that magnesium contents come both from binders and aggregate materials.

The elevated concentrations of MgCO_3 in the plasters from Palenque are consistent with the stone samples from buildings of the site that were also analysed, which also showed a dolomitic composition. Although the geology of the site has not been described in detail, the bedrock of the site has been reported as being dolomitic (Littman 1959). Robertson (1983) includes some pictures

¹ Although results are reported as carbonates, in this case it is likely that magnesium is present as brucite, $\text{Mg}(\text{OH})_2$.

of stone quarrying at Palenque, and although she did not analyse the chemistry of the samples, a dense laminated light reddish appearance can be observed that suggests dolostone (see fig. 7.1).



Fig. 7.1. Stone quarrying at Palenque, likely dolostone (Robertson 1983).

Despite the high contents of MgCO_3 in most of the plaster samples, some samples (Pa2a, Pa47) show a very calcitic composition, with more than 80% CaCO_3 and less than 10% MgCO_3 . This phenomenon has previously been reported by Littman (1959b) and Villaseñor and Price (2008). The latter documented a much higher content in CaCO_3 in limewashes and finishing layers compared to underlying plasters in the sculptures of the Temple of the Inscriptions. A possible explanation for the low contents in MgCO_3 is the use of calcitic deposits within the folded limestone platform of the Chiapas Mountains as raw materials for the plasters. Although it has not been explored in detail, it is likely that parts of this massif are low-magnesium limestones since dolomitization—the replacement of CaCO_3 by MgCO_3 in limestones—does not affect carbonate structures homogeneously (Deelman 2005). However, exploitation of calcitic limestones from the more recent Yucatan platform to the north of Palenque, or the use of shells for lime production is also a possibility.

As described in Chapter 3, shells have been used traditionally in Maya culture as raw materials for lime production in the processing of maize. The snail shells analysed by means of XRF demonstrate that they have a CaCO_3 content of 99% and some contents of Na_2O and K_2O , although they do not have any other diagnostic element that would confirm their usage in lime plasters. Although shells are primarily constituted of aragonite—a polymorph of CaCO_3 —, aragonite is transformed irreversibly to calcite in temperatures above 400°C and it is therefore not possible to detect aragonite in lime plasters made with shells, since the required calcination temperature is around 900°C (Boynton 1980:30). Although fragments of shells were observed in the

plasters of Palenque, no signs of burning were observed, and it is thought they constitute aggregate materials rather than relic material from lime made with shells.

Although the analyses are not conclusive in the identification of raw materials for calcitic limes, it is thought that limestones from non-dolomitized pockets in the Palenque region are the most likely source of raw material for the calcitic plasters of Palenque. The use of snail shells cannot be ruled out, but it is considered that the sheer amounts of shells required to produce architectural plasters makes this idea a less likely hypothesis.

PCA analysis shows that $MgCO_3$ is strongly negatively correlated with $CaCO_3$, which reflects the nature of calcium replacement in dolomite formation. This negative correlation between $MgCO_3$ and $CaCO_3$ results in the vertical tendency that can be seen in the scatter plot (see fig. 6.3, Chapter 6) when compared to the PCA component plot (Fig. A.6.4.3 in appendix A.6).

By looking at fig. 6.1 (Chapter 6), it is not possible to establish a relationship between $MgCO_3/CaCO_3$ ratios in the plasters and the different chronological periods, which indicates that different types of raw materials were employed within the same chronological period and that their selection was more likely related to workability or performance characteristics desired for the plasters than to changes in building traditions through time.

One reason to think that selecting calcitic raw materials was a deliberate option is the fact that dolomitic limes are difficult to slake, especially if they are fired over $900^\circ C$, which causes popping months after the plaster has been applied (Seeley 2000). Related to the slaking practices, archaeologists working at Palenque recently found containers carved into the bedrock of the Picota Group (Cuevas Garcia, personal communication) that may have served for lime slaking. If this is the case, slaking practices at Palenque would have been in clear contrast to the rest of the lowland sites, which most likely used open-air slaking practices, as modern Maya lime production is carried out nowadays (see Chapter 3). The use of lime slaking in containers with a quantity of water is also supported by the observation of small platy crystals that were observed in the binders of the plasters from Palenque (see sample Pa62, appendix A.3.2), which are much smaller than those observed in the samples from Calakmul and Lamanai, which showed rhombohedral prisms. Crystal habits and sizes in lime binders are known to be related to the degree of slaking, since well-slaked lime putties develop small platy crystals of calcium hydroxide that influence the crystal sizes of the carbonated phases (Rodriguez-Navarro et al 1998, Hansen et al 2008, Cazalla et al 2000).

If a thorough slaking is achieved, there is no reason why dolomitic limestones should be avoided as raw materials for lime production. In fact, the large tabular interlocking crystals of brucite that are formed in dolomitic limes have been considered to be responsible for the higher hardness and mechanical behaviour of these types of plasters (Seeley 2000:22). As mentioned in

Chapter 6, large interlocking crystals of brucite were seen with the SEM in the plasters of Palenque (see appendix A.3.1), and they are most likely what makes Palenque's plasters so resistant despite the difficult conservation problems imposed by the extreme weather of the site, a characteristic that is well known to archaeologists (Hernandez Reyes and Peralta Bárcenas 1974).

Given that calcitic and dolomitic limestones (dolostones) are visually different—the dolostone being usually light grey—, it is considered that there was a deliberate selection in the different raw materials, and that the variation in MgCO_3 contents is therefore due to experimentation to obtain specific characteristics in the plasters.

The use of clays and the decline of plaster technology

As mentioned in Chapter 6, cluster analysis and principal component analysis (PCA) of compositional data resulted in a very specific group formed by samples from the Balunté Phase period and from architectural modifications. It is worth noting that in this case PCA analyses groups together different types of samples (i.e. wall renders and floors) of the same period, which suggests that the chronological period rather than the type of samples is the factor influencing the grouping (see appendix A.6.4).

The group formed by Balunté Phase and architectural modification samples is characterised by low contents in carbonates and high contents in Al_2O_3 , SiO_2 , TiO , Fe_2O_3 , NiO , RbO , ZrO and K_2O . As observed in the component plot of the variables (appendix A.6.4), it is clear that there is a strong correlation between these elements, which suggests the presence of clay minerals. The presence of clays was confirmed by the observation of red/brown colours and multiple shrinkage cracks in the matrices under the petrographic microscope. In addition to this, quartz was observed to be the main aggregate material.

Samples from the Balunté phase and from architectural modifications also showed considerable amounts of shells employed as aggregates (see fig. 7.2). Shells were very likely added as an attempt to provide an interlocking effect in the plasters and compensate for the low cohesion of the clayey material in comparison to a lime binder.

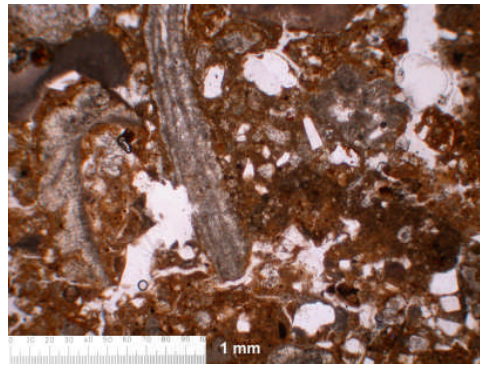


Fig.7.2. Pa56. Clayey matrix with shrinkage cracks. Shell fragment may have been used to compensate for the low cohesion and poor mechanical properties of these plasters. PPL. Scale bar: 1 mm.

Although the dating of the buildings in Palenque cannot be accurately established due to the scarce stratigraphic evidence, it is clear that the structures from which the clayey samples were taken—the North Group and the Bats complex—constitute some of the latest buildings of the site. Temple IV of the North Group, from which samples Pa86 and Pa87 were taken, was the last one to be built at the North Group and shows ceramics from the Balunté phase (Tovalin Ahumada and Ceja Manrique 1993, Rands 1974). The Bats Complex, from which samples Pa53 and Pa54 were taken, is the place where the latest date of the site (799 AD), painted on a ceramic vessel, was discovered (Martin and Grube 2000). Finally, samples Pa40 and Pa80, which also proved to be of clayey composition, were taken from architectural modifications at the Temple of the Foliated Cross and the House D of the Palace respectively. Although these walls cannot be associated with any particular ceramic complex, they were clearly added after the first moment of construction, modifying the plans of the original buildings (Cuevas and Gonzalez 2007), which can be clearly seen on site (see fig. 7.3). The clayey nature of the plasters can sometimes be observed with the naked eye and is characterised by brown colours, a crumbly consistency and the presence of unmixed lime lumps (see fig. 7.4).

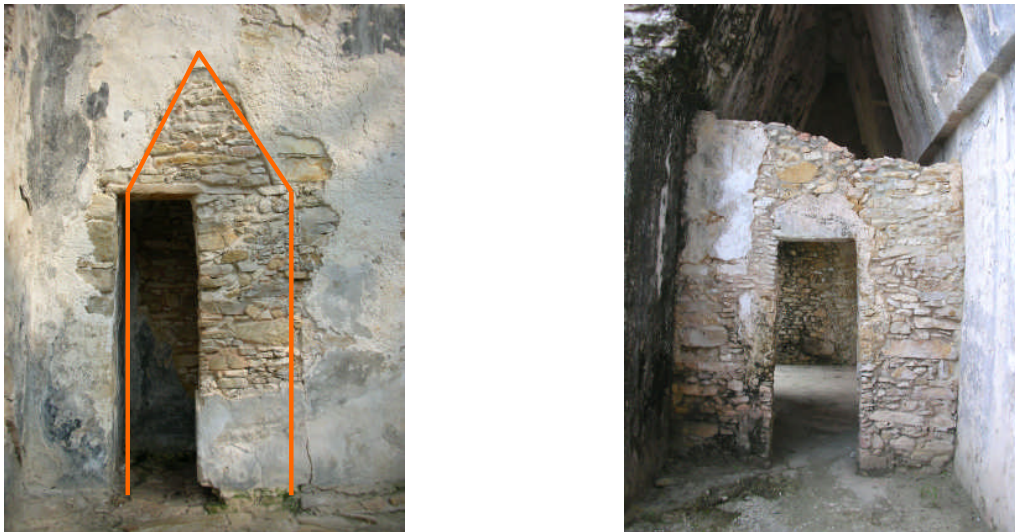


Fig. 7.3. Architectural modifications. Left: modification of a doorway at the Temple of the Foliated Cross with partially lost mud plaster. The orange line shows the original shape of the doorway. Right: dividing wall in the House D of the Palace.



Fig. 7.4. Dividing wall (architectural modification) at the Temple of the Foliated Cross. Mud plaster with unmixed lime lumps. A limewash painted on black can be seen at the left.

In addition to the North Group, the Bats Complex and the architectural modifications, clay-based plasters were seen in the Temple of the Red Queen and the Temple of the Skull, although no samples were taken from the latter two buildings.

It has been suggested that the dividing walls were built by squatters that lived temporarily in Palenque after the site was abandoned (Marken 2006). However, although it is not possible to date these architectural modifications, the compositional and micromorphological similarities between the plasters from dividing walls and those from the North Group and the Bats Complex, which date from the Balunté period, suggests that they are contemporaneous and that the dividing walls were built during the decline of the site. This has implications for the understanding of the decline of the site, and indicates that the people of Palenque were changing the function of the

buildings; this is remarkable for the Temples of the group of the Cross, which were clearly used as ceremonial architecture in earlier periods (see discussion below).

The use of clay-based plasters represents a dramatic change in architectural practices. The distinction between clay-based plasters and the thick pure lime plasters characteristic of earlier periods, even used as joining mortars, can be seen with the naked eye (see fig. 7.4 and 7.5).



Fig 7.5. Thick pure lime plasters used as joining mortars and renders. Left: original wall at Temple of the Foliated Cross (cross section of collapsed wall). Right: original wall in House D of the Palace.

A possible explanation for the breakdown in building traditions and plaster manufacture is related to the socio-economic and political decline of the site, which caused more likely the inability of the managerial elites to order and coordinate building programs, and in general, the inability of the polity to organise production. It is considered that these socio-political changes had an important impact in plaster production given the fact that this industry is very labour-intensive and most likely was organised as a public production, since lime plasters in these cases were destined to public monuments.

A phenomenon that may have occurred together with the former hypothesis is that firewood became a progressively scarce resource and was found away from the site centre where the building works were carried out as the forest retreated due to deforestation. Heavy deforestation has been documented in the late stage of the site's occupation (Liendo-Stuardo 2005), and was most likely caused by over-exploitation of the forest after centuries of dense occupation, which was caused by the transformation of forest into agricultural land, and the exploitation of wood for building and domestic purposes. Furthermore, it is well known that Palenque was one of the most densely occupied Maya sites, and its size was much larger than previously thought (Barnhart 2000). The fact that firewood may have been progressively further away from the site centre must have caused a drastic increase in the transportation costs in lime production, which we know from ethnographic sources is the most labour-demanding activity in a society without wheeled transport (Schreiner

2002). It is believed, however, that if ancient deforestation played a role in the abandonment of building traditions, it was only a secondary aspect that added to the socio-political decline of the site. In this sense it is important to mention the case of Teotihuacan, which made use of limestone sources more than 60 km away for the production of lime (Barba et al in press), which demonstrates that if society is organised and labour is available, the transportation of raw materials from distant locations is possible in societies without the use of wheel.

It is worth noting that despite the breakdown in building traditions during the Terminal Classic period at Palenque, some of the mud plasters show the presence of unmixed lime lumps, as well as a limewash over the surface (see fig. 7.4). This strongly suggests that the craftsmen were trying to emulate the plasters from earlier periods, albeit with much less energy-intensive materials. The incorporation of lime lumps in the mud plasters may have had a symbolic component, in the same way in which Andean metal workers incorporated gold into the bulk of objects, despite the fact that the same effect could have been achieved with a thin layer of gold on the surface (Lechtman and Merrill 1977).

The use of meteoritic material

As mentioned in Chapter 6, many of the samples from Palenque showed glass inclusions, sometimes with clear hydraulic reactions² (see fig. 6.5 and appendices A.2 and A.4). On occasion glass inclusions showed a weathered state, characterised by a yellow or red colour under the polarising microscope. When observed with the naked eye, some of these phases look similar to ceramic inclusions and they might be the “ceramic powder” that De la Fuente (1965:79) mentions when describing the aggregate material that was employed in the plasters of Palenque.

Very often the glass inclusions showed an unusual cracking, bubbles and blebs. When analysed with the EDS attached to the microprobe, these phases also showed unusual compositions with exceptionally high contents in $MgCO_3$ (see discussion below), as well as orange blebs also rich in $MgCO_3$. These characteristics prompted one of my supervisors, Dr. Ruth Siddall, to suggest that these phases may have a meteoritic origin rather than a volcanic nature, since the Maya area is well known from the impact deposits produced by the Chicxulub meteorite, as described in Chapter 2.

The petrographic descriptions and chemical analyses of impactites—rocks formed or transformed by a meteorite impact—of the Chicxulub meteorite from various locations of the Maya area and beyond confirm this interpretation. Altered glass fragments have been reported many times (Fourcade et al 1998, Kring and Boynton 1991, Ocampo et al 2003, Pope et al 2005); exceptionally

² As explained in Chapter 3, hydraulic properties are the result of chemical reactions between lime and reactive silica and alumina, which result in hydrated calcium silicates and aluminates that provide the plasters with improved mechanical properties and the ability to set underwater (Charola and Henriques 1999).

high concentrations of calcium, magnesium and sulphur in yellow glass phases have been reported by Kring and Boynton (1992), Bohor and Glass (1995), and Pope and colleagues (1999), and have been considered as being the result of chemical mixtures with the local target rocks (carbonates and evaporites); and carbonate blebs have also been reported by Tuchscherer and colleagues (2004), who think they could be the result of immiscibility with silicate phases.

The characteristics observed in the quartz grains also support the hypothesis of impactites. In all cases quartz grains show angular or sub-angular edges (see appendix A.2.1), which indicates that they have not been transported long distances by natural mechanisms and therefore do not represent weathered sediments from previous rocks. Another important characteristic is that some of the quartz fragments are shocked, that is, with characteristic sets of cleavages or planar deformation features (PDFs). As can be seen in fig. 6.4 (Chapter 6), a Terminal Classic plaster shows a clast of breccia that has a partially isotropic matrix that supports quartz grains, some of which are clearly shocked. Grains of shocked quartz were seen in many other samples and they can be clearly observed in samples Pa56, Pa89 and Pa53 (see fig. 7.6).

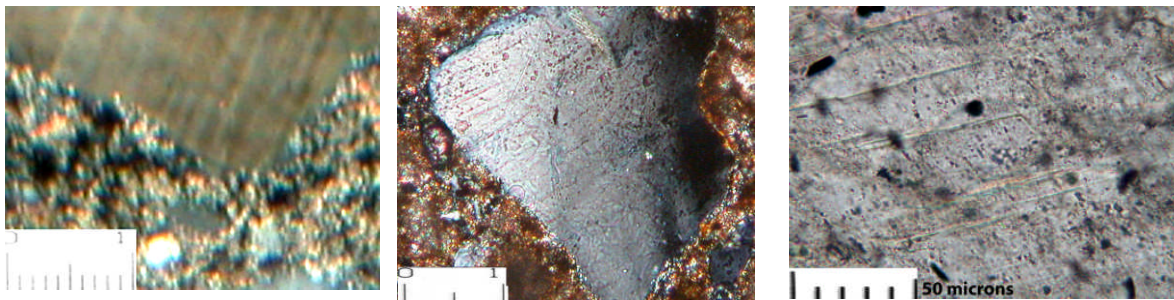


Fig. 7.6 Grains of shocked quartz with visible PDFs. Left: sample Pa56, XPL, scale bar: 100 microns. Center: sample Pa89, XPL, Scale bar: 100 microns. Right: Pa53, PPL, scale bar: 50 microns.

Shocked quartz with PDFs, also known as shock lamellae, was first discovered in nuclear testing, in which pressures up to 35,000 atmospheres are reached (Coes 1953). Shocked quartz was later found in meteorite impact craters, and it was therefore established that this was the only natural environment that would create the necessary pressure to form shocked quartz (Chao et al 1960). Shocked quartz has been considered ever since as a diagnostic feature of impactites.

Regarding the composition of glass phases, it is clear that they differ from the compositions of volcanic glass that are reported in the literature. Whereas volcanic glass has a SiO_2 content of 70% or higher (Tarbuck and Lutgens 2002:70), the glass fragment in sample Pa18 proved to have only 34.6% of SiO_2 , whereas sample Pa27 showed a content of 26%. It is important to mention that these analyses report calcium and magnesium reported as carbonates, which makes SiO_2 appear lower when totals are normalised. However, even if calcium and magnesium contents are reported as oxides, as it is usually reported in the literature, SiO_2 would account for 47.6% in sample Pa18

and 37.4% in sample Pa27, which is still too low for volcanic glass compositions (see table 7.1 and appendix A.4). The composition of these phases therefore reinforces the idea of the meteoritic origin of some of the phases seen in the plasters from Palenque.

| | | Glass phase in Pa18 (wt%) | Glass phase in Pa27 (wt%) |
|--|--------------------------------|---------------------------|---------------------------|
| Major components with Ca and Mg reported as oxides | MgO | 34.1 | 39.4 |
| | SiO ₂ | 47.6 | 37.4 |
| | Al ₂ O ₃ | 9.5 | 12.8 |
| | Fe ₂ O ₃ | 6.9 | 4.3 |
| | CaO | 0.6 | 1.1 |
| Major components with Ca and Mg reported as carbonates | MgCO ₃ | 51.8 | 57.3 |
| | SiO ₂ | 34.6 | 26.0 |
| | Al ₂ O ₃ | 6.9 | 8.9 |
| | Fe ₂ O ₃ | 5.0 | 3.0 |
| | CaCO ₃ | 0.8 | 1.3 |

Table 7.1 Analyses of glass inclusions in samples Pa18 and Pa27. Major components of normalised totals with Ca and Mg reported as oxides and carbonates

Recent geological research has shown that there are many sources of glass materials throughout the lowlands, many of which are not volcanic but were formed as the result of the Chicxulub impact and have therefore a meteoritic origin. These deposits can be found in the central and southern lowlands where outcrops dating from the Cretaceous period are common. Ejecta material from the Chicxulub meteorite has been recovered as far as Haiti in the form of altered glass (tektites and microtektites) and shocked quartz (Kring and Boynton 1991). Impact remains in the form of altered glass have also been detected in breccias that crop out in the Actela section in Guatemala, not far from the border with Belize (Fourcade et al 1998). These breccias are stratigraphically related to the breccias that outcrop in the Bochil and Guayal section in Chiapas, close to Palenque, where also impact ejecta have been found in the form of altered microtektites, nickel-rich spinels and shocked quartz (Arenillas et al 2006). Pope and colleagues (1999) describe the exposed sections of the Albion formation impact ejecta in northern Belize, where altered impact glass and accretionary lapilli have been found, together with impact glass. The Albion formation is 360 km away from the centre of the Chicxulub crater and corresponds to the outer ejecta blanket. A similar 4 m thick exposure has been reported in the Cayo district, covering the Cretaceous Barton Creek dolomite, close to the town of Armenia in Belize (Ocampo et al 2003).

In addition to shocked quartz and yellow glass with unusual compositions, another diagnostic feature was the identification of silicon carbide (SiC)—also known as moissanite—in samples Pa66 and Pa77 with microprobe analyses (see appendix A.4). SiC can only be found in nature in impact deposits, usually in association with diamonds (Hough et al 1997) and it is

therefore a diagnostic feature of impactites. It is worth mentioning, however, that the grinding material employed for sample preparation was made of synthetic SiC, and although samples were ultrasound-cleaned before the analysis, the identification of SiC is not certain.

Based on the presence of shocked quartz, devitrified glass with unusual compositions, carbonate blebs and the possible identification of moissanite, it is possible that 18 out of 57 samples that were analysed from Palenque have meteoritic materials, which suggests that the incorporation of meteoritic material may have been deliberate. Although the reason for the deliberate incorporation of this type of materials is unknown, it is likely that craftsmen were looking for specific workability and/or performance characteristics in the plasters.

As shown in Fig. 6.5 in Chapter 6, some of the devitrified glass inclusions showed clear reaction rims around them when observed under the polarising microscope. Moreover, sample Pa56 showed a large clast of rock with a friable isotropic matrix rich in SiO₂³, which indicates that it is composed very likely of reactive SiO₂. However, reaction rims were not observed in this sample since the plaster around it has a clayey composition.

Many other samples showed hydraulic-looking properties that show few or no content of visible aggregates (see sample Pa61 and Pa63 in appendix A.2). One possibility is that these plasters were made by mixing slaked lime with a SiO₂-rich material similar to the cement of the breccia observed in sample Pa56. As was observed during sample preparation, the cement of this clast was extremely friable and may have been very easy to crush and separate from the quartz grains; therefore, quartz grains could have been sieved and not included in the plaster mixtures, which would have resulted in plasters with no visible aggregates. Moreover, an equally SiO₂-rich material, also very friable and with no phenocrystals was observed in many of the samples from the sequence of floors from the Temple of the Foliated Cross, and it was in one of these samples (Pa66) that a grain of SiC was identified (see fig. 7.7). Therefore, it is very likely that a material similar to the one observed in sample Pa66 was finely ground and mixed with slaked lime, which would have resulted in hydraulic matrices with no visible phenocrystals.

³ Although the matrix of this clast shows a composition of 43% SO₃, 27% CaCO₃ and 24% SiO₂, it is thought that the SO₃ content is due to the mounting resin, which impregnated the porous cement. If SO₃ is not considered in the analysis, a composition of 53% CaCO₃ and 47% of SiO₂ is obtained.

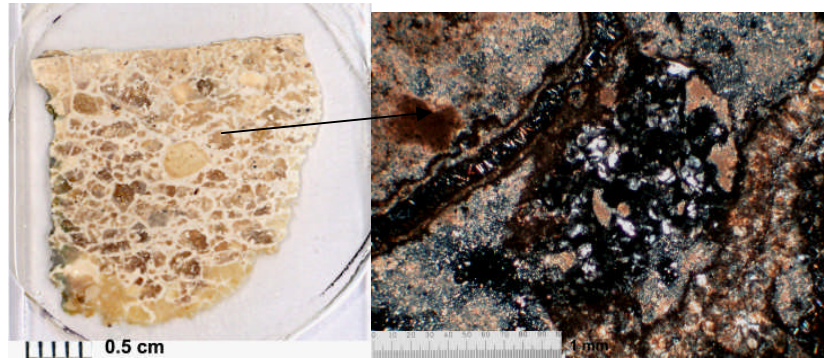


Fig. 7.7. Sample Pa66. Left: visible aggregates in macroscopic scanned view. Right: detail of aggregates constituted by partially isotropic matrix of SiO₂-rich cement and carbonate particles. No phenocrystals can be seen. XPL. Scale bar: 1mm.

Another possible explanation for the samples with hydraulic matrices and few visible aggregates is the use of volcanic ash that reacted readily after thorough mixing with lime. As explained in Chapter 2, there was strong volcanic activity during the Late Cenozoic in the central and northern parts of Chiapas. The Chichón volcano erupted at least 12 times during the last 8000 years, some of which occurred in Pre-Hispanic times (Espíndola et al 2000). These eruptions must have covered extensive areas of the south-western Maya lowlands as happened in 1982, when ash falls reached the states of Veracruz, Tabasco, Oaxaca and Campeche, covering a 100 km area of tephra (Peralta 2004). Therefore, volcanic ash deposits may have been readily available for the craftsmen of Palenque to use and to experiment with the lime mixtures.

It is worth mentioning that many authors (Shepard 1939, 1942, 1954, 1964, Kidder 1937, Simmons and Brem 1979, Rands and Bishops 1980: 23, Jones 1986, Ford and Glicken 1987) have reported the presence of glass phases in lowland Maya ceramics, which has always been interpreted as having a volcanic origin, as discussed below.

It is not possible at this point to discuss whether the glass phases previously reported in Maya ceramics (Shepard 1939, 1942, 1954, 1964, Kidder 1937, Rands and Bishops 1980: 23, Jones 1986, Ford and Glicken 1987) have a meteoritic origin. The studies report fresh glass shards with biotite mica as the main accessory mineral (Shepard 1964, Jones 1984), which does indicate a likely volcanic origin. In the case of Palenque, Rands (1967, 1980) reports that glass fragments are solely accompanied by quartz, which resembles the characteristics of the plasters from Palenque. Jones (1986) also reports a weathered state of the volcanic ash in Maya ceramics, which may indicate a meteoritic origin. In the future, however, diagnostic characteristics such as the presence of shocked quartz and compositional analyses of glass fragments need to be carried out in order to advance our understanding about the presence of glass inclusions in lowland Maya ceramics.

One difficulty for the identification of volcanic ash in hydraulic plasters is that, if thoroughly mixed, it reacts completely with the slaked lime, leaving behind no traces of material that can be observed under the petrographic microscope. Researchers report that often it is possible to observe fragments of volcanic rocks in the lime mixtures, which can be used as evidence of volcanic ash or glass employed as pozzolanic aggregates (Charola and Henriques 1999). In the case of the plasters from Palenque, however, very few fragments of volcanic rocks were seen, and they showed rounded edges that suggest they are mechanically-weathered sediments rather than fragments of volcanic rocks in ash deposits (see sample Pa53 in appendix A.2).

Although the use of volcanic ash for the production of hydraulic plasters in Palenque cannot be ruled out, it is believed that SiO₂-rich materials of meteoritic origin were more often employed to confer some kind of hydraulic properties to the plasters. However, experimental plasters with known meteoritic deposits and slaked lime are required in order to confirm the suspected hydraulic reactions between meteoritic deposits and slaked lime. In the same way, Thermal Analysis (TA) and Thermogravimetric analysis (TGA) could be used in the future to characterise the hydraulic phases present in these plasters (Ellis 1999). It is worth saying that the study and characterisation of meteoritic deposits is a complex field of research and the fact that no other examples of lime plasters with meteoritic materials have been previously documented makes this hypothesis a difficult problem to tackle.

From the point of view of resource procurement, however, the exploitation of meteoritic deposits represents a simpler problem to explain; impactites were very likely within easy reach from Palenque, and their exploitation was therefore of local or regional procurement as mentioned in Chapter 2 (see fig. 2.6 in Chapter 2). The fact that these materials were visually different and appeared as darker bands in the exposed stratigraphies of bedrocks may have prompted the people from Palenque and other sites to experiment with them. In a similar way, for instance, it is known that people from ancient cultures benefited from meteoritic deposits that provided materials with characteristics different from those found in the rest of the local environment. The exploitation of iron meteoritic deposits in the Arctic is one example where people benefited from iron deposits for the manufacturing of tools without the use of smelting technologies (Pringle 1997).

It is not known when meteoritic material was first added to the plasters of Palenque. The earliest sample with seemingly meteoritic inclusions (devitrified isotropic phases and SiC) is sample Pa77, which dates very likely from the reign of K'inich Janaab Pakal I (615-683 AD). However, it is difficult to sample building materials from earlier periods in the architecture of Palenque due to the fact that previous architecture was demolished or razed and covered by later construction. It seems that meteoritic deposits were widely used during Kam Balam II's reign and later. During the

Balunté phase, when plaster technology was declining and lime was replaced by clays, it seems that impactites were still being exploited, since as mentioned before, sample Pa56 showed a large clast of impactite as an aggregate of a clayey plaster and sample Pa53 showed grains of shocked quartz. This suggests that craftsmen were targeting the same deposits that were exploited in previous periods, even when building traditions had changed and when there was perhaps no reason to incorporate these materials in the mixtures, given that lime was not used and hydraulic reactions would therefore not have been obtained.

Soot layers, replastering and the evidence of ritual activity

As described in Chapter 6, the observation of numerous limewash layers in the plasters from Palenque—in some cases up to 60 layers—documents continuous renovation of buildings. This was a very common practice among the ancient Maya and architectural renovations and replasterings were sometimes associated with dedication rituals of buildings. In Maya culture, buildings were likely conceived as animated entities that go through stages of life, death and rebirth, and were awakened by dedication rituals and architectural renovations (Garber et al 1998, Tozzer 1966). Furthermore, ethnographic descriptions and ethnohistorical accounts document that lime and its moment of production are themselves deeply associated with birth, transformation and fertility (Schreiner 2002, 2003, Ruiz de Alarcon 1629). It seems likely, therefore, that the replastering layers and the numerous limewash applications in Palenque, particularly in the Cross Group, represent, in addition to careful maintenance, ritual practices associated with rebirth.

Some of the plaster samples from Palenque show limewash layers alternated with thin black layers. In the case of sample Pa75, from the wall render of the internal central doorway of the Temple of the Foliated Cross, around 60 black layers alternating with limewashes could be seen when a cross section of the sample was examined under the microscope. In the same way, a similar microstratigraphy was seen in sample Pa27, from the internal wall render of the Temple of the Cross, which showed 17 black layers alternated with limewashes. In contrast, however, the wall render from the rear façade of the Temple of the Sun (Pa24) showed several limewashes but no soot layers (see fig. 6.8, 7.8 and 7.9). Littman (1959b) previously noted this characteristic on the wall render of the southeast wall of the Temple of the Cross, which he described as having at least 40 layers, although he did not discuss how this particular microstratigraphy was formed.

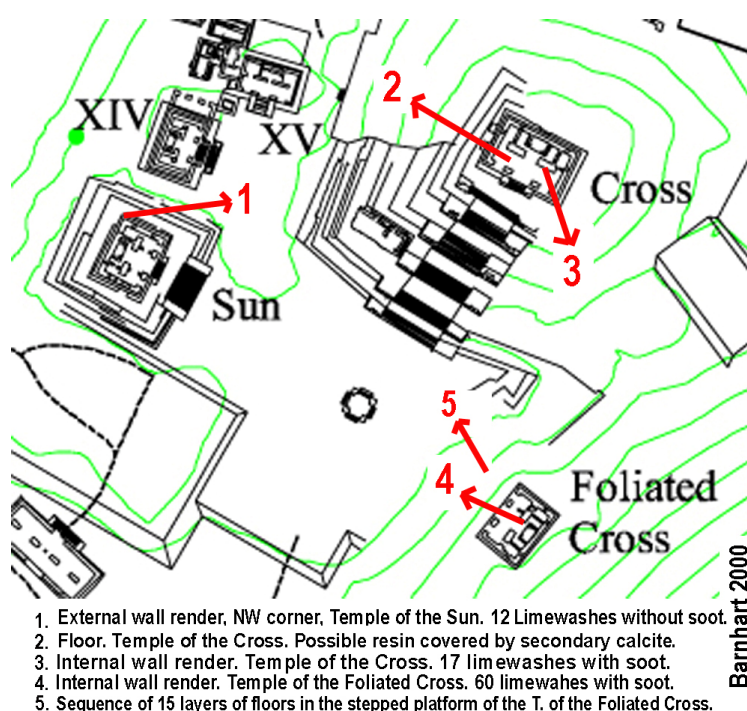


Fig. 7.8. Location of the samples from the temples of the Cross Group.

Based on the extreme thinness of the black layers, I believe they are soot layers deposited by incense or wood burning during ritual practices, as discussed below. As can be observed in fig. 7.9, the layers are much thinner than the one previously reported on the sculptures of the funerary crypt of Pakal by Villaseñor and Price (2008). Whereas the latter measures ca. 15 or 20 μm , the layers that are believed to be soot are so thin that their thickness cannot be measured by means of optical microscopy (see fig. 7.9).

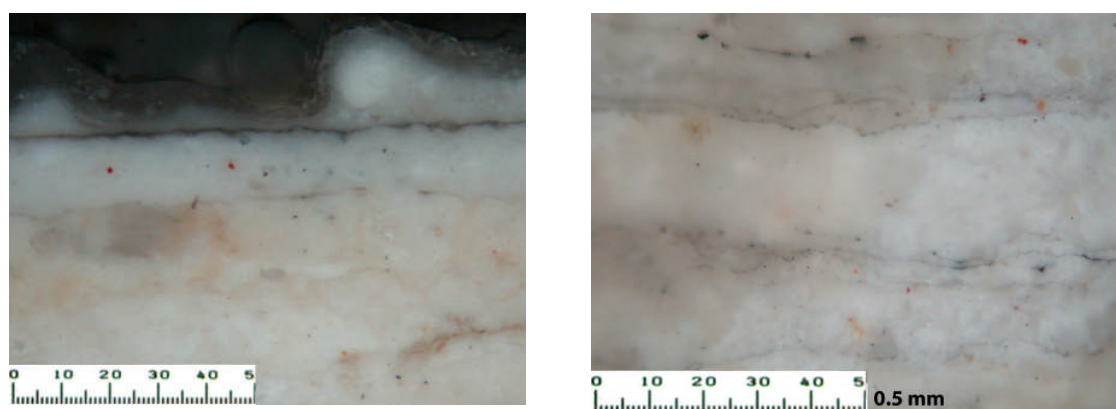


Fig. 7.9. Left: Black paint layer in sculptures of the Temple of the Inscriptions at Palenque (Villaseñor and Price 2008). Right: soot layers in sample Pa75 from wall render of the Temple of the Foliated Cross. Optical reflected polarised light microscopy. Scale bars: 500 microns.

Copal is an aromatic resin obtained from *Bursera* trees often employed in Maya ritual ceremonies, but aromatic wood may also have been used, since it produces a lot of smoke and several offerings of pine associated with construction have been found at Lamanai (Graham 2007).

The practice of incense burning in Maya and other Mesoamerican cultures is well known, and is even mentioned in the Quiché's Popol Vuh as being used for supplication, memorials and as means of expressing gratitude to the gods (Christenson 2003:188,228). Incense burning has also been documented in contemporary Maya rituals, notably in the case of the Lacandons. The Lacandons' incense burning ceremony consists of the ritual killing of god-pots and their subsequent rebirth, which is carried out by smashing the god-pots and manufacturing new ones that are used in the ceremonies for incense burning (Tozzer, 1982; Bruce, 1993). This ceremony symbolises death and rebirth of the god-pots and according to McGee (1998) is the equivalent of ancient ritual practices carried out in ceremonial architecture.

The fact that the soot layers can be seen in the interior renders of the temples but not in the rear facades is probably the result of the fact that ritual practices used to take place inside or at the entrance of the temples. On the other hand, the observation of limewashes without soot layers in the rear façade of the Temple of the Sun (Pa24) suggests that all facades of the buildings were limewashed in a periodic basis, most likely in a complementary manner with the ritual practices, regardless of whether the areas were blackened or not.

In addition to the renovation of wall renders, a sequence of 17 floor layers was seen in the stairs of the Temple of the Foliated Cross (see fig. 6.9 in Chapter 6), and when observed under the microscope, some of the floor layers showed two or three limewashes. This suggests that the replastering of the stepped platform was carried out together with the replastering of the wall renders, and that the whole structure was renovated periodically with ritual purposes.

The hypothesis of incense burning at the Temples of the Cross Group is also supported by the presence of an organic material deposited in the cracks of sample Pa28, from the floor of the Temple of the Cross. This material is isotropic but shows an orange colour under PPL, which suggests the presence of a weathered organic material, likely copal from incense burning ceremonies. The fact that secondary calcite is clearly deposited over this material confirms that the organic material was deposited prior to the abandonment of the site, after which the deposition of secondary calcite most likely took place (see fig. 6.6 in Chapter 6). The formation of secondary minerals as a result of weathering is well known in karst speleology (see Atkinson 1976), and has been described by Villaseñor and Price (2008) in the context of Maya lime plasters. This process consists in the dissolution of carbonates by acidic water, forming calcium hydrogen carbonate that later crystallises as calcium carbonate as the result of the loss of carbon dioxide. The resulting

crystals form in cavities, channels, and as surface crusts and are characterised by large and defined habits. In the case of the plasters from Palenque therefore, the formation of secondary minerals over the surface of archaeological plasters can be used as a microstratigraphic marker to date materials prior to the abandonment of the site, and in the case of sample Pa28 reinforces the idea that the deposition of the resin is Pre-Hispanic in date.

The hypothesis of frequent ritual practices carried out through the burning of incense is also supported by the excavation of over 100 incense burners recovered from the basements of the Temples of the Cross Group (Cuevas Garcia 2000). The iconography of these censers usually represents one of the three gods of the Palenque Triad, namely GI, GII and GIII, which have been interpreted as representations of the Young Sun God, the K'awiil God, and the Old Sun God, all of which reaffirm the concepts of birth, death and renewal (Cuevas Garcia 2000). It is well known that in Maya religion the sun was closely associated with the rulers, who were perhaps the promoters of the idea of them being a manifestation of the sun god (Sharer 2006:739). Based on a thorough analysis of a variety of Maya incense burners, Rice (1999) claims that incense burning was associated with death and rebirth, and the parallel life cycles of the sun and the divine king.

Cuevas Garcia (2000) considers that the incense burners recovered from the Cross Group were used for dedication rituals in a continuous basis. In this way, the censers were conceived as having a life cycle at the end of which they would be buried inside the basement of the structures, but other censers would be manufactured and used for future rituals (Cuevas Garcia 2000), in the same way of the god-pots of the Lacandons mentioned above. Furthermore, most of the incense burners have been found in the west facades of the buildings, which reaffirm the idea that these objects were ritually killed and deposited as caches in the direction that symbolises death, since west is the direction of the dying sun (Cuevas Garcia 2000). This is also supported by the Lacandon renewal ceremonies, where they place the "killed" god-pots in a corner of the god house facing west (McGee 1998).

The inscriptions and imagery of the tablets found inside the sanctuaries of the temples of the Cross Group also support the idea that these temples were deeply associated with the concepts of death and rebirth. The Temple of the Sun, at the west of the group is associated with death and the setting sun. The Temple of the Cross is associated with the Celestial realm because the tablet represents the tree of life that supports the heavens. The Temple of the Foliated Cross, located at the east of the group, is associated with the rising sun and the life-giving direction. The tablet of this temple commemorates the earthly realm and depicts the maize plant, which is the sustainer of life, from which human heads emerge (Sharer 2006, Simon and Grube 2000). For these reasons, it is a consensus among epigraphers that the inscriptions from the sanctuaries inside the Temples of the

Cross Group describe a connection between this architectural group and a mythical birth (Houston 1996).

Houston (1996) suggests that one of the glyphs in the front panel of the Temple of the Cross, represents the word *ku-nu-il* (or *kun-il*), which finds its closest term in the Yucatec Maya *kun* (or *kuun*). This term is defined in the Vienna and the Motul dictionaries as “an oven in which ink is made from smoke”, very likely from carbon that is scraped off the walls (Barrera Vazquez 1980 cited in Houston 1996). Houston’s interpretation of the epigraphy of the Group of the Cross (Houston 1996) concludes that the concepts of oven, burning, heat and smoke, which are also frequently mentioned in the tablets, suggests that these temples were conceived as symbolic sweatbaths in which a mythical birth takes place. However, I believe that it is also possible that the glyphs for heat and burning may represent specific terms for referring to the ritual practice of incense or wood burning, whereas the glyph *kun-il* may refer to the soot deposits that incense burning would produce, and finally, the glyphs related to birth and fertility could refer to the symbolic rebirth of the gods and the temples, which is also supported by Cuevas’ interpretation of the cyclic life of the censers (Cuevas Garcia 2000) and by the architectural renovations in the form of limewashes and plaster layers.

In summary, the observation of several soot layers alternated with limewashes, the numerous incense burners found at the Cross Group, the widespread evidence on the use of incense burning for ritual practices in Mesoamerican cultures, the textual evidence from the inscriptions of this architectural group, and the symbolism given to lime in Maya culture, represent complementary and compelling evidence about ritual practices symbolising death, transformation and rebirth through the burning of aromatic wood or copal and the following renovations of the buildings, and which has perhaps the closest example in contemporary Maya rituals in the renovation ceremonies of the Lacandons.

7.2. Calakmul

In this section I discuss the results of the Calakmul samples. The discussion is organised along several lines: craft specialisation and technological variation through time; hydraulic plasters and the identification of volcanic ash; the use of compacted sascab; crystals in binders as evidence of slaking practices; the identification of ascidians, fecal pellets and amorphous silica plant remains; and characterisation of pigments.

Craft specialisation and technological variation through time

Most of the samples from Calakmul proved to be highly calcareous, with the predominance of subrounded particles of micritic calcite identified as aggregate materials, although few other minerals were also identified. The subrounded particles of micritic calcite are clearly sascab, since samples of sascab from both Calakmul and Lamanai showed in all cases rounded or subrounded edges, and were composed primarily of micritic calcite (see fig. 7.10).

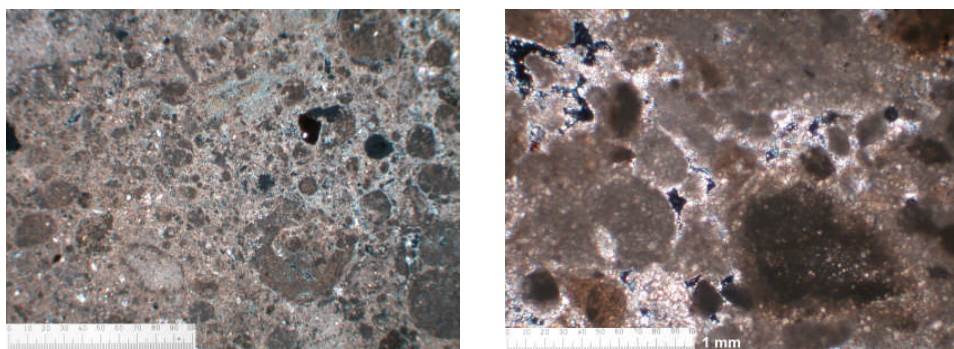


Fig. 7.10. Left: sample Ca10: lime plaster with the clear use of sascab as aggregate, XPL, scale bar: 1 mm. Right: Sascab sample from Calakmul, XPL, scale bar: 1 mm.

Despite the fact that most of the samples from Calakmul are highly calcareous and with the predominance of the use of sascab, important changes were observed in their manufacture according to the different chronological periods

Although point counting was not carried out in this research, based on qualitative microscopic observations it is clear that Preclassic plasters show adequate binder/aggregate ratios, with aggregates entirely surrounded by lime matrices (see fig. 7.10). These plasters also show few visible lime lumps due to optimal mixing (see appendix A.2), as well as exceptional hardness, a characteristic that is well known to archaeologists of the site (R. Carrasco and V. García, personal communication 2006). In addition to this, some of the Preclassic plasters seem to have hydraulic reactions due to the incorporation of pozzolanic aggregates (see discussion below).

Moreover, Preclassic plasters are seen forming layers of considerable thickness in important architectural programs. The modelled frieze of Structure IIC-1, dated towards the end of the Late Middle Preclassic period, measures over 12 m in length and 3 metres height, and the plaster reaches up to 12 cms in thickness (García et al 2006). The architecture of Structure II was one of the highest ever built in Mesoamerica, and it represents, together with the modelled frieze on it, an outstanding example of the advanced architectural practices carried out during the Preclassic Period (see fig. 2.14 in Chapter 2). In the same way, the fact that some of the paint layers of this frieze are extremely thin and homogeneously applied over perfectly flat surfaces (see appendix B.1), as in the case of Ca5, demonstrates the technical achievement that the craftsmen of the Petén had developed

by the Late Middle Preclassic Period as a result of craft specialisation during the emergence of cultural complexity (see Hammond 1986). The analysis of pigments, as discussed below, also demonstrates good technical craftsmanship and knowledge of materials.

The good quality of Preclassic plasters from Calakmul must have played a significant role in the architecture of this period, and may have prompted Maya architects to achieve important architectural innovations, such as the barrel vault of substructure IIc (see fig. 2.16 in Chapter 2).

Following the Preclassic periods, the Early Classic period is not so clear in terms of plaster production. Some of the samples have clayey matrices and sample Ca31, preliminarily dated to the Early Classic, may only be compacted sascab and not burnt lime (see appendix A.2.1). It is not known whether these observations are the result of a decline in plaster technology and architectural practices, or simply a result of unrepresentative sampling. However, these observations seem to correspond well to the scale of architectural practices during the Early Classic period, which is not comparable to those of the Preclassic or Late Classic periods, and includes only the renovation of the façade of Structure II, the Chiick Naab' acropolis and some other smaller scale buildings.

The Late Classic is again a period of outstanding architectural activities, and the archaeological evidence indicates continuous population growth, a clear development of social complexity, economic prosperity and political dominance over many other lowland sites, as described in Chapter 2. The plasters are clearly of good manufacture, and show good mixing, sometimes with many layers of plasters and limewashes, and some of the plasters may also be hydraulic (see discussion below).

The use of unburnt clays and the decline in plaster technology

In contrast to earlier samples, Terminal Classic plasters show considerably less hardness and a general decline in quality of plaster manufacture. The use of earth and clays during the Terminal Classic period at Calakmul was clearly documented by petrography and X-ray fluorescence. The same phenomenon was observed, to some extent, during the Early Classic period, although it is not as clear as in the Terminal Classic samples.

Under the petrographic microscope, clayey plasters were observed as having red brownish matrices, usually with clay pellets, shrinkage cracks, opaque minerals, grains of quartz and plant fibres (see appendix A.2). X-ray fluorescence showed that these samples contain higher amounts of Al_2O_3 and SiO_2 , as well as considerable amounts of Fe_2O_3 , sometimes with detectable amounts of alkaline earths and TiO_2 , which are elements often found in soils. The nature of clayey plasters can be seen very clearly when the samples are plotted in a SiO_2 vs CaCO_3 scatter plot, in which Terminal Classic samples show the highest contents in SiO_2 . Although two samples have an even

higher content of SiO_2 than do the Terminal Classic plasters, this is the result of the presence of quartz and other silicate minerals, and not clayey matrices, as was observed under the petrographic microscope (see fig. 7.11).

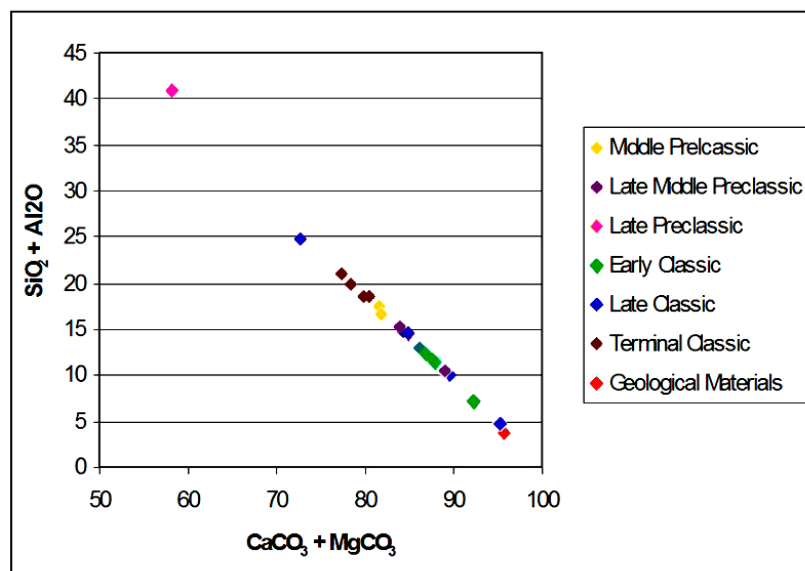


Fig. 7.11. Carbonates vs $\text{SiO}_2 + \text{Al}_2\text{O}_3$ contents in bulk composition of Calakmul plasters.

It is worth noting that these clays were not used as pozzolanic aggregates, since they show no evidence of having been burnt. Instead, they are non-burnt clays collected as local sediments or earth that were mixed with water and applied as mud plasters in architecture. The clayey nature of these plasters can be seen with the naked eye as a darker colour when compared with Preclassic or Late Classic samples, and the colours documented with the Munsell Chart support this observation (see fig. 7.12 and appendix A.1). Moreover, the examination of Terminal Classic plasters with the SEM showed only clay and silt-size calcareous materials in a clayey matrix, without the presence of the characteristic platy and hexagonal prisms of portlandite and recarbonated lime, which suggest that no lime was used in the manufacture of these plasters (see fig. 6.15 in Chapter 6).

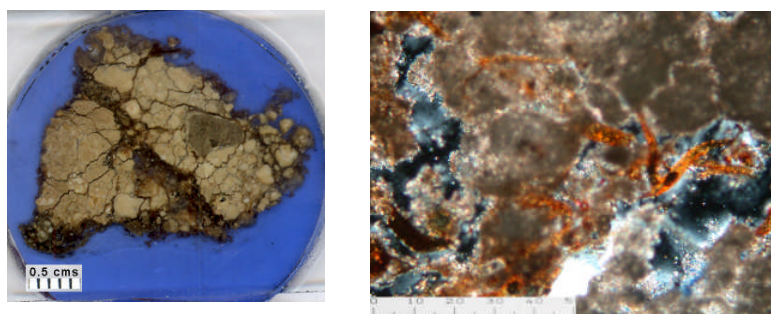


Fig. 7.12. Macroscopic scanned view of sample Ca3 (Terminal Classic) showing multiple cracks and a brown matrix. Scale bar: 0.5 cms. Right: sample Ca3. Clayey matrix with shrinkage cracks and plant fibres. XPL. Scale bar 0.5 mm.

Cluster analyses and PCA analysis of XRF data show a very distinct group formed by the Terminal Classic Samples, Ca 4, Ca33 and Ca34. Sample Ca12, from the Middle Preclassic period was also grouped in this cluster, although this sample was not observed by petrography and it is therefore not known what is causing the similitude in the chemical compositions.

The use of mud plasters at Calakmul has been reported before by Braswell and colleagues (2004) and Folan and colleagues (2001) who describe, based on on-site observations, that Structure IIB of Calakmul was undergoing several additions of earthen-plastered architecture just before the abandonment of the site. Carrasco-Vargas (1999) also mentions that the tomb of Yuknoom Yich'aak K'ak', who died in 695 AD—the same year of the definite defeat of Calakmul by Tikal—was covered with polychrome mud plaster, in contrast to the widespread use of lime plasters of previous periods.

It is possible that the use of clays in architectural plasters occurred as part of a major breakdown in building traditions. The most likely explanation relates to the disruption of the social and political structure of the polity, which has been repeatedly described in the case of Calakmul and many other lowland centres during the Terminal Classic period (Demarest et al 2004, Aimers 2007, Braswell et al 2004). In the case of Calakmul, as mentioned in Chapter 2, many of the buildings that had been previously used for ceremonial purposes, were used for domestic purposes during the Terminal Classic period (Braswell et al 2004), which indicates a disruption of the political and public life of the site. It is very likely therefore that the capacity of the elites to organise public works decreased significantly; high energy industries, such as the production of lime plasters, must have changed dramatically. For that reason, the use of clays in plasters is likely a consequence of the lower labour investment that mud plasters require in comparison to lime plasters, since they do not involve felling the trees or quarrying and burning the limestone, all of which are labour-intensive activities. It is worth noting in this sense that despite the differences in local geological materials of Calakmul and Palenque, the tendency towards the use of mud plasters is a characteristic of both sites during the Terminal Classic period.

In addition to the social and political breakdowns, a phenomenon that may have exacerbated the abandonment of building traditions was likely the increasing difficulties for accessing fuel. As it was shown in Chapter 3, modern Maya lime production makes use of open pyres of wood as a burning method, which is highly demanding in terms of firewood. Based on the widespread ethnohistoric and ethnographic evidence for the use of this technology, as well as the lack of clearly identified enclosed ovens for lime production, it is believed that the burning method of open pyres was the most common choice in Pre-Columbian cultures. Given that these cultures

did not make use of metal tools or wheeled transport, the procurement of raw materials was an energy intensive activity. Specifically, the transportation of firewood must have been the most labour-intensive task, as it is well known in modern indigenous lime production, which results in lime being burnt in areas of available firewood. Based on the evidence of deforestation during the Late and Terminal Classic periods in Calakmul (Gunn et al 2002a), produced by centuries of continued population growth during the Preclassic and Classic periods, it is believed that firewood was obtained further away as deforestation increased, when the forest retreated more and more from the civic and ceremonial centres where the monumental building practices were taking place, in the same way explained above in the case of Palenque. The increasing difficulties for obtaining and transporting raw materials must have resulted in an increase of labour, and the use of less energy-intensive materials, such as non-fired clays, was therefore a suitable choice for building materials in a deforested environment.

Hydraulic plasters and the identification of volcanic ash

It is possible that some of the Preclassic and Late Classic period plasters are slightly hydraulic. This is based on the observation of areas with mottled appearance and less optical activity, as well as the observation of isotropic phases (see fig. 7.13 and samples Ca11, Ca5, Ca7 and Ca18 in appendix A.3). Furthermore, Preclassic plasters, as mentioned above, show exceptional hardness.

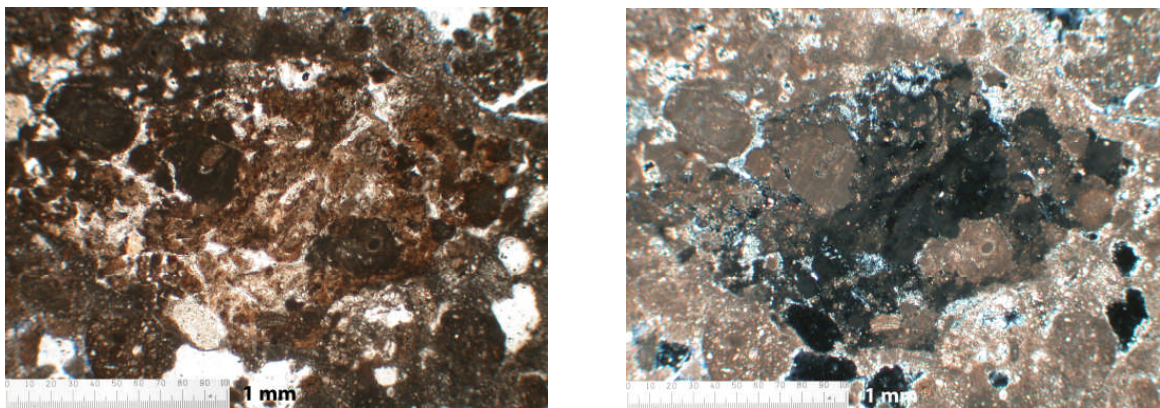


Fig. 7.13. Sample Ca18 showing isotropic phases, most probably volcanic ash.
Left: PPL. Right: XPL. Scale bars: 1 mm.

The presence of acicular crystals also suggests the use of hydraulic plasters (see fig. 7.14). As Charola and Henriques (1999:6) describe, fibrous and acicular crystals are often the most clearly seen evidence of hydraulic components and often grow in C-S-H (calcium silicate hydrate). Acicular phases were seen in many samples but most notably in the Preclassic samples (see appendix A.2). However, it is worth noting that the presence of acicular crystals is not conclusive of

hydraulic plasters because needle-shape crystals of calcite were also observed in the non-archaeological sascab sample, and these habits have also been reported in carbonate rocks of Isla Mujeres, Quintana Roo (Scholle and Ulmer-Scholle 2003:337). However, acicular phases in sample Ca8 were analysed with the microprobe and proved to be composed of 11% SiO₂ and 89% CaCO₃, which does suggests the presence of hydraulic phases (see fig. 7.14 and appendix A.3.2).

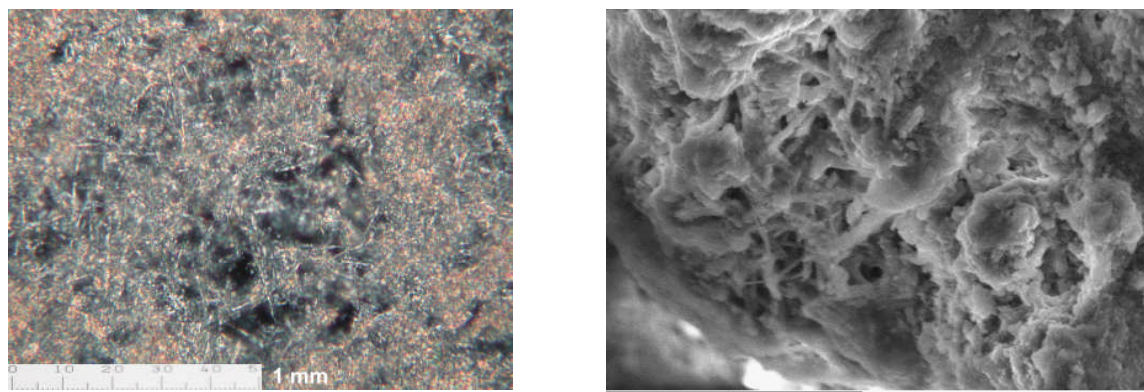


Fig. 7.14. Acicular phases that suggest the use of hydraulic components. Left: sample Ca6. XPL. Scale bar: 1 mm. Right: sample Ca8, BSE image, scale bar: 40 microns.

The bulk composition of the plasters, as obtained by XRF, shows that the plasters with acicular phases from the Late Middle Preclassic period have a slightly higher content in SiO₂ (13-16%) in comparison to the content in the modern sascab from Calakmul (10%) (see appendix A.6.2). Although other samples showed a much higher content in SiO₂ (samples Ca29, Ca16 and Ca26), this proved to be the result of the presence of quartz or clayey matrices rather than hydraulic components. Although the content in SiO₂ in the suspected hydraulic plasters of Calakmul may not seem particularly high, Schäfer and Hilsdorf (1993) define hydraulicity in historic plasters as those with 10 to 25% of hydraulic phases, and between 75 to 90% of carbonates. Furthermore, in the case of the Preclassic and Late Classic samples from Calakmul with seemingly hydraulic properties, hydraulicity may have been favoured by a thorough mixing, which promotes the reaction between lime and pozzolanic aggregates. It is also worth noting that the relatively high content of SiO₂ and Al₂O₃ in the sascab of Calakmul may have moderate hydraulic properties if heat-treated⁴, although no evidence of this was found in the samples.

In addition to the mottled appearance of the plasters' matrices and the presence of acicular crystals that suggest the presence of hydraulic phases, hydraulic reactions were clearly observed in

⁴ SiO₂-rich sascab would have to be heat-treated in order to make the silica reactive, since the silica content in the sascab has a sedimentary origin (clays and other minerals) that does not react with lime to form hydraulic phases. The silica that is present in volcanic ash and glass, on the other hand, is reactive because it is amorphous and therefore does not need heating in order to be used as a pozzolanic aggregate.

sample Ca11. The hydraulic reactions were analysed and proved to have a composition of 38% in SiO₂ and 60% in CaCO₃. This suggests the presence of a calcium silicate hydrate obtained through the use of a pozzolanic aggregate rich in reactive silica, which reacted with the lime and left a pore partially filled with isotropic and acicular phases (see sample Ca11 in appendix A.4).

By looking at the component plots obtained by PCA analysis, it is clear that in the case of Calakmul, SiO₂ and Al₂O₃ are only moderately correlated, in contrast to Palenque and Lamanai, where these elements are strongly correlated (see appendix A.6.4). This suggests that in the case of Calakmul, the presence of SiO₂ originates from different raw materials than Al₂O₃, and that SiO₂ was introduced as a raw material low in Al₂O₃. One possibility of such material is the presence of quartz or the fibrous silicate crystals that were observed in some of the samples (see discussion below). However, samples Ca18, for instance, does not show any of these minerals but only carbonates and isotropic phases, and it has a bulk composition high in SiO₂ and low in Al₂O₃ (see appendix A.2.2 and A.6.2), which suggest the presence of volcanic ash or glass.

By looking at the trace elements obtained by means of XRF, it is clear that SrO and BaCO₃ contents are much higher in the samples with acicular phases and seemingly hydraulic properties, which include Preclassic samples, a Late Classic sample (Ca18), and Terminal Classic samples. In the case of the Late Preclassic and Late Classic samples, it is likely that the high contents of SrO and BaCO₃ are related to the isotropic and hydraulic phases observed in petrography, and which have probably a volcanic origin. In contrast, SrO and BaCO₃ contents in Terminal Classic samples are probably related to use of unburnt clays (see appendix A.6.2).

The presence of globular phases in sample Ca6, primarily composed of SiO₂, also suggests the use of volcanic glass (see appendix A.3.2). Moreover, in the case of Late Classic samples, acicular phases were seen in association with yellow glass (Ca16). The yellow colour in the glass indicates partial devitrification, which is caused by the development of a crystalline structure due to the unstable nature of the glass, as well as by argillization, which is the transformation of materials into clay minerals (Marshall 1961) (see appendix A.4).

Many authors (Shepard 1939, 1942, 1954, 1964, Kidder 1937, Simmons and Brem 1979, Rands and Bishops 1980: 23, Jones 1986, Ford and Glicken 1987) have reported the presence of volcanic ash and glass in lowland Maya ceramics, and the distribution through time of this type of ceramics in the Maya lowlands can be seen in the figure published by Simmons and Brem (1979) (see fig 7.15).



Fig. 7.15. Distribution of ash-tempered ceramics in the Maya lowlands. A: Early classic, B: Late Classic, C: Terminal Classic, D: Postclassic periods. Image: Simmons and Brem (1979).

Although Ispording and Wilson (1974) claimed that the volcanic ash identified by Shepard (1939, 1942, 1954) was palygorskite, re-examination of the materials has confirmed Shepard's identification of vitreous materials in lowlands ceramics (Simmons and Brem 1979). This phenomenon has puzzled archaeologists and has prompted some debate and speculation regarding the provenance of these materials, which usually have been considered to have been traded from the Guatemalan Highlands into the lowlands for use as tempering material, in exchange for salt from the Northern Lowlands (Simmons and Brem 1979).

Ford and Rose (1995) argue that, in order to account for the sheer amounts of volcanic ash found in lowland Maya pottery during Classic times, there must have been local sources of procurement. Ford and Rose consider that this phenomenon is a result of a period of active volcanism that lasted several centuries and produced numerous events of ash falls that covered the Maya lowlands. As they explain, the Chichón volcano may have erupted in Pre-Hispanic times, covering areas of the Western Maya Lowlands as it happened in 1982, when ash falls reached the states of Veracruz, Tabasco, Oaxaca and Campeche, with a diameter of 100 km (Peralta 2004). Graham (1987) has also put an emphasis on availability of local resources before hypothesizing on highlands-lowlands trade, and notes that volcanic deposits in Belize include tuffs in the south of the Pine Ridge Batholith and layers of volcanic ash throughout the outcrop of the Bladen Volcanic Series (Bateson and Hall 1971, Drucker 1978, Hall and Bateson 1972, cited by Graham 1987), as well as pumice fragments along the Belize coast (Graham 1994). Volcanic ash deposits have also been found in core samples from *bajos* in the Petén (Gunn et al 2002a).

The numerous reports of ash-tempered ceramics demonstrate that the Maya were well aware of the properties of volcanic materials and that they were deliberately targeting these deposits. In the case of plaster technology, as mentioned above, the use of volcanic glass or volcanic ash confer hydraulic characteristics to the plasters and it is therefore possible to think that the incorporation of these materials in lime mixtures would be desirable.

Related to this discussion, the examination of sample Ca31, a floor from the Early Classic period, showed a layer over the surface of the plaster that is very likely volcanic ash. The layer measures around 200 micrometres in thickness and it has isotropic properties, which indicates that it is amorphous—without crystalline structure— (see fig. 7.16), a characteristic of volcanic ash and glass. Volcanic ash and glass form during volcanic eruptions when SiO₂- rich magma is cooled down too quickly to allow any crystalline structure to develop (Tarbuck and Lutgens 2002). In addition to the isotropic characteristics, elemental analyses with the microprobe showed that the layer in sample Ca31 is composed primarily of SiO₂, with some contents of Al₂O₃, SO₃ and CaCO₃, which correspond well with the nature of volcanic ash (see appendix A.4 for microprobe analyses). It is important to mention that the application of conservation materials can be ruled out since this floor was covered by a sequence of later floors and fill material.

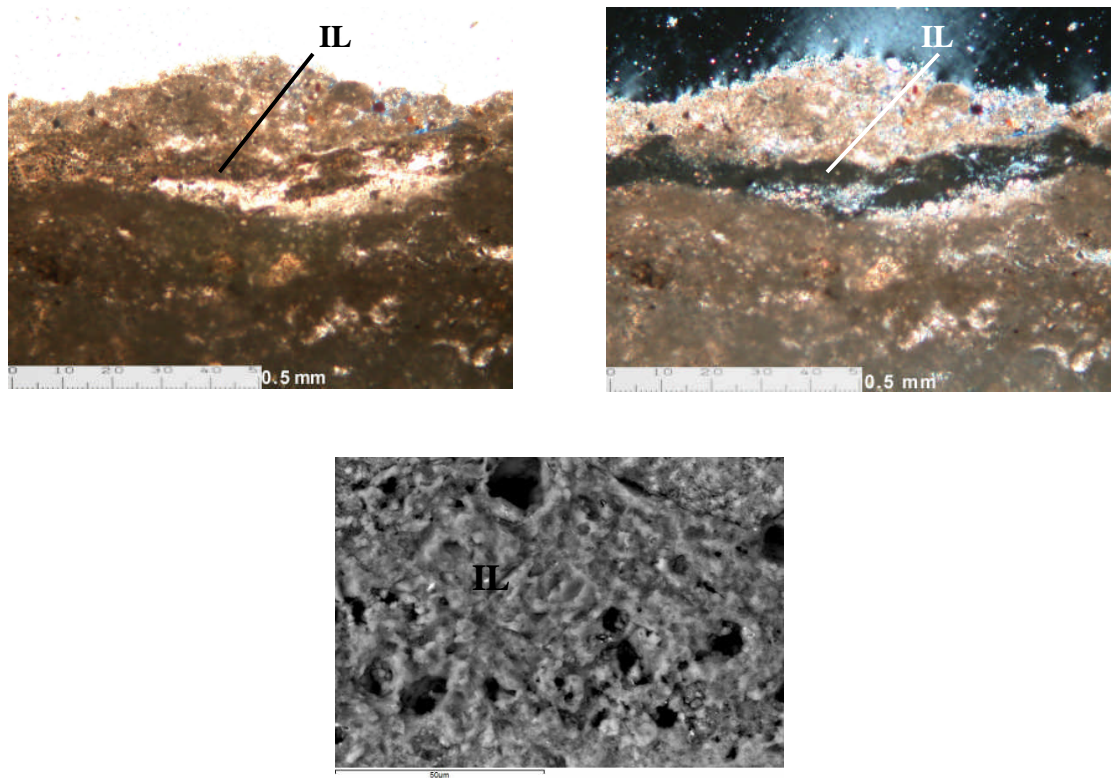


Fig. 7.16. Sample Ca31 Early Classic (?) floor with isotropic layer over the surface (IL). Carbonate material above the isotropic layer is from the fill with which the floor was covered later. Upper left: PPL. Upper right: XPL, scale bars: 0.5 mm. Lower picture: Detail of isotropic layer, BSE image, scale bar: 50 microns.

The layer of volcanic ash observed in sample Ca31 confirms previous reports of ash layers in the Maya lowlands, and indicates this happened during Prehispanic periods. In addition to supporting periods of active volcanism that reached the Maya lowlands, the layer also shows that volcanic ash may have been available for the Maya to use in ceramics and lime technology. Although the layer measures only 200 micrometres in thickness, layer thickness may have been considerably higher at the moment of deposition, and it may have also formed pockets such as those reported in the Bladen Volcanic series (see Graham 1987 and references therein).

Based on the presence of acicular and isotropic phases rich in SiO_2 , the hardness of some of the Calakmul plasters, the layer of volcanic ash and the widespread use of ash-tempered ceramics in the Maya lowlands, it is believed that hydraulic plasters were produced in Calakmul during the Preclassic and Late Classic periods by mixing lime with volcanic ash. However, more research is needed in this respect due to the complexity of the identification of volcanic ash in lime plasters.

The use of compacted sascab

Samples Ca9 and Ca29, from the Middle and Late Preclassic periods respectively, proved to have very different bulk compositions in comparison to the rest of the samples from Calakmul, as shown

by XRF and PCA analyses. Sample Ca9 showed the presence of a silicate mineral with low birefringence and a fibrous habit, which is most likely responsible for the unusual bulk chemistry of the plaster, which proved to be high in SiO_2 as well as with some contents in MgCO_3 , CuO , ZnO , RbO and SrO (see appendix A.6). The sample also showed a micritic cement with no clear presence of aggregates. These characteristics suggest that the floor may be a layer of compacted sascab, that is to say, a layer made by tamping the smaller fraction (clay and silt-size sediments) of carbonate deposits. This is also supported by the crumbly consistency observed during sampling and sample preparation. The sample is the lower layer of a floor stratum and may therefore be a preparation layer for the plastered floor.

Sample Ca29, from the Late Preclassic period, was also the lower layer of a floor stratum, and had the characteristics of non-burnt lime when observed under the petrographic microscope. This sample also showed the presence of a silicate mineral rich in MgCO_3 and without any Al_2O_3 , which indicates a mineral from the serpentine group (see fig. 7.17 and appendix A.4). The sample also had a crumbly consistency when it was taken with the scalpel, which supports the idea that this floor was compacted sascab without any burnt lime, and that this was a common practice in early periods in Calakmul.

The presence of minerals from the serpentine group may be relic material in the soils and carbonate deposits, formed as the result of weathering of serpentinites that have been documented in emplacements in Guatemala (Harlow et al 2004), although serpentine soils have not been reported in the area of Calakmul. However, it is worth saying that these silicate minerals were not observed in the non-archaeological sascab sample analysed from Calakmul.

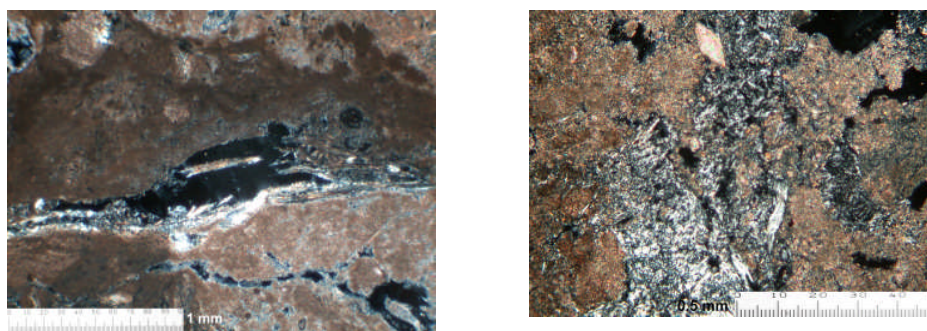


Fig. 7.17. Samples rich in a silicate mineral, likely a mineral from the serpentine group, from lower layers of floors, thought to be compacted sediments (not burnt lime). Left: sample Ca29 (Late Preclassic period). XPL, scale bar: 1 mm. Right: sample Ca9 (Middle Preclassic Period). XPL, scale bar: 0.5 mm.

The practice of laying a preparation layer with tamped sediments before the plastered floors was aimed most likely at obtaining a flat surface with homogeneous characteristics, and indicates good knowledge of the mechanics involved in floors. It is important to mention that the layers that have

been identified as compacted sascab were seen on site as distinctive layers, clearly different from the fill material.

The optical characteristics of the carbonate matrix of sample Ca31, as observed under the polarising microscope, also resemble those of compacted carbonate materials (non-burnt lime), since the matrix only shows silt and clay-size carbonate materials without the apparent use of aggregate material and with cracks running parallel to the surface. In this sample, a silicate mineral with fibrous habit and composed of SiO_2 and some contents of MgCO_3 was also observed. In contrast to samples Ca 9 and Ca29, however, sample Ca31 was an isolated layer, that is, it was not the lower layer of a burnt lime floor, but simply a floor of compacted sascab. It is not known whether the use of compacted non-burnt layers was a common practice during the Early Classic period, since Ca31 was the only layer with these characteristics. It is also unknown whether this was a technological choice or whether it may be related to shortages of fuel or labour.

More research is needed in order to understand the practice of floor construction with tamped sascab. Although Brown (1986e) reported compressive strength of experimental samples of compacted sascab, additional observations and characterisation of experimental floors may inform on the workability and performance characteristics of these floors and their micromorphological characteristics.

Crystals of binders as evidence of slaking practices

The presence of large hexagonal prisms in sample Ca5 and large subhedral and euhedral polyhedrons in samples Ca8 and Ca14 represent lumps of recarbonated lime (see fig. 7.18). The crystal sizes range between 10 and 15 microns, which is much bigger than the platy hexagonal crystals of portlandite or the smaller hexagonal prisms that develop in well slaked lime putties, which measure a few hundred nanometers (see Hansen et al 2008, Rodriguez Navarro et al 2006, Cazalla et al 2000 and appendix A.3.2).

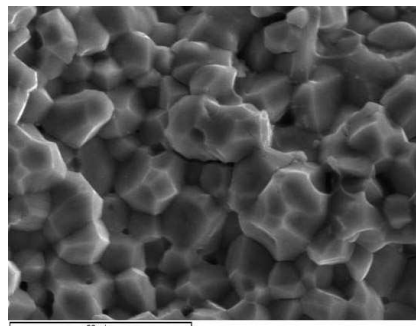


Fig. 7.18. Large recarbonated polyhedrons in sample Ca14. SE image. Scale bar: 30 microns.

Therefore, the observation of large hexagonal prisms of calcite is most likely the result of air-slaking practices whereby CaO is not slaked in a quantity of water but just slaked by the moisture of the air and the rain. From a technological point of view this is not the ideal technique, since optimal properties in plasticity and colloidal behaviour of the lime are not obtained (Hansen et al 2008). However, it is important to emphasise that from an anthropological perspective, air slaking in Maya lime production can be seen as the result of an established set of practices in which tradition, rituals and restrictions in technology (i.e. the lack of draught animals) resulted in open-air burns and the concomitant open air slaking, as discussed in Chapter 3. It is also worth noting that despite the large crystals observed in Late Middle Preclassic samples (Ca5, Ca8), these plasters have been reported by the archaeologists of the site as being of very fine manufacture and the frieze from which the samples were taken was found in excellent preservation, despite being more than 2400 years old.

The identification of ascidians, carbonate pellets and amorphous silica plant remains

In addition to the crystal habits described above, elongated fabrics with rounded edges were observed with the SEM and with high magnifications under the optical microscope (see left and centre images fig. 7.19). These inclusions are most likely ascidians microfossils which unfortunately do not possess any geological information (Scholle and Ulmer-Scholle 2003:303).

The shape of ascidians microfossils resembles that of the faecal pellets frequently found in carbonate rocks, although the latter are much bigger and they are composed of micritic calcite instead of monocrystalline calcite. Carbonate pellets were seen in sample Ca13, as well as in the limestones samples taken from the quarries at Calakmul (Ca25, Ca27 and Ca28). The presence of carbonate pellets in the limestones indicates a rapid sedimentation of carbonate deposits in a low-energy environment (Scholle and Ulmer-Scholle 2003:254), and their presence in lime plasters indicates the nature of aggregate materials; the pellets are not part of the lime binder, since they would have lost their morphology during firing (see fig. 7.19).

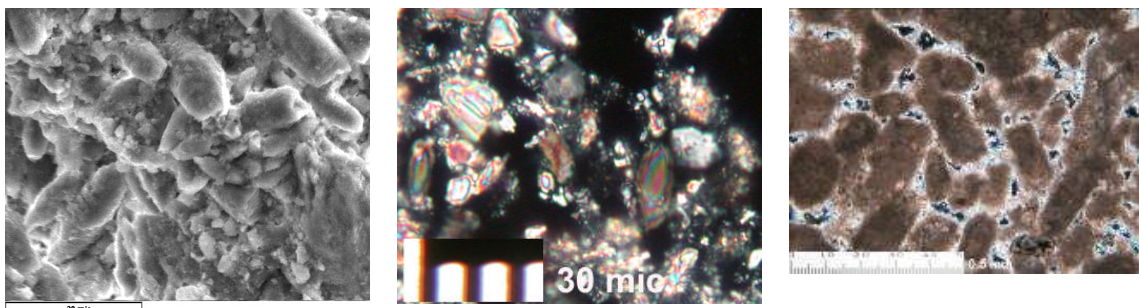


Fig. 7.19. Left: Ascidians in sample Ca8. Secondary electron image. Scale bar: 30 microns. Centre: Ascidians in sample Ca15. XPL, Scale bar: 30 microns. Right: faecal pellets in sample Ca13 composed of micritic calcite. XPL. Scale bar: 500 microns.

Other interesting materials, observed in many samples, mainly from the Preclassic and Terminal Classic periods, were isotropic inclusions with visible cellular structures. These inclusions are composed of amorphous silica and represent the silicic parts of plant remains (see fig. 7.20 and appendix A.4). Although it was not possible to identify the species of the plants, Schreiner (personal communication) has identified similar structures in calcareous deposits of El Mirador, in the Guatemalan Petén, and considers they are the remains of grass species frequently found in the swampy environments of the Petén.

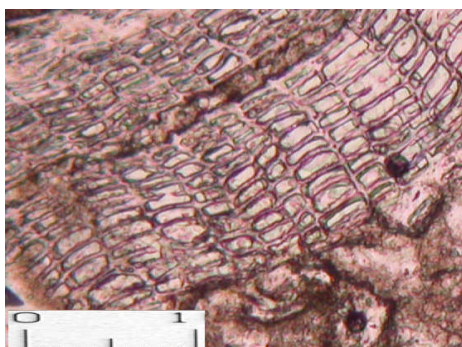


Fig.7.20. Amorphous silica plant remains. Sample Ca30. PPL. Scale bar: 100 microns.

As can be seen in fig. 6.14 (Chapter 6), these isotropic plant remains occur within carbonate grains, which indicate they were part of reworked carbonate deposits that were employed as aggregates in the plasters. These inclusions were also seen in the sascab sample, which further confirms their presence in carbonate deposits. Therefore, these plant remains constitute only accessory materials that were not deliberately added to the plaster and cannot be dated to the moment of plaster production but to the moment when carbonate deposits were reworked and redeposited. Given the secondary nature of these inclusions, they cannot provide any paleoenvironmental information about the time of plaster manufacture.

Characterisation of pigments

The painting techniques observed in the plasters from Calakmul show exceptional quality and knowledge of materials. This is particularly the case with the Late Middle Preclassic samples from the frieze of Substructure IIc-1. Samples Ca5 and Ca7 show very thin red paint layers (ca. 30 μm) applied homogeneously over thin limewashes (see appendix B.1). Pigment dispersions of the paint layer of samples Ca5 and Ca7 show dark red lumps of small birefringent crystals, which indicates the use of hematite (Eastaugh et al 2004), which is also confirmed by the identification of hematite peaks by means of Raman spectroscopy (see appendix B.2).

Hematite was a very widely used pigment in ancient times and is found in the Guatemalan Highlands and in the Maya Highlands of Belize and the rivers that drain them (Graham 1987 and Pendergast 2001). Although there are also nodules of iron oxides in the limestones of the lowlands (E. Graham, N. Hammond, personal communication), the examination of pigments dispersions showed fragments of glass (see appendix B.1), which suggests a volcanic rather than a sedimentary origin.

Samples Ca5 and Ca7 were also analysed by Raman spectroscopy, which yielded peaks similar to those of hematite, although with a rather weak signal, especially in sample Ca5 (see appendix B.2).

The yellow paint layers of samples Ca8 and Ca15 from the frieze of substructure IIC-1 and the Chiik Naab' acropolis respectively, were also analysed by polarising microscopy. Under the microscope, pigment dispersions showed particles of carbonates with small yellow particles, which suggest the presence of goethite mixed with calcite. However, isotropic yellow particles that suggest the use of an organic pigment were also seen (Eastaugh et al 2004). This sample was also processed by Raman spectroscopy, and although a peak similar to hematite was obtained, many other peaks were not identified (see appendix B.1 and B.2). For this reason, more research is needed for the identification of this pigment since no yellow organic pigments have been previously characterised in the Maya area.

The red paint layers in samples Ca14, Ca23 and Ca35, all from the Early Classic period, showed thicker layers less homogeneously applied in comparison to Preclassic samples. When observed under the polarising microscope, red, yellow and black particles were seen, which indicates the use of red ochre as a red pigment. Red ochre is a pigment primarily composed of hematite, although it occurs together with other iron oxides and hydroxides and other impurities such as quartz and clays (Eastaugh et al 2004). When analysed with Raman spectroscopy, many of the characteristic peaks of hematite were clearly detected (see appendix B.1 and B.2).

The black layer of sample Ca35 was analysed with Raman spectroscopy. The spectrum showed the characteristic peaks of graphite at 1300 and 1580 cm^{-1} . This black pigment was very likely obtained from charred pieces of wood, although the recovering of soot deposits is also possible.

Although the study of Calakmul painting techniques was not exhaustive, it is clear that the craftsmen of the Late Middle Preclassic period had sophisticated techniques and a good knowledge of materials, and craft specialisation becomes clear with the likely use of an organic pigment in the case of the yellow paint layer. It is worth mentioning that recent research has characterised a new green pigment employed in Calakmul, veszelyite, which was probably traded from the Central

Mexican Highlands (Garcia Moreno et al 2008). Although the earliest sample with veszelyte dates probably from the Early Classic period, it seems that Calakmul was an important centre of pictorial traditions. More technological studies of painted material need to be carried out on Central Petén sites in order to understand the innovation and development of materials and painting techniques.

7.3. Lamanai

In this section I describe the results of the Lamanai plasters that were presented in Chapter 6. The discussion includes the variation in aggregate materials, the use of non local material during the Late Postclassic/ Spanish Colonial periods, the use of compacted sascab in floors, the presence of large rhombohedral crystals of calcite, the use replastering applications, the evidence of plaster recycling, and the characterisation of pigments and painting techniques.

The variability in aggregate materials

The examination of Lamanai plasters under the polarising microscope allowed the identification of sascab in all of the samples as the main aggregate material, which was identified on the basis of the rounded edges of the particles, in all cases composed of micritic calcite. These characteristics were also observed in the non-archaeological sascab samples that were analysed from Calakmul and Lamanai. Despite the micromorphological similarities, XRD analysis of the sascab from Lamanai showed three peaks that were not present in the plasters from Lamanai (see appendix A.5). This suggests either that the source of sascab employed in the plasters was not the same as the sample of sascab that I analysed, or that the sascab employed in the plasters was sieved and the finer fraction—which is probably richer in clays and other minerals—was removed before mixing it with the lime. However, another possibility is that the concentration of this mineral in the archaeological samples is below the detection limits of the XRD equipment, which is between 3 and 4%.

In addition to the use of sascab, angular fragments of micritic calcite were seen, especially in Late Preclassic samples (see fig. 7.21). Based on the angular edges of these aggregates, it is believed they are crushed limestone, since the analysis of the samples of sascab from Lamanai and Calakmul proved to have rounded edges in all cases. Angular aggregates may have been deliberately added in order to provide the plasters with better mechanical properties, as they create an interlocking effect with the lime binder (Lanas and Alvarez-Galindo 2003). In this sense it is important to mention the modern practice of incorporating quarrying waste (*bak ch'ich* and *bak pek*) to the lime mixtures in the Maya area (V. García, personal communication), which give specific workability properties to the plasters, and which is perhaps a practice with ancient origins.

It is worth noting that the Late Preclassic samples that showed angular aggregates were from lime plaster sculpture. Therefore, the use of angular aggregates is most likely related to the performance characteristics that are desired for the plasters as part of sculpture rather than being diagnostic of raw materials employed during a specific chronological period (see fig. 7.21 and appendix A.2.2).

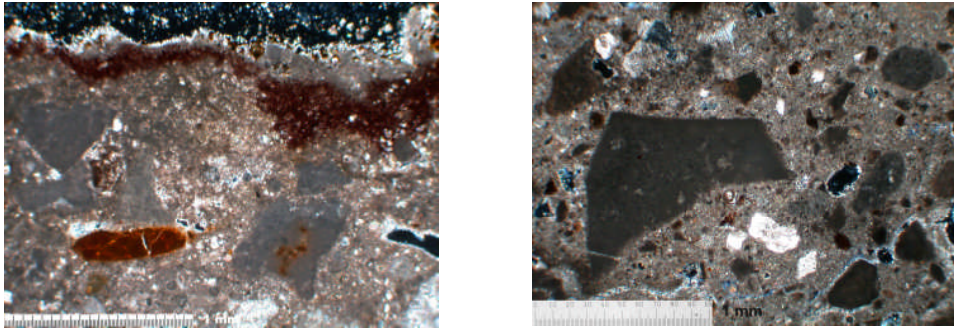


Fig. 7.21. Angular aggregates of micritic calcite (crushed limestone) in Late Preclassic plaster. Left: sample La25. Right: sample La24. XPL. Scale bars: 1 mm.

Limestone fragments were also frequently seen as aggregate materials in Late Classic and Terminal Classic samples, although with much bigger dimensions, as in the case of samples La10 and La11, which show limestone aggregates up to 20 mm in size. In the case of the latter samples, rather than conferring specific mechanical characteristics to the plasters, limestone fragments probably indicate an attempt to economise lime in the mixtures (see appendix A.2.2).

It is important to note that the large limestone fragments observed in the samples of the Late and Terminal Classic periods are composed of crystalline calcite instead of micritic calcite, and correspond very likely to the hard crystalline limestones of Cretaceous deposits. The angular fragments of micritic calcite observed in earlier plasters, on the other hand, are likely soft rocks of the Miocene to Pleistocene epochs that cover crystalline Cretaceous limestones (see McDonald 1978). It is also worth mentioning that during the Terminal Classic period, extensive quarrying of Cretaceous limestones was carried out in order to fill the courtyard of the Ottawa Group N10[3] (Graham 2004). It is possible to speculate, therefore, that the numerous fragments of crystalline limestone observed in the plasters of the Late and Terminal Classic periods were quarrying waste from the infilling works. This is also supported by ethnographic research carried out in the Maya area, which describes that quarrying activities generate up to 50% of limestone waste, which is often incorporated in lime mixtures (Abrams 1994: 46, Morris et al 1931: 215).

Use of non local materials during the Late Postclassic/ Early Spanish colonial periods

As explained in Chapter 6, samples from the Late Postclassic and Early Spanish Colonial periods showed higher contents in SiO_2 and Al_2O_3 in comparison to the rest of the samples. Although samples from other periods that proved to be made of compacted sascab (see discussion below) are also rich in SiO_2 and Al_2O_3 , they do not have the high contents in MnO , Fe_2O_3 , Rb_2O , SrO and ZrO_2 of the Late Postclassic and Early Spanish Colonial samples (see appendix A.6).

Due to this particular composition of the plasters, PCA analysis indicates that Late Postclassic and Early Spanish Colonial samples are the most dissimilar from the rest of the samples and are located away from the local raw materials (i.e. limestones and sascab) although with a high dispersion caused by the different contents in Rb_2O , SrO and ZrO_2 (see fig. 6.17 in Chapter 6 and component plot in appendix A.6.4).

It is worth noting that two of the samples that are preliminarily dated to the Late Postclassic period and which were recovered as debris from a pit dug west of Structure N12-11 (YDLI), may actually be Early Spanish Colonial in date, which is due to the complexity in the history of this structure. Although these samples show some of the characteristics of the Tulum-style temple of the Postclassic, such as the curved mouldings, they also show the considerable thickness and the distinctive yellow tinge of the Spanish Colonial plasters (D. Pendergast, personal communication).

Something that is clear is that the unusual compositions of Late Postclassic / Early Spanish Colonial plasters—high contents in SiO_2 , Al_2O_3 , MnO , Fe_2O_3 , Rb_2O , SrO and ZrO_2 —are the result of numerous devitrified glass fragments that are present in these samples, and which confer the characteristic yellow tinge that Pendergast mentions (see fig. 7.22).

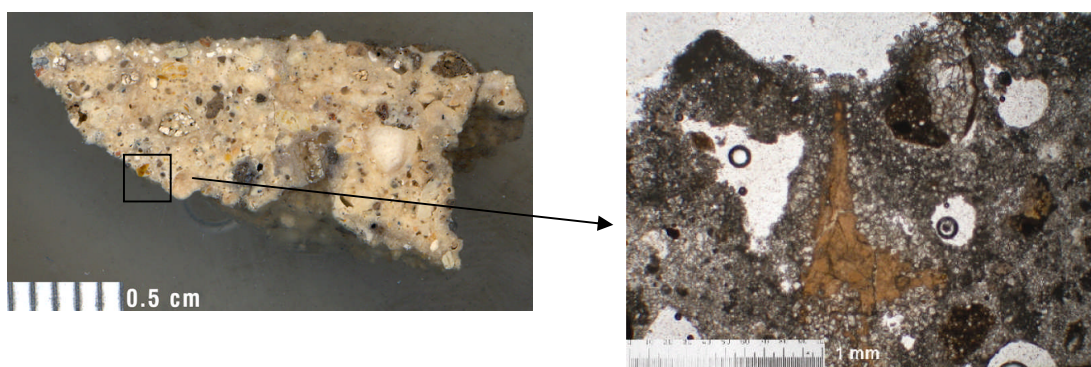


Fig. 7.22. Sample La20. Left: macroscopic scanned view with visible yellow inclusions (scale bar: 0.5 cms). Right: thin section of the same sample with devitrified volcanic glass shard. PPL. Scale bar: 1 mm. (See appendix A.4 for composition).

Some of the fragments of suspected devitrified glass were analysed with the microprobe and proved to have a composition between 46% and 52% of SiO_2 and 23% and 32% of Al_2O_3 , which indicates partial argillization, that is to say, the transformation of glass into clay minerals due to chemical weathering (Tarbuck and Lutgens 2002).

Another frequently seen mineral in Late Postclassic and Spanish Colonial samples was quartz, which was sometimes found embedded in SiO_2 -rich glass. This is a characteristic of acid volcanic rocks, where free quartz is formed. Glass is formed as a result of quick cooling, which prevents the development of a crystalline structure. The glass surrounding quartz crystals in sample Pa49 was also analysed with the microprobe and showed a composition corresponding to that of

devitrified volcanic glass, with 66% of SiO₂ and some contents of Al₂O₃ and CaCO₃ (see fig. 7.23 and appendix A.4).

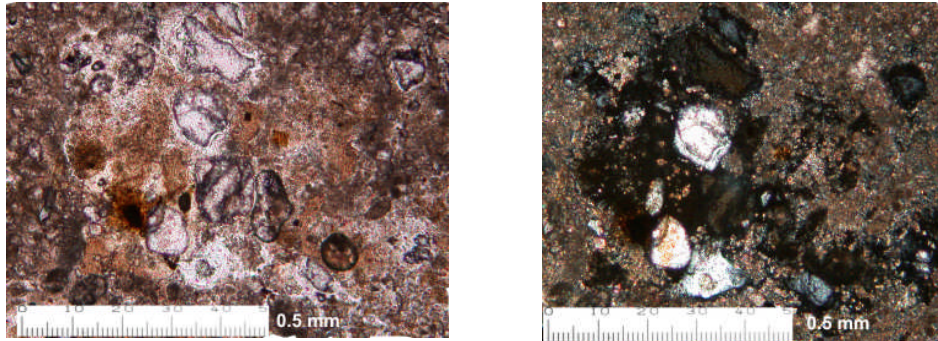


Fig. 7.23. Sample La49 (from Late Postclassic architecture). Quartz grains embedded in devitrified glass.
Left: PPL. Right: XPL. Scale bars: 0.5 mm.

In addition to these characteristics, Late Postclassic and Early Spanish Colonial samples showed some areas with apparent hydraulicity, with the characteristic mottled appearance of the binder (see samples La50 and La22 in appendix A.2.2). Some of these plasters also showed rounded isotropic phases rich in silica, which very likely correspond to alkali-silica gels, a chemical alteration produced by the attack of sodium or potassium to a variety of silica phases in hydraulic limes (St. John et al 2003). Although isotropic phases rich in SiO₂ were more frequently seen in 16th century samples, some inclusions were seen in La9, a floor from the Late/ Terminal Classic period, as well as in sample La36b, from the Late Postclassic (see sample La36b in appendix A.4).

All these characteristics seem to suggest that there was exploitation of siliceous deposits during the Early Spanish Colonial period—and perhaps also in earlier periods—in order to obtain some degree of hydraulicity. This is also supported by the observation of archaeologists of the site that Spanish Colonial plasters show higher hardness in comparison with earlier plasters (D. Pendergast, personal communication, Brown 1986e). Although more research is needed in this respect, it is evident that during the Spanish Colonial period and perhaps during the Late Postclassic, plasters were mixed with materials that were not employed before and are likely from a non local origin. The source of these materials could be the Bladen volcanic series in southern Belize, which is rich in old volcanic deposits (Graham 1987 and references therein).

If volcanic aggregates were indeed employed in Late Postclassic plasters, this could have been the result of the increased trade that is characteristic of this period, and from which Lamanai benefited widely owing its location by the New River lagoon (Graham 2004). In the case of the historic plasters of Lamanai, the incorporation of volcanic materials could have been the result of the continuation in Maya technological practices, or the knowledge brought from European building

traditions, where hydraulic plasters and their description in Classic treatises such as Pliny's and Vitruvius' were well known.

It has to be mention, however, that most of the Late Postclassic/ Spanish Colonial samples were wall renders, in contrast to the rest of the samples of previous periods, which were mainly floors. It is therefore not known whether the incorporation of volcanic materials was a general practice in all Late Postclassic/ Spanish Colonial plasters. In the same way, it is not known whether other types of plasters from previous periods, such as wall renders of sculptures, have volcanic materials.

Use of compacted sascab in floors

As it was mentioned in Chapter 6, 9 out of the 40 samples analysed from Lamanai had matrices entirely composed of micritic calcite and without the clear use of aggregates. These samples, all taken from floors, also showed shrinkage cracks parallel to the surface (see fig. 7.24). When observed on site, these materials showed the same white colour of the burnt lime materials, although with a considerably higher crumbliness, and sometimes as significantly thicker layers, as in the case of the Holiday House (Str. P9-25), which is 20 cms thick (see fig. 7.24).

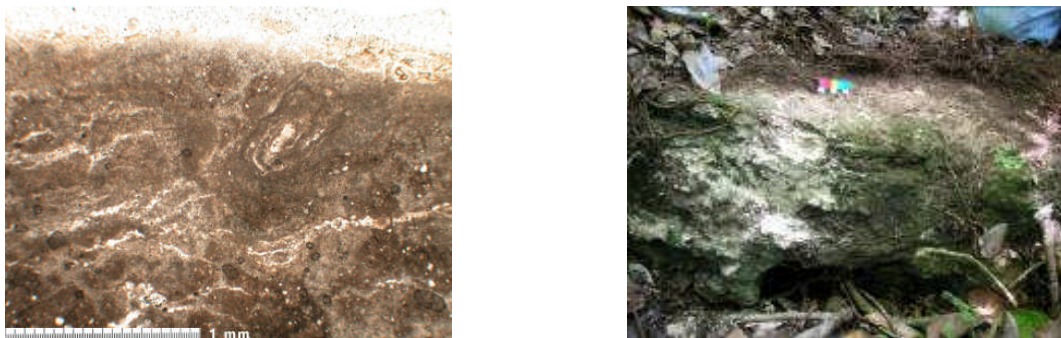


Fig. 7.24. Left: sample La35 (compacted sascab). Micritic calcite with cracks parallel to the surface. PPL. Scale bar: 1 mm. Right: Hyatt floor of the Holiday House (Str. P9-25) characterised as compacted sascab. Scale bar: 5 cms.

As it was discussed in the case of Calakmul, it appears that these characteristics indicate that the floors were not made of burnt lime, but only of compacted sascab. This has been previously noted by Brown (1986:15), who documents the existence of compacted layers of sascab in structure N9-56 and N10-43 of Lamanai. The use of compacted sascab was also noted by Littman (1962:101) at Uaxactun, who explains it as a means of reducing human labour.

Although the use of compacted sascab in floors may at first suggest shortages of fuel, this does not seem to be the case for Lamanai, where lake cores measuring sedimentation rates have not found significant evidence of deforestation (E. Graham, personal communication 2007). An

alternative interpretation is that the use of tamped floors without burnt lime may be related to the exhaustion of limestone sources, which has been noted by Pendergast for Late/Terminal Classic sites in Belize (Pendergast 1988:1656). As mentioned above, despite the vast amounts of stone that were quarried for the infilling works of the Ottawa group courtyard (see Pendergast 1985b:97), they made use of the hard crystalline limestone from Cretaceous formations, which is not suitable for facing and stone carving (E.Graham, personal communication, McDonald 1978). This type of hard crystalline limestone is known in Yucatec Maya as *taman tunich*, and is specifically avoided by the modern Maya for lime burning (Schreiner 2002: 52).

Although a shortage of limestone sources may explain the production of sascab floors during the Late/Terminal Classic periods and onwards, it is worth mentioning that many of the compacted sascab floors are dated to the Late Preclassic period, when there were no shortages in fuel or raw materials for lime production. It is possible to suggest, therefore, that the practice of laying floors with compacted sediments may be an economisation of human labour and resources, or may simply be a result of technological choices made by craftsmen, since tamped sascab provides an adequate surface for floors. This is supported by the fact that the practice of laying floors with non-burnt sediments and clays is often found in vernacular architecture across the world, and it has also been documented in floors in many archaeological sites (see Boivin 2000). Moreover, the construction of floors and roads by tamping sascab is still a common practice in Guatemala, Belize and south-eastern Mexico (see fig. 7.25).



Fig. 7.25. Construction of sascab roads in Belize, close to the site of Lamanai.

Although there are variations in the nature and composition of sascab, Darch and Furley (1983:185) report that samples of sascab from Belmopan, Belize, have up to 72% content in clay-size

sediments, which suggests that it is possible to obtain a hard and, to some extent, durable layer if compacted when it is still wet, as it happens in pottery as a result of drying of the clays before firing (Rice 1987: 65). Brown (1986e) prepared experimental samples of sascab from Lamanai, and reported compressive strengths between 2.1 and 2.8 MPa.

The different characteristics of compacted sascab in comparison to those of mud plasters were sometimes clear in the samples analysed; whereas the former is characterised by small particles of calcite that result in masses of micritic characteristics, the latter is characterised by a reddish colour—both under the microscope and with the naked eye—as well as the presence of clay pellets, quartz grains and opaque minerals. The processing of materials is also presumably different; whereas the compacted sascab requires quarrying the material from pits or tunnels and separating the finer fraction from gravels and boulders, mud plasters are made with clayey soils that are mixed with other materials such as grasses. However, it is important to say that the distinction between tamped sascab, mud plasters and burnt lime materials was not always clear cut in the samples analysed, which is likely due to the fact that there are a range of mixtures of burnt lime materials, mud plasters and compacted sascab, in which different proportions of slaked lime, unburnt clays and carbonate sediments were mixed depending on the resources and human labour invested, or in order to obtain specific characteristics in the mixtures.

The distinction between plasters of burnt lime and layers of tamped sascab in the samples from Lamanai is made only on the basis of optical polarising microscopy, and it is therefore not a definite way of proving the hypothesis. Further examination of crystal habits with the SEM, as well as XRD or thermal analyses, may constitute useful techniques in the future to determine in a more detailed manner the nature of these floors and whether they have any burnt lime mixed with the sascab.

Secondary rhombohedral calcite crystals

A common characteristic of the lime matrices of Lamanai's plasters is the presence of large rhombohedral crystals of calcite (see fig. 6.19 and 6.20 in Chapter 6). This is most likely the result of poor slaking, in which calcium hydroxide is not stored for long enough under excess of water, and lime does not develop the smaller platy hexagonal crystals of calcium hydroxide as explained above (Rodriguez-Navarro et al 1998, Cazalla et al 2000, Hansen et al 2008), which is consistent with the air-slaking practice of modern Maya lime production as described by ethnographic sources (Morris 1931:223, Schreiner 2002:57). Although ethnographic documents state that Maya craftsmen leave the heaps of lime to mature for up to 2 years (Schreiner 2002), air exposure may not be enough to produce a thorough slaking and a decrease in crystal sizes.

Although the presence of large hexagonal prisms of calcite was mentioned in the case of Calakmul, the samples from Lamanai showed extremely large hexagonal prisms up to 100 microns in size. This is thought to be the result of coarsening and aggregation of crystals that is caused when lime loses a certain amount of water, a phenomenon that is not reversible even if it is reintroduced to an excess of water (Rodríguez-Navarro and colleagues 2006) (see fig. 6.18 and 6.20). The large crystals of calcite were observed in samples from all periods, which indicate that open air slaking was a widespread practice at Lamanai. The fact that these crystals were also seen in Spanish Colonial samples, suggests that there was a continuation in the mode of production of lime.

It is worth noting, however, that in sample La21 the large prisms of calcite are cemented together by a mass of smaller crystals, which indicates either that there was a differential slaking of the lime, or that the coarsening and aggregation affected only some of the crystals.

As discussed in the case of Calakmul, open air slaking does not result in optimal workability characteristics of the lime, but must be understood within its own technological context and cultural meaning. This idea is in line with the framework of technological choices proposed by Dobres and Hoffman (1994), as discussed in Chapter 4.

Replastering applications

Several layers of plasters were seen in samples La22 and La36b, from the Late Postclassic period, and sample La19 from the Spanish Colonial period.

In contrast to plasters from other cultural areas, sequences of superimposed layers observed in the plasters of Lamanai proved to be the result of different periods of application. Roman and Renaissance wall renders, for instance, were applied as sequences of progressively thinner layers with smaller aggregates as part of the same plastering application, which is a practice described by Vitruvius (Cowper 1998:161). On the contrary, the plasters of Lamanai that had several layers proved to be the result of applications at different times rather than being graded layers of the same application. This is based on microstratigraphic observations, in which different colours and morphological characteristics of the superimposed layers suggest they were made with different raw materials. Furthermore, in many cases it is clear to see a limewash—which is always applied as a finishing layer—separating two layers of plasters, as in sample La22 from the Tulum-style temple (see fig. 7.26).

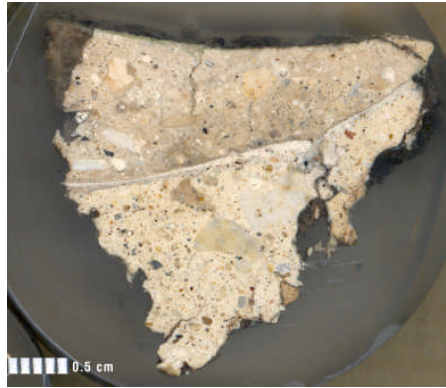


Fig. 7.26. Sample La 22 from Structure N12-12 of the Late Postclassic (Tulum-style temple). Superimposed layers with different characteristics, separated by a limewash. Macroscopic scanned view. Scale bar: 0.5 cms.

Despite this observation of sample La22, it is worth noting the description made by Brown (1986e:13), who mentions that a strong reaction of phenolphthalein was observed in the inner render of the Tulum-style temple. Because a positive phenolphthalein reaction indicates the presence of $\text{Ca}(\text{OH})_2$, this suggests that the first render of the temple was covered soon after it was applied and the new render prevented it from experiencing a full carbonation.

As discussed in the case of Palenque, replastering applications are a common practice in Maya architecture, and in the Cross Group they are clearly associated with ritual practices. In the case of Lamanai, the replastering sequences of the Tulum-style temple (sample La22), and elite residences, such as structure N10-15 and N10-18 (samples La9, La10, La11 and La12), may also be related to renovation rituals.

Recycling of plasters

Fragments of recycled plasters that were employed as aggregate materials for new plasters were seen in sample La6, dated to the Late Classic period. The identification of the recycled fragments of plasters was very clear due to different colours and properties of the matrices, and the fact that, interestingly, the recycled fragments showed a red paint layer overlain by a green/blue paint.

These inclusions of plaster may represent some of the many fragments of an early phase of the destroyed frieze from structure N10-28, which were recovered in the fill material of the Terminal Classic period (Graham 2004). The stratigraphy of the paint layers observed in the recycled plaster is consistent with the description of the frieze, since it has been documented that blue paint layers cover earlier red layers in the body adornments (Shelby 2006).

The reasons for incorporating recycled materials are not known. A practical reason for recycling fragments of destroyed plasters is a possibility, although considering that the fragments

are painted and formed part of a work with a specific iconography and symbolism, the incorporation may have been symbolic.

Characterisation of pigments

Regarding the use of paint layers that were seen overlying the plasters, it is possible to see that the red paint in sample La6 covers an orange layer. The orange layer is most likely a preparation layer, which has been previously reported as a common characteristic of red paint layers in Maya painted plasters (Magaloni 1998).

Pigment dispersions of red paint layers (sample La6 and La25) show dark red, yellow and black particles, which is a common characteristic of red ochre, a natural pigment composed primarily of hematite and other oxides and oxides hydroxides (Eastaugh et al 2004). This pigment can be found in the Maya Mountains and in the rivers that drain them (Graham 1987), in southern Belize, and it is therefore the most likely source of extraction.

As mentioned above and in addition to the red paint layers of sample La6, this sample also showed fragments of earlier plasters that were recycled as aggregates in the new plaster, which showed a red layer overlain by a blue/green paint (see fig. 6.18). The observation of pigments under the polarising microscope—sampled from the thin section—suggests that the blue paint layer is Maya blue, since it shows a translucent blue hue that is fixed into a clay mineral of first order birefringence. The red paint layer showed birefringent red and orange particles with some grains of quartz, which indicate the presence of red ochre (see appendix B.1), likely obtained from the Maya mountains.

8. *Conclusions and Future Research*

In this chapter I summarise and conclude the results presented in Chapter 6 and discussed in Chapter 7. The chapter presents the conclusions of each of the case studies, followed by general concluding remarks and suggestions for future lines of research.

Palenque

Palenque is characterised by a wide range of materials, and the chemistry and mineralogy of the plasters proved to be the most variable of the three sites. High variation of $\text{MgCO}_3/\text{CaCO}_3$ ratios was observed, as well as in SiO_2 and Al_2O_3 contents. Although plasters from Palenque proved to be highly calcareous, other minerals were identified, including quartz, dolomite, hydromagnesite and glass inclusions. It is believed that the variation in the chemical and mineralogical characteristics of the plasters is due to the technical experimentation and exploitation of various resources from the different geological settings around the site, which include the alluvial sediments of the Tabasco plain, the Cretaceous outcrops of the Sierra de Chiapas, and the impact deposits of the Cretaceous/Tertiary (K/T) boundary.

Many altered glass inclusions were observed in the plasters from Palenque. Although volcanic geology is the main source of glass materials in nature, the observation of cracks, bubbles and blebs, as well as the documentation of unusual chemistries of the glass fragments, showed that at least some of the glass phases observed in the plasters from Palenque do not have a volcanic origin but constitute impact materials, likely from the proximal ejecta of the Chicxulub meteorite. This is also supported by the presence of shocked quartz, which is a diagnostic feature of impactites.

Based on the numerous samples that showed impact materials, it is proposed that the ancient Maya deliberately quarried these deposits in order to obtain specific properties of the plasters, possibly to obtain hydraulic plasters. This is supported by the apparent hydraulic reactions observed around isotropic phases and devitrified glass. However, experimental work is needed to study the suspected reactions between slaked lime and impact deposits and to characterise the resulting plasters.

The observation of a fragment of impact breccia in a Terminal Classic sample suggests that these deposits were well known and their exploitation may have continued during the period of decline when clays gradually replaced lime as the binder of architectural plasters.

According to the extensive recent literature, it is likely that impactites were locally available not only at Palenque but at many other locations of the southern Maya lowlands that have Cretaceous and Palaeogene outcrops. It is not possible to determine whether previous glass phases

reported in lowland Maya ceramics also have a meteoritic origin, but the presence of shocked quartz and elemental analyses of glass phases could be used in future studies to illuminate this issue.

Due to the complexity of the identification of volcanic ash and glass in lime plasters given the reaction of these materials with lime, the identification of volcanic ash and glass in the plasters from Palenque cannot be ruled out. However, the few volcanic materials observed in the plasters from Palenque were rounded fragments of volcanic rocks that constitute most likely naturally-transported sediments employed as non-pozzolanic aggregates rather than diagnostic material accompanying volcanic ash or glass.

An important observation of the plasters of Palenque is that crystals of lime binders show smaller sizes in comparison to the binders observed in the samples from Calakmul and Lamanai. This seems to suggest that slaking practices at Palenque were carried out in containers with sufficient water, which would have allowed calcium hydroxide to develop smaller crystal sizes. This is also supported by the recent report of containers carved into the bedrock at the Picota Group, although their excavation is required in order to confirm their use for slaking purposes. The practice of lime slaking in containers might have been prompted by the difficulties shown by poorly slaked magnesian plasters, which to all likelihood were known by the craftsmen of Palenque given the dolomitic nature of the local geology and the high contents of magnesium observed in the plasters.

It is clear that despite the relatively short time span of the plasters analysed from Palenque, important changes in plaster technology were documented. A clear characteristic of the plasters from late periods (Balunte phase) is that they are more clayey than previous plasters. Shells were often seen in these plasters, and were probably added to compensate for the poor mechanical characteristics of the clay binder. It is proposed that the decline in plaster manufacture was the result of the collapse of the socio-political structure of the polity, which resulted in the disruption of building traditions. A likely shortage of firewood might have also contributed to the decrease in the use of lime by increasing the labour required for firewood transportation.

As discussed in Chapter 7, it is believed that the observation of numerous black layers and limewashes in the Cross Group, as well as the observation of an organic substance on the floor of the Temple of the Cross, represent evidence of ritual practices through the burning of aromatic resins or wood. In accordance with many other lines of evidence, it is proposed that these ritual practices had a symbolism related to death and rebirth, which included the ritual rebirth of the temples through their architectural renovation after the ceremony. The numerous layers of lime plasters and limewashes also bespeak a considerable effort from the society to maintain their public

monuments. The Cross Group was an interesting example of how material analyses can complement other sources of evidence to illuminate ancient ritual practices.

Calakmul

The analyses of Calakmul plasters demonstrated the good craftsmanship and technological expertise that was involved in the production of plasters. Although the vast majority of the plasters from Calakmul showed rounded particles of micritic calcite as the main aggregate material, some of the Late Preclassic and Late Classic samples also showed some isotropic phases, which suggest the presence of hydraulic components. Hydraulic components are also suggested by the observation of acicular crystals, reaction rims and a higher hardness in comparison to plasters of other periods. However, a more detailed identification of the hydraulicity of these plasters could be obtained in the future with thermal analysis and wet chemistry (see Bartos et al 1999).

An isotropic layer, entirely composed of SiO₂ over the surface of a floor preliminarily dated to the Early Classic period, was characterised as a layer of volcanic ash. This corresponds well with previous reports of volcanic ash layers at Calakmul, and indicates that there were ash falls during ancient Maya times and that this material was locally available for the Maya to use in their plaster mixtures.

The good quality of Preclassic paint layers, as well as the likely use of a yellow organic pigment, corroborates the technical achievements observed in the plasters and architecture of the same period. These achievements are attributed to the craft specialisation and cultural complexity attained in the Peten area during the Preclassic period. Moreover, the identification of red ochre and hematite indicates trade with other areas, either the Maya Mountains in Belize or the Maya Highlands in Guatemala.

In contrast to Preclassic and Late Classic samples, Terminal Classic plasters are clearly of poorer manufacture. The examination of these plasters under the optical microscope showed plasters rich in clays and with numerous cracks, similar to the Terminal Classic plasters from Palenque. This is interpreted as the result of socio-political decline, which in turn resulted in a decrease in the quality of labour organisation and production, although a shortage of fuel might have also played a role. Early Classic samples also showed a clayey nature, although the phenomenon is not as clear as in the case of Terminal Classic plasters.

The examination of crystal fabrics in the lime binders of Calakmul plasters by means of SEM/EDS showed large polyhedrons and rhombohedral crystals of calcite, which are most likely the result of poor slaking caused by open-air slaking practices. This is supported by ethnographic research, which shows that modern Maya lime production makes use of air slaking. As was

mentioned in Chapter 7, although air slaking does not result in optimal characteristics of the lime, the practice must be understood within its own technological and cultural contexts.

Another feature observed in the plasters from Calakmul was the use of compacted sascab for floors, which was identified on the basis of the micritic appearance of the samples without the apparent use of aggregates and lime binders. Two of the samples were underlying layers of burnt lime floors, and were therefore most likely applied to obtain a flat and stable surface for the laying of floors. Many crystals of a mineral from the serpentine group were observed in the compacted sascab; these crystals are probably relic materials from serpentinites that have been deposited in soils and calcareous deposits.

Numerous fragments of amorphous silica with visible cellular structures were observed in some of the plasters from Calakmul. The examination of these inclusions with the optical and scanning electron microscopes showed that they are silicic remains of plants that were deposited in reworked carbonate deposits, which were later employed as aggregate materials in the plasters. Due to the fact that these plant remains have a secondary origin, they cannot be dated to the moment of plaster manufacture and are therefore not informative of the construction moment.

Carbonate pellets were also frequently seen in the plasters and in the local geological materials from Calakmul. The presence of carbonate pellets indicates the diagenesis of carbonate deposits, which is a rapid sedimentation in shallow waters.

Lamanai

Samples from Lamanai proved to be the most calcitic of the three sites. Despite the time span of 15 centuries of lime plaster technology, this industry showed relatively little variation through time, which is probably related to continued access to local resources—with the exception of Late Postclassic and Spanish Colonial periods—and to the stable political and economic life of this center.

Rounded aggregates of micritic calcite identified as sascab were the most common aggregate materials in the plasters from Lamanai. However, small angular aggregates, also composed of micritic calcite, were identified as crushed limestone in the case of samples from the Late Preclassic period. From the Terminal Classic period onwards, the use of larger aggregates of crystalline calcite becomes more common, which suggests the use of older deposits from lower strata, possibly related to the nature of the quarrying activities that took place during the Terminal Classic period.

The plasters from Late Postclassic and Spanish Colonial periods showed a slightly higher siliceous composition, with higher amounts of quartz and higher contents in SiO₂, Al₂O₃ and

many trace elements. Considerable amounts of devitrified glass were observed in the samples of these periods, which suggest the exploitation of old volcanic deposits, perhaps from the Bladen volcanic series in southern Belize. In the case of Late Postclassic samples, the exploitation of non-local materials could have been the result of an increase in trade, whereas in the case of Spanish Colonial plasters, the use of these materials could have been either a continuation of technological practices from Pre-Hispanic times or the application of European building knowledge described in Classical treatises such as Vitruvius's, which describe the use of pozzolanic aggregates.

Another feature frequently seen in the plasters from Lamanai was the observation of compacted calcareous sediments used in the laying of floors. As discussed in Chapter 7, the micritic appearance of the samples, the absence of aggregate materials and lime lumps, as well as the presence of cracks parallel to the surface of the floors suggests the use of compacted sascab. This technique is a less energy-intensive option in comparison to lime plasters because it does not require the firing of limestones for the production of lime. Based on the identification of sascab floors in many chronological periods, it is believed that this is the result of technological choices rather than shortages of raw materials, fuel or labour. Compacted sascab was only identified in floors, likely because the mechanical characteristics of sascab were adequate for floors but not for wall renders or sculpture.

Another common feature of the Lamanai samples was the observation of large crystals of calcite, which are most likely the result of open-air slaking practices, as was observed in some of the samples from Calakmul. The observation of these crystals in Spanish Colonial samples indicates that there was a continuation of lime production traditions from Pre-Hispanic periods.

Fragments of recycled plasters with visible paint layers, probably from an earlier phase of the destroyed frieze of Structure N10-28, were observed in a Late Classic plaster. Similar fragments with paint layers have been documented before in fill of construction dating to the Terminal Classic period (Graham 2004).

Red ochre was identified in red paint layers of Late Preclassic and Late Classic samples. The pigment was likely obtained from the Maya Mountains or from materials deposited in the rivers that drain these mountains.

Concluding remarks

This study was a coarse-grained approach to the diachronic analysis of Maya lime plasters. It has to be recognised that, due to the broad scope of my research and the large time span of the materials analysed, the results are not the last word on diachronic analyses of plasters from the three case

studies and certainly not on archaeological plasters from the rest of the Maya area. Future research may expand and/or correct some of the ideas and hypotheses presented in my thesis.

Based on the data collected and analysed, it is possible to conclude that there are characteristics that are common to most of the Maya plasters. A distinctive trait is that the vast majority of aggregate materials are calcareous, mostly in the sand-size range or smaller.

The examination of non-archaeological samples of sascab demonstrated that the composition of this material varies according to its provenance. However, the micromorphological characteristics of sascab from Calakmul and Lamanai were very similar and consisted of rounded and subrounded sediments of reworked carbonate materials. These characteristics were also observed in most of the aggregate materials of the archaeological plasters, which demonstrates the presence of sascab. Nevertheless, the distinction between the binder and the silt and clay size fractions of the sascab was not easy, and it was therefore difficult to estimate binder/aggregate ratios based on petrographic observations.

A characteristic frequently observed in the samples was the application of numerous layers of plasters, which proved to be the result of different construction phases, rather than graded layers of the same construction phase. Limewashes were also frequently observed as a finishing layer of the plasters.

Another common feature was the very few fragments of charcoal observed in the plasters. Although it is believed that most or all of the plasters analysed were produced by the method of open kilns in which the lime mixes with the ashes, dearth of charcoal fragments in the plasters is considered to be the result of the use of specific firewoods, such as *chacah*, which leave no charcoal after burning, as explained in Chapter 3.

Despite these common characteristics in the samples analysed, there are noticeable technological changes that reflect the provenance of the samples (i.e. the different sites under study), which is a result of differences in raw materials and local traditions. Changes in technology were also observed in the different chronological periods of each of the case studies, and sometimes showed neat correlations with the broad chronological periods previously established by ceramic typologies, in particular the Terminal Classic periods at Calakmul and Palenque.

The technological variation that was observed in the plasters seems to be related more to chronological variation than to architectural location or the specific function that plasters performed (i.e. floors, wall renders, modeled sculpture or joining mortars). Principal component analyses showed that variation in chemical composition was not related to the specific functions, and different types of samples were spread out across the diagrams, which was very clear in the case of Palenque. This is also supported by petrographic observations, which showed that plasters from the

same periods, regardless of their architectural function or location, showed similar morphological characteristics. However, it is worth noting that the sampling was restricted and some of the periods of some sites included only one type of plaster and no conclusions can therefore be drawn in this respect.

In some cases, it was possible to correlate the characterisation of plasters with human activities that were taking place at the time of the plasters manufacture. In the case of Lamanai, large aggregates of crystalline calcite are probably related to quarrying activities, whereas fragments of recycled plasters with paint layers also reflect a particular activity, which is the destruction of a previous painted plaster. In a similar way, the observation of materials deposited over the plaster surfaces can also constitute valuable information for the interpretation of the use of architecture, as was demonstrated in the case of the soot deposits observed in the samples from the Group of the Cross at Palenque.

It is considered that the continued use of lime plasters is the result of cultural traditions by which the ancient Maya passed on their knowledge of building materials and traditions through generations. However, within the continuation of traditions, technological changes were observed, some of which are considered to be deliberate changes and innovations that are the result of human agency. Examples of this include the experimentation with different calcitic, magnesian and meteoritic resources at Palenque, or the seemingly deliberate use of shells in Terminal Classic plasters to compensate for the poor mechanical properties of the binder. In the same way, there seems to be a deliberate exploitation of siliceous resources at Lamanai during Late Postclassic and Spanish Colonial periods, whereas at Calakmul there is an apparent use of volcanic ash in the plasters and the manufacture of an organic pigment.

The results of this study show that the level of sophistication of plaster technology correlates well with the socio-political and economic contexts of the sites. Plasters from periods of stable and prosperous conditions, as attested by other archaeological sources, proved to be of good manufacture, as in the case of Late Preclassic and Late Classic Calakmul. This is most likely a result of craft specialisation, innovation, understanding of materials and good labour organisation. On the contrary, samples from periods of decline, in particular the Terminal Classic Period at Calakmul and Palenque, clearly showed poor quality plasters with the prevalence of non-burnt clays instead of lime. The good correlation between the quality of plasters and the political and economic conditions at the sites is considered to be the result of the high labour investment that lime production demands, as well as the public sphere in which Maya monumental architecture takes place. The latter characteristic implies that lime plaster manufacture for public architecture depends

on the capacity of the society to organise production, and the ability of the elites to coordinate public works.

The analysis of Maya architectural plasters has produced results that have implications for our understanding of production and the socio-political aspects that it involves. Maya lime-based monumental architecture was a powerful symbol that was effectively used by the ruling elites in ancient Maya times. The production of lime plasters can therefore be seen as an example of relations of production and therefore an important aspect of social and power relations. The three case studies and the different chronological periods under study display noticeable differences regarding the manufacture of plasters, which in turn shows that the different approaches of the sites to the exploitation of natural resources and the creation of a built environment was also different. Lamanai, for instance, showed that tamped sascab was often employed as an alternative to burnt-lime materials, which suggests that the society had a different approach to the use of firewood and/or labour in comparison with Calakmul and Palenque. Calakmul, on the other hand, showed ambitious examples of large-scale architecture with the manufacture of good quality plasters during the Preclassic period, which suggests a highly centralised production of building materials and tight control of the architectural agendas. The case of Palenque, although with smaller architecture in comparison to Calakmul, also made use of large quantities of plasters with good technical craftsmanship. A ritual component in the renovation of plasters of Palenque was also demonstrated, and attempts to continue with technological practices were also evident despite the drastic changes in the production of plasters during the Terminal Classic period.

Even though my research was more concerned with diachronic comparisons within each of the case studies than with synchronic comparisons between sites, it was possible to see some common technological characteristics, not only between the selected sites analysed in my research, but also with previous reports of other Mesoamerican plasters. A relevant example is the case of volcanic materials, which seem to have been identified and deliberately targeted by the Maya and other Mesoamerican cultures. Barba and colleagues (2006) have clearly identified the presence of volcanic glass shards in the plasters of Teotihuacan. In a similar way, the examination of samples in my research showed the presence of volcanic glass fragments in plasters from late periods at Lamanai, as well as the use of volcanic ash in the case of Calakmul. The widespread exploitation of volcanic materials for Maya plasters, as well as for ceramics (Shepard 1939, 1942, 1954, 1964, Kidder 1937, Simmons and Brem 1979, Rands and Bishop 1980, Jones 1986, Ford and Glicken 1987), demonstrates that there was a widespread knowledge of these deposits. It is worth noting in this respect that this technical knowledge on the properties of materials and their exploitation in the

natural environment may have originated not only from the contact with the Maya Highlands, but also from cultural exchange with the Central Mexican Highlands.

The use and production of lime in ancient and modern times are fundamental aspects of Maya culture. In addition to its wide use in architecture, Maya lime production had a rich symbolism and played a fundamental role in the subsistence of Mesoamerican populations, who had, and still have, high consumption of lime-processed maize. Therefore, analyses of lime plasters require discussions of the material and non-material values associated with them in order to avoid overlooking the anthropological dimension of material culture.

Future research

The use of lime was without any doubt a characteristic trait of Maya civilisation and the study and characterisation of lime-based materials should therefore be included in the body of research of Maya archaeology. Lime-based materials provide relevant information for the understanding of building traditions, selection of raw materials and labour investment in architecture. Nevertheless, although archaeological plasters are an important source of information for archaeological investigation, I consider that future studies should analyse these materials together with other sources of evidence to obtain a comprehensive interpretation about the production behind materials and the social aspects related to them. Ethnographic and ethnohistoric sources were used in my research to draw analogies and hypothesize about ancient Maya lime and plaster production. It was also important to review the archaeology of the sites in order to understand the general social and political conditions in which lime plaster production took place. In addition, epigraphy proved to be a very powerful source of evidence in the case of the Cross Group of Palenque and allowed a very rich interpretation of the renewal ceremonies and the use of the buildings of this group. In this sense, it is worth stressing the importance of interdisciplinary work, in which the different subdisciplines of archaeology can contribute to achieve informed interpretations.

Although there are some previous studies on lime plaster characterisation, the lack of standardised procedures and quantitative data is evident, which creates difficulties for comparing the sites and periods under study. Further analyses of architectural lime plasters are therefore required for building a systematic body of data to understand this ancient industry. It is also worth mentioning the relevance of using reference material in order to assess accuracy, as well as reporting standard deviations of quantitative data in order to estimate precision. These parameters are rarely reported in analyses of archaeological materials but are essential for assessing the quality of the data and for drawing comparisons between studies.

Diachronic and synchronic perspectives constitute valuable approaches for the study of technology. Further diachronic perspectives are necessary for understanding the evolution of lime technology within the development of cultural processes. Synchronic perspectives, on the other hand, are required to understand trade of raw materials, technological influences and interaction between sites.

Data on fuel consumption in lime production and its resulting environmental impact with traditional Maya lime burning techniques are very contradictory and result in very different positions regarding estimates of the contribution of this industry to ancient deforestation. The only study that reports in detail the amounts of wood required for producing specific volumes of quicklime was done by Schreiner (2002), and further research should follow this methodology. However, it is worth mentioning that future studies should also consider the different quantities in which lime plasters were used in architecture, depending on the different building traditions of the Maya area.

The origins of lime technology in the Maya area are not clear, neither in terms of location nor in terms of time, and more research is required for compiling and analysing the archaeological evidence in this respect. A frequent problem observed in the literature is the report of “stuccos” without specifying whether they consist of burnt lime plasters or simply compacted sascab. As it was observed in this study, tamped sascab floors can easily be taken as lime plaster floors with the naked eye, and petrography is therefore necessary to draw a distinction between the two. This distinction is also fundamental for understanding architectural practices and for estimating the energy invested in architecture.

One question that remained unresolved in my research was the exploitation of meteoritic deposits in the plasters of Palenque and the seemingly hydraulic reactions observed in the samples. Future research on the topic should consider the prospection of meteoritic deposits close to Palenque in order to confirm Pre-Hispanic exploitation of impactites, as well as the manufacture of experimental plasters with meteoritic materials.

Another future line of research that was not part of my research is the examination of northern lowland plasters. The literature on Maya ceramics reports the frequent use of volcanic glass in many periods and areas of the Maya lowlands, but especially during the Terminal Classic and Postclassic periods in the northern lowlands (Ford and Glicken 1987). This suggests that northern lowland plasters may also contain volcanic glass, and the deliberate production of eminently hydraulic plasters may therefore be confirmed. One specific use that hydraulic plasters may have performed in ancient Maya times is the lining in cisterns or *chultunoob'* in order to reduce permeability and improve water storage. As mentioned in chapter 2, these cisterns, which

were mainly used in the northern lowlands, constituted important features for the subsistence of ancient populations, since the northern lowlands have low rainfall with a long dry season. The examination of inner linings of cisterns is therefore required to evaluate whether hydraulic plasters were employed in order to improve water storage.

Analyses of *sacbeob'* or Maya roads also constitute a future line of research that was not included in my research. The examination of these types of materials would indicate the characteristics of the building materials and whether any burnt lime was employed in their construction.

An important field of research that was not tackled in my thesis is the characterisation of organic binders and additives that were used in lime plaster mixtures and which are reported to have been used in traditional Maya plaster production. Future analyses of archaeological and experimental plasters will expand our knowledge on this topic.

Regarding methodological considerations for future studies of Maya plasters, petrography proved to be the most informative source of information in my research and I consider that this technique should be an essential method for the examination of Maya plasters. Although petrography is often avoided in the study of Maya plasters and ceramics due to the difficulties of sample preparation and the expertise required for the identification of minerals, the technique provided valuable information on the morphological characteristics, nature and origin of the different components of the samples. It also provided information on the microstratigraphic characteristics of the plasters and the materials deposited over their surfaces, all of which is highly informative for the understanding of ancient plaster technology.

Optical reflected microscopy (ORM) was very useful for the examination of colour features, especially soot and paint layers, which could be seen more clearly under ORM than under the petrographic microscope. However, ORM was of little use for the examination of calcareous materials, which constitute the bulk of Maya plasters.

SEM/EDS analyses complemented petrography and allowed the identification of phases that were not identified by petrography. However, it is recommended that future SEM/EDS studies should not be used in isolation since the calcareous nature of the aggregates and the complex nature of sascab are highly misleading when interpreting backscattered electron images of Maya plasters. In a similar way, various minerals that are clearly visible in petrography, such as quartz and feldspars, do not show very clearly in SEM images.

X-ray fluorescence also provided valuable data regarding the bulk composition of the samples, especially regarding elements in trace concentrations. However, it is necessary to complement any analysis of bulk composition with an imaging method, since the former does not

have any spatial information regarding the specific composition of the different components. Regarding the statistical analyses of compositional data, the use of cluster analyses and PCA allowed an adequate examination of the samples' chemistry and of the different variables influencing the groupings.

X-ray diffraction proved to have only limited use for the analysis of Maya plasters. This is due to the fact that Maya plasters are highly calcareous and the peaks of calcite tend to mask the peaks of other minerals that are present in lower amounts. However, dissolving the samples with an acidic solution, a technique followed by García-Solís et al (2006), resulted in stronger peaks of other minerals, such as quartz and dolomite and future XRD analyses should therefore consider this type of sample preparation.

The use of polarising microscopy for the examination of cross sections of painted plasters and pigments dispersions also provided valuable information on the nature of colouring materials. This technique is therefore suggested as a complementary method for the future examination of pigments and painted plasters.

Thermal analysis and wet chemistry were not used in this research due to restrictions in equipment and funding. However, these analyses could be used in the future in order to characterise in a more detailed manner the different hydraulic phases that are present in Maya lime plasters (see Bartos et al 1999).

References

- Abrams, E. M. 1984. Replicative experimentation at Copan, Honduras: implications for ancient economic specialization. *Journal of New World Archaeology* 6(2): p. 39-48.
- _____. 1987. Economic specialization and construction personnel in Classic period Copan, Honduras. *American Antiquity* 52, p. 485-499.
- _____. 1989. Architecture and energy: an evolutionary perspective. In *Archaeological Method and Theory*, edited by Schiffer, M. B., vol. 1, University of Arizona Press, Tucson.
- _____. 1994. *How the Maya built their world: energetics and ancient architecture*. University of Texas Press, Austin, Texas.
- _____. 1996. The evolution of plaster production and the growth of the Copan Maya state. In *Arqueología Mesoamericana: homenaje a William T. Sanders*, p. 193-208. vol. 2, Instituto Nacional de Antropología e Historia, Mexico City.
- _____. 1998. Structures as sites: the construction process and Maya architecture, in: *Function and meaning in Classic Maya architecture*, edited by Houston, S. D., p. 123-138. Dumbarton Oaks, Washington, D.C.
- Abrams, E. M and Bolland, T. W. 1999. Architectural energetics, ancient monuments, and operations management. *Journal of Archaeological Method and Theory*. 6(4), p. 263-291.
- Abrams, E. M and Freter, A. C. 1996. A Late Classic lime-plaster kiln from the Maya centre of Copan, Honduras. *Antiquity* 70, p. 422-428.
- Abrams, E.M. and Rue, D. 1988. The causes and consequences of deforestation among the prehistoric Maya. *Human Ecology* 16, p. 377-395.
- Adams, R. E. W. 1991. Nucleation of population and water storage among the Ancient Maya. *Science* 251(4994): 632.
- Aimers, J. J. 2007. What Maya collapse? The varied transition between the Classic and Postclassic periods in the Maya Lowlands. *Journal of Archaeological Research* 15(4), p. 329-377.
- Altun, I.A. 1999. Influence of heating rate on the burning of cement clinker, in: *Cement and Concrete Research* 29(4): 599-602.
- Andrews, V. E. W. and Hammond, N. 1990. Redefinition of the Swasey Phase at Cuello, Belize. *American Antiquity* 55(3): 570-584.
- Arenillas, I, Arz, J. A, Grajales-Nishimur J.M, Murillo-Muñetón, G, Alvarez, W, Camargo-Zanoguera, A, Molina, E, and Rosales-Domínguez, C. 2006. Chicxulub impact event is Cretaceous/Paleogene boundary in age: New micropaleontological evidence. *Earth and Planetary Science Letters* 249(3-4), p. 241-257.
- ASTM. 2004. *Annual book of ASTM Standard: cement, lime, gypsum*. 4. American Society for Testing and Materials, Philadelphia.
- Atkinson, T. C and Smith, D. I. 1976. The erosion of limestones. In: *the science of speleology*, edited by Ford, T. D and Cullingford, C. H. D, p. 151-177. London: Academic Press, London.

- Baer, P and Merrifield, W. R. 1971. *Two studies on the Lacandonones of Mexico*. Summer Institute of Linguistics of the University of Oklahoma, Norman.
- Baglioni, P and Giorgi, R. 2006. Soft and hard nanomaterials for restoration and conservation of cultural heritage. *Soft Matter* 2, p. 293-303.
- Barba, L, Blancas, J, Manzanilla, L, Ortiz, A, Barca, D, Crisci, J. M, Miriello, D, and Pecci, A. (in press) Provenance of the limestone used in Teotihuacan, Mexico: a methodological approach. *Archaeometry*. Accepted for publication May 2008.
- Barba, L. A and Córdoba Frunz, J. L. 1999. Estudios energéticos de la producción de cal en tiempos Teotihuacanos y sus implicaciones. *Latin American Antiquity* 10(2), pp. 168-179.
- Barba, L. A, Barca, D, Crisci, G. M, Manzanilla, L, Miriello, D, Ortiz, A, and Pecci, A. Characterization of lime plasters from the central patio of Teopancazco, Teotihuacan (Mexico) by optical microscopy, SEM-EDS and ICP-MS Laser ablation. 2006. Poster presented at the International Symposium of Archaeometry, Quebec City.
- Barba, L. A and Manzanilla, L. 1987. Estudio de áreas de actividad. In *Coba, Quintana Roo: análisis de dos unidades habitacionales Mayas*, edited by Manzanilla, L., Universidad Nacional Autónoma de México, México, D.F.
- Barnhart, E. L. 2000. *The Palenque Mapping Project, 1998 - 2000 Final Report* [online] FAMSI. Available at: <http://www.famsi.org/reports/99101/>. [Accessed May 2007]
- Barrera Vazquez, A. 1980. *Diccionario Maya Cordemex Maya-Español, Español-Maya*. Ediciones Cordemex, Mérida, México.
- Bartolini, C, Buffler, R. T, and Blickwede, J. F. 2003. *The Circum-Gulf of Mexico and the Caribbean: hydrocarbon habitats, basin formation, and plate tectonics*. AAPG memoir 79. American Association of Petroleum Geologists, Tulsa, Oklahoma.
- Bartolini, C, Buffler, R. T, and Cantú-Chapa, A. 2001. *The western Gulf of Mexico basin : tectonics, sedimentary basins, and petroleum systems*. American Association of Petroleum Geologists, Tulsa, Oklahoma.
- Bartos, P., Groot, C., Hughes, J.J. (eds) 1999. *International RILEM workshop on historic mortars: characteristics and tests*, proceedings of the Historic mortars: characteristics and tests International workshop, (1999 May :Paisley), Cachan: RILEM.
- Bateson, J. H and Hall, I. H. S. 1977. *The Geology of the Maya Mountains, Belize*. Institute of Geological Sciences. Natural Environment Research Council, London.
- Beach, T. 1998 Soil constraints on Northwest Yucatán, Mexico: Pedoarchaeology and Maya subsistence at Chunchucmil. *Geoarchaeology* 13(8): 759-791.
- Benavides Jaidar, Y. 2006. *Los extractos vegetales usados como aditivos en morteros de cal con fines de conservación*. BSc, INAH-ENCRM, Mexico.
- Benedetti, B, Valetti, S, Bontempi, E, Piccioli, C, and Depero, L. E. 2004. Study of ancient mortars from the Roman Villa of Pollio Felice in Sorrento (Naples). *Applied Physics A: Materials Science & Processing* 79(2), p. 341-345.

-
- Benson, E. (ed) 1980. Fourth Palenque Round Table. *Proceedings of the Cuarta Mesa Redonda de Palenque. June 8-14, 1980*, San Francisco.
- Berdan, F. F and Rieff Anawalt, P. 1992. *The Codex Mendoza*, University of California Press, Los Angeles.
- Bohor, B. F and Glass, B. P. 1995. Origin and diagenesis of K/T impact spherules: from Haiti and Wyoming and beyond. *Meteoritics* 30, p. 182-198.
- Boivin, N. L. 2000. Life rhythms and floor sequences: excavating time in rural Rajasthan and Neolithic Çatalhöyük. *World Archaeology* 31, p. 367-388.
- Boric, D. 2002. The Lepenski Vir conundrum: reinterpretation of the Mesolithic and Neolithic sequences in the Danube Gorges. *Antiquity* 76(294), p. 1026-1039.
- Boynton, R. S. 1980. *Chemistry and technology of lime and limestone*. 2nd edition, Wiley, London, Chichester.
- Braswell, G. E, Gunn, J. D, Dominguez-Carrasco, M. R, Folan, W. J., Fletcher, L, Morales-Lopez, A, and Glascok, M. D. 2004. Defining the Terminal Classic at Calakmul, Campeche. In *The Terminal Classic in the Maya lowlands: collapse, transition, and transformation*, edited by Demarest, A.A., Rice, P. M, and Rice, D. S., Colorado University Press, Colorado.
- Bressani, R. Benavides, V., Acevedo, E., Ortiz, M.A. 1990. Changes in selected nutrient contents and in protein quality in common and quality-protein maize during rural tortilla preparation, in: *Cereal Chemistry* 67(6): 515-518.
- Brook, B. 2001. The Distribution of Carbonate Eolianite. *Earth Science Reviews*, 55, p. 135-164.
- Brown, G. E. 1986a. *Report on the Examination of mortars from Lamanai*. Unpublished report. Concrete Consultants, London, Ontario.
- _____ 1986b. *Report on the Examination of Mortars from Quintana Roo*. Unpublished report, Concrete Consultants, London, Ontario.
- _____ 1986c. *Proposal for the investigation and testing of ancient cementitious construction materials*. Unpublished report, Concrete Consultants, London, Ontario.
- _____ 1986d. *Ancient Mayan Concretes, Mortars and Stuccos: Quintana Roo, Mexico*. Unpublished report, Concrete Consultants, London, Ontario.
- _____ 1986e. *Ancient Maya Concretes, Mortars and Stuccos: Lamanai, Belize*. Unpublished report, Concrete Consultants, London, Ontario.
- Bruce, Robert D. 1993. Incensarios lacandonos. ¿Una cápsula de tiempo de los antiguos mayas? In *Arqueología Mexicana* no. 33, vol. I, pp. 69-73, Raíces-INAH, México.
- Bryant, D. D. Calnek, E.E, Lee, T.A, and Hayden, B. 1988. *Archaeology, ethnohistory, and ethnoarchaeology in the Maya Highlands of Chiapas, Mexico*. p. 54-56 ed. Papers of the New World Archaeological Foundation, New World Archaeological Foundation, Birgham Young University, Provo, Utah.

- Cadogan, C. 2007. Water management in Minoan Crete, Greece: the two cisterns of a Middle Age Bronze settlement. *Water Science and Technology: Water Supply* 7(1), p. 103-11.
- Callebaut, K., Elsen, J., Van Balen, K., Viaene, W. 2001. Nineteen century hydraulic restoration mortars in the Saint Michael's Church (Leuven, Belgium): Natural hydraulic lime or cement? In *Cement and Concrete Research* 31(3): 397-403.
- Carelli, C. W. 2004. The Energetics of royal construction at Early Classic Copan. In *Understanding early Classic Copan*, edited by Bell, E. E., Canuto, M. A., and Sharer, R. J, p. 113-127. Philadelphia, University of Pennsylvania Museum of Archaeology and Anthropology.
- Carmean, K. 1991. Architectural labor investment and social stratification at Sayil, Yucatán, Mexico. *Latin American Antiquity* 2(2), p. 151-165.
- Carrasco-Vargas.R. 1996. Calakmul, Campeche. *Arqueología Mexicana* 3(18), p. 46-51, Raíces-INAH, México.
- _____. 1999. Tumbas reales de Calakmul, ritos funerarios y estructuras de poder. *Arqueología Mexicana* 1999, VII(40) p. 28-31, Raíces-INAH, México.
- _____. 2000. El Cuchcabal de la Cabeza de Serpiente. *Arqueología Mexicana* , VII(42), p. 12-21, Raíces-INAH, México.
- Carrasco-Vargas. R, Boucher, S, Alvarez-Gonzales, P, Tiesler-Blos, V, Garcia-Vierna, V, Garcia-Moreno, R, and Vazquez-Negrete, J. 1999. A dynastic tomb from Campeche, Mexico: new evidence on Jaguar Paw, a ruler of Calakmul. *Latin American Antiquity* 10(1), p. 47-58.
- Carrasco-Vargas. R, Colón González, M. 2005. *El reino de Kaan y la antigua ciudad maya de Calakmul*, in: *Arqueología Mexicana*, Vol. XIII (75): 40-47.
- Castanzo, R. A. 2004. *Tepeaca Kiln Project*. FAMSI [online] Available at <http://www.famsi.org/reports/02021/> [accessed February 2007].
- Castanzo, R. A and Anderson, H. H. 2004. Formative Period lime kilns in Puebla, Mexico. *Mexicon*, XXVI, p. 86-90, [online] [accessed April 2008]. Available at: http://www.mexicon.de/mxv_2604.html
- Castro-Mora, J. 2002. *Monografía Geológico-Mineral del Estado de Campeche*. Secretaria de Economía. Coordinación General de Minería, México.
- Cazalla, O, Rodríguez-Navarro, C., Sebastián, E, Cultrone, G, and de la Torre, M. J. 2000. Ageing of lime putties: effects on traditional lime mortar carbonation. *Journal of the American Ceramic Society* 83(5), p. 1070-1076.
- Chao, E C. T, Shoemaker, E. M, and Madsen, B. M. 1960. First natural occurrence of coesite. *Science* 22(132), p. 220-22.
- Charola, A. E and Henriques, F. M. A. 1999. Hydraulicity in lime mortars revisited. *RILEM TC-167, International Workshop* [online] Paisley, Scotland, RILEM Publications. Available at: <http://www.dec.fct.unl.pt/seccoes/smtc/pub17.pdf> [accessed July 2008].

- Cheek, C. 1986. Construction activity as a measurement of change at Copan, Honduras. In *The Southeast Maya periphery*, edited by Urban, P. A. and Shortman, M, p. 50-71. University of Texas Press., Austin.
- Cherf, W. J. 1984. Procopius, lime mortar C14 dating and the Late Roman fortifications of Thermopylai. *American Journal of Archaeology* 88(4): 594-598.
- Chiavari, C, Fabbri, D, Galletti, G. C, and Mazzeo, R. 1995. Use of analytical pyrolysis to characterize Egyptian painting layers. *Chromatographia* 40(9-10): 594-600.
- Christenson, A. J. 2003. *Popol Vuh. The Sacred Book of the Maya*. O Books, New York.
- Coe, M.D. 1999. *Breaking the Maya code*, revised edition, New York: Thames & Hudson.
- Coe, M. D. 2005 *The Maya*. 7th edition ed. Thames and Hudson, London, New York.
- Coe, S. D. 1994 *America's first cuisines*. University of Texas Press, Austin.
- Coes, L. 1953. A new dense crystalline silica. *Science* 118(3057), p. 131-132.
- Connors, M, Hildebrand, A. R, Pilkington, M, Ortiz-Aleman, C, Chávez, R. E, Urrutia-Fucugauchi, J, Graniel-Castro, E, Camara-Zi, A, Vazquez, J, and Halpenny, J. F. 1996. Yucatán karst features and the size of Chicxulub crater. *Geophysical Journal International* 127(3), p. 11-14.
- Constantinides, I. 1995. Traditional lime plasters: myths, preconceptions and the relevance of good practice, in: *The Building Conservation Directory*, Cathedral Communications Limited, available online: <http://www.buildingconservation.com/articles/plaster/plaster.htm> [Accessed September 2008].
- Cros, P, Michaud, F, Fourcade, E, and Fleury, J. J. 1998. Sedimentological evolution of the Cretaceous carbonate platform of Chiapas (Mexico). *Journal of South American Earth Sciences* 11(4), p. 311-332.
- Cuevas García, M. 2000. Los incensarios del Grupo de las Cruces, Palenque. *Arqueología Mexicana* 2000, VIII(45), p. 54-61, Raíces-INAH, México.
- _____. 2007. *Los incensarios efigie de Palenque. Deidades y rituales mayas*, UNAM, INAH, Centro de Estudios Mayas (IIF), CONACULTA, Serie Testimonios y Materiales Arqueológicos para El Estudios de la Cultura Maya 1.
- Cuevas García, M and González Cruz, A. 2007. A flor de piel: la superficie de los edificios palencanos como fuente de información sobre los últimos momentos de ocupación de la ciudad. Paper presented at *VII Congreso Internacional de Mayistas, Mérida, 8-14 de julio 2007*.
- Dandrau, A. 2000. La peinture murale Minoenne. II: La production des enduits, materiaux et typologie. *Bulletin de Correspondance Hellenique* 12(4), p. 76-97.
- Darch, J and Furley, P. 1983. Observations on the nature of sascab and associated soils in Cayo and Orange Walk District, Belize and El Peten, Guatemala. In *Resources and development in Belize, Occasional Publication*, edited by Furley, P and Robinson, G, p. 179-221. Department of Geography, University of Edinburgh, Edinburgh.
- Davey, N. 1961. *A History of Building Materials*. Poenix House, London.

- De la Fuente, B. 1965. *La Escultura de Palenque*. Instituto de Investigaciones Estéticas-UNAM, México, D.F.
- DeMarrais, E., Castillo, L.J., Earle, T. 1996. Ideology, materialization and power strategies, in: *Current Anthropology*, 37(1): 15-31.
- Deelman, J. C. 2005. Low-temperature Formation of Dolomite and Magnesite [online] Available at: <http://www.jcdeelman.demon.nl/dolomite/bookprospectus.html>. [Accessed December 2007].
- Demarest, A. A., Rice, P. M, and Rice, D. S. 2004. The Terminal Classic in the Maya Lowlands: assessing collapses, terminations, and transformations. In *the Terminal Classic in the Maya Lowlands: collapse, transition and transformation*, edited by Demarest, A. A., Rice, P. M., and Rice, D. S., Colorado University Press, Colorado.
- Dixon, C. G. 1955. *Notes on the geology of British Honduras*. C. G. Dixon Publisher, London.
- Dobres, M. A. 2000. *Technology and social agency: outlining a practice framework for archaeology*. Blackwell Publishers, Oxford.
- Dobres, M. A. and Hoffman, C. R. 1994. Social agency and the dynamics of prehistoric technology. *Journal of Archaeological Method and Theory*. 1(3), p. 211-258.
- Dull, R. A, Southon, J. R, and Sheets, P. 2001. Volcanism, ecology and culture: a reassessment of the volcan Ilopango TBJ eruption in the southern Maya Realm. *Latin American Antiquity* 12, p. 25-44.
- Durán, D. d. 1588. 1994. *The History of the Indies of New Spain*. Translated, annotated, and with an Introduction by Doris Heyden. The Civilization of the American Indian Series 210. University of Oklahoma Press, Norman, Oklahoma.
- Eastaugh, N, Walsh, V, Chaplin, T, and Siddall, R. 2004. *Pigment compendium: a dictionary of historical pigments*. Butterworth Heinemann, London.
- Eaton, J. D. 1991. Tools of ancient Maya builders. Paper presented at *Maya stone tools: selected papers from the second Maya lithic conference*, Prehistory Press, Monographs in World Archaeology 1.
- Ellis, P.R. 1999. Analysis of mortars (to include historic mortars) by differential thermal analysis, in: *Historic mortars: characteristics and tests*, Proceedings of the International RILEM workshop, Paisley, Scotland, edited by P. Bartos, C. Groot, and J. Hughes, RILEM publications, France.
- Elsen, J. 2006. Microscopy of historic mortars: a review. *Cement and Concrete Research*, 36(8), p. 1416-1424.
- Erasmus, C. J. 1977. Monument building: some field experiments. In *Experimental Archaeology*, edited by Ingersoll, D, Yellen, J. E, and Macdonald, W., New York, Columbia University Press, pp. 53-78.
- Escalante Gonzalbo, P.1999 *Los Códices*. Consejo Nacional para la Cultura y las Artes, Serie Tercer Milenio, México, D.F.
- Espindola, J. M, Macías, J. L, Tilling, R. I, and Sheridan, M. F. 2000. Volcanic history of el Chichon Volcano (Chiapas, Mexico) during the Holocene, and its impact on human activity. *Bulletin of Volcanology* 62(9): 90-104.

- Espinosa, L, Ceron, M, and Sulub, Y. A. 1996. Limestone rocks of the Yucatan Peninsula. Description of the lithology and physical properties based on the results of exploration, investigation and laboratory tests. *International Journal of Rock Mechanics and Mining Sciences and Geomechanics Abstracts* 35(4): 410-411.
- Farci, A, Floris, D, and Meloni, P. 2005. Water permeability vs. porosity in samples of Roman mortars. *Journal of Cultural Heritage* 6(1), p. 55-59.
- Fields, V. M. 1985. Fifth Palenque Round Table. *Proceedings of the Fifth Palenque Round Table Conference, June 12-18, 1983 Palenque, Chiapas, Mexico*, San Francisco. Available at: <http://www.mesoweb.com/pari/publications/RT07/index.html>
- _____. 1991. Sixth Palenque Round Table, 1986. Norman, University of Oklahoma Press. Available at: http://www.mesoweb.com/pari/publications/RT08/RT06_00.html
- _____. 1994. Seventh Palenque Round Table, 1989. *Proceedings of the Seventh Palenque Round Table Conference 1989, Palenque, Chiapas, Mexico*, San Francisco. Pre-Columbian Art Research Institute, San Francisco. Available at: <http://www.mesoweb.com/pari/publications/RT09/index.html>
- Flannery, K. V. and Marcus, J. 1990. Borrón y cuenta nueva: setting Oaxaca's archaeological record straight. In *Debating Oaxaca archaeology*, edited by Marcus, J., pp. 17-69. Museum of Anthropology, University of Michigan, Ann Arbor, Michigan.
- Folan, W. J. 1978. Coba, Quintana Roo, Mexico: an analysis of a Prehispanic and contemporary source of sascab. *American Antiquity* 43, p. 79-85.
- _____. 1982. Mining and quarrying techniques of the Lowland Maya. *Anthropology* VI(1,2), p. 149-174.
- Folan, W. J., Gunn, J. D., and Dominguez-Carrasco, M. R. 2001. Triadic temples, central plazas, and dynastic palaces: a diachronic analysis of the royal court complex, Calakmul, Campeche, Mexico. In: *Royal courts of the ancient Maya*, edited by Inomata, T. and Houston, S., p 223-259. Westview, Oxford.
- Folan, W. J., Marcus, J., Pincemin, S, Dominguez-Carrasco, M. R, Fletcher, L, and Morales-Lopez, A. 1995. Calakmul: new data from an ancient Maya capital in Campeche, Mexico. *Latin American Antiquity* 6(4), p. 310-334.
- Folan, W. J. and Morales-Lopez, A. 1996. Calakmul, Campeche, México: la Estructura II-H, sus entierros y otras funciones ceremoniales y habitacionales. *Revista Española de Antropología Americana*, p. 26, p. 9-28.
- Folk, R. L. and Valastro, S. 1976. Successful technique for dating of lime mortar by carbon-14. *Journal of Field Archaeology* 3(2): 203-208.
- Ford, A and Glicken, H. 1987. The significance of volcanic ash tempering in the ceramics of the central Maya Lowlands. Paper presented at *Papers from the 1985 Maya Ceramic Conference*, 345:479-502. Oxford.
- Ford, A and Rose, W. I. 1995. Volcanic ash in ancient Maya ceramics of the limestone lowlands: implications for prehistoric volcanic activity in the Guatemala highlands. *Journal of Volcanology and Geothermal Research* 66(1): 149-162.

- Fourcade, E, Rocchia, R, Gardin, S, Bellier, J. P, Debrabant, P, Masure, E, Robin, E, and Pop, W. T. 1998 Age of the Guatemala breccias around the Cretaceous-Tertiary boundary: relationships with the asteroid impact on the Yucatan. *Comptes Rendus de l'Académie des Sciences - Series IIA - Earth and Planetary Science* 327(1), p. 47-53.
- Franzini, M, Leoni, L, Lezzerini, M, and Sartori, F. 2000. The mortar of the "Leaning Tower" of Pisa. *European Journal of Mineralogy* 12(6), p. 1151-1163.
- Garber, J. F., Driver, W. D, Sullivan, L. A, and Glassman, D. M. 1998. Bloody bowls and broken pots. The life, death, and rebirth of a Maya house. In *The sowing and the dawning: termination, dedication, and transformation in the archaeological and ethnographic record of Mesoamerica*, edited by Mock, S. B, University of New Mexico Press, Albuquerque.
- Garcia-Moreno, R, Granados, J. Tumbas reales de Calakmul, in: *Arqueología Mexicana* (VII):42, p. 28-33, Raíces-INAH, México.
- Garcia-Moreno, R, Mathis, R, Mazel, F, Dubus, M, Calligaro, T, and Strivay, D. 2008. Discovery and characterization of an unknown blue-green Maya pigment: veszelyte. *Archaeometry* 50(4): 658-667.
- Garcia-Solis, C. A, Quintana, P, and Bautista-Zúñiga, F. 2006. La identificación de materiales arcillosos y pétreos utilizados en la manufactura del friso modelado en estuco de la SubII-C1 de Calakmul a través de análisis de difracción de rayos X. In *La ciencia de materiales y su impacto en la arqueología*, edited by Medoza, M, Arenas, J. A, Ruvalcaba, J. L, and Rodríguez, V, p. 237-251. México, D.F.
- Gerhardt, J. C. 1988. *Preclassic Maya Architecture at Cuello, Belize*. 464. BAR, International series, Oxford.
- Gibbons, P.. 2003. Pozzolanas for lime mortars. In: Building Conservation [online]. Available at: <http://www.buildingconservation.com/articles/pozzo/pozzo.htm>. [Accessed February 2008].
- Gill, R.B. 2000. *The great Maya droughts :water, life, and death*, Albuquerque, University of Mexico Press.
- Goodall, R. A, Hall, J, Edwards, H. G. M, Sharer, R. J, Viel, R, and Fredericks, P. M. 2007. Raman microprobe analysis of stucco samples from the buildings of Maya Classic Copan. *Journal of Archaeological Science* 34(4), p. 666-673.
- Goren, Y, Goldberg, P, Stahl, P. W, and Brinker, U. H. 1991. News and short contributions. Petrographic thin sections and the development of Neolithic plaster production in Northern Israel. *Journal of Field Archaeology* 18(1), p. 131-140.
- Gould, A and Watson, P. J. 1982. A dialogue on the meaning and use of analogy in ethnoarchaeological reasoning. *Journal of Anthropological Archaeology* (1)355-381.
- Gourdin, W. H and Kingery, W. D. 1975 The beginnings of pyrotechnology: Neolithic and Egyptian lime plaster. *Journal of Field Archaeology* 2(1): 133-150.
- Graham, E. 1987. Resource diversity in Belize and its implications for models of lowland trade. *American Antiquity* 52(4): 753-767.

-
- _____. 1994. Environment and Land Use. In *The highlands of the lowlands : environment and archaeology in the Stann Creek District, Belize, Central America*, Monographs in world archaeology. Prehistory Press/ Royal Ontario Museum, Madison, Wis., Ontario.
- _____. 2000. Collapse, conquest, and Maya survival at Lamanai, Belize. *Archaeology International*, (4) p. 52-56.
- _____. 2004. Lamanai reloaded: alive and well in the Early Postclassic. Paper presented at *Archaeological investigations in the Eastern Maya Lowlands: papers of the 2003 Belize Archaeology Symposium*. Editors: J. Awe, M. Morris and S. Jones.
- _____. 2007. Lamanai, Belize from Collapse to Conquest – Radiocarbon dates from Lamanai. Paper presented at *106th Meeting of the AAA, 28 November to 2 December*, Washington, D.C.
- _____. 2008. *Lamanai historic monuments conservation project: recording and consolidation of new church architectural features at Lamanai, Belize*. FAMSI [online]. Available at <http://www.famsi.org/reports/06110C/06110CGraham01.pdf> [Accessed August 2008].
- Griffin, G. 1978. Cresterias of Palenque. Paper presented at *Proceedings of the Tercera Mesa Redonda de Palenque, June 11-18, 1978, Palenque, IV: Pre-Columbian Art Research Institute*, Monterey, California. Editors: M.G Robertson and D.C. Jeffers
- Grissom, C. A. 2000. Neolithic statues from Ain Ghazal: construction and form. *American Journal of Archaeology* 104, p. 25-46.
- Grove, D. C. 1987. Raw materials and sources. In *Ancient Chalcatzingo*, edited by Grove, D. C, p. 376-386. University of Texas Press, Austin.
- Grove, D. C and Guillen, A. C. 1987. The Excavations. In: *Ancient Chalcatzingo*, edited by Grove, D. C, pp. 21-55. University of Texas Press, Austin.
- Grube, N. 2006. Volcanoes and Jungle, a Richly Varied Habitat. In *Maya: Divine kings of the rainforest*, edited by Grube, N., Eggebrecht, E, and Seidel, M, Konemann, Koln.
- Gunasekaran, S, Anbalagan, G, and Pandi, S. 2006. Raman and infrared spectra of carbonates of calcite structure. *Journal of Raman Spectroscopy* 37, p. 892-899.
- Gunn, J., Foss, J. F, Folan, W. J., Dominguez-Carrasco, M. R, and Faust, B. B. 2002. Bajo sediments and the hydraulic system of Calakmul, Campeche, Mexico. *Ancient Mesoamerica* 13, p. 297-315.
- Gunn, J. D., Matheny, R. T., and Folan, W. J. 2002. Climate change studies in the Maya area. *Ancient Mesoamerica* 13(1), p. 74-84.
- Hale, J, Heinemeir, J, Lancaster, L, Lindroos, A, and Ringbom, A. 2003. Dating ancient mortar. *American Scientist Online*, 91, p. 130-137. Available at: [http://www.phys.au.dk/ams/hale-jh-2003\(jan17\)datingancientmortar@.pdf](http://www.phys.au.dk/ams/hale-jh-2003(jan17)datingancientmortar@.pdf)
- Hammond, N. 1982a. The Prehistory of Belize. *Journal of Field Archaeology* 9(3): 349-362.
- _____. 1982b.: *Ancient Maya civilization*, Cambridge, Cambridge University Press.
- _____. 1986. New light on the most ancient Maya. *Man* 21(3): 399-413.

- Hammond, N and Ashmore, W. 1981. Lowland Maya Settlement: Geographical and Chronological Frameworks. In *Lowland Maya Settlement Patterns*, p. 19-36. School of American Research, University of New Mexico Press, Albuquerque.
- Hammond, N, Clarke, A, and Donaghey, S. 1995. The long goodbye: Middle Preclassic Maya archaeology at Cuello, Belize. *Latin American Antiquity* 6(2): 120-128.
- Hammond, N, Clarke, A., and Robin, C. 1991. Middle Preclassic buildings and burials at Cuello, Belize: 1990. *Latin American Antiquity* 2(5): 352.
- Hammond, N and Gerhardt, J. C. 1990. Early Maya architectural innovation at Cuello, Belize. *World Archaeology* 21(3): 461-481.
- Hansen, E., Hansen, R. D., and Derrick, M. R. 1995. Los análisis de los estucos y pinturas arquitectónicas de Nakbé: resultados preliminares de los estudios de los métodos y materiales de producción. Paper presented at *VIII Simposio de Investigaciones Arqueológicas en Guatemala 1994*, Guatemala.
- _____. 2005. Technology used in the production of ancient Maya mortars and plasters. Paper presented at *Contemporary and historic uses of lime in mortars, plasters and stuccos*, 1-10. Orlando, Florida.
- Hansen, E. and Rodríguez-Navarro, C. 2001. Los comienzos de la tecnología de la cal en el mundo Maya: innovación y continuidad desde el Preclásico Medio hasta el Clásico Tardío en Nakbé, Petén, Guatemala. Paper presented at *XV Simposio de Investigaciones Arqueológicas en Guatemala*, 183-187.
- Hansen, E., Rodríguez-Navarro, C, and Hansen, R. D. 1997. Incipient Maya burnt lime technology: characterization and chronological variations in Preclassic plaster, stucco and mortar at Nakbe, Guatemala. Paper presented at *Materials Research Society symposium proceedings* , V:207-216. Boston, Massachusetts.
- Hansen, E. F., Rodríguez-Navarro, C., and Van Balen, K. 2008. Lime putties and mortars: insights into fundamental properties. *Studies in Conservation* 5, p. 39-23.
- Hansen, R. D. 1992. *The archeology of ideology: a study of Maya Preclassic Architectural Sculpture at Nakbe, Peten, Guatemala*,. PhD thesis, University of California, Los Angeles.
- _____. 1994. Las dinámicas culturales y ambientales de los orígenes Mayas: estudios recientes del sitio arqueológico Nakbe. Paper presented at *VII Simposio de Investigaciones Arqueológicas en Guatemala 1993*.
- Hansen, R.D. 2000. *Ancient Maya burnt-lime technology: cultural implications of technological styles*. PhD dissertation, Department of Anthropology, University of California, Los Angeles.
- _____. 2000. Ideología y arquitectura: poder y dinámicas culturales de los Mayas del periodo preclásico en las tierras bajas. Paper presented at *2da Mesa Redonda de Palenque, arquitectura e ideología de los antiguos Mayas*.
- Hansen, R. D., Bozarth, S, Jacob, J, Wahl, D, and Schreiner, T. 2002. Climatic and environmental variability in the rise of Maya civilization: A preliminary perspective from northern Peten. *Ancient Mesoamerica* 13(2): 273-295.

- Harlow, G. E, Hemming, S. R, Lallemand, H. G, Sisson, V. B, and Sorensen, S. S. 2004. Two High-pressure-low-temperature serpentinite-matrix mélange belts, Motagua Fault Zone, Guatemala: A record of Aptian and Maastrichtian collisions. *Geology* 32(1): 17-20.
- Haug, G. H., Gunther, D., Peterson, L. C., Sigman, D. M., Hughen, K. A., and Aeschlimann. 2003. climate and the collapse of Maya civilization. *Science* 299, p. 1731-1735.
- Healy, P. F, Emery, K, and Wright, L. E. 1990. Ancient and modern Maya exploitation of the Jute snail (*Pachychilus*). *Latin American Antiquity* 1(2): 170-183.
- Heinemeir, J, Jungner, H, Lindroos, A, Ringbom, A, Von Konow, T., and Rud, N. 1997. AMS 14C Dating of Lime Mortar. *Nuclear Instruments and Methods in Physics Research B* B(123): 487-495.
- Hellmuth, N. 1977. Cholti-Lacandon (Chiapas) and Petén-Ytzá agriculture, settlement pattern and population. In *Social process in Maya prehistory*, edited by Hammond, N, pp. 421-448. Academic Press, London.
- Hernandez-Reyes, C and Peralta-Barcenas, R. 1974. Los estucos modelados de Palenque. *Cultura y Sociedad*, 1(1), p.: 51-53.
- Hildebrand, A. R, Penfield, G. T, Kring, D. A, Pilkington, M, Camargo, M, Jacobsen, S. B, and Boynton, W. V. 1991. Chicxulub Crater: A possible Cretaceous/Tertiary boundary impact crater on the Yucatán Peninsula, Mexico. *Geology* 19(9): 867-871.
- Hodell, D. A., Curtis, J. H, and Brenner, M. 1995. Possible role of climate in the collapse of Classic Maya civilization. *Nature* 372, p. 391-394.
- Hodell, D. A., Quin, R. L., Brenner, M, and Kamenov, G. 2004. Spatial variation of strontium isotopes ($^{87}\text{Sr}/^{86}\text{Sr}$) in the Maya region: a tool for tracking ancient human migration. *Journal of Archaeological Science* 31(5): 585-601.
- Hough, R. M, Gilmour, I, Pillinger, C. T, Langenhorst, F, and Montanari, A. 1997. Diamonds from the iridium-rich K-T boundary layer at Arroyo el Mimbral, Tamaulipas, Mexico. *Geology* 25(11), p. 1019-1022.
- Houston, S. D. 1996. Symbolic Sweatbaths of the Maya: Architectural Meaning in the Cross Group at Palenque, Mexico. *Latin American Antiquity* 7(2): 132-151.
- Houston, S.D. 1998. Finding Function and Meaning in Classic Maya Architecture, in: *Function and Meaning in Classic Maya Architecture*, Washington D.C: Dumbarton Oaks Research Library and Collection.
- Hughes, J. J and Valek, J. 2003. *Mortars in historic buildings : a review of the conservation, technical and scientific literature*. Historic Scotland, Edinburgh.
- INEGI. 2007 Sistema Nacional Estadístico de Información Geográfica [online]. Available at: <http://www.inegi.gob.mx/inegi/default.aspx>
- Isphording, W. C and Wilson, E. M. 1973. Weathering Processes and Physical Subdivisions of Northern Yucatan. Paper presented at *Proceedings of the Association of American Geographers*, 5:117-121.

- Isphording, W. C and Wilson, E. M. 1974. The relationship of volcanic ash, "sak lu'um" and palygorskite in northern Yucatan Maya ceramics. *American Antiquity* 39(3).
- Jones, L. D. 1986. *Lowland Maya pottery: the place of petrological analysis*. B.A.R. International Series. 288. British Archaeological Reports, Oxford.
- Karkanias, P. 2007. Identification of lime plaster in prehistory using petrographic methods: A review and reconsideration of the data on the basis of experimental and case studies, in: *Geoarchaeology* 22(7): 775-796.
- Katz, S. H, Hediger, M. L, and Valleroy, L. A. 1974. Traditional maize processing techniques in the New World. *Science* 184(4138), p. 765-773.
- Kerstin, E., Rodríguez Navarro, C., Pardo, E.S., Hansen, E., Cazzalla, O. 2002. Lime mortars for the conservation of historic buildings, in: *Studies in Conservation* 46(4): 62-75.
- Kidder, A. V. 1937. Ceramic Technology- Anna O. Shepard, in: *The reports on the Investigations of the Divisions of Historical Research*, Carnegie Institute of Washington, Washington DC.
- King, B. 2000. A Brief Introduction to Pozzolanas, in: *Alternative construction - contemporary natural building methods*, edited by Elizabeth, L. and Adams, C., John Wiley and Sons.
- King, D. T and Petryny, L. W. 2003. Stratigraphic and sedimentology of coarse impactoclastic breccia units within the Cretaceous-Tertiary Boundary Section, Albion Island, Belize. In *Impact Markers in the Stratigraphic Record*, edited by Koeberl, C and Martinez Ruiz, F. C, Springer, Berlin, London.
- Kingery, W. D, Vandiver, P. B., and Prickett, M. 1988. The beginnings of pyrotechnology, part II: production and use of lime and gypsum plaster in the Pre-pottery Neolithic Near East. *Journal of Field Archaeology* 15(2): 219-244.
- Kowalski, J.K (ed). 1999. *Mesoamerican architecture as a cultural symbol*, Oxford: Oxford University Press.
- Kring, D. A and Boynton, W. V. 1991 Altered spherules of impact melt and associated relic glass from K/T boundary sediments in Haiti. *Geochimica et Cosmochimica Acta* 55:1737-1742.
- Kring, D. A and Boynton, W. V. 1992. Petrogenesis of an augite-bearing melt rock in the Chicxulub structure and its relationship to K/T impact spherules in Haiti. *Nature* 358(141): 144.
- Lacadena García-Gallo, A. 2004. *The glyphic corpus from Ek' Balam, Yucatán, México*, FAMSI [online]. Available at: <http://www.famsi.org/reports/01057/section04.htm> [accessed July 2008].
- Lamprecht, H. O. 1993. *Opus Caementitium: bautechnik der Romer*. Beton-Verlag, Dusseldorf.
- Lanas, J and Alvarez Galindo, J. I. 2003 Masonry repair lime-based mortars: factors affecting the mechanical behavior. *Cement and Concrete Research* 33(11), p. 1867-1876.
- Lechtman, H.N, Merrill, R.S. 1977. *Material culture : styles, organization, and dynamics of technology*, in: Proceedings of the American Ethnological Society, Detroit, Apr. 3-4, 1975 , St. Paul, West Pub co.

- Leroi-Gourhan, A. 1965. *Préhistoire de L'art Occidental*. Art et les grandes civilisations Éditions d'art, Paris.
- Lewenstein, S. M. 1987. *Stone tool use at Cerros : the ethnoarchaeological and use-wear evidence*. University of Texas Press, Austin.
- _____. 1995. La albañilería maya: herramientas, tareas y aportaciones en la península Yucateca durante el Clásico y Posclásico. Paper presented at *Memorias del segundo congreso Internacional de Mayistas*, p. 210-223. Instituto de Investigaciones Filológicas, UNAM, Mexico,.
- Liendo Stuardo, R. 2005. An archaeological study of settlement distribution in the Palenque Area, Chiapas, Mexico. *Anthropological Notebooks*, Slovene Anthropological Society 11, p. 31-44.
- Littman, E. R. 1957 Ancient Mesoamerican mortars, plasters and stuccos. Comalcalco part I. *American Antiquity* 23(2): 135-139.
- _____. 1958a. Ancient Mesoamerican mortars, plasters and stuccos: the composition and origin of sascab. *American Antiquity* 24(2): 172-176.
- _____. 1958b. Ancient Mesoamerican mortars, plasters and stuccos. Comalcalco part II. *American Antiquity* 23(3): 292-296.
- _____. 1959a. Ancient Mesoamerican mortars, plasters and stuccos. Las Flores, Tampico. *American Antiquity* 25(1): 117-119.
- _____. 1959b. Ancient Mesoamerican mortars, plasters and stuccos. Palenque, Chiapas. *American Antiquity* 25(2): 264-266.
- _____. 1960a. Ancient Mesoamerican mortars, plasters and stuccos. The Puuc area. *American Antiquity* 25(3): 407-412.
- _____. 1960b. Ancient Mesoamerican mortars, plasters and stuccos. The use of bark extracts. *American Antiquity* 25(4): 593-597.
- _____. 1962 Ancient Mesoamerican Mortars, Plasters, and Stuccos: Floor Constructions at Uaxactun. *American Antiquity* 28(1): 100-103.
- _____. 1966 The classification and analysis of ancient calcareous materials. *American Antiquity* 31(6): 875-878.
- _____. 1967. Patterns in Maya floor construction. *American Antiquity* 32(4): 523-533.
- _____. 1979. Preliminary Report on Plaster Floors at Cuello, in: *Cuello Project 1978 Interim Report*, pp. 79-87. Archaeological Research Program. Douglass College, Rutgers University, New Brunswick.
- _____. 1990. *Observations on the Floors of Platforms 5D-1 and 5D-4 (Group 5D-2)*.
- López Bravo, R. 2000. La veneración de los ancestros en Palenque. *Arqueología Mexicana* VIII(45), p. 38-43, Raíces-INAH, México.

- Macías, J. L., Arce, J. L., Mora, J. C., Espindola, J. M., and Saucedo, R. 2003. A 550-year old Plinian eruption at el Chichon Volcano, Chiapas, Mexico: explosive vulcanism due to reheating of the magna reservoir. *Journal of Geophysical Research* 108(3): 1-18.
- Mackinnon, J. J. and May, E. M. 1990. Small scale Maya lime making in Belize, ancient and modern. *Ancient Mesoamerica* 1: 197-203.
- Magaloni, D. 1995. Técnicas de la pintura mural en Mesoamérica. *Arqueologia Mexicana* 3(16), p. 16-23, Raíces-INAH, México.
- _____. 1998. El arte en el hacer: técnica pictórica y color en las pinturas de Bonampak. In *La pintura mural prehispánica en México. II. Bonampak.*, edited by De la Fuente, B and Staines, L, pp. 49-80. Instituto de Investigaciones Estéticas, UNAM, Mexico, D.F.
- Magaloni, D., Falcón, T., Cama, J., Siegel, R. W., Lee, R., Pancella, R., Baños, L., and Castaño, V. 1992. Electron microscopy studies of the chronological sequences of Teotihuacan plaster technique. Paper presented at *Materials Research Society symposium proceedings*, Materials Research Society, (3) p. 997-1005.
- Magaloni, D., Newman, R., Castano Banos, R., Pancella, R., and Fruh, Y. 1995. An analysis of Mayan painting techniques at Bonampak, Chiapas, Mexico. Paper presented at *Materials Issues in Art and Archaeology IV, Materials Research Society Symposium proceedings*, 352, p. 381-388. Pittsburgh, P.A.
- Magaloni, D., Pancella, R., Fruh, R., Cañetas, J., and Castaño, V. 1995. Studies on the Maya mortars technique. Paper presented at *Materials Issues in Art and Archaeology IV, Materials Research Society symposium proceedings*, p. 483-489. Pittsburg, Pennsylvania.
- Marken, D. B and Lanham, M. D. 2006. *Palenque: recent investigations at the Classic Maya Center*, Altamira press, Lanham, M.D.
- Martin, S. and Grube, N. 2000. *Chronicle of the Maya kings and queens: deciphering the dynasties of the ancient Maya*. Thames and Hudson, London.
- Matheny, R. T. 1982. Ancient Lowland and Highland Maya water and soil conservation strategies. In *Maya subsistence. Studies in memory of Dennis E. Puleston*, edited by Flannery, K. V., Studies in archaeology, Academic Press, New York, London.
- Mathews, P. 2000. *Who's who in the Classic Maya World. The royal genealogy of Palenque*. FAMSI, [online] Available at: http://research.famsi.org/whos_who/royal_gen_images.php?id=3 [Accessed September 2008].
- Mathews, P and Biró, P. 2005. Maya hieroglyph dictionary. FAMSI [online]. Available at: http://research.famsi.org/mdp/mdp_index.php [accessed March 2008].
- Mathews, R. A. S. 2002. *Geology, environment and lime production variation in the Maya Lowlands*. MSc, University of Texas.
- Mazzullo, S. J, Teal, C. S, and Graham, E. 1994. Mineralogic and crystallographic evidence of lime processing, Santa Cruz Maya Site (Classic to Postclassic), Ambergris Caye, Belize. *Journal of Archaeological Science* 21(6): 785-795.

- McDonald, R. 1978. Preliminary Report on the physical geography of northern Belize. In *Cuello Project 1978 Interim Report*, pp. 79-87. Edited by N. Hammond, Archaeological Research Program. Douglass College, Rutgers University, New Brunswick.
- McGee, R. J. 1998. The Lacandon incense burner renewal ceremony. Termination and dedication ritual among the contemporary Maya. In *the Sowing and the Dawning. Termination, Dedication and Transformation in the Archaeological and Ethnographic Record of Mesoamerica*, edited by Mock, S. B, University of New Mexico Press, Albuquerque.
- Middendorf, B. and Knöfel, D. 1998. Characterization of historic mortars from buildings in Germany and the Neatherlands in: *Conservation of Historic Brick Structures*, edited by N.S. Baer, S. Fitz., and R.A. Livingston, pp. 179-196, Donhead: Dorset.
- Miller, M.E. 2006. Maya painting in a major and minor key, in: *Anales del Instituto de Investigaciones Estéticas* (89): 59-70.
- Moraa, J. C, Jaimes-Vierab, M. C, Garduño-Monroy, V. H, Layerd, P. W, Pompa-Merab V, and Godínez, M. L. 2007. Geology and geochemistry characteristics of the Chiapanecan Volcanic Arc (Central Area), Chiapas Mexico. *Journal of Volcanology and Geothermal Research* 162(1-2): 43-72.
- Moropoulou, A., Bakolas, A., Bisbikous, K., 1995. Characterization of ancient byzantine and later historical mortars by thermal and X-ray diffraction techniques, in: *Thermochimica Acta* 20: 779-795.
- Moropoulou, A, Casmak, A. S, Biscontin, G, Bakolas, A, and Zendri, E. 2002. Advanced Byzantine cement based composites resisting earthquake stresses: the crushed brick/lime mortars of Justinian's Hagia Sophia. *Construction and Building Materials* 16(8), p. 543-552.
- Morris, E. H, Charlot, J, and Morris, A. A. 1931. *The Temple of the Warriors at Chichen Itzá, Yucatán*. 1 ed. Carnegie Institute of Washington, Washington D.C.
- Murakami, T, Hodgins, G. W. L, Vonarx, a. J, and Simon, A. 2006. Radiocarbon dating Mesoamerican plasters: studies from Teotihuacan. Paper presented at *International Symposium of Archaeometry*, Quebec City, Canada, May 2nd - 6th.
- Nations, J. D. 1979. Snail shells and maize preparation: A Lacandon Maya analogy. *American Antiquity* 44(3): 568-571.
- Nipper, M, Sánchez Chávez, J. A, and Tunnell, J. W. 2008. Gulf base: resource database for Gulf of Mexico Research. Available online: <http://www.gulfbase.org/> [Accessed July 2008].
- Ocampo, A. C, Ames, D, Pope, K. O., and Smit, J. 2003. New location of Chicxulub's impact ejecta in Central Belize. *Geophysical Research Abstracts*, EGS - AGU - EUG Joint Assembly, Abstracts from the meeting held in Nice, France, 6 - 11 April 2003, abstract #6925.
- Oleson, J. P, Brandon, C, Cramer, S. M, Cucitore, R, Gotti, E, and Hohlfelder, R. L. 2004. The ROMACONS Project: a contribution to the historical and engineering analysis of Hydraulic concrete in Roman maritime structures. *International Journal of Nautical Archaeology* 33(2): 199-229.
- Ortiz, S. 1994. Work, the division of labour and co-operation. In *Companion Encyclopedia of Anthropology*, edited by Ingolt, T, Routledge, London.

- Ower, L. H. 1928 *Geology of British Honduras*. Clarion Limited, Chicago.
- Pacheco, L. E. 2007. Viaje al corazón de Calakmul. *Letras Libras* 2007: 52-59.
- Paine, R. R. and Freter, A. 1996. Environmental degradation and the Classic Maya collapse at Copan, Honduras (AD 600-1250): evidence from studies of household survival. *Ancient Mesoamerica* 7:37-47.
- Palladio, A. 1998. *The Four Books on Architecture*. translated by Robert Tavernor and Richard Schofield. MIT Press, Cambridge, Mass. London.
- Pendergast, D. M. 1985a. Lamanai, Belize: an updated view. In *The Lowland Maya Postclassic*, edited by Chase, A. F. and Rice, P. M., pp. 91-103. University of Texas Press, Austin.
- _____. 1985b. Stability through change: Lamanai, Belize, from the ninth to the seventeenth century. In *Late Lowland Maya Civilization, Classic to Postclassic*, edited by Sabloff, J. A. and Andrews, E. W., A School of American Research Book. University of New Mexico Press, Albuquerque.
- _____. 1988. Engineering problems in ancient Maya architecture: past, present, and future. Paper presented at *The engineering geology of ancient works, monuments and historical sites: preservation and protection: proceedings of an international symposium, Athens, 19-23 September 1988*, 3:1652-1660. Rotterdam.
- _____. 1990. Up from the dust: the central lowlands Postclassic as seen from Lamanai and Marco Gonzalez, Belize. In *Vision and revision in Maya studies*, edited by Clancy, F. S. and Harrison, P. D., University of New Mexico Press, Albuquerque.
- _____. 2001. Cinnabar and hematite. In *Archaeology of ancient Mexico and Central America : an encyclopedia*, edited by Evans, S. T. Webster D. L. ed, pp. 145. Garlands, New York, London.
- Peralta, O. 2004 El Chichonal. *El Faro*, III(35), p. 8-9, Coordinación de Investigación Científica, UNAM, Mexico.
- Pfaffenberger, B. 1988. Fetichised objects and human nature: towards an anthropology of technology, in: *Man* 23(2): 236-252.
- Pichler, H. and Schmitt-Riegraf, C. 1997 *Rock-forming Minerals in Thin Section*. Chapman and Hall, London.
- Pollard, A. M. 2007. *Analytical chemistry in Archaeology*. Cambridge University Press, Cambridge.
- Pope, K. O. and Dahlin, B. H. 1989. Ancient Maya Wetland Agriculture: New insights from ecological and remote sensing research. *Journal of Field Archaeology* 16:87-105.
- Pope, K. O., Ocampo, A. C., and Duller, C. E. 1993 Superficial Geology of the Chicxulub Impact crater, Yucatan, Mexico. *Earth, Moon and Planets* 63:93-104.
- Pope, K. O., Ocampo, A. C., Fischer, A. G., Alvarez, W., Fourke, B. W., Webster, C. L., Vega, F. J., Smit, J., Fritsche, A. E., and Claeys, P. 1999. Chicxulub impact ejecta from Albion Island, Belize. *Earth and Planetary Science Letters* 170(4), p. 351-364.

- Pope, K. O., Ocampo, A. C., Fischer, A. G., Vega, F. J., Ames, D., King, D. T jr., Fouke, B. W., Wachtman, R. J., and Kletetschka, G. 2005. Chicxulub impact ejecta deposits in southern Quintana Roo, Mexico, and central Belize. In *Large Meteorite Impacts III*, edited by Kenkmann, T, Horz, F, and Deutsch, A, pp. 171-190. Special Paper 394. The Geological Society of America.
- Pope, K. O., Pohl, M. D, Jones, J. G, Lentz, D. L., Von Nagy, C, Vega, F. J, and Quitmyer, I. R. 2001. Origin and Environmental Setting of Ancient Agriculture in the Lowlands of Mesoamerica . *Science* 18, p. 1370-1373.
- Pringle, H. 1997. New respect for metal's role in ancient Arctic cultures. *Science* 277(5327): 766-767.
- Rathje, W.L. 1971. The origin and development of Lowland Classic Maya Civilisation, in *American Antiquity* 36(3), pp. 275-285.
- Rands, B.C., Rands, R.L. 1959. The incensario complex of Palenque, Chiapas, *American Antiquity* 25(2): 234-236.
- Rands, R. L. 1974. A Chronological framework for Palenque. [online] Pebble Beach, California: Robert Louis Stevenson School, Pre-Columbian Art Research. Available at: www.mesoweb.com/pari/publications/RT01/Chronological.pdf [accessed July 2008].
- Rands, R. L and Bishop, R. L. 1980. Resource procurement zones and patterns of ceramic exchange in the Palenque region, Mexico. In *Models and methods in regional exchange*, edited by Fry, R. E, SSA Papers No. 1. Society for American Archaeology, Washington D.C.
- Redfield, R and Villa, R. 1934. *Chan Kom: a Maya village*. Carnegie Institute of Washington, publication 448, University of Chicago Press.
- Reese-Taylor, K and Koontz, R. 2001. The cultural poetics of power and space in ancient Mesoamerica. In *Landscape and power in ancient Mesoamerica*, edited by Koontz, R, Reese-Taylor, and Headrick, A, Westview Press, Boulder, CO.
- Rice, P. M. 1987. *Pottery Analysis*. University of Chicago Press, Chicago, London.
- _____ 1999. Rethinking Classic Lowlands Maya pottery censers, in: *Ancient Mesoamerica* 10, p. 25-50.
- Roberts, R. J and Irving, E. M. Mineral Deposits of Central America. 1957, *Geological Survey Bulletin* (1034). Washington D.C, U.S Government Printing Office.
- Robertson, M.G. 1974. First Palenque Round Table, Part I. Paper presented at *A conference on the art, iconography, and dynastic history of Palenque, Palenque, Chiapas, Mexico. December 14-22, 1973*, Pebble Beach, California.
- _____ 1967. *Ancient Maya relief sculpture*. Museum of Primitive Art, New York.
- _____ 1975. Stucco techniques employed by ancient sculptors of the Palenque Piers. Paper presented at *Actas del XLI Congreso Internacional de Americanistas 2-7 Septiembre 1974*, 1.
- _____ 1976. Second Palenque Round Table, part III. Paper presented at *The art, iconography & dynastic history of Palenque, part III, December 14-21, Palenque 1974*, Pebble Beach, California.

- _____. 1979. A sequence for Palenque painting techniques. In *Maya archaeology and ethnohistory*, edited by Hammond, N and Willey, G. R., pp. 149-171. University of Texas Press, Texas and London.
- _____. 1980. Third Palenque Round Table, part 2. *Proceedings of the tercera Mesa Redonda de Palenque. June 11-18, 1978, Palenque*, Austin, Texas.
- _____. 1983. *The Sculpture of Palenque*. IV. Princeton University Press, Princeton, New Jersey.
- Robertson, M. G and Jeffers, D. C. (eds) 1979. *Proceedings of the tercera mesa redonda de Palenque, June 11-18, 1978, Palenque. A conference on the art, hieroglyphics, and historic approaches of the Late Classic Maya*, Monterey, California.
- Rodriguez-Navarro, C., Hansen, E., and Ginell, W. S. 1998. Calcium hydroxide crystal evolution upon ageing of lime putty. *Journal of the American Ceramic Society* 81(11): 3032-3034.
- Rodríguez Campero, O. 2000. La Gran Plaza de Calakmul, in: *Arqueología Mexicana*, Vol. VII (42), p. 22-39, Raíces-INAH, México.
- _____. 2008. *La arquitectura Petén en Calakmul: una comparación regional*. FAMSI [online]. Available at: <http://www.famsi.org/reports/02070es/index.html> [accessed November 2007].
- Rojas González-Castilla. 2000. La reserva de la biosfera de Calakmul, in: *Arqueología Mexicana*, Vol. VII (42), p. 46-51, Raíces-INAH, México.
- Roys, R. L. 1934. *The engineering knowledge of the Maya*. 436 ed. Carnegie Institute of Washington, Washington, D.C.
- Ruiz de Alarcón, H. 1629 *Treatise on the heathen superstitions that today live among the Indians native to this New Spain, 1629*. translated and edited by J. Richard Andrews and Ross Hassig ed. The civilization of the American Indian series University of Oklahoma Press.
- Russell, B., Dahlin, B.H. 2007. Traditional burnt-lime production at Mayapán, Mexico, in: *Journal of Field Archaeology*, vol. 32: 407-423.
- _____. 2008. *Postclassic Settlement on the Rural-Urban Fringe of Mayapán, Yucatán, Mexico: Results of the Mayapán Periphery Project*, doctoral dissertation, University at Albany, State University of New York.
- Ruz-Lhuillier, A. 1973. *El Templo de las Inscripciones, Palenque*. Colección Científica INAH, Mexico City.
- Salvador, A. 1991 *The Gulf of Mexico Basin*. The geology of North America, Geological Society of America, Boluder, Colorado.
- Sanders, W. T. 1977. Environmental heterogeneity and the evolution of Lowland Maya civilization. In *The origins of Maya Civilization*, edited by Adams, R. E. W., pp. 287-295. University of New Mexico Press, Albuquerque.
- Scholle, P. A and Ulmer-Scholle, D. S. 2003. *A colour guide to the petrography of carbonate rocks: grains, textures, porosity and diagenesis*. The American Association of Petroleum Geologists, Tulsa, Oklahoma.

- Schönian, F, Tagle, R., Stöffler, D, and Kenkmann, T. 2005. Geology of Southern Quintana Roo (Mexico) and the Chicxulub ejecta blanket. *Lunar and Planetary Science XXXVI*.
- Schreiner, T. 2001. Fabricación de cal en Mesoamérica: implicaciones para los mayas del Preclásico en Nakbé, Petén. Paper presented at *XIV Simposio de Investigaciones Arqueológicas en Guatemala*, p. 405-418.
- _____. 2002 *Traditional Maya lime production: environmental and cultural implications of a native American technology*. PhD, Department of Architecture, University of California, Berkeley.
- _____. 2003. Aspectos rituales de la producción de cal en Mesoamerica: evidencias y perspectivas de las Tierras Bajas Mayas. Paper presented at *Simposio de Investigaciones Arqueológicas en Guatemala, 2002*, 480-487.
- Seeley, N. J. 2000. Magnesian and dolomitic lime mortars in building conservation. *Journal of architectural conservation* 6(2): 21-29.
- Sendova, M, Zhelyaskov, V, Scalera, M, and Ramsey, M. 2005. Micro-Raman spectroscopic study of pottery fragments from the Lapatsa tomb, Cyprus, ca. 2500 BC. *Journal of Raman Spectroscopy* 36, p. 829-833.
- Shafer J and Hilsdorf, H. K. 1993. Ancient and new lime mortars- the correlation between their composition, structure and properties. Paper presented at *Proceedings of the International RILEM/UNESCO Congress*, 605-612. London.
- Sharer, R. J. 2002. Early Classic dynastic origins in the Southeastern Maya Lowlands. In *Incidents of archaeology in Central America and Yucatán. Essays in honor of Edwin M. Shook*, edited by Love, M, Popenoe de Hatch, M., and Escobedo, H. L, University Press of America.
- _____. 2006 with Traxler, L.P. *The Ancient Maya*. 6th ed. Stanford University Press, Stanford, California.
- Sharer, R. J, Traxler, L. P., Sedat, D. W, Bell, E. E., Canuto, M. A., and Powell, C. 1999. Early Classic architecture beneath the Copan Acropolis. *Ancient Mesoamerica* 10(1): 3-23.
- Shaw, J. M. 2003. Climate change and deforestation, implications for the Maya Collapse. *Ancient Mesoamerica* 14, p. 157-167.
- Shelby, T. M. 2006. *Report of the 1998 and 1999 investigations on the Archaeology and Iconography of the Polychrome Stucco Facade of Structure 10-28, Lamanai, Belize*. FAMSI [online]. Available at: <http://www.famsi.org/reports/98037/section04.htm>, [accessed July 2008].
- Shennan, S. 1997. *Quantifying Archaeology*. Second edition ed. Edinburgh University Press, Edinburgh.
- Shepard, A. O. 1939. Technological Notes on the Pottery of San Jose. In *Excavations at San Jose, British Honduras*, edited by Thomson, J. E. S, pp. 251-277, Carnegie Institute of Washington, publication 506, Washington DC.
- _____. 1952. *Ceramic Technology*. Carnegie Institute of Washington, publication 51, Washington D.C.
- _____. 1954. *Ceramics for the Archaeologists*. Carnegie Institute of Washington, publication 609, Washington D.C.

-
- _____. 1964. Temper identification: "Technological sherd-splitting" or an unanswered challenge. *American Antiquity* 29(4): 518-520.
- Siddall, R. 2000. The use of volcanoclastic material in Roman hydraulic concretes: a brief review. In *The Archaeology of Geological Catastrophes*, edited by McGuire, B., Griffiths, D, and Stewart, I, pp. 339-344. Special Publications. vol. 171, Geological Society, London.
- Siemens, A. H. 1978. Karst and the Pre-Hispanic Maya in the Southern Lowlands. In *Pre-Hispanic Maya Agriculture*, p. 117-143, edited by Harrison, P. D and Turner, B. L, University of New Mexico Press, Albuquerque.
- Sillar, B. and Tite, M. 2000. The challenge of technological choices for material science approaches in archaeology. *Archaeometry* 2-20.
- Simmons, M. P and Brem, G. F. 1979. The analysis and distribution of ash-tempered pottery in the Lowland Maya area. *American Antiquity* 44(1): 79-91.
- St John, D. A, Poole, A. B, and Sims, I. 2003 *Concrete petrography: a handbook of investigative techniques*. Kovel, Norwich.
- Stefanidou, M and Papayiani, I. 2005. The role of aggregates on the structure and properties of lime mortars. *Cement and Concrete Composites* 27(9-10), p. 914-919.
- Sykes, M. 1985. Diego Rivera and the Hotel Reforma murals. *Archives of American Art Journal*, the Smithsonian Institution 25(1/2): 29-40.
- Tarback, E. J and Lutgens, F. K. 2002. *The earth: an introduction to physical geology*. 7th ed. Prentice Hall, Upper Saddle River, N.J.
- Terry, R, Fernandez, F, Parnell, J. J, and Inomata, T. 2004. The story in the floors: chemical signatures of ancient and modern Maya activities at Aguateca, Guatemala. *Journal of Archaeological Science* 31(9): 1237-1250.
- Thompson, J.E.S. 1970. *Maya history and religion*, Norman, Oklahoma: :University of Oklahoma Press.
- Thompson, R. H. 1974. *Modern Yucatecan Maya Pottery Making*. Reprint of the 1958 edition published by the Society for American Archaeology, Salt Lake City. Memoirs of the Society for American Archaeology Kraus Reprint Co, Millwood, N.Y.
- Tilling, R. I, Rubin, M, Sigurdsson, H, Carey, S, Duffield, W. A, and Rose, W. I. 1984. Holocen eruptive activity of el Chichon Volcano, Chiapas, Mexico. *Science* , 18 (224), p. 747-749.
- Tovalín Ahumada, A and Ceja Manrique, G. 1993. Desarrollo Arquitectónico del Grupo Norte de Palenque. Paper presented at *Eighth Palenque Round Table 1993* Vol X: San Francisco. [online versión]. Available at: <http://www.mesoweb.com/pari/publications/RT10/Desarrollo.pdf>
- Tovalín Ahumada, A and López Bravo, R. 2001 Excavaciones en el norte del Palacio, Palenque. *Revista Pueblos y Fronteras* 2001, 1, p. 131-146.
- Tozzer, A. M. 1966 (c. 1941). *Landa's relación de las cosas de Yucatán*. Papers of the Peabody Museum of Archaeology and Ethnology, Harvard University XVIII. Kraus, New York.

-
- _____. 1982. *Mayas y Lacandones. Un estudio comparativo*. Instituto Nacional Indigenista, Clásicos de las Antropología no. 13, México.
- Tuchscherer, M. G, Reimold, W. U, Koeberl, C, Gibson, R. L., and Bruin, D. 2004. First petrographic results on impactites from the Yaxcopoil-1 borehole, Chicxulub structure, Mexico. *Meteoritics and Planetary Science* 39(6), p. 899-930.
- UNAM. *Mapa Geológico de México*. 1990. Instituto de Geología, Universidad Nacional Autónoma de México.
- Van Balen, K. 2005. Carbonation reaction of lime, kinetics at ambient temperature. *Cement and Concrete Research*, 35, p. 647-657.
- Van Balen, K., Van Gemert, D. 1994. Modelling lime mortar carbonation, *Materials and Structure*, 27, p. 393-398.
- Van Balen, K., Toumbakari, E.E., Blanco, M.T. Aguilera, J., Puertas, F., Sabbioni, C, Zappia, G, Riontino, C, Gobi, G. Procedure for a mortar type identification: a proposal, 1999. in: *Historic mortars: Characteristics and tests*, RILEM TC-167, International Workshop, Paisley, Scotland, RILEM Publications.
- Van Nice, R. L. 1948. Hagia Sophia: New Types of Structural Evidence. *The Journal of the Society of Architectural Historians* .
- Vidano, R. P and Fischbach, D. B. 1978. New lines in the Raman spectra of carbons and graphite. *Journal of the American Ceramic Society* 61(1-2): 13-17.
- Villaseñor, I and Price, C. 2008. Technology and decay of magnesian lime plasters: the sculptures of the funerary crypt of Palenque, Mexico. *Journal of Archaeological Science* 35(4): 1030-1039.
- Villegas, M, Vázquez, X, Ríos, D, Baños, L, and Magaloni, D. 1995. Relative dating of the stucco relieves at Palenque, Chiapas based on variation of material preparation. Paper presented at *Materials Research Society symposium proceedings*, 352:469-481.
- Vitruvius, P. 1999. *Ten books of architecture*. Translation by Ingrid D. Rowland Cambridge University Press, Cambridge.
- Ward, W. C, Keller, G, Stinnesbeck, W, and Adatte, T. 1995. Yucatan subsurface stratigraphy; implications and constraints for the Chicxulub impact. *Geology* 23(10): 873-876.
- Ward, W. C, Weidie, A. E, and Back, W. 1985. *Geology and hydrogeology of the Yucatan and Quaternary geology of Northeastern Yucatan Peninsula*. New Orleans, New Orleans Geological Society.
- Webster, D. 1999. The Archaeology of Copán, Honduras. *Journal of Archaeological Research* 7(1): 1-53.
- Webster, D and Kirker, J. 1995. Too many Maya, too few buildings: investigation construction potential at Copán, Honduras. *Journal of Anthropological Research* 51, p. 363-387.
- Weidie, A. E. 1985. Geology of Yucatan Platform. In *Geology and hydrogeology of the Yucatan and quaternary geology of northeastern Yucatan peninsula*, edited by Ward, W. G, Weidie, A. E, and Back, W, pp. 1-22. New Orleans Geological Society, New Orleans.

- White, L. A. 1949. Energy and the evolution of culture. In *The science of culture*, p.. 363-393. Grove Press, New York.
- Wilbert, J. 1987. *Tobacco and shamanism in South America*, Yale University Press: New Haven.
- Willys, A. E. 1973. *Archaeological evidence on social stratification and commerce in the Northern Maya lowlands: two masons' tool kits from Muna and Dzibilchaltun, Yucatan*. Tulane University, New Orleans.
- Wright, A.C.S.; Romney, D.H.; Arbuckle, R.H.; Vial, V.E.; (ed) 1959. *Land in British Honduras. Report of the British Honduras Land Use Survey Team*, Colonial Research Publication 24. Her Majesty's Stationery Office, London.
- Wright, L. E. 1999. The elements of Maya diets, alkaline earth baselines and paleodietary reconstruction in the Pasión region. In *Reconstructing ancient Maya diet*, edited by White, C. D, p. 197-219. University of Utah Press, Salt Lake City.

A.1. Munsell Colours

| Sample | Munsell Colour Dry | Munsell Colour Wet | Sample | Munsell Colour Dry | Munsell Colour Wet |
|-------------------------------------|--------------------|--------------------|-----------|--------------------|--------------------|
| Ca1 | 10YR 8/4 | 10YR 8/4 | La5 | 10YR 8/2 | 10YR 8/3 |
| Ca2 | 10YR 7/2 | 10YR 6/2 | La6 | 10YR 8/2 | 10YR 8/3 |
| Ca3 | 10YR 7/3 | 10YR 6/3 | La7 | 10YR 8/1 | 10YR 8/2 |
| Ca4 | 10YR 7/2 | 10YR 6/2 | La8 | 10YR 7/2 | 10YR 6/3 |
| Ca5 | 10YR 8/1 | 10YR 8/2 | La9 | 10YR 8/2 | 10YR 8/3 |
| Ca6 | 10YR 8/2 | 10YR 7/2 | La10 | 10YR 8/1 | 10YR 8/2 |
| Ca7 | 10YR 8/1 | 10YR 8/2 | La11 | 10YR 8/1 | 10YR 8/3 |
| Ca8 | 10YR 8/2 | 10YR 8/2 | La12 | 10YR 8/1 | 10YR 8/3 |
| Ca9 | 10YR 8/1 | 10YR 8/2 | La13 | 10YR 8/2 | 10YR 8/3 |
| Ca10 | 10YR 8/2 | 10YR 8/2 | La14 | 10YR 8/2 | 10YR 8/3 |
| Ca11 | 10YR 8/1 | 10YR 8/2 | La15 | 10YR 8/1 | 10YR 8/2 |
| Ca12 (The sample crumbled when wet) | 10YR 8/1 | 10YR 8/2 | La16 | 10YR 8/1 | 10YR 8/2 |
| Ca13 | 10YR 6/2 | 10YR 6/2 | La17 | 10YR 8/2 | 10YR 8/3 |
| Ca14 | 10YR 8/1 | 10YR 7/2 | La18 | 10YR 8/2 | 10YR 7/3 |
| Ca15 | 10YR 8/2 | 10YR 7/2 | La19 | 10YR 8/2 | 10YR 7/4 |
| Ca16 | 10YR 7/2 | 10YR 7/1 | La20 | 10YR 8/2 | 10YR 8/3 |
| Ca17 | 10YR 8/1 | 10YR 7/2 | La21 | 10YR 8/1 | 10YR 8/3 |
| Ca18 | 10YR 8/2 | 10YR 8/3 | La22 | 10YR 8/1 | 10YR 8/3 |
| Ca19 | 10YR 8/1 | 10YR 7/2 | La23 | 10YR 8/1 | 10YR 8/2 |
| Ca20 (The sample crumbled when wet) | 10YR 7/2 | 10YR 7/2 | La24 | 10YR 8/1 | 10YR 8/2 |
| Ca21 | 10YR 8/1 | 10YR 7/2 | La25 | 10YR 8/1 | 10YR 8/2 |
| Ca22 | 10YR 8/1 | 10YR 7/2 | La26 | 10YR 8/2 | 10YR 8/3 |
| Ca23 | 10YR 8/1 | 10YR 7/2 | La27 | 10YR 8/1 | 10YR 8/2 |
| Ca24 | 10YR 8/1 | 10YR 7/1 | La29 | 10YR 7/2 | 10YR 6/2 |
| Ca25 | 10YR 8/2 | 10YR 8/2 | La30 | 10YR 8/1 | 10YR 8/2 |
| Ca26 | 10YR 8/2 | 10YR 8/2 | La31 | 10YR 8/1 | 10YR 8/2 |
| Ca27 | 10YR 8/2 | 10YR 8/3 | La32a | 10YR 6/1 | 10YR 6/3 |
| Ca28 | 10YR 8/2 | 10YR 8/2 | La33 | 10YR 8/1 | 10YR 8/3 |
| Ca29 | 10YR 8/2 | 10YR 8/2 | La34 | 10YR 8/1 | 10YR 8/2 |
| Ca30 | 10YR 8/1 | 10YR 8/2 | La35 | 10YR 8/1 | 10YR 8/3 |
| Ca31 | 10YR 8/1 | 10YR 8/2 | La36a | 10YR 5/1 | 10YR 4/1 |
| Ca32 | 10YR 8/2 | 10YR 8/2 | La36b | 10YR 8/2 | 10YR 8/3 |
| Ca33 | 10YR 6/2 | 10YR 6/2 | La39 | 10YR 8/1 | 10YR 8/3 |
| Ca34 | 10YR 7/2 | 10YR 6/2 | La Sascab | 10YR 8/1 | 10YR 7/2 |
| Ca35 | 10YR 8/2 | 10YR 7/2 | | | |
| Ca36 | 10YR 8/1 | 10YR 7/2 | Pa1 | 10YR 8/1 | 10YR 8/2 |
| CaSascab | 10YR 8/1 | 10YR 8/2 | Pa2a | 10YR 8/2 | 10YR 8/3 |
| La1 | 10YR 8/1 | 10YR 8/3 | Pa2b | 10YR 8/1 | 10YR 8/2 |
| La2 | 10YR 8/2 | 10YR 8/3 | Pa3 | 10YR 8/1 | 10YR 8/3 |
| La3 | 10YR 8/3 | 10YR 8/3 | Pa4 | White fragment | 10YR 8/1 |
| La4 | 10YR 8/2 | 10YR 8/3 | | Dark soil | 10YR 4/2 |
| | | | Pa5 | 10YR 8/1 | 10YR 8/4 |

| Sample | Munsell Colour Dry | Munsell Colour Wet | Sample | Munsell Colour Dry | Munsell Colour Wet | |
|--------|---------------------|--------------------|--------|--------------------|--------------------|----------|
| Pa6 | 10YR 8/1 | 10YR 8/1 | Pa47 | 10YR 8/2 | 10YR 7/2 | |
| Pa7 | 10YR 8/2 | 10YR 8/3 | Pa48 | 10YR 8/2 | 10YR 8/3 | |
| Pa8 | 10YR 8/1 | 10YR 8/1 | Pa49 | 10YR 8/1 | 10YR 8/2 | |
| Pa9 | 10YR 8/1 | 10YR 8/2 | Pa50 | Upper layer | 10YR 8/1 | 10YR 8/2 |
| Pa10 | 10YR 8/1 | 10YR 8/1 | | Lower layer | 10YR 8/2 | 10YR 7/2 |
| Pa11 | 10YR 8/1 | 10YR 8/2 | Pa51 | 10YR 6/3 | 10YR 6/4 | |
| Pa12 | 10YR 7/2 | 10YR 7/4 | Pa52 | 10YR 8/2 | 10YR 7/3 | |
| Pa13 | 10YR 8/1 | 10YR 7/4 | Pa53 | 10YR 7/2 | 10YR 5/3 | |
| Pa14 | 10YR 8/2 | 10YR 6/2 | Pa54 | 10YR 6/4 | 10YR 5/2 | |
| Pa16 | 10YR 8/1 | 10YR 7/2 | Pa55 | 10YR 8/2 | 10YR 7/3 | |
| Pa17 | 10YR 8/1 | 10YR 8/2 | Pa56 | Plaster | 10YR 6/3 | 10YR 5/4 |
| Pa18 | 10YR 8/1 | 10YR 8/2 | | Clast of breccia | 10YR 8/1 | 10YR 8/2 |
| Pa19 | 10YR 8/1 | 10YR 7/2 | Pa57 | 10YR 7/2 | 10YR 7/3 | |
| Pa20 | Upper darker layer | 10YR 8/2 | Pa58 | 10YR 7/3 | 10YR 5/4 | |
| | Lower lighter layer | 10YR 8/1 | Pa59 | 10YR 8/1 | 10YR 8/1 | |
| Pa21 | 10YR 8/1 | 10YR 8/2 | Pa60 | 10YR 8/1 | 10YR 8/1 | |
| Pa22 | 10YR 8/2 | 10YR 8/3 | Pa61 | 10YR 8/1 | 10YR 8/1 | |
| Pa23 | 10YR 8/1 | 10YR 8/2 | Pa62 | 10YR 8/1 | 10YR 8/3 | |
| Pa24 | 10YR 8/1 | 10YR 8/1 | Pa63 | 10YR 8/1 | 10YR 8/2 | |
| Pa25 | 10YR 8/1 | 10YR 8/1 | Pa64 | 10YR 8/1 | 10YR 8/1 | |
| Pa26 | 10YR 7/2 | 10YR 7/2 | Pa65 | 10YR 8/1 | 10YR 8/1 | |
| Pa27 | 10YR 8/1 | 10YR 8/2 | Pa66 | 10YR 8/1 | 10YR 8/1 | |
| Pa 28 | 10YR 8/2 | 10YR 8/3 | Pa67 | 10YR 8/1 | 10YR 8/1 | |
| Pa29 | 10YR 8/1 | 10YR 8/1 | Pa68 | 10YR 8/1 | 10YR 8/1 | |
| Pa30 | 10YR 7/2 | 10YR 7/2 | Pa69 | 10YR 8/1 | 10YR 8/2 | |
| Pa31 | 10YR 8/1 | 10YR 8/2 | Pa70 | 10YR 8/1 | 10YR 8/2 | |
| Pa32 | 10YR 8/1 | 10YR 8/3 | Pa71 | 10YR 8/1 | 10YR 8/1 | |
| Pa33 | 10YR 8/2 | 10YR 8/3 | Pa72 | 10YR 8/1 | 10YR 8/2 | |
| Pa34 | 10YR 8/1 | 10YR 8/3 | Pa73 | 10YR 8/1 | 10YR 8/3 | |
| Pa35 | 10YR 5/2 | 10YR 4/2 | Pa74 | 10YR 8/1 | 10YR 8/1 | |
| Pa36 | 10YR 8/1 | 10YR 7/2 | Pa75 | 10YR 8/2 | 10YR 7/2 | |
| Pa37 | 10YR 8/2 | 10YR 7/3 | Pa76 | 10YR 8/1 | 10YR 8/1 | |
| Pa38 | 10YR 8/1 | 10YR 8/2 | Pa77 | 10YR 8/1 | 10YR 8/2 | |
| Pa39 | 10YR 8/1 | 10YR 8/1 | Pa78 | 10YR 8/1 | 10YR 8/2 | |
| Pa40 | 10YR 6/6 | 10YR 5/4 | Pa79 | 10YR 6/3 | 10YR 5/6 | |
| Pa41 | 10YR 8/1 | 10YR 8/2 | Pa80 | 10YR 7/4 | 10YR 6/3 | |
| Pa42 | 10YR 7/4 | 10YR 7/4 | Pa81 | 10YR 8/1 | 10YR 8/3 | |
| Pa43 | 10YR 8/2 | 10YR 7/2 | Pa82 | 10YR 8/3 | 10YR 6/4 | |
| Pa44 | 10YR 7/2 | 10YR 7/3 | Pa83 | 10YR 7/3 | 10YR 6/4 | |
| Pa45 | 10YR 7/4 | 10YR 6/3 | Pa84 | 10YR 8/1 | 10YR 8/1 | |
| Pa46 | 10YR 8/1 | 10YR 8/3 | Pa85 | 10YR 7/2 | 10YR 6/4 | |

Colours listed:

10YR 3/2 Very dark grayish brown
10YR 4/2 Dark grayish brown
10YR 5/2 Grayish brown
10YR 5/3 Brown
10YR 5/4 Yellowish brown
10YR 5/6 Yellowish brown
10YR 6/1 Gray
10YR 6/2 Light brownish gray
10YR 6/3 Pale brown
10YR 6/4 Light yellowish brown
10YR 6/6 Brownish yellow
10YR 7/1 Light gray
10YR 7/2 Light gray
10YR 7/3 Very pale brown
10YR 7/4 Very pale brown
10YR 8/1 White
10YR 8/2 White
10YR 8/3 Very pale brown
10YR 8/4 Very pale brown

A.2.1. Petrographic Observations

| A.2.1. Petrographic Observations | | | | | | | | | | | | | | | | | | | | | | | |
|----------------------------------|------|------------------|-----------------------------|---------------------------------------|-----------------|---|----------------------------------|-----------------|---------------|---------|--------------------------------|----------------------|---------|---|---|---------|----------------------|-------------|-------------------------------------|----------------------------------|-----------------|--------------------|---|
| General | | | | | | Carbonate Matrix | | | | | | | | Aggregates and other materials | | | | | | | | | |
| Sample | Type | Period/ ruler | Layers sequence | Lime washes | Paint layers | Matrix (hydraulic/ non hydraulic/ clayey) | Pores shape | Biggest pore | Lime lumps | Mixing | Calcite hexagonal prisms | Acicular crystals | Fossils | Aggregates mineralogy | Roundness and sphericity. | Sorting | Biggest aggregate | Aggregate % | Charcoal | Isotropic plant structures | Plant fibres | Opakes | Observations |
| Pa4 | JM | Cas | NA | Yes | No | Non-hydraulic | Elongated and cracks | 0.25 mm | No | Good | No | No | No | Mic cal, crys cal, shells, Q in isot, ShocQz. | Subangular, tabular | Bad | 7 mm | 35% | No | No | No | Few | Muddy matrix. Fragment of ceramic with quartz. Recrystallized. |
| Pa49 | WR | Ot | Upper | No | No | Clayey | Rounded and vesicular | 0.25 mm | No | Good | No | No | No | Qz, crys cal. | Angular | Regular | 1 mm | 40% | No | No | No | Yes | |
| Pa49 | WR | Ot | Lower | No | No | Hydraulic | Cracks | 0.25 mm | Not clear | Good | No | No | No | Mic cal, crys cal*, Qz and isot in clay pel. Isot. | Subangular, subspherical | Bad | 8 mm | 30% | No | No | No | No | |
| Pa50 | F | Ot | NA | No | No | Hydraulic | Elongated | 0.2mm | Yes | Regular | No | No | No | Mic cal*, crys cal, isot, clay pel with musc, qz and Fe oxides.. | Subrounded, subspherical | Bad | 8 mm | 40% | No | No | No | No | Clayey inclusions with musc, felds and isot. Mud plaster layer over the surface. |
| Pa77 | WR | Pak II | Two layers in the sample | | No | Hydraulic | Rounded and elongated | | No | Good | No | No | No | Mic cal*, isot, Sil Car? Horn? Oliv? | Subangular, subspherical | Good | 3 mm | 30% | No | No | Yes | No | Isotropic phase without reaction rim. |
| Pa78 | WR | Pak II | NA | No | No | Non hydraulic/ slightly hydraulic | Rounded | 0.15 mm | Not | Regular | No | No | No | Mic and crys cal, clay pel with qz, dev glass, polyc qz, shoc qz? | Calcareous: subrounded, Quartz: angular. | Good | 2 mm | 30% | No | No | Yes | Very few. | |
| Pa22 | F | Kam Bal | NA | | No | Hydraulic | Rounded, elongated. | 0.3 mm | No | Good | No | No | No | Mic cal, crys cal, Qz, Qz in isot, Clay pel with Qz and isot. | Calcareous: subrounded, Quartz: angular. | Bad | 13 mm | 25% | No | No | No | No | matrix and quartz inclusions. Many different types of aggregates. |
| Pa23 | F | Kam Bal | NA | No | No | Non hydraulic | Rounded | 0.25 mm | No | Good | No | No | No | Mic cal, crys cal. | Subrounded, subspherical | Bad | 8 mm | 25% | No | No | No | No | |
| Pa24 | WR | Kam Bal | NA | 12 layers | No | Hydraulic | Few, rounded and elongated | 0.5 mm | No | Good | No | No | No | Mic cal, crys cal, Qz, Clay pel, isot, Spar, Mudstone. | Subrounded, subspherical | Reg | 3 mm | 25% | Yes, small | No | No | No | Several layers of limewashes. Soot alternated with limewashes. Slight hydraulic reactions around isotropic phases |
| Pa27 | WR | Kam Bal | NA | 17 layers alternated with soot. | No | Slightly hydraulic. Very clear in some areas. | Rounded and elongated | 1 mm | No? | Good | No | No | No | Mic cal, crys cal, Qz in isot, dev glass. | Subrounded, subspherical | Good | 3 mm | 30% | Small fragment. | No | No | No | |
| Pa28 | F | Kam Bal | NA | No | No | Hydraulic | Elongated and cracks | 0.5 mm | Yes | Good | No | No | No | Mic cal, crys cal*, spar, shells, clay pellet with qz, micas, Fe oxides, plag feld, shoc Qz in isot. | Subangular, tabular | Bad | 4 mm | 30% | Small one. Probably hardwood. | No | No | Few | Organic substance in cracks, probably a resin. Shocked quartz? |
| Pa52 | F | Kam Bal? | NA | No | No | Moderately hydraulic. | Few, rounded | 0.4 mm | Yes | Good | No | No | No | cal*, qz, isot, igneous? | Subrounded, spherical | Good | 1.5 | 40% | No | No | No | Very few. | |
| Pa59 | F | Kam Bal | Upper | No | No | Non hydraulic/Slightly hydraulic | Rounded | 0.25 mm | No | Good | No | Yes | No | Mic cal, dev glass. | Calcareous: subrounded, subspherical | Good | 0.75 mm | 35% | No | Yes | No | No | It does not have the reactions seen in the other samples from this sequence. |
| Pa59 | F | Kam Bal | Lower | 1 layer | No | Hydraulic | Rounded and elongated | 0.5 mm | Not clear | Good | No | Yes | No | Mic cal, dev glass, isot, qz*. | Calcareous: subrounded, subspherical | Regular | 4 mm | 30% | No | Yes | No | Few | |
| Pa60 | F | Kam Bal | NA | 3 layers | No | Hydraulic around pozzolanic aggregates | Rounded and elongated | 0.5 mm | No | Regular | No | Yes | No | Mic cal, isot, dev glass. | Subrounded, subspherical | Good | 4 mm | Not clear | No | No | No | Few iron oxides | Hydraulic reactions around some aggregates. |
| Pa61 | F | Kam Bal | NA | 3 layers | No | Hydraulic? | Rounded | 2 mm | No | Good | No | No | No | Mic and crys cal, isot. | Subrounded, subspherical | Good | 0.5 mm | Not clear | No | No | No | No | Some cracks. |

Abbreviations type of material: F: Floor, JM: Joining mortar, WR: Wall render, S: sculpture, L: Limestone, S: sculpture, Sas: sascab. Abbreviations rulers and periods: Cas: Cascada Phase, Ot: Otulum Phase, Pak II: K'inich Janaab' Pakal, Kam Bal: K'inich Kam Balam II, Joy Chit: Joy Chitam II, Kuk Bah: K'inich Kuk Bahlam II, Balun: Balunte Phase, Arch mod: architectural modifications. Abbreviations mineralogy: Mic cal: micritic calcite, crys cal: crystalline calcite, spar: sparite, qz: quartz, shoc qz: shocked quartz, isot: isotropic, pol qz: polycrystalline quartz, dev glass: devitrified glass, clay pel: clay pellets, plag feld: plagioclase feldspars, musc: muscovite mica, horn: hornblende, sil car: silicon carbide, oliv: olivine. Dominant phases are marked with *.

| General | | | | | | Carbonate Matrix | | | | | | | Aggregates and other materials | | | | | | | | | | Observations |
|---------|------|------------------|----------------------------|---|-----------------|---|----------------------------------|-----------------|---------------|---------|--------------------------------|----------------------|--------------------------------|--|--|---------|----------------------|-------------|------------|----------------------------------|-----------------|--------------------------------|--|
| Sample | Type | Period/ ruler | Layers sequence | Lime washes | Paint layers | Matrix (hydraulic/ non hydraulic/ clayey) | Pores shape | Biggest pore | Lime lumps | Mixing | Calcite hexagonal prisms | Acicular crystals | Fossils | Aggregates mineralogy | Roundness and sphericity | Sorting | Biggest aggregate | Aggregate % | Charcoal | Isotropic plant structures | Plant fibres | Opakes | |
| Pa62 | F | Kam Bal | NA | 2 layers | No | Hydraulic | Elongated and cracks | 1 mm | No | Regular | No | No | No | Mic cal*, cryst cal, isot*, dev glass. | Subrounded, subspherical | Good | 1.5 mm | Not clear | No | No | No | Few iron oxides | around pozzolanic aggregates. |
| Pa63 | F | Kam Bal | NA | 2 layers | No | Hydraulic | Elongated and cracks | 1 mm | No? | Good? | No | No | No | Mic cal*, crys cal, plag feld, qz, isot*. | Subrounded and subspherical. | Regular | 4mm | Not clear | No | No | No | Some iron oxides | Hydraulic reactions around pozzolanic aggregates. |
| Pa65 | F | Kam Bal | NA | No | No | Hydraulic? | Rounded and cracks | 1 mm | Not clear | Good | No | No | No | Mic calc*, isot*. | Subrounded, subspherical | Good | 4 mm | Not clear | No | No | No | No | Hydraulic reactions around pozzolanic aggregates. |
| Pa66 | F | Kam Bal | NA | 1 layer | No | Hydraulic around meteoritic inclusions. | Elongated and cracks | 1.5 mm | No | Good? | No | Yes | No | Mic cal, qz in isot, zircon, silicon carbide? (microprobe) | subrounded and subshperical. | Regular | 3 mm | Not clear | No | No | No | No | Hydraulic reactions around pozzolanic aggregates. |
| Pa67 | F | Kam Bal | NA | 1 layer | No | Hydraulic | Elongated and cracks | 1mm | No? | Good? | No | No | No | Mic cal*, isot*, dev glass. | Subrounded, subangular | Good | 3 mm | Not clear | No | No | No | No | Hyd. reactions around pozzolanic aggregates. Orange blebs in isotropic phase. |
| Pa68 | F | Kam Bal | NA | 1 layer | No | Hydraulic. Partly isotropic with reactions around cracks. | Elongated and cracks | 0.5 mm | No | Good? | No | No | No | Mic and crys cal, isot, dev glass. | Subrounded, subspherical | Bad | 7 mm | Not clear | No | No | No | No | Hydraulic reactions around pozzolanic aggregates. Blebs in fragments of limestone. |
| Pa70 | F | Kam Bal | NA | 3 layers | No | Hydraulic around glassy (devitrified) aggregates | Rounded and cracks | 1.5 mm | No | Regular | No | No | No | Mic and crys cal, dev glass, isot. | Subrounded, subspherical | Good | 4 mm | Not clear | No | No | No | Yes, (iron in clay pellets) | Hydraulic reactions around pozzolanic aggregates. |
| Pa71 | F | Kam Bal | NA | 2 layers | No | Hydraulic | Rounded and around cracks | 1 mm | No | Good | No | No | No | Mic cal*, cryst cal, isot*, igneous? | Calcareous: subangular, subspherical | Good | 6 mm | Not clear | No | No | No | No | Hydraulic reactions around pozzolanic aggregates. |
| Pa72 | F | Kam Bal | NA | 4 layers ca. 60 layers alternated with soot | No | Perhaps slightly hydraulic | Rounded | 1 mm | No | Good | No | No | No | Mic, calc, qz, isot. | Subrounded, subspherical | Regular | 2.5 mm | 30% | No | No | No | No | Impact glass and hydraulic reactions. |
| Pa75 | WR | Kam Bal | Sequence of lime washes | ca. 60 layers alternated with soot | No | Some of the layers perhaps slightly hydraulic | Very small. Rounded. | 0.5 mm | No | Good | No | No | No | Mic cal*, isot, qz, igneous? | Sobrounded, subspherical | Good | 0.3 mm | 10% | No | No | No | No | Only layers of limewashes alternated with soot. |
| Pa18 | F | Joy Chit? | NA | No | No | Slightly hydraulic Non hydraulic. Lower limewash may be hydraulic. | Few, rounded | 0.2mm | Yes | Reg | No | No | No | Mic cal*, Qz, Clay pel with Qz and isot, DevGalss, isot*. | Subrounded, subspherical | Regular | 10 mm | 25% | Yes. | No | No | Yes | Devitrified glass: dark orange under PPL and XPL |
| Pa19 | WR | Joy Chit? | NA | 2 layers | No | Perhaps slightly hydraulic. | Few, rounded | 0.25 mm | No | Good | No | No | No | Mic cal, crys cal, clay pel, Qz, isot, musc. | Subrounded, subspherical | Reg | 3 mm | 30% | No | No | No | Very few. | |
| Pa43 | WR | Joy Chit? | NA | No | No | Perhaps slightly hydraulic. | Rounded | 0.25 mm | No | Good | No | No | No | Mic cal, crys cal, qz in isot. | calcareous: rounded. Quartz: angular | Good | 0.75mm | 35% | No | No | No | Very few. | |
| Pa1 | WR | Kuk Bahl | NA | 8 layers. No soot. | Black paint | Slightly hydraulic | Rounded and elongated | | Yes | Good | No | No | No | Mic cal*, qz, isot. | Subrounded, subspherical | Bad | 9 mm | 35% | Bo | No | No | No | A grain of polycryst qz embedded in a fragment of limestone. |
| Pa2a | F | Kuk Bahl | NA | No | No | Hydraulic. Partly isotropic. | Few, rounded and elongated | 500 µm | No | Regular | No | No | No | Mic cal, Shoc Qz?. | Angular, subspherical. | Bad | 4mm | 35% | No | No | No | No | Isotropic layer on the surface (plant remains?). |
| Pa2b | F | Kuk Bahl | NA | No | No | Slightly hydraulic | Rounded and elongated | 750 µm | Not clear | Regular | No | Yes | No | Mic cal*, crys cal, isot, Sil Car? | Subrounded, subspherical | Bad | 12 mm | 20% | Yes, small | No | No | Very few. | Very few aggregates. |
| Pa12 | WR | Kuk Bahl? | NA | No | No | Slightly hydraulic | Few, rounded | 0.5 mm | No | Good | No | No | Forams. | Mic cal, crys cal, Qz, PoiQz, Dev glass, sanidine, bone? | Calcareous: rounded. Quartz: angular | Regular | 6 mm | 25% | Yes | No | No | Yes. | |
| Pa53 | WR | Balun? | NA | No | No | Non hydraulic/ clayey | Few elongated and cracks | | Yes, 1 mm | Regular | No | No | No | Crys cal, Sho Qz, igneous? Micas, Plag feld, Fe oxides, clay pel. | Angular | Regular | 4 mm | 30% | No | No | No | Yes | Recrystallized calcite in cracks. Same fabric as Pa86. |

Abbreviations type of material: F: Floor, JM: Joining mortar, WR: Wall render, S: sculpture, L: Limestone, S: sculpture, Sas: sascab. **Abbreviations rulers and periods:** Cas: Cascada Phase, Ot: Otulum Phase, Pak II: K'inich Janaab' Pakal, Kam Bal: K'inich Kam Balam II, Joy Chit: Joy Chitam II, Kuk Bahl: K'inich Kuk Bahlam II, Balun: Balunte Phase, Arch mod: architectural modifications. **Abbreviations mineralogy:** Mic cal: micritic calcite, Cryst cal: crystalline calcite, Spar: sparite, qz: quartz, Shoc qz: shocked quartz, isot: isotropic, pol qz: polycrystalline quartz, dev glass: devitrified glass, clay pel: clay pellets, plag feld: plagioclase feldspars, musc: muscovite mica horn: hornblende, sil car: silicon carbide, oliv: olivine. Dominant phases are marked with *.

| General | | | | | | Carbonate Matrix | | | | | | | | Aggregates and other materials | | | | | | | | Observations | | |
|----------------------------|------|------------------|--------------------|----------------|--|---|-------------------------------|---------------------|---------------|---------|--------------------------------|----------------------|---------|---|--|---------|----------------------|-------------|-------------------------|----------------------------------|-----------------|--|---|--|
| Sample | Type | Period/ ruler | Layers sequence | Lime washes | Paint layers | Matrix (hydraulic/ non hydraulic/ clayey) | Pores shape | Biggest pore | Lime lumps | Mixing | Calcite hexagonal prisms | Acicular crystals | Fossils | Aggregates mineralogy | Roundness and sphericity. | Sorting | Biggest aggregate | Aggregate % | Charcoal | Isotropic plant structures | Plant fibres | | Opaques | |
| Pa56 (plaster) | F | Balun? | NA | No | No | Clayey with glassy phases | Elongated | 1 mm | No | Good | No | No | Forams. | Isot. Shoc Qz?, tourmaline? | subangular | Good | 25 mm | 30% | No | No | No | No | It has a fragment of impact breccia with a partly isotropic matrix. | |
| Pa56 (impact clast). | F | Balun? | NA | NA | NA | Partly isotropic | Round | 3mm | NA | NA | No | No | No | Plag feld, pol qz. Matrix partially isot. | NA | Good | NA | NA | NA | NA | NA | No | Shocked quartz. Partly isotropic matrix | |
| Pa86 | WR | Balun? | NA | No | No | Clayey | Cracks | Only cracks | Yes, 15 mm | Bad | No | No | No | Qz, some mic and crys cal, plag feld and pyrox. shells, opaques. | Angular and subshperical | Bad | 7 mm | 35% | No | No | No | Very few. | Muddy matrix with numerous grains of quartz | |
| Pa87 | WR | Balun? | NA | No | No | Clayey | Elongated and cracks | 0.5 mm | No | Good | No | No | Foram. | Qz, mic and crys cal, shoc qz?, shell. | Subrounded, subshperical | Bad | 8 mm | 25% | No | No | No | Very few. | | |
| Pa88 | WR | Balun? | NA | 1 layer | No | Clayey | Rounded and cracks | 0.5 mm | No | Reg | No | No | No | Mic and crys cal, qz, shoc qz, isot, micas. | Subrounded, subangular, spherical | Bad | 10 mm | 30% | No | No | No | No | Muddy matrix with many cracks | |
| Pa44 | WR | Arch mod | NA | | No | Clayey | Cracks | 0.5 mm | Yes | Regular | No | No | No | Qz and opaques, plag feld, crys cal*, pol qz, coral, shoc Qz, shell. | Angular, subshperical | Bad | 5 mm | 35% | No | No | No | Few | | |
| Pa45 | JM | Arch mod | NA | No | No | Clayey | Vesicular and cracks | 0.75 mm | Yes, 6 mm | Bad | No | no | No | Mic cal, qz, shell. | Calcareous: subrounded. Qz: subangular. | Regular | 5 mm | 25% | No | No | No | Yrd | Quartz grains around 0.25 mm. | |
| Pa5 | L | Cas | NA | NA | NA | NA | NA | No visible pores | NA | NA | NA | NA | NA | NA | NA | NA | NA | NA | NA | NA | NA | No | Crystalline limestone | |
| Pa26 | L | Kam Bal | NA | NA | NA | NA | NA | NA | NA | NA | NA | NA | No | NA | NA | NA | NA | NA | NA | NA | NA | NA | No | Crystalline calcite with veins of recrystallized calcite and iron oxides. |
| Pa48 | L | Joy Chit | NA | NA | NA | NA | NA | NA | NA | NA | NA | NA | NA | Cryst calcite | NA | NA | NA | NA | NA | NA | NA | NA | No | Crystalline limestone |
| Pa55 | L | Balun? | NA | NA | NA | NA | No visible pores | No visible pores | NA | NA | NA | NA | NA | NA | NA | NA | NA | NA | NA | NA | NA | NA | No | Crystalline calcite with veins or iron oxides. Small quartz inclusions. |
| Ca9 | F | M Prec | NA | No | No | Non hydraulic | Rounded | 0.3 mm | No | Regular | No | Yes | No | Mic cal, qz, serp?, isot. | Mainly subrounded subspherical. Also angular. | Regular | 12 mm | Not clear. | No | No | No | No | No | Several inclusions of silicate (serpentine mineral?) |
| Ca10 | F | M Prec | NA | 1 layer | No | Slightly hydraulic | Related to cracks | 0.3 mm | No | Regular | Yes. | Yes, many. | No | Mic and crys cal, shell, isot. | Subrounded and subspherical. | Bad | 5 mm | 15% | Yes, small fragment. | Yes | No | Yes | Yes | Inclusion of silicate (serpentine mineral?) |
| Ca11 | WR | M Prec | NA | No | No | Hydraulic? | Elongated and vesicular | 0.75 mm | No | Good | Yes | Yes, very large | No | Mic cal, isot, dev glass. | Subrounded, subshperical. | Good | 0.5 mm | 25% | No | Yes | No | No | Texture with several isotropic inclusions and acicular crystals. | |
| Ca5 | S | LM Prec | NA | 1 layer | Red paint. Very well applied. | Slightly hydraulic | Rounded | 0.3 mm | Yes | Good | No | Yes | No | Mic cal*, crys cal, pol qz, isot, serp? | Subrounded, subspherical | Good | 4 mm. | 20% | One small fragment | No | No | Yes, few. | It has an extremely thin perfectly applied paint layer over the surface. | |
| Ca6 | WR | LM Prec | Upper layer | 1 layer | No | Non hydraulic | Rounded | 1 mm | Yes | Good | Yes | Yes | No | Mic cal*, crys cal*, isot, serp? | Subrounded subspherical but also angular. | Good | 2 mm | 15% | No | Yes | No | Yes, 1 iron oxide inclusion, 1 mm | With an amorphous layer overlain by a lime layer of 20 µm over the surface | |
| Ca6 | WR | LM Prec | Lower layer | No | No | Non hydraulic. | Rounded | 1 mm | No | Good | No | Yes | No | Mic cal* and crys cal, mudstone, serp?, Dev glass* | Mainly subrounded, subspherical | Regular | 6 mm | 15% | Small fragment. | Yes | No | No | | |
| Ca7 | S | LM Prec | NA | 1 layer | Red paint. | Slightly hydraulic | Rounded | 0.5 mm | No | Good | Yes. Few | Not clear | No | Mic cal*, crys cal, serp? Isot* | Subrounded and subspherical | Good | 3 mm | 15% | No | No | No | Yes, few. | | |
| Ca8 | S | LM Prec | NA | No | No | Non hydraulic | Rounded | 1mm | No | Good | No | No | No | Mic cal*, muscov. isot, dev glass. | Subrounded and subspherical | Good | 2.5 | 20% | No | Yes | No | Few. | Considerable amounts of glass and devitrified glass. | |

Abbreviations type of material: F: Floor, JM: Joining mortar, WR: Wall render, L: Limestone, Sas: sascab, S: sculpture. MPrec: Middle Preclassic, LMPrec: Late Middle Preclassic, LPrec: Late Preclassic, ECias: Early Classic, LCias: Late Classic, TCias: Terminal Classic.
 Abbreviations mineralogy: Mic cal: micritic calcite, crys cal: crystalline calcite, spar: sparite, qz: quartz, shoc qz: shocked quartz, isot: isotropic, pol qz: polycrystalline quartz, dev glass: devitrified glass, clay pel: clay pellets, plag feld: plagioclase feldspars, musc: muscovite mica, met cal: metamorphic calcite, horn: hornblende, sil car: silicon carbide, oliv: olivine, serp: serpentine, metam calc: metamorphic calcite. Dominant phases are marked with *.

| General | | | | | | Carbonate Matrix | | | | | | | | Aggregates and other materials | | | | | | | | | |
|---------|------|------------------|--------------------|----------------|-----------------|---|---|-----------------|---------------|-----------------|--------------------------------|------------------------------|----------------------|---|--|--------------|----------------------|-------------|--|--------------------------------------|-----------------|---------------------------|---|
| Sample | Type | Period/ ruler | Layers sequence | Lime washes | Paint layers | Matrix (hydraulic/ non hydraulic/ clayey) | Pores shape | Biggest pore | Lime lumps | Mixing | Calcite hexagonal prisms | Acicular crystals | Fossils | Aggregates mineralogy | Roundness and sphericity. | Sorting | Biggest aggregate | Aggregate % | Charcoal | Isotropic plant structures | Plant fibres | Opaques | Observations |
| Ca29 | F | L Prec | NA | No | No | Some areas with apparent hydraulic reactions. | Vesicular | 2 mm | No | Regular | No | Yes | No | Mic cal*, micas, serp?*, dev glass, isot. | Calcareous: subrounded. subspherical. Silicates: fibrous | Regular | 2 mm | Not clear. | No | Yes | No | No | Very different sample from the rest. Presence of serpentine mineral. |
| Ca30 | F | L Prec | Upper layer | No | No | Non hydraulic/ com | Rounded and | 1 mm | No | Good | Yes | Yes | No | Mic cal, Cryst cal | Subrounded and | Regularly sd | 1 mm | 15% | No | No | No | No | Few small g Layer thickness: 1.5 cm |
| Ca30 | F | L Prec | Lower layer | No | No | Non hydraulic | Elongated | 1 mm | No | Bad | Yes | Yes | Not clear | Mic cal, Cryst cal, sd | Subrounded and | Regularly sd | 2 mm | 15% | No | Yes, within mic | No | No | Small inclusions. |
| Ca31 | F | E Clas? | NA | Yes | No | Non hydraulic/Com | Elongated an | 0.6 mm | No | Regular | No | Not clear. | No | Mic cal*, isot (angul | Subrounded sub | Regularly sd | 3 mm | Not clear | No | No | No | No | Isotropic layer over the |
| Ca1 | WR | E Clas | NA | No | No | Slightly clayey | Rounded | 0.25 mm | No | Good | Yes, around 25 µm | Yes but very localized | No | Mic cal*, clay pel*, qz. | Subrounded, subspherical | Good | 1 mm | 20% | No | No | No | No | |
| Ca2 | F | E Clas | NA | No | No | Non hydraulic? | Few. Rounded. | 0.2 mm | NA | Good | Yes. | Yes | No | Mic cal*, qz. | Subrounded, subspherical | Bad | 20 mm | NA | Small fragments. | No | No | No | Dark brown matrix. |
| Ca13 | F | E Clas | NA | No | No | Non hydraulic/ slightly clayey. | Rounded. | 0.3 mm | No | Regular | No | Yes | No | Mic cal*. | Subrounded and subspherical | Regular | 10 mm | Not clear. | Yes | No | No | No | |
| Ca14 | WR | E Clas | NA | No | Red paint. | Perhaps slightly hydraulic | Rounded | 0.25 mm | No | Good | No | No | No | Mic cal, cryst cal, serp? Qz, isot. | Subrounded subspherical. | Regular | 2.5 mm. | Not clear. | Yes | Yes | No | Yes | |
| Ca15 | WR | E Clas | NA | No | Red paint. | Non hydraulic | Rounded and elongated. Few cracks. | 0.75 mm | Yes | Good | Yes | Yes. | Limited to areas. | Mic cal* | Subrounded and subshpherical | Good | 2 mm | 20% | Yes | Yes but within a sascab grain. | No | No | There is an aggregate with an isotropic plant structure within it. |
| Ca19 | F | E Clas | NA | No | No | Non hydraulic | Rounded. | 0.5 mm | No | Regular | Yes | Yes | No | Mic cal*, crys cal, isot. | Subrounded and subspherical. | Bad | 4 mm | 20% | No | No | No | No | |
| Ca22 | F | E Clas | NA | No | Red paint. | Non hydraulic/clayey | Related to cracks | 0.5 mm | No | Regular | No | No. | No | Mic cal* | Subrounded and subspherical | Poor | 12 mm | Not clear. | No | No | No | Yes, many iron oxides | |
| Ca23 | WR | E Clas | NA | No | Red paint. | Non hydraulic | Rounded | 1 mm | No | Good | No | Yes. Limited to areas. | No | Mic cal*, qz, isot. | Calcareous: subrounded, quartz: angular | Bad | 0.75 mm | 20% | No | Probably yes | No | No | Chaotic texture. Several isotropic inclusions with cellular structures and acicular crystals. |
| Ca24 | ? | E Clas? | NA | Yes | No | Non hydraulic | Rounded. | 1 mm | No | Good. | No | Not clear. | No | Mic and cryst cal*, pol qz, serp? | Subrounded and subspherical but also subangular. | Good | 1 mm | 20% | Yes, some fragments with visible features | No | No | Yes, some iron oxides. | Isotropic layer over the surface (resin?) |
| Ca16 | WR | L Clas | Upper | No | No | Non hydraulic | Vesicular | 0.25 mm | Yes | Good | No | No | No | Mic cal*, crys cal, shell. | Subrounded and subspherical. | Good | 1 mm | Not clear | No | No | No | Few | |
| Ca16 | WR | L Clas | Medium | 2 layers | No | Probably slightly hydraulic | Rounded | 1 mm | Yes | Good | No | No | Foram | Mic cal*, isot, serp? | Subrounded and subspherical. | Regular | 1.5 mm | 20% | Yes, no visible features. | No | No | Yes | Many inclusions of glass and devitrified glass. |
| Ca16 | WR | L Clas | Lower | 2 layers | No | Slightly hydraulic | Vesicular and elongated | 1.5 mm | Yes | Good | No | Yes | No | Mic cal*, dev glass, alk feld, isot. | Subrounded and subspherical | Good | 1.5 mm | 35% | No | No | No | Few | Many inclusions of isot and dev glass. |
| Ca18 | F | L Clas | Upper | No | No | Perhaps slightly hydraulic | Rounded. | 0.2mm | No | Regular | Yes, small crystals. | Yes | No | Mic cal*, dev glass, qz. | Subrounded and subspherical. | Regular | 1 mm | 20% | No | No | No | No | Isot layer over the surface (resin?) |
| Ca18 | F | L Clas | Lower | No | No | Non hydraulic | Around aggregates. | 2 mm | No | Regular | Yes | Yes | No | Mic cal* and crys cal, clay pel. | Subrounded and subspherical. | Regular | 3 mm | 25% | Yes, with visible structures. | No | No | No | |
| Ca21 | F | L Clas | NA | No | No | Non hydraulic | Rounded. | 3 mm | No | Regular/b ad | No | Apparently yes. | No | Mic cal, muscov? | Subrounded and subspherical. | Regular | 3 mm | 20% | No | No | No | Yes, iron oxides. | Many opaques. |
| Ca26 | WR | L Clas | NA | No | No | Non hydraulic | Vesicular | 0.5 mm | Not clear | n | No | No | No | Mic cal*, cryst cal*, qz*, dev glass, isot. | Calcareous: subrounded, quartz: angular | Regular | 3 mm | 20% | No | Not clear. | No | No | |

Abbreviations type of material: F: Floor, JM: Joining mortar, WR: Wall render, L: Limestone, S: sculpture, Sas: sascab, MPrec: Middle Preclassic, LPrec: Late Preclassic, EClas: Early Classic, LClas: Late Classic, TClas: Terminal Classic.
 Abbreviations mineralogy: Mic cal: micritic calcite, cryst cal: crystalline calcite, spar: sparite, qz: quartz, shoc qz: shocked quartz, isot: isotropic, pol qz: polycrystalline quartz, dev glass: devitrified glass, clay pel: clay pellets, plag feld: plagioclase feldspars, musc: muscovite mica, met cal: metamorphic calcite, horn: hornblende, sil car: silicon carbide, oliv: olivine, serp: serpentinite, metam calc: metamorphic calcite. Dominant phases are marked with *.

| General | | | | | | Carbonate Matrix | | | | | | | | Aggregates and other materials | | | | | | | | Observations | |
|-----------|------|------------------|---------------------------------|----------------|-----------------|---|-------------------------------|-----------------|---------------|-------------|--------------------------------|------------------------|---------|--|---|---------|----------------------|-------------|-------------------------------|----------------------------------|-----------------------------|-------------------------------|---------|
| Sample | Type | Period/ ruler | Layers sequence | Lime washes | Paint layers | Matrix (hydraulic/ non hydraulic/ clayey) | Pores shape | Biggest pore | Lime lumps | Mixing | Calcite hexagonal prisms | Acicular crystals | Fossils | Aggregates mineralogy | Roundness and sphericity | Sorting | Biggest aggregate | Aggregate % | Charcoal | Isotropic plant structures | Plant fibres | | Opaques |
| Ca36 | WR | L Clas | NA | | No | Non hydraulic | Small subrounded pores | 1.5 mm | Yes | Good | No | Not clear | No | Mic cal*, cryst cal, isot. | Subrounded and subspherical. | Regular | 4 mm | 15% | Yes, several fragments | No | No | Yes | |
| Ca3 | F | T Clas | NA | | No | Clayey, Compacted sascab? | Cracks | Only cracks | No | Regular | No | Yes | No | Mic cal*, serp? | Subrounded, subspherical | Regular | 5 mm | Not clear. | Small fragment | No | Yes, many. | Yes, iron oxides. | |
| Ca4 | F | T Clas | Yes, one layer over the surface | | No | Clayey | Cracks | Only cracks | No | Good | No | No | No | Mic cal*, cryst cal*, qz, shell. | Subrounded, subspherical | Good | 4 mm | 30% | No | Yes | Yes | Yes, few. | |
| Ca33 | F | T Clas | NA | | No | Non hydraulic/clayey | Rounded and adjacent to pores | 1 mm | No | Bad | No | Apparently yes. | No | Mic cal* | Subrounded and subspherical | Good | 5 mm | 35% | Yes | Yes | Yes, mixed with the matrix. | Yes, some iron oxides. | |
| Ca34 | WR | T Clas | NA | | No | Clayey | Rounded and as cracks | 1 mm | No | Regular/bad | No | Yes. | No | Mic cal*, isot | Subrounded and subspherical but also subangular. | Poor | 15 mm | 30% | Yes | Yes | No | Yes, some iron oxides. | |
| Ca Sascab | Sas | NA | NA | NA | NA | NA | NA | NA | NA | NA | NA | NA | NA | NA | NA | Bad | NA | NA | NA | Yes | NA | No | |
| Ca25 | L | L Clas | NA | NA | NA | NA | Rounded | 0.2mm | No | NA | No | No | No | Mic cal. | NA | NA | NA | NA | NA | NA | NA | NA | No |
| Ca27 | L | NA | NA | NA | NA | NA | Vesicular | 0.2mm | No | NA | No | No | No | Mic cal | NA | NA | NA | NA | NA | NA | NA | NA | No |
| Ca28 | L | NA | NA | NA | NA | NA | Vesicular | 0.2mm | No | NA | No | No | No | Mic cal | NA | NA | NA | NA | NA | NA | NA | NA | No |
| La24 | WR | L Prec | NA | | No | Thin red paint layer. Non hydraulic? Slightly hydraulic? | Rounded | 0.2 mm | No | Good | No | Yes | No | Mic cal, cryst cal, mudstone, isot. | Subrounded and subspherical. Also angular. | Good | 2 mm. | 25% | Yes, but no visible features. | No | No | Yes | |
| La25 | WR | L Prec | NA | | No | Red paint layer (300 µm) Non hydraulic | Rounded | 1 mm | No | Good | No | No | No | Mic cal, pelloids, crys cal, dev glass?. | Subrounded and subspherical. Also angular. | Regular | 5 mm | 30% | No | No | No | Few | |
| La28 | F | L Prec | NA | | No | Non hydraulic | Rounded | 0.2mm | No | Good | No | Yes | No | Mic cal, crys cal, isot. | Subrounded. | Regular | 5 mm | 25% | No | No | No | No | |
| La 29 | F | L Prec? | NA | | No | Clayey | Elongated | 0.25 mm | No | Good | Yes | No | No | Mic and crys cal. | Subrounded, subspherical | Regular | 3 mm | 35% | No | No | No | No | |
| La31 | F | L Prec | NA | | No | compacted sascab? | Vesicular | 0.75 mm | NA | NA | NA | NA | NA | Met cal | Mic cal and rec. calcite (no visible aggregates) | NA | NA | No | No | No | No | Few. | |
| La32a | F | L Prec | NA | | No | Clayey | Elongated and cracks | 0.75 mm | No | Good | Yes | No | No | Mic cal*, metam cal*, qz* | Calcareous: subrounded and subspherical. | Regular | 3 mm | 35% | Yes but no visible structures | No | No | Few charcoal and iron oxides. | |
| La32b | F | L Prec | NA | | No | Non hydraulic | Elongated | 0.5 mm | Not clear | Good | Yes. | No | No | Mic cal, cryst cal*, qz, shoc qz? | Subrounded, subspherical. Polycrystalline: angular. | Good | 1.5 mm | 25% | No | No | No | Few. | |
| La34 | F | L Prec | NA | | No | Compacted sascab? | Elongated | 0.25 mm | No | Not clear | Yes | No | No | Mic cal*, no clear presence of aggregates. | NA | NA | NA | NA | No | No | No | No | |
| La46 | F | L Prec? | NA | | No | Compacted sascab? | Elongated and vesicular | 0.75 mm | No | N/A | Yes, but few. | Yes but very localized | No | No clear presence of aggregates. Qz. | NA | NA | NA | N/A | No | No | No | No | |

Abbreviations type of material: F: Floor, JM: Joining mortar, WR: Wall render, S: sculpture, L: Limestone, S: sculpture, Sas: sascab. Abbreviations Period/ ruler: LPrec: Late Preclassic, EClas: Early Classic, LClas: Late Classic, TClas: Terminal Classic. EPos: Early Postclassic, LPost: Late Postclassic. SCol: Spanish Colonial. Abbreviations mineralogy: Mic cal: micritic calcite, cryst cal: crystalline calcite, spar: sparite, qz: quartz, shoc qz: shocked quartz, isot: isotropic, pol qz: polycrystalline quartz, dev glass: devitrified glass, clay pel: clay pellets, plag feld: plagioclase feldspars, musc: muscovite mica, horn: hornblende, sill car: silicon carbide, oliv: olivine, metam calc: metamorphic calcite. Dominant phases are marked with *.

| General | | | | | | Carbonate Matrix | | | | | | | | Aggregates and other materials | | | | | | | | Observations | |
|---------|------|-------------------|--------------------|----------------|---------------------------------------|---|--|-----------------|---------------|-----------|----------------------------------|----------------------|-------------------------|--|---|-------------|----------------------|-------------|--|----------------------------------|--------------------------|---|---|
| Sample | Type | Period/ ruler | Layers sequence | Lime washes | Paint layers | Matrix (hydraulic/ non hydraulic/ clayey) | Pores shape | Biggest pore | Lime lumps | Mixing | Calcite hexagonal prisms | Acicular crystals | Fossils | Aggregates mineralogy | Roundness and sphericity | Sorting | Biggest aggregate | Aggregate % | Charcoal | Isotropic plant structures | Plant fibres | Opaques | Observations |
| La47 | F | L Prec? | NA | No | No | Compacted sascab | Elongated | 0.25 mm | NA | N/A | Yes | No | No | Mic cal*, no clear presence of aggregates. | NA | NA | NA | NA | No | No | No | No | Chaotic texture of micritic calcite. Sample underneath La46. |
| La45 | F | E Clas | NA | No | No | Non hydraulic | Rounded | 0.5 mm | No | Regular | Yes | No | No | Mic and crys cal, qz, isot. | Subrounded, subspherical. | Regular | 1.5 mm | 20% | Yes, 2mm tangential section. | No | No | Very few. | |
| La48 | WR | E Clas | NA | No | No | Slightly hydraulic | Rounded | 2 mm | Yes | Good | Yes, many and very big | No | No | Mic cal*, crys cal* qz in isot, dev glass. | Subrounded, subspherical. | Regular | 4 mm | 15% | No | Yes | No | No | |
| La3 | F | L Clas | NA | No | No | Compacted sascab | Related with cracks | NA | NA | NA | NA | NA | No | Mic calc* | NA | NA | NA | NA | NA | NA | NA | NA | NA |
| La4 | F | L Clas | NA | No | No | Non hydraulic | Adjacent to aggregates. | 1 mm | Yes, 4 mm. | Good | No | No | Formas. | Mic cal*, crys cal*. | Subrounded and subspherical | Bad | 4 mm | 30% | No | No | No | Yes, iron oxides. Probably plant remains. | Dark matrix. |
| La6 | F | L Clas | NA | 1 layer | Yes. Red over orange paints. | Slightly hydraulic? | Rounded | 0.8 mm | Yes. | Good | No | No | No | Mic cal, Qz, Mudstone, recycled plaster*, angular opaques, isot in clay pel. | Subrounded and subspherical but also angular. | Well sorted | 8 mm | 30% | Yes, many but not visible features | No | Probably y remains | Yes, iron oxides | It has a fragment of plaster as aggregate with green and red paint layers. The red paint layer has an isotropic inclusion. |
| La7 | F | L Clas | NA | No | No | Compacted sascab? | Related to crakes. | 2 mm | No | Good | No | Yes | Shell fragments ? | Mic cal, isot, qz, shell. | Subrounded and subspherical | Well sorted | 0.5 mm | NA | No | No | No | Yes, iron oxides. | Considerable amounts of quartz |
| La14 | F | L Clas | NA | 1 layer | No | Compacted sascab? | Vesicular | 5 mm. | NA | NA | Yes. | Yes. | No | Mic cal*, crys cal, shell, isot. | NA | NA | 10 mm | NA | No | NA | NA | Very few. | |
| La15 | F | L Prec | NA | No | No | Non hydraulic | Rounded | 0.5 mm | No | Good | Yes | Not clear. | No | Mic cal, crys cal, qz. | Subrounded and subspherical. One angular. | Good | 3 mm | 20% | No | No | No | Very few, apparently plant remains. | Isotropic layer applied over the surface. |
| La16 | F | L Clas | NA | No | No | Non hydraulic? | Elongated Many, adjacent to aggregates and cracks. | 0.8 mm | | Bad | Yes | No | Foram | Mic cal, crys cal*, isot. | Subrounded Subrounded and subspherical. | Bad | 5 mm | 30% | No | No | No | Yes | Lump of hexagonal prisms of calcite (dolomite?) |
| La17 | F | L Clas | NA | No | No | Non hydraulic? | | 0.5 mm | No | Regular | Yes, many | Yes | No | Mic cal*, rec. calc* | Also angular. | Bad | 15 mm | 25% | Yes, a small fragment | No | No | No | It is only a thin layer that covers a fragment of sascab. |
| La35 | F | L Clas | NA | No | No | Compacted sascab. | Elongated | 0.25 mm | No | Not clear | Yes | No | No | Mic cal*, rec calc*, no clear presence of aggregates. | NA | NA | NA | NA | No | No | No | No | |
| La9 | F | L Clas/ T Clas | NA | 1 layer | No | Slightly hydraulic? | Rounded and vesicular | 10 mm | Yes, 10 mm | Bad | Yes, many. | Probably yes. | No | Mic cal, crys cal, qz, qz in isot. | Subangular. Also subrounded and subspherical. | Bad | 8 mm | 30% | Yes. Few fragments but not visible features. | No | No | Yes, iron oxides. | Chaotic texture. Oxide stains in some limestone fragments (fragments with glass and shocked quartz). Floor on top of La10. Large hexagonal prisms of calcite in the matrix. Floor layer below La9. |
| La10 | F | L Clas/ T Clas | NA | No | No | Non hydraulic | Rounded | 0.5 mm | No | Regular | Yes, crystals up to 100 µm | Yes | No | Mic cal, crys cal*, qz in isot. | Angular. Also subrounded and subspherical. | Bad | 20 mm | 30% | No | No | Yes | No | |
| La11 | F | T Clas/ E Post | NA | No | No | Non hydraulic | Related to cracks | 0.3 mm | No | Good | No | Yes. | No | Mic cal*, crys cal. | Angular. Also subrounded and subspherical. | Bad | 15 mm | 35% | No | No | No | Yes, few iron oxides. | Isotropic layer over the surface. Sample on top of La12. |
| La12 | F | T Clas/ E Post | NA | No | No | Non hydraulic | Adjacent to aggregates. | 0.2 mm | No | Good | Yes | Not clear. | No | Mic and crys cal, mudstone, isot. | Angular, subr. and subspherical. | Regular | 5 mm | 25% | Apparently yes. | No | Yes | No | Large hexagonal prisms of calcite. Sample under La11. |

Abbreviations type of material: F: Floor, JM: Joining mortar, WR: Wall render, S: sculpture, L: Limestone, S: sculpture, Sas: sascab. Abbreviations Period/ ruler: LPrec: Late Preclassic, EClas: Early Classic, LClas: Late Classic, TClas: Terminal Classic, EPos: Early Postclassic, LPost: Late Postclassic. SCol: Spanish Colonial. Abbreviations mineralogy: Mic cal: micritic calcite, crys cal: crystalline calcite, spar: sparite, qz: quartz, shoc qz: shocked quartz, isot: isotropic, pol qz: polycrystalline quartz, dev glass: devitrified glass, clay pel: clay pellets, plag feld: plagioclase feldspars, musc: muscovite mica, horn: hornblende, sil car: silicon carbide, oliv: olivine, metam calc: metamorphic calcite. Dominant phases are marked with *.

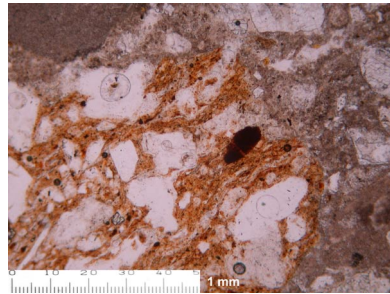
| General | | | | | | Carbonate Matrix | | | | | | | | Aggregates and other materials | | | | | | | | Observations | | | |
|-----------|------|---------------|-----------------|-------------|--------------|---|---------------------------------|--------------|------------|---------|--------------------------|-------------------|---------|---|--|---------------------------------|-----------------------|---|---|----------------------------|--------------|--------------------------|---|---|--|
| Sample | Type | Period/ ruler | Layers sequence | Lime washes | Paint layers | Matrix (hydraulic/ non hydraulic/ clayey) | Pores shape | Biggest pore | Lime lumps | Mixing | Calcite hexagonal prisms | Acicular crystals | Fossils | Aggregates mineralogy | Roundness and sphericity | Sorting | Biggest aggregate | Aggregate % | Charcoal | Isotropic plant structures | Plant fibres | Opakes | Observations | | |
| La 2 | F | E Pos/ M Pos | NA | No | No | Compacted sascab | Related with cracks. | 0.3 mm | NA | Good | No | Yes | No | Mic cal*, qz. Recrystallized calcite* | Subrounded and subspherical. | Good (only clay size sediments) | 1 mm | NA | No | No | No | Some iron oxides. | | | |
| La22 | WR | L Post | Upper | 1 layer | No | Slightly hydraulic | Rounded | 1 mm. | Yes, 1mm. | Bad. | Yes | No | No | Mic cal*, crys cal*, dev glass*, isot. Met cal? | Surrounded. Isot: angular. | Regular | 4 mm | 25% | Yes but no visible features. | No | No | Yes | | | |
| La22 | WR | L Post | Lower | 1 layer | No | Slightly hydraulic | Rounded | 2 mm. | Yes | Bad. | Yes | No | No | Mic cal*, crys cal, dev glass* | Subangular | Regular | 5 mm. | 20% | Yes. | No | No | Few | | | |
| La36a | WR? | L Post? | NA | No | No | Non hydraulic? | Rounded. | 0.7 mm | Yes, 2 mm. | Regular | Yes | Not clear. | No | Mic cal*, crys cal*, isot. | Angular. Also subrounded and subspherical. | Regular | 4 mm | 25% | Yes but no visible features. | No | No | Very few | | | |
| La36b | WR? | L Post? | Upper | 2 layers | No | Non hydraulic | Rounded. | 1 mm | Yes | Good | Yes | Not clear. | No | Mic cal, crys cal*, dev glass*. | Subrounded and subangular. | Good | 2 mm | 20% | No | No | No | Yes, many iron oxides | Layer thickness: 1 cm | | |
| La36b | WR? | L Post? | Medium | 1 layer | No | Slightly hydraulic | Rounded and cracks. | 1 mm. | No | Regular | Yes | Yes | No | Mic cal*, crys cal*, dev glass*, qz, isot. | Subrounded, subspherical. | Good | 3 mm | 25% | Yes | No | No | Yes, iron oxides. | | | |
| La36b | WR? | L Post? | Lower | No | No | Non hydraulic | Rounded. | 3 mm | NA | Good | Yes | No | No | Mic and crys cal. clay pel. | No visible aggregates | No visible aggregates | No visible aggregates | 25% | No | No | No | No | | | |
| La49 | F | L Post | NA | 1 layer | No | Slightly hydraulic and non-hydraulic mixtures | Rounded and elongated | 0.75 mm | Yes, 2 mm. | Regular | Yes but few | No | No | Mic cal, crys cal*, qz in isot*, shoc qz?, coral? | Subrounded, subspherical. | Regular | 3 mm | 25% | Small fragment. No visible structures. | No | No | Few iron oxides | Layer on top of La50 | | |
| La50 | F | L Post | NA | No | No | Slightly hydraulic? | Rounded | 0.5 mm | No | Good | Yes | No | No | Mic cal, crys cal*, clay pel, dev glass*, isot. | Subrounded, subspherical. Gig aggregate: angular | Bad | 20 mm | 80% (big fragment of crystalline limestone) | Yes but no visible structures | No | No | No | A very large aggregate of crystalline calc. Layer under La49. | | |
| La19 | F | S Col | Upper | No | No | Slightly hydraulic | Rounded | 0.3 mm | Yes | Good | Yes | No | No | Mic cal, crys cal*, dev glass*, isot. musc. | Subrounded and subspherical. | Good | 1 mm | 20% | Yes, one small fragment | No | No | Yes, few | | | |
| La19 | F | S Col | Lower | 1 layer | No | Slightly hydraulic | Rounded | 2 mm. | No | Good | Yes. | Yes | No | Mic cal, isot. | Subrounded and subspherical. | Good | 4 mm | 35% | Yes, few inclusions. No visible features. | No | No | Yes, few. | Isotropic layer between the two plasters. | | |
| La20 | JM | S Col | NA | No | No | Slightly hydraulic | Rounded | 1 mm. | Yes | Good. | Yes, big crystals. | Yes | No | Mic cal*, qz in opaques, dev glass*. | Subrounded and subspherical. | Regular | 2 mm | 25% | No | No | No | Yes | | | |
| La21 | WR | S Col | NA | No | No | Slightly hydraulic? | Rounded | 1.5 mm. | Yes, 2 mm. | Good. | Yes, big crystals. | Yes | No | Mic cal*, crys cal, isot, met cal?, dev glass*. | Angular. | Regular | 5 mm | 20% | No | No | No | Yes. | Isotropic layer over the surface. | | |
| La40 | WR | S Col | NA | No | No | Perhaps slightly hydraulic | Rounded | 0.75 mm | Yes | Good | Yes | No | No | Mic cal*, crys cal, dev glass, isot. | subrounded, subspherical | 1 mm | 1.5 mm | 25% | No | No | No | Angular fragment 1.5 mm. | | | |
| La Sascab | Sas | NA | NA | NA | NA | NA | NA | NA | NA | NA | NA | Yes | No | Mic cal* | NA | NA | NA | NA | NA | No | No | NA | Recrystallized calcite. | | |
| La13 | L? | L Clas | No | NA | No | Compacted sascab? | Vesicular? | 0.25 mm | NA | NA | No | Yes | No | Mic cal* | Subrounded and subspherical. | Good | 2 mm | Not clear | No | No | No | No | No | | |
| La23 | L | S Col | NA | NA | NA | NA | Vesicular | 0.3 mm | NA | NA | NA | NA | No | Mic cal* (no visible aggregates). | NA | NA | 3 mm | NA | NA | NA | NA | NA | NA | Pelmicrite. Pelloids in micritic cement | |
| La27 | L | L Prec | NA | NA | NA | NA | Vesicular rounded and vesicular | 0.3 mm | NA | NA | NA | NA | NA | NA | NA | NA | NA | NA | NA | NA | NA | NA | NA | Micritic calcite with quartz grains. | |
| La39 | L | L Post | NA | NA | NA | NA | NA | 0.3 mm | NA | NA | NA | NA | NA | NA | NA | NA | NA | NA | NA | NA | NA | NA | NA | NA | micritic calcite. Some quartz grains and clasts of crystalline |

Abbreviations type of material: F: Floor, JM: Joining mortar, WR: Wall render, L: Limestone, Sas: sascab, S: sculpture, MPrec: Middle Preclassic, LPrec: Late Preclassic, EClas: Early Classic, LClas: Late Classic, TClas: Terminal Classic.

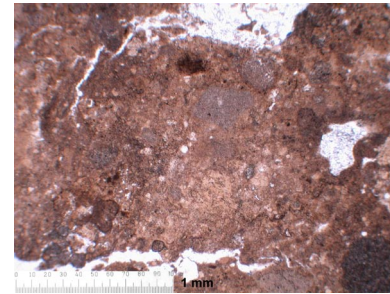
Abbreviations mineralogy: Mic cal: micritic calcite, crys cal: crystalline calcite, spar: sparite, qz: quartz, shoc qz: shocked quartz, isot: isotropic, pol qz: polycrystalline quartz, dev glass: devitrified glass, clay pel: clay pellets, plag feld: plagioclase feldspars, musc: muscovite mica, met cal: metamorphic calcite, horn: hornblende, sil car: silicon carbide, oliv: olivine, serp: serpentinite, metam calc: metamorphic calcite. Dominant phases are marked with *.

A.2.2. Photomicrographs and Fabric Groups

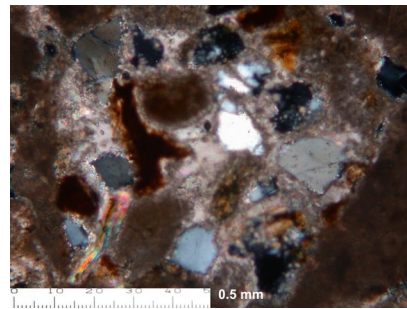
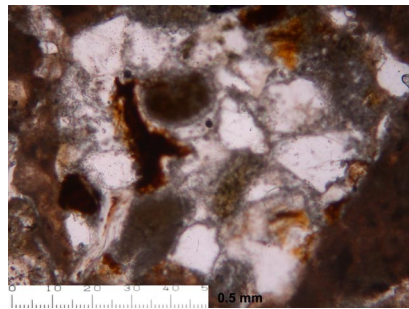
Palenque



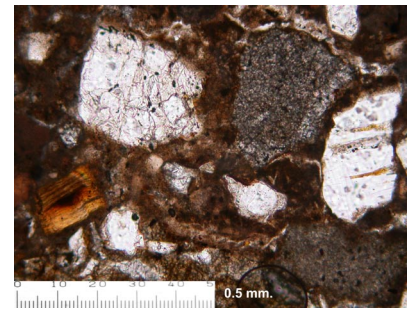
Pa 4. Joining mortar. Cascada Phase. Fragment of quartz-tempered ceramics (?) employed as aggregate. Left: PPL. Right: XPL. Scale bar: 0.5 mm.



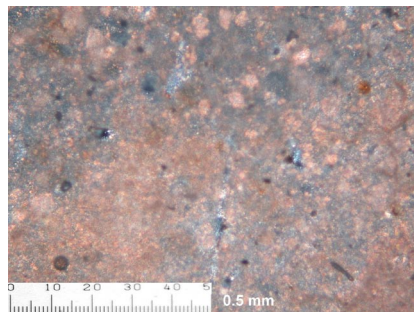
Pa49. Wall render. Otulum Phase. Hydraulic matrix, aggregates of micritic calcite and grain of quartz. Left: PPL. Right: XPL. Scale bar: 1 mm.



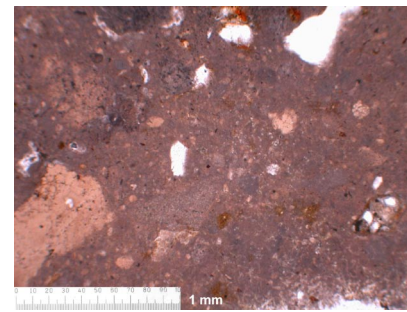
Pa50. Floor. Otulum phase? Rounded reworked sediment with quartz, micas and altered feldspars. Left: PPL. Right: XP. Scale bar: 0.5 mm.



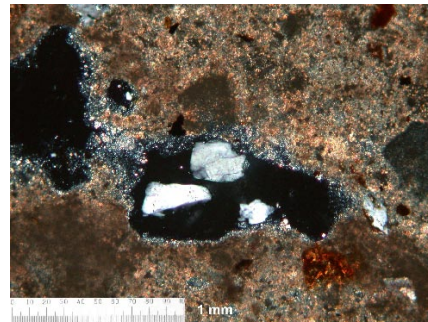
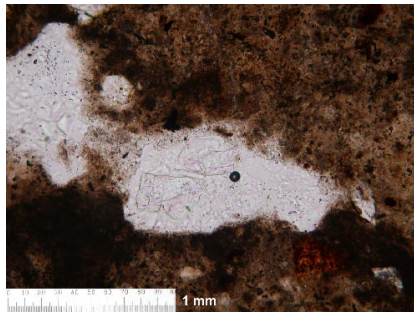
Pa88. Wall render. Otulum phase? Aggregates of crystalline calcite, polycrystalline quartz, feldspars and micas. Left: PPL. Right: XP. Scale bar: 0.5 mm.



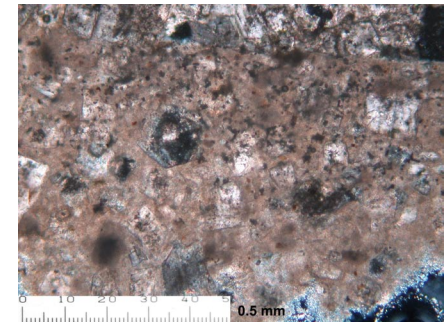
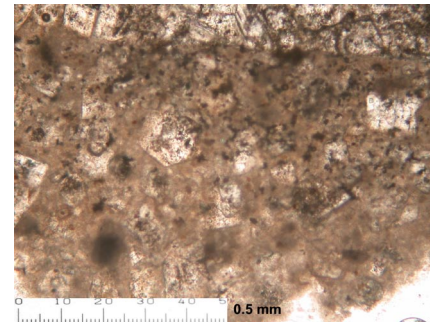
Pa77. Wall render. K'inich Janaab Pakal I. Silt-size aggregates of micritic calcite in hydraulic matrix.



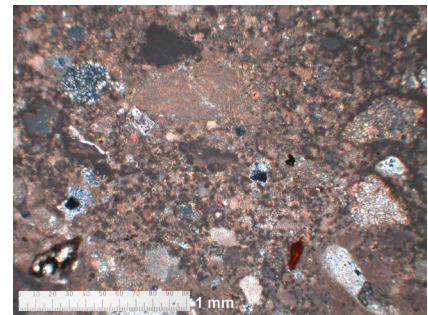
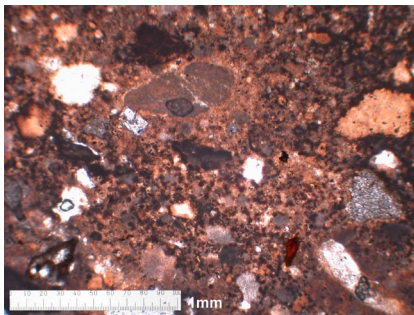
Pa78. Wall render. K'inich Janaab Pakal I. Aggregates of quartz and micritic calcite. A lime lump can be seen at the lower left corner. Left: PPL. Right: XP. Scale bar: 1 mm



Pa22. Floor. K'inich Kam Balam II. Aggregates of isotropic phases with quartz. Likely volcanic origin. Left: PPL. Right: XP. Scale bar: 1 mm.



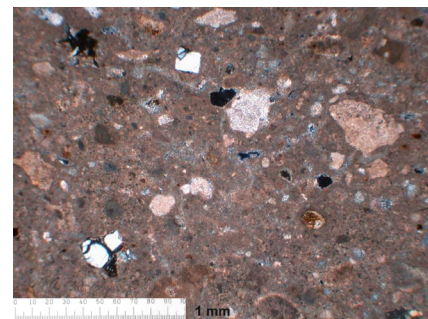
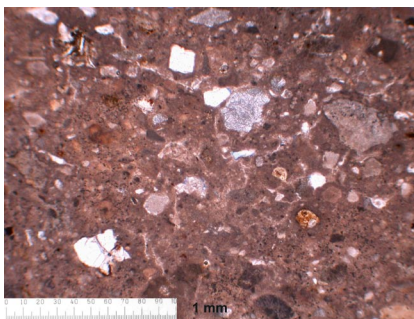
Pa23. Floor. K'inich Kam Balam II. Large crystals of dolomite (?) employed as aggregate materials. Left: PPL. Right: XP. Scale bar: 0.5 mm.



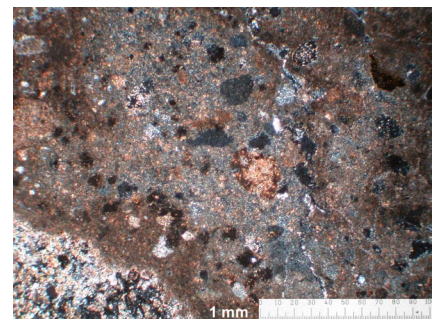
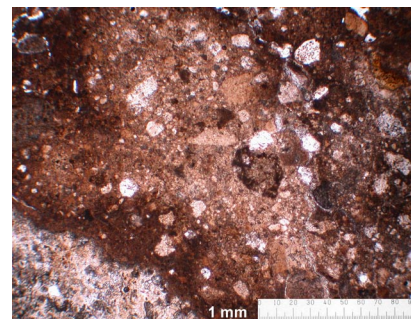
Pa24. Wall render. K'inich Kam Balam II. Micritic and crystalline calcite. Visible lime lumps. Left: PPL. Right: XP. Scale bar: 1 mm.



Pa27. Wall render. K'inich Kam Balam II. Impact glass with yellowish colour. Cracks, bubbles and sanidine grain can be seen. Hydraulic matrix. Left: PPL. Right: XPL. Scale bar: 0.5 mm. See appendix A.4 for composition of glass.



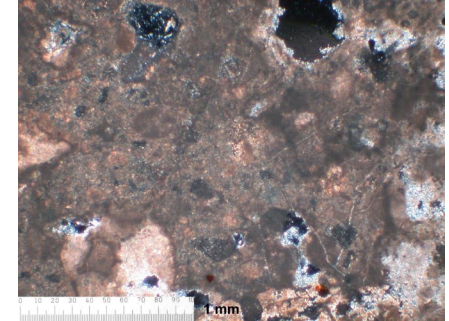
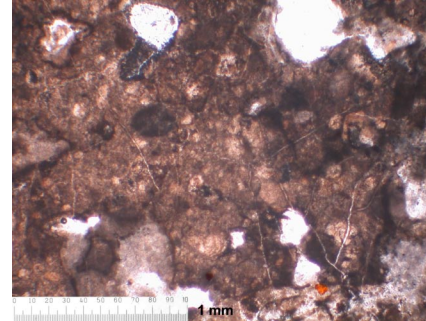
Pa52. Floor. K'inich Kam Balam II? Slightly hydraulic matrix with quartz lined isotropic materials. Micritic and crystalline calcareous aggregates. Left: PPL. Right: XP. Scale bar: 1 mm.



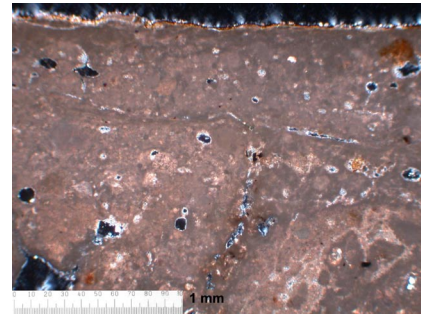
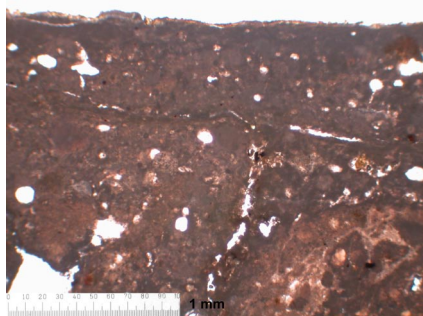
Pa 59. Floor. K'inich Kam Balam II. Slightly hydraulic matrix. Left: PPL. Right: XPL. Scale bar: 1 mm.



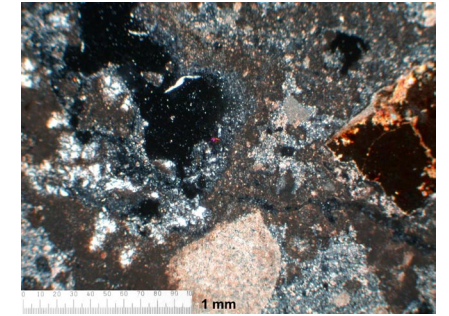
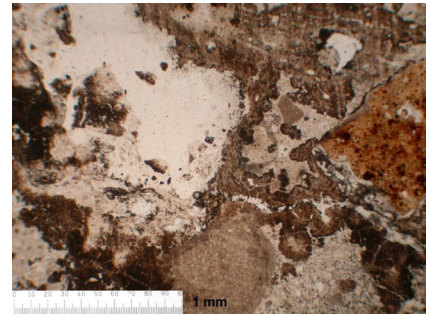
Pa28. Floor. K'inich Kam Balam II. Rounded reworked volcanic inclusion and rounded grain of biosparite. Clayey matrix. Left: PPL. Right: XP. Scale bar: 1 mm.



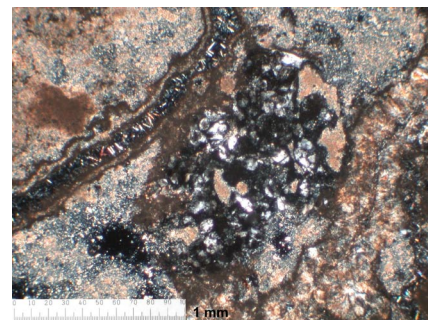
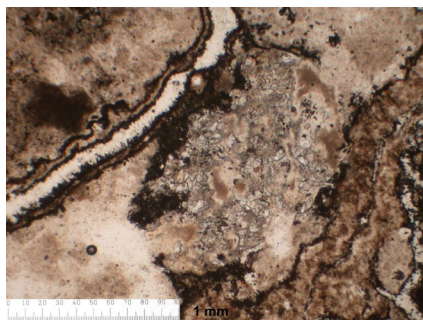
Pa61. Floor. K'inich Kam Balam II. Hydraulic matrix with few calcareous aggregates. Left: PPL. Right: XP. Scale bar: 1 mm.



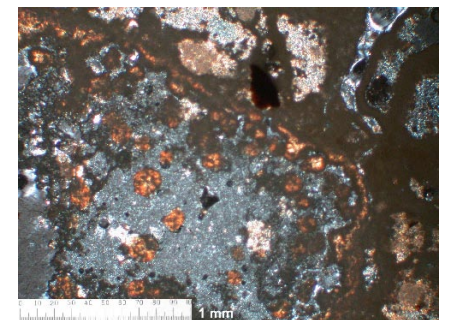
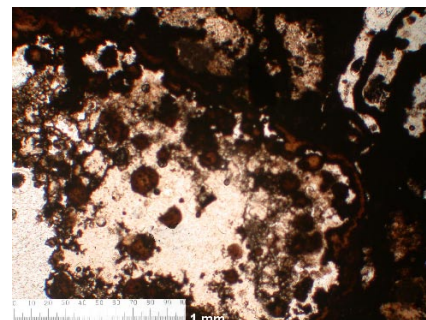
Pa63. Floor. K'inich Kam Balam II. Two layers with hydraulic matrix. Few visible aggregates. Left: PPL. Right: XP. Scale bar: 1 mm.



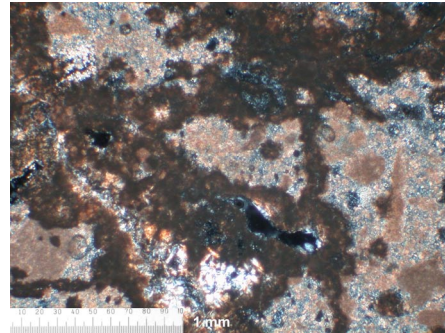
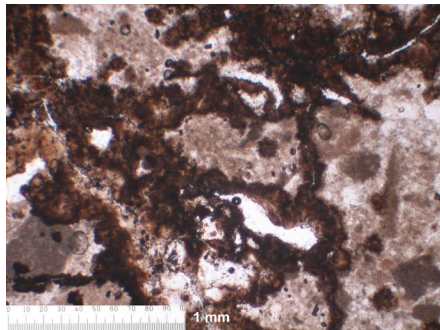
Pa65. Floor. K'inich Kam Balam II. Hydraulic matrix with isotropic phases and devitrified glass. Left: PPL. Right: XP. Scale bar: 1 mm.



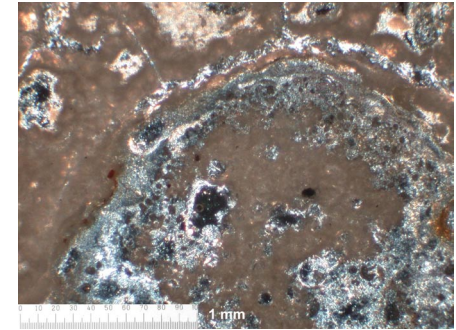
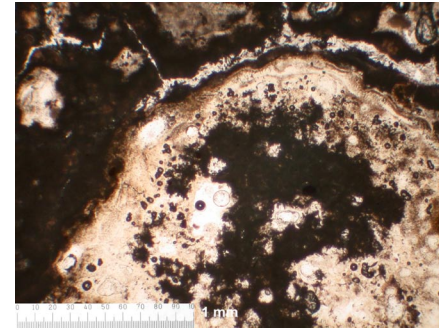
Pa66. Floor. K'inich Kam Balam II. Hydraulic reactions and isotropic phases. Recrystallized (secondary) minerals in crack. Left: PPL. Right: XP. Scale bar: 1 mm.



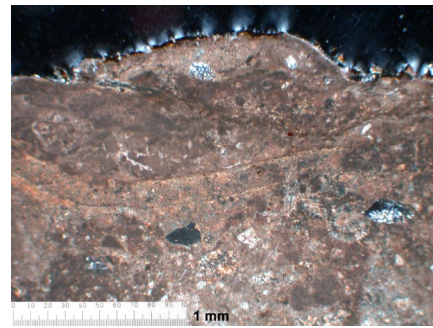
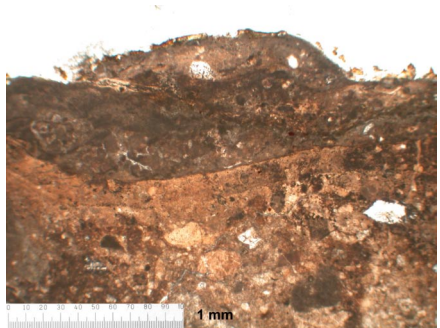
Pa67. Floor. K'inich Kam Balam II. Isotropic phases with orange blebs. Hydraulic reactions can be seen surrounded the isotropic phase. Left: PPL. Right: XPL. Scale bar: 1 mm.



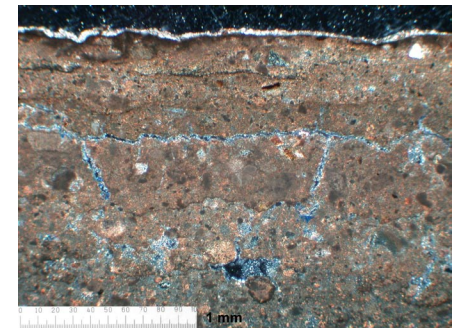
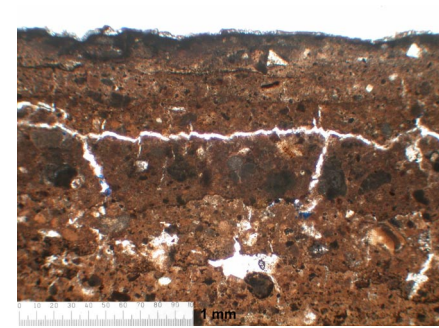
Pa 68. Floor. K'inich Kam Balam II. Hydraulic reactions around partially isotropic phases with carbonate particles. Left: PPL. Right: XP. Scale bar: 1 mm.



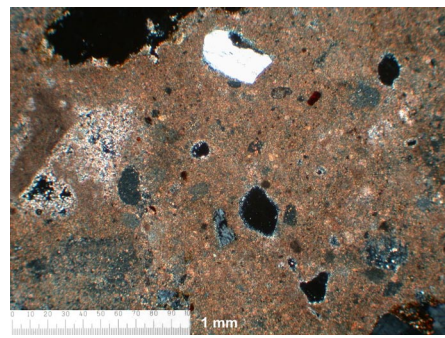
Pa71. Floor. K'inich Kam Balam II. Hydraulic reactions and isotropic phases. Left: PPL. Right: XP. Scale bar: 1 mm.



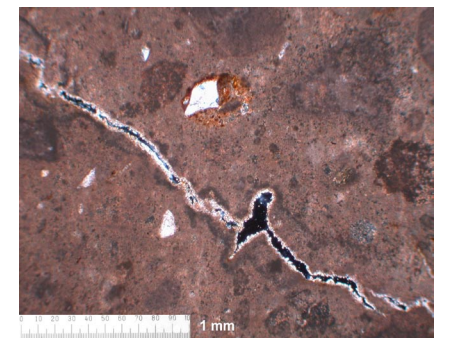
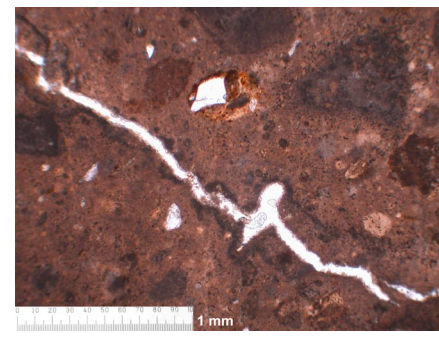
Pa72. Floor. K'inich Kam Balam II. Slightly hydraulic matrix and two visible limewash layers. Left: PPL. Right: XP. Scale bar: 1 mm.



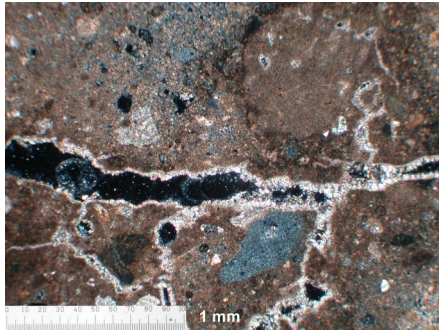
Pa75. Floor. K'inich Kam Balam II. Sequence of limewashes with slightly hydraulic matrices. Left: PPL. Right: XP. Scale bar: 1 mm.



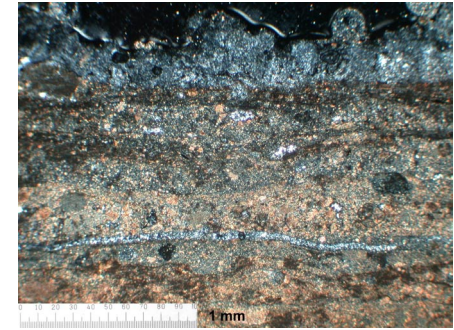
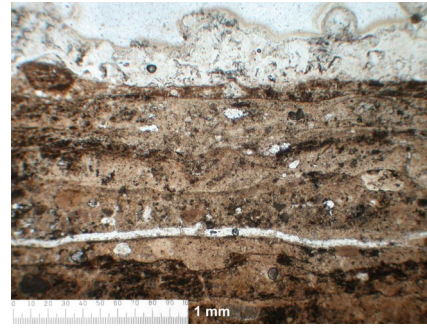
Pa18. Floor. Joy Chitam II? Quartz and devitrified glass. Left: PPL. Right: XP. Scale bar: 1 m.m.



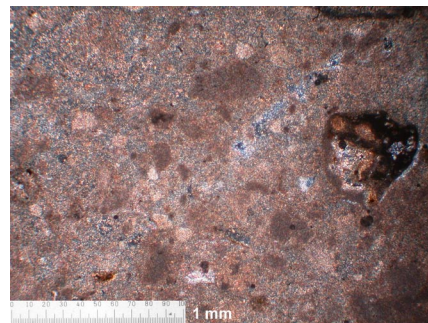
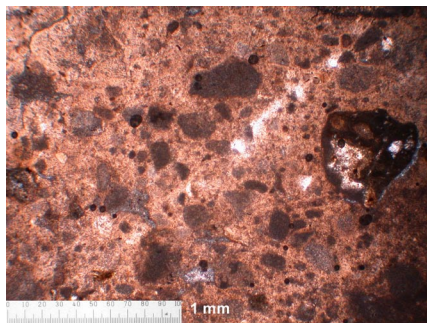
Pa19. Wall render. Joy Chitam II? Calcareous aggregates (micritic) and pellet with quartz. Left: PPL. Right: XP. Scale bar: 1 mm.



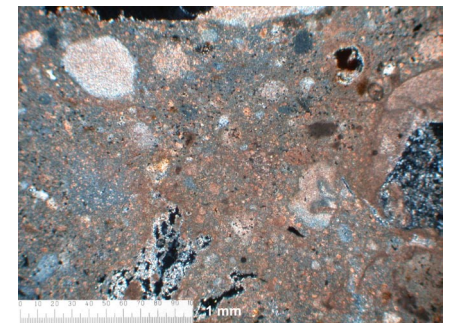
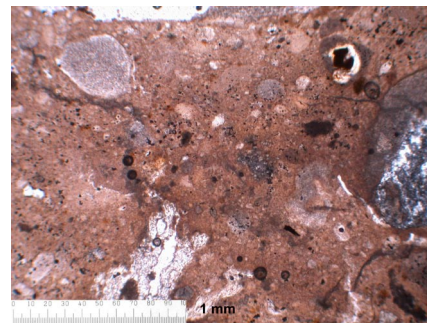
Pa43. Wall render. Joy Chitam? Calcareous aggregates and recrystallized calcite. XPL. Scale bar: 1 mm.



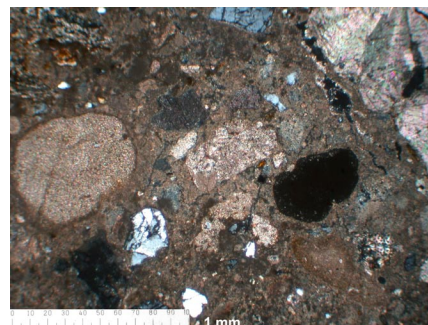
Pa1. Wall render. K'inich Kuk Bahlam II (Aka Kuk). Silt size calcareous aggregates and numerous limewash layers. Secondary minerals in accretion layer. Left: PPL. Right: XP. Scale bar: 1 mm.



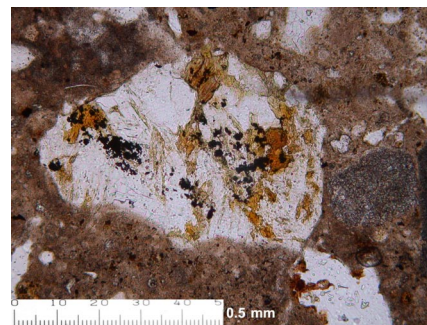
Pa2a. Floor. K'inich Kuk Bahlam II (Aka Kuk). Rounded calcareous aggregates (micritic). Left: PPL. Right: XP. Scale bar: 1 mm.



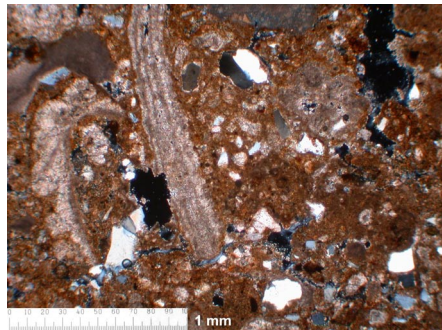
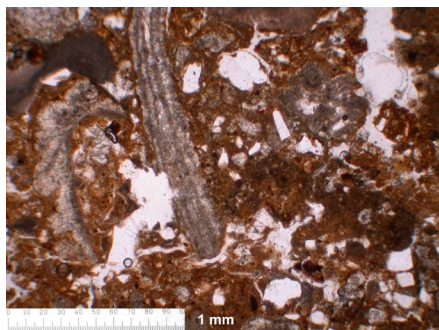
Pa2b. Floor. K'inich Kuk Bahlam II (Aka Kuk). Hydraulic matrix with calcareous aggregates. Left: PPL. Right: XP. Scale bar: 1 mm.



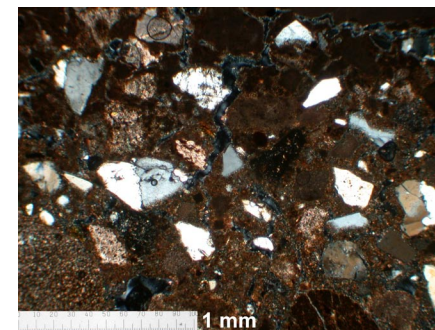
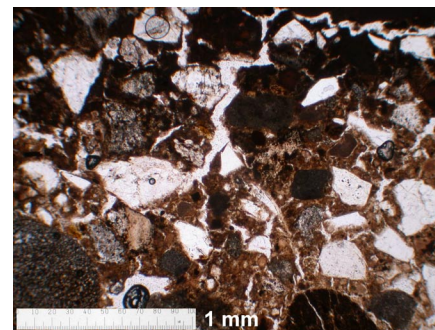
Pa12. Wall render. K'inich Kuk Bahlam II (Aka Kuk). Micritic and crystalline aggregates (some rounded) and isotropic phases. Left: PPL. Right: XP. Scale bar: 1 mm.



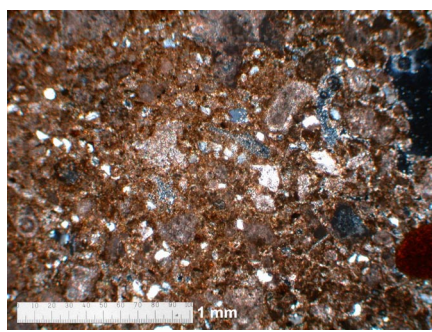
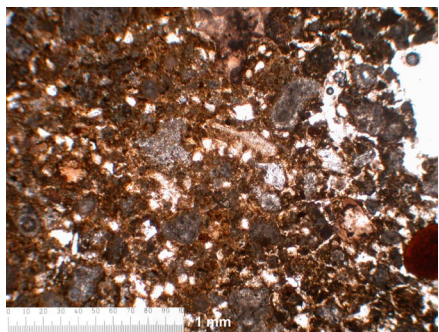
Pa53. Wall render. Balunté Phase. Rounded igneous rock with biotite mica, feldspars and opaques. Left: PPL. Right: XP. Scale bar: 0.5 mm.



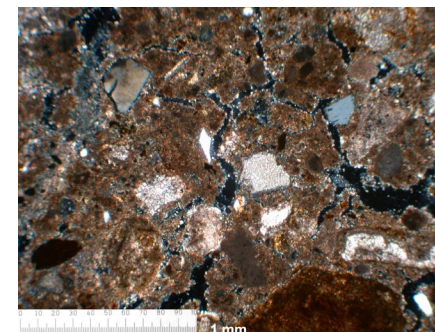
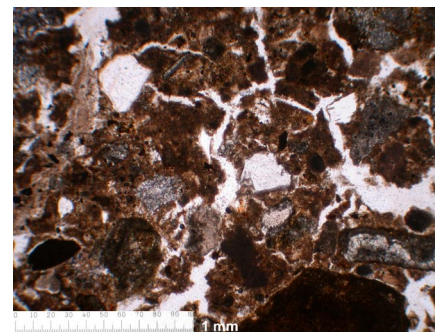
Pa56. Floor. Balunté Phase. Clayey matrix rich in iron oxides. Quartz and shells as aggregates. Left: PPL. Right: XP. Scale bar: 1 mm.



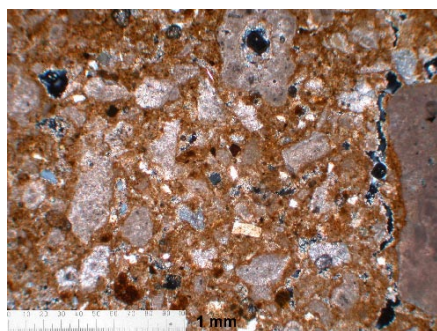
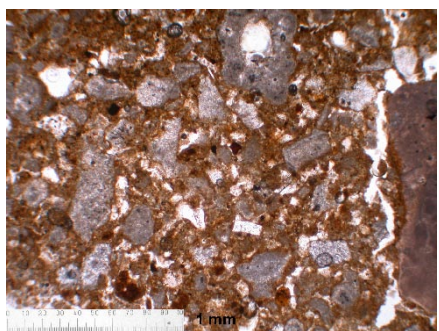
Pa86. Wall render. Balunté Phase. Clayey matrix with numerous shrinkage cracks. Aggregates of angular quartz. Left: PPL. Right: XP. Scale bar: 1 mm.



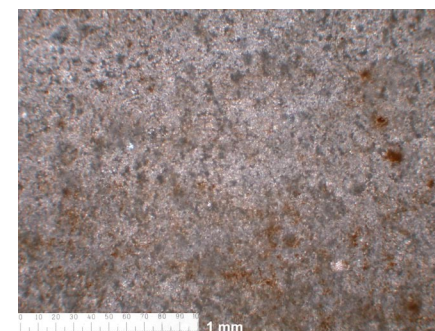
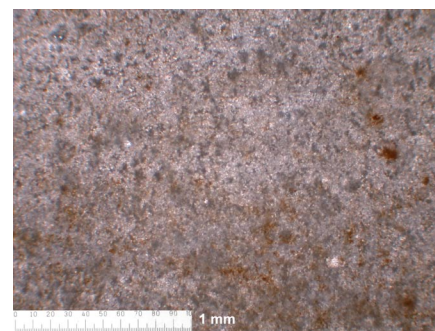
Pa87. Wall render. Balunté Phase. Clayey matrix with small subangular quartz aggregates. Left: PPL. Right: XP. Scale bar: 1 mm.



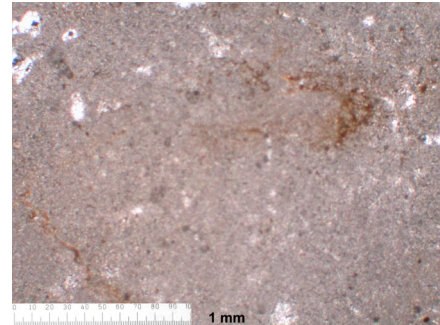
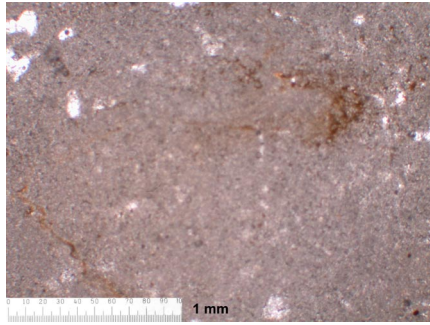
Pa44. Wall render. Architectural modifications. Clay-rich matrix, quartz and crystalline calcite (dolomite?). Visible shrinkage cracks in the matrix. Left: PPL. Right: XP. Scale bar: 1 mm.



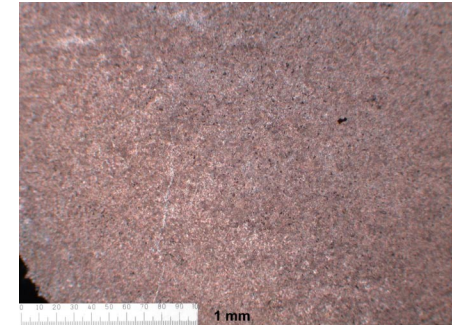
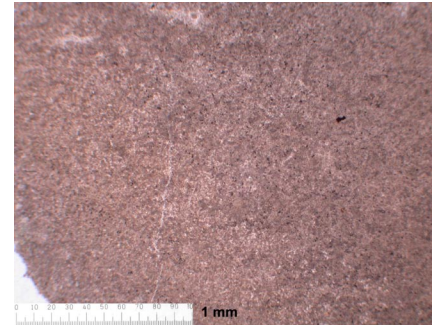
Pa45. Joining mortar. Architectural modifications. Clayey matrix with cracks and crystalline and micritic calcareous aggregates. Left: PPL. Right: XP. Scale bar: 1 mm.



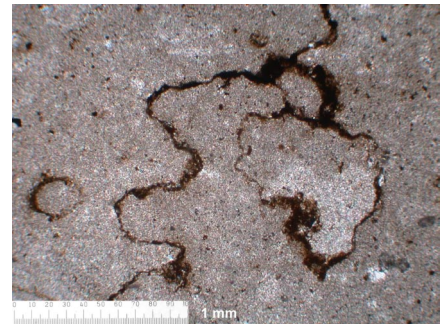
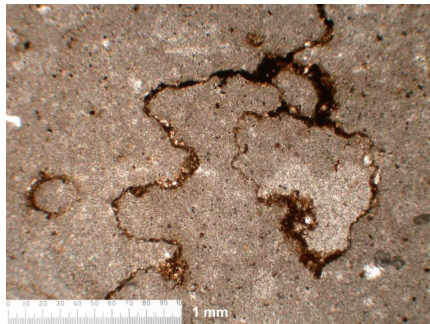
Pa5. Crystalline limestone. Micritic and sparry calcite (dolomite?). Left: PPL. Right: XP. Scale bar: 1 mm. See appendix A.6 for bulk composition.



Pa26. Crystalline limestone with iron oxides. Left: PPL. Right: XP. Scale bar: 1 mm. See appendix A.6 for bulk composition.

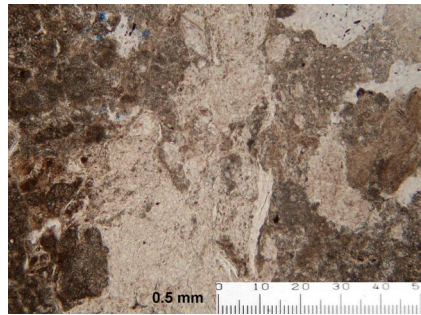


Pa48. Crystalline limestone. Left: PPL. Right: XP. Scale bar: 1 mm. See appendix A.6 for bulk composition.



Pa 55. Crystalline limestone with veins of iron oxides. Left: PPL. Right: XP. Scale bar: 1 mm. See appendix A.6 for bulk composition.

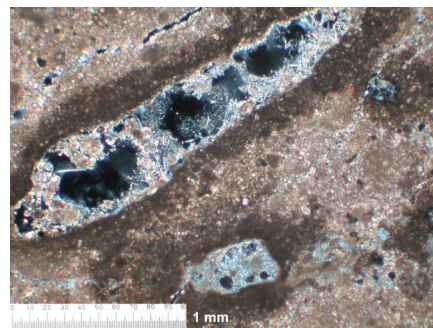
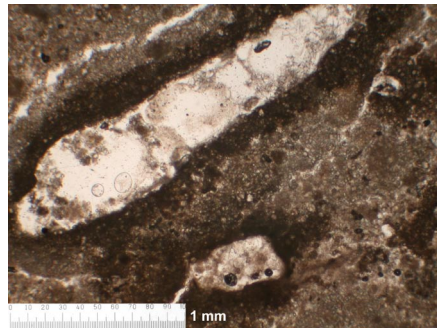
Calakmul



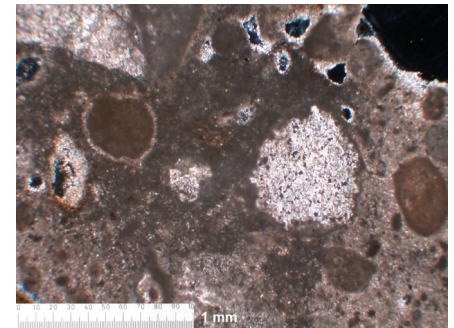
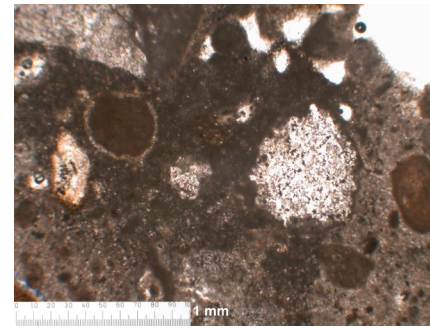
Ca9. Floor. Middle Preclassic. Masses of serpentine group mineral. Compacted sascab? Late Middle Preclassic. Left: PPL. Right: XP. Scale bar: 0.5 mm.



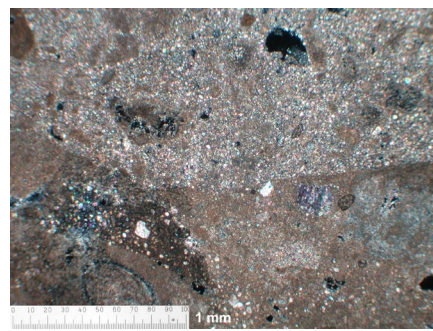
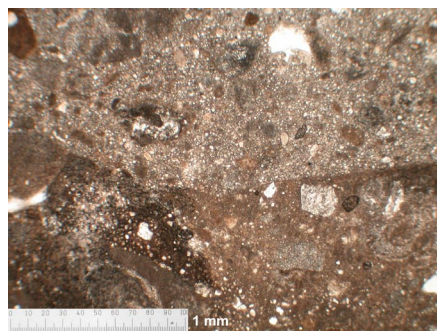
Ca10. Floor. Middle Preclassic. Inclusion of *Cyrenia* shell. Floor. Middle Preclassic. Left: PPL. Right: XP. Scale bar: 0.5 mm.



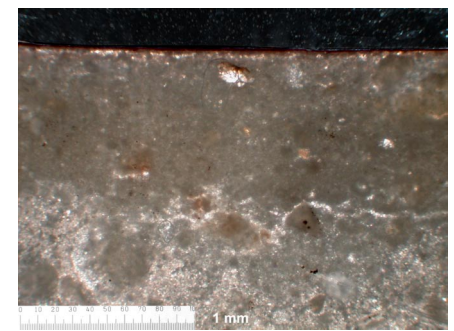
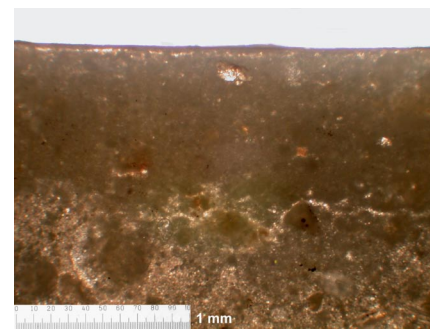
Ca11. Wall render. Middle Preclassic. Hydraulic reactions and acicular phases. Wall render. Middle Preclassic. Left: PPL. Right: XP. Scale bar: 1 mm. See appendix A.4 for composition.



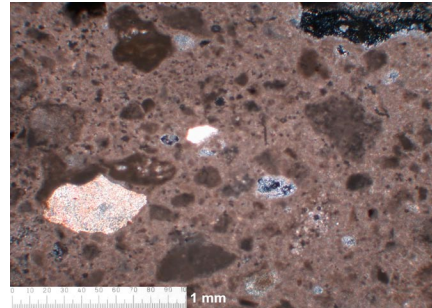
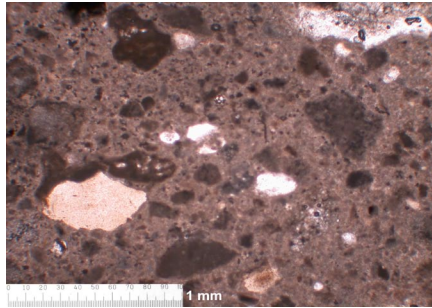
Ca5. Sculpture. Late Middle Preclassic. Micritic and polycrystalline calcareous aggregates, isotropic phase and areas of hydraulic reaction. Sculpture. Late Middle Preclassic. Left: PPL. Right: XP. Scale bar: 1 mm.



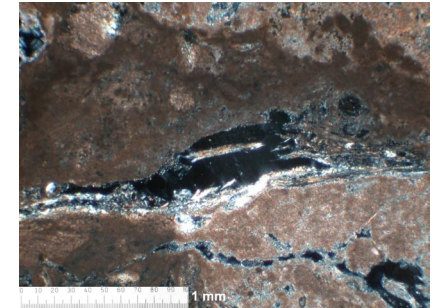
Ca6. Wall render. Late Middle Preclassic. Interfase of replastering application. Left: PPL. Right: XP. Scale bar: 1 mm.



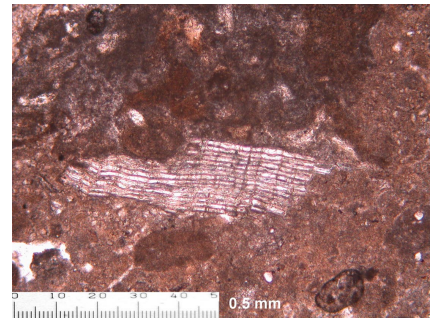
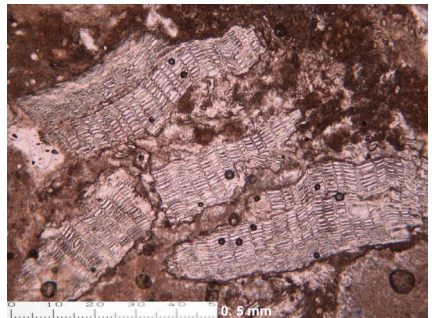
Ca7. Sculpture. Late Middle Preclassic. Fine limewash with thin red paint layer. Sculpture. Late Middle Preclassic. Left: PPL. Right: XP. Scale bar: 1 mm. See appendix B.1 for pigment dispersions.



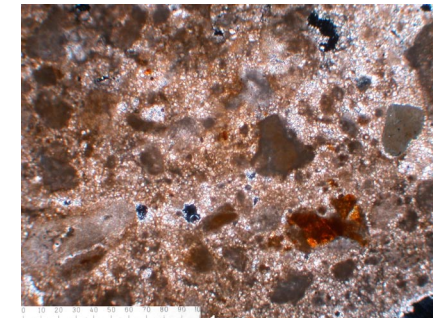
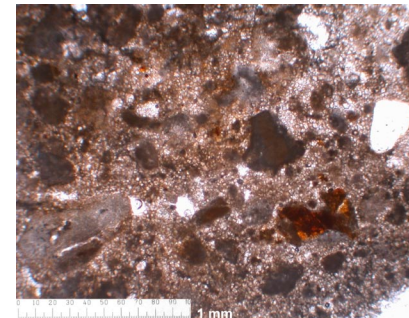
Ca8. Late Middle Preclassic. Sculpture. Calcareous aggregates, isotropic phases and likely devitrified glass. Sculpture. Late Middle Preclassic. Left: PPL. Right: XP. Scale bar: 1 mm.



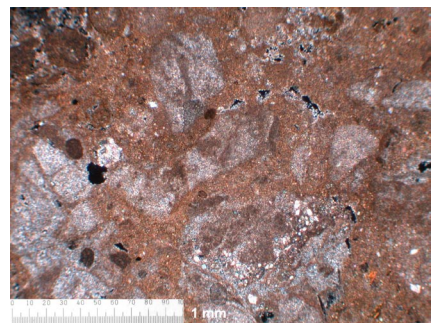
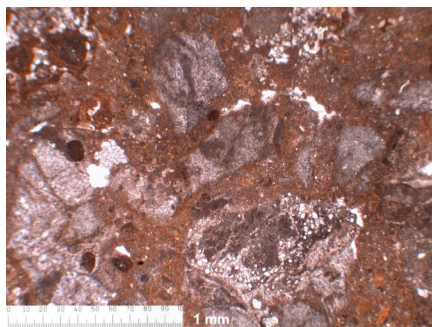
Ca29. Floor. Mineral from serpentine group. Left: PPL. Right: XP. Scale bar: 1 mm. See appendix A.4 for composition.



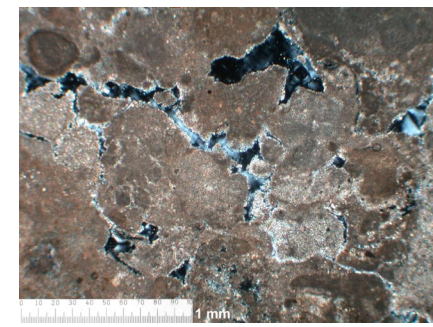
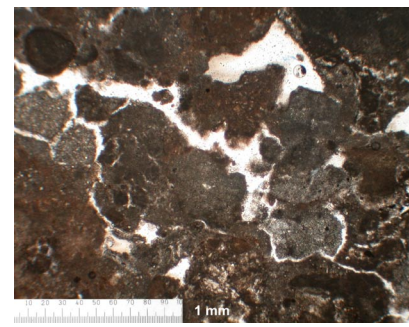
Ca30. Floor. Late Preclassic. Amorphous silica plant remains. Scale bar: 0.5 mm.



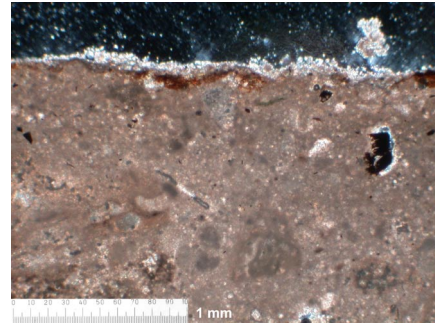
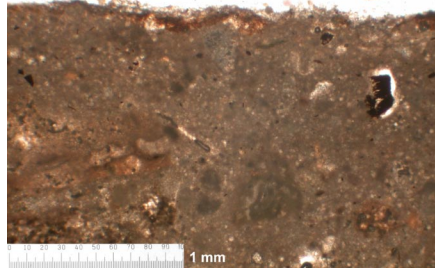
Ca1. Wall render. Early Classic. Fine sand-size micritic aggregates and iron oxides. Wall render. Early Classic. Left: PPL. Right: XP. Scale bar: 1 mm.



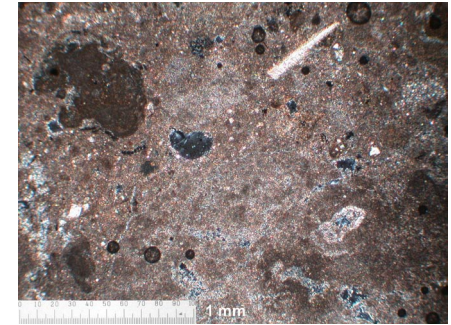
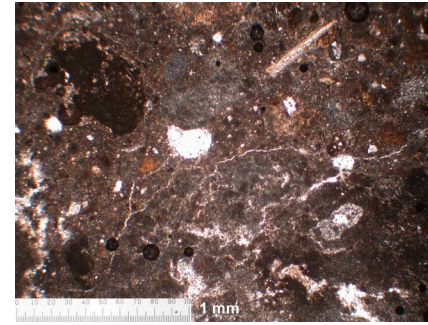
Ca2. Floor. Early Classic. Sand-size sparry aggregates and iron-rich matrix. Floor. Early Classic. Left: PPL. Right: XP. Scale bar: 1 mm.



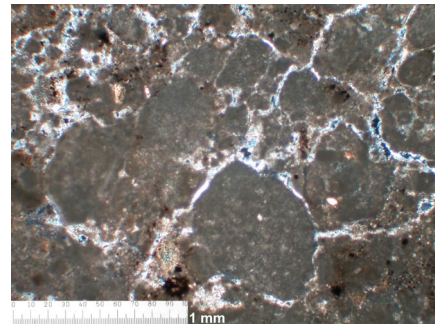
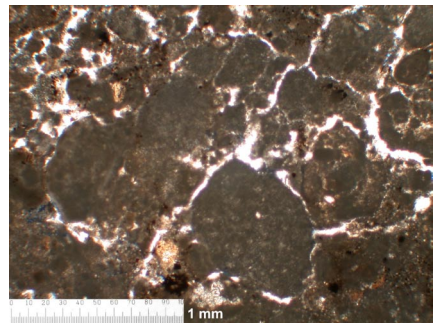
Ca13. Floor. Early Classic?. Calcareous aggregates and cracks in the matrix. Floor. Early Classic. Left: PPL. Right: XP. Scale bar: 1 mm.



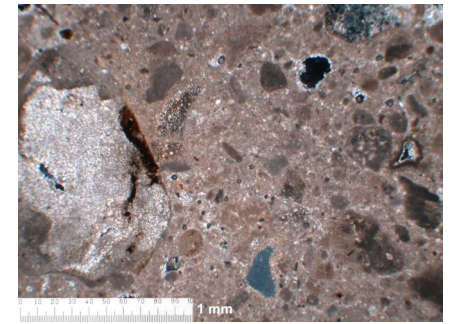
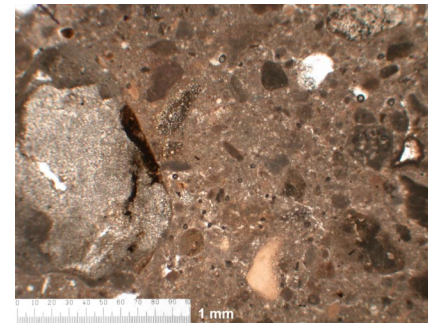
Ca14. Wall render. Early Classic? Red paint layer. Visible fragment of charcoal. Left: PPL. Right: XP. Scale bar: 1 mm.



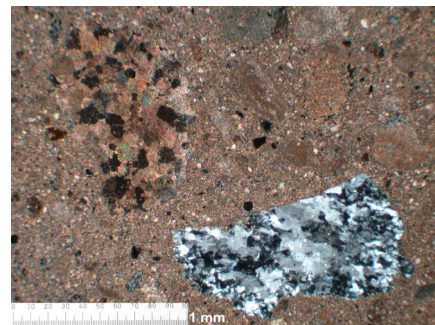
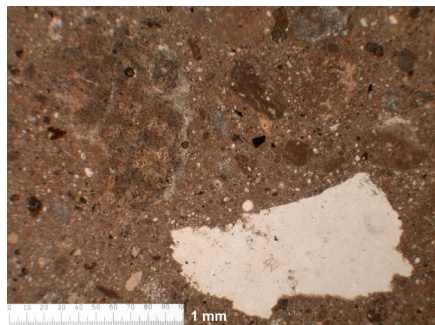
Ca19. Floor. Early Classic. Non hydraulic plaster with rounded aggregates. Left: PPL. Right: XP. Scale bar: 1 mm.



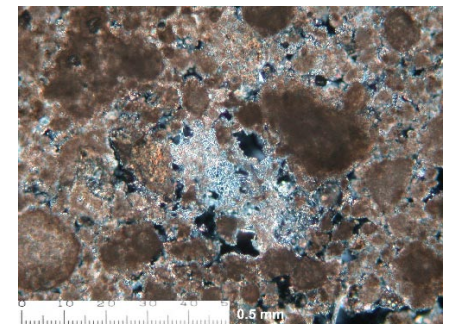
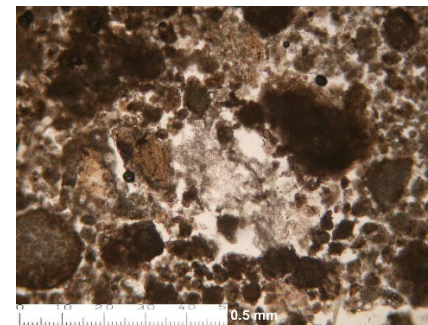
Ca22. Floor. Early Classic. Calcareous aggregates in slightly clayey matrix, yellow mineral and cracks in matrix. Left: PPL. Right: XP. Scale bar: 1 mm.



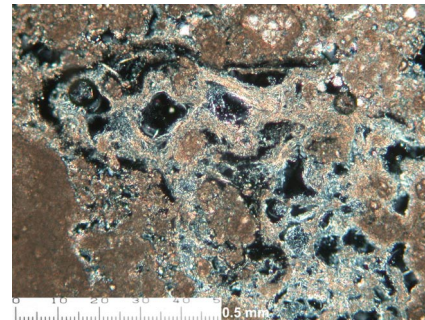
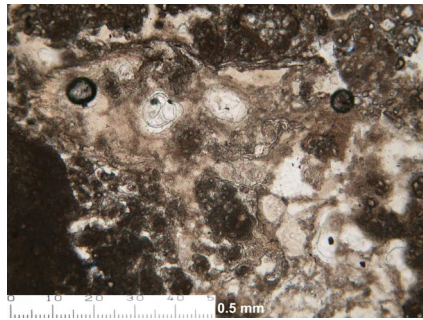
Ca23. Wall render. Early Classic. Micritic and crystalline calcite. Left: PPL. Right: XP. Scale bar: 1 mm.



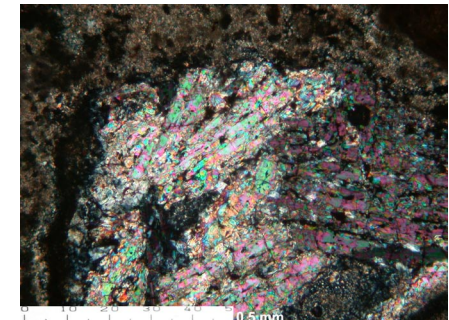
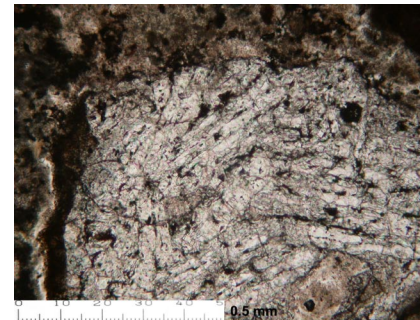
Ca24. Early Classic. Quartzite and dolomite employed as aggregates. Early Classic or earlier. Left: PPL. Right: XP. Scale bar: 1 mm.



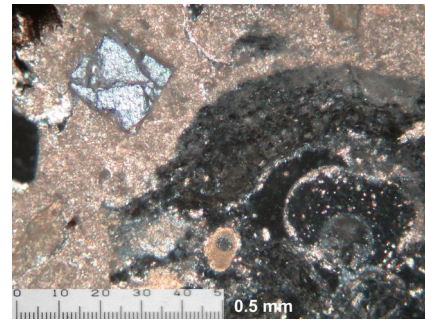
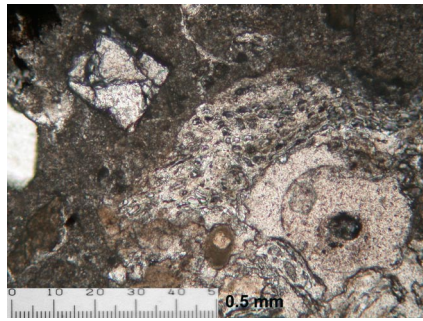
Ca16. Wall render. Late Classic. Devitrified glass in association with acicular phases. Wall render. Late Classic. Left: PPL. Right: XP. Scale bar: 0.5 mm. See appendix A.4 for composition.



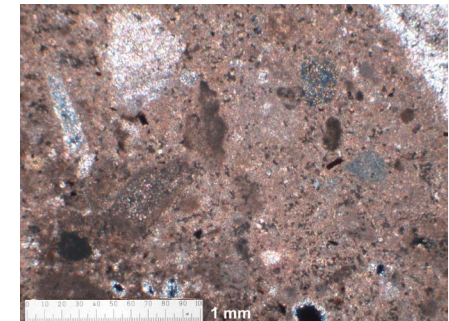
Ca18. Floor. Late Classic. Acicular crystals in association with isotropic phases. Left: PPL. Right: XP. Scale bar: 0.5 mm. See appendix A.4 for composition.



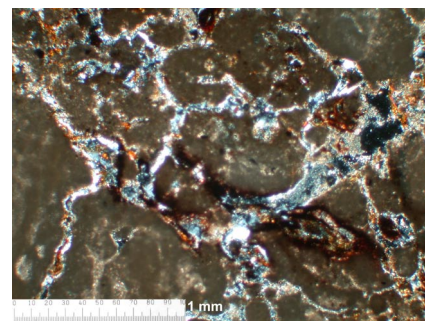
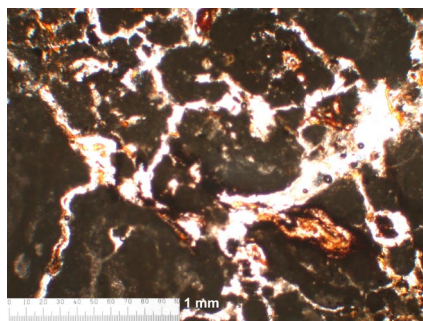
Ca21. Floor. Late Classic. Rounded fragment of schist. Left: PPL. Right: XP. Scale bar: 0.5 mm.



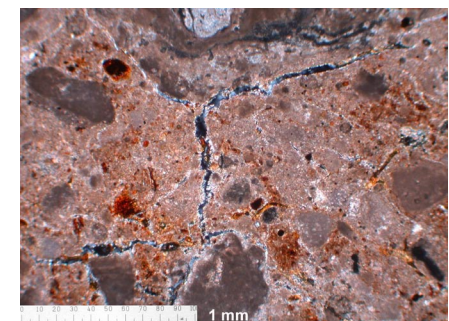
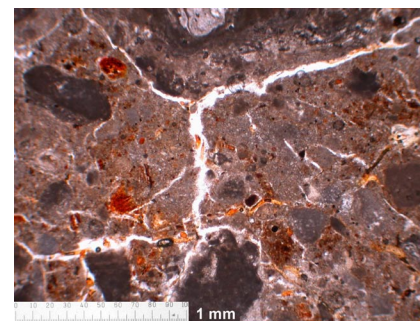
Ca26. Wall render. Late Classic. Quartz and isotropic phase with amorphous silica plant remains. Left: PPL. Right: XP. Scale bar: 0.5 mm. See appendix A.4 for composition.



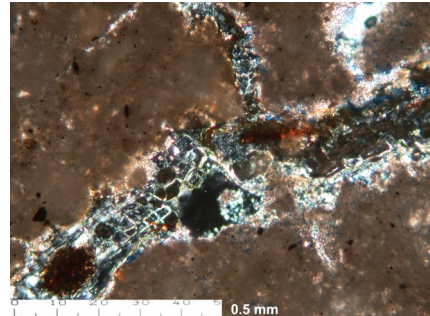
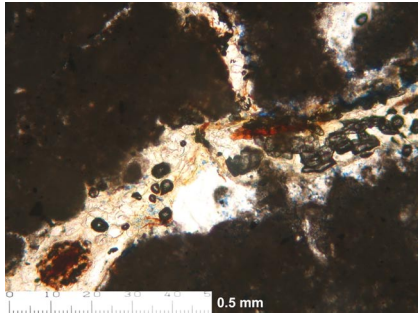
Ca36. Wall render. Late Classic. Micritic and crystalline calcareous aggregates. Lime lumps. Left: PPL. Right: XP. Scale bar: 1 mm.



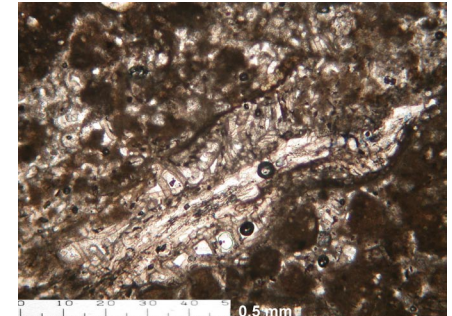
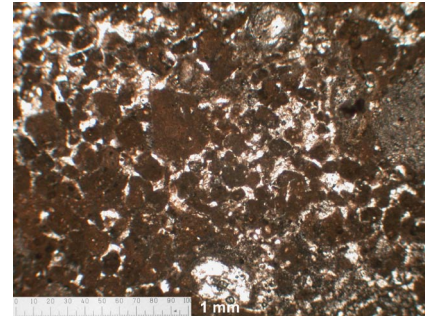
Ca3. Floor. Terminal Classic. Micritic clayey matrix with cracks and plant fibers. Left: PPL. Right: XP. Scale bar: 1 mm.



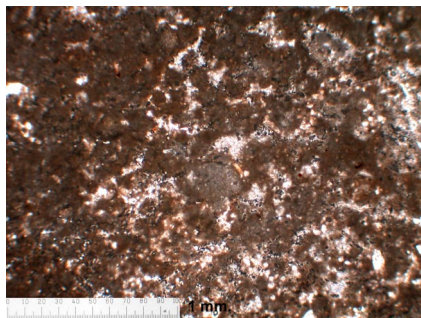
Ca4. Floor. Terminal Classic. Clayey matrix with iron oxides, cracks and plant roots. Left: PPL. Right: XPL. Scale bar: 1 mm.



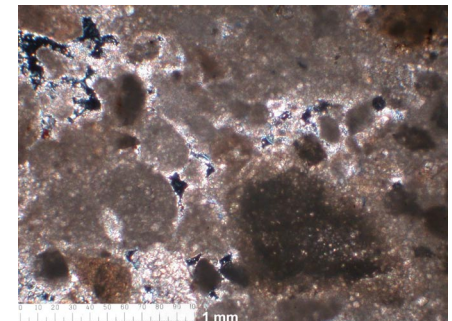
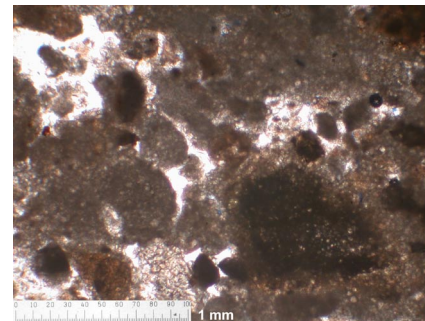
Ca34. Terminal Classic. Clayey plaster with cracks and plant roots. Left: PPL. Right: XP. Scale bar: 0.5 mm.



Ca25. Limestone. Modern material. Pelloidal limestone. Left: visible pelloids. PPL. Scale bar: 1 mm. Right: fossil. PPL. Scale bar: 0.5 mm.

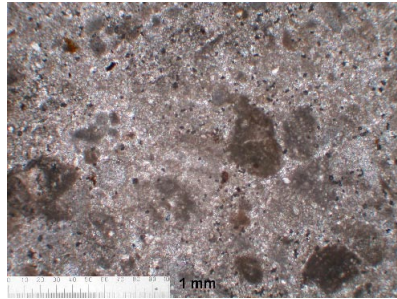
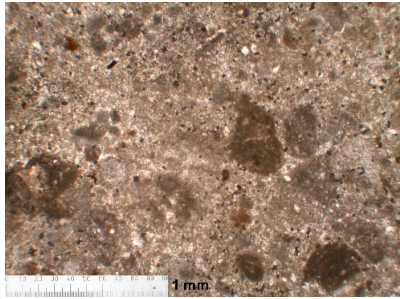


Ca28. Limestone. Modern material. Pelloidal limestone. PPL. Scale bar: 1 mm. See appendix A.6 for bulk composition.

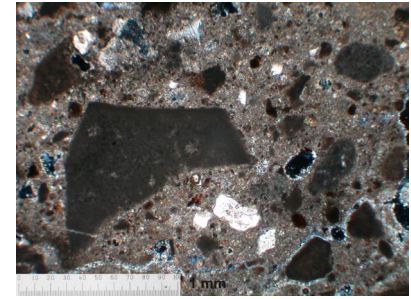
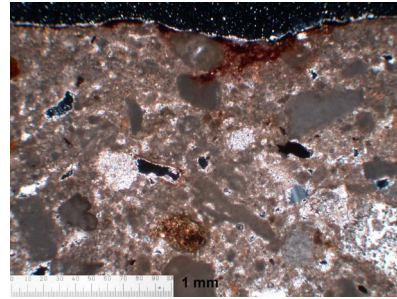


CaSascab. Local modern material. Rounded reworked sediments of micritic calcite. Left: PPL. Right: XP. Scale bar: 1 mm. See appendix A.6 for bulk composition.

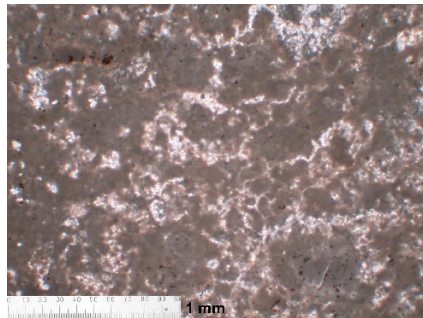
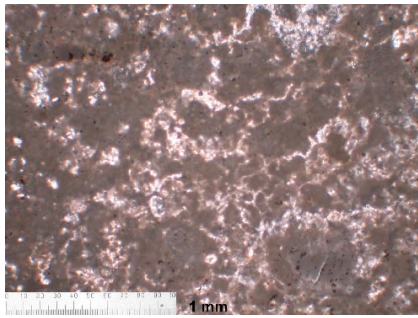
Lamanai



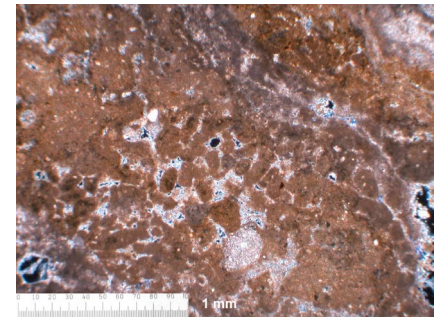
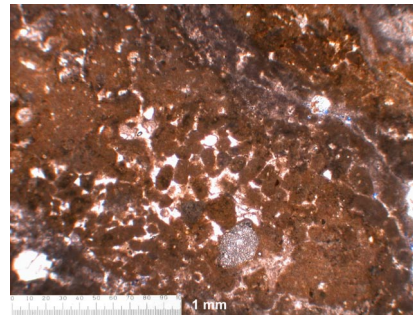
La 15. Floor. Late Preclassic. Subrounded aggregates of micritic calcite. Left: PPL. Right: XPL. Scale bar: 1mm.



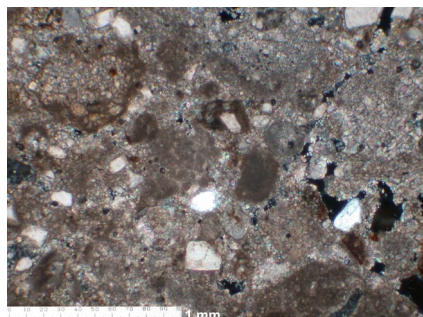
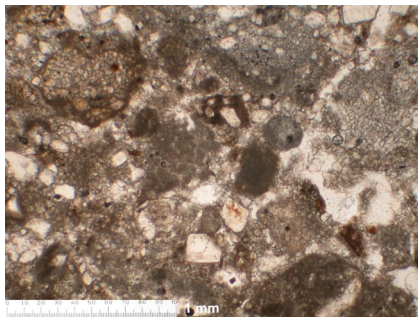
La 24. Floor. Late Preclassic. Left: subounded aggregates of micritic and crystalline calcite. Red paint layer. XPL, scale bar: 1 mm. Right: Angular aggregates of micritic calcite (crushed limestone). XPL, scale bar: 1 mm.



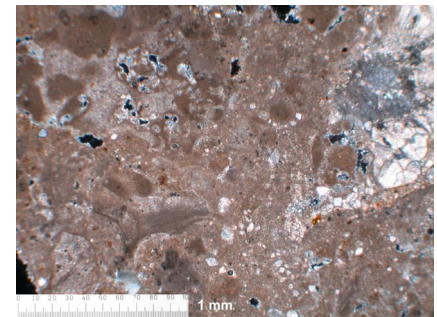
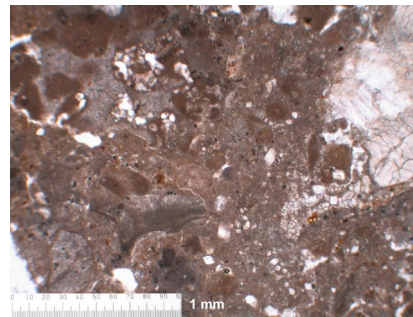
La28. Floor. Late Preclassic. Pelloids and cement of micritic calcite. Compacted sascab? Left: PPL. Right: XPL. Scale bar: 1 mm.



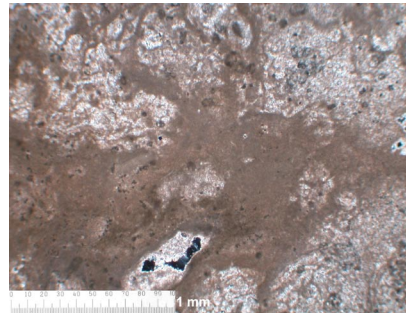
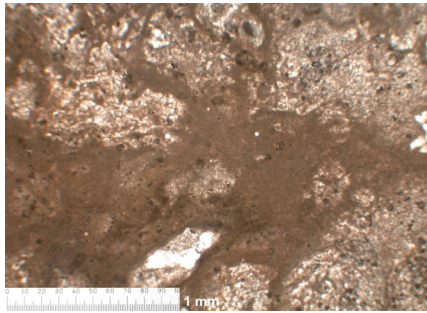
La29. Floor. Late Preclassic. Pelloids and sediments of micritic calcite. No clear presence of aggregates. Left: PPL, Right: XP. Scale bar: 1 mm.



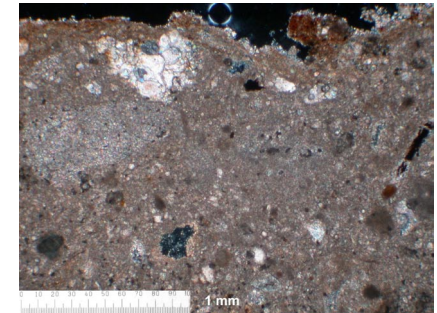
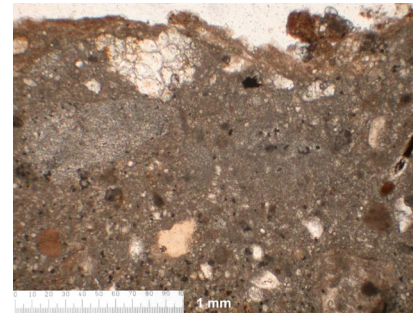
La32b. Floor. Late Preclassic. Rhombohedral calcite and quartz. Left: PPL. Right: XP. Scale bar: 1 mm.



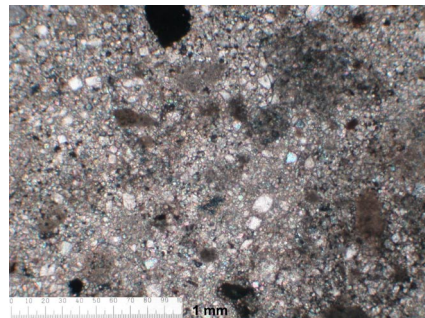
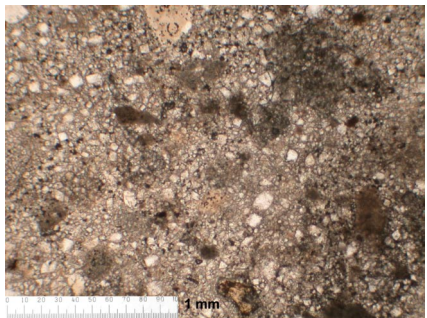
La46. Floor. Late Preclassic/ Early Classic. Crystalline limestone and aggregates of micritic calcite. Left: PPL. Right: 1 mm. Scale bar: 1 mm.



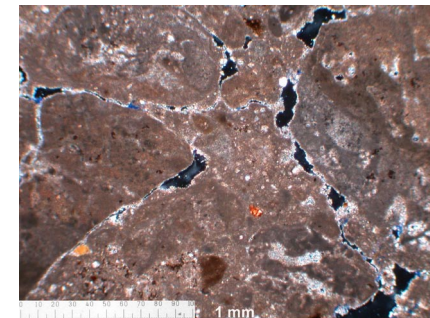
La47. Tamped floor underlying a burnt lime floor. Late Preclassic/
Early Classic. Chaotic texture of micritic calcite. Compacted sascab?
Left: PPL. Right: Xp. Scale bar: 1 mm.



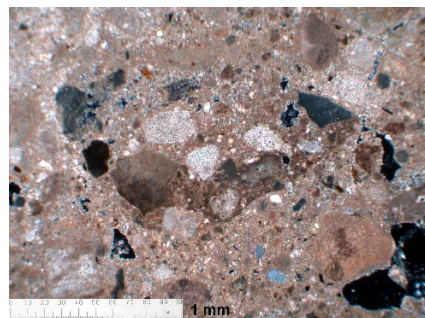
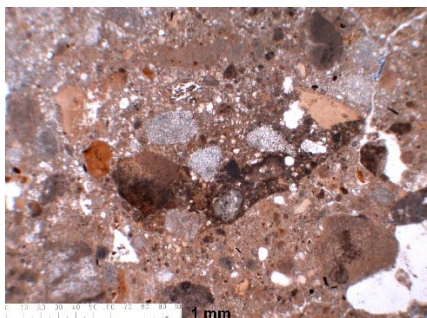
La45. Floor. Early Classic. Aggregates of crystalline and micritic
calcite, and isotropic phases. Floor. Early Classic. Left: 1 mm. Right:
1 mm.



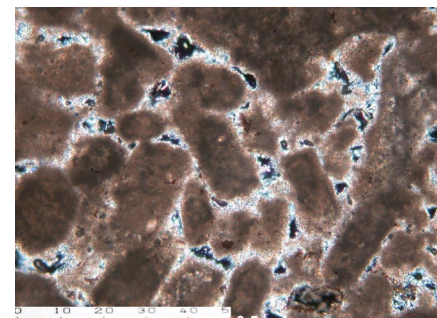
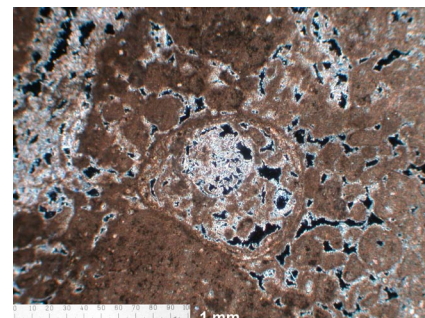
La48. Sculpture. Early Classic. Calcareous aggregates, isotropic phases
and rhombohedral calcite crystals. Left: PPL. Right: XP. Scale bar: 1 mm.



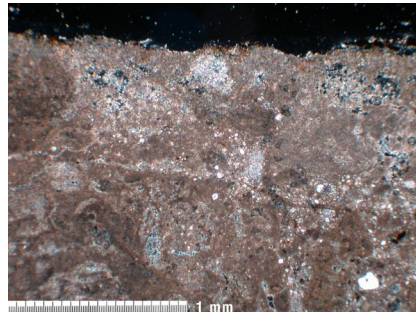
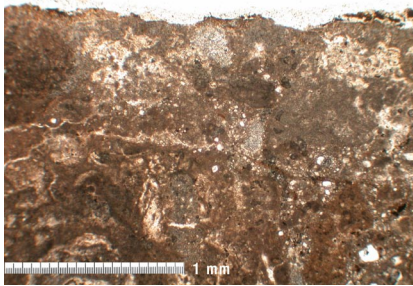
La4 Floor. Late Classic. Subrounded and subangular
aggregates of micritic calcite. XPL. Scale bar: 1mm.



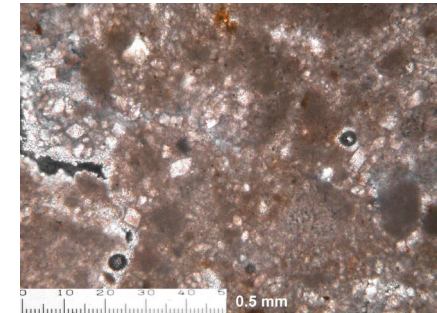
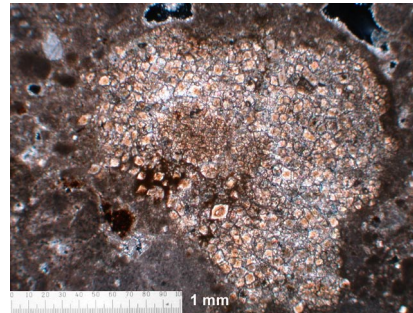
La6. Floor. Late Classic. Fragment of earlier plaster
recycled as aggregate. Left: PPL. Right: XPL. Scale
bar: 1 mm.



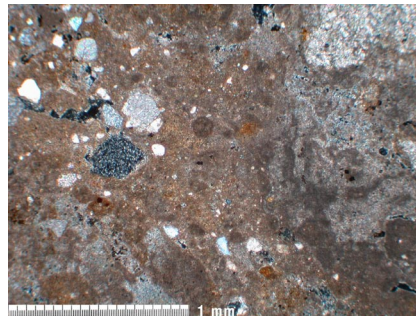
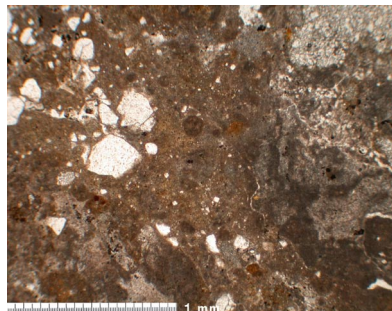
La13. Floor. Late Classic. Fragment of pelloidal limestone.
Left: XPL. Scale bar: 1 mm. Right: XPL. Scale bar: 0.5



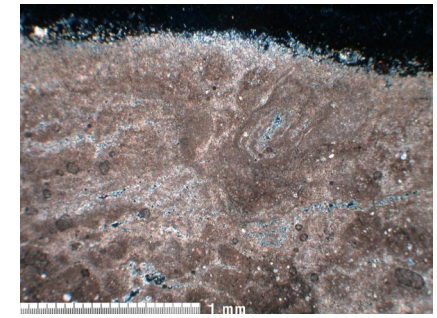
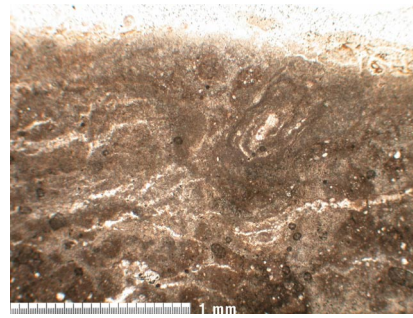
La14. Floor. Late Classic? Micritic cement with rhombohedral calcite crystals. Left: PPL. Right: XP. Scale bar: 1 mm.



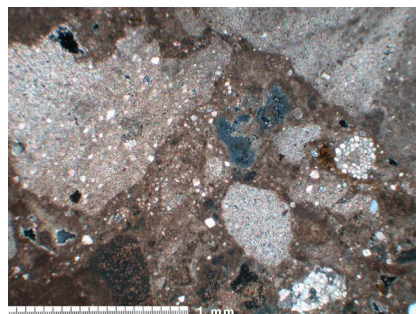
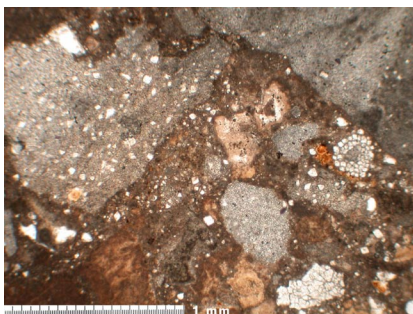
La 16. Floor. Late Classic? Left: Rhombohedral crystals, likely dolomite. XPL. Scale bar: 1 mm. Right: Micritic matrix with rhombohedral crystals of calcite. XPL. Scale bar: 1mm.



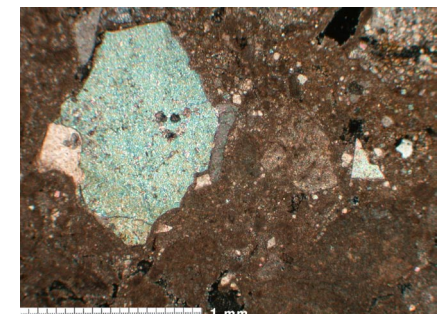
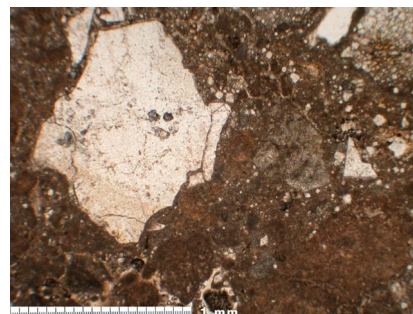
La17. Floor. Late Classic. Micritic calcite cement, iron oxides and aggregates of crystalline calcite. Left: PPL. Right: XP. Scale bar: 1 mm.



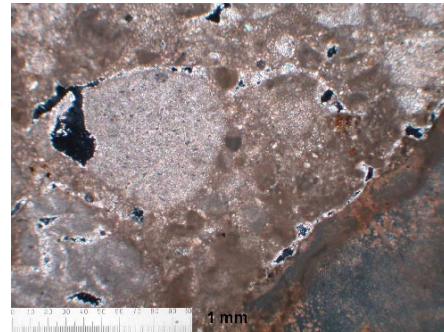
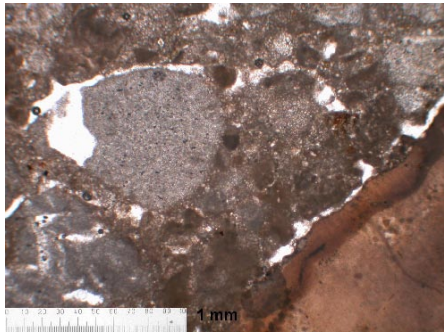
La35. Floor. Late Classic. Micritic cement with no visible aggregates. Crack parallel to the surface. Compacted sascab? Left: PPL. Right: XPL. Scale bar: 1 mm.



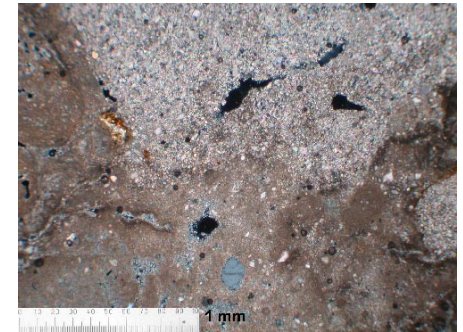
La9. Late/Terminal Classic or later. Aggregates of crystalline limestone and visible lime lumps. Left: PPL. Right: XP. Scale bar: 1 mm



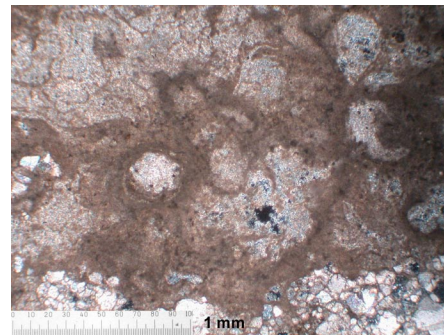
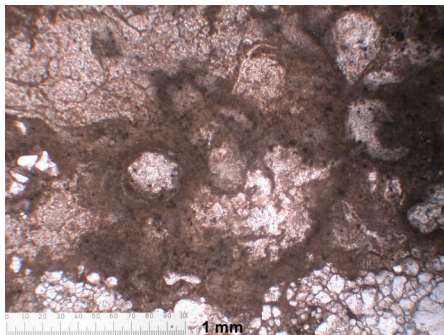
La10. Late/ Terminal Classic or later. Large fragments of crystalline calcite and crystals of rhombohedral calcite in the matrix. Left: PPL. Right: Xp. Scale bar: 1 mm.



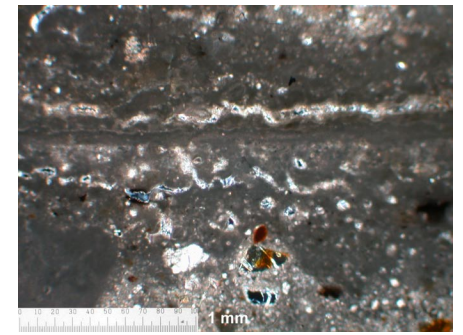
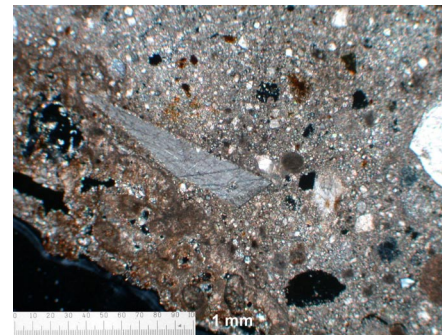
La 12. Floor. Terminal Classic/ Early Postclassic. Crystalline calcite employed as aggregates and visible lime lumps. Left: PPL. Right: XPL. Scale bar: 1 mm.



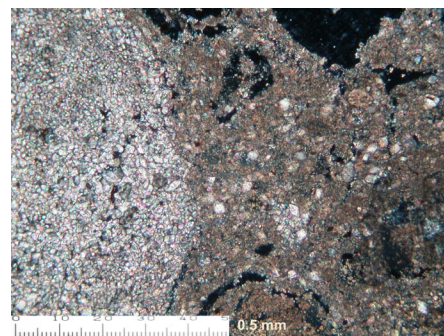
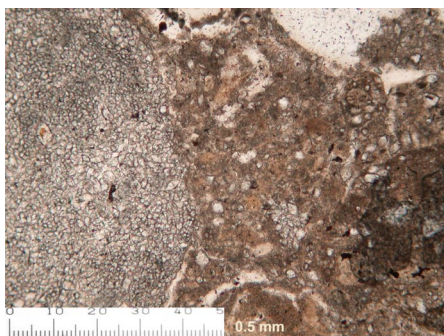
La 11. Floor. Terminal Classic/ Early Postclassic. Aggregate of crystalline calcite. XPL. Scale bar: 1mm.



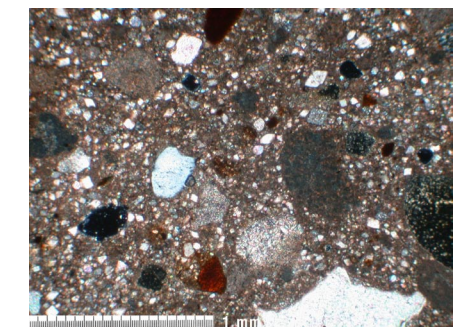
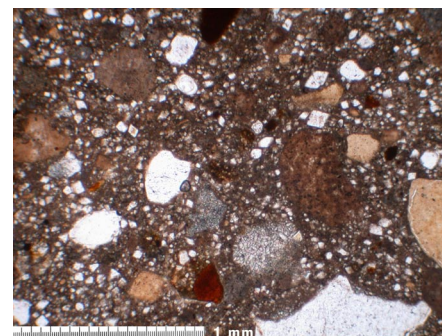
La2. Floor. Early/Middle Postclassic. Micritic cement with recrystallized minerals (compacted sascab?) Left: PPL, Right: XPL. Scale bar: 1mm.



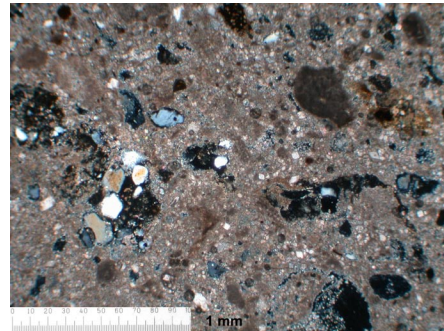
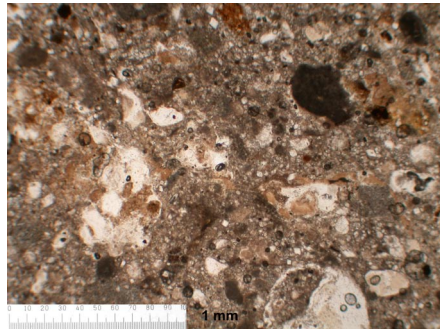
La22, Wall render. Late Postclassic. Left: Angular fragment of crystalline calcite and clay pellets. XPL, scale bar: 1mm. Right: Interface between two layers. Slightly hydraulic matrix. XPL. Scale bar: 1 mm.



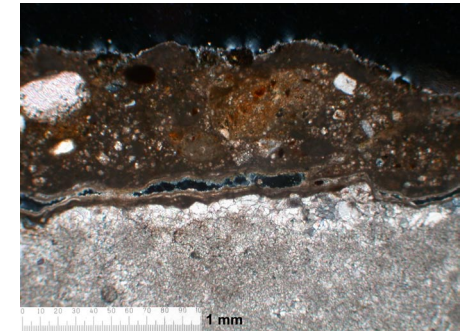
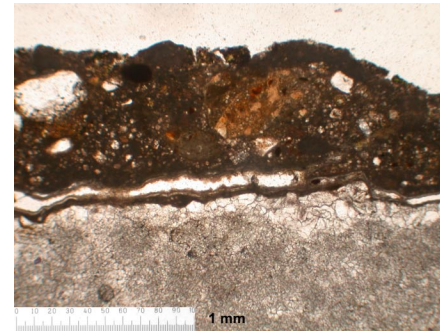
La36a. Wall render? Late Postclassic/ Early Spanish Colonial. Isotropic phases and large fragment of crystalline limestone. Left: PPL. Right: XP. Scale bar:



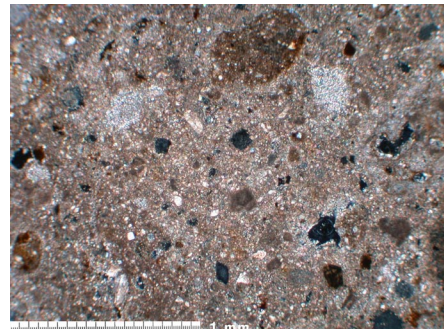
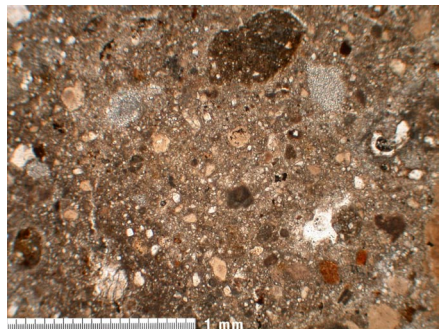
La36b. Wall render? Late Postclassic/ Early Spanish Colonial. Angular isotropic phases, iron oxides, crystalline calcite and quartz. Left: PPL. Right: XP. Scale bar: 1 mm.



La49. Floor. Late Postclassic. Quartz in isotropic phases (devitrified glass). Left: PPL. Right: XP. Scale bar: 1 mm.



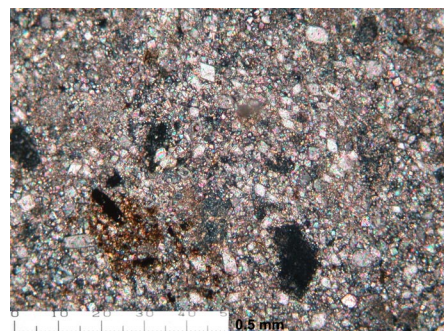
La50. Floor. Late Postclassic. Aggregates of crystalline calcite and clayey aggregates in slightly hydraulic matrix. Plaster laid over a crystalline limestone. Left: PPL. Right: XP. Scale bar: 1 mm.



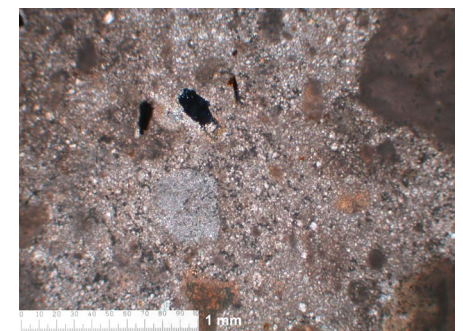
La19. Floor. Early Spanish Colonial. Rounded aggregates of micritic and crystalline calcite, iron oxides and numerous isotropic phases. Left: PPL. Right: XP. Scale bar: 1 mm.



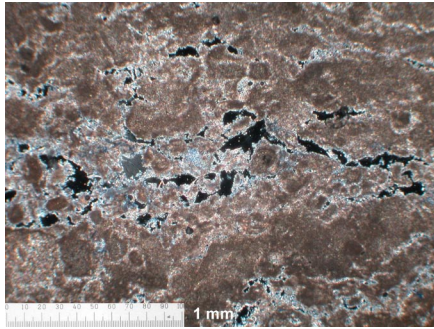
La20. Joining mortar. Early Spanish Colonial. Visible isotropic phases (likely silica gel). Left: PPL. Right: XP. Scale bar: 1 mm.



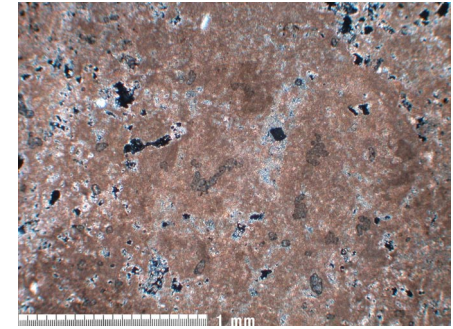
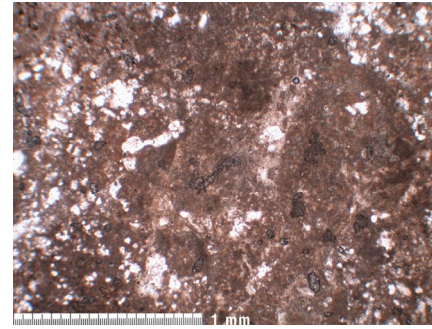
La21. Wall render. Early Spanish Colonial. Rhombohedral calcite, isotropic phases and clay pellets. Left: PPL. Right: XP. Scale bar: 0.5



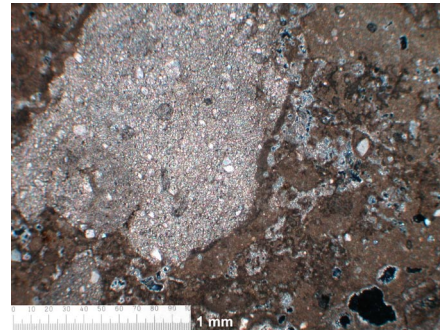
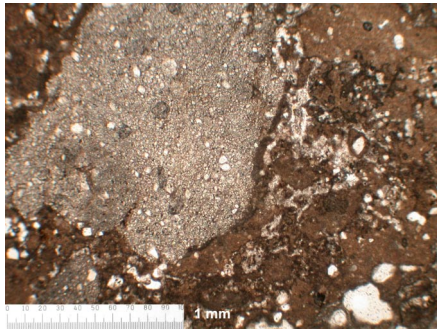
La40. Wall render. Early Spanish Colonial. Calcareous aggregates and orange partially isotropic phases (devitrified glass?). Left: PPL. Right: XP. Scale bar: 1 mm.



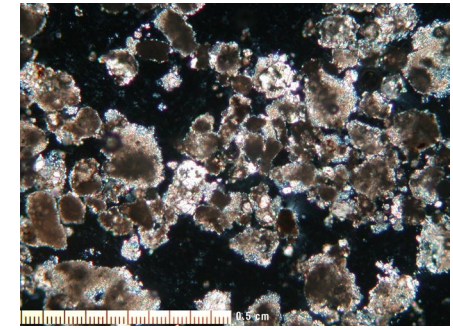
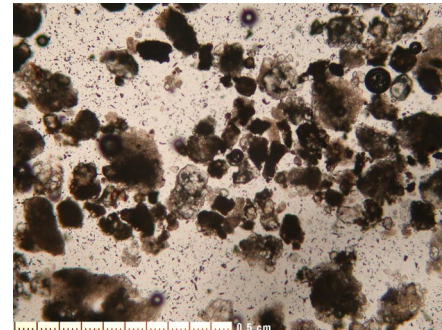
La 23. Limestone. Pelmicrite. XPL. Scale bar: 1 mm.



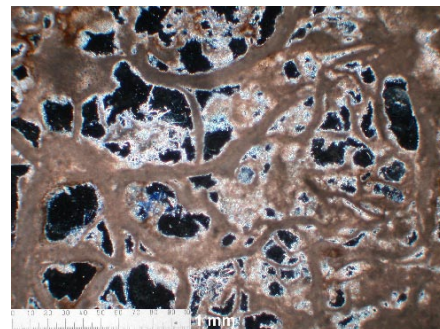
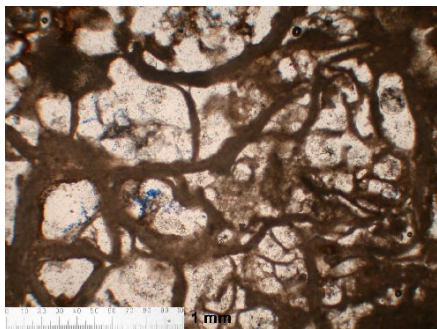
La27. Micritic limestone. Left: PPL. Right: XP. Scale bar: 1 mm.



La39. Limestone inclusion of crystalline calcite and rhombohedral calcite crystals in micritic matrix. Limestone from Late Postclassic building. Left: PPL. Right: XP. Scale bar: 1 mm.



La Sascab. Subrounded sediments of micritic and crystalline calcite. Left: PPL. Right: XP. Scale bar: 0.5 mm.



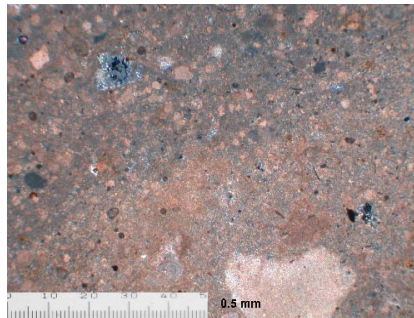
LaSascab (gravel-size sediment). Walls of micritic calcite with acicular phases. 40x. Left: PPL. Right: XPL.

Fabric Groups

Samples were classified in fabric groups, based on mineralogic and micromorphological characteristics, as observed by petrography.

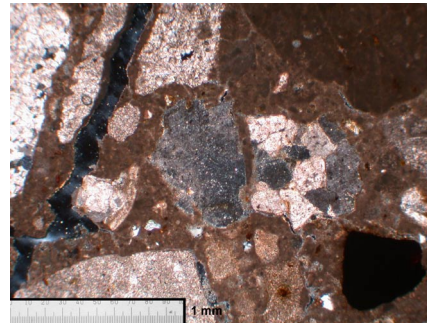
Palenque

Group 1: Characterised by aggregates of micritic calcite, in occasions with moderate hydraulic matrix. Absence of quartz. Samples in this group include: Pa1, Pa2a, Pa75, Pa77.



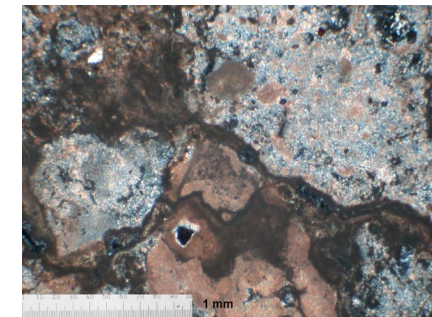
Pa77. Aggregates of micritic calcite in hydraulic matrix. Scale bar: 0.5mm. XPL.

Group 2: Characterised by aggregates of micritic and polycrystalline calcite, in occasions with moderate hydraulic matrix. Absence of quartz. Samples in this group include: Pa2b, Pa4, Pa28, Pa43, Pa28, Pa44, Pa59, Pa24, Pa23.



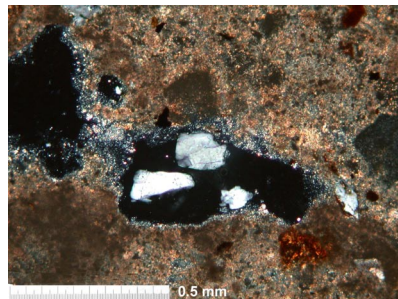
Pa28. Aggregates of micritic and polycrystalline calcite and sparite. Scale bar: 1mm. XPL.

Group 3: Characterised by aggregates composed of a silicon-rich cement and hydraulic reactions around them. Occasional presence of devitrified glass. Absence of quartz. Samples in this group include: Pa62, Pa59, Pa60, Pa61, Pa62, Pa66, Pa67, Pa70, Pa71.



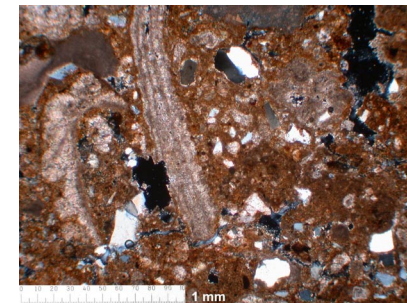
Pa62. Silicon-rich cement and hydraulic reactions. Scale bar: 1mm. XPL.

Group 4: Characterised by inclusions of glass, shocked quartz and hydraulic reactions. Occasional presence of alkali and plagioclase feldspars and muscovite micas. Samples in this group include: Pa4, Pa12, Pa18, Pa19, Pa22, Pa27, Pa28, Pa43, lower layer of Pa49, lower layer of Pa50, Pa52, Pa63, Pa72, Pa78.



Pa22. Quartz in isotropic material. Scale bar: 0.5 mm. XPL.

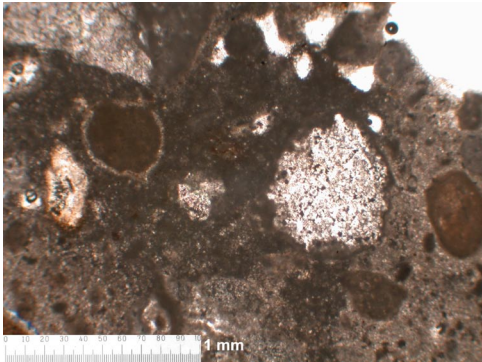
Group 5: Characterised by a clayey matrix and the abundant presence of quartz. Many shrinkage cracks in matrix. Inclusions of iron oxides. Occasional use of shell as aggregates. Rounded sediments of volcanic rocks. Exemplified by sample Pa44, upper layer of Pa49, upper layer of Pa50, Pa53, Pa56, Pa86, Pa87, Pa88.



Pa56. Quartz and shells in a clayey matrix. Scale bar: 1mm. XPL.

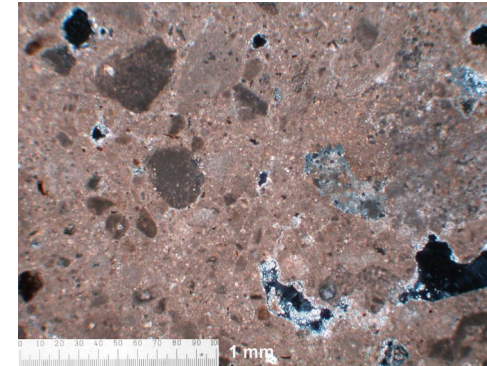
Calakmul

Group 1. Characterised by localised hydraulic reactions, large acicular phases, micritic and crystalline calcite employed as aggregate, isotropic materials and occasional presence of devitrified glass: Ca5, Ca7, Ca8, Ca10, Ca11, Ca14, Ca6, Ca16, upper layer of Ca18.



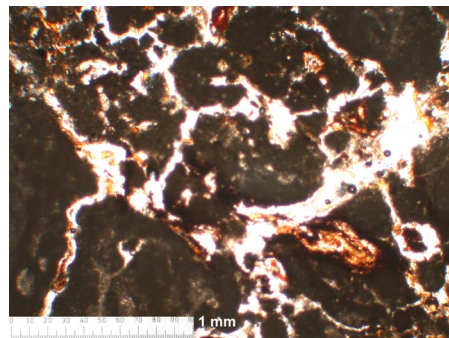
Ca5. Localised hydraulic reactions, aggregates of micritic and crystalline calcite, likely devitrified glass. PPL. Scale bar: 1 mm.

Group 2. Characterised by non-hydraulic matrix and the predominance of subrounded aggregates of micritic calcite. Occasional presence of acicular phases, polycrystalline quartz and isotropic materials. Samples Ca9, Ca14, Ca15, lower layer of Ca18, Ca19, Ca21, Ca23, Ca24, Ca26, Ca30, Ca31.

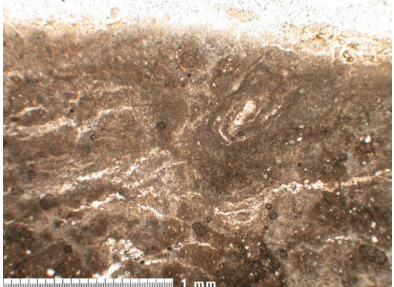
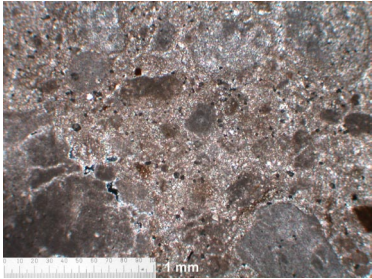
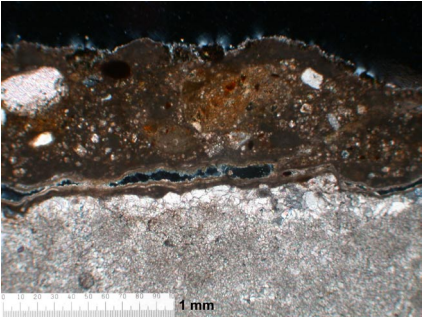
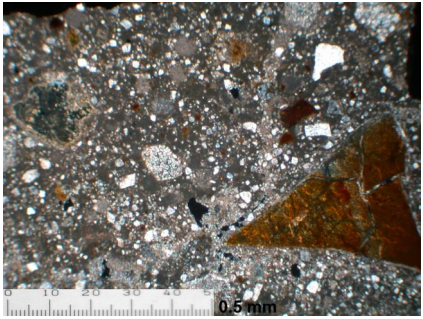


Ca15. Non hydraulic matrix with rounded aggregates of micritic calcite.

Group 3. Characterised by clayey matrices, presence of iron oxides, multiple cracks in the matrix, plant roots and the occasional presence of quartz. Samples Ca1, Ca3, Ca4, Ca13, Ca22, Ca33 and Ca34



Ca3. Clayey matrix with shrinkage cracks and plant roots.

| Lamanai | |
|---|--|
| <p>Group 1. Characterised by clay-size calcareous sediments (micritic calcite). The sediments are compacted and often show a parallel structure to the surface of the floor. Very likely compacted sascab (non-burnt lime). Samples La2, La3, La7, La13, La14, La 31, La34, La35, La46, La47.</p>  <p>La35. Compacted clay-size sediments of micritic calcite. PPL. Scale bar: 1 mm.</p> | <p>Group 2. Characterised by the use of subrounded aggregates of micritic calcite, although crystalline calcite may also be present. Occasional presence of quartz and isotropic phases. Samples La4, La6, La15, La16, La17, La24, La25, La28, La32b, La45, La48, La11?, La12?</p>  <p>La15. Subrounded aggregates of micritic calcite. XPL. Scale bar: 1 mm.</p> |
| <p>Group 3. Characterised by the prevalence in the use of large aggregates of crystalline calcite, although micritic calcite may also be present. Presence of clay pellets and quartz, sometimes within isotropic materials. Localised slight hydraulic reactions. Samples La9 and La10, La22, La36a, La49 and La50.</p>  <p>La50. Large aggregate of crystalline calcite (lower area), slight hydraulic reactions, quartz and clay pellets.</p> | <p>Group 4. Similar to group 3. Also characterised by the use of aggregates of crystalline calcite and the presence of quartz. Higher amounts of rounded clay pellets and numerous angular fragments of devitrified glass. Slight hydraulic reactions. Samples La19, La20, La21, La40, upper and medium layer of La36b.</p>  <p>Medium layer of La36b. Slight hydraulic matrix, isotropic phases (silica gel), quartz, iron oxides and angular fragment of devitrified glass. XPL. Scale bar: 0.5 mm.</p> |

A.3.1. EDS Analyses

| Sample | Chron | Area | Na ₂ O | MgCO ₃ | Al ₂ O ₃ | SiO ₂ | P ₂ O ₅ | SO ₃ | K ₂ O | CaCO ₃ | TiO ₂ | MnO | Fe ₂ O ₃ | Br | SrO | MoO ₃ | BaCO ₃ | NiO | Sum |
|--------|---------|----------------------------|-------------------|-------------------|--------------------------------|------------------|-------------------------------|-----------------|------------------|-------------------|------------------|-----|--------------------------------|-----|-----|------------------|-------------------|-----|-----|
| Pa49 | Otulum | Matrix | 0.2 | 37.9 | 0.3 | 3.4 | 0.0 | 4.4 | 0.0 | 53.8 | 0.0 | 0.0 | 0.0 | 0.0 | 0.0 | 0.0 | 0.0 | 0.0 | 100 |
| Pa49 | Otulum | Aggregate | 0.0 | 5.8 | 0.6 | 1.5 | 0.4 | 9.0 | 0.0 | 82.7 | 0.0 | 0.0 | 0.0 | 0.0 | 0.0 | 0.0 | 0.0 | 0.0 | 100 |
| Pa49 | Otulum | Matrix | 0.0 | 28.4 | 0.7 | 2.0 | 0.0 | 0.0 | 0.2 | 68.7 | 0.0 | 0.0 | 0.0 | 0.0 | 0.0 | 0.0 | 0.0 | 0.0 | 100 |
| Pa49 | Otulum | Aggregate | 0.3 | 51.3 | 2.3 | 6.1 | 0.5 | 1.4 | 0.0 | 38.1 | 0.0 | 0.0 | 0.0 | 0.0 | 0.0 | 0.0 | 0.0 | 0.0 | 100 |
| Pa75 | Kam Bal | Limewash | 0.0 | 47.8 | 0.7 | 2.2 | 0.0 | 0.0 | 0.0 | 49.4 | 0.0 | 0.0 | 0.0 | 0.0 | 0.0 | 0.0 | 0.0 | 0.0 | 100 |
| Pa75 | Kam Bal | Limewash | 0.0 | 41.1 | 0.0 | 3.8 | 0.0 | 0.0 | 0.0 | 54.3 | 0.0 | 0.0 | 0.8 | 0.0 | 0.0 | 0.0 | 0.0 | 0.0 | 100 |
| Pa75 | Kam Bal | Aggregate | 1.1 | 0.0 | 0.0 | 7.9 | 0.0 | 88.8 | 0.0 | 2.2 | 0.0 | 0.0 | 0.0 | 0.0 | 0.0 | 0.0 | 0.0 | 0.0 | 100 |
| Pa75 | Kam Bal | Limewash | 0.5 | 55.1 | 0.0 | 0.9 | 0.0 | 0.0 | 0.0 | 43.5 | 0.0 | 0.0 | 0.0 | 0.0 | 0.0 | 0.0 | 0.0 | 0.0 | 100 |
| Pa75 | Kam Bal | Limewash | 0.0 | 51.8 | 0.4 | 1.3 | 0.0 | 9.6 | 0.0 | 36.9 | 0.0 | 0.0 | 0.0 | 0.0 | 0.0 | 0.0 | 0.0 | 0.0 | 100 |
| Pa1 | Kuk Bal | Clast cement (meteoritic?) | 0.0 | 3.2 | 0.0 | 8.2 | 0.0 | 87.3 | 0.0 | 1.3 | 0.0 | 0.0 | 0.0 | 0.0 | 0.0 | 0.0 | 0.0 | 0.0 | 100 |
| Pa1 | Kuk Bal | Shocked quartz in clast | 0.0 | 0.0 | 0.0 | 100.0 | 0.0 | 0.0 | 0.0 | 0.0 | 0.0 | 0.0 | 0.0 | 0.0 | 0.0 | 0.0 | 0.0 | 0.0 | 100 |
| Pa1 | Kuk Bal | Aggregate | 0.0 | 0.0 | 0.0 | 0.4 | 0.0 | 99.4 | 0.0 | 0.0 | 0.0 | 0.0 | 0.0 | 0.2 | 0.0 | 0.0 | 0.0 | 0.0 | 100 |
| Pa1 | Kuk Bal | Matrix | 0.0 | 47.2 | 0.5 | 2.4 | 0.0 | 0.0 | 0.0 | 49.9 | 0.0 | 0.0 | 0.0 | 0.0 | 0.0 | 0.0 | 0.0 | 0.0 | 100 |
| Pa1 | Kuk Bal | Limewash | 0.3 | 53.7 | 1.3 | 5.7 | 0.5 | 4.8 | 0.0 | 33.7 | 0.0 | 0.0 | 0.0 | 0.0 | 0.0 | 0.0 | 0.0 | 0.0 | 100 |
| Pa1 | Kuk Bal | Limewash | 0.5 | 39.8 | 0.0 | 1.2 | 0.0 | 3.4 | 0.0 | 54.7 | 0.0 | 0.0 | 0.4 | 0.0 | 0.0 | 0.0 | 0.0 | 0.0 | 100 |
| Pa1 | Kuk Bal | Secondary mineral | 0.0 | 94.3 | 0.0 | 1.9 | 0.0 | 0.0 | 0.0 | 2.7 | 0.0 | 0.0 | 0.0 | 0.0 | 0.0 | 1.1 | 0.0 | 0.0 | 100 |
| Pa1 | Kuk Bal | Aggregate | 0.0 | 26.0 | 0.7 | 3.1 | 0.0 | 0.4 | 0.0 | 69.8 | 0.0 | 0.0 | 0.0 | 0.0 | 0.0 | 0.0 | 0.0 | 0.0 | 100 |
| Pa1 | Kuk Bal | Matrix | 0.0 | 21.8 | 0.6 | 0.9 | 0.0 | 41.1 | 0.0 | 35.6 | 0.0 | 0.0 | 0.0 | 0.0 | 0.0 | 0.0 | 0.0 | 0.0 | 100 |
| Pa1 | Kuk Bal | Aggregate | 0.0 | 33.4 | 4.8 | 1.3 | 8.4 | 0.0 | 0.0 | 51.6 | 0.5 | 0.0 | 0.0 | 0.0 | 0.0 | 0.0 | 0.0 | 0.0 | 100 |
| Pa24 | Kam Bal | Secondary mineral | 0.0 | 97.8 | 0.0 | 0.0 | 0.3 | 0.6 | 0.3 | 1.0 | 0.0 | 0.0 | 0.0 | 0.0 | 0.0 | 0.0 | 0.0 | 0.0 | 100 |
| Pa24 | Kam Bal | Limewash | 0.6 | 36.0 | 0.0 | 1.4 | 0.3 | 0.0 | 0.0 | 61.7 | 0.0 | 0.0 | 0.0 | 0.0 | 0.0 | 0.0 | 0.0 | 0.0 | 100 |
| Pa24 | Kam Bal | Aggregate | 0.1 | 46.1 | 4.0 | 6.4 | 0.0 | 18.5 | 0.0 | 24.1 | 0.0 | 0.0 | 0.7 | 0.0 | 0.0 | 0.0 | 0.0 | 0.0 | 100 |
| Pa24 | Kam Bal | Aggregate | 0.0 | 7.3 | 0.4 | 1.7 | 0.0 | 0.6 | 0.0 | 89.8 | 0.2 | 0.0 | 0.0 | 0.0 | 0.0 | 0.0 | 0.0 | 0.0 | 100 |
| Pa24 | Kam Bal | Aggregate2 | 0.2 | 25.9 | 5.0 | 0.7 | 0.3 | 0.0 | 0.0 | 67.7 | 0.2 | 0.0 | 0.0 | 0.0 | 0.0 | 0.0 | 0.0 | 0.0 | 100 |
| Pa2a | Kuk Bal | Aggregate | 0.0 | 10.0 | 0.6 | 2.6 | 0.0 | 21.0 | 0.1 | 65.4 | 0.0 | 0.1 | 0.2 | 0.0 | 0.0 | 0.0 | 0.0 | 0.0 | 100 |
| Pa2a | Kuk Bal | Matrix | 0.1 | 11.1 | 0.6 | 3.2 | 0.0 | 11.7 | 0.0 | 72.4 | 0.0 | 0.0 | 0.3 | 0.0 | 0.0 | 0.0 | 0.4 | 0.2 | 100 |
| Pa2a | Kuk Bal | Matrix | 0.0 | 9.2 | 0.5 | 4.6 | 0.2 | 14.6 | 0.0 | 70.1 | 0.0 | 0.0 | 0.3 | 0.2 | 0.0 | 0.0 | 0.0 | 0.2 | 100 |
| Pa2a | Kuk Bal | Aggregate | 0.1 | 5.2 | 0.0 | 0.9 | 0.2 | 4.6 | 0.1 | 88.3 | 0.1 | 0.0 | 0.0 | 0.4 | 0.1 | 0.0 | 0.0 | 0.0 | 100 |
| Pa53 | Balunte | Matrix | 0.0 | 8.8 | 5.6 | 10.9 | 0.0 | 0.0 | 0.4 | 72.7 | 0.0 | 0.0 | 1.6 | 0.0 | 0.0 | 0.0 | 0.0 | 0.0 | 100 |
| Pa53 | Balunte | Aggregate | 0.6 | 0.0 | 0.6 | 6.8 | 1.1 | 89.5 | 0.0 | 1.0 | 0.4 | 0.0 | 0.0 | 0.0 | 0.0 | 0.0 | 0.0 | 0.0 | 100 |
| Pa53 | Balunte | Matrix | 0.0 | 12.7 | 2.1 | 10.8 | 0.0 | 20.6 | 0.2 | 53.2 | 0.0 | 0.0 | 0.0 | 0.0 | 0.0 | 0.0 | 0.0 | 0.4 | 100 |
| Pa53 | Balunte | Aggregate | 0.0 | 0.0 | 0.0 | 100.0 | 0.0 | 0.0 | 0.0 | 0.0 | 0.0 | 0.0 | 0.0 | 0.0 | 0.0 | 0.0 | 0.0 | 0.0 | 100 |
| Pa53 | Balunte | Lime lump | 0.0 | 4.8 | 0.0 | 1.8 | 0.0 | 0.0 | 0.0 | 93.4 | 0.0 | 0.0 | 0.0 | 0.0 | 0.0 | 0.0 | 0.0 | 0.0 | 100 |
| Pa53 | Balunte | Matrix | 0.0 | 5.4 | 0.8 | 3.2 | 0.0 | 0.4 | 0.0 | 90.2 | 0.0 | 0.0 | 0.0 | 0.0 | 0.0 | 0.0 | 0.0 | 0.0 | 100 |
| Pa86 | Balunte | Matrix | 0.0 | 34.6 | 2.6 | 18.6 | 0.1 | 0.4 | 0.2 | 42.9 | 0.0 | 0.0 | 0.6 | 0.0 | 0.0 | 0.0 | 0.0 | 0.1 | 100 |
| Pa86 | Balunte | Aggregate | 0.0 | 1.2 | 0.7 | 0.0 | 0.3 | 0.0 | 0.0 | 97.8 | 0.0 | 0.0 | 0.0 | 0.0 | 0.0 | 0.0 | 0.0 | 0.0 | 100 |
| Pa86 | Balunte | Matrix | 0.0 | 31.3 | 3.7 | 24.3 | 0.4 | 0.3 | 0.3 | 37.9 | 0.0 | 0.0 | 1.5 | 0.0 | 0.0 | 0.0 | 0.0 | 0.3 | 100 |
| Pa86 | Balunte | Aggregate | 0.0 | 0.0 | 0.0 | 100.0 | 0.0 | 0.0 | 0.0 | 0.0 | 0.0 | 0.0 | 0.0 | 0.0 | 0.0 | 0.0 | 0.0 | 0.0 | 100 |

Chronology: Otulum: Otulum Phase (620/700 AD), **Kam Bal:** Kinich Kan Balam II (684-702 AD), **Kuk Bal:** K'inich Kuk Balam II (Aka Kuk) (764-799 AD), **Balunte:** Balunte Phase: (770-850 AD).
Values in blue indicate higher concentrations in comparison to the rest of the samples.

| Sample | Chron | Area | Na ₂ O | MgCO ₃ | Al ₂ O ₃ | SiO ₂ | P ₂ O ₅ | SO ₃ | K ₂ O | CaCO ₃ | TiO ₂ | MnO | Fe ₂ O ₃ | Br | SrO | MoO ₃ | BaCO ₃ | NiO | Sum |
|--------|---------------|-----------------|-------------------|-------------------|--------------------------------|------------------|-------------------------------|-----------------|------------------|-------------------|------------------|-----|--------------------------------|-----|-----|------------------|-------------------|-----|-----|
| Ca10 | M Prec | Matrix | 0.0 | 0.8 | 0.8 | 8.1 | 0.0 | 8.3 | 0.1 | 80.1 | 0.0 | 0.0 | 0.2 | 0.0 | 0.2 | 1.4 | 0.0 | 0.0 | 100 |
| Ca10 | M Prec | Matrix | 0.1 | 1.0 | 0.9 | 4.4 | 0.0 | 7.1 | 0.1 | 85.3 | 0.0 | 0.1 | 0.3 | 0.2 | 0.0 | 0.0 | 0.4 | 0.0 | 100 |
| Ca10 | M Prec | Aggregate | 0.0 | 0.3 | 0.2 | 10.0 | 0.0 | 0.6 | 0.1 | 87.4 | 0.1 | 0.0 | 0.1 | 0.0 | 0.0 | 0.0 | 1.1 | 0.1 | 100 |
| Ca10 | M Prec | Aggregate | 0.1 | 0.7 | 0.0 | 23.4 | 0.0 | 0.3 | 0.0 | 74.6 | 0.0 | 0.0 | 0.1 | 0.0 | 0.0 | 0.3 | 0.5 | 0.0 | 100 |
| Ca10 | M Prec | Bright spots | 0.2 | 0.3 | 0.0 | 1.2 | 0.0 | 11.6 | 0.1 | 56.5 | 0.0 | 0.0 | 0.0 | 0.0 | 0.6 | 0.0 | 29.3 | 0.1 | 100 |
| Ca6 | LM Prec | Cordierite? | 0.2 | 7.3 | 14.1 | 57.0 | 0.0 | 7.4 | 0.9 | 3.7 | 0.3 | 0.0 | 8.9 | 0.0 | 0.0 | 0.0 | 0.0 | 0.2 | 100 |
| Ca6 | LM Prec | Matrix | 0.2 | 1.9 | 2.2 | 9.7 | 0.0 | 0.5 | 0.1 | 83.4 | 0.0 | 0.2 | 1.7 | 0.0 | 0.0 | 0.0 | 0.0 | 0.0 | 100 |
| Ca6 | LM Prec | Matrix | 0.0 | 0.6 | 2.1 | 8.7 | 0.0 | 1.5 | 0.6 | 85.7 | 0.0 | 0.0 | 0.7 | 0.0 | 0.0 | 0.0 | 0.0 | 0.0 | 100 |
| Ca6 | LM Prec | Aggregate | 0.0 | 1.0 | 0.2 | 1.3 | 0.0 | 0.6 | 0.0 | 96.7 | 0.0 | 0.0 | 0.0 | 0.0 | 0.0 | 0.0 | 0.0 | 0.2 | 100 |
| Ca6 | LM Prec | Aggregate | 0.2 | 0.9 | 0.0 | 0.5 | 0.0 | 1.2 | 0.0 | 97.1 | 0.0 | 0.0 | 0.1 | 0.0 | 0.0 | 0.0 | 0.0 | 0.0 | 100 |
| Ca29 | L Prec | Crystal | 0.4 | 2.5 | 0.0 | 9.1 | 0.0 | 13.6 | 0.3 | 71.8 | 0.0 | 0.0 | 0.5 | 1.5 | 0.0 | 0.0 | 0.0 | 0.3 | 100 |
| Ca29 | L Prec | Matrix (resin?) | 0.0 | 0.0 | 0.0 | 0.0 | 0.0 | 54.4 | 0.4 | 45.6 | 0.0 | 0.0 | 0.0 | 0.0 | 0.0 | 0.0 | 0.0 | 0.0 | 100 |
| Ca29 | L Prec | Crystal | 0.0 | 4.5 | 1.5 | 9.7 | 0.0 | 0.3 | 0.0 | 83.0 | 0.0 | 0.0 | 1.0 | 0.0 | 0.0 | 0.0 | 0.0 | 0.0 | 100 |
| Ca13 | E Clas | Matrix | 0.0 | 1.2 | 0.3 | 1.7 | 0.5 | 1.1 | 0.0 | 94.9 | 0.0 | 0.3 | 0.0 | 0.0 | 0.0 | 0.0 | 0.0 | 0.0 | 100 |
| Ca13 | E Clas | Matrix | 0.0 | 3.6 | 9.9 | 47.9 | 0.3 | 0.3 | 0.8 | 34.1 | 0.0 | 0.0 | 3.0 | 0.0 | 0.0 | 0.0 | 0.0 | 0.0 | 100 |
| Ca13 | E Clas | Aggregate | 0.0 | 0.9 | 0.7 | 38.9 | 0.0 | 0.0 | 0.2 | 59.3 | 0.0 | 0.0 | 0.0 | 0.0 | 0.0 | 0.0 | 0.0 | 0.0 | 100 |
| Ca13 | E Clas | Aggregate | 0.0 | 1.3 | 0.3 | 17.3 | 0.0 | 0.4 | 0.1 | 80.6 | 0.0 | 0.0 | 0.0 | 0.0 | 0.0 | 0.0 | 0.0 | 0.0 | 100 |
| Ca36 | L Clas | Aggregate | 0.4 | 23.9 | 1.0 | 2.2 | 0.3 | 0.6 | 0.2 | 70.9 | 0.0 | 0.0 | 0.5 | 0.0 | 0.0 | 0.0 | 0.0 | 0.0 | 100 |
| Ca36 | L Clas | Aggregate | 0.0 | 0.4 | 0.8 | 2.2 | 0.0 | 0.3 | 0.0 | 96.1 | 0.2 | 0.0 | 0.0 | 0.0 | 0.0 | 0.0 | 0.0 | 0.0 | 100 |
| Ca36 | L Clas | Matrix | 0.0 | 1.1 | 0.0 | 3.6 | 0.6 | 0.4 | 0.4 | 92.5 | 0.0 | 0.0 | 0.0 | 1.4 | 0.0 | 0.0 | 0.0 | 0.0 | 100 |
| Ca18 | L Clas | Matrix | 0.0 | 0.6 | 0.4 | 2.2 | 0.0 | 6.0 | 0.1 | 90.5 | 0.0 | 0.0 | 0.2 | 0.0 | 0.0 | 0.0 | 0.0 | 0.0 | 100 |
| Ca18 | L Clas | Matrix | 0.0 | 0.4 | 0.1 | 0.5 | 0.0 | 0.3 | 0.0 | 98.4 | 0.0 | 0.0 | 0.3 | 0.0 | 0.0 | 0.0 | 0.0 | 0.0 | 100 |
| Ca18 | L Clas | Aggregate | 0.0 | 0.0 | 0.0 | 0.0 | 0.0 | 0.6 | 0.0 | 99.4 | 0.0 | 0.0 | 0.0 | 0.0 | 0.0 | 0.0 | 0.0 | 0.0 | 100 |
| Ca3 | T Clas | Amorp. plant | 0.0 | 0.0 | 0.0 | 100.0 | 0.0 | 0.0 | 0.0 | 0.0 | 0.0 | 0.0 | 0.0 | 0.0 | 0.0 | 0.0 | 0.0 | 0.0 | 100 |
| Ca3 | T Clas | Matrix | 0.3 | 1.0 | 0.2 | 3.5 | 0.0 | 3.7 | 0.0 | 91.3 | 0.0 | 0.0 | 0.0 | 0.0 | 0.0 | 0.0 | 0.0 | 0.0 | 100 |
| Ca3 | T Clas | Aggregate | 0.0 | 0.8 | 0.0 | 0.0 | 0.2 | 1.1 | 0.1 | 97.8 | 0.0 | 0.0 | 0.0 | 0.0 | 0.0 | 0.0 | 0.0 | 0.0 | 100 |
| Ca3 | T Clas | Matrix | 0.0 | 0.4 | 1.1 | 21.3 | 0.0 | 1.3 | 0.3 | 74.6 | 0.0 | 0.3 | 0.7 | 0.0 | 0.0 | 0.0 | 0.0 | 0.0 | 100 |
| Ca3 | T Clas | Aggregate | 0.0 | 1.4 | 0.0 | 0.5 | 0.0 | 0.1 | 0.0 | 97.5 | 0.0 | 0.0 | 0.0 | 0.0 | 0.0 | 0.0 | 0.0 | 0.5 | 100 |
| Ca33 | T Clas | Matrix (resin?) | 0.1 | 0.6 | 0.2 | 0.7 | 0.0 | 40.6 | 0.0 | 57.6 | 0.0 | 0.0 | 0.2 | 0.0 | 0.0 | 0.0 | 0.0 | 0.0 | 100 |
| Ca33 | T Clas | Matrix * | 0.0 | 0.7 | 0.0 | 15.7 | 0.2 | 2.6 | 0.1 | 79.1 | 0.0 | 0.0 | 0.0 | 0.0 | 0.0 | 0.0 | 1.6 | 0.0 | 100 |
| Ca33 | T Clas | Bright spots | 0.0 | 0.0 | 0.1 | 0.1 | 0.0 | 27.7 | 0.0 | 3.2 | 0.0 | 0.0 | 0.0 | 0.0 | 2.1 | 0.0 | 66.8 | 0.0 | 100 |
| Ca33 | T Clas | Aggregate * | 0.0 | 0.9 | 0.0 | 37.9 | 0.0 | 1.6 | 0.1 | 58.9 | 0.3 | 0.0 | 0.2 | 0.0 | 0.0 | 0.0 | 0.0 | 0.1 | 100 |
| Ca33 | T Clas | Aggregate * | 0.0 | 1.8 | 1.3 | 42.5 | 0.0 | 0.6 | 0.1 | 52.9 | 0.0 | 0.1 | 0.7 | 0.0 | 0.0 | 0.0 | 0.0 | 0.0 | 100 |
| CaSas | Modern (geol) | Bulk | 0.2 | 0.6 | 0.0 | 0.0 | 0.0 | 0.8 | 0.0 | 97.2 | 0.5 | 0.0 | 0.7 | 0.0 | 0.0 | 0.0 | 0.0 | 0.0 | 100 |
| Ca Sas | Modern (geol) | Bulk | 0.3 | 13.2 | 8.9 | 48.3 | 0.0 | 14.3 | 0.9 | 8.5 | 0.2 | 0.0 | 5.3 | 0.0 | 0.0 | 0.0 | 0.0 | 0.0 | 100 |
| Ca Sas | Modern (geol) | Bulk | 0.6 | 2.5 | 1.7 | 13.3 | 0.0 | 9.1 | 0.0 | 72.4 | 0.0 | 0.0 | 0.3 | 0.0 | 0.0 | 0.0 | 0.0 | 0.0 | 100 |

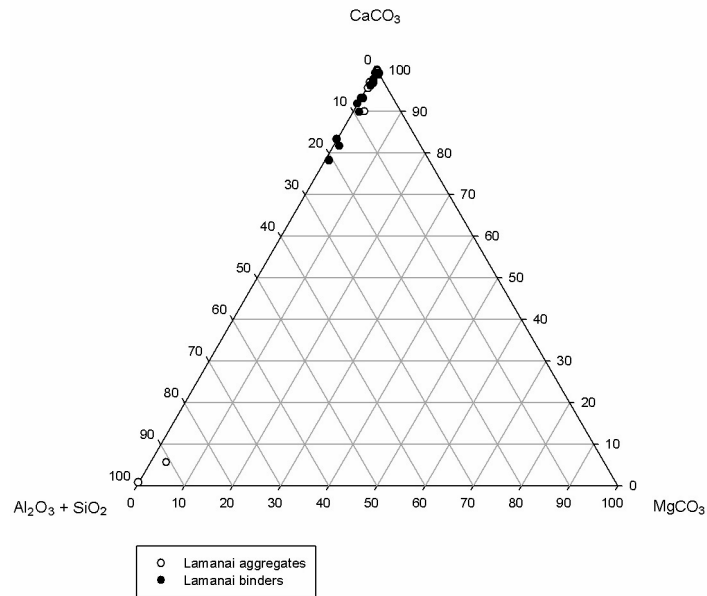
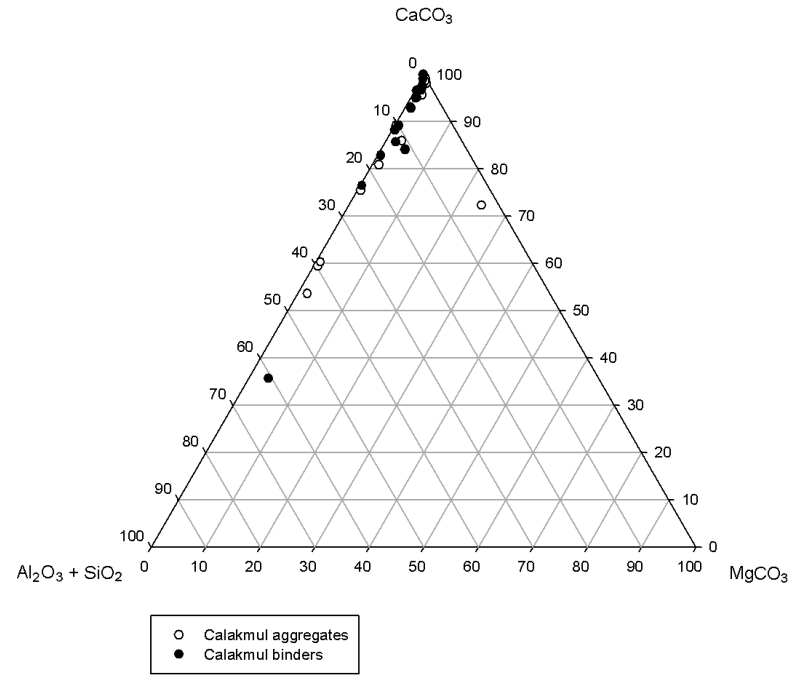
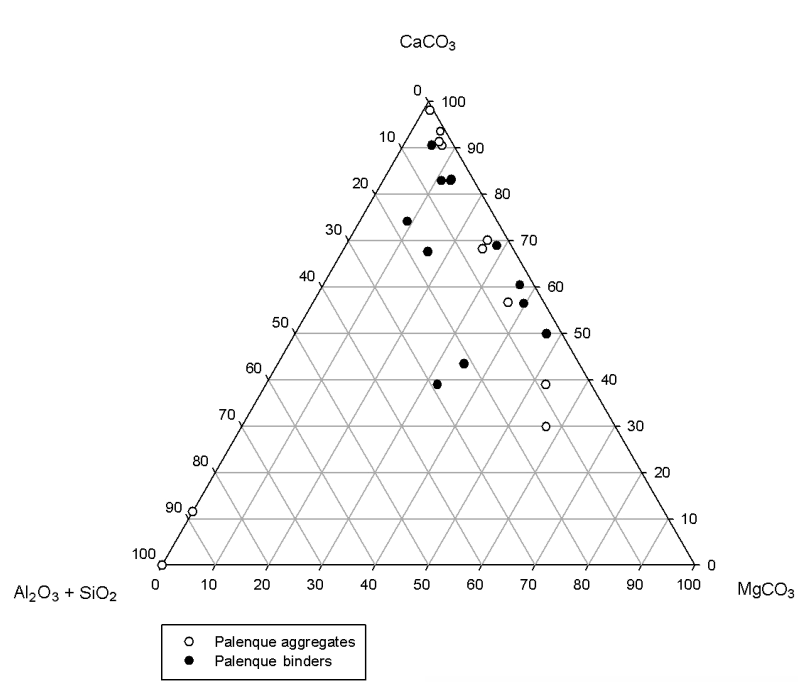
Chronology: M Prec: Middle Preclassic, LM Prec: Late Middle Preclassic, L Prec: Late Preclassic, E Clas: Early Classic, L Clas: Late Classic, T Clas: Terminal Classic, Modern (geo): modern geological materials.
Values in blue indicate higher concentrations in comparison to the rest of the samples. *Distinction between aggregate and matrix is not clear in sample Ca33.

| Sample | Chron | Area | Na ₂ O | MgCO ₃ | Al ₂ O ₃ | SiO ₂ | P ₂ O ₅ | SO ₃ | K ₂ O | CaCO ₃ | TiO ₂ | MnO | Fe ₂ O ₃ | Br | SrO | MoO ₃ | BaCO ₃ | NiO | Sum |
|--------|-------------|------------------------|-------------------|-------------------|--------------------------------|------------------|-------------------------------|-----------------|------------------|-------------------|------------------|-----|--------------------------------|-----|-----|------------------|-------------------|-----|-----|
| La 30 | L Prec | Bulk | 0.8 | 0.7 | 0.0 | 1.5 | 0.0 | 0.4 | 0.0 | 96.6 | 0.0 | 0.0 | 0.0 | 0.0 | 0.0 | 0.0 | 0.0 | 0.0 | 0.8 |
| La 30 | L Prec | Aggregate | 0.0 | 0.3 | 0.4 | 0.5 | 0.0 | 0.3 | 0.0 | 98.5 | 0.0 | 0.0 | 0.0 | 0.0 | 0.0 | 0.0 | 0.0 | 0.0 | 0.0 |
| La 30 | L Prec | Matrix | 0.3 | 0.5 | 1.0 | 2.2 | 0.0 | 0.4 | 0.0 | 95.3 | 0.0 | 0.0 | 0.3 | 0.0 | 0.0 | 0.0 | 0.0 | 0.0 | 0.3 |
| La 31 | L Prec | Aggregate | 0.0 | 0.8 | 1.1 | 1.3 | 0.0 | 0.0 | 0.0 | 96.8 | 0.0 | 0.0 | 0.0 | 0.0 | 0.0 | 0.0 | 0.0 | 0.0 | 0.0 |
| La 31 | L Prec | Matrix | 0.0 | 0.9 | 0.1 | 0.1 | 0.0 | 0.0 | 0.0 | 98.9 | 0.0 | 0.0 | 0.0 | 0.0 | 0.0 | 0.0 | 0.0 | 0.0 | 0.0 |
| La 31 | L Prec | Bulk | 0.0 | 0.9 | 1.6 | 2.3 | 0.0 | 0.0 | 0.0 | 94.8 | 0.0 | 0.0 | 0.3 | 0.0 | 0.0 | 0.0 | 0.0 | 0.0 | 0.0 |
| La 17 | L Clas | Bulk | 0.0 | 0.7 | 0.2 | 0.0 | 0.0 | 0.2 | 0.0 | 98.9 | 0.0 | 0.0 | 0.0 | 0.0 | 0.0 | 0.0 | 0.0 | 0.0 | 0.0 |
| La 17 | L Clas | Aggregate | 0.0 | 0.0 | 0.0 | 0.0 | 0.0 | 0.0 | 0.0 | 100.0 | 0.0 | 0.0 | 0.0 | 0.0 | 0.0 | 0.0 | 0.0 | 0.0 | 0.0 |
| La 35 | L Clas | Aggregate | 0.0 | 0.5 | 1.5 | 1.7 | 0.0 | 0.0 | 0.0 | 96.3 | 0.0 | 0.0 | 0.0 | 0.0 | 0.0 | 0.0 | 0.0 | 0.0 | 0.0 |
| La 35 | L Clas | Matrix | 0.0 | 0.7 | 1.0 | 1.2 | 0.0 | 0.0 | 0.0 | 97.1 | 0.0 | 0.0 | 0.0 | 0.0 | 0.0 | 0.0 | 0.0 | 0.0 | 0.0 |
| La 9 | LClas/TClas | Matrix | 0.0 | 0.0 | 0.0 | 0.7 | 0.0 | 0.4 | 0.0 | 98.9 | 0.0 | 0.0 | 0.0 | 0.0 | 0.0 | 0.0 | 0.0 | 0.0 | 0.0 |
| La 9 | LClas/TClas | Bulk | 0.0 | 0.0 | 0.5 | 0.6 | 0.0 | 0.0 | 0.0 | 98.9 | 0.0 | 0.0 | 0.0 | 0.0 | 0.0 | 0.0 | 0.0 | 0.0 | 0.0 |
| La 9 | LClas/TClas | Aggregate | 0.0 | 0.0 | 0.0 | 0.6 | 0.0 | 0.0 | 0.0 | 99.4 | 0.0 | 0.0 | 0.0 | 0.0 | 0.0 | 0.0 | 0.0 | 0.0 | 0.0 |
| La 10 | LClas/TClas | Aggregate | 0.0 | 0.0 | 0.0 | 99.0 | 0.0 | 0.2 | 0.0 | 0.8 | 0.0 | 0.0 | 0.0 | 0.0 | 0.0 | 0.0 | 0.0 | 0.0 | 0.0 |
| La 10 | LClas/TClas | Bulk | 0.0 | 1.0 | 2.0 | 1.9 | 0.0 | 0.4 | 0.0 | 94.7 | 0.0 | 0.0 | 0.0 | 0.0 | 0.0 | 0.0 | 0.0 | 0.0 | 0.0 |
| La 10 | LClas/TClas | Matrix | 0.0 | 0.0 | 9.3 | 7.3 | 0.0 | 0.0 | 0.0 | 82.3 | 0.0 | 0.0 | 1.1 | 0.0 | 0.0 | 0.0 | 0.0 | 0.0 | 0.0 |
| La 22 | L Post | Matrix upper layer | 0.0 | 0.5 | 3.7 | 2.6 | 0.0 | 0.0 | 0.0 | 93.2 | 0.0 | 0.0 | 0.0 | 0.0 | 0.0 | 0.0 | 0.0 | 0.0 | 0.0 |
| La 22 | L Post | Aggregate upper layer | 0.0 | 0.3 | 2.4 | 1.6 | 0.0 | 0.0 | 0.0 | 95.7 | 0.0 | 0.0 | 0.0 | 0.0 | 0.0 | 0.0 | 0.0 | 0.0 | 0.0 |
| La 22 | L Post | Limewash | 0.0 | 1.1 | 0.6 | 0.6 | 0.0 | 0.5 | 0.0 | 97.2 | 0.0 | 0.0 | 0.0 | 0.0 | 0.0 | 0.0 | 0.0 | 0.0 | 0.0 |
| La 22 | L Post | Aggregate lower layer | 0.0 | 0.0 | 1.5 | 1.5 | 0.0 | 0.0 | 0.0 | 96.8 | 0.0 | 0.0 | 0.2 | 0.0 | 0.0 | 0.0 | 0.0 | 0.0 | 0.0 |
| La 22 | L Post | Matrix lower layer | 0.0 | 1.3 | 7.7 | 9.1 | 0.0 | 0.0 | 0.2 | 80.7 | 0.0 | 0.0 | 1.0 | 0.0 | 0.0 | 0.0 | 0.0 | 0.0 | 0.0 |
| La36b | LPost? | Aggregate upper layer | 0.0 | 2.4 | 4.4 | 3.2 | 0.0 | 0.0 | 0.0 | 90.0 | 0.0 | 0.0 | 0.0 | 0.0 | 0.0 | 0.0 | 0.0 | 0.0 | 0.0 |
| La36b | LPost? | Matrix supper layer | 0.0 | 0.4 | 0.9 | 1.0 | 0.0 | 0.0 | 0.0 | 97.7 | 0.0 | 0.0 | 0.0 | 0.0 | 0.0 | 0.0 | 0.0 | 0.0 | 0.0 |
| La36b | LPost? | Aggregate medium layer | 0.0 | 0.0 | 0.0 | 0.0 | 0.0 | 0.0 | 0.2 | 99.8 | 0.0 | 0.0 | 0.0 | 0.0 | 0.0 | 0.0 | 0.0 | 0.0 | 0.0 |
| La36b | LPost? | Matrix medium layer | 0.0 | 0.9 | 9.5 | 10.9 | 0.0 | 0.6 | 0.4 | 76.6 | 0.0 | 0.0 | 1.1 | 0.0 | 0.0 | 0.0 | 0.0 | 0.0 | 0.0 |
| La36b | LPost? | Aggreg. lower layer | 0.0 | 0.3 | 0.0 | 0.0 | 0.0 | 0.0 | 0.0 | 99.7 | 0.0 | 0.0 | 0.0 | 0.0 | 0.0 | 0.0 | 0.0 | 0.0 | 0.0 |
| La 19 | S Col | Matrix | 0.0 | 0.0 | 3.4 | 3.2 | 0.0 | 0.3 | 0.0 | 92.4 | 0.0 | 0.0 | 0.6 | 0.0 | 0.0 | 0.0 | 0.0 | 0.0 | 0.0 |
| La21 | S Col | Aggregate | 0.2 | 0.8 | 0.0 | 0.0 | 0.0 | 0.2 | 0.0 | 98.8 | 0.0 | 0.0 | 0.0 | 0.0 | 0.0 | 0.0 | 0.0 | 0.0 | 0.2 |
| La21 | S Col | Matrix | 0.0 | 0.0 | 2.5 | 5.5 | 0.6 | 0.0 | 0.9 | 90.5 | 0.0 | 0.0 | 0.0 | 0.0 | 0.0 | 0.0 | 0.0 | 0.0 | 0.0 |
| La21 | S Col | Bulk | 0.0 | 0.7 | 2.5 | 7.3 | 0.0 | 0.6 | 0.5 | 87.8 | 0.0 | 0.0 | 0.5 | 0.0 | 0.0 | 0.0 | 0.0 | 0.0 | 0.0 |
| La20 | S Col | Aggregate | 0.6 | 3.1 | 29.1 | 53.7 | 0.0 | 0.0 | 3.4 | 5.2 | 0.8 | 0.0 | 4.1 | 0.0 | 0.0 | 0.0 | 0.0 | 0.0 | 0.6 |
| La20 | S Col | Matrix | 0.0 | 1.3 | 3.7 | 4.9 | 0.0 | 0.0 | 0.6 | 88.9 | 0.0 | 0.0 | 0.6 | 0.0 | 0.0 | 0.0 | 0.0 | 0.0 | 0.0 |
| La20 | S Col | Bulk | 0.0 | 1.0 | 6.3 | 8.0 | 0.0 | 0.0 | 0.6 | 82.6 | 0.0 | 0.0 | 1.5 | 0.0 | 0.0 | 0.0 | 0.0 | 0.0 | 0.0 |
| Sasc 1 | Modern(geo) | Bulk | 0.0 | 0.0 | 0.3 | 0.2 | 0.4 | 0.0 | 0.0 | 99.1 | 0.0 | 0.0 | 0.0 | 0.0 | 0.0 | 0.0 | 0.0 | 0.0 | 0.0 |
| Sasc2 | Modern(geo) | Bulk | 0.0 | 0.0 | 0.0 | 0.9 | 0.0 | 0.0 | 0.0 | 99.1 | 0.0 | 0.0 | 0.0 | 0.0 | 0.0 | 0.0 | 0.0 | 0.0 | 0.0 |
| Sasc 3 | Modern(geo) | Bulk | 0.0 | 0.7 | 1.6 | 17.8 | 0.0 | 0.0 | 0.0 | 79.9 | 0.0 | 0.0 | 0.0 | 0.0 | 0.0 | 0.0 | 0.0 | 0.0 | 0.0 |

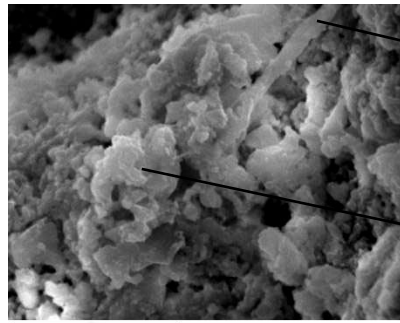
Chronology: **L Prec**: Late Preclassic, **E Clas**: Early Classic, **L Clas**: Late Classic, **T Clas**: Terminal Classic, **L Post**: Late Postclassic, **S Col**: Spanish Colonial. **Modern (geo)**: modern geol. materials.

Values in blue indicate higher concentrations in comparison to the rest of the samples.

Ternary Diagrams. EDS data.



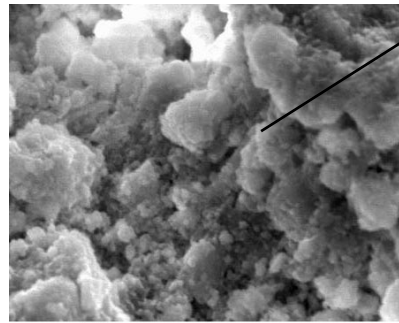
Palenque



Acicular
 CaCO₃ 61.7%
 MgCO₃ 24.5%
 SiO₂ 13.1%
 SO₃ 0.7%

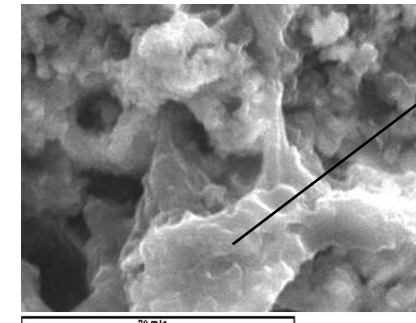
Agglomeration of
 anhedral crystals
 CaCO₃ 52.9%
 MgCO₃ 44.8%
 SiO₂ 2.3%

Pa18. Scale bar: 15 microns



Agglomeration of
 anhedral crystals
 CaCO₃ 61.6 %
 MgCO₃ 29.2%
 SiO₂ 6.2%
 Al₂O₃ 2.1%
 SO₃ 1.0%

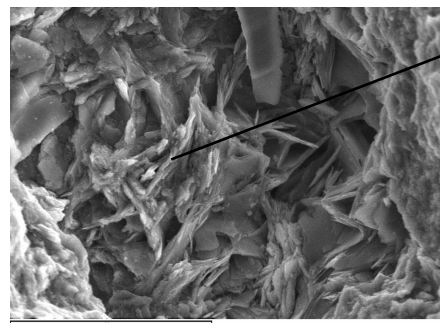
Pa18. Scale bar: 15 microns



Agglomeration
 of platy crystals
 in limewash
 CaCO₃ * 89.9%
 MgCO₃ 8.1%
 SiO₂ 1.5%

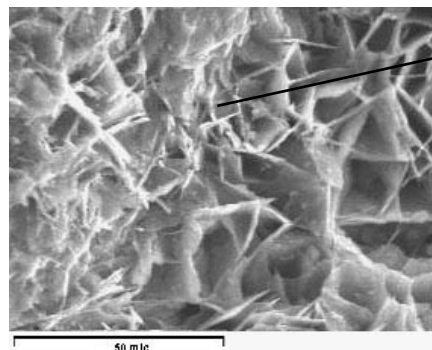
*Likely present
 as Ca(OH)₂.

Pa62. Scale bar: 20 microns



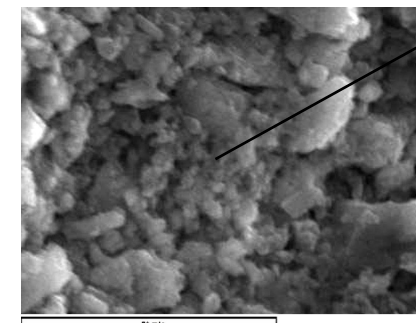
Tabular crystals
 MgCO₃ 100%

Pa68. Scale bar: 60 microns.



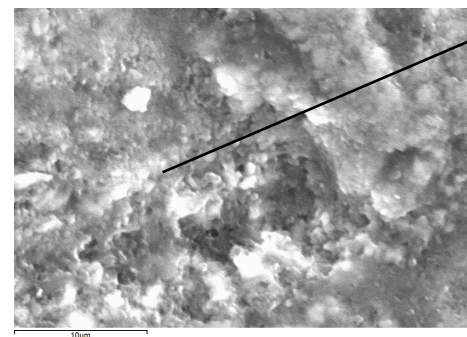
Tabular crystals
 MgCO₃ 100%

Pa70. Scale bar: 50 microns



Anhedral
 crystals
 MgCO₃ 86.5%
 CaCO₃ 7.4%
 SiO₂ 3.9%
 Al₂O₃ 2.1%

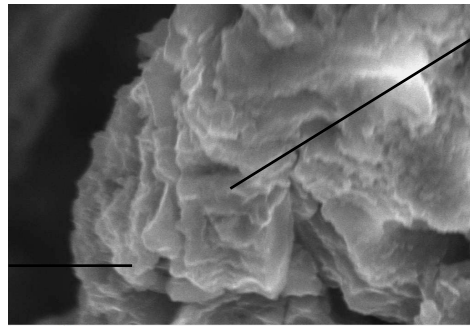
Pa70. Scale bar: 20 microns.



Anhedral crystals
 in limewash
 CaCO₃ 82.7%
 MgCO₃ 7.7%
 SiO₂ 3.9%

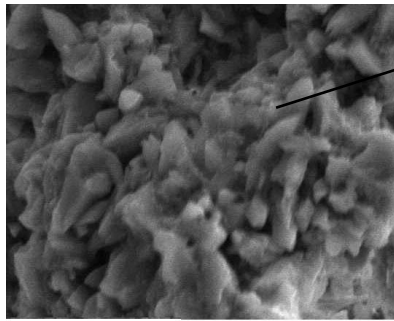
Pa71. Scale bar: 10 microns

Calakmul



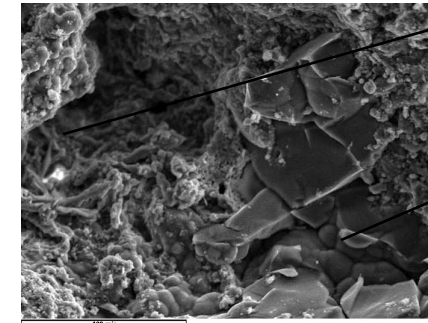
Foliated crystals
 SiO_2 71.1%
 CaCO_3 13.1%
 Al_2O_3 15.8%

Ca5. Scale bar: 10 microns



Hexagonal prisms
 CaCO_3 95.5%
 MgCO_3 3.4%
 SiO_2 2.2%

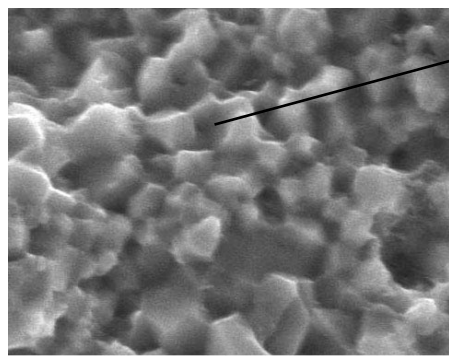
Ca5. Scale bar: 20 microns.



Acicular crystals
 CaCO_3 92.6%
 SiO_2 6.9%
 SO_3 0.5%

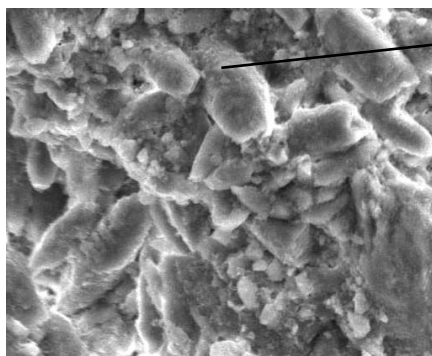
Globular/
 amorphous
 SiO_2 98.8%
 CaCO_3 1.2%

Ca6. Scale bar: 100 microns.



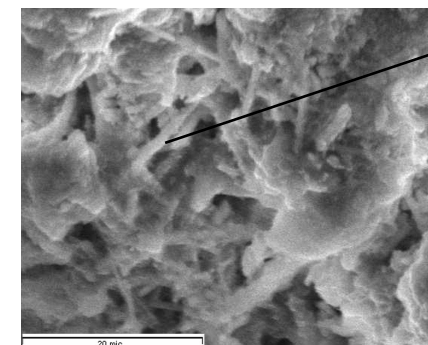
Equant prisms
 CaCO_3 98.9%
 SiO_2 1.1%

Ca8. Scale bar: 15 microns

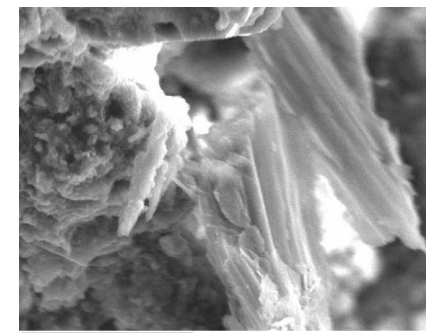


Ascidians?
 CaCO_3 90.1%
 MgCO_3 5.4%
 SiO_2 4.6%

Ca8. Scale bar: 30 microns

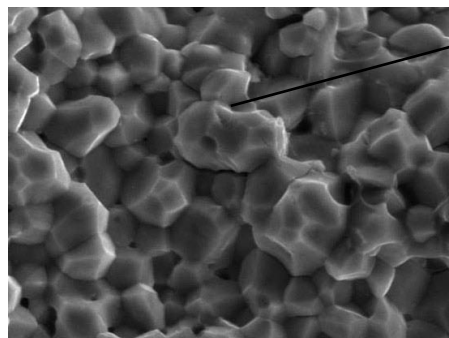


Acicular
 CaCO_3 88.6%
 SiO_2 11.2%



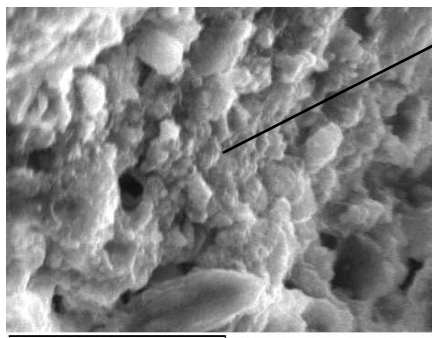
Bladed crystals
 CaCO_3 88.2
 SiO_2 9.2
 MgCO_3 1.8
 Al_2O_3 0.8

Ca15. Scale bar: 20 microns



Agglomerations of
 polyhedrons
 CaCO_3 100%

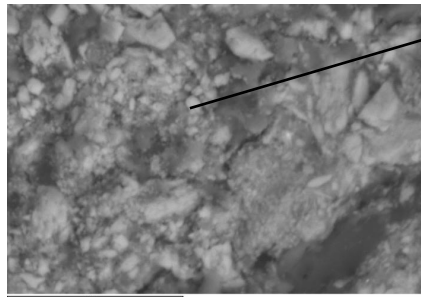
Ca14. Scale bar: 30 microns



Agglomeration of
 anhedral crystals
 CaCO_3 93.5%
 SiO_2 5.1%
 Al_2O_3 1.0%
 K_2O 0.4%

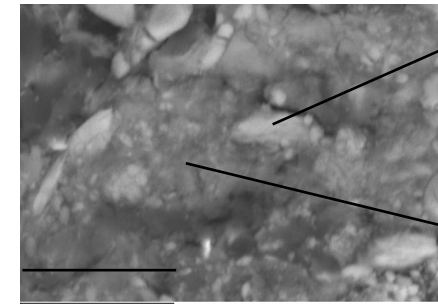
Ca15. Scale bar: 20 microns

Calakmul



Anhedral crystals
CaCO₃ 79.1%
SiO₂ 15.7 %
SO₃ 2.6 %
BaCO₃ 1.6%

Ca3. Scale bar: 20 microns.

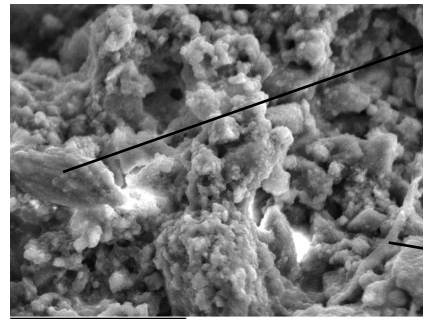


Anhedral crystal
CaCO₃ 97.8%
MgCO₃ 1.6%
SiO₂ 0.6%

Clay-size cement:
CaCO₃ 64.8%
SiO₂ 20.5%
MgCO₃ 6.6%
Al₂O₃ 4.1%

Ca4. Scale bar: 20 microns.

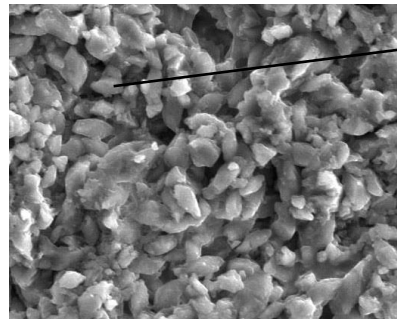
Lamanai



Prism with smaller crystals:
 CaCO_3 92.4%
 SiO_2 4.3%
 Al_2O_3 2.5%
 SO_3 0.8%

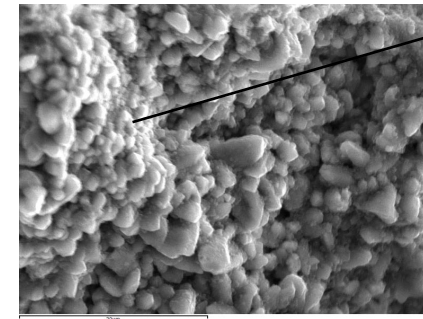
Fibrous:
 CaCO_3 69.4%
 SiO_2 19.2%
 Al_2O_3 8.1%

La4. Scale bar: 40 microns



Prismatic
 CaCO_3 99.7%
 SiO_2 0.3%

La9. Scale bar: 30 microns



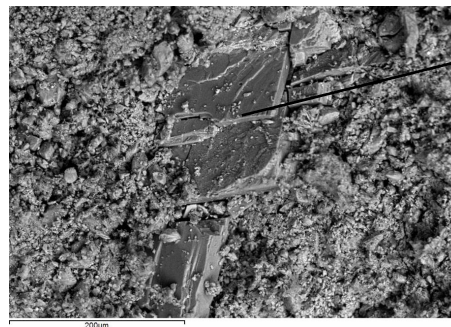
Prismatic
 CaCO_3 99.5%
 SiO_2 0.5%

La9. Scale bar: 30 microns



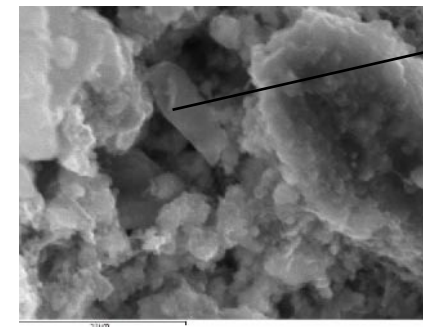
Rhombohedral
 CaCO_3 : 98.2
 SiO_2 1.1%
 Al_2O_3 0.7%

La10. Scale bar: 100 microns



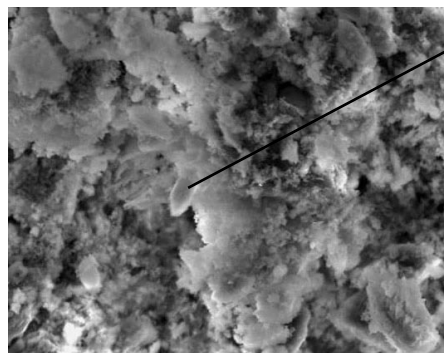
Foliated
 CaCO_3 100%

La10. Scale bar: 200 microns



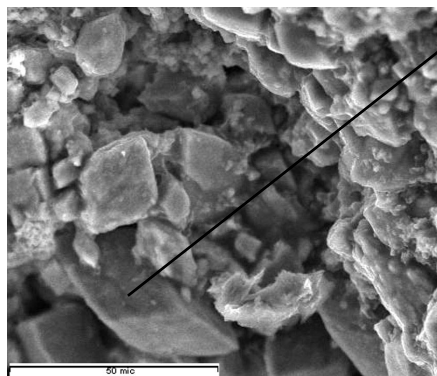
Elongated
 CaCO_3 87.5%
 SiO_2 7.9%
 Al_2O_3 2.8%

La19. Scale bar: 10 microns



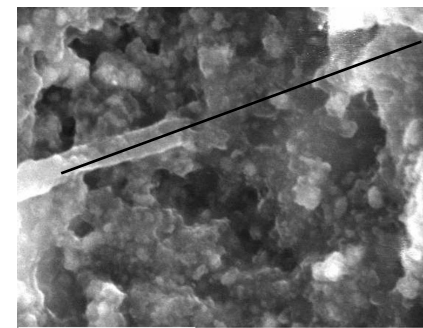
Elongated:
 CaCO_3 94.5%
 SiO_2 2.8%
 Al_2O_3 1.9%

La19. Scale bar: 30 microns



Large rhombohedrons cemented by masses of smaller crystals
 CaCO_3 100%

La21. Scale bar: 50 microns



Elongated
 CaCO_3 86.7%
 SiO_2 4.7%
 SO_3 2.9%
 MgCO_3 9.2%

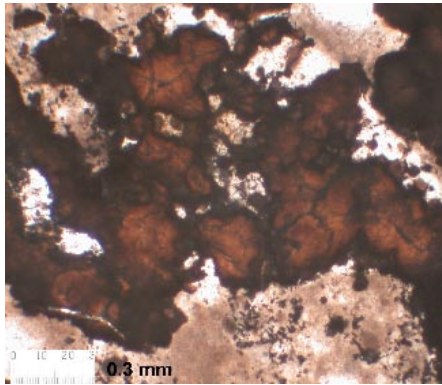
La28. Scale bar: 10 microns

Accuracy of the equipment. Comparison of certified values of Basalt Columbia River, BCR-2, and measurements of Jeol superprobe JXA-8600

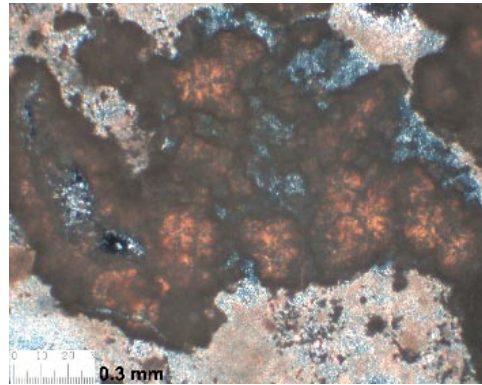
| | Na ₂ O | MgO | Al ₂ O ₃ | SiO ₂ | K ₂ O | CaO | TiO ₂ | FeO | |
|--------------------------|-------------------|-----|--------------------------------|------------------|------------------|------|------------------|------|-------|
| Certified values | 3.2 | 3.3 | 13.5 | 54.1 | 1.8 | 7.1 | 2.3 | 13.8 | 99.02 |
| Analysis with superprobe | 3 | 3.6 | 12.8 | 56.8 | 1.9 | 6.9 | 2.2 | 12.8 | 100 |
| s.d. | 0.2 | 0.1 | 0.2 | 0.1 | 0.2 | 0.1 | 0.2 | 0.3 | |
| δ absolute | -0.2 | 0.3 | -0.7 | 2.7 | 0.1 | -0.3 | -0.1 | -1 | |
| δ relative | -6.3 | 9.1 | -5.2 | 5 | 5.6 | -4.2 | -4.3 | -7.2 | |

Palenque

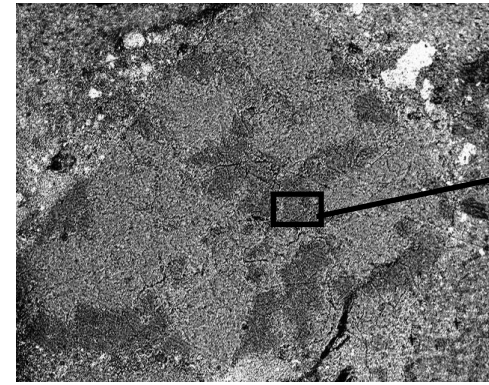
Pa 60. Floor. K'inich Kan Balam II (684-702)



PPL. Scale bar: 0.3 mm.



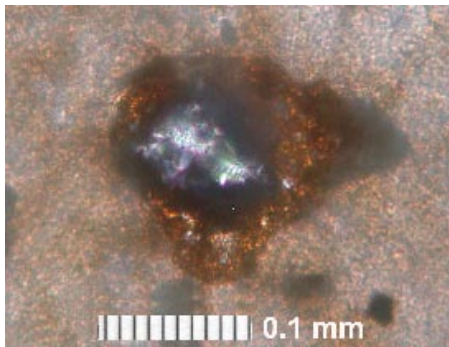
XPL. Scale bar: 0.3 mm.



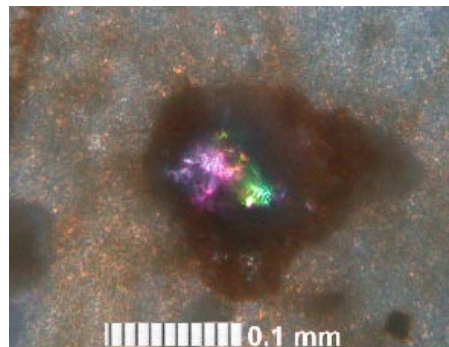
Orange blebs
MgCO₃ 85%
CaCO₃ 12%
SiO₂ 2%

BSE

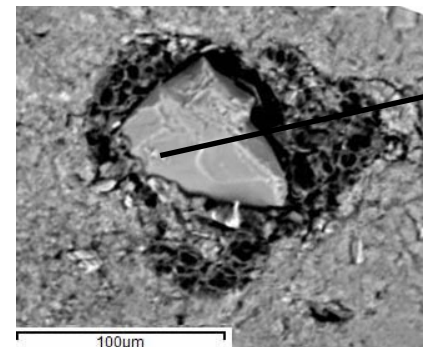
Pa66. Floor. K'inich Kan Balam II (684-702)



PPL. Scale bar: 0.1 mm.



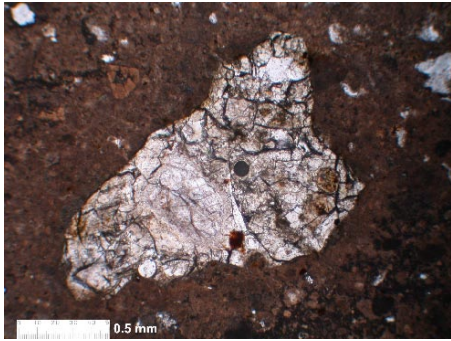
XPL. Scale bar: 0.1 mm.



Silicon carbide
C 35.1%
Si 64.9 %
(all elements measured without stoichiometry)

BSE

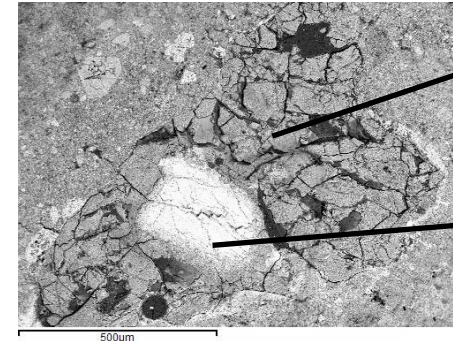
Pa27. Wall render. K'inich Kan Balam II



PPL. Scale bar: 0.5 mm.



XPL. Scale bar: 0.5 mm.

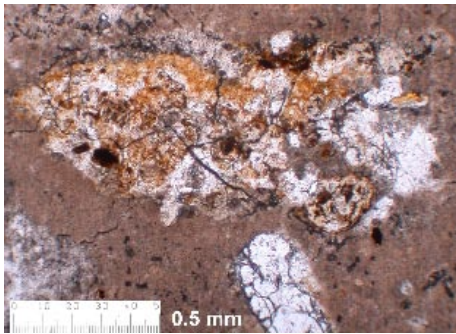


BSE

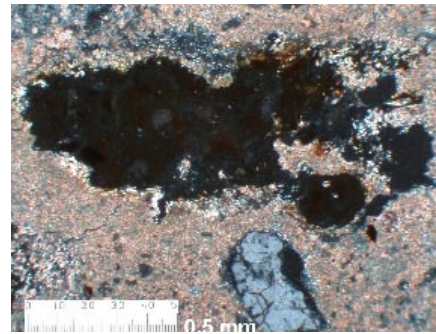
Glass Matrix
 MgCO_3 56%
 SiO_2 25%
 Al_2O_3 9%

K feldspar
 SiO_2 66%
 Al_2O_3 17%
 K_2O 17%

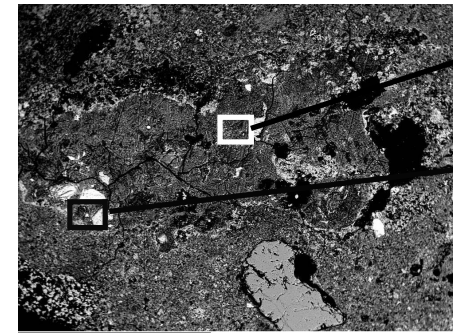
Pa18. Floor. Joy Chitam II or K'inich Kan Balam II



PPL. Scale bar: 0.5 mm.



XPL. Scale bar: 0.5 mm.

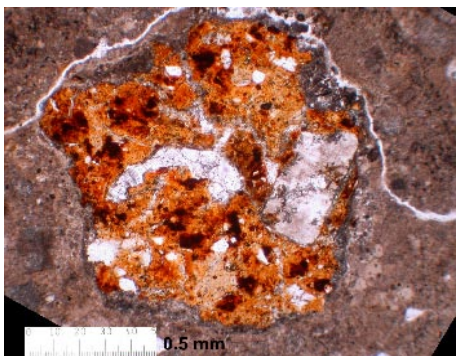


BSE

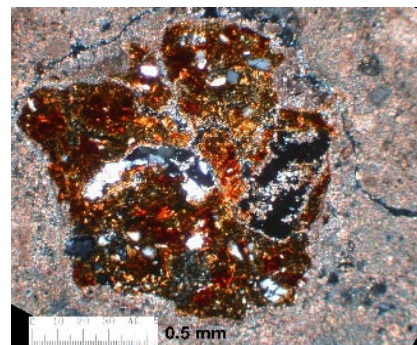
Glass Matrix
 MgCO_3 52%
 SiO_2 35%
 Al_2O_3 7%
 Fe_2O_3 5%

Opaque Mineral
 SiO_2 34%
 Fe_2O_3 14%
 MgCO_3 20%
 Al_2O_3 18%

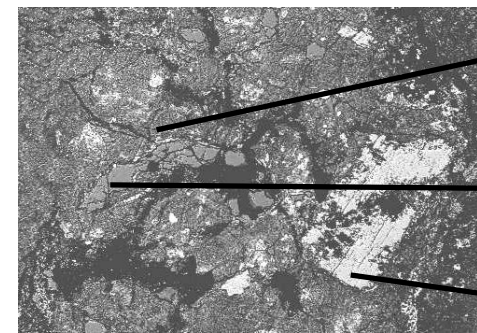
Pa18. Joy Chitam II or K'inich Kan Balam II



PPL. Scale bar: 0.5 mm.



XPL. Scale bar: 0.5 mm.



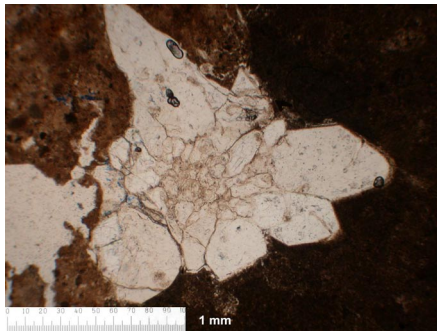
BSE

Devitrified glass
 MgCO_3 44%
 SiO_2 29%
 Al_2O_3 19%
 Fe_2O_3 5%

Quartz
 SiO_2 100%

K feldspar
 SiO_2 66%
 Al_2O_3 17%
 K_2O 15%

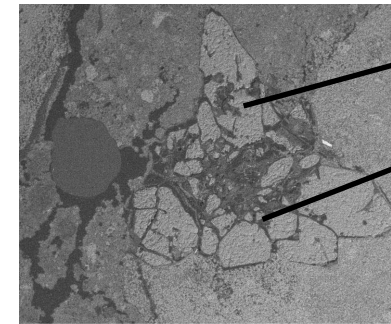
Pa1. K'inich Kuk Bahlam II (Aka Kuk)



PPL. Scale bar: 1 mm.



XPL. Scale bar: 1 mm.

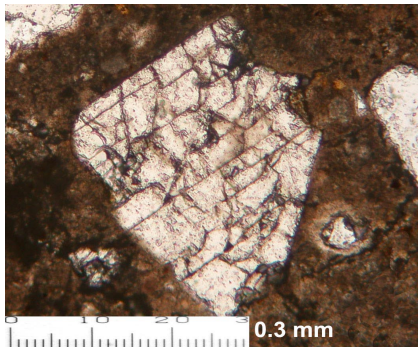


BSE

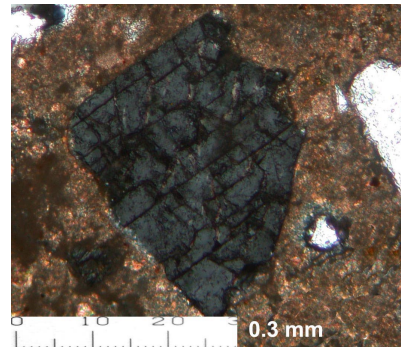
Shocked quartz
SiO₂ 100%

Isotropic matrix
SO₃ 85%
SiO₂ 8%
MgCO₃ 7%

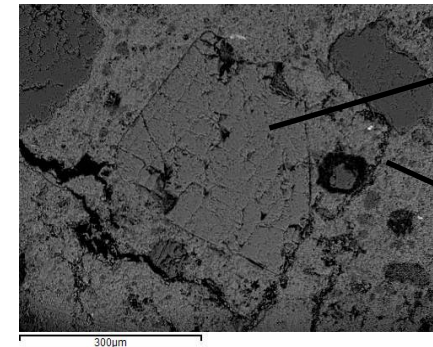
Pa12. K'inich Kuk Bahlam II (Aka Kuk)?



PPL. Scale bar: 0.3 mm.



XPL. Scale bar: 0.3 mm.

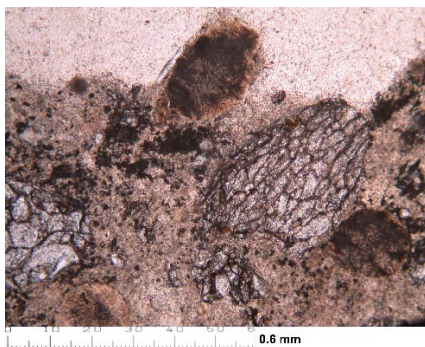


BSE

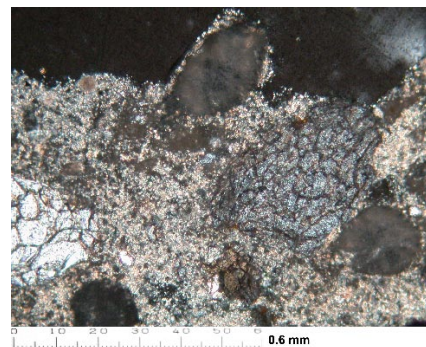
K feldspar
SiO₂ 67%
Al₂O₃ 18%
K₂O 11%

Isotropic phase
around quartz
Glass melt?
MgCO₃ 33%
SO₃ 26%
SiO₂ 21%

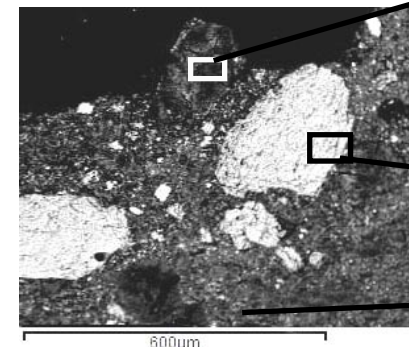
Pa56. Floor. Balunte Phase. Detail of breccia clast.



PPL. Scale bar: 0.6 mm.



XPL. Scale bar: 0.6 mm.



BSE

Brown inclusion
CaCO₃ 41%
SO₃ 40%
Al₂O₃ 12%
SiO₂ 6%

Shocked quartz.
SiO₂ 99.7%
SO₃ 0.3%

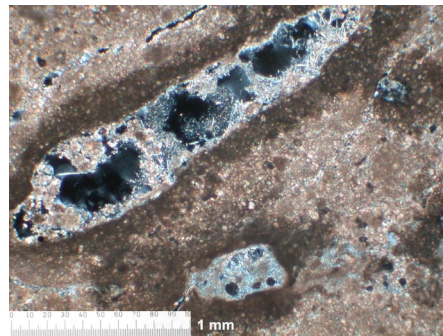
Cement of clast
SO₃ 43%
CaCO₃ 27%
SiO₂ 24%

Calakmul

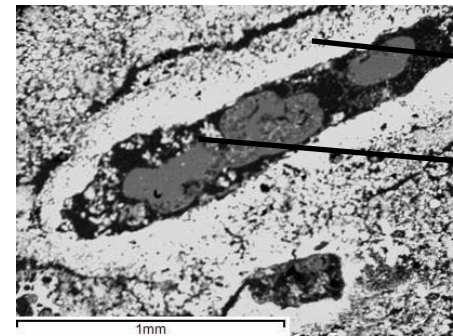
Ca11. Wall render. Middle Preclassic.



PPL. Scale bar: 1 mm.



XPL. Scale bar: 1 mm.

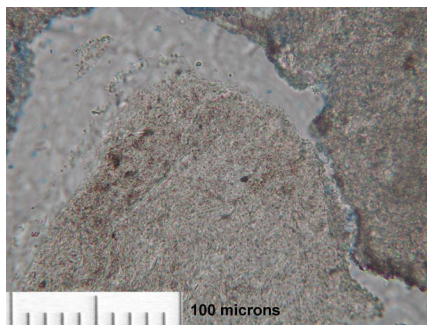


BSE

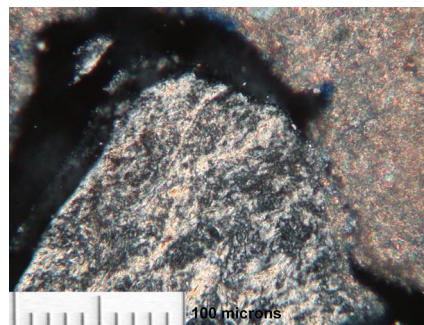
Reaction rim
 CaCO_3 60%
 SiO_2 38%

Acicular phases
 CaCO_3 86%
 SiO_2 9%
 Al_2O_3 2%

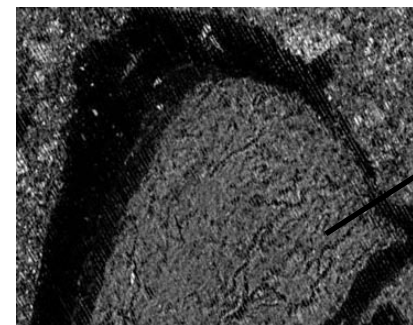
Ca6. Wall render. Late Middle Preclassic.



PPL. Scale bar: 0.1 mm.



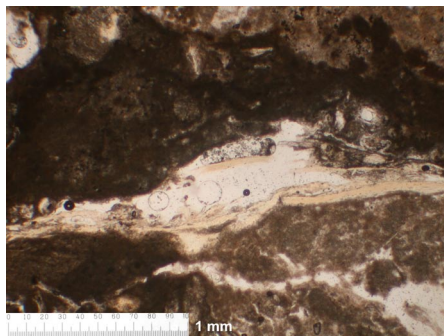
XPL. Scale bar: 0.1 mm.



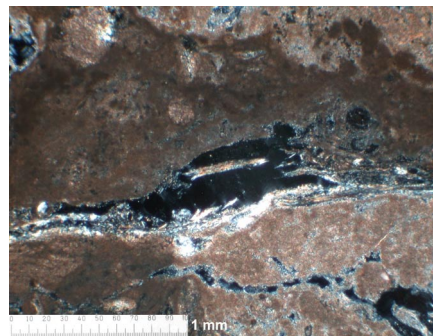
BSE

Cordierite?
 SiO_2 58%
 Al_2O_3 14%
 SO_3 8%
 Fe_2O_3 9%
 MgCO_3 8%

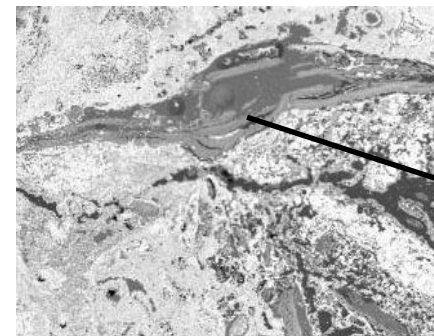
Ca29. Floor. Late Preclassic.



PPL. Scale bar: 1 mm.



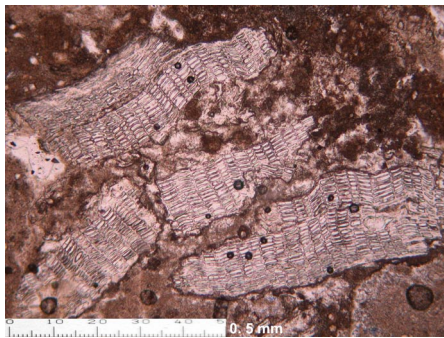
XPL. Scale bar: 1 mm.



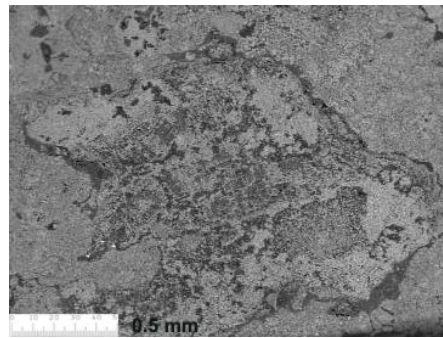
BSE

Silicate mineral
 from the serpentine
 group?
 SiO_2 45%
 MgCO_3 40%
 CaCO_3 8%
 F 5%

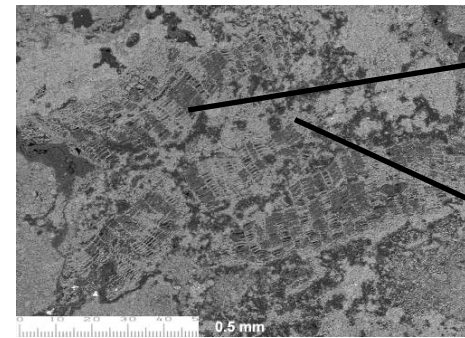
Ca30. Floor. LatePreclassic?



PPL. Scale bar: 0.5 mm.



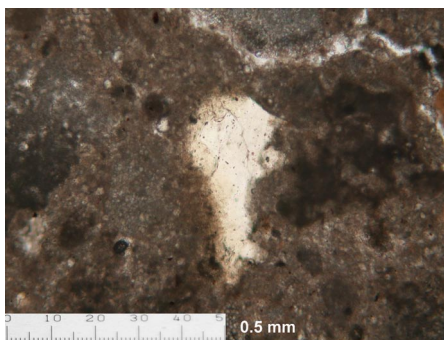
XPL. Scale bar: 0.5 mm.



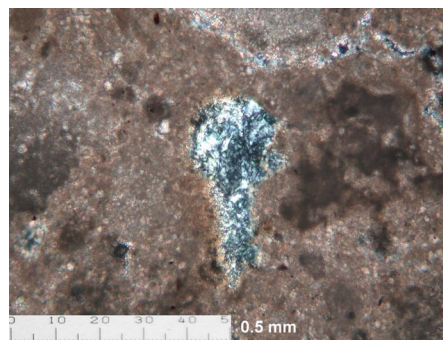
BSE

Remains of plants with visible cellular structure
 SiO_2 100%
 Matrix of inclusion
 SiO_2 70%
 CaCO_3 28%
 F 1%

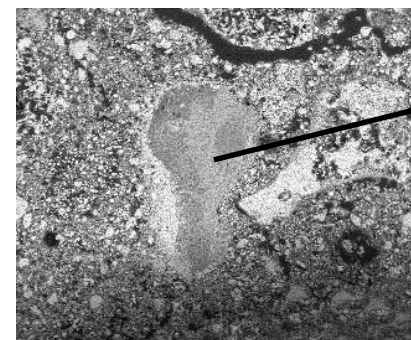
Ca14. Wall render. Early Classic.



PPL. Scale bar: 0.5 mm.

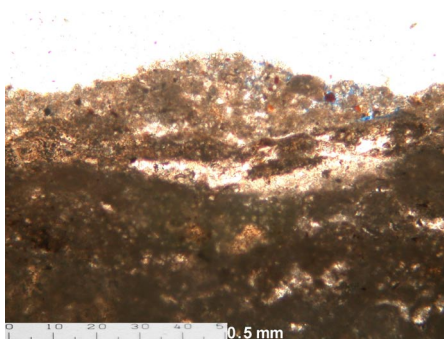


XPL. Scale bar: 0.5 mm.

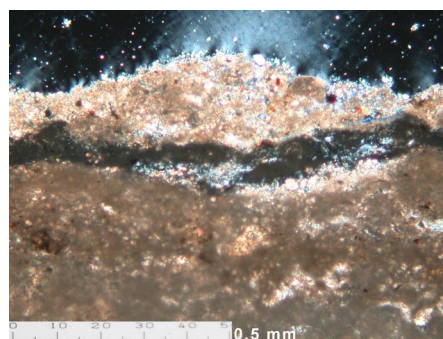


BSE

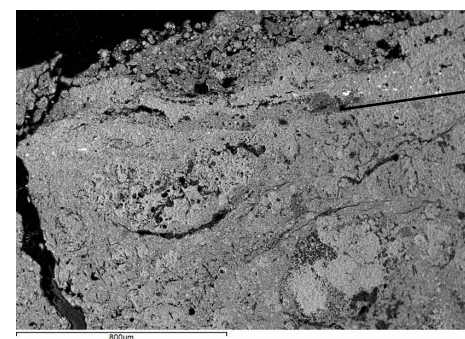
Cordierite?
 SiO_2 77%
 MgCO_3 20%
 Al_2O_3 2%



PPL. Scale bar: 0.5 mm.



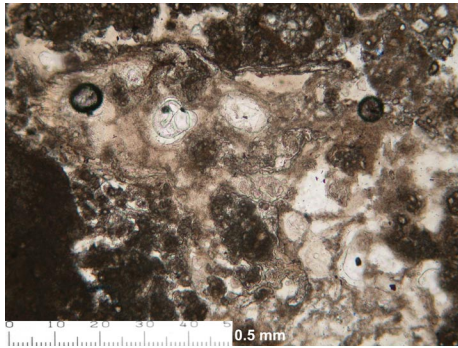
XPL. Scale bar: 0.5 mm.



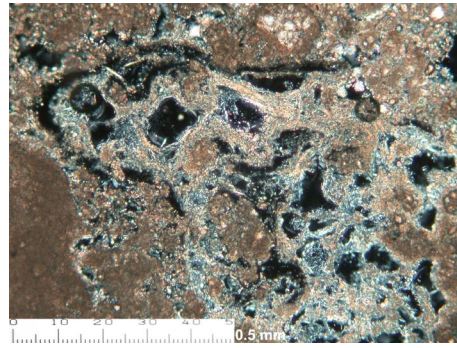
BSE

Isotropic layer (volcanic ash)
 SiO_2 91%
 Al_2O_3 2%
 CaCO_3 5%
 MgCO_3 01%
 Fe_2O_3 0.4%
 SO_3 0.6%

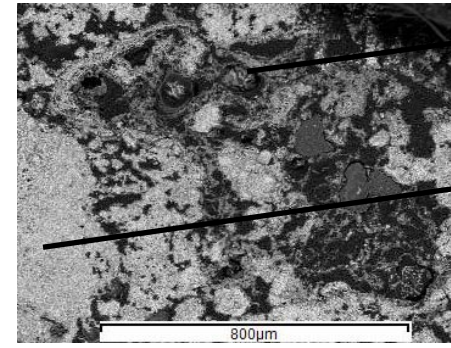
Ca18. Floor. Late Classic.



PPL. Scale bar: 0.5 mm.



XPL. Scale bar: 0.5 mm.

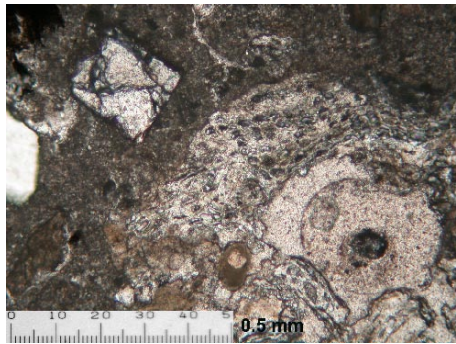


BSE

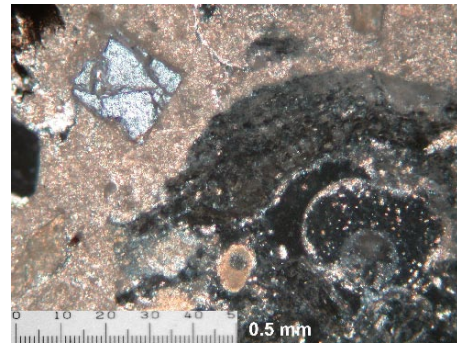
Acicular calcite
CaCO₃ 99%
SO₃ 1%

SiO₂-rich matrix
CaCO₃ 67%
SiO₂ 31%
MgCO₃ 1%

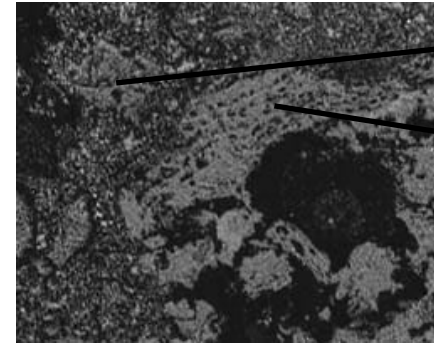
Ca26. Wall render. Late Classic.



PPL. Scale bar: 0.5 mm.



XPL. Scale bar: 0.5 mm.

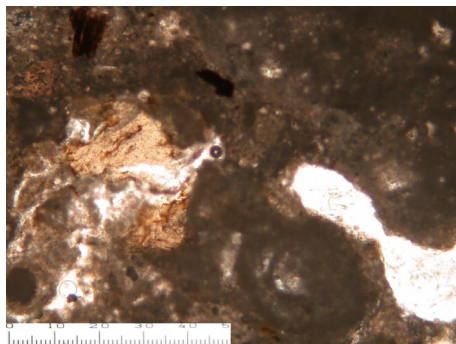


BSE

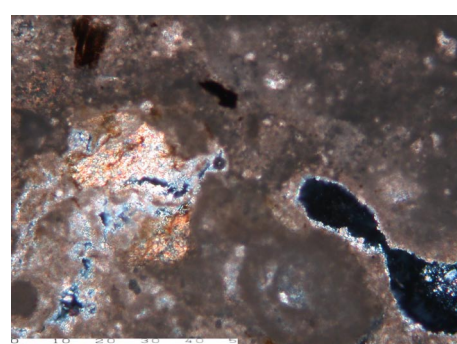
Quartz
SiO₂ 100%

Amorphous silica plant remain.
SiO₂ 100%

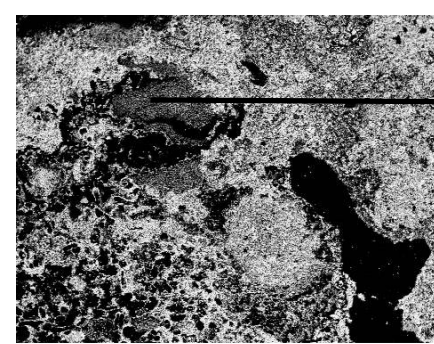
Ca16. Wall render. Late Classic.



PPL. Scale bar: 0.5 mm.



XPL. Scale bar: 0.5 mm.

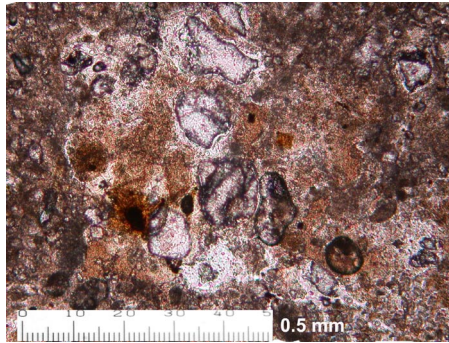


BSE

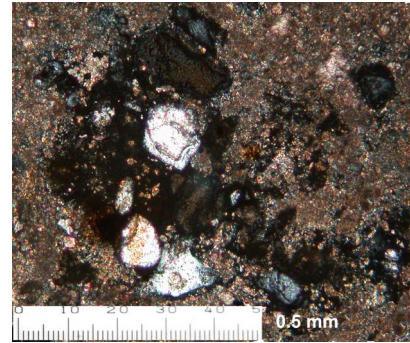
Devitrified glass
SiO₂ 65%
MgCO₃ 17%
Al₂O₃ 10%
Fe₂O₃ 3%
CaCO₃ 3%

Lamanai

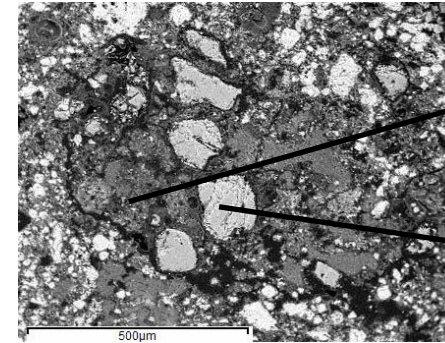
La49. Floor. Late Postclassic.



PPL. Scale bar: 0.5 mm.



XPL. Scale bar: 0.5 mm.



BSE

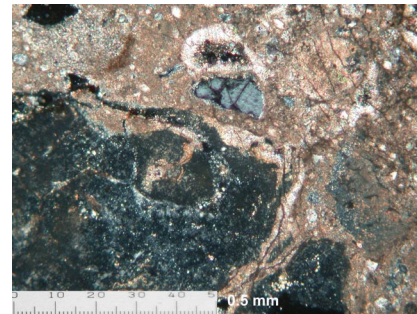
Devitrified glass
 SiO_2 66%
 Al_2O_3 16%
 CaCO_3 15%

Quartz
 SiO_2 100%

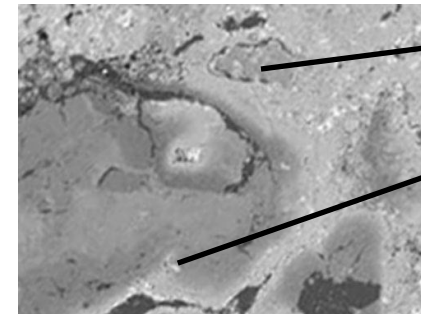
La49. Floor. Late Postclassic.



PPL. Scale bar: 0.5 mm.



XPL. Scale bar: 0.5 mm.

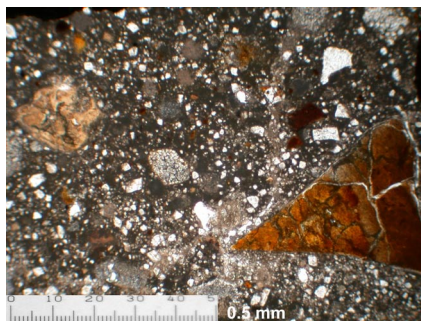


BSE

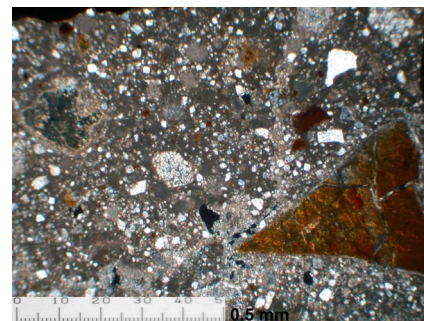
Quartz
 SiO_2 100%

Lime lump
 CaCO_3 85%
 SO_3 10%
 SiO_2 3%

La36b. Wall render? Late Postclassic? Spanish Colonial?



PPL. Scale bar: 0.5 mm.



XPL. Scale bar: 0.5 mm.



BSE

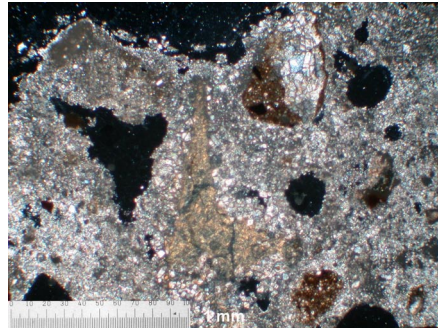
Silica gel.
 SiO_2 50%
 Al_2O_3 37%
 CaCO_3 4%

Devitrified/
 argillized glass.
 SiO_2 52%
 Al_2O_3 26%
 Fe_2O_3 15%

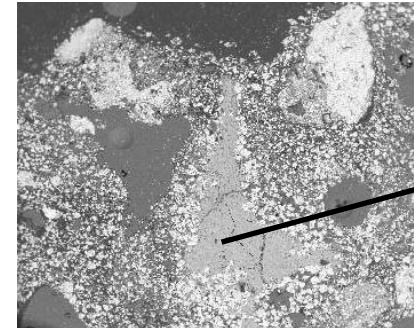
La20. Joining mortar. Spanish Colonial.



PPL. Scale bar: 1 mm.



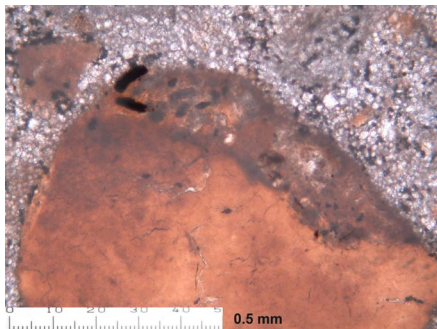
XPL. Scale bar: 1 mm.



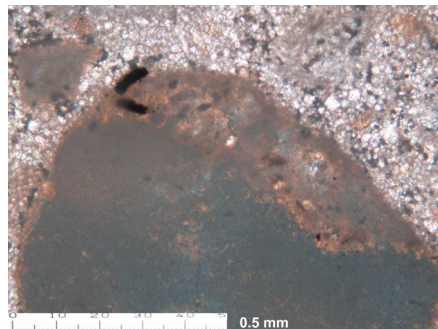
BSE

Devitrified/argillized
glass shard
SiO₂ 54%
Al₂O₃ 33%
Fe₂O₃ 4%

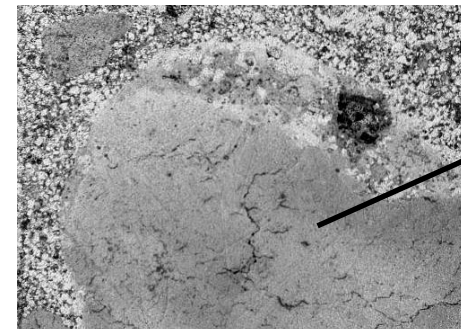
La40. Wall render. Spanish Colonial.



PPL. Scale bar: 0.5 mm.



XPL. Scale bar: 0.5 mm.



BSE

Lime lump
CaCO₃ 84%
SO₃ 10%

A.5. X Ray Diffraction

| Sample | Daresbury | Ingold Lab | Acidic dissolution | Main peaks 2θ with 1.54056 | | | | | | |
|-----------|-----------|------------|--------------------|---|--|--|---|---|--|--|
| | | | | Calcite pdf: 862334 Main Peaks 2θ: 29.4, 48.5, 39.4. | Quartz pdf: 862237. Main Peaks 2θ: 26.6, 20.8, 39.4. | Dolomite pdf: 791346. Main Peaks 2θ: 31.5, 41.6, 45.4. | Hydromagnesite Pdf: 050211. Main Peaks 2θ: 15.2, 30.8, 41.9. | Montmorillonite 15A pdf: 291498. Main Peaks 2θ: 5.8, 19.7, 29.5. | Nickel Pdf: 011258 Main peaks: 44.3, 92.1, 51.6 | Unidentified peaks (2 theta values for 1.54506). |
| Ca3 | | * | | * | | | | | | |
| Ca7 | | * | | * | | | | | | |
| Ca9 | * | | | * | | | | | | |
| Ca10 | | | * | * | | | | | | |
| Ca13 | * | | | * | | * | | | | 8.3, 26.9, 30.9, 33.8, 50.9, 67.4 |
| Ca18 | | * | | * | | | | | | |
| Ca21 | * | | | * | | | | | | |
| Ca22 | | * | | * | | | | | | |
| Ca29 | | | * | * | | | | | | |
| Ca33 | * | | * | * | * | | | * | | |
| CaSacab | * | | | * | | | | | | |
| La39 | * | | | * | | | | | | |
| La14 | * | | | * | | | | | | |
| La4 | * | | | * | | | | | | |
| La12 | * | | | * | | | | | | |
| La21 | | * | * | * | * | | | | | |
| La22 | * | | | * | | | | | | |
| La19 | * | | | * | | | | | | |
| La25 | * | | | * | | | | | | |
| La49 | | * | | * | * | | | | | |
| La sascab | * | | | * | | | | | | 44.8, 50.9 |
| Pa33 | * | | | * | | | | | | |
| Pa34 | * | | | * | | | | | | |
| Pa44 | * | | | * | * | | | | *??? | 75.8 |
| Pa60 | | | * | * | * | | | | | |
| Pa63 | | * | | * | | * | * | | | |
| Pa70 | | * | | * | | | * | | | |
| Pa76 | * | | | * | | | | | | |
| Pa88 | * | | | * | | * ??? | | | *??? | 50.9, 91.9 |
| Pa89 | * | * | | * | * | * | | | | |

Table A.5.1. Minerals identified by XRD .

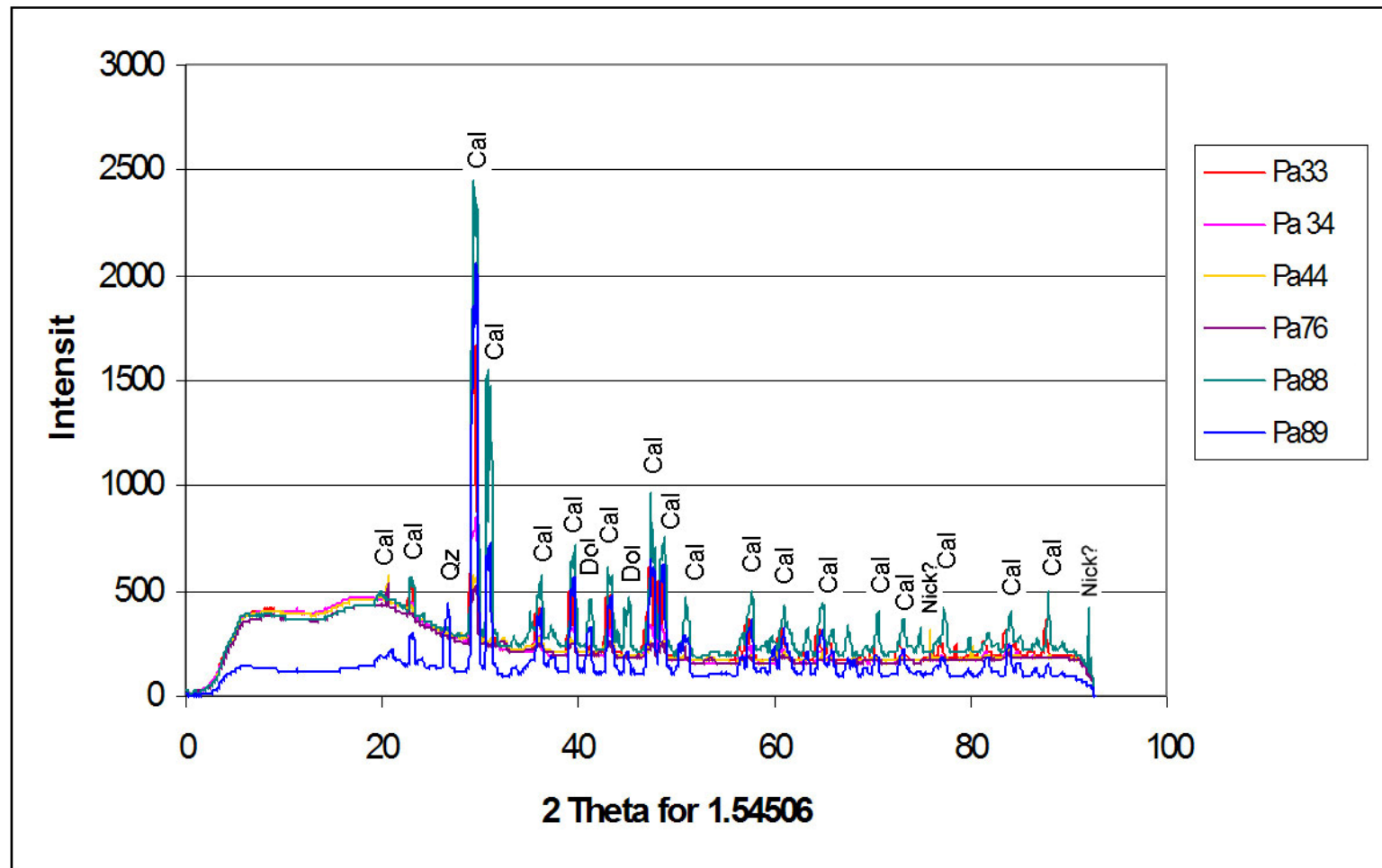


Fig. A.5.1. Palenque samples analysed at Daresbury (without acid dissolution).
Cal: calcite, Qz: quartz, Dol: dolomite, Nick: nickel.

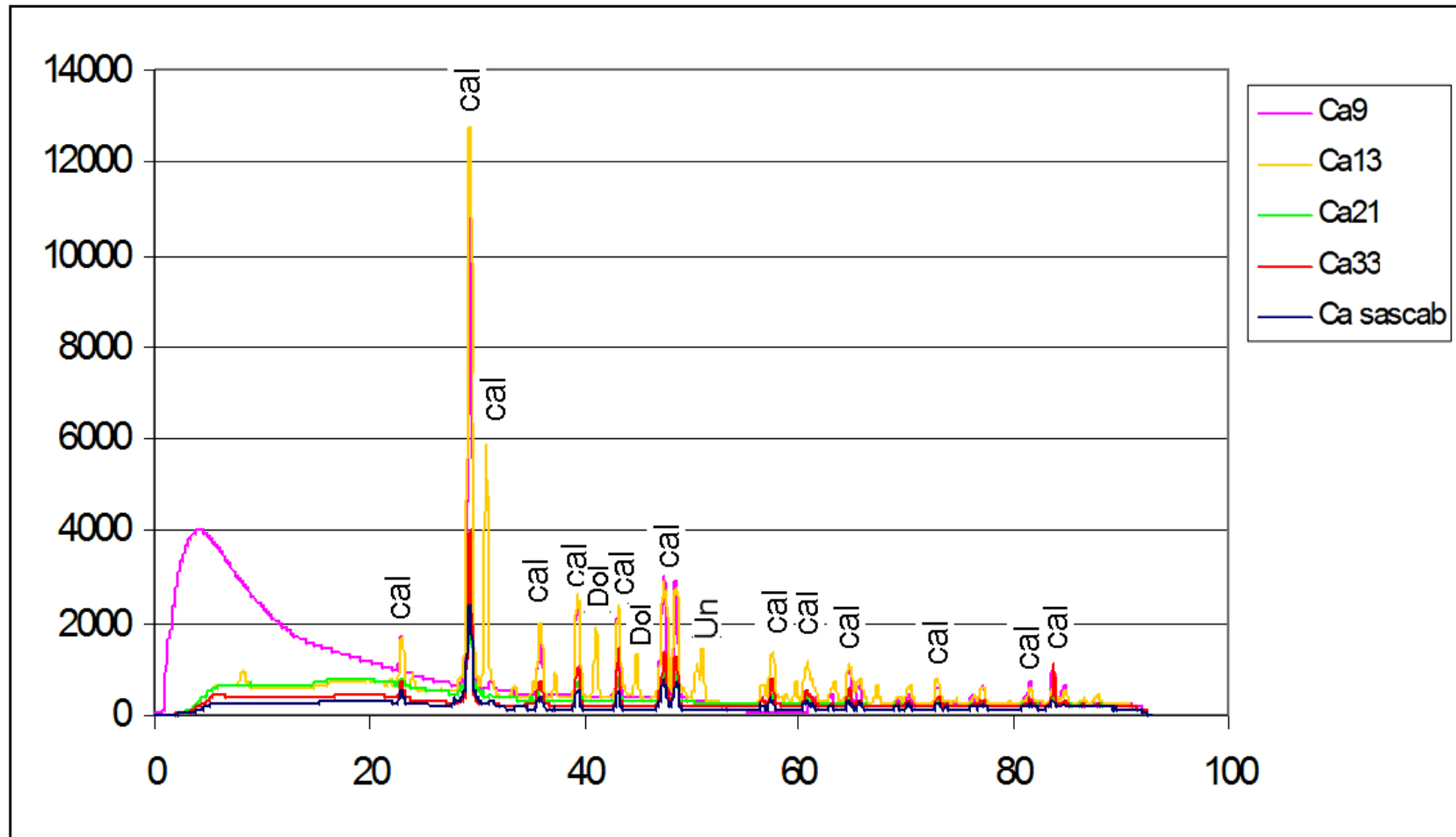


Fig. A.5.2. Calakmul samples analysed at Daresbury (without acid dissolution).
Cal: calcite, Dol: dolomite, Un: unidentified peaks.

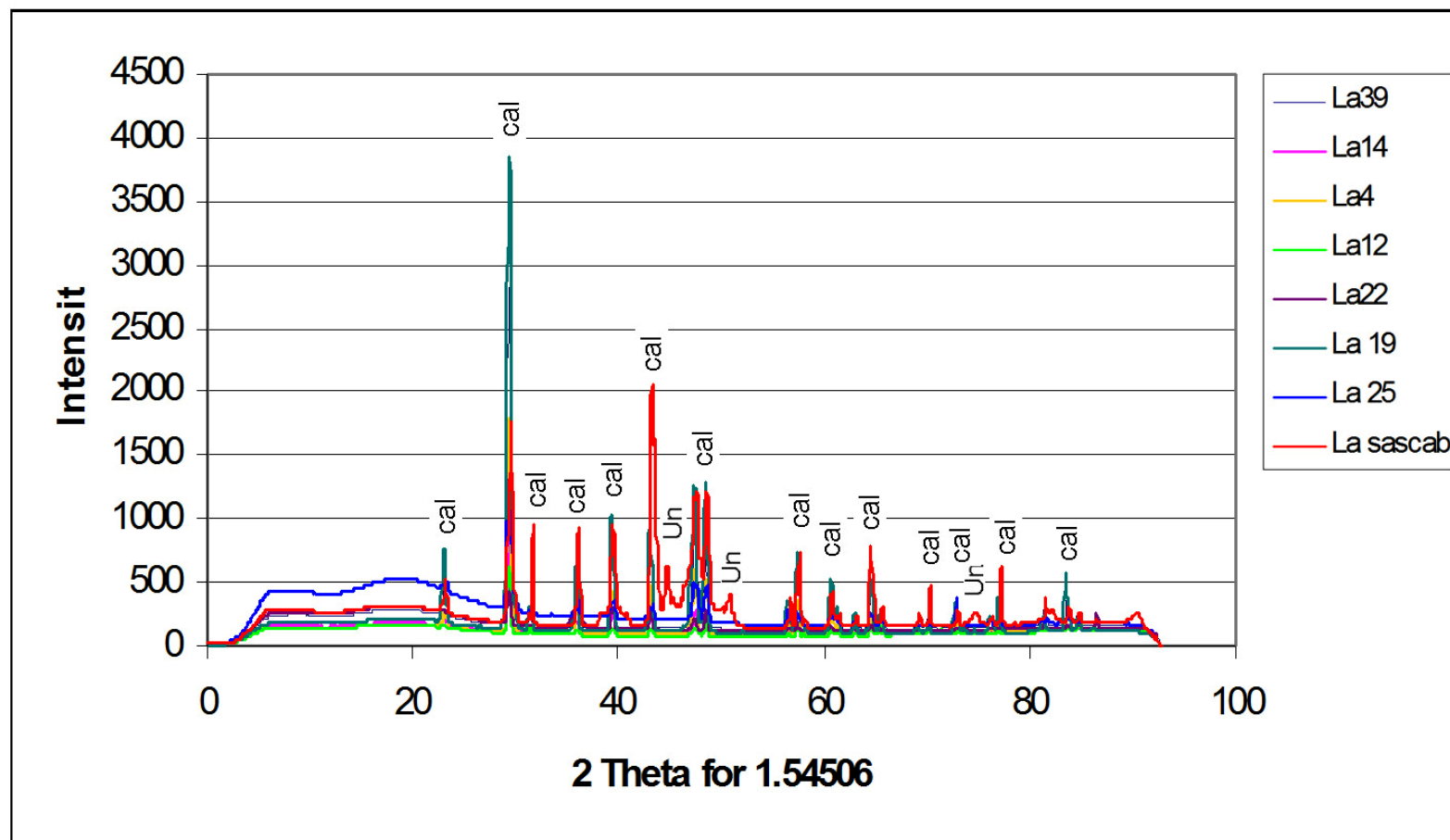


Fig. A.5.3. Lamanai samples analysed at Daresbury (without acid dissolution).
Cal: calcite, Un: unidentified peaks.

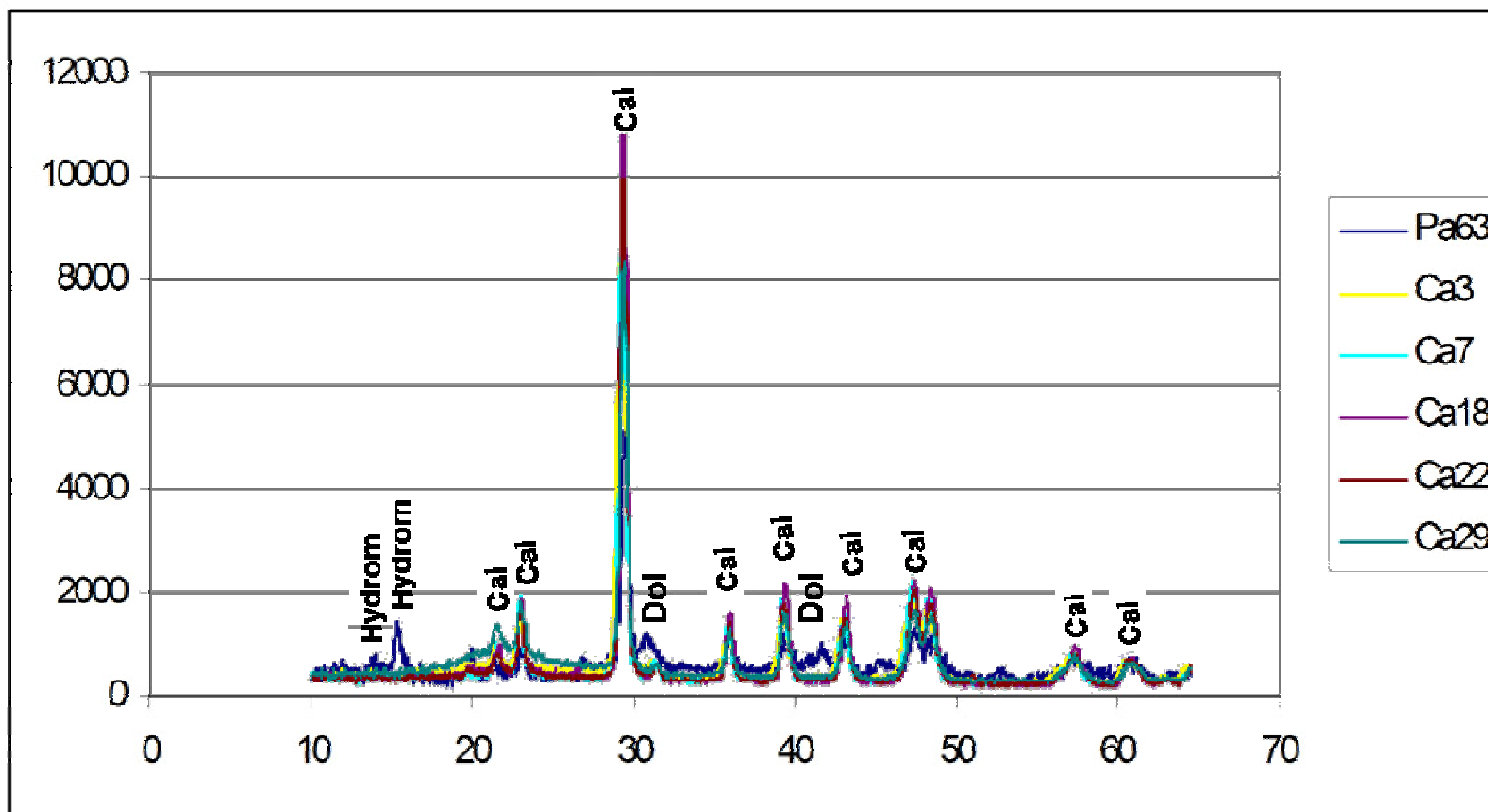


Fig. A.5.4. XRD spectra of samples analysed at Ingolds Laboratory (without acid dissolution).
Cal: calcite, Dol: dolomite, Hydrom: Hydromagnesite.

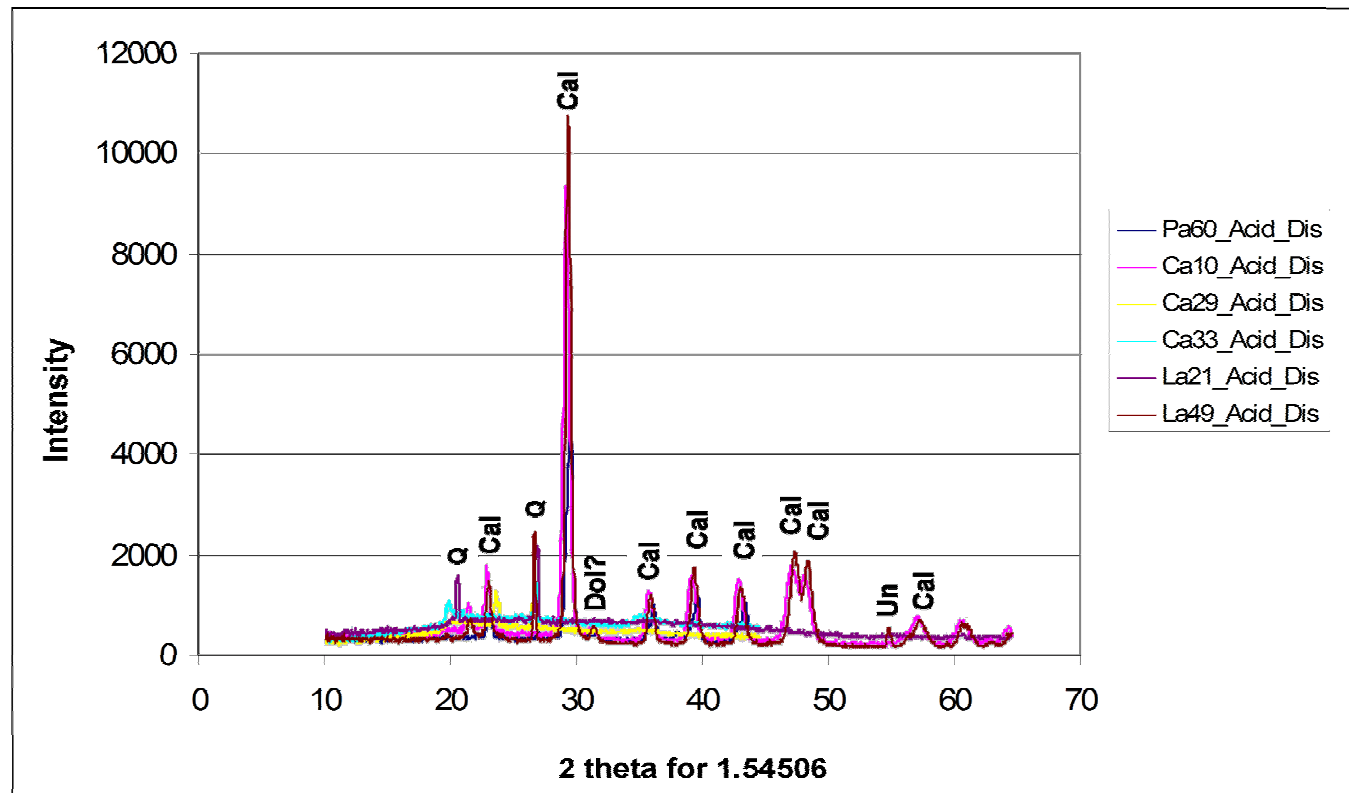


Fig. A.5.5. XRD spectra of samples analysed at Ingolds Laboratory (with acid dissolution).
Cal: calcite, Dol: dolomite, Q: quartz.

A.6.1. Quality of the Data

In order to evaluate the accuracy and precision of the XRF equipment, the certified and analysed compositions of British Chemical Standards (BCS 353 and BCS 393) are presented. The analysed compositions are presented as obtained from the XRF equipment and normalized to the totals of the analytical standards. Cr₂O₃ and SrO are not presented in BCS 393 since they are not reported by the British Chemical Standards and they fall under the detection limits of the XRF equipment.

| Sample | SiO ₂ % | Al ₂ O ₃ % | TiO ₂ % | Fe ₂ O ₃ % | Cr ₂ O ₃ % | CaO% | MgO% | K ₂ O% | P ₂ O ₅ % | SrO% | Sum |
|---|--------------------|----------------------------------|--------------------|----------------------------------|----------------------------------|-------|-------|-------------------|---------------------------------|-------|-------|
| BCS 353 Certified composition | 20.5 | 3.77 | 0.16 | 4.82 | 0.02 | 64.8 | 2.42 | 0.49 | 0.08 | 0.23 | 97.29 |
| BCS 353 Analysed | 22.12 | 3.91 | 0.12 | 4.86 | 0.02 | 56.76 | 2.12 | 0.75 | 0.056 | 0.24 | 94.26 |
| Standard deviation (σ) BCS 353 Analysed | 0.083 | 0.25 | 0.0005 | 0.009 | 0.002 | 0.19 | 0.38 | 0.0025 | 0.004 | 0.002 | NA |
| BCS 353 Analysed. Normalised to totals of certified standards | 22.83 | 4.04 | 0.12 | 5.02 | 0.02 | 58.58 | 2.19 | 0.77 | 0.06 | 0.25 | 97.29 |
| δ (Analysed composition- certified composition) | 2.33 | 0.27 | -0.04 | 0.20 | 0.00 | -6.22 | -0.23 | 0.28 | -0.02 | 0.02 | NA |
| Relative δ (%) (δ / certified composition)*100. | 11.37 | 7.16 | -25 | 4.15 | 0 | -9.60 | -9.50 | 57.14 | -25 | 8.70 | NA |

Certified and analysed compositions of British Chemical Standard (BCS) 353 (Sulphate resisting Portland cement).

| Sample | SiO ₂ % | Fe ₂ O ₃ % | Mn ₂ O ₃ % | CaO% | Sum |
|---|--------------------|----------------------------------|----------------------------------|-------|-------|
| BCS 393 Certified composition | 0.7 | 0.045 | 0.01 | 55.4 | 56.16 |
| BCS 393 Analysed | 0.83 | 0.063 | 0.01 | 51.43 | 52.33 |
| Standard dev. (σ) BCS 393 Analysed | 0.01 | 0.00 | 0.00 | 0.08 | NA |
| BCS 393 Analysed. Normalised to totals of certified standards | 0.89 | 0.07 | 0.01 | 55.19 | 56.16 |
| δ (Analysed composition-certified composition) | 0.19 | 0.02 | 0.00 | -0.21 | 0.00 |
| Relative δ (%) (δ / certified composition)*100. | 27.23 | 50.22 | 7.30 | -0.39 | 0 |

Certified and analysed compositions of British Chemical Standard (BCS) 393 (Limestone).

| Sample | Chron | Type | Na ₂ O | MgO ₃ | Al ₂ O ₃ | SiO ₂ | K ₂ O | CaCO ₃ | TiO ₂ | MnO | Fe ₂ O ₃ | Co ₃ O ₄ | NiO | CuO | ZnO | Rb ₂ O | SrO | ZrO ₂ | BaCO ₃ | Sum |
|--------|----------|------|-------------------|------------------|--------------------------------|------------------|------------------|-------------------|------------------|------|--------------------------------|--------------------------------|------|------|------|-------------------|------|------------------|-------------------|------|
| | | | % (wt) | | | | | | | | | ppm (part per million) (wt) | | | | | | | | |
| Pa6 | Otulum | WR | 0 | 35.03 | 0.93 | 3.88 | 0.16 | 59.47 | 0.02 | 0.02 | 0.46 | 0 | 10 | 20 | 20 | 0 | 240 | 0 | 39 | 100 |
| σ | | | 0 | 0.06 | 0.00 | 0.02 | 0.00 | 0.10 | 0.00 | 0.00 | 0.00 | 0 | 0.00 | 0.00 | 0.00 | 0 | 0.00 | 0 | 0.00 | 0.00 |
| Pa49 | Otulum | WR | 0 | 35.27 | 0.77 | 2.78 | 0.05 | 60.80 | 0.02 | 0.01 | 0.27 | 0 | 20 | 20 | 10 | 0 | 200 | 10 | 51 | 100 |
| σ | | | 0 | 0.08 | 0.01 | 0.02 | 0.00 | 0.09 | 0.00 | 0.00 | 0.00 | 0 | 0.00 | 0.00 | 0.00 | 0 | 0.00 | 0.00 | 0.00 | 0.00 |
| Pa24 | Kam Bal | WR | 0 | 37.43 | 1.35 | 3.53 | 0.07 | 57.15 | 0.04 | 0.01 | 0.40 | 10 | 10 | 10 | 20 | 0 | 130 | 10 | 26 | 100 |
| σ | | | 0 | 0.11 | 0.02 | 0.01 | 0.00 | 0.08 | 0.00 | 0.00 | 0.01 | 0.00 | 0.00 | 0.00 | 0.00 | 0 | 0.00 | 0.00 | 0.00 | 0.00 |
| Pa 52 | KamBal? | F | 0 | 12.98 | 1.33 | 5.93 | 0 | 78.97 | 0.04 | 0.03 | 0.66 | 0 | 20 | 10 | 30 | 0 | 540 | 20 | 64 | 100 |
| σ | | | 0 | 0.07 | 0.02 | 0.02 | 0 | 0.07 | 0.00 | 0.00 | 0.01 | 0 | 0.00 | 0.00 | 0.00 | 0 | 0.00 | 0.00 | 0.00 | 0.00 |
| Pa59 | Kam Bal | F | 0 | 23.80 | 0.74 | 5.03 | 0 | 70.01 | 0.02 | 0.01 | 0.37 | 0 | 0 | 10 | 20 | 0 | 120 | 0 | 39 | 100 |
| σ | | | 0 | 0.04 | 0.01 | 0.03 | 0 | 0.08 | 0.00 | 0.00 | 0.00 | 0 | 0 | 0.00 | 0.00 | 0 | 0.00 | 0 | 0.00 | 0.00 |
| Pa65 | Kam Bal | F | 0 | 63.36 | 1.36 | 4.06 | 0 | 30.61 | 0.04 | 0.02 | 0.54 | 0 | 30 | 10 | 20 | 0 | 90 | 10 | 0 | 100 |
| σ | | | 0 | 0.14 | 0.01 | 0.02 | 0 | 0.06 | 0.00 | 0.00 | 0.00 | 0 | 0 | 0 | 0 | 0 | 0 | 0 | 0 | 0 |
| Pa71 | Kam Bal | F | 0 | 47.34 | 1.95 | 6.70 | 0 | 42.95 | 0.06 | 0.04 | 0.93 | 0 | 40 | 20 | 30 | 0 | 180 | 10 | 39 | 100 |
| σ | | | 0 | 0.17 | 0.01 | 0.02 | 0 | 0.06 | 0.00 | 0.00 | 0.00 | 0 | 0.00 | 0.00 | 0.00 | 0 | 0.00 | 0.00 | 0.00 | 0.00 |
| Pa18 | JoyChit? | F | 0 | 34.67 | 1.06 | 5.42 | 0.25 | 58.06 | 0.03 | 0.02 | 0.44 | 0 | 20 | 10 | 20 | 0 | 270 | 10 | 142 | 100 |
| σ | | | 0 | 0.17 | 0.03 | 0.05 | 0.01 | 0.10 | 0.00 | 0.00 | 0.00 | 0 | 0.00 | 0.00 | 0.00 | 0 | 0.00 | 0.00 | 0.00 | 0.00 |
| Pa43 | JoyChit? | WR | 0 | 9.09 | 1.08 | 4.34 | 0 | 84.92 | 0.03 | 0.02 | 0.47 | 0 | 0 | 10 | 20 | 0 | 330 | 10 | 51 | 100 |
| σ | | | 0 | 0.06 | 0.02 | 0.02 | 0 | 0.17 | 0.00 | 0.00 | 0.00 | 0 | 0 | 0.00 | 0.00 | 0 | 0.00 | 0.00 | 0.00 | 0.00 |
| Pa47 | JoyChit? | F | 0 | 10.81 | 1.10 | 4.59 | 0 | 82.98 | 0.04 | 0.02 | 0.42 | 0 | 0 | 10 | 20 | 0 | 290 | 10 | 51 | 100 |
| σ | | | 0 | 0.04 | 0.01 | 0.01 | 0 | 0.08 | 0.00 | 0.00 | 0.00 | 0 | 0 | 0.00 | 0.00 | 0 | 0.00 | 0.00 | 0.00 | 0.00 |
| Pa1 | Kuk Bal | WR | 0 | 41.94 | 0.84 | 2.89 | 0 | 53.93 | 0.02 | 0.01 | 0.34 | 10 | 20 | 10 | 20 | 0 | 170 | 0 | 0 | 100 |
| σ | | | 0 | 0.21 | 0.02 | 0.01 | 0 | 0.07 | 0.00 | 0.00 | 0.01 | 0.00 | 0.00 | 0.00 | 0.00 | 0 | 0.00 | 0 | 0 | 0 |
| Pa2a | Kuk Bal | F | 0 | 9.71 | 0.76 | 4.32 | 0 | 84.55 | 0.02 | 0.06 | 0.55 | 0 | 20 | 10 | 20 | 0 | 210 | 0 | 64 | 100 |
| σ | | | 0 | 0.07 | 0.02 | 0.04 | 0 | 0.31 | 0.00 | 0.00 | 0.00 | 0 | 0.00 | 0.00 | 0.00 | 0 | 0.00 | 0 | 0.00 | 0.00 |
| Pa53 | Balunte | WR | 0 | 12.05 | 3.57 | 14.59 | 0.16 | 68.13 | 0.10 | 0.04 | 1.32 | 20 | 50 | 20 | 30 | 10 | 180 | 40 | 142 | 100 |
| σ | | | 0 | 0.025 | 0.025 | 0.035 | 0.004 | 0.04 | 0.00 | 0.00 | 0.01 | 0.00 | 0.00 | 0.00 | 0.00 | 0.00 | 0.00 | 0.00 | 0.00 | 0.00 |
| Pa56 | Balunte | F | 0.16 | 9.14 | 6.37 | 21.68 | 0.47 | 59.48 | 0.18 | 0.03 | 2.40 | 40 | 140 | 20 | 50 | 30 | 400 | 70 | 167 | 100 |
| σ | | | 0.05 | 0.07 | 0.03 | 0.03 | 0.01 | 0.09 | 0.00 | 0.00 | 0.01 | 0.00 | 0.00 | 0.00 | 0.00 | 0.00 | 0.00 | 0.00 | 0.00 | 0.00 |
| Pa86 | Balunte | WR | 0 | 19.88 | 3.14 | 18.16 | 0.30 | 56.64 | 0.10 | 0.07 | 1.65 | 30 | 60 | 20 | 30 | 20 | 250 | 60 | 167 | 100 |
| σ | | | 0 | 0.03 | 0.02 | 0.04 | 0.01 | 0.07 | 0.00 | 0.00 | 0.01 | 0.00 | 0.00 | 0.00 | 0.00 | 0.00 | 0.00 | 0.00 | 0.00 | 0.00 |
| Pa87 | Balunte | WR | 0 | 16.84 | 4.86 | 19.87 | 0.35 | 55.71 | 0.17 | 0.03 | 2.10 | 20 | 130 | 10 | 40 | 20 | 230 | 70 | 129 | 100 |
| σ | | | 0 | 0.09 | 0.04 | 0.04 | 0.01 | 0.06 | 0.00 | 0.00 | 0.00 | 0.00 | 0.00 | 0.00 | 0.00 | 0.00 | 0.00 | 0.00 | 0.00 | 0.00 |

Values in blue indicate significantly higher contents of the element in comparison with other samples.

| Sample | Chron | Type | Na ₂ O | MgO ₃ | Al ₂ O ₃ | SiO ₂ | K ₂ O | CaCO ₃ | TiO ₂ | MnO | Fe ₂ O ₃ | Co ₃ O ₄ | NiO | CuO | ZnO | Rb ₂ O | SrO | ZrO ₂ | BaCO ₃ | Sum | |
|----------|----------|------|-------------------|------------------|--------------------------------|------------------|------------------|-------------------|------------------|------|--------------------------------|--------------------------------|------|------|------|-------------------|------|------------------|-------------------|------|--|
| | | | % (wt) | | | | | | | | | ppm (part per million) (wt) | | | | | | | | | |
| Pa40 | Arch mod | JM | 0 | 11.79 | 5.51 | 13.71 | 0.68 | 65.93 | 0.15 | 0.04 | 2.13 | 30 | 120 | 20 | 40 | 30 | 230 | 60 | 103 | 100 | |
| σ | | | 0 | 0.05 | 0.01 | 0.08 | 0.01 | 0.11 | 0.00 | 0.00 | 0.01 | 0.00 | 0.00 | 0.00 | 0.00 | 0.00 | 0.00 | 0.00 | 0.00 | 0.00 | |
| Pa44 | Arch mod | WR | 0 | 39.83 | 1.87 | 7.68 | 0.46 | 48.87 | 0.05 | 0.02 | 1.18 | 10 | 50 | 10 | 20 | 10 | 220 | 20 | 77 | 100 | |
| σ | | | 0 | 0.07 | 0.01 | 0.03 | 0.00 | 0.08 | 0.00 | 0.00 | 0.00 | 0.00 | 0.00 | 0.00 | 0.00 | 0.00 | 0.00 | 0.00 | 0.00 | 0.00 | |
| Pa80 | Arch mod | JM | 0.34 | 15.05 | 4.65 | 12.54 | 0.75 | 64.42 | 0.14 | 0.04 | 2.01 | 30 | 130 | 20 | 40 | 30 | 250 | 40 | 90 | 100 | |
| σ | | | 0.13 | 0.05 | 0.02 | 0.02 | 0.01 | 0.03 | 0.00 | 0.00 | 0.00 | 0.00 | 0.00 | 0.00 | 0.00 | 0.00 | 0.00 | 0.00 | 0.00 | 0.00 | |
| Pa82 | Arch mod | WR | 0.21 | 33.99 | 2.37 | 9.84 | 0.39 | 51.83 | 0.07 | 0.05 | 1.21 | 0 | 50 | 20 | 30 | 10 | 200 | 20 | 90 | 100 | |
| σ | | | 0.12 | 0.16 | 0.02 | 0.06 | 0.00 | 0.14 | 0.00 | 0.00 | 0.01 | 0 | 0.00 | 0.00 | 0.00 | 0.00 | 0.00 | 0.00 | 0.00 | 0.00 | |
| PaShells | Modern | Geo | 0.42 | 0.00 | 0.18 | 0.35 | 0.15 | 98.81 | 0 | 0 | 0.04 | 0 | 0 | 10 | 20 | 0 | 390 | 0 | 0 | 100 | |
| σ | | | 0.06 | 0 | 0.00 | 0.01 | 0.00 | 0.13 | 0 | 0 | 0.00 | 0 | 0 | 2.55 | 0.71 | 0.06 | 2.76 | 0 | 0 | 0 | |
| Pa3 | CasP | L | 0 | 40.56 | 1.00 | 2.18 | 0 | 56.10 | 0.02 | 0.01 | 0.12 | 0 | 0 | 10 | 10 | 0 | 120 | 0 | 0 | 100 | |
| σ | | | 0 | 0.09 | 0.03 | 0.02 | 0 | 0.07 | 0.00 | 0.00 | 0.00 | 0 | 0 | 0.00 | 0.00 | 0 | 0.00 | 0 | 0 | 0 | |
| Pa5 | CasP | L | 0 | 40.70 | 1.04 | 2.53 | 0 | 55.46 | 0.02 | 0.01 | 0.23 | 0 | 0 | 10 | 10 | 0 | 130 | 0 | 0 | 100 | |
| σ | | | 0 | 0.04 | 0.013 | 0.02 | 0 | 0.09 | 0 | 0 | 0 | 0 | 0 | 0.00 | 0.00 | 0 | 0.00 | 0 | 0 | 0 | |
| Pa7 | OtP | L | 0 | 37.57 | 0.48 | 2.40 | 0.43 | 58.89 | 0 | 0.01 | 0.19 | 10 | 10 | 50 | 60 | 0 | 160 | 10 | 39 | 100 | |
| σ | | | 0 | 0.02 | 0.01 | 0.01 | 0.00 | 0.02 | 0 | 0.00 | 0.00 | 0.00 | 0.00 | 0.00 | 0.00 | 0 | 0.00 | 0.00 | 0.00 | 0.00 | |
| Ca10 | M Prec | F | 0 | 1.03 | 1.09 | 13.61 | 0 | 83.08 | 0.04 | 0.01 | 0.34 | 0 | 20 | 20 | 10 | 0 | 1428 | 0 | 6516 | 100 | |
| σ | | | 0 | 0.04 | 0.00 | 0.02 | 0 | 0.18 | 0.00 | 0.00 | 0.00 | 0 | 0.00 | 0.00 | 0.00 | 0 | 0.00 | 0 | 0.00 | 0.00 | |
| Ca9 | M Prec | F | 0 | 3.08 | 1.71 | 15.71 | 0 | 78.43 | 0.05 | 0.01 | 0.68 | 20 | 0 | 80 | 120 | 20 | 2089 | 0 | 901 | 100 | |
| σ | | | 0 | 0.03 | 0.03 | 0.02 | 0 | 0.08 | 0.00 | 0.00 | 0.01 | 0.00 | 0 | 0.00 | 0.00 | 0.00 | 0.00 | 0 | 0.00 | 0.00 | |
| Ca12 | M Prec | F | 0 | 1.93 | 2.24 | 14.59 | 0 | 79.86 | 0.06 | 0.02 | 0.83 | 10 | 60 | 20 | 20 | 0 | 1299 | 20 | 3280 | 100 | |
| σ | | | 0 | 0.01 | 0.02 | 0.04 | 0 | 0.06 | 0.00 | 0.00 | 0.00 | 0.00 | 0.00 | 0.00 | 0.00 | 0 | 0.00 | 0.00 | 0.00 | 0.00 | |
| Ca6 | LM Prec | WR | 0 | 1.83 | 1.66 | 13.64 | 0 | 81.97 | 0.08 | 0.02 | 0.49 | 0 | 20 | 10 | 10 | 0 | 1030 | 0 | 2007 | 100 | |
| σ | | | 0 | 0.04 | 0.03 | 0.02 | 0 | 0.03 | 0.00 | 0.00 | 0.00 | 0 | 0.00 | 0.00 | 0.00 | 0 | 0.00 | 0 | 0.00 | 0.00 | |
| Ca7 | LM Prec | S | 0 | 1.00 | 1.69 | 10.20 | 0 | 86.26 | 0.07 | 0.02 | 0.53 | 10 | 20 | 10 | 10 | 0 | 620 | 0 | 1660 | 100 | |
| σ | | | 0 | 0.04 | 0.01 | 0.05 | 0 | 0.03 | 0.00 | 0.00 | 0.01 | 0.00 | 0.00 | 0.00 | 0.00 | 0 | 0.00 | 0 | 0.00 | 0.00 | |
| Ca5 | LM Prec | S | 0 | 0.83 | 1.11 | 9.20 | 0 | 88.12 | 0.03 | 0.02 | 0.32 | 0 | 0 | 10 | 10 | 0 | 1039 | 0 | 2598 | 100 | |
| σ | | | 0 | 0.05 | 0.03 | 0.03 | 0 | 0.03 | 0.01 | 0.00 | 0.00 | 0 | 0 | 0.00 | 0.00 | 0.00 | 0.00 | 0 | 0.00 | 0.00 | |
| Ca8 | LM Prec | S | 0 | 1.58 | 1.42 | 11.03 | 0 | 85.08 | 0.03 | 0.01 | 0.44 | 0 | 20 | 20 | 10 | 0 | 1269 | 0 | 2753 | 100 | |
| σ | | | 0 | 0.02 | 0.03 | 0.04 | 0 | 0.09 | 0.00 | 0.00 | 0.00 | 0 | 0.00 | 0.00 | 0.00 | 0 | 0.00 | 0 | 0.00 | 0.00 | |

Values in blue indicate significantly higher contents of the element in comparison with other samples.

| Sample | Chron | Type | Na ₂ O | MgO ₃ | Al ₂ O ₃ | SiO ₂ | K ₂ O | CaCO ₃ | TiO ₂ | MnO | Fe ₂ O ₃ | Co ₃ O ₄ | NiO | CuO | ZnO | Rb ₂ O | SrO | ZrO ₂ | BaCO ₃ | Sum | |
|--------|---------|------|-------------------|------------------|--------------------------------|------------------|------------------|-------------------|------------------|------|--------------------------------|--------------------------------|------|------|------|-------------------|------|------------------|-------------------|-----|--|
| | | | % (wt) | | | | | | | | | ppm (part per million) (wt) | | | | | | | | | |
| Ca29 | L Prec | F | 0.38 | 2.25 | 1.22 | 39.65 | 0 | 55.95 | 0.04 | 0 | 0.37 | 0 | 40 | 20 | 10 | 0 | 720 | 0 | 618 | 100 | |
| σ | | | 0.09 | 0.03 | 0.01 | 0.09 | 0 | 0.04 | 0.00 | 0 | 0.00 | 0 | 0.00 | 0.00 | 0.00 | 0 | 0.00 | 0 | 0.00 | | |
| Ca13 | E Clas | F | 0 | 2.90 | 1.71 | 10.05 | 0.07 | 84.51 | 0.06 | 0.02 | 0.50 | 0 | 20 | 20 | 30 | 10 | 850 | 0 | 888 | 100 | |
| σ | | | 0 | 0.01 | 0.01 | 0.05 | 0.00 | 0.12 | 0.00 | 0.00 | 0.00 | 0 | 0.00 | 0.00 | 0.00 | 0.00 | 0.00 | 0 | 0.00 | | |
| Ca19 | E Clas | F | 0 | 0.99 | 1.11 | 10.25 | 0 | 86.97 | 0.07 | 0.01 | 0.35 | 0 | 10 | 20 | 20 | 0 | 720 | 0 | 1737 | 100 | |
| σ | | | 0 | 0.01 | 0.01 | 0.04 | 0 | 0.03 | 0.00 | 0.00 | 0.00 | 0 | 0.00 | 0.00 | 0.00 | 0 | 0.00 | 0 | 0.00 | | |
| Ca22 | E Clas | F | 0 | 1.75 | 1.37 | 11.26 | 0 | 84.86 | 0.06 | 0.01 | 0.44 | 0 | 20 | 20 | 20 | 0 | 860 | 10 | 1634 | 100 | |
| σ | | | 0 | 0.01 | 0.00 | 0.06 | 0 | 0.15 | 0.00 | 0.00 | 0.00 | 0 | 0.00 | 0.00 | 0.00 | 0 | 0.00 | 0.00 | 0.00 | | |
| Ca24 | E Clas? | NA | 0 | 0.76 | 1.10 | 6.12 | 0 | 91.45 | 0.05 | 0.01 | 0.34 | 0 | 0 | 10 | 20 | 0 | 280 | 10 | 1390 | 100 | |
| σ | | | 0 | 0.01 | 0.00 | 0.04 | 0 | 0.14 | 0.00 | 0.00 | 0.00 | 0 | 0 | 0.00 | 0.00 | 0 | 0.00 | 0.00 | 0.00 | | |
| Ca17 | L Clas | WR | 0 | 0.40 | 0.73 | 3.64 | 0 | 94.84 | 0.03 | 0.01 | 0.23 | 0 | 0 | 10 | 10 | 0 | 390 | 0 | 836 | 100 | |
| σ | | | 0 | 0.02 | 0.01 | 0.02 | 0 | 0.05 | 0.00 | 0.00 | 0.00 | 0 | 0 | 0.00 | 0.00 | 0 | 0.00 | 0 | 0.00 | | |
| Ca26 | L Clas | WR | 0.50 | 2.00 | 3.84 | 21.08 | 0.15 | 70.62 | 0.12 | 0.02 | 1.46 | 20 | 120 | 20 | 30 | 10 | 660 | 30 | 1235 | 100 | |
| σ | | | 0.03 | 0.02 | 0.02 | 0.03 | 0.00 | 0.03 | 0.00 | 0.00 | 0.00 | 0.00 | 0.00 | 0.00 | 0.00 | 0.00 | 0.00 | 0.00 | 0.00 | | |
| Ca18 | L Clas | F | 0 | 1.00 | 1.01 | 13.45 | 0 | 83.84 | 0.03 | 0.01 | 0.32 | 0 | 10 | 10 | 10 | 0 | 500 | 0 | 2830 | 100 | |
| σ | | | 0 | 0.02 | 0.02 | 0.02 | 0 | 0.06 | 0.01 | 0.00 | 0.00 | 0 | 0.00 | 0.00 | 0.00 | 0 | 0.00 | 0 | 0.00 | | |
| Ca36 | L Clas | WR | 0 | 1.14 | 0.94 | 9.04 | 0 | 88.34 | 0.05 | 0.01 | 0.27 | 0 | 0 | 20 | 20 | 0 | 770 | 0 | 1338 | 100 | |
| σ | | | 0 | 0.01 | 0.01 | 0.04 | 0 | 0.07 | 0.00 | 0.00 | 0.00 | 0 | 0 | 0.00 | 0.00 | 0 | 0.00 | 0 | 0.00 | | |
| Ca3 | T Clas | F | 0 | 1.46 | 1.60 | 16.91 | 0 | 78.97 | 0.05 | 0.01 | 0.57 | 0 | 30 | 10 | 20 | 0 | 1219 | 0 | 3074 | 100 | |
| σ | | | 0 | 0.03 | 0.01 | 0.01 | 0 | 0.02 | 0.00 | 0.00 | 0.00 | 0 | 0.00 | 0.00 | 0.00 | 0 | 0.00 | 0 | 0.00 | | |
| Ca34 | T Clas | WR | 0.27 | 2.02 | 3.00 | 15.49 | 0.26 | 77.69 | 0.07 | 0.02 | 0.87 | 20 | 50 | 20 | 20 | 10 | 900 | 0 | 2122 | 100 | |
| σ | | | 0.09 | 0.02 | 0.01 | 0.08 | 0.00 | 0.11 | 0.00 | 0.00 | 0.00 | 0.00 | 0.00 | 0.00 | 0.00 | 0.00 | 0.00 | 0 | 0.00 | | |
| Ca33 | T Clas | F | 0 | 2.10 | 3.38 | 16.56 | 0.06 | 76.28 | 0.08 | 0.03 | 1.13 | 20 | 70 | 20 | 30 | 10 | 1550 | 20 | 2097 | 100 | |
| σ | | | 0 | 0.01 | 0.02 | 0.06 | 0.00 | 0.03 | 0.00 | 0.00 | 0.01 | 0.00 | 0.00 | 0.00 | 0.00 | 0.00 | 0.00 | 0.00 | 0.00 | | |
| Ca4 | T Clas | F | 0 | 2.27 | 3.12 | 17.85 | 0 | 75.13 | 0.08 | 0.02 | 1.07 | 10 | 70 | 30 | 30 | 10 | 1949 | 20 | 2508 | 100 | |
| σ | | | 0 | 0.02 | 0.02 | 0.12 | 0 | 0.21 | 0.00 | 0.00 | 0.01 | 0 | 0.00 | 0.00 | 0.00 | 0.00 | 0.00 | 0.00 | 0.00 | | |
| Ca27 | Modern | Geo | 0 | 0.87 | 0.77 | 2.95 | 0 | 94.78 | 0.02 | 0.01 | 0.20 | 0 | 0 | 10 | 20 | 0 | 1039 | 0 | 3010 | 100 | |
| σ | | | 0 | 0.01 | 0.01 | 0.02 | 0 | 0.09 | 0.01 | 0.00 | 0.00 | 0 | 0 | 0.00 | 0.00 | 0 | 0.00 | 0 | 0.00 | | |
| Ca28 | Modern | Geo | 0 | 0.77 | 0.93 | 2.87 | 0 | 95.03 | 0.03 | 0.01 | 0.27 | 0 | 0 | 10 | 20 | 10 | 440 | 0 | 425 | 100 | |
| σ | | | 0 | 0.02 | 0.02 | 0.02 | 0 | 0.34 | 0.00 | 0.00 | 0.00 | 0 | 0 | 0.00 | 0.00 | 0.00 | 0.00 | 0 | 0.00 | | |
| Ca Sas | Modern | Geo | 0 | 2.31 | 2.08 | 10.83 | 0 | 83.76 | 0.09 | 0.02 | 0.64 | 0 | 20 | 10 | 20 | 0 | 370 | 20 | 2238 | 100 | |
| σ | | | 0 | 0.03 | 0.02 | 0.06 | 0 | 0.04 | 0.00 | 0.00 | 0.00 | 0 | 0.00 | 0.00 | 0.00 | 0 | 0.00 | 0.00 | 0.00 | | |

Values in blue indicate significantly higher contents of the element in comparison with other samples.

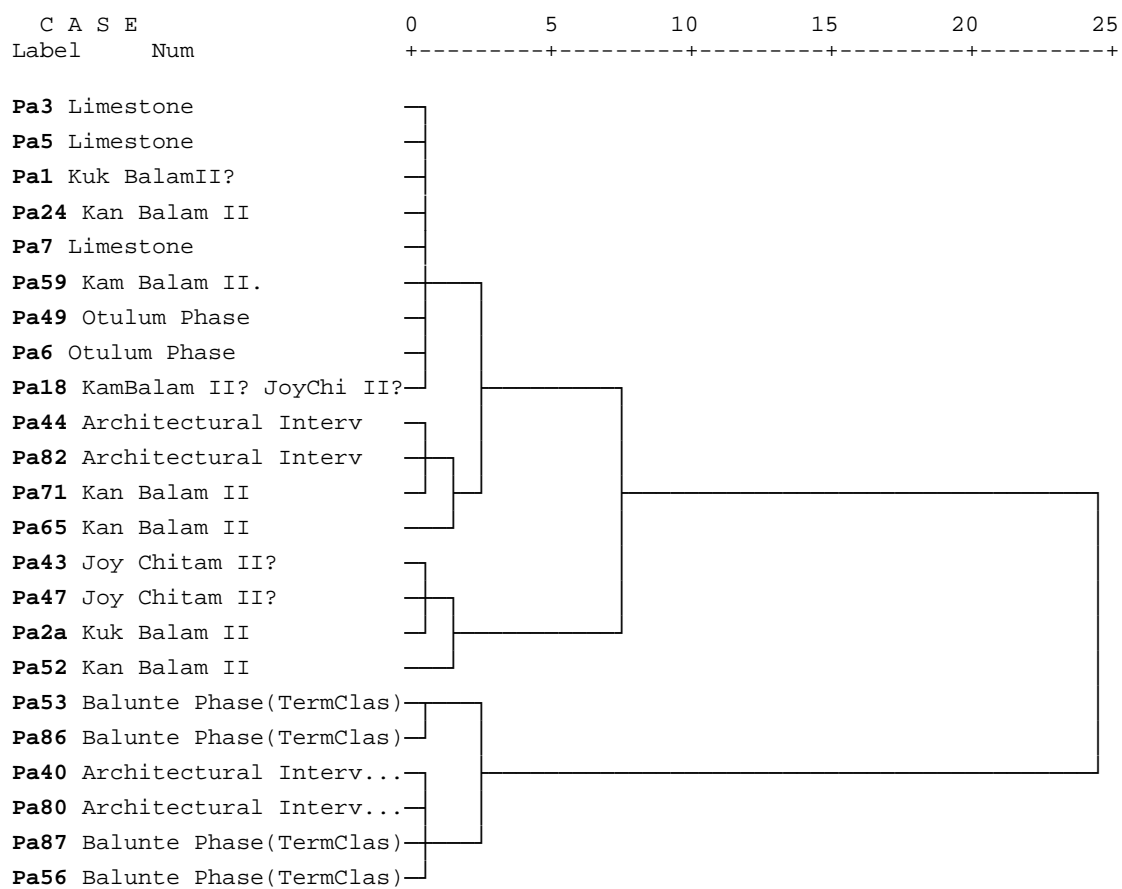
| Sample | Chron | Type | Na ₂ O | MgO ₃ | Al ₂ O ₃ | SiO ₂ | K ₂ O | CaCO ₃ | TiO ₂ | MnO | Fe ₂ O ₃ | Co ₃ O ₄ | NiO | CuO | ZnO | Rb ₂ O | SrO | ZrO ₂ | BaCO ₃ | Sum |
|--------|----------------|----------|-------------------|------------------|--------------------------------|------------------|------------------|-------------------|------------------|------|--------------------------------|--------------------------------|-----|------|------|-------------------|------|------------------|-------------------|-----|
| | | | % (wt) | | | | | | | | | ppm (part per million) (wt) | | | | | | | | |
| La15 | L Pre | F | 0 | 0.90 | 1.68 | 4.40 | 0 | 92.53 | 0.03 | 0.01 | 0.42 | 0 | 0 | 10 | 10 | 0 | 130 | 10 | 90 | 100 |
| σ | | | 0 | 0.02 | 0.02 | 0.01 | 0 | 0.03 | 0.00 | 0.00 | 0.01 | 0 | 0 | 0 | 0.00 | 0 | 0.00 | 0 | 0 | |
| La34 | L Pre | F (CSas) | 0 | 0.33 | 0.48 | 1.15 | 0 | 97.92 | 0.01 | 0 | 0.09 | 0 | 0 | 10 | 10 | 0 | 50 | 0 | 103 | 100 |
| σ | | | 0 | 0.00 | 0.00 | 0.00 | 0 | 0.04 | 0.00 | 0 | 0.00 | 0 | 0 | 0.00 | 0.00 | 0 | 0.00 | 0.00 | 0.00 | |
| La45 | E Clas | F | 0 | 0.62 | 1.18 | 2.25 | 0 | 95.67 | 0.02 | 0.01 | 0.23 | 0 | 0 | 20 | 20 | 0 | 90 | 10 | 103 | 100 |
| σ | | | 0 | 0.04 | 0.01 | 0.01 | 0 | 0.23 | 0.00 | 0.00 | 0.00 | 0 | 0 | 0.00 | 0.00 | 0 | 0.00 | 0.00 | 0.00 | |
| La44 | E Clas | F (CSas) | 0 | 0.68 | 2.38 | 5.86 | 0 | 90.52 | 0.05 | 0.02 | 0.47 | 0 | 0 | 10 | 20 | 0 | 90 | 20 | 103 | 100 |
| σ | | | 0 | 0.01 | 0.02 | 0.03 | 0 | 0.17 | 0.00 | 0.00 | 0.00 | 0 | 0 | 0.00 | 0.00 | 0 | 0.00 | 0.00 | 0.00 | |
| La48 | E Clas | S | 0 | 0.73 | 1.56 | 4.06 | 0 | 93.33 | 0.03 | 0.01 | 0.25 | 0 | 0 | 10 | 10 | 0 | 100 | 10 | 193 | 100 |
| σ | | | 0 | 0.02 | 0.02 | 0.02 | 0 | 0.04 | 0.00 | 0.00 | 0.00 | 0 | 0 | 0.00 | 0.00 | 0 | 0.00 | 0.00 | 0.00 | |
| La13 | L Clas | F (CSas) | 0 | 0.61 | 1.66 | 3.62 | 0 | 93.69 | 0.03 | 0.01 | 0.35 | 0 | 0 | 10 | 20 | 10 | 130 | 10 | 90 | 100 |
| σ | | | 0 | 0.03 | 0.02 | 0.01 | 0 | 0.03 | 0.00 | 0.00 | 0.00 | 0 | 0 | 0.00 | 0.00 | 0.00 | 0.00 | 0.00 | 0.00 | |
| La17 | L Clas | F | 0 | 0.57 | 1.62 | 3.24 | 0 | 94.14 | 0.03 | 0.01 | 0.37 | 0 | 0 | 10 | 10 | 0 | 70 | 10 | 142 | 100 |
| σ | | | 0 | 0.01 | 0.02 | 0.03 | 0 | 0.12 | 0.00 | 0.00 | 0.00 | 0 | 0 | 0.00 | 0.00 | 0 | 0.00 | 0.00 | 0.00 | |
| La3 | L Clas | F (CSas) | 0 | 0.75 | 2.10 | 6.16 | 0 | 90.48 | 0.04 | 0.01 | 0.43 | 0 | 0 | 10 | 20 | 10 | 80 | 30 | 116 | 100 |
| σ | | | 0 | 0.03 | 0.03 | 0.03 | 0 | 0.12 | 0.00 | 0.00 | 0.00 | 0 | 0 | 0.00 | 0.00 | 0.00 | 0.00 | 0.00 | 0.00 | |
| La6 | L Clas | F | 0 | 0.50 | 1.60 | 3.87 | 0 | 93.49 | 0.03 | 0.02 | 0.46 | 0 | 0 | 10 | 20 | 10 | 160 | 20 | 116 | 100 |
| σ | | | 0 | 0.01 | 0.03 | 0.02 | 0 | 0.11 | 0.00 | 0.00 | 0.00 | 0 | 0 | 0.00 | 0.00 | 0.00 | 0.00 | 0.00 | 0.00 | |
| La9 | L Clas/ T Clas | F | 0 | 0.25 | 1.03 | 2.35 | 0 | 96.03 | 0.02 | 0.01 | 0.28 | 0 | 0 | 10 | 10 | 0 | 130 | 10 | 103 | 100 |
| σ | | | 0 | 0.01 | 0.01 | 0.02 | 0 | 0.17 | 0.00 | 0.00 | 0.00 | 0 | 0 | 0.00 | 0.00 | 0 | 0.00 | 0.00 | 0.00 | |
| La10 | L Clas/ T Clas | F | 0 | 0.66 | 1.74 | 3.36 | 0 | 92.58 | 1.11 | 0.01 | 0.52 | 0 | 0 | 10 | 10 | 0 | 110 | 10 | 103 | 100 |
| σ | | | 0 | 0.02 | 0.01 | 0.02 | 0 | 0.07 | 0.00 | 0.00 | 0.00 | 0 | 0 | 0.00 | 0.00 | 0 | 0.00 | 0.00 | 0.00 | |
| La11 | T Clas/ E Post | F | 0 | 0.44 | 1.62 | 3.21 | 0 | 94.27 | 0.03 | 0.01 | 0.39 | 0 | 0 | 20 | 20 | 10 | 90 | 20 | 116 | 100 |
| σ | | | 0 | 0.01 | 0.01 | 0.02 | 0 | 0.07 | 0.00 | 0.00 | 0.00 | 0 | 0 | 0.00 | 0.00 | 0.00 | 0.00 | 0.00 | 0.00 | |
| La12 | T Clas/ E Post | F | 0 | 0.75 | 1.50 | 3.46 | 0 | 93.90 | 0.03 | 0.01 | 0.32 | 0 | 0 | 20 | 20 | 10 | 100 | 10 | 116 | 100 |
| σ | | | 0 | 0.02 | 0.01 | 0.04 | 0 | 0.02 | 0.00 | 0.00 | 0.00 | 0 | 0 | 0.00 | 0.00 | 0.00 | 0.00 | 0.00 | 0.00 | |

Values in blue indicate significantly higher contents of the element in comparison with other samples.

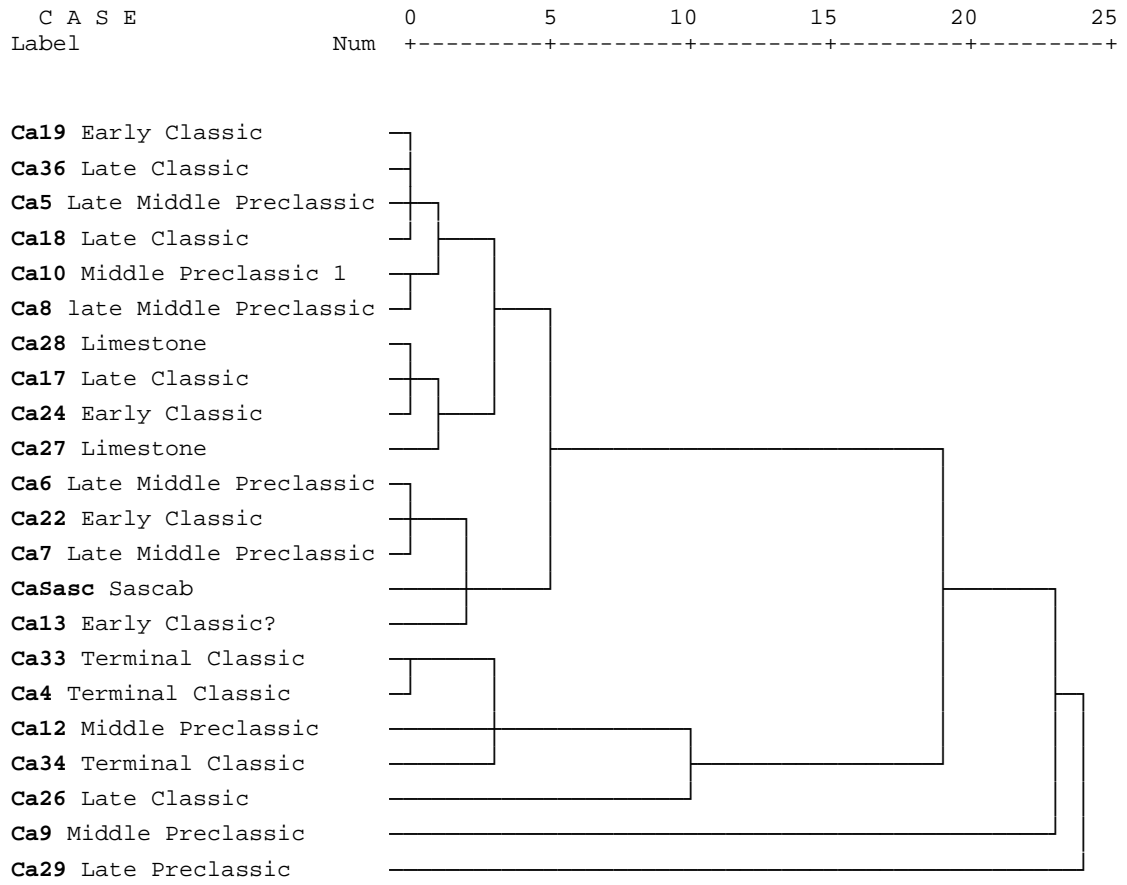
| Sample | Chron | Type | Na ₂ O | MgO ₃ | Al ₂ O ₃ | SiO ₂ | K ₂ O | CaCO ₃ | TiO ₂ | MnO | Fe ₂ O ₃ | Co ₃ O ₄ | NiO | CuO | ZnO | Rb ₂ O | SrO | ZrO ₂ | BaCO ₃ | Sum | |
|---------|---------------|-------------|-------------------|------------------|--------------------------------|------------------|------------------|-------------------|------------------|------|--------------------------------|--------------------------------|-----|------|------|-------------------|------|------------------|-------------------|------|--|
| | | | % (wt) | | | | | | | | | ppm (part per million) (wt) | | | | | | | | | |
| | E Pos/ M Post | F (Com Sas) | | | | | | | | | | | | | | | | | | | |
| La2 | | | 0 | 0.66 | 0.98 | 2.18 | 0 | 95.93 | 0.02 | 0.01 | 0.19 | 0 | 0 | 10 | 10 | 0 | 120 | 10 | 116 | 100 | |
| σ | | | 0 | 0.01 | 0.01 | 0.01 | 0 | 0.05 | 0.00 | 0.00 | 0.00 | 0 | 0 | 0.00 | 0.00 | 0 | 0.00 | 0.00 | 0.00 | 0.00 | |
| La49 | L Post | F | 0 | 0.73 | 1.23 | 3.60 | 0 | 94.13 | 0.03 | 0.01 | 0.24 | 0 | 0 | 10 | 10 | 0 | 150 | 10 | 90 | 100 | |
| σ | | | 0 | 0.01 | 0.01 | 0.01 | 0 | 0.12 | 0.00 | 0.00 | 0.00 | 0 | 0 | 0.00 | 0.00 | 0 | 0.00 | 0.00 | 0.00 | 0.00 | |
| La36b | L Post? | WR | 0 | 0.50 | 3.67 | 6.03 | 0 | 88.58 | 0.08 | 0.02 | 1.08 | 20 | 0 | 10 | 20 | 0 | 170 | 30 | 116 | 100 | |
| σ | | | 0 | 0.01 | 0.03 | 0.04 | 0 | 0.15 | 0.00 | 0.00 | 0.00 | 0.00 | 0 | 0.00 | 0.00 | 0.00 | 0.00 | 0.00 | 0.00 | 0.00 | |
| La36a | L Post? | WR | 0 | 0.88 | 6.54 | 12.42 | 0 | 78.20 | 0.15 | 0.07 | 1.70 | 0 | 0 | 30 | 50 | 20 | 120 | 60 | 142 | 100 | |
| σ | | | 0 | 0.01 | 0.04 | 0.05 | 0 | 0.08 | 0.00 | 0.00 | 0.01 | 0 | 0 | 0.00 | 0.00 | 0.00 | 0.00 | 0.00 | 0.00 | 0.00 | |
| La23 | S Col | Geo | 0 | 0.95 | 1.37 | 4.01 | 0.10 | 93.34 | 0.01 | 0.01 | 0.19 | 0 | 0 | 10 | 10 | 20 | 70 | 10 | 64 | 100 | |
| σ | | | 0 | 0.03 | 0.02 | 0.01 | 0.01 | 0.06 | 0.00 | 0.00 | 0.00 | 0 | 0 | 0.00 | 0.00 | 0.00 | 0.00 | 0.00 | 0.00 | 0.00 | |
| La19 | S Col | F | 0 | 0.63 | 3.49 | 6.47 | 0 | 88.39 | 0.07 | 0.02 | 0.89 | 0 | 0 | 20 | 30 | 0 | 110 | 20 | 270 | 100 | |
| σ | | | 0 | 0.02 | 0.01 | 0.01 | 0 | 0.02 | 0.00 | 0.00 | 0.00 | 0 | 0 | 0.00 | 0.00 | 0 | 0.00 | 0.00 | 0.00 | 0.00 | |
| La20 | S Col | JM | 0 | 0.76 | 2.78 | 6.00 | 0.06 | 89.39 | 0.07 | 0.05 | 0.86 | 0 | 0 | 20 | 30 | 10 | 110 | 30 | 77 | 100 | |
| σ | | | 0 | 0.01 | 0.03 | 0.02 | 0.01 | 0.13 | 0.00 | 0.00 | 0.01 | 0 | 0 | 0.00 | 0.00 | 0.00 | 0.00 | 0.00 | 0.00 | 0.00 | |
| La21 | S Col | WR | 0 | 0.88 | 1.78 | 4.59 | 0.02 | 92.17 | 0.04 | 0.03 | 0.46 | 0 | 0 | 20 | 20 | 10 | 100 | 10 | 116 | 100 | |
| σ | | | 0 | 0.03 | 0.02 | 0.00 | 0.00 | 0.02 | 0.00 | 0.00 | 0.00 | 0 | 0 | 0.00 | 0.00 | 0.00 | 0.00 | 0.00 | 0.00 | 0.00 | |
| La Cret | Modern | L | 0 | 0.00 | 0.37 | 0.60 | 0 | 98.93 | 0 | 0 | 0.09 | 0 | 0 | 10 | 10 | 0 | 80 | 0 | 0 | 100 | |
| σ | | | 0 | 0 | 0.01 | 0.01 | 0 | 0.21 | 0 | 0 | 0.00 | 0 | 0 | 0.00 | 0.00 | 0 | 0.00 | 0 | 0 | 0 | |
| La Sas1 | Modern | Sas | 0 | 0.39 | 0.92 | 2.29 | 0 | 96.17 | 0.02 | 0 | 0.19 | 0 | 0 | 10 | 20 | 0 | 70 | 10 | 51 | 100 | |
| σ | | | 0 | 0.01 | 0.04 | 0.02 | 0 | 0.07 | 0.00 | 0 | 0.00 | 0 | 0 | 0.00 | 0.00 | 0 | 0.00 | 0.00 | 0.00 | 0.00 | |
| La Sas2 | Modern | Sas | 0 | 0.31 | 0.40 | 0.78 | 0 | 98.41 | 0 | 0 | 0.09 | 0 | 0 | 10 | 10 | 0 | 50 | 0 | 64 | 100 | |
| σ | | | 0 | 0.01 | 0.01 | 0.01 | 0 | 0.24 | 0 | 0 | 0.00 | 0 | 0 | 0.00 | 0.00 | 0 | 0.00 | 0 | 0.00 | 0.00 | |

Values in blue indicate significantly higher contents of the element in comparison with other samples.

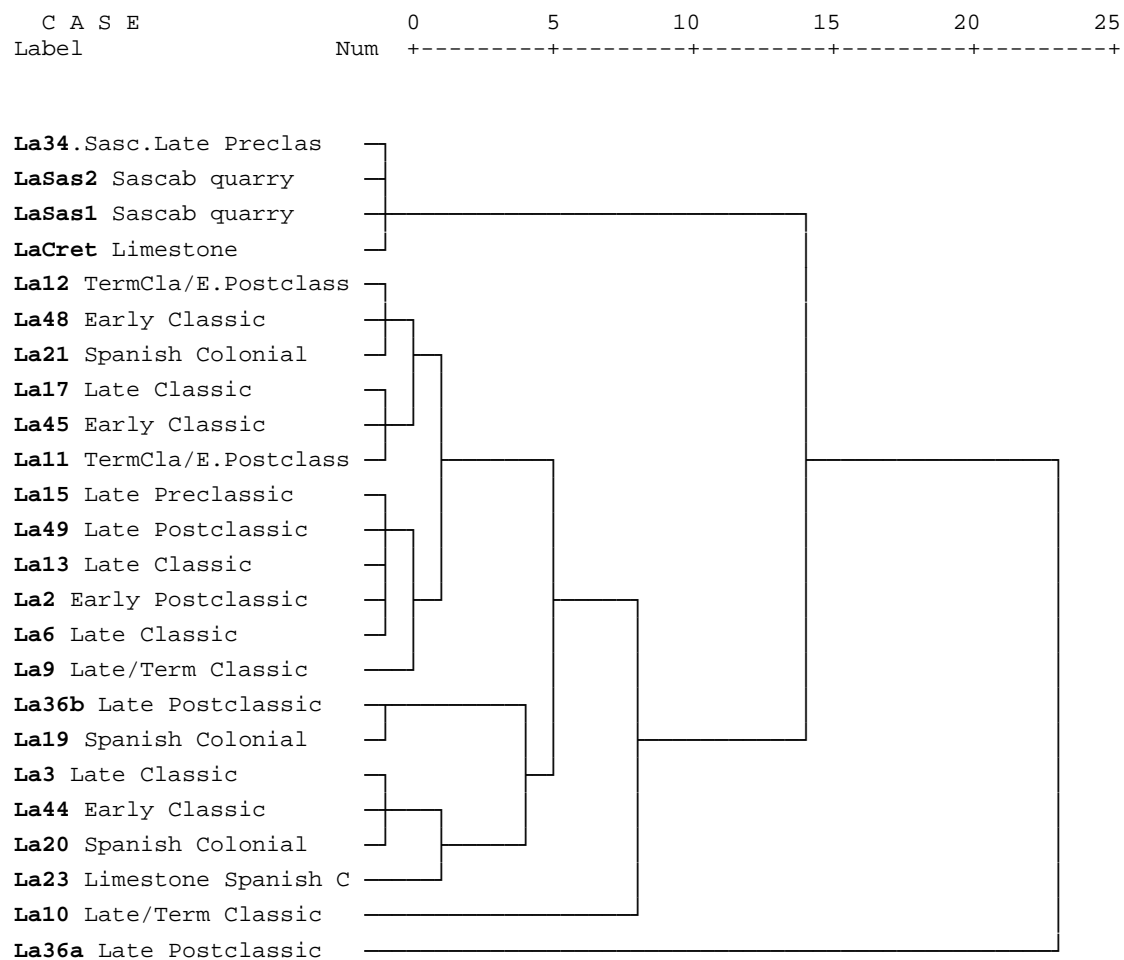
Palenque (bulk elemental data obtained by XRF)



Cluster analysis Calakmul (bulk elemental data obtained by XRF)



Cluster analysis Lamanai (bulk elemental data obtained by XRF)



A.6.4. Principal Component Analyses of XRF data

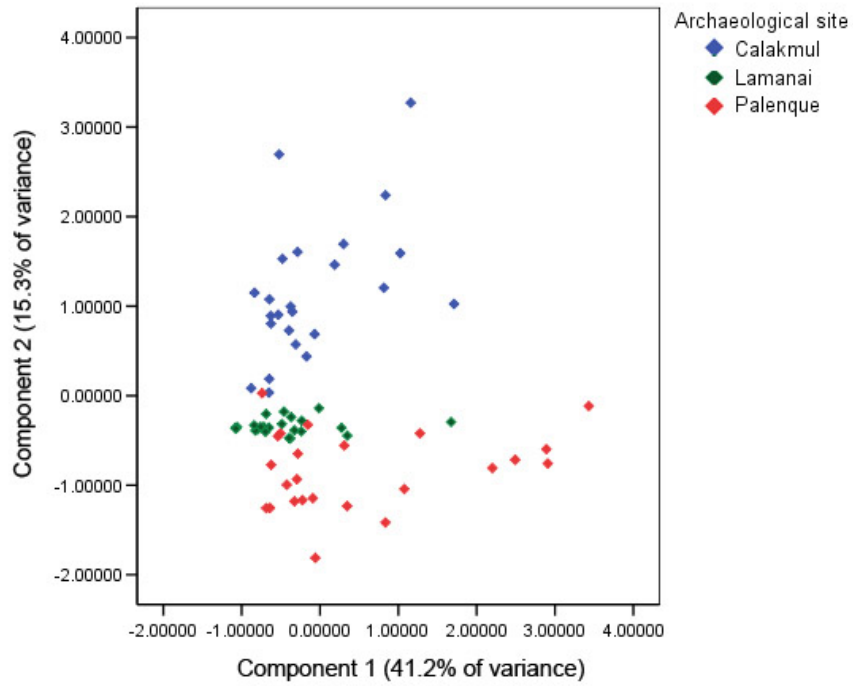


Fig. A.6.4.1. PCA analysis of compositional variation according to sites.

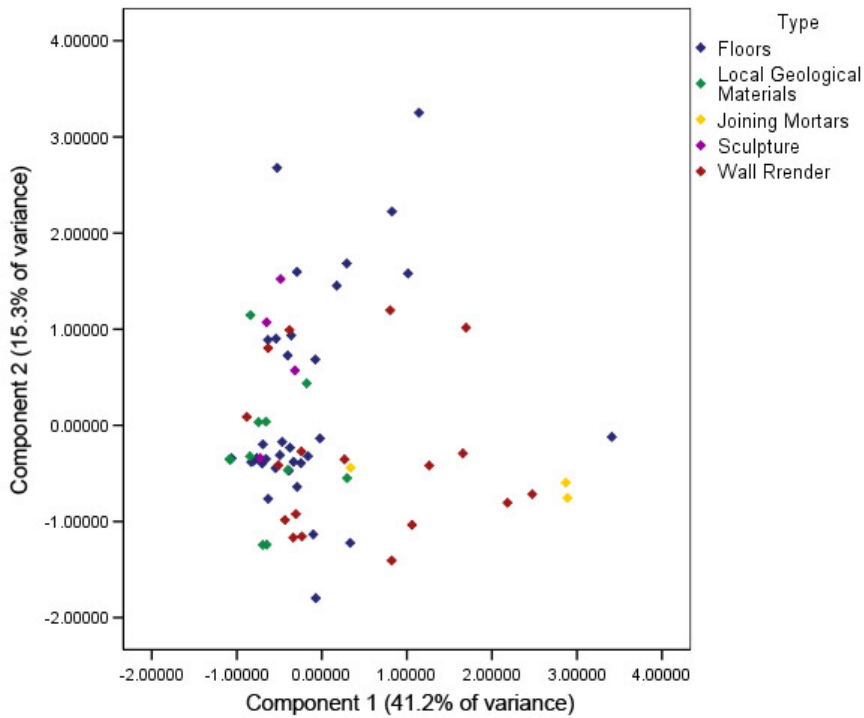


Fig. A.6.4.2. PCA analysis of compositional variation according to type of plaster (all sites).

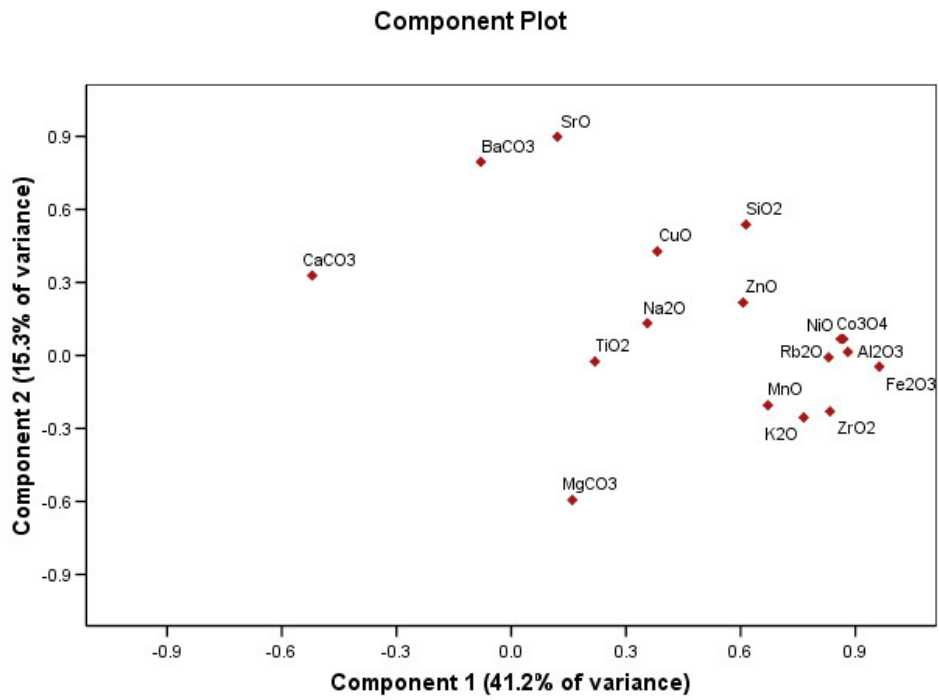


Fig. A.6.4.3. Component plot of compositional variation (all sites).

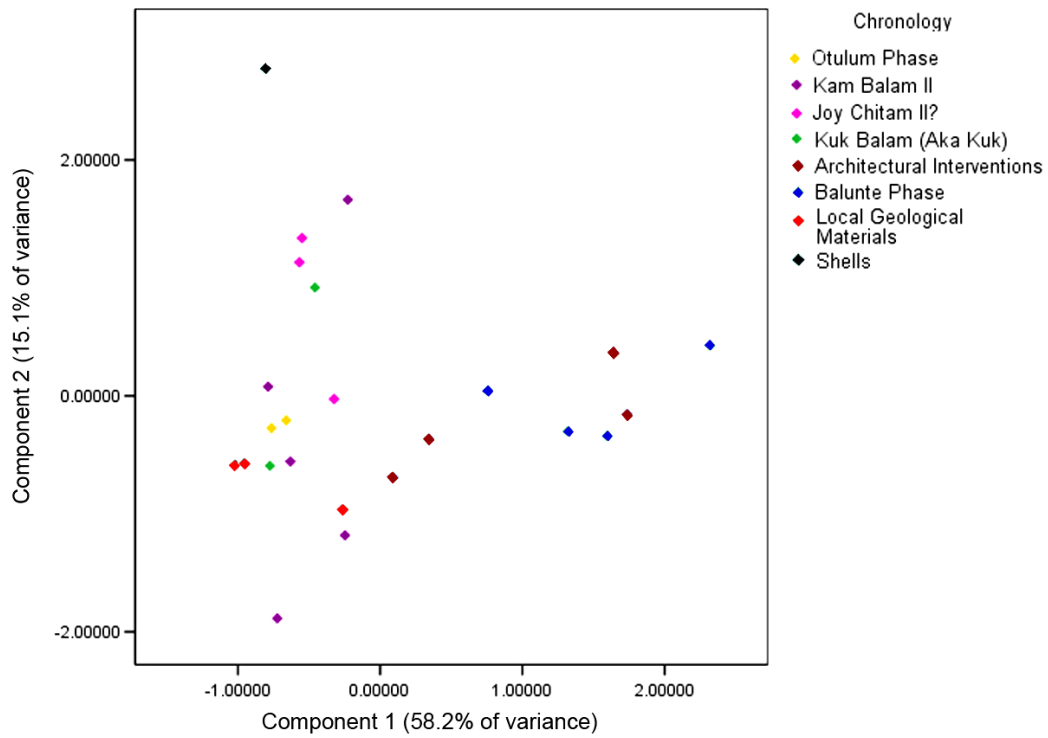


Fig. A.6.4.4. PCA analysis of compositional variation according to chronology (Palenque)

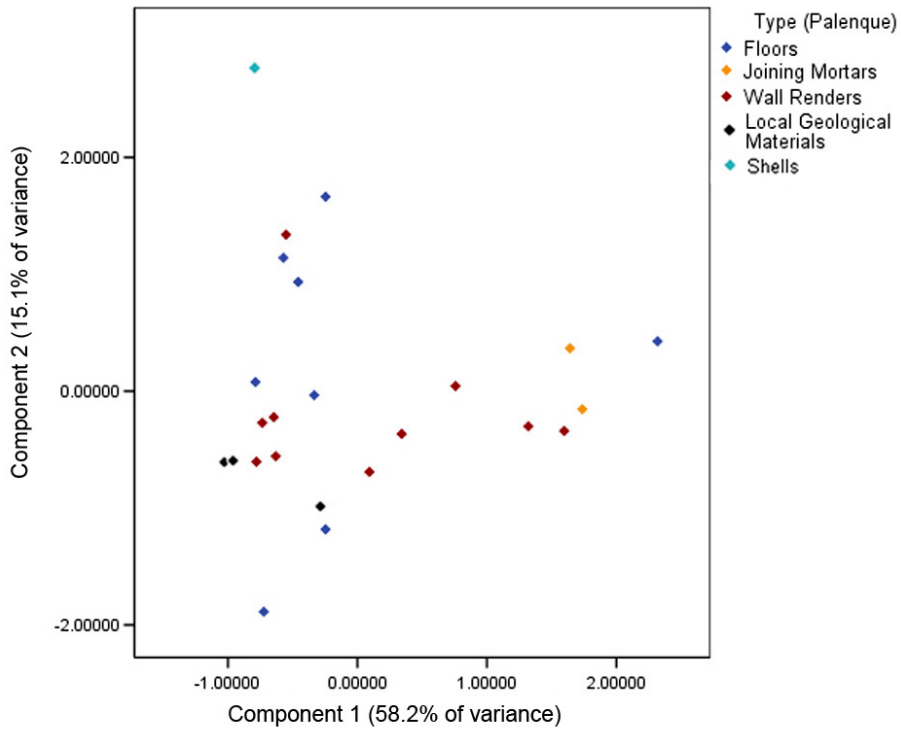


Fig. A.6.4.5. PCA analysis of compositional variation according to type (Palenque)

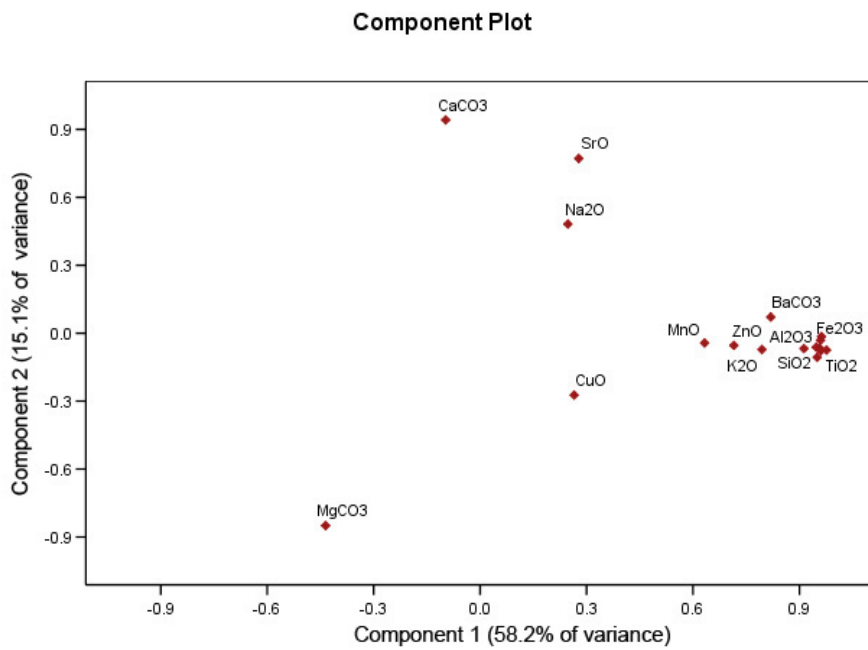


Fig. A.6.4.6. Component plot of compositional variation (Palenque).

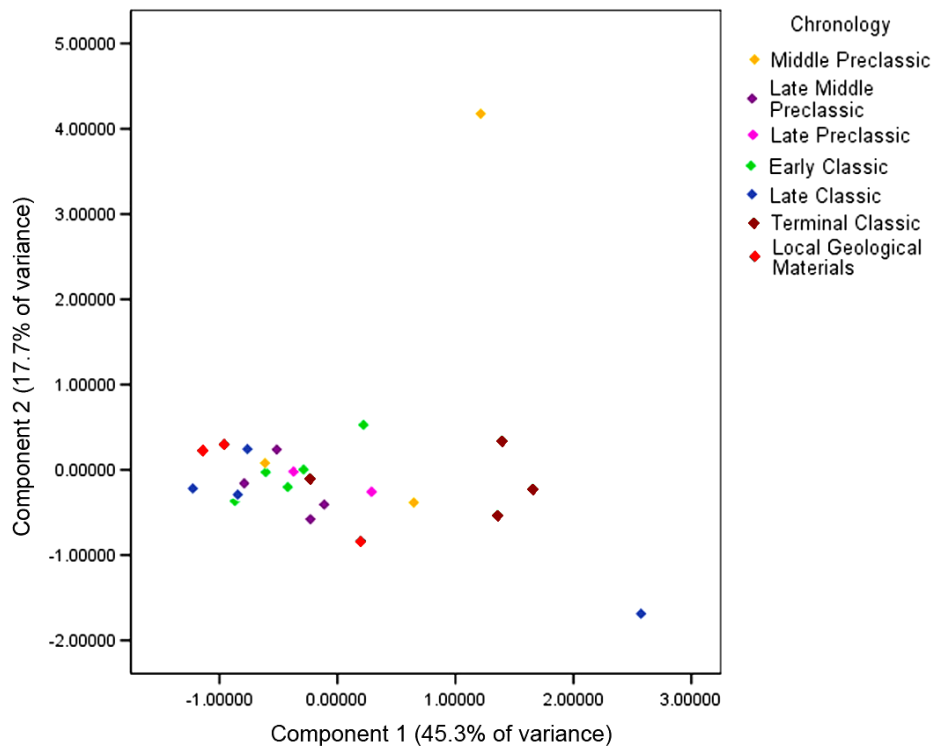


Fig. A.6.4.7. PCA analysis of compositional variation according to chronology (Calakmul).

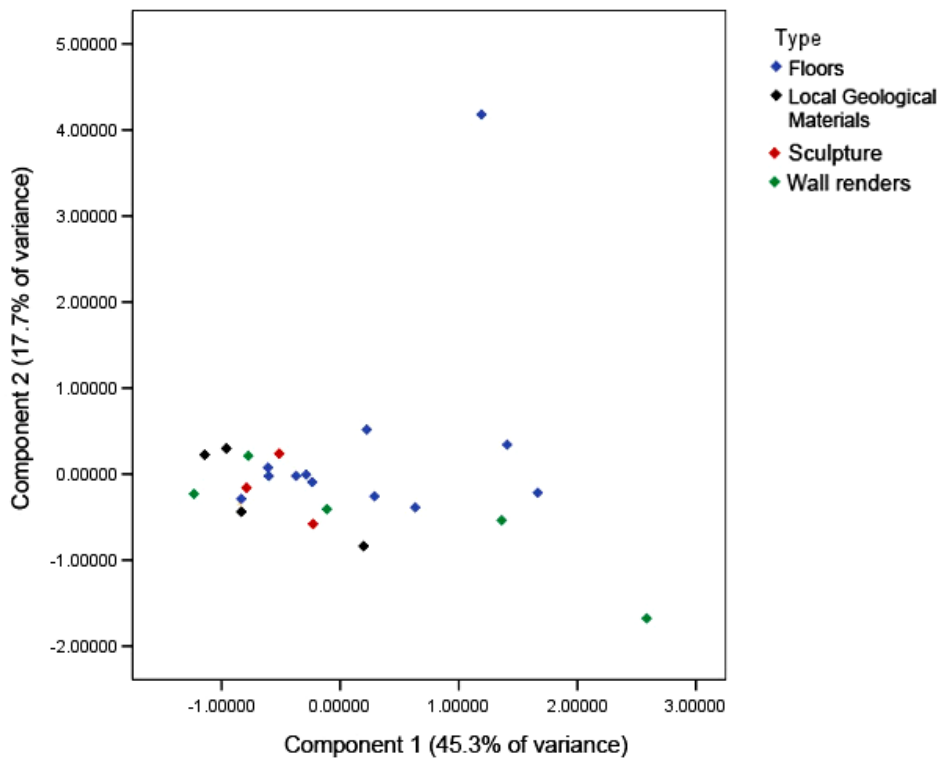


Fig. A.6.4.8. PCA analysis of compositional variation according to type (Calakmul)

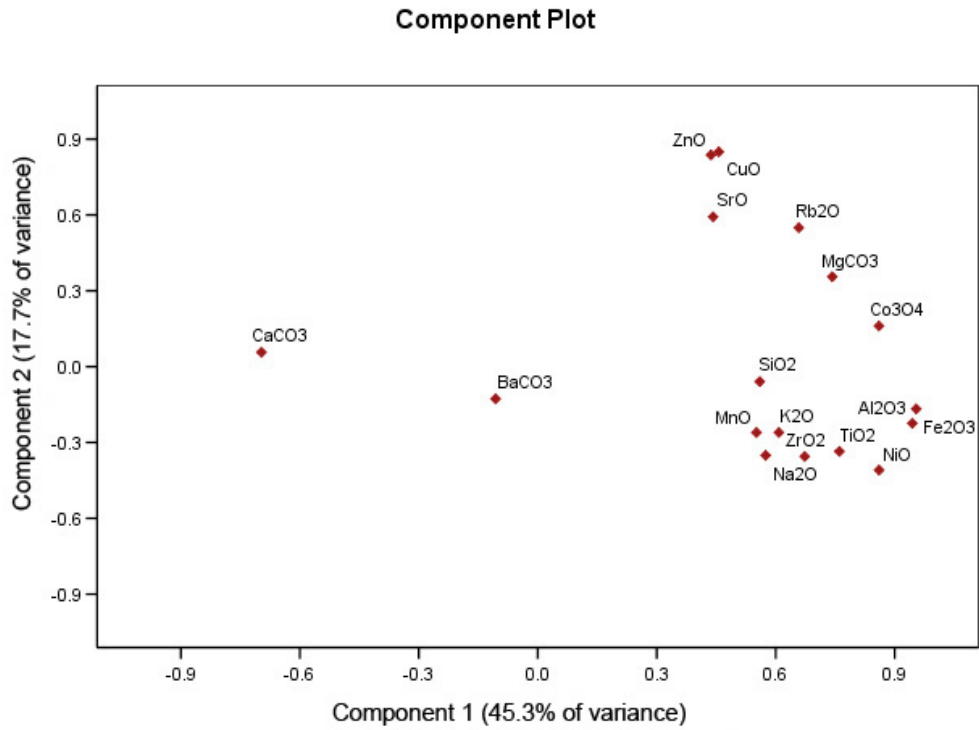


Fig. A.6.4.9. Component plot of compositional variation (Calakmul).

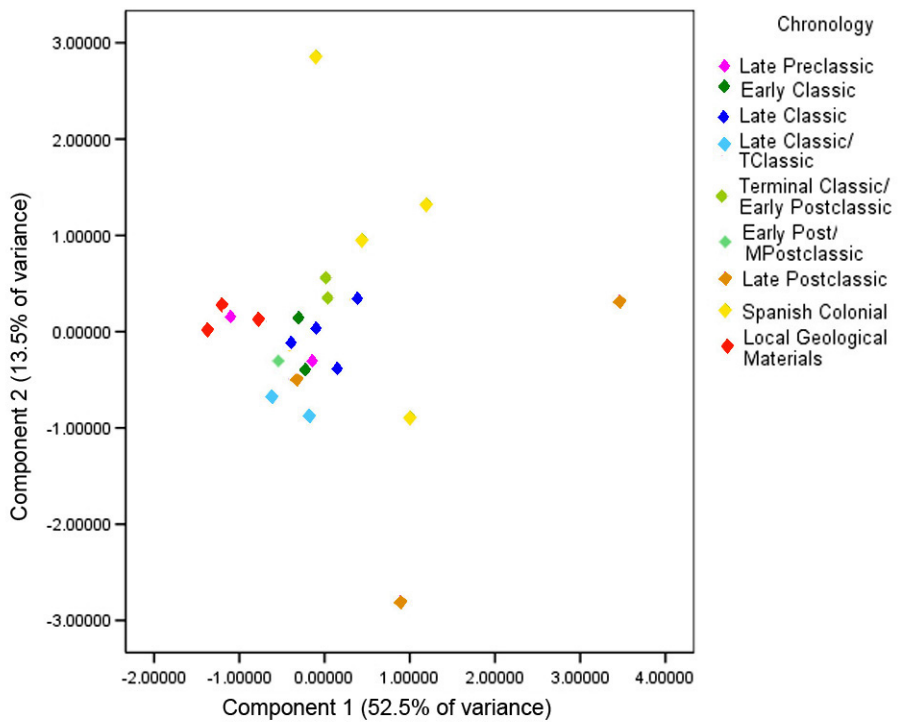


Fig. A.6.4.10 PCA analysis of compositional variation according to chronology (Lamanai).

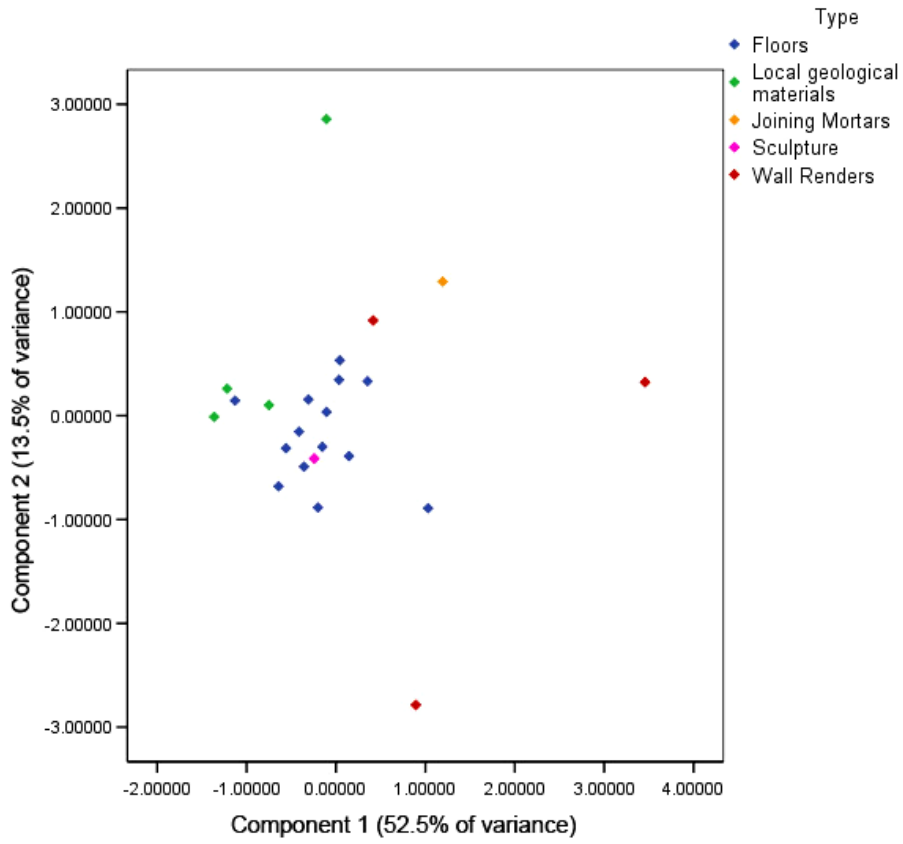


Fig. A.6.4.11. PCA analysis of compositional variation according to type (Lamanai).

Component Plot

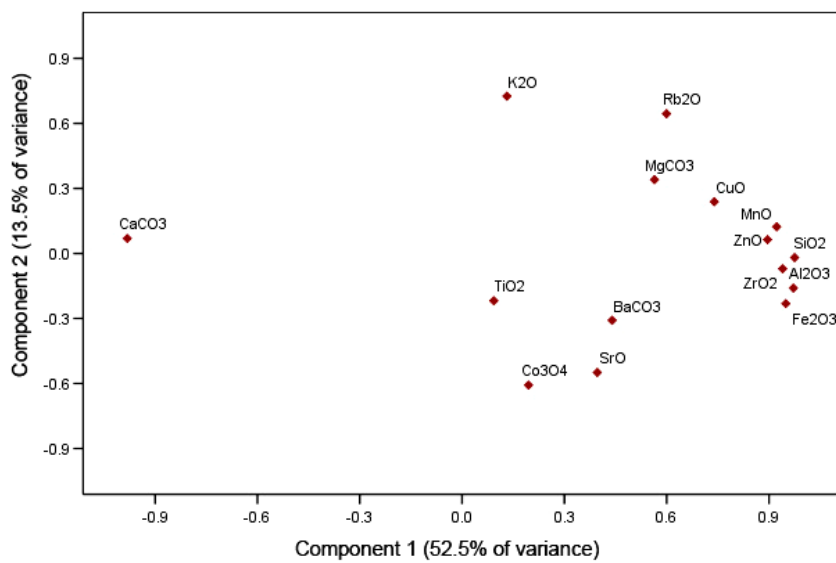
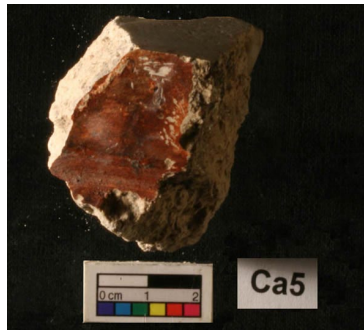
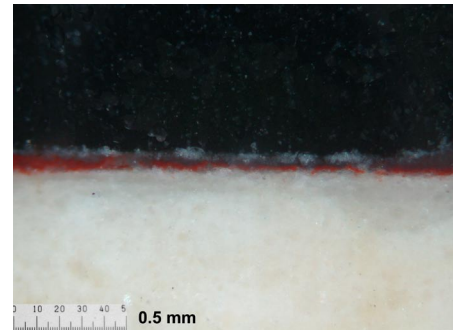


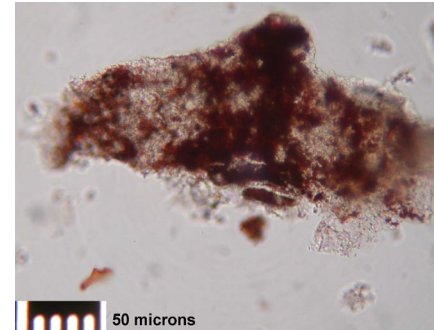
Fig. A.6.4.12. Component plot of compositional variation (Lamanai).



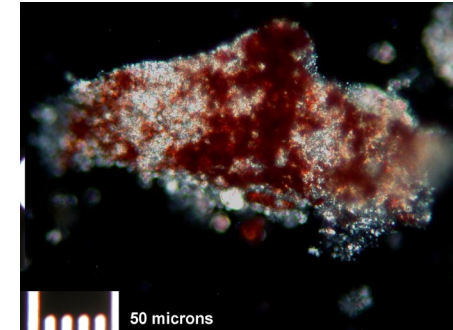
Ca5. Red paint layer.



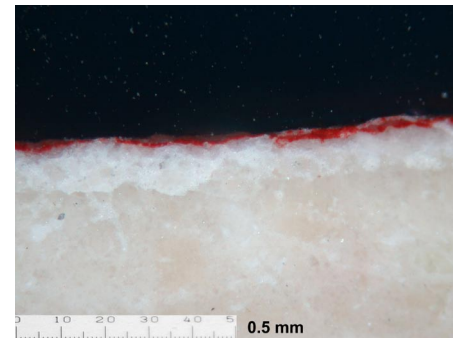
Ca5. Red paint layer over limewash. (hematite) RXPL. Scale bar: 0.5 mm.



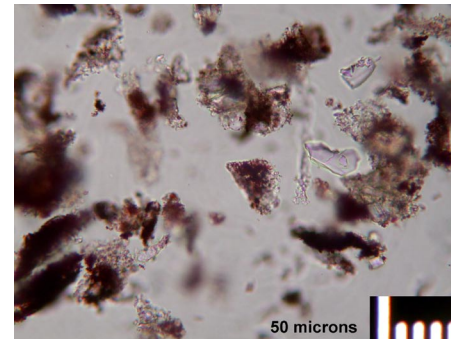
Ca5. Particle with dark red areas. Birrefringence of red particles can be observed in the edges. Characterization: hematite. Left: PPL. Right: XPL. Scale bar: 50 microns.



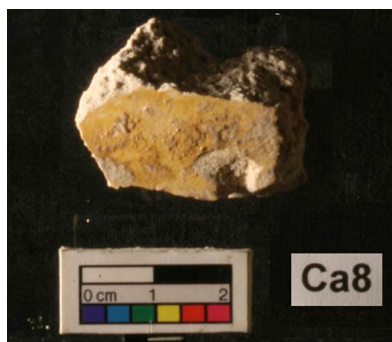
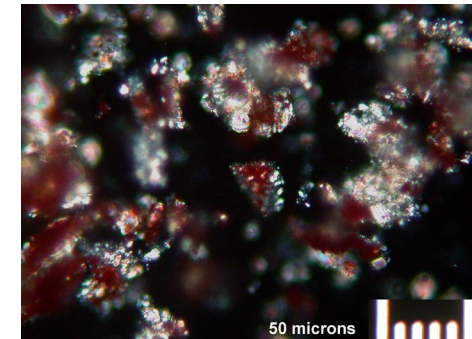
Ca7. Red paint layer. Scale bar: 2 cms.



Ca7. Red paint layer over limewash. RXPL. Scale bar: 0.5 mm.



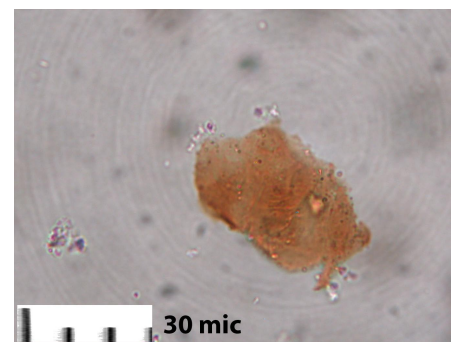
Ca7. Particles with dark red areas; small particles of birefringent red. Isotropic phases. Characterization: hematite. Left: PPL. Right: XPL/ Scale bar: 50 microns.



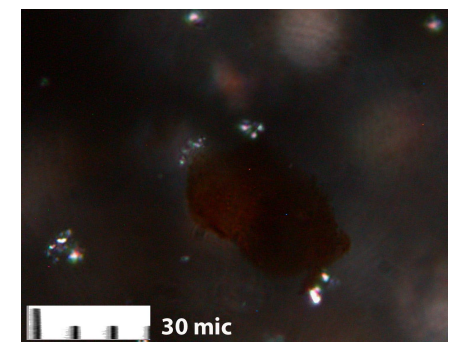
Ca8. Yellow paint layer. Scale bar: 2 cms.

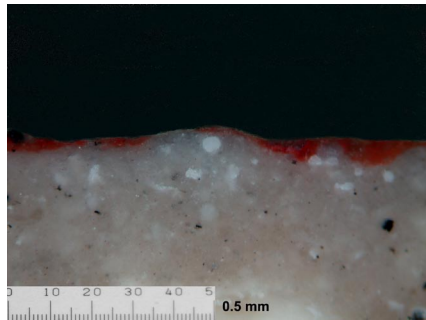


Ca8. Translucent pale yellow layer with orange-yellow particles. Scale bar: 0.5 mm

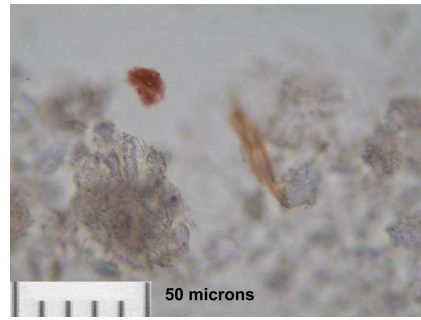


Ca8. Yellow isotropic particle that suggests the production of an organic pigment. Small birefringent particles can also be seen in other areas of the sample. Characterization: unknown. Likely goethite and organic pigment. Left: PPL, right: XPL. Scale bar: 30 microns.

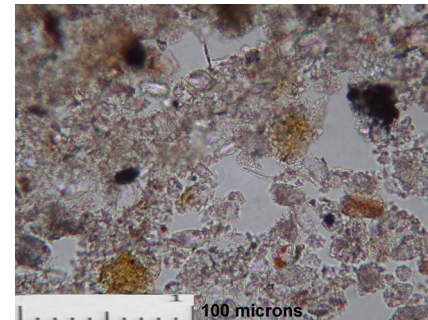




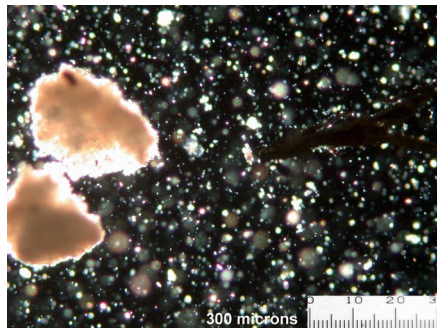
Ca14. Red paint layer. Scale bar: 0.5 mm. RXPL.



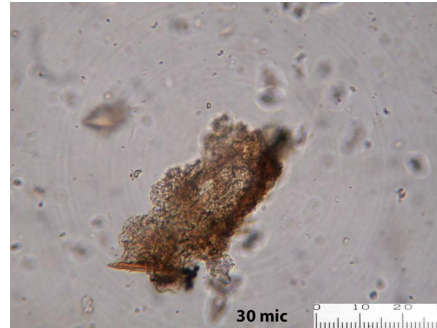
Ca14. Red and yellow particles. Scale bar: 50 microns. PPL.



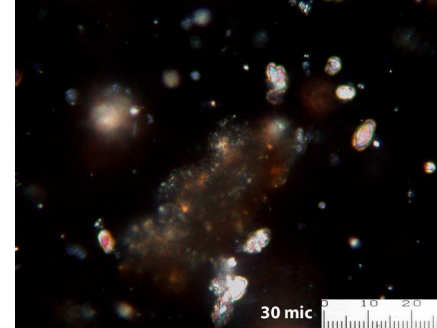
Ca14. Red, yellow and black particles. Characterization: red ochre. PPL. Scale bar: 100 microns.



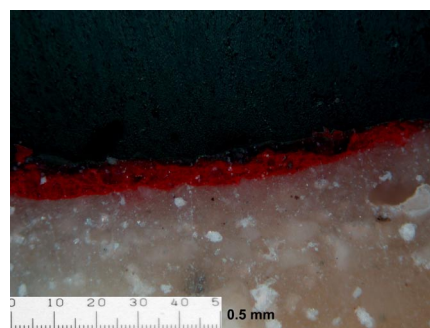
Ca15. Yellow-stained carbonate particles. XPL. Scale bar: 300 microns



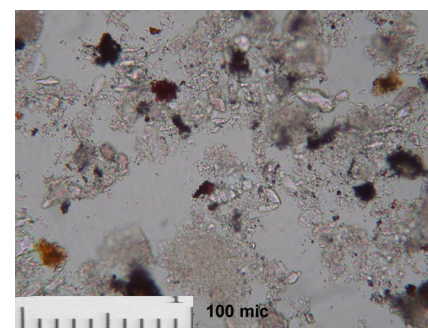
Ca15. Yellow and orange isotropic particles. Small birefringent particles can also be seen in other areas of the sample. Characterization: unknown. Likely goethite and organic pigment. Left: PPL, scale bar: 30 microns. Right: XP, scale bar: 30 microns.



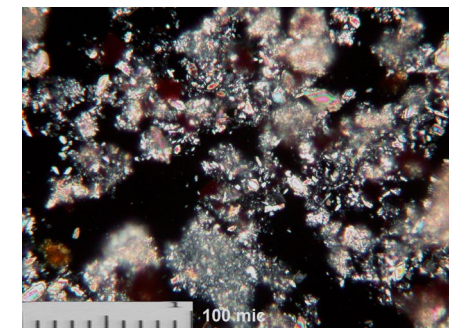
Ca23. Red paint layer. Scale bar: 2 cms.



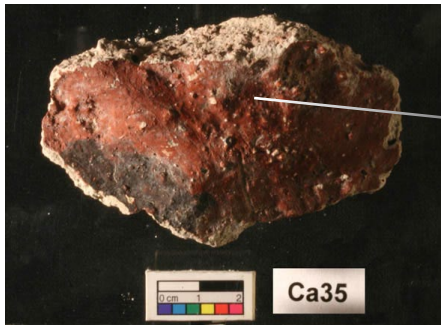
Ca23. Dark red over medium red paint layer. Scale bar: 0.5 mm. RXPL.



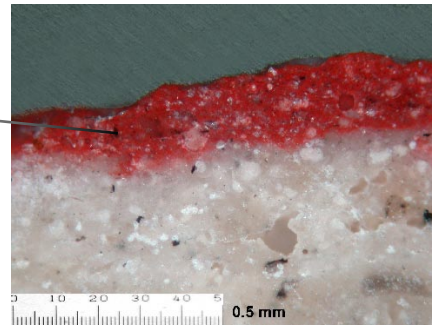
Ca23. Red, yellow and black particles. Scale bar: 100 microns. Left: PPL. Right: XP.



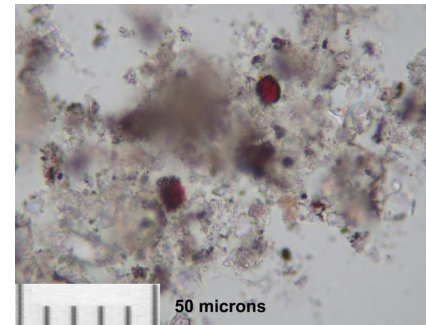
Ca23. Dark red (birrefringent), yellow and black particles. Identification: red ochre. Left: PPL. Right: XP.



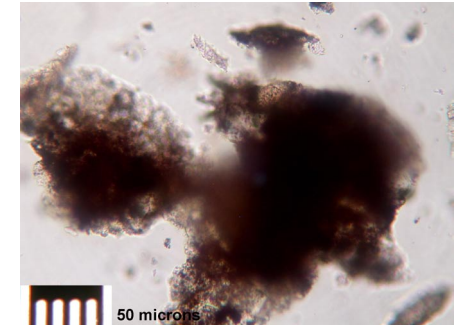
Ca35. Black and red paint layers.
Scale bar: 2 cms.



Ca35. Red paint layer. RXPL.



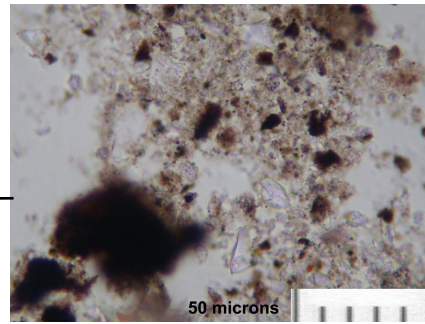
Ca35. Red and yellow particles. PPL.
Scale bar: 50 microns. PPL.



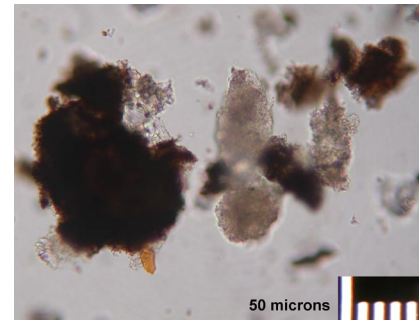
Ca35. Pure dark red particle. Characterization: hematite. PPL. Scale bar: 500 microns.



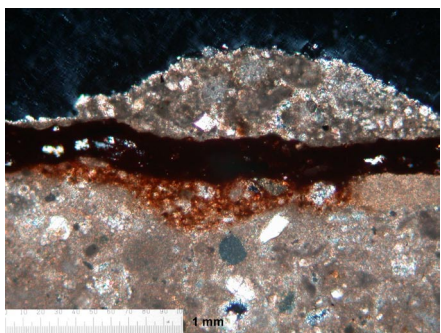
Ca35. Black and red paint layers.
Scale bar: 2 cms.



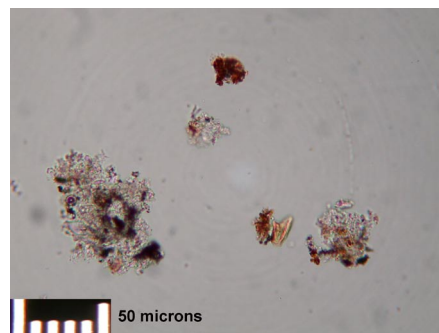
Ca35. Black and dark brown particles. PPL. Scale bar: 50 microns.



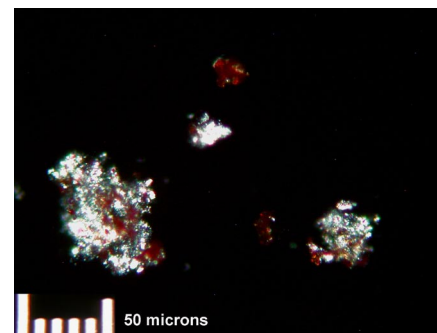
Ca35. Black and dark brown particles with impurities (isotropic non-pleochroic yellow areas). PPL. Scale bar: 50 microns. Characterization: graphite.

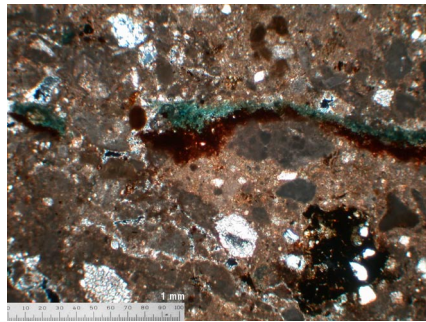


La6. Red over orange paint layers.
XPL. Scale bar: 1 mm.

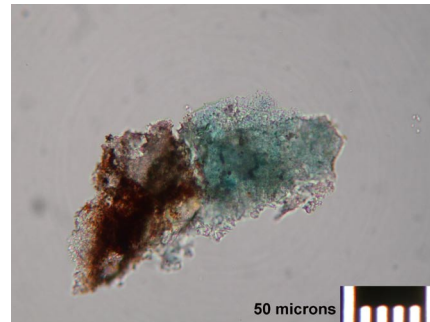


La6. Red, yellow and brown birrefringent particles. Characterization: red ochre. Left: PPL. Right: XPL. Scale bar: 50 microns.

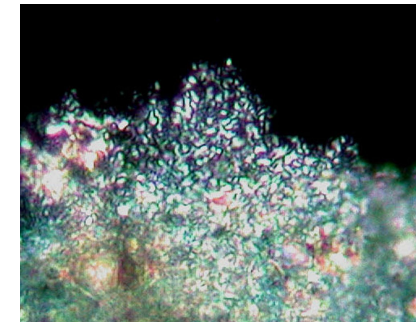
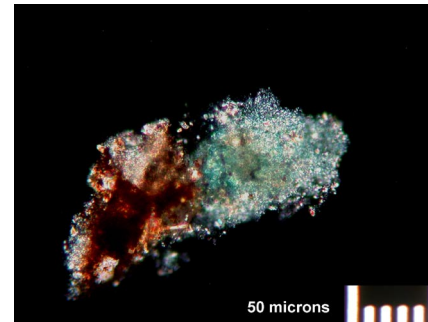




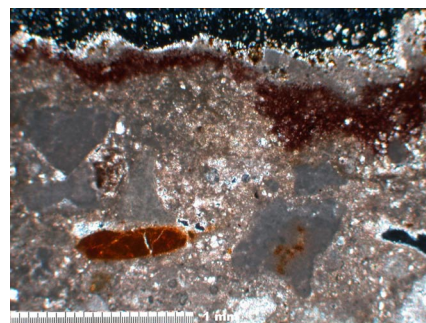
La6. Fragments of recycled plaster with paint layers. XPL. Scale bar: 1 mm.



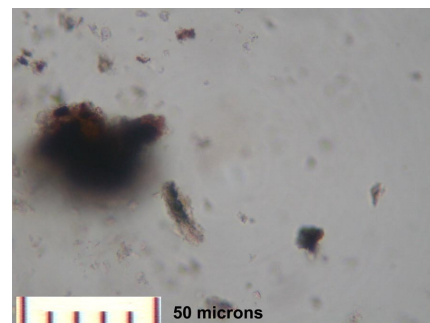
La6. Paint layers from recycled plaster. Blue layer: translucent blue fixed in clay mineral. Characterization: Maya blue. Red layer: dark red with orange hues. Likely hematite. Left: PPL. Right: XPL. Scale bar: 50 microns.



Zoom of the clay mineral in substrate of blue layer. Width of picture: ca. 50 microns.



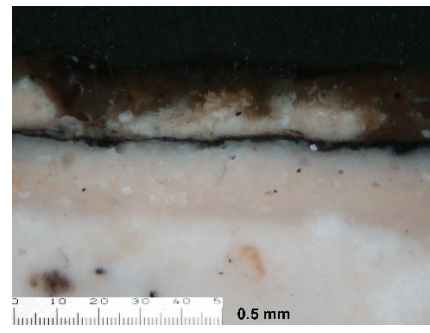
La25. Red paint layer. Scale bar: 1 mm. XPL.



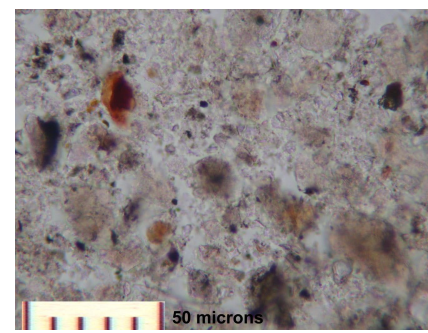
La25. Lump of red birefringent particles. Likely hematite. PPL. Scale bar: 50 microns.



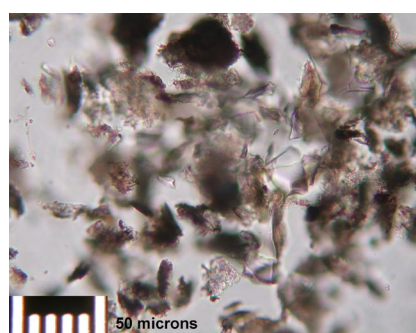
Pa41. Scale bar: 2 cms.



Pa41. Black paint layer with and application of limewash.



Pa41. Red and black particles. Scale bar: 50 microns.



Pa41. Dark brown particles with impurities. Isotropic phases. Characterisation: Graphite with fragments of glass. PPL. Scale: 50 microns.

| Sample | Peaks detected in samples | Hematite | | | | | | Graphite | | Calcite | | | Observations |
|-------------------|--|-----------------------------|-----------------------------|-----------------------------|-----------------------------|-----------------------------|-----------------------------|--|-------------------------------------|----------------------------------|-----------------------------|------------------------------|--|
| | | 226 (Sendova et al 2005) | 246 (Sendova et al 2005) | 294 (Sendova et al 2005) | 411 (Sendova et al 2005) | 505 (Sendova et al 2005) | 612 (Sendova et al 2005) | 1550-1580 G line (crystalline graphite) (Vidano and Fischbach 1978) | 1300 (Vidano and Fischbach 1978) | 288 (Gunasekaran et al 2006). | 712 (Sendova et al 2005) | 1086 (Sendova et al 2005) | |
| Ca5 Red paint | 226*, 246*, 409, 262, 263, 283, 301, 340, | * | * | *(283) | *? | | | | | | | | Weak peaks but 226 and 246 are clear. |
| Ca7 Red paint I | 291, 320, 408*, 415, 420, 425, 608, 696, 711, 1086* | | | *(291) | *(408) | | * | | | | * | * | Very strong peaks at 408 and 1086. |
| Ca8 Yellow paint | 250,265,279,282*,293,318,332,336,332,390,408*,1086*, 1772* | | | * | *(408) | | | | | *(282) | | * | Many peaks between 200 and 400. Organic dye? |
| Ca14 Red paint | 225, 247, 292, 409, 495, 609, 711, 861, 1087 | * | * | * | * | (495?) | * | | | | * | * | |
| Ca23 Red paint | 226, 293, 409, 1086, 938? 582? | * | | * | * | | | | | | | * | |
| Ca35 red paint | 225, 285, 292, 390, 411, 1005, 1086. | * | | * | * | | | | | * | | * | |
| Ca35 black paint | 1360, 1560. | | | | | | | * | | | | | |
| Pa41 Black layer | 1300, 1555. | | | | | | | * | | | | | |
| Pa75 Black layer | 370?, 1085, 1270?, 1560?, 1751? | | | | | | | * | * | | | | |
| Pa 85 Black paint | 1086, 1280, 1560 | | | | | | | * | * | | | * | |

Table B.2.1. Pigment identification.

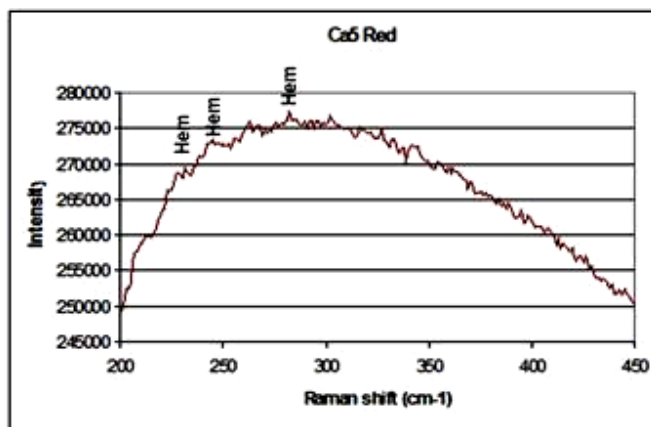


Fig. B.2.1. Sample Ca5. Red paint layer with some of the characteristic peaks of hematite (226, 246, 283) and unidentified peaks (262 and 300)

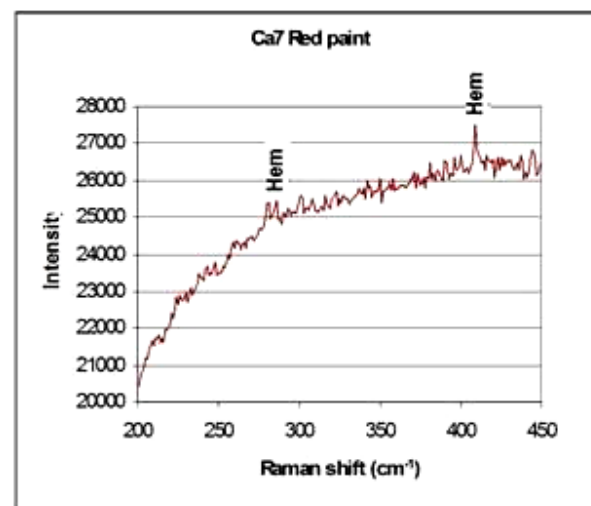
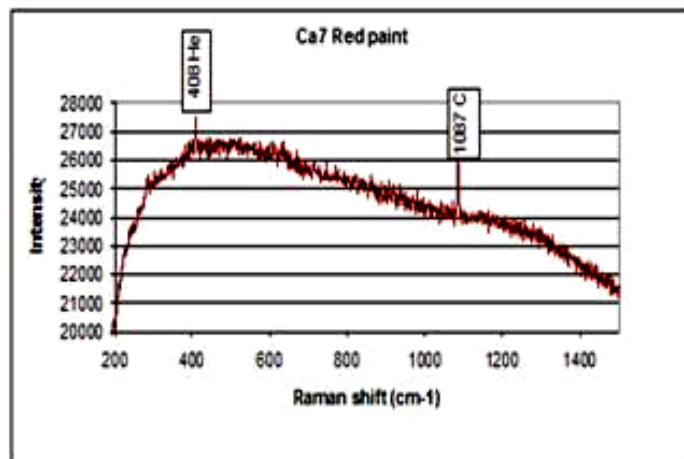


Fig. B.2.2. Sample Ca7. Red paint layer with some of the characteristic peaks of hematite (283 and 409) and calcite (1087).

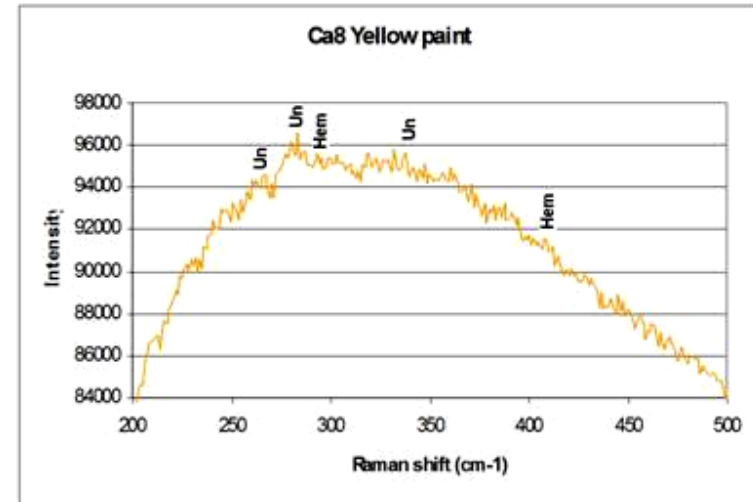
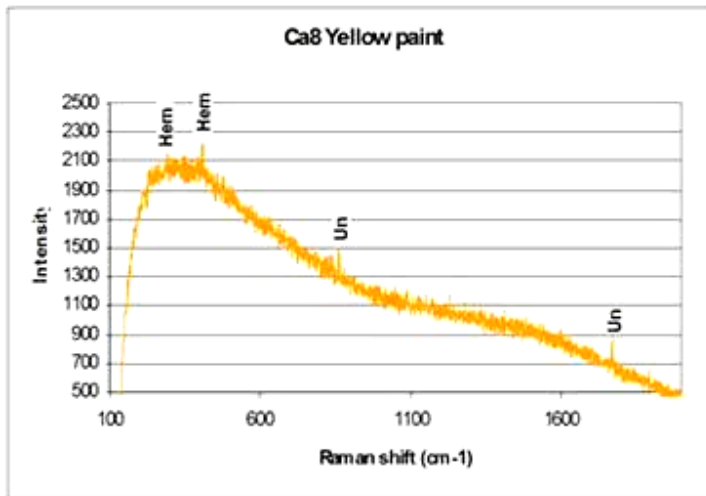


Fig. B.2.3. Sample Ca8. Yellow paint layer with some of the characteristic peaks of hematite (291 and 409) and unidentified peaks (282, 838 and 1772).

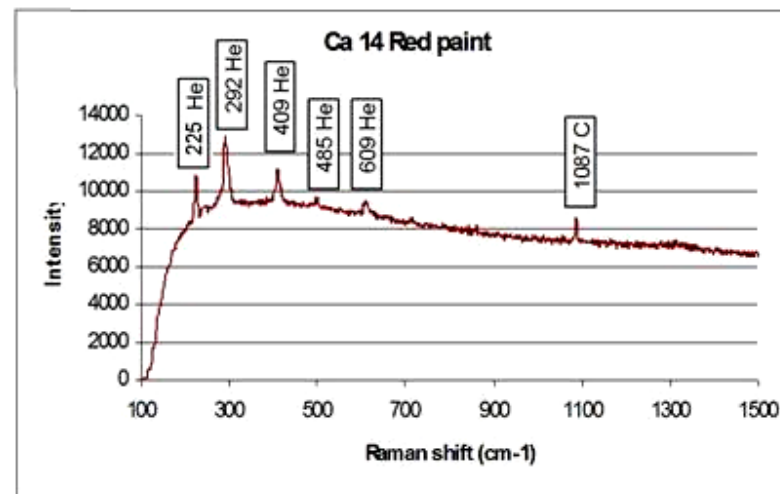


Fig. B.2.4. Sample Ca14. Red paint layer with some of the characteristic peaks of hematite (225, 292, 409, 486, 609) and calcite (1087).

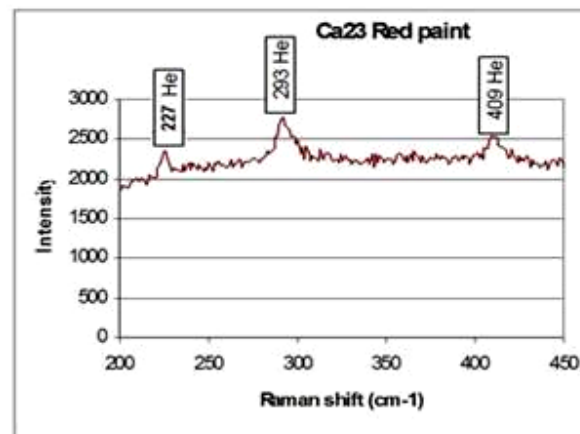
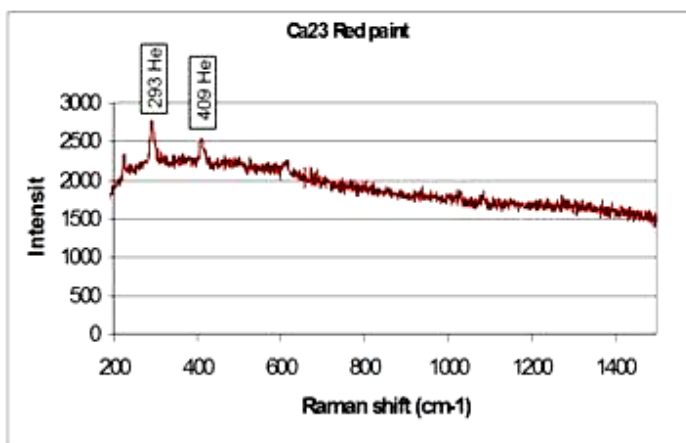


Fig. B.2.5. Sample Ca23. Red paint layer with some of the characteristic peaks of hematite (227, 293, 409) and calcite (1087).

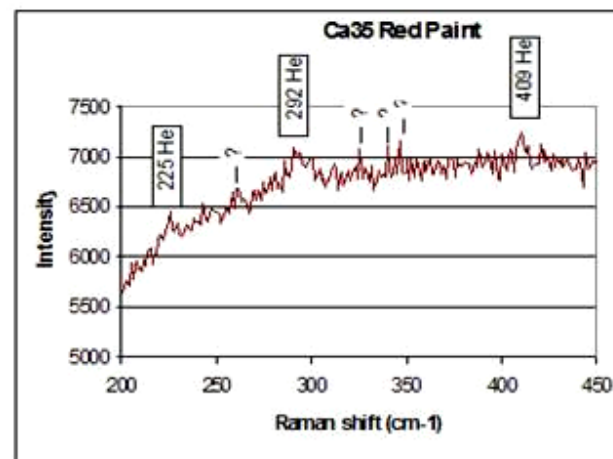
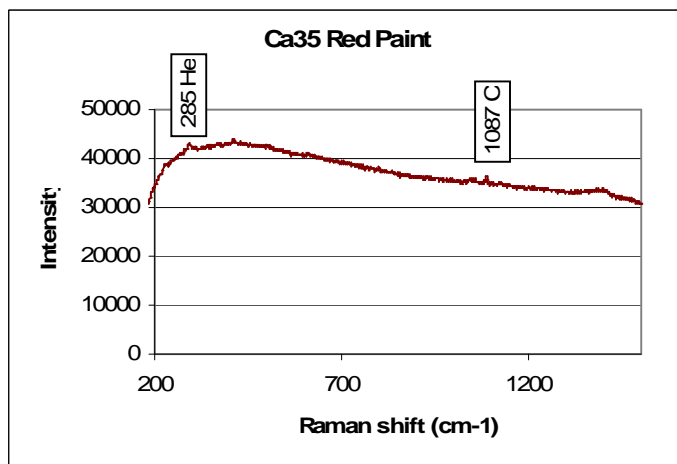


Fig. B.2.6. Sample Ca35. Red paint layer with some of the characteristic peaks of hematite (227, 292, 409) and calcite (1087), and unidentified peaks (260, 325, 339 and 346).

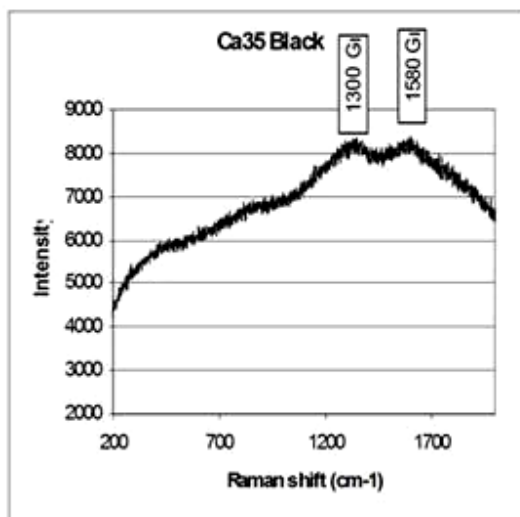


Fig. B.2.7. Sample Ca35. Black paint layer with the characteristic peaks of graphite (1300 and 1580).

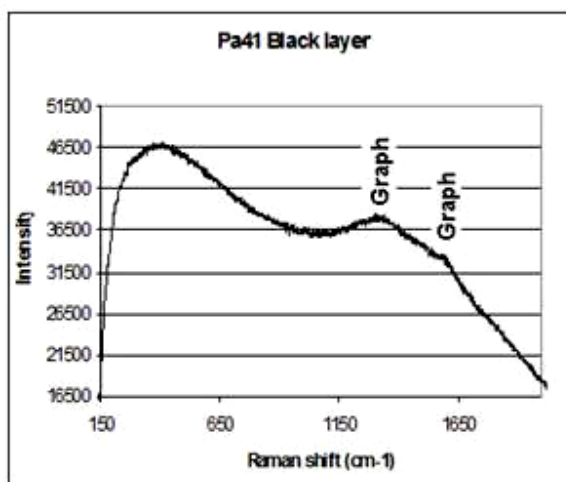


Fig. B.2.8. Sample Pa41. Black paint layer with the characteristic peaks of graphite (1300 and 1580).

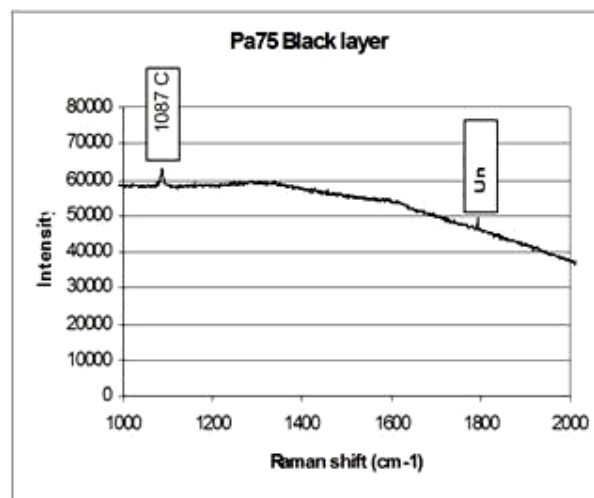


Fig. B.2.9. Sample Pa75. Black paint layer with the peak of calcite (1087) and unidentified peak (1763).

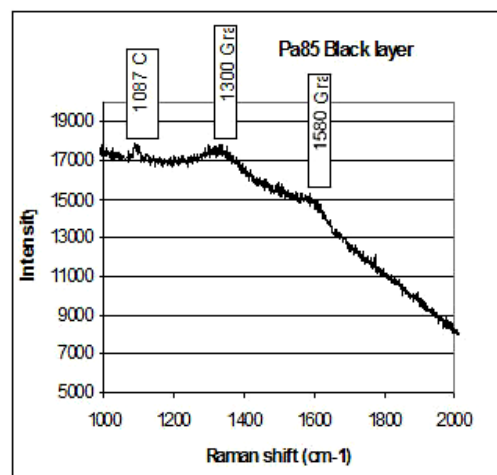


Fig. B.2.10. Sample Pa85. Black paint layer with the peaks of calcite (1087) and graphite (1300, 1580).

Glossary

Acicular: Needle- shaped. A type of crystal habit.

Accretionary lapilli: Material that is aggregated into rounded particles during volcanic eruptions or impact events due to moisture or other factors. Lapilli include particles between 2 mm and 64 mm in diameter.

Aggregate: Material that is mixed with a binder and water in the manufacture of plasters and mortars. The type of aggregates and the aggregate/binder ratio have a fundamental role in the mechanical properties of the plasters.

Anhedral: Crystals with no defined external faces.

Argillization: Alteration by which certain minerals or glass are transformed into clay minerals.

Bak ch'ich': Yucatec Maya term for denoting a stone powder obtained as the waste material from quarrying activities. In modern days masons combine *bak chich* with sascab in order to obtain a more durable material in the plasters mixtures (V. García, personal communication 2005).

Bak pek: Yucatec Maya term for denoting gravel-size fragments of stone that are obtained as waste from quarrying activities. *Bak pek* is employed in modern times in the Maya area as aggregate material in the manufacture of plasters. It is also employed as a compacted layer before a layer of *bak ch'ich'* during the construction of floors (V. García, personal communication 2005).

Breccia: Rock composed of angular fragments of preexisting rocks or minerals cemented by a microcrystalline matrix (Tarbuck and Lutgens 1999).

Cement: A microcrystalline material that sets independently and can bind other materials together. The term is usually employed to refer to Portland cement, the most common cement employed in modern masonry construction. In petrology, the cement of a rock is the microcrystalline mass that binds bigger minerals or clasts together.

Chicxulub: The name of an impact crater that is buried underneath the Yucatan Peninsula in Mexico. It is named after the town of the same name, which is located roughly at the centre of the impact crater. The impact occurred roughly 65 million years ago and it is considered to have played a major role in the mass extinction at the end of the Cretaceous period (Arenillas 2006),

Clast: A fragment of preexisting rock. The term is usually employed in sedimentary rocks.

Clay: The term “clay” is applied to both a particle size range and a group of minerals. Clay-size particles are those that measure less than .002 mm in diameter. Clay minerals are aluminium phyllosilicates with some contents of iron, magnesium, alkali metals, alkali earths and other cations.

Cocciopesto: Italian for “crushed earthenware”. In plaster manufacture *cocciopesto* refers to the Roman technique for producing a durable material by adding crushed fragments or dust of bricks or terracotta to the slaked lime in order to obtain a hydraulic set.

Component plot: In statistical analyses of data reduction, a component plot is diagram that illustrates how variables are interrelated and how they influence the grouping of the samples.

Concrete: A mixture of binder, aggregates and water. It is usually employed to refer to thick layers or to mixtures with cobble-size aggregates. Concrete also refers to the mixtures in which Portland cement is employed as binder. The term is not employed in my thesis.

Chultun (pl. *chultunoob'*): Yucatec Maya for water/rain and precious stone (Alvarez 1984:52). In Maya archaeology a *chultun* is a container built under the floor, usually plastered, that is found most commonly in sites of the Northern Maya lowlands. *Chultunoob'* are considered to have been used as cisterns and for food storage.

Devitrification: The development of a crystalline structure in an originally amorphous material, usually glass, due to the unstable nature of this material in environmental conditions.

Dolomite: Mineral composed of calcium magnesium carbonate, $\text{Ca.Mg}(\text{CO}_3)_2$. Dolomite is the major component of dolostones and dolomitic limestones.

Dolostone: Sedimentary rock composed primarily of the mineral dolomite. Dolostones are thought to have been formed from limestones by the replacement of calcium by magnesium based on the fact that most dolostones are of considerable age.

Ejecta: Material that is expelled during a volcanic eruption or a meteorite impact and which is deposited long distances away after traveling by air or under water.

Euhedral: Crystals with well-formed crystal faces.

Habit: The appearance of a crystal as a result of its crystal faces. It is usually employed for individual crystals that have grown freely without encountering any pre-existing solids.

Hydraulic lime: Lime produced by the reaction of reactive silica and alumina with lime to form calcium and silicate and aluminates hydrates, which results in a hard material that sets under water. Hydraulic limes can be produced by burning a limestone with clay content (natural hydraulic lime) or by deliberately adding siliceous materials to the limestone before calcination (artificial hydraulic limes). A hydraulic set can also be obtained by adding pozzolanic aggregates to the slaked lime.

Impactite: A rock that has been created or modified by a meteorite. Impactites include melts, target rocks affected by shock metamorphism, and sedimentary rocks with impact components.

Isotropic: A material that has the same properties in all directions. In optical microscopy, an isotropic material is the one that is not affected by polarised light and remains dark under crossed polars. There are few isotropic minerals and they all belong to the cubic system (Gribble and Hall 1992). Other isotropic materials include amorphous, such as glass and organic matter.

Lake pigment: A pigment that is manufactured by precipitating a dye over an inert medium.

Limewash: A thin coat of lime that is applied by brushing over lime plaster layers.

Micritic calcite: Calcite crystals that are less than 4 microns in size and form a cement in some limestones. Under the optical microscope, individual crystals of calcite cannot be seen.

Mortar: The plaster that is employed to bind masonry blocks together. Sometimes it is also used as a generic term interchangeable with plaster, although its use in this thesis is limited to the plasters employed for joining masonry blocks.

Pak luum: Maya term for denoting the earth plaster that is used in traditional Maya wattle and daub architecture. From *pak* (wall) and *luum* (earth) (Alvarez 1984:232).

Plaster: Mixture of aggregates, binder and water that is employed as a cementing, rendering or joining material in construction. The term is usually employed for lime-based materials. In this thesis it is employed as an umbrella term, regardless of the aggregate size observed or the architectural function or location.

Phenocrystal or phenocryst: In volcanic rocks, the term refers to a crystal that is distinctively larger than those of the groundmass. Phenocrysts are found in porphyritic rocks as a result of two-stage cooling of the magma.

Polity: term originally employed to refer to the Greek city-states. In Maya archaeology, the term refers to the sites with assumed autonomous political organisation.

Pozzolanas and pozzolanic aggregates: Materials rich in silica and alumina that are added to the lime during slaking to produce a chemical reaction that results in calcium silicate and aluminate hydrates. The resulting material is known as hydraulic lime.

Sascab: Maya term for denoting calcareous sediments produced as an in-situ weathering of limestone. Sascab includes a range of sediment sizes, from clay-size sediments to boulders. Sascab is usually found under a hardened carapace or under the soil in the karstic terrain of the Maya lowlands.

Shocked quartz: The type of quartz in which the crystalline structure has been deformed along planes due to immense pressure but limited temperature. Shocked quartz is produced during nuclear testing or meteorite impacts.

Sintering temperature: Temperature at which powder particles adhere to each other, forming a coherent mass without melting. In cement chemistry, sinterization of limestone and clays occurs in temperatures above 1,400°C (Callebaut 2001).

Stelae: Carved stone slabs used in the Maya area and other cultural areas of the ancient world. In the Maya area they were primarily used during the Classic period to record dynastic sequences and political events with the use of Maya writing and the long count calendar.

Stoichiometry: The calculation of the quantities and relationships of reactants and products involved in a chemical reaction. A compound converted by stoichiometry refers to the calculation of the molecular weight of a certain compound based on the molecular weight of the compound from which it is converted and the relationship (proportion) of each of the elements of both compounds.

Stucco: Umbrella term in Mesoamerican archaeology that refers to any lime-based plaster that is employed in masonry architecture, regardless of its location, quality or appearance. Outside Mesoamerican archaeology the term refers more specifically to modelled decorations. The term stucco is not employed in my thesis.

T'aan: Yucatec Maya term to denote both ash and lime. In order to remove the ambiguity the prefix *ku* is employed with *t'aan* to refer to lime, whereas the prefix *dzi* is employed to refer to ash (*ku t'aan*: lime; *dzi t'aan*: ash) (Alvarez 1984, Bolles 2001).

Tektite: Natural glass objects that are formed as a result of large meteorites impacting on the earth's surface.

Tephra: Material that falls from the air in volcanic eruptions, regardless of its composition or particle size.

Tzaal: Term used by the Itzaj Maya to identify the porous soft and easily quarried limestone that underlies the region and which is preferred over other types of limestone as raw material for lime production. A corruption of this Maya word results in the Spanish term "piedra de sal" or "stone of salt" (Hofling 1997 in Schreiner 2002:51).

Abbreviations and Acronyms

Å: Ångstrom. Unity of length. 1 Å= 0.1 nanometers.

BSE: Backscattered electrons. In scanning electron microscopy, these electrons are reflected or backscattered in elastic scattering (i.e. the scattering that does not lose energy but changes the direction of propagation). Backscattered electron images are employed for observing differences in composition, since heavy atoms backscatter electrons more strongly and therefore appear brighter in the images (Pollard 2007).

CCLRC: Central Laboratory of the Research Councils.

CNCPC: Coordinación Nacional de Conservación del Patrimonio Cultural.

CONACYT: Consejo Nacional de Ciencia y Tecnología, México.

IIA: Instituto de Investigaciones Antropológicas.

INAH: Instituto Nacional de Antropología e Historia, México.

LA-ICP-MS: laser ablation inductively coupled plasma mass spectrometry.

µm: Micron or micrometer. Unity of length. 1 mm= 1,000 µm

MPa. Megapascal. Multiple of Pascal, the main unit of pressure of the International System of Units. Megapascals are used for pressures applied in small areas.

OM: Optical microscopy.

ORPLM: Optical reflected polarised light microscopy.

PCA. Principal component analysis. Statistical analysis that is used for data reduction. PCA reduces the number a variables to a smaller number of artificial variables that are not correlated with one another. It provides useful information for the understanding of the relationship between variables, the relationship between units, and indicates which variables are involved in the trends (Shennan 1997).

PPL. Plane polarised light. In optical microscopy, PPL refers to light that has been filtered by a polariser, which results in wavelengths travelling in a single plane. PPL is employed to observe colour, pleochroism, habit, cleavage and relief of minerals.

σ: Lower case of the Greek letter sigma. In statistics, it is employed to refer to standard deviation.

SE: Secondary electron. In scanning electron microscopy, secondary electrons are the ones produced as a result of inelastic scattering (i.e. scattering in which there is a change in energy). Secondary electron images provide information about the topography of samples since edges and raised areas generate more secondary electrons and consequently appear brighter.

SEM-EDS. Scanning electron microscopy/ Energy dispersive spectrometry. Scanning electron microscopy is an analytical technique for the observation of materials at high magnifications. Energy dispersive spectrometry is a device attached to the scanning electron microscope that is employed to obtain semi-quantitative elemental compositions.

UNAM: Universidad Nacional Autónoma de México.

XPL. Cross polarised light. In optical microscopy, XPL is obtained when, in addition to the polariser that is employed in plane polarised light, an analyser is inserted into the optical path. XPL is employed to observe isotropism, birefringence, extinction angle, twinning and zoning of minerals.

XRD: X-ray diffraction. Analytical technique that is employed for the characterisation of crystalline materials. XRD is based on the diffraction of light as it interacts with the crystalline structure of samples.

XRF. X-ray fluorescence. Analytical technique for the characterisation of elemental composition of materials. XRF is based on the interaction of X-rays with the atoms that make up the samples.

List of Figures

Chapter 1

Fig. 1.1. Location of case studies and other Maya sites.

Chapter 2

Fig 2.1. Physiography of the Maya area.

Fig. 2.2. Physiographic variation in the Maya area. Cross section South-North.

Fig.2.3 Geology of the Maya area.

Fig.2.4. Physiographic areas of the Yucatan Peninsula.

Fig.2.5. Age of the rocks and sediments in the Maya area and locations of the three case studies.

Fig.2.6. Chicxulub crater center and outcrops of impact ejecta. Location of Chichón volcano.

Fig. 2.7. Chicxulub ejecta deposits. Left: Cretaceous/Palaeogene boundary at Guayal. Right: Quarry at Albion Island with visible K/T deposits.

Fig. 2.8. View of a sascab quarry (sascabera) in Indian Church, Lamanai, Belize and detail of chert nodule in sascab quarry at Indian Church.

Fig. 2.9. Location of Palenque showing the geological diversity of the region.

Fig. 2.10. Palenque Map.

Fig. 2.11. Temple of the Sun, Palenque.

Fig. 2.12. Calakmul. View of Structure I.

Fig.2.13. Central area of Calakmul with hydraulic system of canals and reservoirs.

Fig.2.14. Building phases of Structure II, Calakmul.

Fig. 2.15. Drawing of lime plaster frieze in substructure IIc1, Calakmul.

Fig. 2.16. Barrel vault of Substructure IIc, Calakmul.

Fig. 2.17. Structure N10-43, the High Temple, Lamanai.

Fig. 2.18. Plan of Lamanai.

Fig. 2.19. Structure YDLII. Remains of the 16th century Spanish church, Lamanai.

Chapter 3

Fig. 3.1. Chemical reactions that occur in the lime cycle.

Fig. 3.2. Drawing of a sascab mine or sascabera.

Fig. 3.3. Structure 327 of Cuello showing postholes and numerous layers of lime plasters dating from the Swasey and Bladen phases.

Fig. 3.4. Partially lost lime plaster relief sculpture showing scratched design on the wall at Palenque.

Fig. 3.5. Sak Nuk[ul] Nah glyph.

Fig. 3.6. Sak Xok Naah glyph (The white house for counting) in Vault number 19 of Ek'Balam: Right: Detail of Ek' Balam's structure 35.

Fig. 3.7. Depiction of 4,000 loads of lime in the Mendoza codex.

Fig. 3.8. Left: Calera construction in the early 20th at Chichén Itzá. Right: After the burn the lime is left to slake in the open air. Pictures: Morris and colleagues (1931).

Fig. 3.9. Lime burning at Chan Kom. Picture: Redfield and Villa (1934).

Chapter 4.

Fig. 4.1. Possible sequence or *chaîne opératoire* of lime plaster production.

Fig. 4.2. Schematic representation of technological choices and the factors that influence decision-making throughout the sequence of production.

Chapter 6

Fig. 6.1. CaCO₃ vs MgCO₃ scatter plot (weight %). XRF data of Palenque samples.

Fig. 6.2. CaCO₃ + MgCO₃ vs SiO₂ + Al₂O₃ scatter plot (weight %). XRF data of Palenque samples.

Fig. 6.3. Scatter plot of the two principal components (PCA) of bulk compositional XRF data of Palenque samples.

Fig. 6.4. Left: Sample Pa56: clay-based plaster with a clast of breccia, Right: clast of breccia with angular grains of shocked quartz supported by a partially isotropic matrix.

Fig. 6.5. Reaction rims around devitrified glass. Left: sample Pa67. Right: sample Pa70.

Fig. 6.6. Sample Pa28. Organic substance with secondary calcite recrystallised over it.

Fig. 6.7. Sample Pa75. Wall render, interior wall of the Temple of the Foliated Cross. Left: Mosaic of pictures showing 60 black layers. Right: detail with limewashes alternated with visible black layers.

Fig. 6.8. Sample Pa24. External wall from the rear façade of the Temple of the Sun. Limewashes with no visible black layers.

Fig. 6.9. Sequence with 15 layers of floors in the stepped platform of the Temple of the Foliated Cross. Left: General view. Right: detail.

Fig. 6.10. CaCO₃ + MgCO₃ Vs SiO₂ + Al₂O₃ scatter plot (weight %) of Calakmul samples.

Fig. 6.11. Principal component analysis of XRF compositional data of Calakmul samples.

- Fig. 6.12.** Aggregate formed by aluminosilicate crystals, likely cordierite. Sample Ca9. XPL. Scale bar: 0.5 mm.
- Fig. 6.13.** Sample Ca16. Yellow mineral associated with acicular phases.
- Fig. 6.14.** Sample Ca30. Inclusions with cellular structure. Left: PPL. Scale bar: 500 microns. Right: BSE image that shows they are part of a carbonate aggregate. Scale bar: 500 μ m.
- Fig. 6.15.** Clay-size calcareous materials. Left: sample Ca3, BSE image. Right: Sample Ca4. BSE image.
- Fig. 6.16.** $\text{CaCO}_3 + \text{MgCO}_3$ Vs $\text{SiO}_2 + \text{Al}_2\text{O}_3$ scatter plot of bulk XRF data of Lamanai samples.
- Fig. 6.17.** Principal component analysis of bulk XRF data of Lamanai samples.
- Fig. 6.18.** Sample La6. Fragment of plaster recycled as aggregate. Red and blue/green paint layers can be seen, and possibly the use of ceramic as aggregate in the recycled plaster.
- Fig. 6.19.** Hexagonal prisms of calcite. Left: Sample La9, isolated crystals in matrix. Right: sample La31, crystals in channel.
- Fig. 6.20.** Left: sample La21. Large rhombohedral prisms cemented by smaller crystals. SE image. Right: sample La19. Large rhombohedral crystal with smaller platy crystals in its faces.
- Fig. 6.21.** Left: two layers of floors in Str. N10-15. Right: five thick layers in debris recovered in the pit west of Str. N12-11 (YDLI).

Chapter 7

- Fig. 7.1.** Stone quarrying at Palenque, likely dolostone.
- Fig. 7.2.** Sample Pa56. Clayey matrix with shrinkage cracks and shell fragments.
- Fig. 7.3.** Architectural modifications. Left: modification of a doorway at the Temple of the Foliated Cross with partially lost mud plaster. The orange line shows the original shape of the doorway. Right: dividing wall in the House D of the Palace.
- Fig. 7.4.** Dividing wall (architectural modification) at the Temple of the Foliated Cross. Mud mortar with unmixed lime lumps. A limewash painted on black can be seen at the left.
- Fig. 7.5.** Thick pure lime plasters used as joining mortars and renders. Left: original wall at Temple of the Foliated Cross (cross section of collapsed wall). Right: original wall in House D at the Palace.
- Fig. 7.6** Grains of shocked quartz with visible PDFs. Left: sample Pa56. Centre: sample Pa89. Right: Pa53.
- Fig. 7.7.** Sample Pa66. Left: visible aggregates in macroscopic scanned view. Right: detail of aggregates constituted by partially isotropic matrix of SiO_2 -rich cement and carbonate particles. No phenocrystals can be seen.

- Fig. 7.8.** Location of the samples from the temples of the Cross Group.
- Fig. 7.9.** Left: black paint layer in sculptures of the Temple of the Inscriptions at Palenque (Villaseñor and Price 2008). Right: soot layers in sample Pa75 from wall render of the Temple of the Foliated Cross.
- Fig. 7.10.** Left: sample Ca10: lime plaster with the clear use of sascab as aggregate. Right: sascab sample from Calakmul.
- Fig. 7.11.** Carbonates vs $\text{SiO}_2 + \text{Al}_2\text{O}_3$ contents in bulk composition of Calakmul plasters.
- Fig. 7.12.** Macroscopic scanned view of sample Ca3 (Terminal Classic) showing multiple cracks and a brown matrix. Right: sample Ca3. Clayey matrix with shrinkage cracks and plant fibres.
- Fig. 7.13.** Sample Ca18 showing isotropic phases.
- Fig. 7.14.** Acicular phases that suggest the use of hydraulic components. Left: sample Ca6. Right: sample Ca8.
- Fig. 7.15.** Distribution of ash-tempered ceramics in the Maya lowlands.
- Fig. 7.16.** Sample Ca31 Early Classic (?) floor with isotropic layer over the surface.
- Fig. 7.17.** Samples rich in a silicate mineral, likely a mineral from the serpentine group, from lower layers of floors, thought to be compacted sediments (not burnt lime). Left: sample Ca29 (Late Preclassic period). Right: sample Ca9 (Middle Preclassic Period).
- Fig. 7.18.** Large recarbonated polyhedrons in sample Ca14. SE image.
- Fig. 7.19.** Left: Ascidiens in sample Ca8. SE image. Centre: Ascidiens in sample Ca15. Right: faecal pellets in sample Ca13 composed of micritic calcite.
- Fig. 7.20.** Amorphous silica plant remains. Sample Ca30.
- Fig. 7.21.** Angular aggregates of micritic calcite (crushed limestone) in Late Preclassic plaster. Left: sample La25. Right: sample La24.
- Fig. 7.22.** Sample La20. Left: macroscopic scanned view with visible yellow inclusions. Right: thin section of the same sample with devitrified volcanic glass shard
- Fig. 7.23.** Sample La49 (from Late Postclassic architecture). Quartz grains embedded in devitrified glass.
- Fig. 7.24.** Left: sample La35 (compacted sascab). Micritic calcite with cracks parallel to the surface. Right: Hyatt floor of the Holiday House (Str. P9-25), characterised as compacted sascab.
- Fig. 7.25.** Construction of sascab roads in Belize, close to the site of Lamanai.
- Fig. 7.26.** Sample La 22 from Structure N12-12 of the Late Postclassic (Tulum-style temple). Superimposed layers with different characteristics, separated by a limewash.

List of Tables

Chapter 1

Table 1.1. Plaster samples analysed in this research.

Chapter 2

Table 2.1. Geologic timescale of the Phanerozoic Eon.

Table 2.2. Mesoamerican chronology.

Table 2.3. Dynastic history of Palenque.

Chapter 5

Table 5.1. Inventory of samples analysed.

Table 5.2. Analyses carried out.

Chapter 7

Table 7.1 Analyses of glass inclusions in samples Pa18 and Pa27. Major components of normalised totals with Ca and Mg reported as oxides and carbonates.